IDAHO
DEPARTMENT OF ENVIRONMENTAL QUALITY

PARTIAL PERMIT FOR HWMA STORAGE and TREATMENT

for the

LIQUID WASTE MANAGEMENT SYSTEM at the IDAHO NUCLEAR TECHNOLOGY & ENGINEERING CENTER

on the

IDAHO NATIONAL LABORATORY

EPA ID NO. ID4890008952

Effective Date: October 18, 2004
Revision Date: December 2, 2013
Book 4 of 4

RCRA PERMIT

FOR THE

IDAHO NATIONAL LABORATORY

Volume 14
INTEC Liquid Waste Management System

Appendix IV

Final Report for Organics Partitioning Resulting from Operation of an INTEC Double Needle Sampler
(INEEL/EXT-03-00774)

Revision Date: October 29, 2008

INEEL/EXT-03-00774

Final Report for Organics Partitioning Resulting from Operation of an INTEC Double Needle Sampler

Mike Heiser
and
Science Applications International Corporation

June 2003

Idaho National Engineering and Environmental Laboratory

Idaho Falls, Idaho 83415

Prepared for the
U.S. Department of Energy
Assistant Secretary for Environmental Management
Under DOE Idaho Operations Office
Contract DE-AC07-99ID13727

SAIC SCIENCE TECHNOLOGY
APPLICATIONS RESEARCH CENTER

FINAL REPORT FOR ORGANICS PARTITIONING RESULTING FROM OPERATION OF AN INTEC DOUBLE NEEDLE SAMPLER

Revision 1
September 24, 2002

Prepared for :
Bechtel BWXT Idaho, LLC
Idaho National Engineering and Environmental Laboratory
Idaho Falls, ID 83415

Prepared by:
Science Applications International Corporation
950 Energy Drive
Idaho Falls, ID 83401
Contract No. 00000127, Release No. 1

Acronym List

cc	cubic centimeter
EE	End Effector
g	gram
GC/MS	Gas Chromatograph/Mass Spectrometer
IDEQ	State of Idaho Department of Environmental Quality
INEEL	Idaho National Engineering and Environmental Laboratory
INTEC	Idaho Nuclear Technology and Engineering Center
l	liter
LDUA	Light Duty Utility Arm
M	Molar
mg	milligram
ml	milliliter
N	Normal
ng	nanogram
NWCF	New Waste Calcining Facility
PEWE	Process Equipment Waste Evaporator
psig	pounds per square inch gage
ppb	part per billion
ppm	part per million
RCRA	Resource Conservation and Recovery Act
STAR	Science Technology Applications Research (Center)
TCA	1,1,1-Trichloroethane
TFF	Tank Farm Facility
TOC	total organic carbon
μl	microliter
VOC	volatile organic constituents

Table of Contents

1.0 BACKGROUND 1

1.1. Previous Organic Partitioning Tests 1
1.2. Conclusions from Previous Organic Partitioning Tests 2
1.2.1. Bench-Scale Evaporator Conclusions 2
1.2.2. LDUA End Effector Conclusions 3

2.0 TEST OBJECTIVES 4

3.0 BENCH-SCALE PROCESS EQUIPMENT 4

4.0 DOUBLE NEEDLE SAMPLER TEST SUMMARY 7

4.1. Feed Preparations 7
4.2. Test Methodology and Sample Collection 8
4.2.1. Sample Collection Using the Double Needle Sampler 9
4.2.2. Sample Collection from the Feed Tank Drain 10
4.3. Analytical Results 11

5.0 DATA INTERPRETATION 12

5.1. Double Needle Sampler Test Data 12
5.2. Comparison with Previous Organic Partitioning Tests 18
5.3. Comparison with INTEC Sampling 18

6.0 CONCLUSIONS 19

7.0 REFERENCES 20

List of Figures

Figure 1-1: PEWE Volatile Organic Partitioning 2
Figure 1-2: PEWE Semi-Volatile Organic Partitioning 3
Figure 1-3: LDUA Sample EE Volatile Organic Partitioning 3
Figure 3-1: STAR Center Bench-Scale Evaporator System 4
Figure 3-2: Bench-Scale Evaporator System Diagram 5
Figure 3-3 Double Needle Sampler 6
Figure 3-4 Double Needle Sampler with Sample Bottle 7
Figure 5-1: Comparison of Time Relative Sample Analysis for CS_2 Data 15
Figure 5-2: Comparison of Time Relative Sample Analysis for 1,1,1-Trichloroethane Data 16
Figure 5-3: Comparison of Time Relative Sample Analysis for Toluene Data 17

List of Tables

Table 4-1: Double Needle Sampler Feed Solutions (for 44 Liters of feed) 8
Table 4-2: Double Needle Sampling System – Sampling Requirements 9
Table 5-1. Analysis of Double Needle Sampler versus Direct Feed Tank Samples for Volatile Organic Constituents. 13

1.0 BACKGROUND

The double needle sampler testing is a continuation of previous test series that investigated the fate of organic species in the Process Equipment Waste Evaporator (PEWE) system at the Idaho Nuclear Technology and Engineering Center (INTEC). This test series was designed to investigate the effects of operation of the double needle sampling systems on volatile organic constituents in an acidic feed matrix.

The PEWE, located in CPP-604, reduces the volume of mixed waste sent to the Tank Farm Facility at the INTEC. The PEWE system consists of feed tanks for accumulation of waste solutions, two evaporator trains for processing the waste solution, a bottoms collection vessel, and condensate collection vessels. The waste solutions are transferred from the feed tanks to the evaporator vessel, where the solution is heated and circulated through the evaporator. The overhead vapors generated in the evaporator are condensed and transferred to the PEW condensate collection tanks. The condensate is accumulated in the condensate collection tanks for further processing at the Liquid Effluent Treatment and Disposal Facility, CPP-1618. The remaining solution is circulated through the evaporator until procedurally designated limits are met, at which time the solution is transferred to the bottoms collection vessel. The bottoms are eventually transferred to the Tank Farm Facility for storage.

Although extensive process information is available regarding wastes processed in the PEWE, there is less information regarding hazardous organic constituents. Hazardous organic species have been discharged to the PEWE system as a result of past operating practices. Studies were conducted to determine the fate of the organic compounds in the INTEC Tank Farm,[1] but these studies did not address the effects of the evaporation process on the fate of the organics. SAIC has conducted four bench-scale evaporator and two Light Duty Utility Arm tests to evaluate the fate of spiked organics in a high and low molarity nitric acid simulated feeds. The results of these tests indicated that INTEC sample collection and handling procedures do not significantly effect the concentration of volatile organic or semi-volatile organic constituents in the waste stream.[2]

1.1. Previous Organic Partitioning Tests

In 1998 a series of organic partitioning tests were initiated at SAIC's Science Technology Applications Research (STAR) Center located in Idaho Falls, Idaho. These tests were designed to support the Idaho National Engineering and Environmental Laboratory (INEEL) INTEC permitting, regulatory, and closure decision makers. Primary test objectives included:

- Quantify organic partitioning that results from STAR Center bench-scale evaporator operation,
- Quantify organic losses that result from operation of the Light Duty Utility Arm (LDUA) sampler end effector, and
- Determine organic losses that may be attributed to INTEC sampling procedures.

1.2. Conclusions from Previous Organic Partitioning Tests

Test series conclusions were based on quantitative data analysis as well as qualitative observations. Results provided a representation of the fate of organics in the PEWE system and LDUA sample end effector.

1.2.1. Bench-Scale Evaporator Conclusions

Analytical data revealed that up to 75% of the volatile organics and 40% of the semi-volatile organics spiked to the PEWE feedstock were destroyed, decomposed, reacted, or volatilized prior to evaporator processing. This percentage may be dependent upon the physical properties (e.g. vapor pressure) of each compound.[2]

Bench-scale PEWE bottoms were virtually free of volatile organic compounds. Given that the bench-scale feedstock was spiked with 3-4 orders of magnitude higher volatile organic constituent (VOC) concentrations than found at INTEC, it is reasonable to conclude that detectable VOC concentrations will not be present in the TFF and were not introduced to the calciner. It is likely, however, that semi-volatile compounds processed through the PEWE will be present in the TFF and calciner feed.

Analytical data did not conclusively indicate that INTEC sample collection and handling procedures effect VOC or SVOC concentrations. Figures 1-1 and 1-2 below present simplified partitioning mass balances, from bench-scale evaporator operation, of volatile and semi-volatile organics.[2]

Figure 1-1: PEWE Volatile Organic Partitioning
[Basis = 100 mass units]

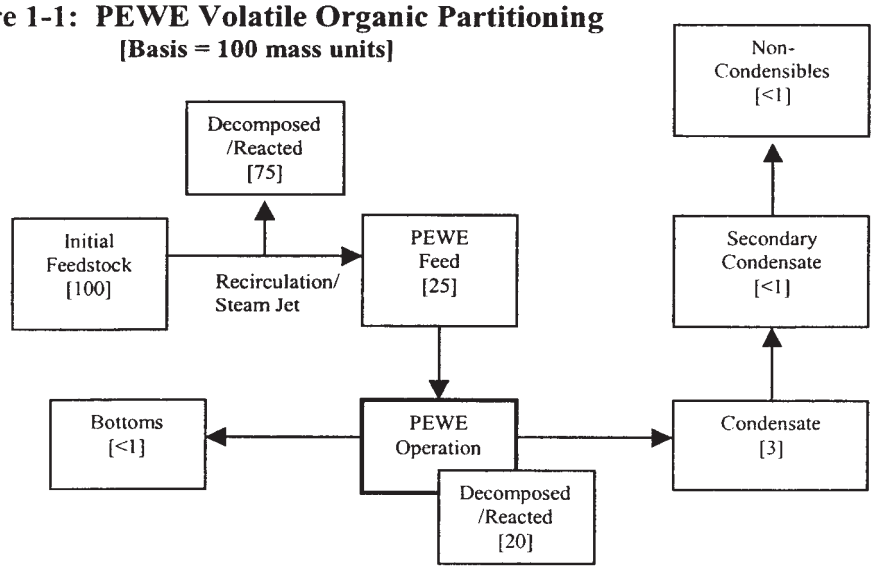

Figure 1-2: PEWE Semi-Volatile Organic Partitioning
[Basis = 100 mass units]

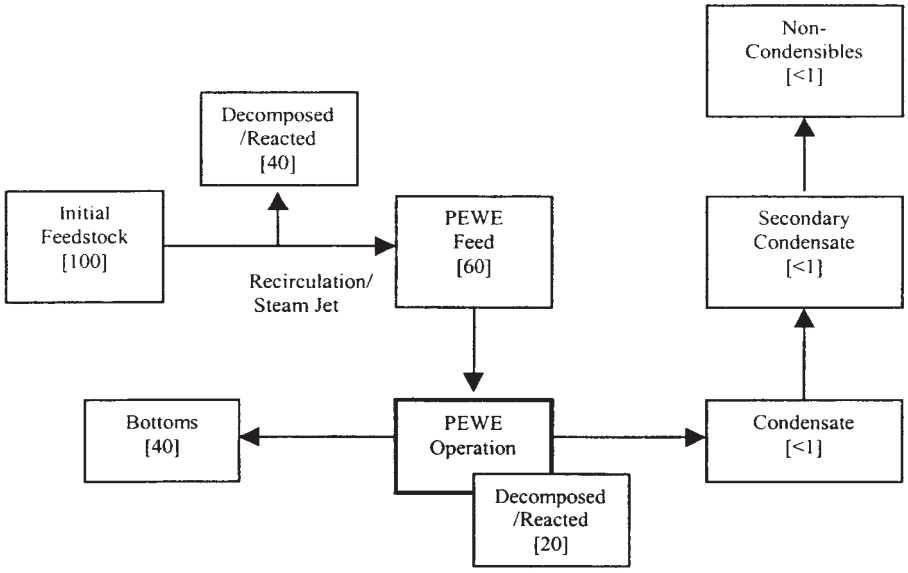

1.2.2. LDUA End Effector Conclusions

Analytical data indicated that LDUA sample EE operating vacuums effect volatilization of organic species in simulated tank heel residue. Each operating vacuum yielded consistent data resulting in a good material balance about the end effector. The data indicated that the higher the operating vacuum, the greater the resulting volatile organic volatilization. Based on LDUA testing, it was recommended that the end effector be operated at the lowest operating vacuum allowed by the heel matrix. Figure 1-3 below presents a simplified volatile organic balance about the LDUA sample EE.[2]

Figure 1-3: LDUA Sample EE Volatile Organic Partitioning
[Basis = 100 mass units]

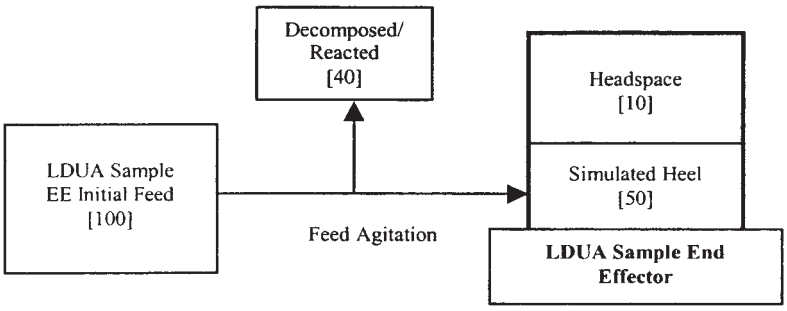

An independent evaluation of INTEC analytical procedures (Analytical Chemistry Methods) compared to SW-846 specified methods was conducted to identify variances, should they exist, between the analytical protocols. Identified variances were satisfactorily addressed by the INTEC Remote Analytical Laboratory thereby establishing analytical equivalency.

2.0 TEST OBJECTIVES

In February 2001, the results of previous organic partitioning testing were presented to the State of Idaho Department of Environmental Quality (IDEQ). At this time, the IDEQ requested that additional testing be performed to statistically quantify potential losses of volatile organic species that may be attributed to the double needle sampling systems currently utilized at INTEC. As such, the double needle sampler testing was designed to determine the effects of operation of the double needle sampling systems on volatile organic species that have potentially been introduced into the PEWE system.

3.0 BENCH-SCALE PROCESS EQUIPMENT

The bench-scale PEWE system was been designed and constructed at the SAIC Science and Technology Applications Research (STAR) Center to model typical PEWE system operations. The bench-scale system consists of a feed tank, evaporator vessel with an attached thermosiphon reboiler, bottoms collection tank, condensate collection tank, and tank sampling station.

Testing of the double needle sampler system utilized the feed tank, sample station, and vessel off-gas systems only. An image of the STAR Center bench-scale evaporator system is presented as Figure 3-1 and a flow diagram of the bench-scale system is shown in Figure 3.2. The only modification to the bench-scale evaporator system for double needle sampler testing was the addition of a mechanical mixer to the feed tank

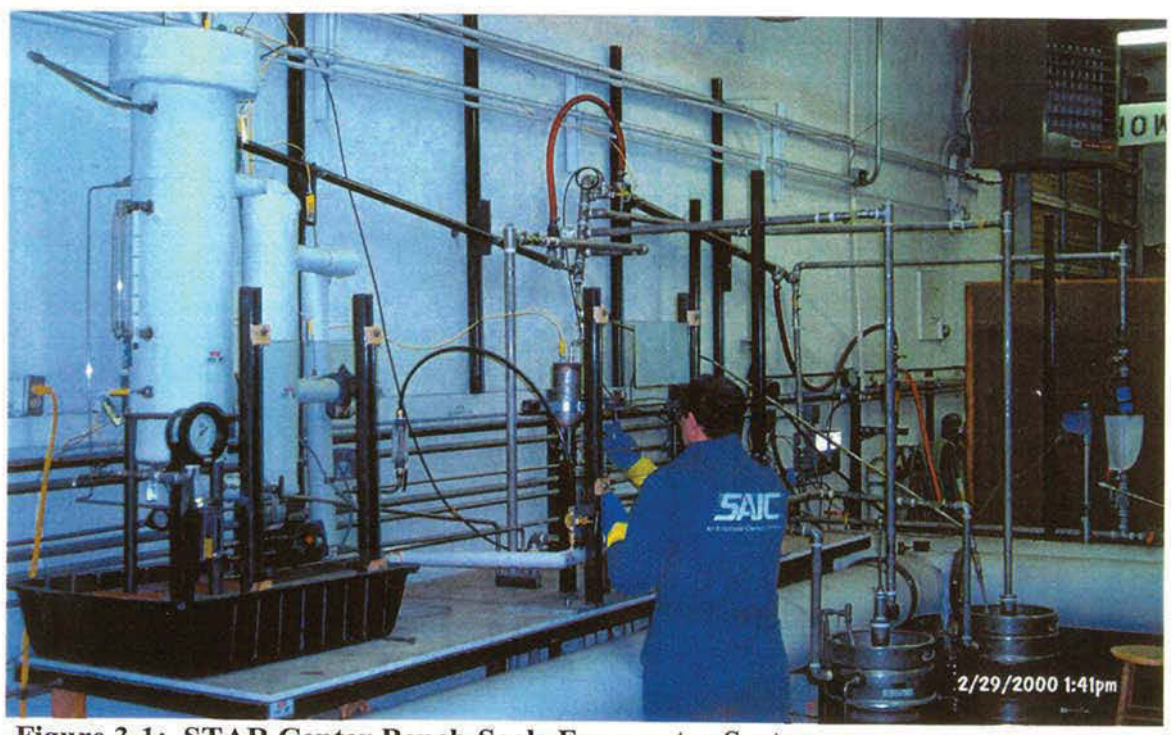

Figure 3-1: STAR Center Bench-Scale Evaporator System

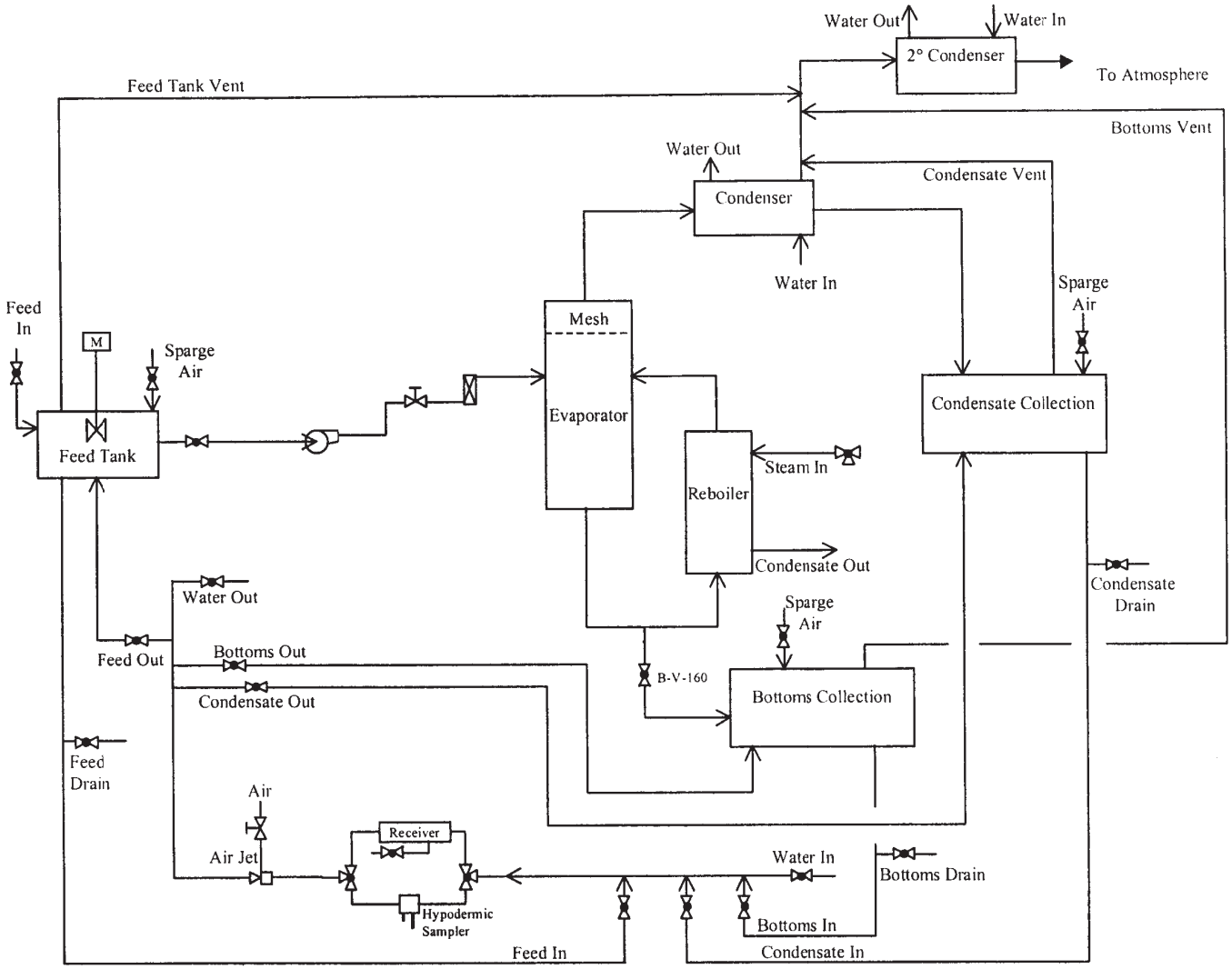

Figure 3-2: Bench-Scale Evaporator System Diagram

A sampling station and associated piping was assembled as part of the bench-scale system for the previous test series. The sample station was designed to model existing sample stations at INTEC. The double needle sample assembly was supplied by INTEC and is identical to the sample assemblies used at INTEC.

The sampling station can sample solutions from the feed tank, bottoms tank, and condensate tank. The sample station consists of a double hypodermic needle sampler and a larger volume sample receiver. An air jet is used to initiate sample flow through the sample station and recirculate the sample back to the respective tank. The hypodermic needle sampler consists of a double hypodermic needle sample assembly to which a sample bottle, fitted with a neoprene or Teflon diaphragm, can be attached. When the air jet is actuated, the sample flows into the sample bottle through one needle (the long needle) and exits through the other (the short needle), filling the sample bottle. This sampling method results in headspace in the top of the sample bottle. The double needle sampler was used exclusively throughout this testing. Figure 3-3 and 3-4 are images of the double needle sampling system.

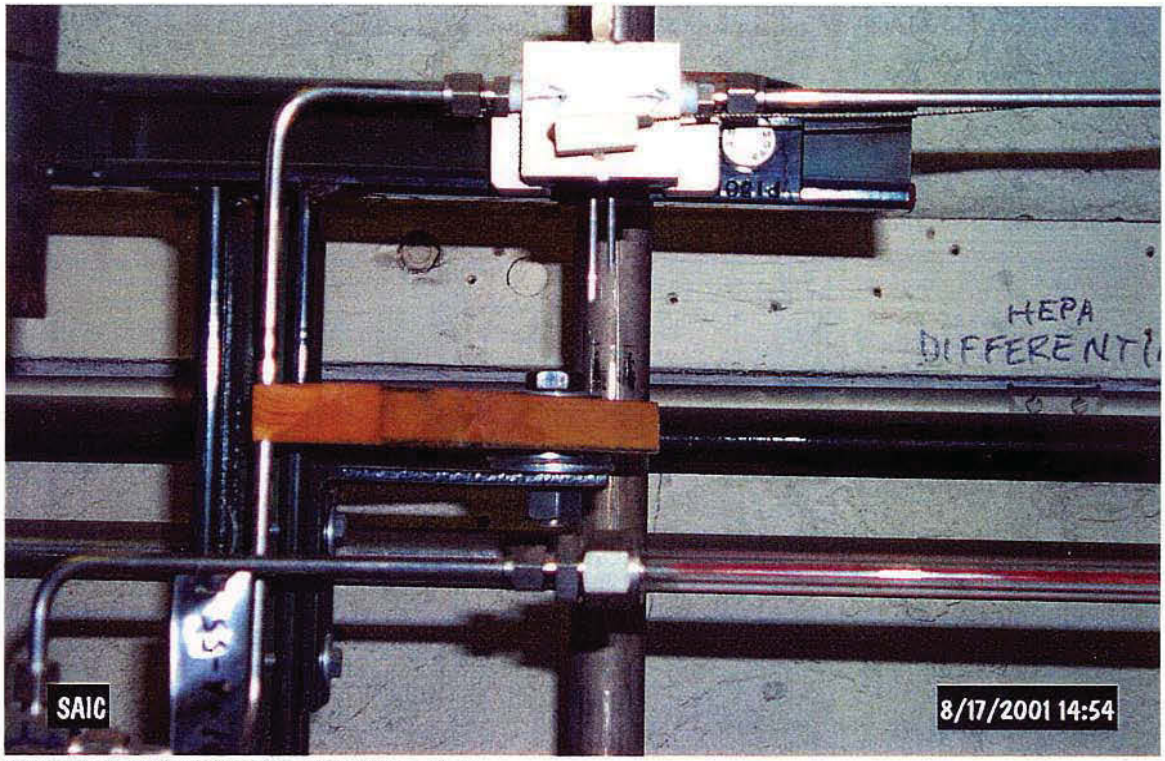

Figure 3-3 Double Needle Sampler

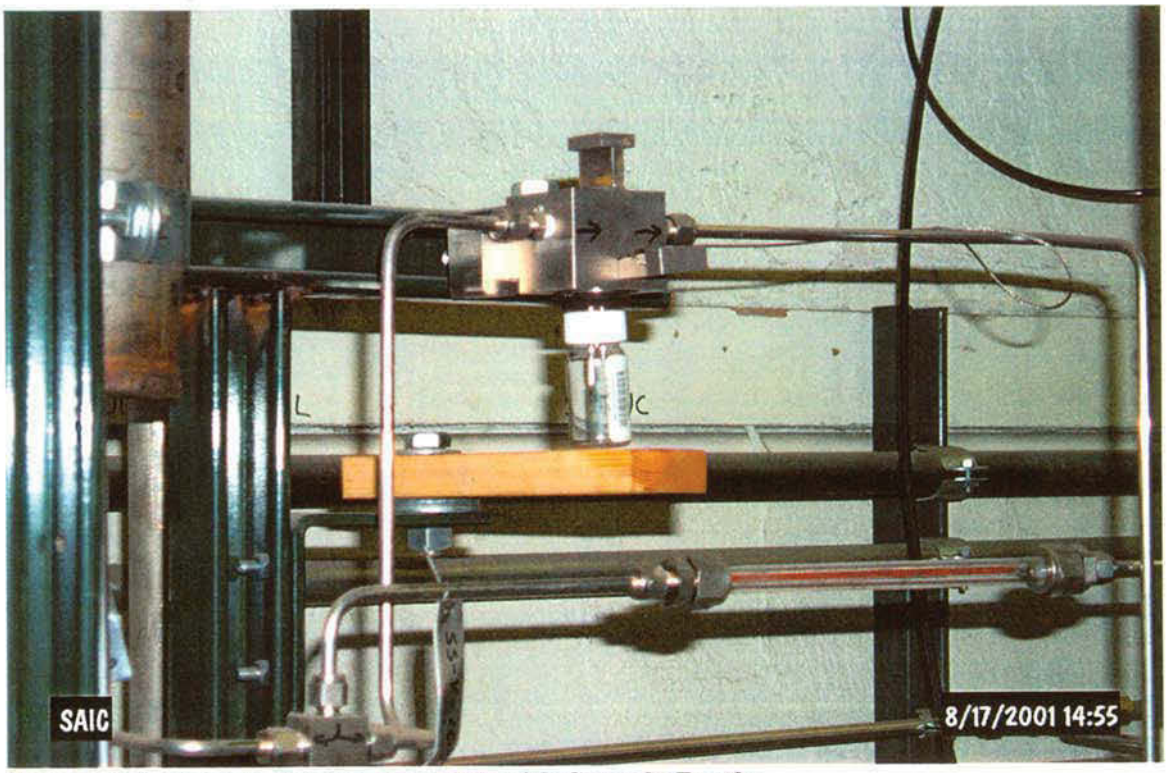

Figure 3-4 Double Needle Sampler with Sample Bottle

4.0 DOUBLE NEEDLE SAMPLER TEST SUMMARY

4.1. Feed Preparations

Previous organic partitioning testing at the SAIC STAR Center was used to determine organic species spiking concentrations. Bench-scale evaporator tests in September, 1998, (Test 1 and 2) spiked target organic constituents to a concentration of 1,000 mg/l in the feed, which is 3-4 orders of magnitude higher than concentrations typical of INTEC waste streams. Data analysis revealed that this concentration could be lowered while still maintaining acceptable detection limits for the target organic constituents.

Additional organic partitioning tests in both the bench-scale evaporator system and with the LDUA end effector (from October 1998 to March 2000) utilized target organic constituents that were spiked to a concentration of 100 mg/l in the feed. These concentrations were still an order of magnitude higher than typical INTEC waste streams, but were required to help ensure detection of the target organics by the analytical laboratory.

The concentration of organic and inorganic constituents in the feed solution for the double needle sampler testing was similar to previous organic partitioning tests. Operations and sampling procedures were provided in a test plan entitled *Organics Partitioning Resulting from Operation of an INTEC Double Needle Sampler*[3] which is

provided as Attachment 1. Double needle sampler testing was conducted the week of July 9, 2001. All key operational and sampling procedures/parameters as well as significant testing observations were documented in a bound logbook. Copies of the logbook entries and datasheets are provided as Attachment 2.

Simulated feed materials were generated at the STAR Center to model known acid waste feed solutions processed in the PEWE system at INTEC. Organics were spiked into 44 liters of nitrated acid feed to concentrations of 100 mg/l. Organic constituents were added in greater concentrations than are typically found in INTEC waste streams. This helps ensure that the analytical methods applied to the sample solutions are capable of detecting the organic constituents present in the solutions. Table 4.1 shows the chemical species that are present in the simulated waste stream, the desired concentrations of the chemical, and the quantity of chemical required to obtain the desired concentration. The target volatile organics for this testing were carbon disulfide, toluene, and 1,1,1-trichloroethane.

Table 4-1: Double Needle Sampler Feed Solutions (for 44 Liters of feed)

Species	Chemical Formula	MW (g/mole)	Acid Feed		
			Desired Conc.	Units	Required Quantity (g)
Acid		63.01	1.2	N	3.34 L
Nitrate					
Aluminum	$Al(NO_3)_3$ Solution	2.2 Molar	5.4	g/l	4.00 L
Calcium	$Ca(NO_3)_2*4H_2O$	236.15	0.166	g/l	43.0
Iron	$Fe(NO_3)*9H_2O$	404.02	0.008	g/l	2.55
Sodium/Potassium	$NaNO_3$	85.01	3.954	g/l	643.0
Carbon Disulfide	CS_2	76.14	100	mg/l	3.48 ml
Toluene	$C_6H_5CH_3$	92.14	100	mg/l	5.08 ml
1,1,1-Trichloroethane	CH_3CCl_3	133.40	100	mg/l	3.29 ml

The organic species present in the waste stream were spiked directly to the feed tank after negative pressure to the system had been established. The feed solution was mechanically mixed to help ensure the feed homogeneity prior to performance of the double needle sampler testing.

4.2. Test Methodology and Sample Collection

After completion of feed preparation activities, the feed solution was mechanically mixed for 4 1/2 hours. The sampling rational for the double needle sampler testing was to collect a total of twenty feed solution samples for comparison of volatile organic constituent concentrations. Ten samples were collected using the double needle sample system and ten samples were collected from the feed tank drain.

For comparison purposes, one sample was collected using the double needle sampling system and a second sample was immediately collected from the feed tank drain (spigot sample). This procedure was repeated until the full twenty samples were collected. Table 4-2 lists the samples identification number, sample location, analysis

type, and required sample volume for the double needle sampler testing. The samples collection methods for the double needle sampler system and the feed tank are discussed in the following sections.

Table 4-2: Double Needle Sampling System – Sampling Requirements

Sample ID No.	Description	Analytes	Volume
Feed Tank Sample			
05-FT-01	Direct Feed Tank Sample	Target	120 ml
05-FT-02	Direct Feed Tank Sample	Target	120 ml
05-FT-03	Direct Feed Tank Sample	Target	120 ml
05-FT-04	Direct Feed Tank Sample	Target	120 ml
05-FT-05	Direct Feed Tank Sample	Target	120 ml
05-FT-06	Direct Feed Tank Sample	Target	120 ml
05-FT-07	Direct Feed Tank Sample	Target	120 ml
05-FT-08	Direct Feed Tank Sample	Target	120 ml
05-FT-09	Direct Feed Tank Sample	Target	120 ml
05-FT-10	Direct Feed Tank Sample	Target	120 ml
Double Needle Samples			
05-DN-11	Double Needle Sample	Target	120 ml
05-DN-12	Double Needle Sample	Target	120 ml
05-DN-13	Double Needle Sample	Target	120 ml
05-DN-14	Double Needle Sample	Target	120 ml
05-DN-15	Double Needle Sample	Target	120 ml
05-DN-16	Double Needle Sample	Target	120 ml
05-DN-17	Double Needle Sample	Target	120 ml
05-DN-18	Double Needle Sample	Target	120 ml
05-DN-19	Double Needle Sample	Target	120 ml
05-DN-20	Double Needle Sample	Target	120 ml
Field Blank Sample			
05-QC-21	Distilled Water Field Blank	TOC	80 ml
05-QC-22	Distilled Water Trip Blank	TOC	80 mL
05-QC-23	Cross Contamination Sample	TOC	80 ml

4.2.1. Sample Collection Using the Double Needle Sampler

The double needle sample station was designed and fabricated to model existing PEWE sampling capabilities. The double needle sampler and air jet were supplied by INTEC. Operation of the sampling station was similar to the approved INTEC liquid sampling procedures.

To begin sampling, the sample bottle was connected to the sample station by piercing the diaphragm with a double-hypodermic needle sampling assembly. Once connected, the sample stream was circulated through the sample bottle with the use of an air jet and air lift. The sample stream flowed into the bottle through one needle and exited through the other, filling the bottle. The sample stream was recirculated for 10 minutes on the first sample bottle. The double needle sampler was then isolated by

closing the inlet and outlet isolation valves, the sample bottle was removed from the double needle sampler, a new sample bottle was connected to the sample station, and the sample stream was recirculated through the second bottle for 5 minutes. This procedure was repeated until four samples bottles were filled using the double needle sampler.

As shown in Table 4-2, the analytical laboratory required 120-ml of sample volume for performance of the volatile organic analysis. Since sampling with the double needle sampler results in head space being present in the sample vials, four 40-ml sample vials were required for each sample series using the double needle sampling system. Sample collection and analysis of volatile organic species requires that no head space be present in the sample containers. Therefore, the fourth sample vial collected was used to fill the first three sample vials, the punctured septa were replaced, and the resultant sample volume was 120-ml.

Previous studies at INTEC have analyzed and recommended operating conditions for jet transfer systems. The preferred minimum sample circulation rate is 100 ml/min and a rate of 200 – 300 ml/min is considered a good circulation rate.[4] The flow rate of the sample stream through the double needle sampler was measured at the conclusion of the double needle sampler testing. The flow rate was measured by placing a 1 liter graduated cylinder on the sample return line and recording the volume of liquid that was transferred to the cylinder in 1 minute. The sample stream flow rate was determined to be 270 ml/min and would be considered a good recirculation rate.

The double needle sample system was operated with an initial sample recirculation time of 10 minutes and three subsequent recirculation times of 5 minutes each. The 10 minute recirculation would result in 2700 ml (2.7 l) of sample stream recirculating through the double needle sampler, which was approximately 6 percent of the total feed volume. Each subsequent 5 minute recirculation would result in 1350 ml (1.35 l) of sample stream recirculating through the sample system, which was approximately 3 percent of the total feed volume.

Overall, 6750 ml (2700 ml + 3*1350 ml) of sample stream was recirculated through the double needle sampler to obtain the 120-ml of sample volume required for analysis. This equates to approximately 15 percent of the total feed volume being recirculated for each sample series obtained using the double needle sampler.

4.2.2. Sample Collection from the Feed Tank Drain

The feed tank samples were collected directly into 40-ml amber glass vials with Teflon lined septum. Three amber glass vials were required for each sample to obtain the desired 120-ml of total sample volume. The procedure for collecting direct feed tank samples is listed below:

1. Place a container below the feed tank drain valve .
2. Open the feed tank drain valve and allow feed solution to flush the drain line, then close the feed tank drain valve

3. Place an empty sample container below the feed tank drain valve.
4. Open the feed tank drain valve and allow the solution to gravity flow into sample container.
5. When the sample container is full, close the drain valve.
6. Put the lid on the sample container, verify zero headspace, and place the sample container in the required shipping device for shipment to the analytical laboratory.

4.3. Analytical Results

All samples were analyzed by Hauser Laboratories located in Boulder, CO. Liquid organic samples were analyzed with a gas chromatograph/mass spectrometer (GC/MS) in accordance with SW 846-8260 guidelines. Liquid sample calibration curves for each analyte ranged from 50 ng to 400 ng. The chain of custody forms and the analytical package received from Hauser is included in Attachment 3. Hauser Laboratories conducted the analyses for the previous organic partitioning studies and is familiar with the intricacies of performing volatile organic analyses in an acidic matrix. Although every effort was made to minimize data uncertainty, the following factors potentially contributed to error.

1. Feed homogeneity: It was thought that with adequate mechanical feed mixing (5 hours), the spiked organics would be thoroughly dispersed/homogenized within the feed mixture. During collection of the initial feed tank sample, organic globules were visible in the sample bottle. The organic globules were also observed during previous bench-scale evaporator tests that utilized a recirculation pump for mixing. The initial feed tank sample was returned to the feed tank and mechanical mixing was reinitiated. In addition, a small amount of sparge air was introduced to the feed tank to promote mixing.

2. Chemical Reaction: Organic partitioning testing resulting from typical INTEC operations has been conducted since 1998. This testing has resulted in both qualitative and quantitative determinations for the partitioning of organics in INTEC systems. However, the rates of reaction and mechanisms between nitric acid and volatile organic constituents have not been fully quantified for the various INTEC operating scenarios.

5.0 DATA INTERPRETATION

5.1. Double Needle Sampler Test Data

The primary objective of the double needle sampler testing was to determine the effects of operation of INTEC double needle sampling systems on volatile organic species that were spiked in known concentrations to a typical PEWE feed solution. The target organic constituents (carbon disulfide, 1,1,1-trichloroethane, and toluene) were spiked to a concentration of 100 mg/l in the feed solution, which is an order of magnitude greater than concentrations typically anticipated for INTEC waste streams. This spiking concentration helps ensure detection of the target organic constituents by the analytical laboratory.

The feed was then mechanically mixed for approximately 4 1/2 hours to homogenize the acid matrix and the organics. After mixing, an initial feed tank sample was obtained using the procedure described in Section 4.2.2. The feed tank drain line was flushed into a new, clean container. Organic globules were present in the solution drained from the feed tank which indicated in a non-homogenous feed mixture. The samples were added back to the feed tank and the feed tank solution was allowed to mix for an additional 30 minutes. A small amount of air sparge was also applied to the feed tank to assist with mixing.

Sampling activities were then reinitiated with the double needle sampling system. Four 40-ml sample bottles were required for each data series collected using the double needle sampler. A feed tank sample series was collected immediately following the double needle sampler operation. Three 40-ml sample bottles were required for each direct feed tank sample.

Table 5-1 lists the analytical results from the double needle sampler testing. The results have been arranged in the order the samples were collected to assist with the comparison of the double needle sampler and the direct feed tank samples.

Table 5-1. Analysis of Double Needle Sampler versus Direct Feed Tank Samples for Volatile Organic Constituents.

Sample ID	Sample Location	Time of Day	CS_2 (ng/uL)	1,1,1-TCA (ng/uL)	Toluene (ng/uL)
05-FT-01A	Feed Tank	9:45	3.2	3.69	3.74
05-DN-11A	Double Needle	9:20 - 09:45	9.92	10.52	10.32
05-DN-11A (dup)	Double Needle	9:20 - 09:45	9.6	10.16	9.96
05-FT-02A	Feed Tank	10:11	0.74	0.82	0.68
05-DN-12A	Double Needle	09:51 - 10:16	1.31	1.87	1.93
05-FT-02B	Feed Tank	10:11	0.49	0.6	0.64
05-DN-12B	Double Needle	09:51 - 10:16	0.74	1.12	1.26
05-FT-02B (dup)	Feed Tank	10:11	0.5	0.63	0.65
05-FT-03A	Feed Tank	10:37	0.48	0.39	0.17
05-DN-13A	Double Needle	10:12 - 10:37	0.2	0.31	0.37
05-FT-04A	Feed Tank	11:03	0.23	0.18	0.05
05-DN-14A	Double Needle	10:38 - 11:03	0.05	0.07	0.1
05-FT-05A	Feed Tank	11:30	0.14	0.1	bloq
05-DN-15A	Double Needle	11:05 - 11:30	bloq	bloq	bloq
05-FT-06A	Feed Tank	11:56	0.12	0.11	nd
05-DN-16A	Double Needle	11:31 - 11:56	nd	nd	nd
05-FT-07A	Feed Tank	12:22	0.08	0.07	nd
05-DN-17A	Double Needle	11:57 - 12:22	nd	nd	nd
05-FT-08A	Feed Tank	12:48	nd	nd	nd
05-DN-18A	Double Needle	12:23 - 12:48	nd	nd	nd
05-FT-09A	Feed Tank	13:14	0.06	0.08	nd
05-DN-19A	Double Needle	12:49 - 13:14	nd	nd	nd
05-FT-10A	Feed Tank	13:40	0.09	0.09	nd
05-DN-20A	Double Needle	13:15 - 13:40	nd	nd	nd

dup = duplicate
nd = not detected (detection limit = 0.025 ng/ul
bloq = below limit of quantitation (0.050 ng/ul)
1,1,1-TCA = 1,1,1-trichloroethane

The most obvious trend in the volatile organic data was the consistent decrease in the concentration of the organic constituents with each sample series until most of the organic species were below the analytical detection limit. The detection limit for the organic constituents was 0.050 ng/µl or 50 parts per billion. This would suggest that the nitric acid solution was reacting/decomposing the spiked volatile organic constituents and/or the organic constituents were being stripped from solution by the air jet, air sparge, air lift. Both of these mechanisms most likely played a role in decreasing the volatile organic concentrations in the feed solution.

It should be noted that the spiked concentration of the volatile organics (100 mg/L) was significantly greater than the concentrations that would be typical of INTEC waste streams. The higher concentrations were required to ensure that detectable quantities of volatile organics would be present for analysis. It appears that some air

stripping of volatile organic constituents may occur during operation of the double needle samplers, however, the air stripping occurs after sample collection and should not significantly effect the sample validity. The effectiveness of air stripping techniques is dependent on a number of variables (such as volatile organic concentration, operating temperatures, Henry's Law constants, and flow rates) and the higher spiking concentrations in the feed solution may have contributed to observed air stripping effects.[6]

Figures 5-1, 5-2, and 5-3 graphically show the reduction in concentration of the target volatile organics for both spigot and double needle samples. It can be seen that all three of the organic constituents follow the same general curve for reduction in concentration. Comparison of the analytical results relative to the time of day the samples were obtained results in a good correlation between the double needle and spigot samples. The mean time for the double needle sample period (25 minutes each) was utilized to compare the sample results. Attachment 4 contains photos of the bench-scale evaporator system at the SAIC STAR Center.

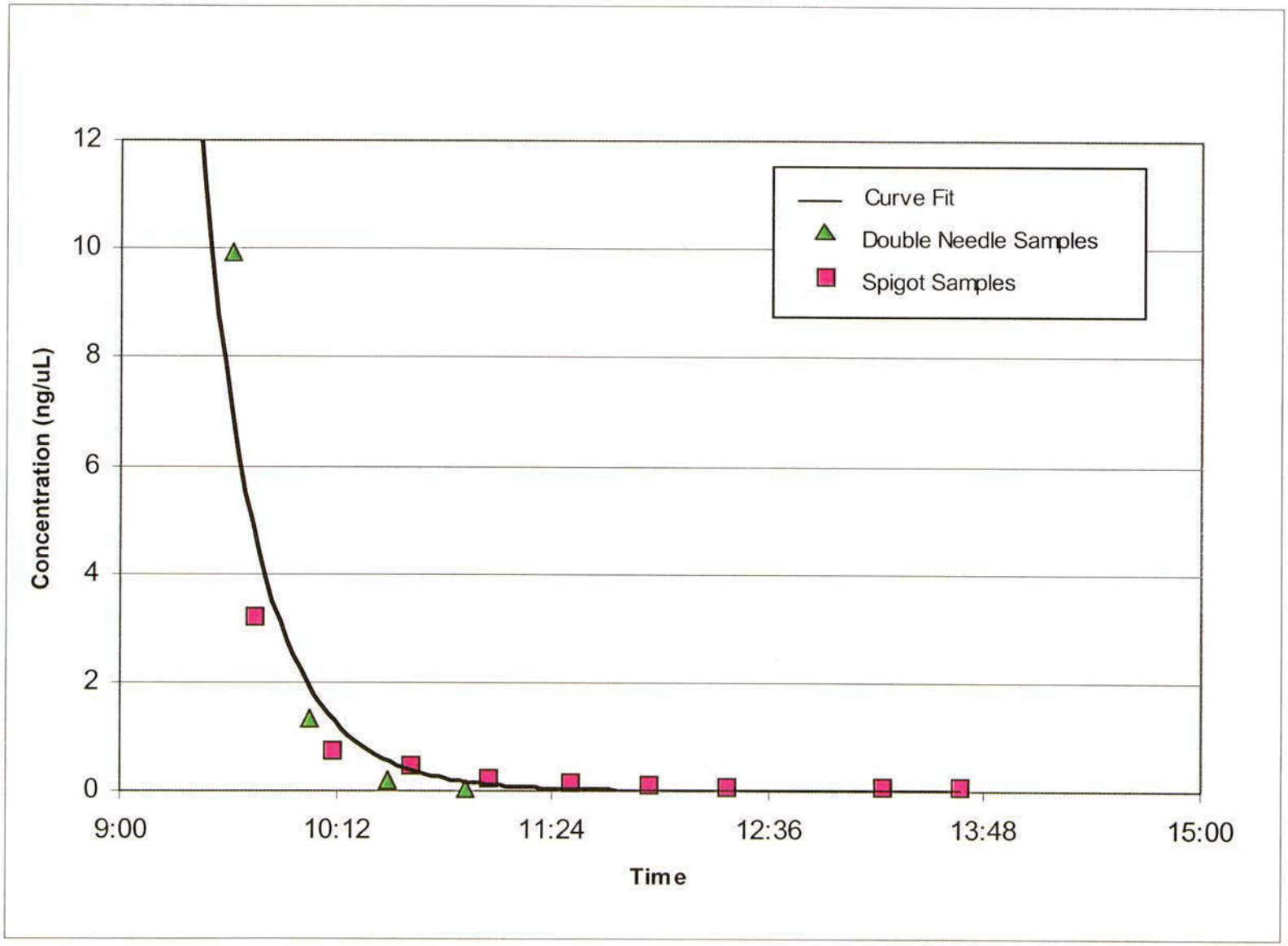

Figure 5-1: Comparison of Time Relative Sample Analysis for CS_2 Data.[7]

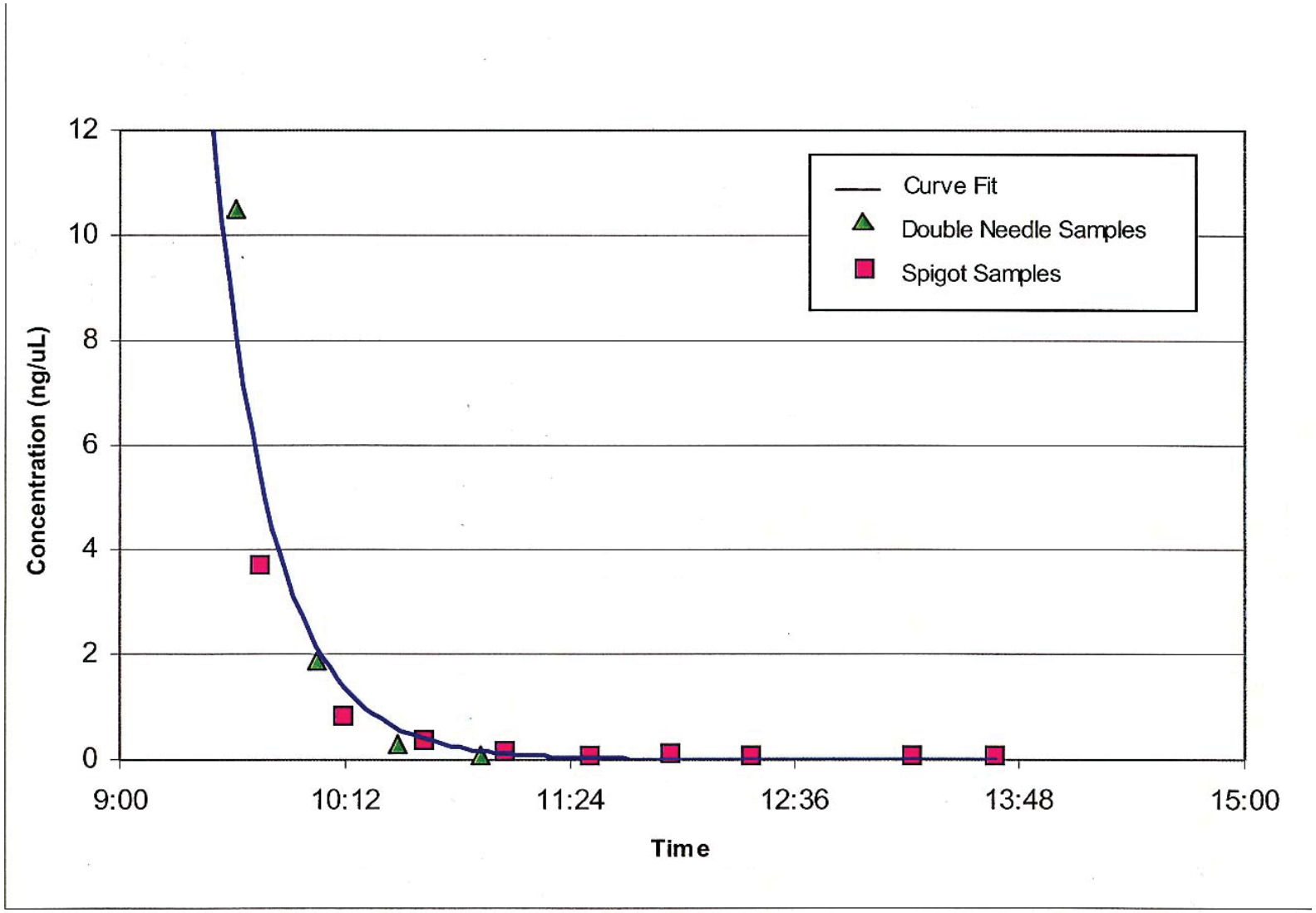

Figure 5-2: Comparison of Time Relative Sample Analysis for 1,1,1-Trichloroethane Data.[7]

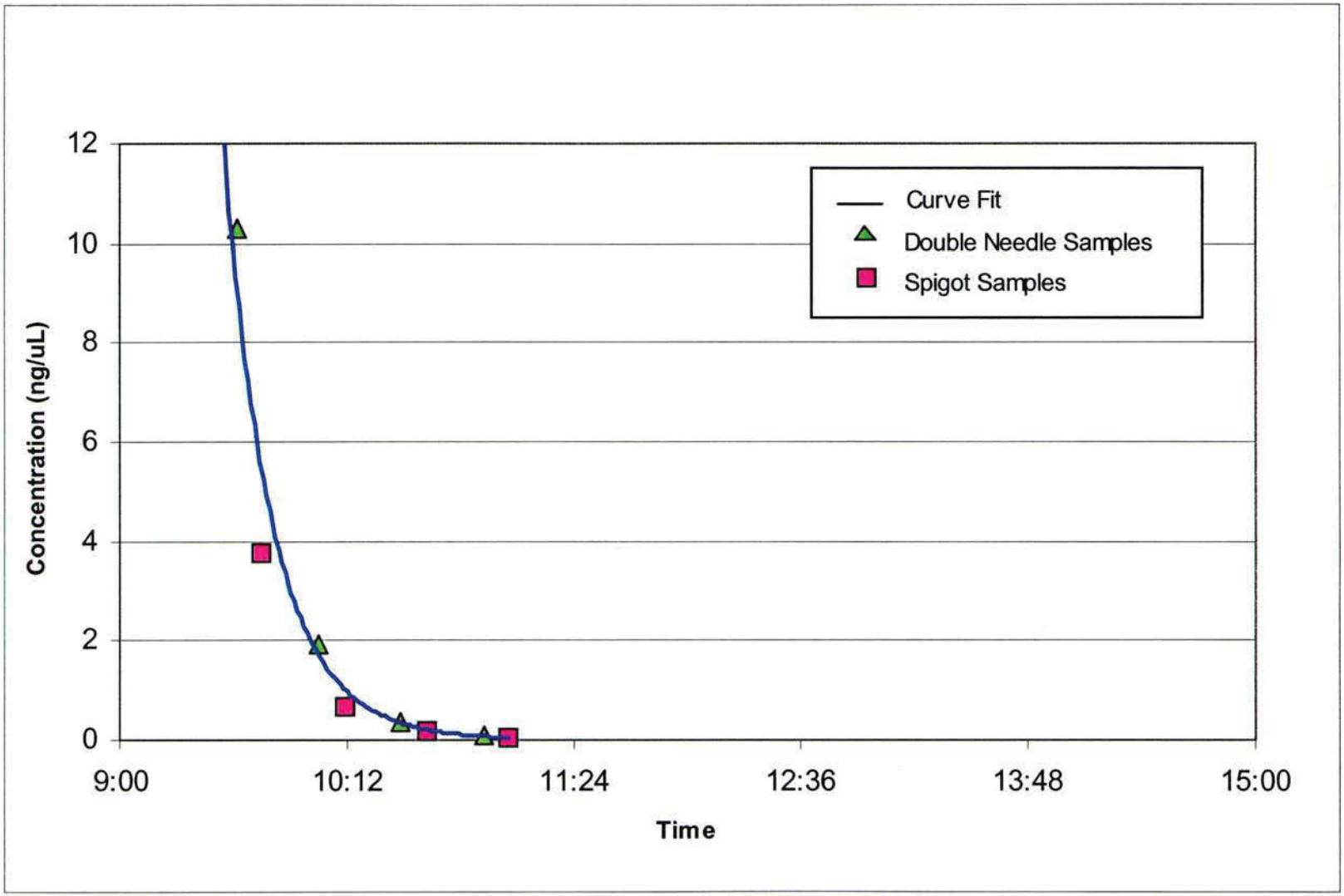

Figure 5-3: Comparison of Time Relative Sample Analysis for Toluene Data[7]

5.2. Comparison with Previous Organic Partitioning Tests

Previous bench-scale evaporator tests concluded that up to 75 percent of the volatile organic species spiked to the feedstocks were destroyed, decomposed, reacted, or volatilized prior to evaporator processing. The bench-scale evaporator feeds were steam jetted and air sparged prior to being sampled and fed to the evaporator.

For the LDUA test series, the concentration of the organic constituents in the feed solution was 100 mg/l. The analytical data from Test 2 with the LDUA end effector yielded volatile organic constituent concentrations of 0.2 to 1 mg/l, which is a 99 percent reduction in the volatile organic constituents concentrations. The LDUA Test 2 feed stock was mechanically mixed for 5 hours prior to sampling with the end effector.

The double needle sampler testing resulted in a reduction of approximately 90 percent of the volatile organic constituents after five hours of mechanical mixing (including 20 minutes of air sparge) and almost complete reduction by the end of the test. This is consistent with the conclusions documented from previous organic partitioning tests (bench-scale evaporator and LDUA EE operation) and indicates that the acidic nature of the solution plays a key role in the reduction of VOC concentrations in typical INTEC waste streams.

5.3. Comparison with INTEC Sampling

The double needle sampler test was designed to be a bench-scale operation (44 liter tank volume) for ease of sample collection and to minimize hazardous waste generation. The proportions utilized in the double needle sampler test are quite different from those present in the INTEC waste processing system.

The blend and hold tanks (VES-NCC-101, -102, and –103) typically hold 3,000 to 4,000 gallons. The sparge volume and the volume of air supplied to the airlift may be comparable and may similarly affect the solution transported to the sampler. The PEW tanks do receive the sample return from the double needle sampling system and could be affected by the air-jet, but this effect would be small due to the large volume of the tanks (the evaporator feed sediment tank , VES-WL-132 and the evaporator feed collection tank, VES-WL-133 have 4,700 gallon and 19,000 gallon capacities, respectively).[9]

Analysis of INTEC tank farm facility solutions for volatile organic constituents have been consistently less than the minimum quantification level of 10 ng/ml.[5] Based on the results of the organic partitioning test series conducted at the SAIC STAR Center, it is reasonable to infer that any volatile organic constituents introduced to the INTEC waste system have been destroyed, decomposed, reacted, or volatilized as a result of typical plant conditions and reactions with the nitric acid waste matrix.

6.0 CONCLUSIONS

Test series conclusions are based on quantitative data analysis as well as qualitative observations. The results provide representation of the fate of volatile organic constituents and the validity of samples the have been collected using INTEC double needle samplers.

Direct statistical comparison of the double needle and spigot samples is difficult due to decomposition, reaction, and/or volatilization of the target organic constituents. However, a good correlation between the double needle and spigot samples is observed by graphical representation of the analytical data relative to the time of day the samples were collected. This data indicates that samples collected utilizing a double needle sampler are comparable to spigot samples.

After 4 1/2 hours of mixing with a mechanical mixer, organic globules were still visible in a sample. Then after air sparging and mechanical mixing for 30 minutes, the first samples were taken and a sequence of sampling every few minutes was initiated. More than 90% of the organics were destroyed by the first sample and roughly 60-80% of the remaining quantities were destroyed in each 25-minute period through the remainder of the test.

Analytical data, compiled for previous organic partitioning studies (tests 1 through 4 in the bench scale evaporator and LDUA end effector testing), indicated that volatile organic constituents would be destroyed, decomposed, reacted, or volatilized as a result of typical INTEC plant conditions. The bench-scale evaporator utilized steam recirculation and air sparging to mix the tank contents, while the LDUA tests employed a mechanical mixer. A reduction of up to 99 percent of the volatile organic constituents concentration was observed in these tests. The rapid reduction of volatile organics concentrations, as evidenced in bench-scale evaporator, LDUA EE, and double needle sampler testing, suggests that nitric acid digestion plays a key role in the reduction of volatile organic concentrations in typical INTEC waste streams.

Based on the reduction of volatile organic constituents and previous sampling of INTEC tank farm facility solutions, it is reasonable to infer that volatile organic constituents introduced to the INTEC waste system are most likely destroyed, decomposed, reacted, or volatilized as a result of typical plant conditions and/or reactions with the nitric acid waste matrix and will be below quantification limits. The double needle and spigot samples both yielded comparative results. The double needle sampler may contribute to some air stripping of organics, but is negligible compared to the rapid degradation of the volatile organic compounds in nitric acid waste solutions. It is unlikely that trace volatile organic concentrations could be detected, in INTEC waste streams, utilizing any sampling method.

7.0 REFERENCES

1. Radian Corporation, *Results of a Laboratory Study to Assess the Fate of Organic Compounds in Synthetic ICPP Tank Farm Waste*, July 17, 1995.

2. SAIC, *PEWE and LDUA Bench-Scale Test Series, Organic Partitioning Comprehensive Final Report*, July 23, 2000.

3. SAIC, *Double Needle Sampling System Test Plan, Organic Partitioning Resulting from Operation of an INTEC Double Needle Sampler,* June 25, 2001.

4. Houck, E. D., *Design and Operation of Process Liquid Samplers,* Westinghouse Idaho Nuclear Company, WINCO-1022, January 1986.

5. Schindler, R.E., *Independent Validation of Upper-Envelope NWCF Emissions for Screening-Level Risk Analysis,* Schi-14-97, June 1997.

6. SAIC, *INEEL High Level Waste and Facilities Disposition Environmental Impact Statement, ICPP Delisting Study*, April, 1998.

7. Millet, C.B., letter to M.B. Heiser, "Organic Analysis with Double Needle Samplers", August 16, 2002.

ATTACHMENT 1

Double Needle Sampling System Test Plan

Double Needle Sampling System

Test Plan

Organics Partitioning Resulting from Operation of an INTEC Double Needle Sampler

Test 5, Double Needle Sampler Statistical Testing

SAIC STAR Center

June 25, 2001

Prepared for:
Bechtel BWXT Idaho, LLC
Idaho National Engineering and Environmental Laboratory
Idaho Falls, ID 83415

Prepared by:
Science Applications International Corporation
950 Energy Drive
Idaho Falls, ID 83401
Contract No. K00-564414, TO 10

Double Needle Sampling System

Test Plan

Organics Partitioning Resulting from Operation of an INTEC Double Needle Sampler

Test 5, Double Needle Sampler Statistical Testing

SAIC STAR Center

Approval Signature | Date

7-6/01/2001

T. D. Thomson
SAIC, Senior Engineer/Project Manager

7/9/01

J. D. Atkinson
SAIC, Applications Engineer

7/1/01

M. B. Heiser
HLW Program, Advisory Engineer

Test 5, Double Needle Sampler Statistical Testing

Table of Contents

1.0 BACKGROUND 4
2.0 TEST OBJECTIVES 4
3.0 BENCH-SCALE SYSTEM DESIGN 5
4.0 SYSTEM OPERATIONS 7
4.1 Feed Preparation 7
4.2 Start-up Instructions 7
4.2.1 Pre-Start 7
4.2.2 Feed Preparation 8
4.3 Sample Collection Instructions 8
4.3.1 Sample Collection from Tank Drains 8
4.3.2 Sample Station Sample Collection 9
4.4 System Cleaning 11
4.5 Health and Safety Requirements 12
4.6 Waste Management 12
5.0 SAMPLE AND ANALYSIS RATIONALE 13
5.1 Data Quality Objectives 13
5.1.1 Problem Statement 13
5.1.2 Data Users 14
5.1.3 Study Boundaries and Decisions 14
5.2 Target Analytes 14
5.3 Organic Spiking Concentrations 14
5.4 Quality Control 15
6.0 REPORTING 15
7.0 REFERENCES 16

1.0 BACKGROUND

The Process Equipment Waste Evaporator (PEWE), located in CPP-604, reduces the volume of mixed waste sent to the Tank Farm Facility at the Idaho Nuclear Technology and Engineering Center (INTEC). The PEWE system consists of feed tanks for accumulation of waste solutions, two evaporator trains for processing the waste solution, a bottoms collection vessel, and condensate collection vessels. The waste solutions are transferred from the feed tanks to the evaporator vessel, where the solution is heated and circulated through the evaporator. The overhead vapors generated in the evaporator are condensed and transferred to the PEW condensate collection tanks. The condensate is accumulated in the condensate collection tanks for further processing at the Liquid Effluent Treatment and Disposal (LET&D) Facility, CPP-1618. The remaining solution is circulated through the evaporator until procedurally designated limits are met, at which time the solution is transferred to the bottoms collection vessel. The bottoms are eventually transferred to the Tank Farm for storage.

Hazardous organic species have been discharged to the PEWE system as a result of past operating practices. Studies have been conducted to determine the fate of the organic compounds in the INTEC Tank Farm,[1] but these studies did not address the effects of the evaporation process on the fate of the organics. SAIC has conducted four bench-scale studies to evaluate the fate of spiked organics in a high and low molarity nitric acid simulated feeds. These results of these tests indicated that INTEC sample collection and handling procedures do not significantly effect the concentration of volatile organic or semi-volatile organic constituents in the waste stream.[2] This test (Test 5) is designed to validate the sample collection (double needle sampler systems) and handling procedures currently employed by INTEC operations.

2.0 TEST OBJECTIVES

The purpose of Test 5 is to determine the effects of operation of the double needle sampling systems on volatile organic species that have been introduced into the PEWE system. Data will be evaluated to quantify the fate of organic constituents due to sampling system operation. Results will be incorporated into a final report designed to support INTEC RCRA compliance activities. This will be accomplished as follows:

1) A mechanical mixer will be added to the PEWE feed tank. The mechanical mixer will ensure a homogenous feed solution for sampling operations.

2) Samples will be collected and analyzed for spiked organic-constituents. This will involve collecting feed samples directly from the feed tank and also using the double needle sampling system. Samples will then be analyzed for spiked organic constituents as well as total organic carbon.

3) Evaluate the effects of the double needle sampling system on spiked organic constituents. This is accomplished by collecting approximately ten direct samples and ten double needle samples, in a planned test series, for comparison.

4) Verify conclusions drawn from previous bench-scale tests. Fill in double needle sampling system data gaps necessary to support organic partitioning hypotheses.

3.0 BENCH-SCALE SYSTEM DESIGN

A bench-scale PEWE system has been designed and constructed at the SAIC Science and Technology Applications Research (STAR) Center to model typical PEWE system operations. The bench-scale system consists of a feed tank, evaporator vessel with an attached thermosiphon reboiler, bottoms collection tank, condensate collection tank, and tank sampling station. A flow diagram of the bench-scale system is shown in Figure 3.1. The only modification to the bench-scale evaporator system for this test was the addition of a mechanical mixer to the feed tank.

A sampling station and associated piping has been assembled as part of the bench-scale system. The sampling station can sample solutions from the feed tank, bottoms tank, and condensate tank. The sample station consists of a double hypodermic needle sampler and a larger volume sample receiver. An air jet is used to initiate sample flow through the sample station and recirculate the sample back to the respective tank. The hypodermic needle sampler consists of a double hypodermic needle sample assembly to which a sample bottle, fitted with a neoprene or Teflon diaphragm, can be attached. When the air jet is actuated, the sample flows into the sample bottle through one needle and exits through the other, filling the sample bottle. This sampling method will result in headspace in the top of the sample bottle.

The sample receiver is a section of stainless steel pipe with an inlet and an outlet for the sample solution. When the air jet is actuated the sample flows into the bottom of the sample receiver and exits through the top, filling the receiver. The sample is then drained from the receiver into sample bottles by opening the drain valve located at the bottom of the receiver.

Figure 3.1 – Bench-Scale System Diagram

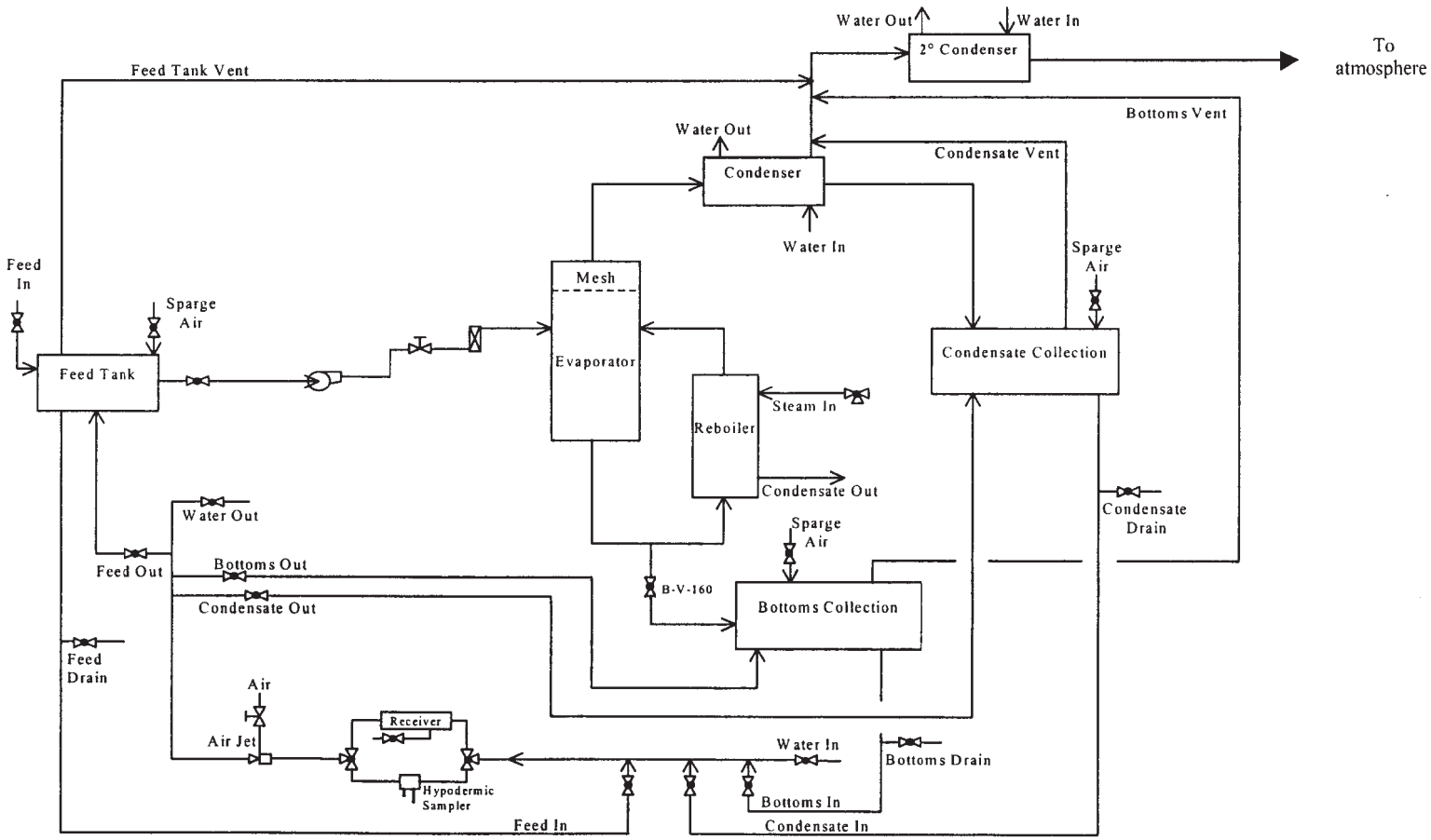

4.0 SYSTEM OPERATIONS

The following subsections provide the Test 5 operations details. These include feed preparation, sampler system operation, sample collection, and system cleaning procedures. Additional subsections address health and safety and waste management.

4.1 Feed Preparation

Simulated feed materials will be generated at the STAR Center to model known acid waste feed solutions processed in the PEWE system at INTEC. Organic constituents will be spiked in the feed material to determine the partitioning of these species as a result of double needle sampling system operation. Organic constituents are added in greater concentrations than are typically found in INTEC waste streams. This helps ensure that the analytical methods applied to the sample solutions are capable of detecting the organic constituents present in the solutions. Table 4.1-1 shows the chemical species that are present in the simulated waste stream, the desired concentrations of the chemical, and the quantity of chemical required to obtain the desired concentration.

Table 4.1-1: Test 5 Feed Solutions (for 44 Liters of feed)

Species	Chemical Formula	MW (g/mole)	Acid Feed		
			Desired Conc.	Units	Required Quantity (g)
Acid		63.01	1.2	N	3.34 L
Nitrate					
Aluminum	$Al(NO_3)_3$ Solution	2.2 Molar	5.4	g/l	4.00 L
Calcium	$Ca(NO_3)_2*4H_2O$	236.15	0.166	g/l	43.0
Iron	$Fe(NO_3)*9H_2O$	404.02	0.008	g/l	2.55
Sodium/Potassium	$NaNO_3$	85.01	3.954	g/l	643.0
Carbon Disulfide	CS_2	76.14	100	mg/l	3.48 ml
Toluene	$C_6H_5CH_3$	92.14	100	mg/l	5.08 ml
1,1,1-Trichloroethane	CH_3CCl_3	133.40	100	mg/l	3.29 ml

The organic species present in the waste stream will be spiked directly to the feed tank after negative pressure to the evaporator vessels has been established. The feed solution will be mechanically mixed to help ensure the feed is homogenous prior performance of the double needle sampler test series.

4.2 Start-up Instructions

4.2.1 Pre-Start

4.2.1.1 Turn on the exhaust blower and adjust the bleed air supply valve (OG-V-127) to provide vacuum in the evaporator system. The evaporator should be operated at slightly negative conditions (~3 inches WC).

4.2.1.2 Verify the sample station equipment is properly configured for operation. Verify all vessel drain, sample supply, sample return, and air sparge valves are closed. The peristaltic pump and isolation ball valve (F-V-121) provide isolation of feed solution to the evaporator and must be turned off and closed, respectively..

4.2.1.3 Turn on the STAR Center cooling tower to initiate cooling water flow to the primary and secondary condensers.

4.2.1.4 Verify that feed preparations activities have been completed, and that the feed tank contains the required volume of feed for the test.

4.2.2 Feed Preparation

4.2.2.1 Add the pre-measured organic species to the feed vessel through the organic addition valve (F-V- 125) located on the top of the feed vessel.

4.2.2.2 Turn on the mechanical mixing device and allow the feed solution to mix for approximately 5 hours.

4.3 Sample Collection Instructions

Samples will be collected to determine organic partitioning associated with double needle sample system operations and perform material balances on the constituents present in the simulated feeds. Table 4.3-1 shows a matrix of the required samples, the sample location, and volume of sample that will be collected during testing. Special instructions for sampling activities will be included in the PEWE Bench-Scale Testing Logbook.

4.3.1 Sample Collection from Tank Drains

Samples will be collected from tank drains for comparison to double needle sampling system samples. This will enable direct comparison of the effects of the double needle sampler on the removal of organics.

4.3.1.1 Place a container below the feed tank drain valve (F-V-124).

4.3.1.2 Open the feed tank drain valve (F-V-124) and allow feed solution to flush the drain line, then close the feed tank drain vale (F-V-124).

4.3.1.3 Place an empty sample container below the feed tank drain valve.

4.3.1.4 Open the feed tank drain valve (F-V-124) and allow the solution to gravity flow into sample container.

4.3.1.5 When the sample container is full, close the drain valve.

4.3.1.6 Put the lid on the sample container, verify zero headspace, and place the sample container in the required shipping device for shipment to the analytical laboratory.

Table 4.3-1: Double Needle Sampler System Sampling Requirements

Sample ID No.	Description	Analytes	Volume
Feed Tank Sample			
05-FT-01	Direct Feed Tank Sample	Target	120 ml
05-FT-02	Direct Feed Tank Sample	Target	120 ml
05-FT-03	Direct Feed Tank Sample	Target	120 ml
05-FT-04	Direct Feed Tank Sample	Target	120 ml
05-FT-05	Direct Feed Tank Sample	Target	120 ml
05-FT-06	Direct Feed Tank Sample	Target	120 ml
05-FT-07	Direct Feed Tank Sample	Target	120 ml
05-FT-08	Direct Feed Tank Sample	Target	120 ml
05-FT-09	Direct Feed Tank Sample	Target	120 ml
05-FT-10	Direct Feed Tank Sample	Target	120 ml
Double Needle Samples			
05-DN-11	Double Needle Sample	Target	120 ml
05-DN-12	Double Needle Sample	Target	120 ml
05-DN-13	Double Needle Sample	Target	120 ml
05-DN-14	Double Needle Sample	Target	120 ml
05-DN-15	Double Needle Sample	Target	120 ml
05-DN-16	Double Needle Sample	Target	120 ml
05-DN-17	Double Needle Sample	Target	120 ml
05-DN-18	Double Needle Sample	Target	120 ml
05-DN-19	Double Needle Sample	Target	120 ml
05-DN-20	Double Needle Sample	Target	120 ml
Field Blank Sample			
05-QC-21	Distilled Water Field Blank	TOC	80 ml
05-QC-22	Distilled Water Trip Blank	TOC	80 mL
05-QC-23	Cross Contamination Sample	TOC	80 ml

4.3.2 Sample Station Sample Collection

A sample station has been designed and fabricated to model existing PEWE sampling capabilities. Operation of the sampling station will be similar to PEWE sampling procedures. The sample station is equipped with a double hypodermic needle sampler and a larger sample receiver. An air jet is used to draw the sample from the respective tank through the sample station. The feed, bottoms, and condensate tanks can be sampled using either the hypodermic needle sampler or the sample receiver.

Sampling will occur after the feed tank has been thoroughly mixed using a mechanical mixer. The feed tank and the hypodermic needle sampler will be used exclusively for this test series. Table 4.3-1 shows the required number of samples and the sample volume.

4.3.2.1 Verify the sample receiver drain (SS-V-108) and vent valves (SS-V-107) are closed.

4.3.2.2 Attach a sample bottle to the hypodermic sample assembly. Align the long hypodermic needle next to the sample bottle cap's edge with the short hypodermic needle as near the center of the septum as possible.

4.3.2.3 Push the sample bottle up (with hand positioned on the bottom half of the sample bottle) until it is firmly seated against the needle block gasket.

4.3.2.4 Position the sample station three-way valves (SS-V-109 and SS-V-110) to route sample solution through the hypodermic sampler.

4.3.2.5 Open the sample supply and sample return isolation valves from the tank to be sampled as shown in the table below.

Note: Feed tank valves (SS-V-112A and SS-V-112B) will be used exclusively for this test series.

Table 4.3-2: Sample Station Valve Line-up

Open Supply Valve	Tank To Be Sampled	Open Return Valve
SS-V-112A	Feed Tank	SS-V-112B
SS-V-113A	Condensate Tank	SS-V-113B
SS-V-111A	Bottoms Tank	SS-V-111B

4.3.2.6 Adjust the air flow to the sample station airlift to about 0.5 scfh.

4.3.2.7 Initiate airflow to the sample station air jet to start circulating solution through the sample station by throttling valve AIR-V-106. Record the air supply pressure and air flow rate to the air jet. The air flow through the jet should be between 5 and 20 scfh.

4.3.2.8 Allow the sample to recirculate through the sample station for 10 minutes. If multiple samples are required from the same tank, circulate solution for each subsequent sample through the sample station for 5 minutes.

4.3.2.9 After the sample has circulated for the specified period of time, shut off the air supply to the air jet by closing valve AIR-V-106.

4.3.2.10 Shut off the air supply to the sample station air lift.

4.3.2.11 Shut the respective sample station supply and return valves as shown in Table 4.3-2.

4.3.2.12 Disconnect the sample bottle from the sampling apparatus and install a new sample bottle (if required).

Note: When removing the sample bottle from the hypodermic sampler, lower the sample bottle so that both needles are in the headspace above the liquid. Wait 30 – 60 seconds (until the needles stop dripping). Quickly pull the sample bottle straight down and away from the needles.

4.3.2.13 If more sample volume is required, repeat steps 4.3.2.1 through 4.3.2.9 as necessary.

4.3.2.14 Upon completing sampling activities for each tank, drain the sample lines and sample station equipment into a collection vessel.

4.3.2.15 Open the water supply (SS-V-114A) and return (SS-V-114B) isolation valves to the sample station and thoroughly rinse the sample station lines. Collect the water in a collection vessel.

4.3.2.16 Close the water supply (SS-V-114A) and return (SS-V-114B) isolation valves to the sample station and drain the remaining water from the sample station.

4.3.2.17 Transfer the solution collected from the sampling operations into the VOA sample vials to be supplied to the analytical laboratory and verify that zero headspace is present in the sample vials.

4.4 System Cleaning

The feed tank and sampling system will require cleaning prior to Test 5 to prevent potential cross contamination of trace concentration of organic residues from previous testing. Water, dilute nitric acid , and/or steam will be employed to clean the evaporator system. The system will be cleaned after all sampling activities associated with the operation have been completed.

4.4.1 Verify that all tanks have been completely drained of test solutions.

4.4.2 Supply steam to the evaporator vessel, to steam clean the evaporator system, by opening the steam supply valve to the evaporator. Turn on the steam generator and allow steam to circulate through the evaporator and associated vessels for approximately 30 minutes.

4.4.3 Charge the feed tank and evaporator vessel with water or dilute nitric acid solution.

4.4.4 Heat and circulate the solution through the evaporator by following the evaporator startup instructions.

4.4.5 After cleaning the evaporator, drain the rinse solution remaining in the evaporator vessel to the bottoms collection vessel.

4.4.6 Circulate the rinsate through the sample lines and the sample station as described in the sample collection instructions.

4.4.7 Drain all solutions from the evaporator and associated vessels. A sample of the solution will be obtained to verify that no cross contamination of organics has occurred.

4.5 Health and Safety Requirements

Hazardous chemicals will be used during bench-scale system tests and will include nitric acid and organic species. Personnel protective equipment will be provided to mitigate potential exposure to these substances.

When handling acidic solutions, personnel shall wear neoprene gloves and a face shield. In addition, Draeger sample tubes will be used to monitor the presence of nitric acid vapors in the operating area.

When handling dry chemicals, all measurement of chemicals shall be conducted in a ventilated area. The dry chemicals will then be added to the liquid feed makeup vessel. Gloves shall be worn during all dry chemical handling operations.

When handling organic species, perform all liquid measurements in a ventilated area. The organic species will then be added to the liquid feed makeup vessel. Gloves shall be worn during all organic species handling operations. Once the feed solution has been added to the feed tank, maintain the evaporator system at slightly negative conditions to prevent organic vapors from entering the operating area. Additionally, Draeger sample tubes will be used to monitor the for the presence of organic vapors in the operating area.

The evaporator system will contain surfaces that are maintained at elevated temperatures. Heated surfaces shall be insulated to protect personnel during evaporator operation. Signs will be posted to notify personnel of potentially hot surfaces.

4.6 Waste Management

The double needle sampler test series will require generation of simulated INTEC waste streams. The total volume of simulated waste solutions and rinse waters will not exceed 50 gallons. Simulated solutions from double needle sampler testing will remain in the feed for use during a Paint Filter Leach Test (PFLT) of the PEWE system off-gas. The

PFLT will be performed after completion of the double needle sampler test series. Waste management and disposal is detailed in the test plan for the PFLT.

5.0 SAMPLE AND ANALYSIS RATIONALE

The primary objective of the double needle sampler test series is to quantify organic partitioning which results from INTEC sample collection and handling procedures. As such, the sampling system operation and sampling strategy has been designed to simulate INTEC operations. Prior to previous tests, it was postulated that organic partitioning results from the following operational/sampling activities:

- air sparging of evaporator feed, condensate and bottoms tanks,
- steam jet transfer of liquid waste to PEWE feed tanks,
- air jet transfer and hypodermic needle sample collection,
- sample transfer from sample collection bottles to no-headspace organic vials, and
- >4° C temporary storage following sample collection.

These tests (Tests 1 through 4) demonstrated that the effects of air sparging and simulated steam jetting on spiked organic concentrations was significantly greater than the effects of air jetted sample collection and sample handling. After air sparging and steam jetting of feed solutions, approximately 75 percent of the spiked VOCs were reacted, decomposed, or volatilized and were no longer present in the feed solution.

This test has been designed to verify the effects of operation of the double needle sampling system only. As such, air sparge and steam jet operations will not be conducted.

5.1 Data Quality Objectives

The US Environmental Protection Agency (EPA) developed the Data Quality Objectives (DQOs) process as a system-based tool to support decision making which often follows characterization activities. Although the double needle sampler testing does not affect remedial or corrective actions, elements of the DQO process are helpful in clearly defining and bounding characterization, ultimately resulting in defensible data. The following subsections address relevant DQO issues.

5.1.1 Problem Statement

Quantification of volatile organic losses due to operation of double needle sampling systems is unachievable at INTEC due to high radioactivity and sampling/analysis logistics. PEWE bottoms are transferred to the tank farm, and PEWE condensate serves as feed to the LET&D. These systems are subject to regulatory scrutiny; bench-scale sampling and analysis will contribute to the INTEC characterization database to be used for permitting and to demonstrate permit compliance.

5.1.2 Data Users

Double needle sampling system data will be used to support permitting activities conducted by BBWI and DOE-ID for the State of Idaho. Data may also be used by INTEC personnel to better understand the fate of organics due to double needle sampler operations.

5.1.3 Study Boundaries and Decisions

All reasonable efforts have been made to simulate INTEC operations and sampling protocols during sampler system testing. Target analytes (Table 5.2-1 below) were determined by evaluating PEWE feed data and selecting representative spike constituents. Spiking concentrations were bounded by analytical quantitation limits. Nitric acid and inorganic feedstock molarity was determined by evaluating and simulating PEWE feed.

Data generated by this test is anticipated to verify/validate that current INTEC sampling methods (i.e. double needle sampler operation) do not result in significant losses of volatile organic species. This data will be used to supplement INTEC process knowledge and ongoing RCRA sampling and analysis in generating a characterization database which will be used for operational permitting and to demonstrate permit compliance.

5.2 Target Analytes

Table 5.2-1 below lists test target analytes. Target analytes were chosen to best represent expected PEWE feed constituents with regard to vapor pressures. TOC analysis will be used for trip blanks and detection of potential cross contamination.

Table 5.2-1: Target Analytes

Volatile Organics	Other Analysis
1,1,1-trichloroethane	Total Organic Carbon (TOC)
toluene	
carbon disulfide	

5.3 Organic Spiking Concentrations

Whereas spiking concentrations of inorganics is predicated upon simulating INTEC liquid waste feed molarities and specific gravity, organic spiking concentrations are dependent upon test objectives and analytical detection limits. Based on previous tests, detection limits are expected to vary between 1 and 10 mg/l. To help ensure detection in all samples, organic spiking concentrations will be 10 times expected detection, or 100

mg/l. The volume of organics to be added to a 44 liter feedstock is provided in table 5.3-1 below.

Table 5.3-1: Organic Volumes per 46 Liter Feedstock

Spiked Organic	Volume
1,1,1-Trichloroethane	3.48 ml
Carbon disulfide	5.08 ml
Toluene	3.29 ml

5.4 Quality Control

Two quality control (QC) samples will be collected. The first quality control sample is a trip blank to monitor for organic cross contamination that may occur during sample shipping. The second QC sample will be collected following pre-cleaning to monitor for cross contamination.

The analytical laboratory maintains and adheres to a quality control manual that can be provided upon request.

6.0 REPORTING

A detailed operations/sample logbook will be maintained. All operational observations and any deviations from procedure will be recorded. All pertinent sample collection information (date of sample, quantity of sample, observations, etc.) will be recorded. Following the receipt and evaluation of analytical data, a comprehensive final report will be generated which will include:

- operations and sampling description,
- data reduction spreadsheet,
- organic partitioning calculations,
- statistical analysis of sampling data,
- conclusions,
- additional study recommendations, if any,
- copy of logbook, and
- Attachment 1 data sheets.

7.0 REFERENCES

1. Radian Corporation, *Results of a Laboratory Study to Assess the Fate of Organic Compounds in Synthetic ICPP Tank Farm Waste*, July 17, 1995.

2. Science Applications International Corporation, *PEWE and LDUA Test Series, Orangics Partitioning Comprehensive Final Report*, Revision 0, June 2000.

Attachment A

Double Needle Sampler Data Sheets

Double Needle Sampler Data Sheets

Data to be Taker prior to and During Sampling

DATE:_____

Time	System Pressure (In. WC)	Feed Tank Level (L)	Feed Tank Temp(°F)	Primary Cond. Exit Temp. (°C)	Cooling Water Supply Temp. (°F)	Primary Cond. Supply Temp. (°F)	Cooling Water Exit Temp. (°F)	Cooling Water Flow	Sampling Operations Readings			
									Sample ID	Air Jet Flow	Air Pressure	Air Lift Flow
	E-PI-1	F-SG-101	E-TC-10	E-TC-9	E-TE-11	E-TE-12	E-TE-13	E-FI-13		AIR-FI-106		AIR-FI-116

RCRA PERMIT

FOR THE

IDAHO NATIONAL LABORATORY

Volume 14
INTEC Liquid Waste Management System

Appendix V

Standard Double Needle
Remote Sampling Protocol

Revision Date: October 29, 2008

STANDARD DOUBLE NEEDLE REMOTE SAMPLING PROTOCOL

1.0 Air Sparge Vessel Prior to Sampling

1.0.1 Air sparge the vessel for a specified time or per Shift Supervision instructions.

1.1 Sample Solution Using the Double-Needle Sampling Method

1.1.1 Open the following valves:

A. sample liquid discharge valve
B. sampler jet air valve
C. sampler supply valve.

1.1.2 Lower the sampler bottle lift mechanism and remove and save the drip bottle.

1.1.3 Prepare sampler.

1.1.3.1 Place sample bottle in holder.

1.1.3.2 Move the bottle lift mechanism into its full up position.

1.1.3.3 Visually ensure that the needles have pierced the septum and that the bottle is seated against the needle block stop gasket.

1.1.4 Open the appropriate jet pressure control valve, adjusting the valve until the appropriate psig is obtained.

1.1.5 If applicable, open the airlift flow control valve and set the rotameter as indicated.

1.1.6 Recirculate the solution through the sample bottle.

1.1.7 Visually ensure the solution is recirculating through the bottle.

1.1.8 Recirculate the solution for the minimum of 20 minutes for the first bottle and 5 minutes for the subsequent bottle(s).

1.1.9 Shut off the airlift and jet valves in the sampling corridor.

1.1.10 Ensure the sample vial is at least seventy-five percent (75%) full when the sample will be analyzed for organics.

1.1.11 Repeat steps 1.0.1 through 1.1.10 for additional samples.

1.1.12 Shut off valves opened in step 1.1.1 A, B, and C and airlift when sampling is complete.

1.1.13 Replace the saved drip bottle and raise the sampler bottle lift mechanism.

1.1.14 Transport sample from the cubicle to the lab using appropriate methods.

RCRA PERMIT

FOR THE

IDAHO NATIONAL ENGINEERING AND ENVIRONMENTAL LABORATORY

Volume 14
INTEC Liquid Waste Management System

Appendix VI

EDF-1747 Hydrodynamic and Structural Analysis of the Flood Hazards at CPP-659 During a Peak Flow in the Big Lost River

Revision Date: October 29, 2008

Document ID: EDF-1747
Revision ID: 0

Engineering Design File

Hydrodynamic and Structural Analysis of Flood Hazards at CPP-659 During a Peak Flow in the Big Lost River

Prepared for:
U.S. Department of Energy
Idaho Operations Office
Idaho Falls, Idaho

INEEL
Idaho National Engineering & Environmental Laboratory
BECHTEL BWXT IDAHO, LLC

Form 412.14
10/05/99
Rev. 02

Hydrodynamic and Structural Analyses of Flood Hazards at CPP-659 During A Peak Flow in the Big Lost River

The following Engineering Design File (EDF) were prepared under the responsible charge of the Professional Engineer as indicated by the seal and signature provided on this page. The Professional Engineer is registered in the State of Idaho to practice Civil and Structural Engineering.

PROFESSIONAL ENGINEER
REGISTERED
4003
1/17/2001
STATE OF IDAHO
SCOTT ALAN JENSEN

431.02
06/29/2000
Rev. 07

ENGINEERING DESIGN FILE

Functional File No. _____
EDF No. 1747
Page 1 of 13

1. Project File No.: _____ 2. Project/Task: CPP-659 Flood Hazard Analysis

3. Subtask: Hydrodynamic and Structural Analyses of Flood Hazards at CPP-659

4. Title: Hydrodynamic and Structural Analyses of Flood Hazards at CPP-659 During a Peak Flow in the Big Lost River

5. Summary: This summary briefly describes the problem to be addressed, gives a summary of the analyses performed in addressing the problem, and states the results, conclusions, and recommendations.

A study performed by the INEEL in 1986 estimated the flow volumes and water-surface elevations which occur during a peak flow in the Big Lost River at the INEEL. The INEEL study assumed that the 100-year peak flow and failure of Mackay Dam occur simultaneously, and estimated that the peak flow is equal to 28,500 ft^3/s at the diversion dam in the southwestern part of the INEEL. Building CPP-659—the New Waste Calcining Facility—lies within this hypothetical flood plain boundary based on the computed water elevation. The purpose of this analysis is to provide information to Idaho DEQ, in order to ensure compliance with RCRA regulations that require determination of hydrodynamic and hydrostatic forces expected to occur at the site and a description of flood protection devices at the facility and how these will prevent washout. The analysis consists of three parts: (1) A hydrodynamic analysis to compute the pressure exerted on the building by flood water; (2) A field investigation and structural analysis to determine whether the concrete foundation of CPP-659 can withstand the presence of flood water and to assess the likelihood of water infiltration; (3) A hydraulic analysis to examine the potential for sediment transport and erosion.

The results of this analysis lead to the following conclusions. Hydrostatic and hydrodynamic forces due to flood water above grade are negligible in comparison to lateral earth pressure. However, the weight of water in saturated soil considerably increases the lateral earth pressure. The lateral earth pressure of saturated soil was computed and shown to be 2 times larger than the pressure of dry soil. However, the strength of the below-grade retaining walls is adequate to support the increase in lateral earth pressure which may occur as a consequence of the flood postulated by the INEEL. Another major factor affecting the structural adequacy of the building is the method of construction, particularly the methods used to prevent water infiltration during a flood. A field investigation showed that construction of CPP-659 follows many of the methods described in the ACI Manual of Concrete Practice to assure a watertight structure. However, some minor water seepage was observed during the field investigation. Water accumulation is insignificant, which indicates that the rate of seepage is very low. Water that may seep into CPP-659 through pipe or utility penetrations is handled by flood protection devices that are designed to route water to the hot sump or valve cubicle so that water does not come into direct contact with waste piles or containerized hazardous wastes stored in the building. In particular, the flood protection devices are designed to preclude washout of hazardous waste from the building. Furthermore, a hydraulic analysis indicates that sediment transport and erosion at CPP-659 may occur. However, the likelihood of erosion is reduced by flood control devices that divert water to storage basins, asphalt and concrete that cover the gravel sediment found in the stream bed, and structures such as roads and buildings that slow and divert the flow.

6. Distribution (complete package): P. E. Murray, MS 3760; N. C. Hutten, MS 3428; S. A. Davies, MS 3650; S. A. Jensen, MS 3650; S. L. Austad, MS 3650
Distribution (summary package only): None

7. Review (R) and Approval (A) Signatures:

	R/A	Printed Name/Organization	Signature	Date
Author	R	P. E. Murray/6790	P. E. Murray	1/17/01
Reviewer	R	S. A. Jensen/6780	SA Jensen	1/17/2001
Project Manager	A	N. C. Hutten/7312	N. C. Hutten	1/17/2001
Project Engineer	R	S. A. Davies/6710	Stan Davies	1/17/01
Engineering Supervisor	A	S. L. Austad/6780	SLAustad	1/17/2001

Introduction

In 1986, the INEEL published a report containing calculated flow volumes and water-surface elevations which occur during a peak flow in the Big Lost River at the INEEL (1). The INEEL study included the assumption that the 100-year peak flow and failure of Mackay Dam occur simultaneously, and thereby estimated that the peak flow in the Big Lost River is equal to 28,500 ft^3/s at the INEEL diversion dam. However, there are conflicting scientific opinions regarding the magnitude of the 100-year peak flow in the Big Lost River, and the INEEL Natural Phenomena Hazards Committee is currently addressing this issue. Presently, the water surface profile associated with a 28,500 ft^3/s flow is considered to be an upper bound on potential flooding at the INEEL. The particular water surface profile obtained from the INEEL study is used as a basis for the present analysis.

In the INEEL study, 57,740 ft^3/s was estimated to occur at Mackay Dam. The flow is attenuated downstream, and the INEEL diversion dam located in the southwestern part of the INEEL was estimated to receive 28,500 ft^3/s. The diversion dam was assumed to be unable to retain that flow, and so a large part of the discharge flows onto the site. The remaining water was assumed to flow through the diversion channel and into spreading areas. A hydraulic model was used to compute the flow volumes and water elevations within a 18 mile reach downstream of the diversion dam. Building CPP-659—the New Waste Calcining Facility at INTEC—lies within the hypothetical flood plain boundary that is based on computed water elevations given in the 1986 INEEL report (1).

The purpose of this engineering analysis is to provide information to Idaho DEQ regarding the hydrodynamic and structural effects of a peak flow. This analysis is performed to ensure compliance with RCRA regulations (2) that require an "engineering analysis to indicate the various hydrodynamic and hydrostatic forces expected to result at the site as a consequence of a 100-year flood," and "structural or other engineering studies showing the design of operational units and flood protection devices at the facility and how these will prevent washout." In the RCRA regulations (2), the term "washout" is defined as "the movement of hazardous waste from the active portion of a facility as a result of flooding."

This analysis is performed to ensure compliance with the following specific requirements stemming from application for a RCRA permit for mixed hazardous waste treatment in CPP-659 and to address issues presented in the DEQ letter received 9/27/00 requesting this study:

1. A description of building CPP-659 construction parameters which prevent run-on to the units described in the Volume 18 Part B permit application;
2. A professional engineer (PE) certification that CPP-659 could withstand hydrodynamic or hydrostatic forces applied to the building as a result of the hypothetical 100-year flood event described in the 1986 INEEL report (1);
3. PE certification that the design of operational units and/or flood protection devices in CPP-659 are adequate to prevent washout;
4. A discussion of the controls within the building that provide protection against washout.

This analysis consists of three parts:

1. Hydrodynamic and hydrostatic analyses were used to compute the pressure exerted on the building by stationary and moving flood water;
2. A field investigation and structural analysis are used to determine whether the concrete foundation of CPP-659 can withstand the presence of flood water and to assess the likelihood of water infiltration;
3. A hydraulic analysis is used to examine the potential for erosion and washout of hazardous waste.

Background

Peak Flow Analysis

Koslow and Van Haaften (1) examined the consequences of a failure of Mackay Dam and performed a hydraulic analysis to determine the extent of the flood plain for several scenarios. Their analysis included a predicted 100-year flood and simultaneous piping failure at Mackay Dam, which leads to a breach of the dam, overtopping of the INEEL diversion dam, and flooding of the INEEL site. This scenario results in a peak flow released from the dam that was calculated to be 57,740 ft^3/s. This flow between Mackay Dam and the INEEL is attenuated by storage, agricultural diversion, and channel infiltration. The calculated flow at the INEEL diversion dam is 28,500 ft^3/s. Since the diversion dam is unable to retain the high flow, most of the flood water is assumed to flow onto the site.

Flow Routing Analysis

The peak flow estimated by Koslow and Van Haaften (1) was used in a flow routing analysis to determine the extent of the flood plain at the INEEL site. The geometry of the channel was determined from USGS topographical maps, and the Big Lost River stream bed was examined to determine surface roughness. The Bernoulli equation for ideal flow and the Manning relation for energy loss in open channels were used to compute the peak flow and water elevation at each cross-section. The INTEC site was surveyed by INEEL engineers to determine building and ground elevations. All vertical elevations are in reference to the National Geodetic Vertical Datum of 1929 (NGVD29). Of particular interest in this study is Building CPP-659 located at the INTEC facility. The leading edge of the flood wave is estimated to arrive at INTEC approximately 17.1 hours after breach of the dam. The peak flow is attenuated to 24,870 ft^3/s, and the peak water velocity is estimated to be 2.2 ft/s. Since the area surrounding INTEC is very flat, flood water will spread easily and so the flood plain is wide and shallow. The elevation of the stream bed is 4911 feet and the calculated water elevation is 4916 feet. The lowest ground elevation at CPP-659 is 4912.1 feet and occurs at the east side of the building. These results suggest that the depth of flood water may reach 4 feet at the building's foundation. Therefore, a water depth equal to 4 feet is used in the following hydrodynamic and hydrostatic analyses.

Koslow and Van Haaften (1) also performed an analysis to examine the potential for overland flooding due to localized heavy rain and snowmelt. It was found that localized flooding due to a 25-year peak rainfall and simultaneous snowmelt lead to a peak flow equal to 32 ft^3/s. This runoff can be accommodated by the drainage basin at INTEC and flood control devices such as culverts, dikes, and ditches. Meanwhile, flood water may collect in low-elevation areas at

INTEC. The following hydrodynamic and hydrostatic analyses of 4 feet of water at the foundation of CPP-659 may also be used to assess the effect of overland flooding due to localized precipitation.

Hydrostatic and Hydrodynamic Analyses

Hydrostatic Forces

The results of the INEEL study (1) were used to determine that the depth of flood water may reach 48 inches at the CPP-659 building foundation during a peak flow in the Big Lost River streambed adjacent to INTEC. At a depth of 48 inches, the hydrostatic pressure on the foundation is

$$P_{water} = \gamma_{water} \cdot d = 62.4 \frac{lb}{ft^3} \cdot 4\ ft = 249.6 \frac{lb}{ft^2},$$

where P_{water} is the hydrostatic pressure, γ_{water} is the weight of water, and d is the water depth. The resultant force per unit width of foundation is

$$F_{water} = \frac{1}{2} P_{water} \cdot d = 499.2 \frac{lb}{ft},$$

where F_{water} is the resultant force that occurs at a height above grade equal to $d/3$, as is shown in Fig. 1.

The lateral earth pressure of saturated soil includes the effect of water pressure and soil pressure. The at-rest earth pressure due to the weight of soil is

$$P_{soil} = K_o(\gamma_{sat} \cdot H - \gamma_{water} \cdot H) = 0.375 \cdot \left(135 \frac{lb}{ft^3} - 62.4 \frac{lb}{ft^3}\right) \cdot H = 27.2 \frac{lb}{ft^3} \cdot H,$$

where P_{soil} is the earth pressure, γ_{sat} is the weight of saturated soil, H is the soil depth, and K_o is the earth pressure coefficient. The at-rest earth pressure coefficient was obtained from the relation

$$K_o = 1 - \sin\phi,$$

where ϕ is the angle of internal friction which is equal to 43° according to the NWCF soils report (3). The weight of saturated soil at NWCF is assumed to be equal to the weight of dense, mixed-grain sand given by Peck et al (4). The resultant force per unit width is

$$F_{soil} = \frac{1}{2} P_{soil} \cdot H = 13.6 \frac{lb}{ft^3} \cdot H^2,$$

where F_{soil} is the resultant force that occurs at a height equal to $H/3$ from the base of the retaining wall. The hydrostatic pressure due to the presence of water is

$$P_{wet\ soil} = \gamma_{water} \cdot H = 62.4 \frac{lb}{ft^3} \cdot H,$$

where $P_{wet\ soil}$ is the hydrostatic pressure. The resultant force per unit width of retaining wall is

$$F_{wet\ soil} = \frac{1}{2} P_{wet\ soil} \cdot H = 31.2 \frac{lb}{ft^3} \cdot H^2,$$

where $F_{wet\ soil}$ is the resultant force that occurs at a height equal to $H/3$ from the base of the retaining wall. The total resultant force per unit width of retaining wall is

$$F_{total} = F_{soil} + F_{wet\ soil} = 44.8 \frac{lb}{ft^3} \cdot H^2,$$

where F_{total} is the total resultant force that occurs at a height equal to $H/3$ from the base of the retaining wall, as is shown in Fig. 1.

In the case of dry soil, the resultant force per unit width of retaining wall is

$$F_{dry\ soil} = \frac{1}{2} \cdot K_o \cdot \gamma_{dry} \cdot H^2 = \frac{1}{2} \cdot 0.375 \cdot 118 \frac{lb}{ft^3} \cdot H^2 = 22.1 \frac{lb}{ft^3} \cdot H^2.$$

The density of dry soil is given in the NWCF soils report (3).

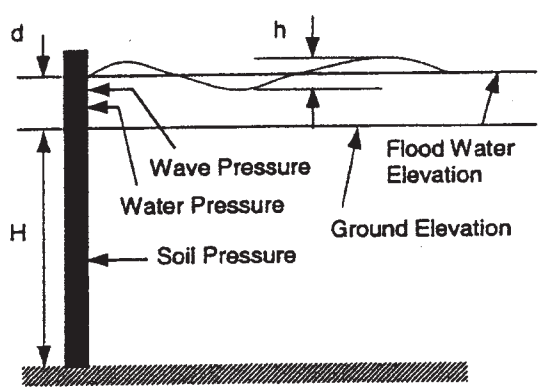

Fig. 1. Various forces acting on a retaining wall during a flood.

Hydrodynamic Forces

The force of moving flood water is calculated by considering the impact of shallow water waves caused by a high wind. A graph that shows the relation between wind velocity, water depth, wave height, and wave period is given in Fig. 10-16 on page 10-36 in Brater and King (5). Assuming a wind velocity equal to 60 mph and a water depth equal to 4 feet, the graph shows that the wave height is 2.0 feet and the wave period is 3.4 seconds. The relation between wave period and wavelength of shallow water waves is

$$\frac{L}{T} = \sqrt{g \cdot d},$$

where L is the wavelength, T is the wave period, d is the water depth, and g is the gravitational acceleration. Assuming a water depth equal to 4 feet and a wave period equal to 3.4 seconds, the wavelength is

$$L = T\sqrt{g \cdot d} = 3.4\,\text{s}\sqrt{32.2\frac{\text{ft}}{\text{s}^2} \cdot 4\,\text{ft}} = 38.6\,\text{ft},$$

and the wave velocity is

$$\frac{L}{T} = \frac{38.6\,\text{ft}}{3.4\,\text{s}} = 11.35\frac{\text{ft}}{\text{s}}.$$

In comparison, the velocity of flood water as estimated by Koslow and Van Haaften (1) is 2.2 ft/sec. Therefore, the velocity of moving flood water is small in comparison to the velocity of wind-generated waves.

The resultant force per unit width of retaining wall, which is caused by wind-generated waves, is calculated from an empirical relation described on page 10-41 in Brater and King (5). Assuming a wave height equal to 2.0 feet, the pressure exerted by the wave is

$$P_{wave} = \gamma_{water} \cdot h = 62.4\frac{\text{lb}}{\text{ft}^3} \cdot 2.0\,\text{ft} = 124.8\frac{\text{lb}}{\text{ft}^2}.$$

According to Fig. 10-21 on page 10-42 in Brater and King (5), the pressure distribution is uniform from the ground to the still-water height, and hydrostatic from the still-water height to a height above still water equal to $1.66 \cdot h$. Assuming a water depth equal to 4 feet, the force of the wave is

$$F_{wave} = P_{wave}\left(d + 0.5 \cdot 1.66 \cdot h\right) = 124.8\frac{\text{lb}}{\text{ft}^2}\left(4\,\text{ft} + 0.5 \cdot 1.66 \cdot 2.0\,\text{ft}\right) = 706.4\frac{\text{lb}}{\text{ft}},$$

and occurs at a height above grade equal to 2.9 feet, as is shown in Fig. 1.

The results of these calculations show that the hydrostatic and hydrodynamic forces are small in comparison to the lateral earth pressure. Furthermore, hydrostatic and hydrodynamic forces have a negligible effect on the overturning moment. However, a substantial increase in the earth pressure occurs when the soil becomes saturated—the dry soil force is equal to $22.1 \cdot H^2$ lb/ft and the saturated soil force is equal to $44.8 \cdot H^2$ lb/ft. Since the topmost 40 feet of soil at the NWCF is mostly sandy gravel that is dry and permeable (3), the assumption of saturated soil may be very conservative. Therefore, the calculated earth pressure is an upper bound on the actual earth pressure that would occur during a flood.

Structural Analysis

The second and third levels of CPP-659 are below grade and contain an inner cell structure encased in a 4 feet thick shielded concrete wall. The cell structure is surrounded by corridors and various utility rooms. The retaining walls on the second and third levels support gravel backfill and are 1 1/3 to 2 feet thick concrete. The first level is 3 feet above grade and contains a maintenance area leading to the cell structure and an outer office area built on gravel backfill. The exterior retaining wall supporting the first level is 1 1/6 feet thick concrete.

The structural features of the concrete foundation at CPP-659 were examined during a field investigation. The following features were examined: footing and foundation structures; type of concrete used during construction; soil grading and drainage systems; exterior wall construction, including joints and the method of sealing penetrations; openings such as doorways that enable water to easily infiltrate; the use of water stops and sealant to prevent water infiltration; and the occurrence of water seeping through cracks and penetrations. The ACI Manual of Standard Practices (6) provides guidance on construction of watertight concrete structures. The result of the field investigation shows that construction of the NWCF follows many of these standard practices, though some minor water seepage was observed.

The following list of construction practices were used to assure a watertight foundation and to provide adequate drainage during a flood.

(1) The retaining walls that support lateral earth pressure were made using high-density, low-permeability concrete.

(2) Soil surrounding the foundation is graded to slope away from the building.

(3) All joints are fitted with carbon steel water stops to prevent water infiltration.

(4) The first level is at an elevation higher than the flood water elevation.

(5) Visible cracks in the above-grade, exterior concrete foundation were not observed.

(6) Water entering the building drains to the hot sump tank located below the third level.

The following list of observations suggest the potential for water infiltration during a flood, particularly seepage caused by water infiltration through pipe penetrations and other openings. The field study investigated the potential for water infiltration through the utility piping tunnel, tank farm waste pipe, concrete hatches, doorways and other openings.

(1) All the INTEC utility piping is carried in an underground tunnel that sometimes contains water because the tunnel has manholes that provide an opening for runoff. Despite the presence of level alarms and a pump in the utility tunnel, the water in the utility tunnel occasionally seeps into the utility corridor located at the second level of CPP-659. Seepage occurs through pipe penetrations into the utility corridor. Seeping water is collected by a floor drain in the utility corridor and flows into VES-NCC-122—the non-fluoride hot sump tank. This tank has a maximum capacity of 4300 gallons and is equipped with level monitoring and control equipment. If seeping water enters the building as a result of a prolonged flood event, VES-NCC-122 can be sampled and its contents transferred to VES-

WL-133—the Process Equipment Waste Evaporator (PEWE) feed tank. The contents of tank VES-NCC-122 can also be transferred to VES-NCC-119—the fluoride hot sump tank—or the Tank Farm Facility if the PEWE cannot accept the liquid. Water is transferred through steam jets that have a capacity equal to 20 gal/min each.

(2) A 3 inch stainless steel pipe carrying waste from the tank farm is the only pipe that penetrates the inner cell structure. This pipe is encased in a larger pipe that is well sealed, and water infiltration through the pipe penetration has not been observed. If flood water enters the building at this location, the flood protection devices are designed to route water to a sump in the valve cubicle which is equipped with leak detection devices. From this sump the water may be pumped to a variety of other tanks, such as VES-NCC-119, VES-NCD-123, and VES-NCD-129. These tanks are equipped with level monitors and overflow alarms.

(3) Concrete hatches located in the maintenance area at the first level lead to the cell structure. These hatches are not watertight, but flood water will not reach the maintenance area since the first level is at an elevation equal to 4917 feet, which is 1 foot higher than the flood level.

(4) The lowest elevation of an entry into the building is a doorway on the north side, which is at an elevation equal to 4914.3 feet. This is 1.7 feet less than the flood water elevation. The doorway leads to the first level, which is at an elevation equal to 4917 feet. The exterior retaining wall at this doorway is located 20 feet from the closest retaining wall on the second and third levels. If a person enters the exterior door at the north side of CPP-659, he must walk up steps to an elevation of 4917 feet to reach the first level, and then walk 20 feet toward the center of the building to be above the second level. Therefore, water entering the exterior doorway may only infiltrate the gravel backfill underneath because there is no path for water to infiltrate the levels below grade.

Another important consideration is the ability of the retaining walls to withstand lateral earth pressure. In the section on hydrodynamic analysis, the at-rest lateral earth pressure of saturated soil was computed and shown to be 2 times larger than the pressure of dry soil. This particular flood hazard affects all below-grade retaining walls that support backfill. The structural design of the second and third levels of CPP-659 is complex, and the concrete retaining walls have a variable height, width, and thickness. Surcharge loads are present in addition to lateral earth pressure. Furthermore, the strength of reinforced concrete depends on the exact size, number, and placement of the steel bars. Therefore, a thorough assessment of the effect of soil saturation on the stress in retaining walls is a complex structural analysis that is beyond the scope of this study. However, the following simple calculation demonstrates that the strength of the below-grade retaining walls are more than adequate to support the increase in lateral earth pressure which may occur as a consequence of a flood.

The building structure consists of two levels below grade, and the height of each level is 17 feet. The first level is 3 feet above grade. Therefore, the depth of soil at the base of the first level retaining wall is 14 feet. Consider a concrete beam fixed at both ends and acted on by a distributed force, as is shown in Fig. 2. This particular beam loading represents the lateral earth pressure acting on a section of retaining wall, and leads to a conservative estimate of the shear force and the bending moment. To examine the loading on the weakest section of retaining wall, assume that the length of the beam is equal to 8 feet—the maximum spacing between supports—

and the thickness of the beam is equal to 16 inches—the minimum thickness of the foundation walls. Using the results calculated previously in the section entitled *Hydrostatic Forces*, the force per unit area of beam is equal to

$$P = P_{soil} + P_{wet\ soil} = 27.2\frac{lb}{ft^3}\cdot H + 62.4\frac{lb}{ft^3}\cdot H = 89.6\cdot H\,lb/ft^2,$$

where H is measured in feet. At the base of the beam where H is equal to 14 feet, the pressure is equal to $1250\,lb/ft^2$. To examine the maximum loading on the beam, assume that this pressure is uniformly distributed on the entire length of the beam.

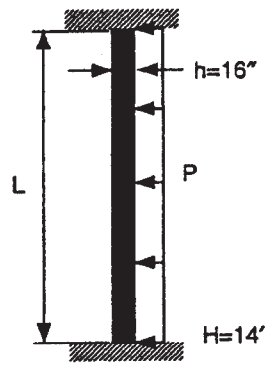

Fig. 2. Lateral earth pressure acting on a retaining wall.

The maximum shear force and bending moment occurs at the ends of the beam, and are obtained from the following formulas found in ACI 318 (7):

$$M = \frac{P\,L^2}{12} = 6690\frac{ft-lbs}{ft},$$

$$V = \frac{P\,L}{2} = 5020\frac{lbs}{ft}.$$

The actual force and moment are multiplied by a load factor equal to 1.7, as specified in ACI 318 (7), to give $M_u = 11{,}400\ lb\ ft$ and $V_u = 8{,}500\ lb$ per 1 foot width of beam.

To compute the allowable shear and moment capacity of the concrete beam, assume the minimum required reinforcement according to ACI 318-77 (7), which was the building code for reinforced concrete at the time the NWCF was built. For reinforcement with a yield strength equal to 40,000 psi, assume #4 bar spaced 8 inches center to center, and assume top and bottom covers equal to 1 inch. This meets the requirements that the area of vertical reinforcement shall not be less than 0.0015 times the wall area and the reinforcement layers shall not be placed more than 1/3 the wall thickness from the surface, as described in Sections 14.2.11 and 14.2.12 of ACI 318 (7). Furthermore, the concrete is assumed to have a compressive strength equal to 4000 psi.

The computation of moment and shear capacity are based on ACI 318 (7) and the CRSI Design Handbook (8). The shear capacity is obtained from Section 11.3.1.1 of ACI 318 (7):

$$V_c = 0.85\, 2\sqrt{f_c'}\, b\, d,$$

where f_c' is the compressive strength of concrete, b is the width of the beam, and d is the distance from the extreme compression fiber to the centroid of the tension reinforcement. The moment capacity for a single layer of tension reinforcement is obtained from page 5-7 in the CRSI Design Handbook (8):

$$M_n = 0.90\, A_s\, f_y\, (d - a/2),$$

where A_s is the area of tension reinforcement, f_y is the yield strength of the reinforcement, and a is the depth of the concrete compression block which is obtained from a balance of concrete compression and bar tension:

$$A_s\, f_y = 0.85\, f_c'\, b\, a.$$

The moment capacity and shear capacity for the concrete beam are $M_n = 13{,}100$ lb ft and $V_c = 19{,}000$ lb per 1 foot width of beam, which are larger than the factored moment and shear computed above. In fact, the retaining walls at the NWCF are stronger than this simple example indicates, owing to the presence of intersecting walls, columns, and slabs anchored to each section of retaining wall.

Hydraulic Analysis

Transport of sediment caused by moving flood water may lead to erosion of the stream bed. The type of soil needs to be known to assess the potential for erosion. A previous study (3) found that the topmost 40 feet of soil at the NWCF is mostly sandy gravel and some silt. Below the topmost layer is a 0 to 10 feet intermediate layer of clay soil containing silt and sand, and below the intermediate layer is basalt bedrock. A sieve analysis performed on the topmost layer of soil showed that the 75th percentile of the particle diameter distribution is approximately equal to 0.4 inches to 0.8 inches (3), which means that 75% of the particles by weight are that size or finer. In the case of a non-cohesive soil with a particle diameter larger than approximately 0.05 inches, the critical shear stress for sediment transport may be obtained from the following relation given on page 7-26 in Brater and King (5):

$$\tau_{critical} = 0.4 \cdot D,$$

where D is the 75th percentile of the particle diameter distribution measured in inches, and the critical shear stress is measured in lb/ft^2. Assuming a particle diameter equal to 0.6 inches,

$$\tau_{critical} = 0.4 \cdot 0.6\text{ in} = 0.24 \frac{\text{lb}}{\text{ft}^2}.$$

The shear stress due to uniform flow of water in a channel having a small slope may be obtained from the following relation given on page 7-25 in Brater and King (5):

$$\tau = \gamma_{water} \cdot d \cdot s,$$

where d is the water depth and s is the channel slope. In the Big Lost River stream bed near INTEC, the channel slope is approximately equal to 16 feet per mile. Since the flood water depth at CPP-659 is approximately equal to 4 feet, the shear stress due to moving flood water near the building is

$$\tau = 62.4\frac{\text{lb}}{\text{ft}^3} \cdot 4\text{ ft} \cdot \frac{16}{5280} = 0.76\frac{\text{lb}}{\text{ft}^2}.$$

Since $\tau > \tau_{critical}$, compute the particle size needed to resist erosion. Assuming a particle diameter equal to 2.0 inches,

$$\tau_{critical} = 0.4 \cdot 2.0\text{ in} = 0.80\frac{\text{lb}}{\text{ft}^2}.$$

Therefore, erosion of sand and rock with a diameter smaller than 2 inches may occur. However, the likelihood of erosion is greatly reduced because much of the sandy gravel sediment found in the stream bed has been covered with asphalt and concrete at INTEC. Furthermore, the likelihood of erosion is reduced by the presence of flood control devices that divert water to storage basins and structures such as roads and buildings that slow and divert the flow. Since the main foundations are deep and the gravel has some larger rock, erosion of the soil is not likely to cause damage to critical structural components.

Conclusions

An engineering analysis was used to calculate the various hydrodynamic and hydrostatic forces expected to result at Building CPP-659 as a consequence of a 100-year flood coinciding with a failure of Mackay Dam. A structural study was used to describe the design of CPP-659 and its flood protection devices and how these will prevent washout of hazardous waste. Specific details are given below.

An engineering analysis was used to determine whether CPP-659 can withstand a peak flow in the Big Lost River adjacent to INTEC. Hydrostatic and hydrodynamic forces due to flood water above grade are negligible in comparison to lateral earth pressure, but the weight of water in saturated soil considerably increases the lateral earth pressure. In fact, the lateral earth pressure of saturated soil was computed and shown to be 2 times larger than the pressure of dry soil. However, the strength of the below-grade retaining walls is adequate to support the increase in lateral earth pressure which may occur as a consequence of a flood.

Another major factor affecting the structural adequacy of the building is the method of construction, particularly the methods used to prevent water infiltration during a flood. A field investigation showed that construction of the NWCF follows many of the methods described in the ACI Standard Practices to assure a watertight structure. Furthermore, the field investigation

examined the potential for water infiltration through the utility piping tunnel, tank farm waste pipe, concrete hatches, doorways and other openings. The first level of CPP-659 contains a pathway for water to enter the concrete hatches in the maintenance area. Since the elevation of the first level is one foot above the elevation of the hypothetical 100-year flood, water entry through these openings will not occur. However, some minor water seepage from a below-grade utility tunnel was observed during the field investigation. The rate of water seepage is very low and water accumulation is insignificant. Water that may seep into CPP-659 through pipe or utility penetrations is handled by flood protection devices that are designed to route water to the hot sump tank so that water does not come into direct contact with waste piles or containerized hazardous wastes. In particular, the flood protection devices are designed to preclude "washout" or movement of hazardous waste from the building as a result of flooding.

Another issue concerns the potential for erosion and sediment transport. The shear stress of moving flood water near CPP-659 is larger than the critical shear stress needed to cause sediment transport, and so erosion at CPP-659 may occur. However, the likelihood of erosion is greatly reduced because much of the sandy gravel sediment found in the stream bed has been covered with asphalt and concrete at INTEC. Furthermore, the likelihood of erosion is reduced by the presence of flood control devices that divert water to storage basins and structures such as roads and buildings that slow and divert the flow. Since the main foundations are deep and the gravel has some larger rock, erosion of the soil is not likely to cause damage to critical structural components.

References

1. K. N. Koslow and D. H. Van Haaften, *Flood Routing Analysis for a Failure of Mackay Dam*, EGG-EP-7184, June, 1986.
2. *Code of Federal Regulations*, 40 CFR Ch. 1, Sect. 270.14(b), Para. 11(iv) A, August 1, 2000.
3. *Soil and Foundation Investigation, Proposed New Waste Calcining Facility*, Prepared for The Energy Research and Development Administration, Fluor Contract No. 453504, Dames and Moore, 1976.
4. R. B. Peck, W. E. Hanson, and T. H. Thornburn, *Foundation Engineering*, 2nd Edition, John Wiley & Sons, NY, 1974.
5. E. F. Brater and H. W. King, *Handbook of Hydraulics*, 6th Edition, McGraw-Hill, NY, 1976.
6. *Environmental Engineering Concrete Structures*, ACI 350.2R-97, American Concrete Institute, 2000.
7. *Building Code Requirements for Reinforced Concrete*, ACI 318-77, American Concrete Institute, 1978.
8. *CRSI Design Handbook*, 3rd Edition, Concrete Reinforcing Steel Institute, 1978.

RCRA PERMIT

FOR THE

IDAHO NATIONAL LABORATORY

Volume 14
INTEC Liquid Waste Management System

Appendix VII

EDF-2613, Hydrodynamic and Structural Analyses of Flood Hazards at the PEWE and LET&D Buildings During a Peak Flow in the Big Lost River

Revision Date: October 29, 2008

Document ID: EDF-2613
Revision ID: 0

Engineering Design File

Hydrodynamic and Structural Analysis of Flood Hazards at the PEWE and LET&D Buildings During a Peak Flow in the Big Lost River

Prepared for:
U.S. Department of Energy
Idaho Operations Office
Idaho Falls, Idaho

INEEL
Idaho National Engineering & Environmental Laboratory
BECHTEL BWXT IDAHO, LLC

Form 412.14
10/05/99
Rev. 02

Hydrodynamic and Structural Analyses of Flood Hazards at the PEWE and LET&D Buildings During a Peak Flow in the Big Lost River

The following Engineering Design File (EDF) was prepared under the responsible charge of the Professional Engineer as indicated by the seal and signature provided on this page. The Professional Engineer is registered in the State of Idaho to practice Civil and Structural Engineering.

PROFESSIONAL ENGINEER
REGISTERED
4003
5/2/01
STATE OF IDAHO
SCOTT ALAN JENSEN

431.02
06/29/2000
Rev. 07

ENGINEERING DESIGN FILE

Functional File No. _____
EDF No. 2613
Page 1 of 14

1. Project File No.: _____ 2. Project/Task: INTEC Flood Hazard Analysis

3. Subtask: Hydrodynamic and Structural Analyses of Flood Hazards at INTEC

4. Title: Hydrodynamic and Structural Analyses of Flood Hazards at the PEWE and LET&D Buildings During a Peak Flow in the Big Lost River

5. Summary: This summary briefly describes the problem to be addressed, gives a summary of the analyses performed in addressing the problem, and states the results, conclusions, and recommendations.

A study performed by the INEEL in 1986 estimated the flow volumes and water-surface elevations which would occur during a peak flow in the Big Lost River at the INEEL. This study assumed that the 100-year peak flow and failure of Mackay Dam occur simultaneously, which leads to a conservative estimate of the floodplain. The PEWE (CPP-604, CPP-605) and LET&D (CPP-1618) buildings lie within this flood plain boundary based on the computed water elevation. The purpose of this analysis is to provide information to Idaho DEQ, in order to ensure compliance with RCRA regulations that require determination of hydrodynamic and hydrostatic forces expected to occur at the site and a description of flood protection devices at the facility and how these will prevent washout. The analysis consists of three parts:

(1) A hydrostatic analysis was used to compute the pressure exerted on the building by stationary flood water and saturated soil.
(2) A hydrodynamic analysis was used to compute the pressure exerted on the building by moving flood water caused by wind-generated water waves.
(3) A structural analysis was used to determine whether the concrete foundation of the buildings can withstand the presence of flood water and to assess the extent of water infiltration.

The results of this analysis lead to the following conclusions:

(1) The most important feature of the building construction is whether the first level finished floor elevation is higher than the flood water elevation. Only CPP-1618 meets this requirement, but with a contingency. For CPP-1618, the elevation of wind-generated water waves is higher than the first level floor elevation, and so a barrier is needed to stop waves splashing onto the doorways. For CPP-604 and CPP-605, the flood water elevation is higher than the first level floor elevation, and so additional flood protection devices are needed to prevent water infiltration.
(2) The construction of the buildings follows many of the standard practices used to assure a watertight foundation and to provide adequate drainage during a flood, though some minor water seepage currently occurs through pipe penetrations at CPP-604. Water entering the tank vault and pump pit drains to a sump and is transferred by steam jets to the evaporator feed tank. The jets have enough capacity to transfer the maximum seepage rate expected to occur during a flood.
(3) An important consideration in regard to flood protection is the ability of the retaining walls to withstand lateral earth pressure and water pressure. The exterior retaining walls of the CPP-604 and CPP-605 buildings are considerably stronger with regard to hydrodynamic and hydrostatic forces than are those of the CPP-1618 building. Therefore, for the purposes of this study, information on the strength of the building CPP-1618 retaining wall is provided to represent the minimum wall strength of all three buildings. A structural analysis of the CPP-1618 retaining wall demonstrates that the building can withstand hydrostatic forces caused by the maximum credible flooding event in the Big Lost River on the INEEL.

6. Distribution (complete package): P. E. Murray, MS 3760; N. C. Hutten, MS 3428; S. A. Davies, MS 3650; S. A. Jensen, MS 3650; S. L. Austad, MS 3650

7. Review (R) and Approval (A) Signatures:
(Minimum reviews and approvals are listed. Additional reviews/approvals may be added.)

	R/A	Printed Name/Organization	Signature	Date
Author	R	P. E. Murray/6790	P. E. Murray	5/23/01
Checker	R	S. A. Jensen /6780	S. A. Jensen	5/23/01
Project Engineer	A	S. A. Davies /6710	[illegible]	5/23/01
Project Manager	A	N. C. Hutten/7312	Neil C. Hutten	5/24/01
Engineering Supervisor	A	S. L. Austad/6780	[illegible]	5/23/01

Introduction

In 1986, the INEEL published a report containing calculated flow volumes and water-surface elevations which would occur during a peak flow in the Big Lost River at the INEEL (1). The INEEL study included the assumption that the 100-year peak flow and failure of Mackay Dam occur simultaneously, and thereby estimated that the peak flow in the Big Lost River is equal to 28,500 ft^3/s at the INEEL diversion dam. However, there are conflicting scientific opinions regarding the magnitude of the 100-year peak flow in the Big Lost River, and the INEEL Natural Phenomena Hazards Committee is currently addressing this issue. Presently, the water surface profile associated with a 28,500 ft^3/s flow is considered to be an upper bound on potential flooding at the INEEL. The particular water surface profile obtained from the INEEL study is used as a basis for the present analysis.

In the INEEL study, 57,740 ft^3/s was estimated to occur at Mackay Dam. The flow is attenuated downstream, and the INEEL diversion dam located in the southwestern part of the INEEL was estimated to receive 28,500 ft^3/s. The diversion dam was assumed to be unable to retain that flow, and so a large part of the discharge flows onto the site. The remaining water was assumed to flow through the diversion channel and into spreading areas. A hydraulic model was used to compute the flow volumes and water elevations within a 18 mile reach downstream of the diversion dam. Several RCRA-regulated buildings lie within the maximum credible flood plain boundary that is based on computed water elevations given in the 1986 INEEL report (1).

The purpose of this engineering analysis is to provide information to Idaho DEQ regarding the hydrodynamic and structural effects of a peak flow. This analysis is performed to ensure compliance with RCRA regulations (2) that require an "engineering analysis to indicate the various hydrodynamic and hydrostatic forces expected to result at the site as a consequence of a 100-year flood," and "structural or other engineering studies showing the design of operational units and flood protection devices at the facility and how these will prevent washout." In the RCRA regulations (2), the term "washout" is defined as "the movement of hazardous waste from the active portion of a facility as a result of flooding."

This analysis is performed to ensure compliance with the following specific requirements stemming from application for a RCRA permit for mixed hazardous waste treatment in the Process Equipment Waste Evaporator (PEWE) and Liquid Effluent Treatment and Disposal (LET&D) facilities:

1. A description of building construction parameters which prevent water infiltration into the units described in the RCRA Volume 14 Part B permit application;
2. A professional engineer (PE) certification that the buildings could withstand hydrodynamic and hydrostatic forces as a result of the flood event described in the 1986 INEEL report (1);
3. PE certification that the design of operational units and/or flood protection devices in the buildings are adequate to prevent washout;
4. A discussion of the controls within the buildings that provide protection against washout.

This analysis consists of three parts:

1. A hydrostatic analysis was used to compute the pressure exerted on the building by stationary flood water and saturated soil;

2. A hydrodynamic analysis was used to compute the pressure exerted on the building by moving flood water generated by a 60 mph wind;
3. A structural analysis was used to determine whether the concrete foundation of the buildings can withstand the presence of flood water and to assess the extent of water infiltration.

Background

Peak Flow Analysis

Koslow and Van Haaften (1) examined the consequences of a failure of Mackay Dam and performed a hydraulic analysis to determine the extent of the flood plain for several scenarios. Their analysis included a predicted 100-year flood and simultaneous piping failure at Mackay Dam, which leads to a breach of the dam, overtopping of the INEEL diversion dam, and flooding of the INEEL site. This scenario results in a peak flow released from the dam that was calculated to be 57,740 ft^3/s. This flow between Mackay Dam and the INEEL is attenuated by storage, agricultural diversion, and channel infiltration. The calculated flow at the INEEL diversion dam is 28,500 ft^3/s. Since the diversion dam is unable to retain the high flow, most of the flood water is assumed to flow onto the site.

Flow Routing Analysis

The peak flow estimated by Koslow and Van Haaften (1) was used in a flow routing analysis to determine the extent of the flood plain at the INEEL site. The geometry of the channel was determined from USGS topographical maps, and the Big Lost River stream bed was examined to determine surface roughness. The Bernoulli equation for ideal flow and the Manning relation for energy loss in open channels were used to compute the peak flow and water elevation at each cross-section. All vertical elevations are in reference to the National Geodetic Vertical Datum of 1929 (NGVD29). Of particular interest in this study are the RCRA-regulated buildings located at the INTEC facility. The leading edge of the flood wave is estimated to arrive at INTEC approximately 17.1 hours after breach of the dam. The peak flow is attenuated to 24,870 ft^3/s, and the peak water velocity is estimated to be 2.2 ft/s. Since the area surrounding INTEC is very flat, flood water will spread easily and so the flood plain is wide and shallow. The elevation of the stream bed in the vicinity of INTEC is 4911 feet and the corresponding calculated water elevation is 4916 feet. The ground elevation at INTEC varies from 4912 ft to 4914 ft. These results suggest that the depth of flood water may reach 4 feet at some locations. Therefore, a maximum water depth equal to 4 feet is used in the following hydrodynamic and hydrostatic analyses.

Koslow and Van Haaften (1) also performed an analysis to examine the potential for overland flooding due to localized heavy rain and snowmelt. It was found that localized flooding due to a 25-year peak rainfall and simultaneous snowmelt lead to a peak flow equal to 32 ft^3/s. This runoff can be accommodated by the drainage basin at INTEC and flood control devices such as culverts, dikes, and ditches. Meanwhile, flood water may collect in low-elevation areas at INTEC. The following hydrodynamic and hydrostatic analyses may also be used to assess the effect of overland flooding due to localized precipitation.

Description of Buildings

The following structures comprise the PEWE and LET&D facilities and have been analyzed for flood hazards:

CPP-604	Process Equipment Waste Evaporator (PEWE) Building
CPP-605	Atmospheric Protection System Fan Building (attached to PEWE)
CPP-1618	Liquid Effluent Treatment and Disposal (LET&D) Building

An important consideration is the first level finished floor elevation, which must be above the flood water elevation in order to prevent infiltration of water through unsealed doorways and other openings. Vertical elevations are currently measured in reference to the National Geodetic Vertical Datum of 1929 (NGVD29). The first level finished floor elevations, as shown on the as-built drawings, are listed in Table 1. The PEWE buildings were constructed in the 1950s, and the datum used then was not NGVD29. Therefore, the INTEC site was recently surveyed by INEEL engineers to determine building and ground elevations using NGVD29. These results are also listed in Table 1. The recent elevation measurements using NGVD29 are approximately one foot less than the elevation shown on the as-built drawings. Note that the PEWE buildings (CPP-604 and CPP-605) are connected and are essentially one building.

Table 1. Building elevations in feet above sea level.

Building	First Level Floor Elevation (shown on as-built drawing)	First Level Floor Elevation (in reference to NGVD29)
CPP-604	4913	4912.0
CPP-605	4913	4912.0
CPP-1618	4917	4916.1

The first level finished floor elevations of CPP-604 and CPP-605 are below the hypothetical flood water elevation. In this case, flood water may infiltrate through exterior doorways and enter the cells. Therefore, additional flood protection devices are needed to prevent washout of hazardous waste in the event of a flood.

Hydrostatic and Hydrodynamic Analyses

In this section, hydrostatic and hydrodynamic analyses will be used to compute the pressure exerted on a building foundation by stationary flood water, saturated soil, and wind-generated water waves.

Hydrostatic Forces

The lateral earth pressure of saturated soil includes the effect of water pressure and soil pressure. Using the method described in Section 2.4 in Peck et al (3), the at-rest earth pressure due to the weight of soil is

$$P_{soil} = K_o\left(\gamma_{sat} \cdot H - \gamma_{water} \cdot H\right) = 0.375 \cdot \left(135\frac{lb}{ft^3} - 62.4\frac{lb}{ft^3}\right) \cdot H = 27.2\frac{lb}{ft^3} \cdot H,$$

where P_{soil} is the earth pressure, γ_{sat} is the weight of saturated soil, γ_{water} is the weight of water, H is the soil depth, and K_o is the at-rest earth pressure coefficient. The earth pressure coefficient is obtained from the relation

$$K_o = 1 - \sin\phi,$$

where ϕ is the angle of internal friction which is equal to 43° according to the INEEL soils report (4). The weight of saturated soil at the INEEL is assumed to be equal to the weight of saturated, dense, mixed-grain sand, as is given in Table 1.4 in Peck et al (3). The resultant force per unit width of retaining wall is

$$F_{soil} = \frac{1}{2} P_{soil} \cdot H = 13.6 \frac{lb}{ft^3} \cdot H^2,$$

where F_{soil} is the resultant force that occurs at a height equal to $H/3$ from the base of the retaining wall, as is shown in Fig. 1. The hydrostatic pressure due to the presence of water is

$$P_{water} = \gamma_{water} \cdot (H + d) = 62.4 \frac{lb}{ft^3} \cdot (H + d),$$

where P_{water} is the hydrostatic pressure, and d is the water depth. The resultant force per unit width of retaining wall is

$$F_{water} = \frac{1}{2} P_{water} \cdot (H + d) = 31.2 \frac{lb}{ft^3} \cdot (H + d)^2,$$

where F_{water} is the resultant force that occurs at a height equal to $(H + d)/3$ from the base of the retaining wall, as is shown in Fig. 1. The total resultant force per unit width of retaining wall is

$$F_{total} = F_{soil} + F_{water} = 44.8 \frac{lb}{ft^3} \cdot H^2 + 31.2 \frac{lb}{ft^3} \left(2 \cdot H \cdot d + d^2\right),$$

where F_{total} is the total resultant force that includes the weight of soil and water.

In the case of saturated soil and a water depth equal to zero, the resultant force per unit width of retaining wall is obtained from the preceding equation by setting $d = 0$:

$$F_{sat\ soil} = 44.8 \frac{lb}{ft^3} \cdot H^2.$$

In the case of dry soil, the resultant force per unit width of retaining wall is

$$F_{dry\ soil} = \frac{1}{2} \cdot K_o \cdot \gamma_{dry} \cdot H^2 = \frac{1}{2} \cdot 0.375 \cdot 118 \frac{lb}{ft^3} \cdot H^2 = 22.1 \frac{lb}{ft^3} \cdot H^2.$$

The density of dry soil is given in the INEEL soils report (4). These results show that a substantial increase in lateral earth pressure occurs when the soil becomes saturated. In fact, the at-rest lateral earth pressure of saturated soil is approximately two times larger than the pressure of dry soil. Since the topmost 40 feet of soil at INTEC is mostly sandy gravel that is dry and permeable (4), the assumption of saturated soil is very conservative. Therefore, the calculated earth pressure is an upper bound on the actual earth pressure that would occur during a flood.

The results of the Koslow and Van Haaften study (1) show that the depth of flood water may reach 4 feet at INTEC during a peak flow in the Big Lost River. Assuming a water depth equal to 4 feet, the total resultant force per unit width of retaining wall is

$$F_{total} = 44.8\frac{lb}{ft^3}\cdot H^2 + 249.6\frac{lb}{ft^2}\cdot H + 499.2\frac{lb}{ft}.$$

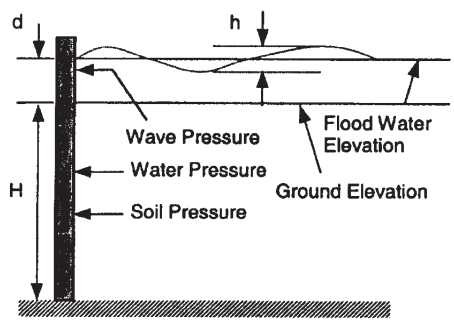

Fig. 1. Various forces acting on a retaining wall during a flood.

Hydrodynamic Forces

The force of moving flood water is calculated by considering the impact of shallow water waves caused by a high wind. A graph that shows the relation between wind velocity, water depth, wave height, and wave period is given in Fig. 10-16 on page 10-36 in Brater and King (5). Assuming a wind velocity equal to 60 mph and a water depth equal to 4 feet, the graph in Brater and King (5) shows that the wave height is 2.0 feet and the wave period is 3.4 seconds. The relation between wave period and wavelength of shallow water waves is

$$\frac{L}{T} = \sqrt{g\cdot d},$$

where L is the wavelength, T is the wave period, d is the water depth, and g is the gravitational acceleration. Assuming a water depth equal to 4 feet and a wave period equal to 3.4 seconds, the wavelength is

$$L = T\sqrt{g\cdot d} = 3.4\,s\sqrt{32.2\frac{ft}{s^2}\cdot 4\,ft} = 38.6\,ft,$$

and the wave velocity is

$$\frac{L}{T} = \frac{38.6\,\text{ft}}{3.4\,\text{s}} = 11.35\frac{\text{ft}}{\text{s}}.$$

In comparison, the velocity of flood water as estimated by Koslow and Van Haaften (1) is 2.2 ft/sec. Therefore, the velocity of moving flood water is small in comparison to the velocity of wind-generated waves.

The resultant force per unit width of retaining wall, which is caused by wind-generated waves, is calculated from an empirical relation described on page 10-41 in Brater and King (5). Assuming a wave height equal to 2.0 feet, the pressure exerted by the wave is

$$P_{wave} = \gamma_{water} \cdot h = 62.4\frac{\text{lb}}{\text{ft}^3} \cdot 2.0\,\text{ft} = 124.8\frac{\text{lb}}{\text{ft}^2},$$

where h is the wave height. According to Fig. 10-21 on page 10-42 in Brater and King (5), the pressure distribution is uniform from the ground to the still-water height, and hydrostatic from the still-water height to a height above still water equal to $1.66 \cdot h$. This particular distribution represents the pressure that is produced by a non-breaking wave reflected from a vertical wall. Superposition of approaching and reflecting waves lead to standing waves that have a height approximately equal to $2\,h$. Assuming a water depth equal to 4 feet, the force of the wave is

$$F_{wave} = P_{wave}\left(d + 0.5 \cdot 1.66 \cdot h\right) = 124.8\frac{\text{lb}}{\text{ft}^2}\left(4\,\text{ft} + 0.5 \cdot 1.66 \cdot 2.0\,\text{ft}\right) = 706.4\frac{\text{lb}}{\text{ft}},$$

and occurs at a height above grade equal to 2.9 feet, as is shown in Fig. 1. The preceding equation for the wave force is the total hydrodynamic force per unit width of retaining wall.

Comparison of Hydrostatic and Hydrodynamic Forces

The hydrostatic and hydrodynamic forces have been calculated using a flood water depth equal to 4 ft and several values of saturated soil depth. The results are shown in Fig. 2.

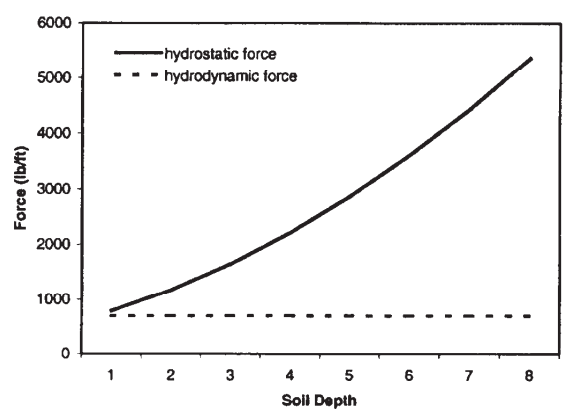

Fig. 2. Hydrostatic and hydrodynamic forces per unit width of foundation.

These results show that for a saturated soil depth larger than several feet, the hydrodynamic force due to waves is small in comparison to the hydrostatic force due to lateral earth pressure and water pressure.

Structural Analysis

In this section, structural analyses will be used to determine whether the concrete foundations of the buildings can withstand the presence of flood water, and to assess the extent of water infiltration through pipe penetrations and exterior doorways.

Foundation Walls

An important consideration in regard to flood protection is the ability of the retaining walls to withstand lateral earth pressure. In the section on hydrostatic analysis, the at-rest lateral earth pressure of saturated soil was computed and shown to be 2 times larger than the pressure of dry soil. This particular flood hazard affects all below-grade retaining walls that support backfill. The structural design of the building foundation is complex, and the concrete retaining walls have a variable height, width, and thickness. Surcharge loads are present in addition to lateral earth pressure. Furthermore, the strength of reinforced concrete depends on the exact size, number, and placement of the steel bars. Therefore, a thorough assessment of the effect of soil saturation on the stress in retaining walls is a complex structural analysis that is beyond the scope of this study. However, the following observations suggest a simple way to assess the strength of the below-grade retaining walls and to demonstrate that the walls are more than adequate to support the increase in lateral earth pressure which may occur as a consequence of a flood.

The buildings comprising the PEWE and LET&D facilities are much different in design. Building CPP-604 includes three levels: one level above grade and two levels below grade. The lower levels contain an inner cell structure surrounded by corridors, storage tank vaults, and various utility rooms. The retaining walls on the lower levels are 1 to 4 feet thick reinforced concrete. Building CPP-605 is attached to CPP-604 and contains a control room and off-gas equipment, but does not have levels below grade. The smallest exterior retaining wall of CPP-605 is 9 in. thick concrete supported by a concrete footing located 5 ft below the first level slab. Building CPP-1618 has three levels that are above grade and none below grade. The exterior retaining wall of CPP-1618 is 8 in. thick concrete supported by a concrete footing located 9 ft below the first level slab. The exterior retaining walls of the CPP-604 and CPP-605 buildings are considerably stronger with regard to hydrodynamic and hydrostatic forces than are those of the CPP-1618 building. Therefore, for the purposes of this study, information on the strength of the building CPP-1618 retaining wall is provided to represent the minimum wall strength for all three buildings. The following structural analysis of a concrete retaining wall uses the design of CPP-1618 to demonstrate that the buildings can withstand hydrostatic forces caused by the maximum credible flood.

The distance from the footing to the first level slab is 7 ½ ft. The first level slab is 3 ½ ft above grade, and so the depth of soil at the base of the retaining wall is 4 ft. Since the flood water elevation coincides with the first level slab elevation, as shown in Table 1, the depth of flood water is 3 ½ ft.

Consider a concrete beam pinned at both ends and acted on by hydrostatic forces, as is shown in Fig. 3. This particular beam loading represents the lateral earth and water pressure acting on a section of retaining wall. Simple supports are assumed since an angular displacement may occur at the ends of the beam where the wall is anchored to the slab and footing. Furthermore, the soil pressure at the inside of the wall is assumed to be equal to the at-rest earth pressure of dry soil.

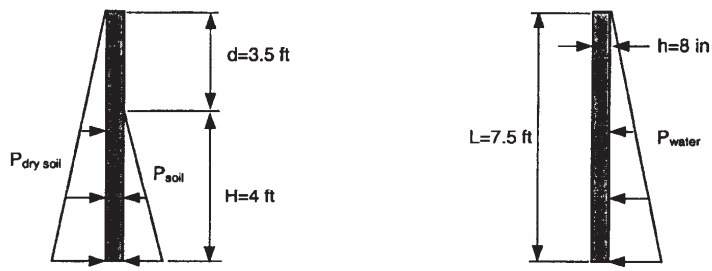

Fig. 3. Lateral earth and water pressure acting on a retaining wall.

The length of the beam is equal to 7 ½ ft and the thickness of the beam is equal to 8 in. Using the hydrostatic pressure calculated previously, the pressure at the base of the beam is equal to

$$P = P_{soil} + P_{water} - P_{dry\ soil} = 27.2\frac{lb}{ft^3}\cdot H + 62.4\frac{lb}{ft^3}\cdot(H+d) - 44.3\frac{lb}{ft^3}\cdot(H+d) = 245\,lb/ft^2,$$

where $H = 4\ ft$ and $d = 3.5\ ft$. To examine the loading on the beam, assume that the pressure varies linearly from zero to 245 lb/ft^2 over the length of the beam, as shown in Fig. 4.

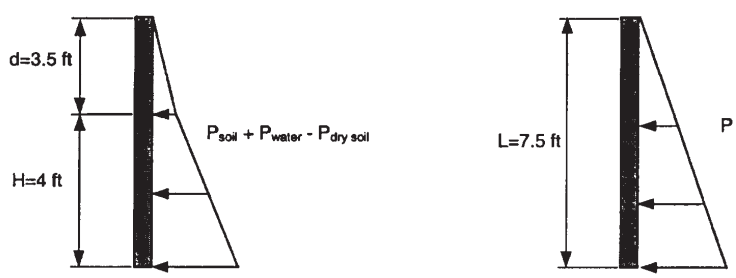

Fig. 4. Actual and assumed pressure acting on a retaining wall.

The maximum shear force and bending moment occur at the base of the beam, and are obtained from the following formulas found in Roark and Young (6), Table 3, Case 2e:

$$M = 0.0641\,P\,L^2 = 883\frac{ft-lbs}{ft},$$

$$V = \frac{PL}{3} = 613 \frac{\text{lbs}}{\text{ft}}.$$

The actual force and moment are multiplied by a load factor equal to 1.7, as specified in ACI 318 (7), to give $M_u = 1501$ lb ft and $V_u = 1042$ lb per 1 foot width of beam.

To compute the allowable shear and moment capacity of the concrete beam, assume that the beam includes vertical reinforcement only and neglect the presence of horizontal reinforcement. The vertical reinforcement is a single layer of #4 bar spaced 10 inches center to center. This meets the requirement that the area of vertical reinforcement shall not be less than 0.0015 times the wall area, as described in Sections 14.2.11 of ACI 318 (7), which was the building code for reinforced concrete at the time CPP-1618 was built. Since the bar is placed in the center of the slab, the top and bottom covers are equal to 4 inches. The concrete has a minimum compressive strength equal to 3000 psi. Furthermore, it is assumed that the yield strength of reinforcement bar is equal to 40,000 psi.

The computation of moment and shear capacity are based on ACI 318 (7) and the CRSI Design Handbook (8). The shear capacity is obtained from Section 11.3.1.1 of ACI 318 (7):

$$V_c = 0.85\, 2\sqrt{f_c'}\, b\, d,$$

where f_c' is the compressive strength of concrete, b is the width of the beam, and d is the distance from the extreme compression fiber to the center of mass of the tension reinforcement. The moment capacity for a single layer of tension reinforcement is obtained from page 5-7 in the CRSI Design Handbook (8):

$$M_n = 0.90\, A_s\, f_y\, (d - a/2),$$

where A_s is the area of tension reinforcement, f_y is the yield strength of the reinforcement, and a is the depth of the concrete compression block which is obtained from a balance of concrete compression and bar tension:

$$A_s\, f_y = 0.85\, f_c'\, b\, a.$$

The moment capacity of the concrete beam is $M_n = 2767$ lb ft per 1 foot width of beam, which exceeds the factored moment computed above. The shear capacity of the beam is $V_c = 4470$ lb per 1 foot width of beam, which exceeds the factored shear computed above. In fact, the retaining walls at CPP-1618 are stronger than this simple example indicates, owing to the presence of intersecting walls and columns anchored to each section of retaining wall, and the presence of horizontal reinforcement.

Water Infiltration Through Pipe Penetrations

The waste treatment process at INTEC includes a complex system of pipes that transfer waste between buildings for treatment. This observation suggests the potential for seepage

caused by water infiltration through pipe penetrations located below the flood level. A field investigation found that seepage currently occurs through pipe penetrations into the waste tank vault and waste pump pit located at CPP-604. Seepage occurs only at pipes entering the tank vault and pump pit through penetrations located at the roof of the concrete enclosure. As a result of rain, snowmelt, and runoff, the soil above the concrete enclosure becomes wet and seepage occurs. Seeping water is currently a minor nuisance, but the potential exists for additional infiltration into CPP-604 during a flood. This infiltration will be handled by sumps and jets designed to route water to storage tanks that are equipped with level monitors and overflow alarms. It is important to note that seepage does not penetrate the inner cell structure nor penetrate the pipes carrying waste. A waste pipe is encased in a larger pipe that is well sealed, which produces a secondary containment that keeps the seepage and waste stream separated.

Seepage into CPP-604 has been recently monitored by tracking the amount of water transferred to the evaporator feed tank. The total volume of water includes sump water, process water, and steam condensation. By subtracting the process water and steam condensation from the total, the amount of water transferred from the sumps had been calculated. However, the sump water had included leakage from steam valves. In November 2000, the steam system was turned off between transfers to prevent steam leakage. Since then, data on water seepage has been available because the sump receives only the water seepage through pipe penetrations.

The tank vault consists of four separate concrete enclosures. The penetrations into the enclosure containing tank VES-WM-100 leak, and the penetrations into the enclosure containing tanks VES-WL-101 and VES-WL-102 leak. The penetrations into the enclosure containing the pumps also leak. The pump pit and each tank enclosure have a sump and a steam jet. Water infiltrating the tank vault and pump pit travels directly to the sump, where the jets are used to transfer the sump water to VES-WL-132 and VES-WL-150, and then to VES-WL-133 (the evaporator feed tank). The seepage for each month from November 2000 through February 2001 is shown in Fig. 5.

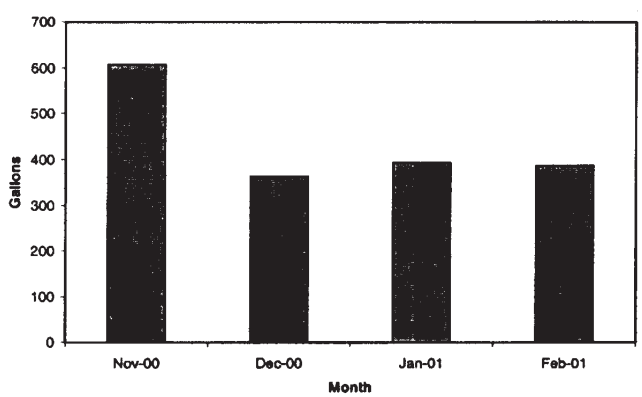

Fig. 5. Seepage through pipe penetrations in CPP-604.

The concrete enclosures are buried under an earth embankment that is at the same elevation as the first floor roof of CPP-604. The difference in elevation between the pipe penetrations and the top of the embankment is 32 ft. The difference in elevation between the ground level and the top of the embankment is 14 ft. Therefore, the difference in elevation between the pipe penetrations and the ground level is 18 ft.

The maximum seepage rate expected to occur during the hypothetical flood is estimated in the following manner. Note that the maximum seepage occurred in November and was equal to 20 gal/day or 0.833 gal/hr. Assume that the hydraulic head causing this seepage is equal to 18 ft, which is the difference in elevation between the pipe penetrations and the ground level. Since the embankment has been observed to be wet during the winter and spring seasons, it is plausible that part of the embankment is saturated. Furthermore, it is assumed that the embankment is totally saturated during a flood, and so in that case the hydraulic head is equal to 32 ft.

Since the hydraulic pressure in soil is proportional to the hydraulic head, the hydraulic pressure increases by a factor equal to

$$\frac{h_{max}}{h} = \frac{32}{18} = 1.8 .$$

Note that this is a conservative estimate of the increase in hydraulic pressure because it is assumed that the embankment is totally saturated with water. Since the seepage rate is proportional to the hydraulic pressure, the maximum seepage expected during a flood is

$$Q = 0.833 \frac{gal}{hr} \cdot 1.8 = 1.5 \frac{gal}{hr} .$$

The capacity of a steam jet depends on several factors that include steam pressure, pipe size, suction lift, and discharge head. The jets in the tank vault have a 1 in. inlet line, 1½ in. suction line, and 1½ in. discharge line. The jet in the pump pit has a ¾ in. inlet line, 1 in. suction line, and 1 in. discharge line. To calculate the pump capacity, consider the small jet in the pump pit, which is a Penberthy jet model GL-1 or equivalent. The upper bounds on the lift and head needed to transfer water from the sump to the evaporator feed tank are a suction lift equal to 5 feet and a discharge head equal to 20 feet. The minimum operating steam pressure needed to operate at this suction lift and discharge head is equal to 80 psig at a suction water temperature of 80°F. The steam pressure can be adjusted to increase the flow rate if needed. According to the Penberthy technical data (9), model GL-1 at these conditions has a discharge capacity equal to 7.9 gal/min. Since the small jet can transfer much more than the calculated maximum seepage, the flood protection devices have enough capacity to handle the maximum seepage that is expected to occur at CPP-604 during a flood.

Water Infiltration Through Doorways

In most cases, openings such as doors, stairs, and elevators on the first level lead to the inner cell structure. Since these openings are not watertight, it is necessary that the first level finished floor elevation be located above the flood water elevation in order to prevent infiltration of water through unsealed doorways and other openings. Generally, flood water will not enter the

building if the first level is at an elevation at least equal to 4917 ft, which is the flood water level (4916 ft) plus the wave height (1 ft). The data in Table 1 show that neither building meets this requirement. Since the first level finished floor elevation of CPP-1618 is 4916 ft, infiltration of water can be prevented by using a barrier to stop waves splashing onto the doorways. For the other buildings, additional flood protection devices are needed to prevent water infiltration.

Conclusions

An engineering analysis was used to calculate the various hydrodynamic and hydrostatic forces expected to result at the PEWE and LET&D buildings as a consequence of a 100 year flood coinciding with a failure of Mackay Dam. A structural study was used to describe the design of these buildings and their flood protection devices and how these will prevent washout of hazardous waste. Specific details are given below.

The following structural features of the buildings comprising the PEWE and LET&D facilities were examined: footing and foundation structures; openings such as doorways that enable water to easily infiltrate; and the occurrence of water seepage through pipe penetrations. The following results were obtained:

(1) The most important feature of the building construction is whether the first level finished floor elevation is higher than the flood water elevation. Only CPP-1618 meets this requirement, but with a contingency. For CPP-1618, the elevation of wind-generated water waves is higher than the first level floor elevation, and so a barrier is needed to stop waves splashing onto the doorways. For CPP-604 and CPP-605, the flood water elevation is higher than the first level floor elevation, and so additional flood protection devices are needed to prevent water infiltration.

(2) The construction of the buildings follows many of the standard practices used to assure a watertight foundation and to provide adequate drainage during a flood, though some minor water seepage currently occurs through pipe penetrations at CPP-604. Water entering the tank vault and pump pit drains to a sump and is transferred by steam jets to the evaporator feed tank. The jets have enough capacity to transfer the maximum seepage rate expected to occur during a flood.

(3) An important consideration in regard to flood protection is the ability of the retaining walls to withstand lateral earth pressure and water pressure. For the purposes of this study, the exterior retaining wall of CPP-1618 was chosen to represent the minimum wall strength of the three buildings evaluated, with regard to withstanding hydrostatic forces acting on a foundation wall. A structural analysis of the CPP-1618 retaining wall demonstrates that the building can withstand hydrostatic forces caused by a maximum credible flooding event.

References

1. K. N. Koslow and D. H. Van Haaften, *Flood Routing Analysis for a Failure of Mackay Dam*, EGG-EP-7184, June, 1986.
2. *Code of Federal Regulations*, 40 CFR Ch. 1, Sect. 270.14(b), Para. 11(iv) A, August 1, 2000.
3. R. B. Peck, W. E. Hanson, and T. H. Thornburn, *Foundation Engineering*, 2nd Edition, John Wiley & Sons, NY, 1974.
4. *Soil and Foundation Investigation, Proposed New Waste Calcining Facility*, Prepared for The Energy Research and Development Administration, Fluor Contract No. 453504, Dames and Moore, 1976.
5. E. F. Brater and H. W. King, *Handbook of Hydraulics*, 6th Edition, McGraw-Hill, NY, 1976.
6. R. J. Roark and W. C. Young, *Formulas for Stress and Strain*, 5th Edition, McGraw-Hill, NY, 1975.
7. *Building Code Requirements for Reinforced Concrete*, ACI 318-77, American Concrete Institute, 1978.
8. *CRSI Design Handbook*, 3rd Edition, Concrete Reinforcing Steel Institute, 1978.
9. *Penberthy Jet Pump Technical Data – Pumping Liquids*, Bulletin 1200, May, 1987.

RCRA PERMIT

FOR THE

IDAHO NATIONAL LABORATORY

Volume 14
INTEC Liquid Waste Management System

Appendix VIII

EDF-2470, Analysis of Hydrostatic Forces on INTEC Liquid Waste Tanks During a 100-Year Flood

Revision Date: October 29, 2008

Document ID: EDF-2470
Revision ID: 0
Effective Date: 09/12/02

Engineering Design File

Analysis of Hydrostatic Forces on INTEC Liquid Waste Tanks During a 100-Year Flood

Prepared for:
U.S. Department of Energy
Idaho Operations Office
Idaho Falls, Idaho

INEEL
Idaho National Engineering and Environmental Laboratory

Form 412.14
07/24/2001
Rev. 03

431.02
02/26/2002
Rev. 10

ENGINEERING DESIGN FILE

EDF- 2470
Rev. No. 0
Page 1 of 14

1. Title: Analysis of Hydrostatic Forces on INTEC Liquid Waste Tanks During a 100-Year Flood

2. Project File No.:

3. Index Codes:
Building/Type PEWE, LET&D SSC ID _____ Site Area INTEC

4. Summary:

The purpose of this engineering analysis is to provide data regarding the hydrostatic, hydrodynamic, and structural effects of a 100-year peak flood. This analysis is performed to ensure compliance with requirements stemming from application for a RCRA permit for mixed hazardous waste treatment in the Process Equipment Waste Evaporator (PEWE) and Liquid Effluent Treatment and Disposal (LET&D) facilities. RCRA regulations require an engineering analysis to determine the various hydrodynamic and hydrostatic forces expected to result at the site as a consequence of a 100-year flood, and structural or other engineering studies showing the design of operational units and flood protection devices at the facility and how these will prevent washout of hazardous waste.

Previous analyses suggest that the PEWE and LET&D facilities may be exposed to floodwater infiltration. The scope of the present analysis is to determine the hydrostatic and hydrodynamic forces of floodwater acting on the tanks and ancillary piping in the PEWE and LET&D systems, and to determine if these forces will damage the tanks and piping and allow hazardous waste to escape.

Data on tank capacity, dimensions, supports and anchorage was presented for each liquid waste tank in the PEWE and LET&D systems that may be exposed to floodwater forces. These forces include buoyancy and hydrostatic pressure. The buoyancy force acting on the tank may lead to flotation, and external fluid pressure may lead to collapse of the tank wall. Since the buoyancy force on piping is negligible in comparison to those forces on large, empty tanks, it is only necessary to ensure that the tanks are adequately anchored to prevent uplift. It is also necessary to show that the tanks have enough strength to resist collapse of the tank walls.

The results of the analysis showed that the tanks are able to withstand hydrostatic forces resulting from the postulated 100-year flood. These tanks are located in cells that are accessible by an access corridor and a series of doorways that are normally closed. Although water infiltration into the cells is possible by seepage through the edge of doorways, all tanks in the cells are adequately anchored to prevent uplift and have enough strength to resist collapse of the tank walls. Therefore the tanks and piping will not be damaged as a result of floodwater infiltration.

RCRA tanks that are located in concrete vaults are not exposed to water infiltration because the access hatches and pipe penetrations are watertight. The access hatches are always closed except when performing maintenance in the vault, and all pipe penetrations are grouted and sealed to be watertight. Water transfers from the sumps are continually monitored, and if access hatches or pipe penetrations are found to be leaking, sealant or grout is reapplied in order to maintain a watertight vault. Therefore washout of hazardous waste from these tanks will be prevented.

5. Review (R) and Approval (A) and Acceptance (Ac) Signatures:

	R/A	Name/Organization	Signature	Date
Author		P. E. Murray/5225	P. E. Murray	9/5/02
Checker	R	N. B. Smith/5225	N B Smith	9/5/02
Supervisor	A	S. R. Jensen/5225	S. R. Jensen	9/12/02
Project Engineer	Ac	P. A. Holmes/5225	P A Holmes	9/13/02
Requestor	Ac	N. C. Hutten/7310	N. C. Hutten	9/13/02
Doc. Control				

6. Distribution: (Name and Mail Stop) P. E. Murray, MS 5106

431.02
02/26/2002
Rev. 10

ENGINEERING DESIGN FILE

EDF- 2470
Rev. No. 0
Page 2 of 14

7.	Does document contain sensitive unclassified information? ☐ Yes ☒ No If Yes, what category:
8.	Can document be externally distributed? ☒ Yes ☐ No
9.	Uniform File Code: 0286 Disposition Authority: A17-30-c-1 Record Retention Period: Until Dismantlement or disposal of equipment, or when superceded or obsolete.
10.	For QA Records Classification Only: ☒ Lifetime ☐ Nonpermanent ☐ Permanent Item and activity to which the QA Record apply:
11.	NRC related? ☐ Yes ☒ No
12.	Registered Professional Engineer's Stamp PROFESSIONAL ENGINEER REGISTERED 9181 9-13-08 STATE OF IDAHO PATRICK A. HOLMES

Purpose

The purpose of this engineering analysis is to provide data needed in support of a Volume 14 RCRA permit application to comply with Idaho DEQ requirements for operation of the PEWE and LET&D systems. This analysis is performed to ensure compliance with RCRA regulations that require an engineering analysis to determine the various hydrodynamic and hydrostatic forces expected to result at the site as a consequence of a 100-year flood, and structural or other engineering studies showing the design of operational units and flood protection devices at the facility and how these will prevent washout. In the RCRA regulations, washout is defined as the movement of hazardous waste from the active portion of a facility as a result of flooding.

Scope

A structural evaluation of tanks in the PEWE and LET&D facilities is needed to demonstrate that the tanks and piping will not be damaged as a result of hydrodynamic and hydrostatic forces, which may occur as a result of water infiltration during a 100-year flood. The tanks are located in building CPP-601, CPP-604, CPP-605, CPP-641, CPP-649 and CPP-1618. A previous structural analysis [3] showed that these buildings are exposed to floodwater infiltration through doorways and other openings that are below the floodwater level associated with a 100-year flood coincident with a Mackay Dam Failure [1]. The issue is complicated because there are many different tanks and piping systems involved.

This task includes an evaluation of the PEWE and LET&D buildings to determine if the tanks and attached piping are exposed to flooding. If the tanks are exposed, a structural evaluation is performed to determine if the tanks are adequately anchored to prevent uplift due to buoyancy, and to determine if the tanks have enough strength to resist collapse of the tank walls due to external pressure.

This Engineering Design File (EDF) includes a description of all the affected structures, tank and piping systems, including details on the tank anchorage. The tanks included in this evaluation are those specified in Section D-2c of the RCRA Part B Permit Application, Volume 14. This EDF also includes calculations to determine the hydrostatic force of floodwater tending to cause flotation of the tanks and collapse the tank walls, and calculations to determine restraining forces at the tank supports.

Safety and Performance Categories

Safety categories are used for systems, structures, and components (SSC) to establish a graded approach to design and analysis based on the safety function performed by the SSC. Similarly, performance categories are used for an SSC exposed to natural phenomena hazards to establish a graded approach to design and analysis based on the importance of the SSC. However, the safety category and performance category are not used in this analysis since the design basis flood event and scope of the analysis are governed by RCRA regulations.

Background on 100-Year Flood

Koslow and Van Haaften [1] examined the consequences of a failure of Mackay Dam and performed a hydraulic analysis to determine the extent of the flood plain for several scenarios. Their analysis included a 100-year flood and simultaneous piping failure at Mackay Dam, which leads to a breach of the dam, overtopping of the INEEL diversion dam, and flooding of the INEEL site. This scenario results in a peak flow released from the dam that was calculated to be 57,740 ft^3/s. This flow between Mackay Dam and the INEEL is attenuated by storage, agricultural diversion, and channel infiltration. The calculated flow at the INEEL diversion dam is 28,500 ft^3/s. Since the diversion dam is unable to retain the high flow, most of the floodwater is assumed to flow onto the site.

The peak flow estimated by Koslow and Van Haaften [1] was used in a flow routing analysis to determine the extent of the flood plain at the INEEL site. A hydraulic analysis of open channel flow was used to compute the peak flow and water elevation at each cross-section of the Big Lost River channel. All vertical elevations are in reference to the National Geodetic Vertical Datum of 1929 (NGVD29). Of particular interest in this study are the PEWE and LET&D buildings located at the INTEC facility. The leading edge of the flood wave is estimated to arrive at INTEC approximately 17.1 hours after breach of the dam. The peak flow is attenuated to 24,870

ft^3/s, and the peak water velocity is estimated to be 2.2 ft/s. Since the area surrounding INTEC is very flat, floodwater will spread easily and so the flood plain is wide and shallow. The elevation of the streambed in the vicinity of INTEC is 4911 ft and the calculated water elevation is 4916 ft. Since the minimum ground elevation at the PEWE and LET&D buildings is approximately 4912 ft, the depth of floodwater may reach 4 ft at some locations.

Koslow and Van Haaften [1] also performed an analysis to examine the potential for overland flooding due to localized heavy rain and snowmelt. It was found that localized flooding due to a 25-year peak rainfall and simultaneous snowmelt lead to a peak flow estimated to be 32 ft^3/s. Although this runoff can be accommodated by the drainage basin at INTEC and flood control devices such as culverts, dikes, and ditches, floodwater may collect in low-elevation areas at the PEWE and LET&D buildings.

Description of Structures

The following buildings comprise the PEWE and LET&D facilities:

CPP-604	Process Equipment Waste Evaporator (PEWE) Building
CPP-605	Atmospheric Protection System Building (adjoining PEWE)
CPP-708	Main Stack for PEWE and LET&D Systems
CPP-1618	Liquid Effluent Treatment and Disposal (LET&D) Building
CPP-649	Off-gas Equipment and HEPA Filter Building
CPP-601	Process Building
CPP-641	Waste Hold-up Tank Building

The first level finished floor elevations, as shown on the as-built drawings, are listed in Table 1. Elevations are currently measured in reference to the National Geodetic Vertical Datum of 1929 (NGVD29). However, the buildings were constructed when the datum was not NGVD29. Recent elevation measurements in reference to NGVD29, which are approximately 1 ft. less than those shown on the as-built drawings, are listed in Table 1.

Table 1. Building elevation in feet above sea level.

Building	First level floor elevation (shown on as-built drawing)	First level floor elevation - (in reference to NGVD29)	INEEL Drawing Number
CPP-604	4913.0	4912.0	103223
CPP-605	4913.0	4912.0	128821
CPP-1618	4917.0	4916.1	347771
CPP-649	4912.8	4911.9	128837; 128840
CPP-601	4917.0	4916.0	103062
CPP-641	4916.0	4915.0	111809

The floodwater elevation for the postulated 100-year flood coincident with a Mackay Dam failure is 4916 ft in reference to NGVD29 (Koslow and Van Haaften, [1]). The wave height of shallow water waves generated by a 60 mph wind with a water depth equal to 4 ft is approximately 2 ft from crest to trough (Fig. 10-16 in Brater and King [2]). In many cases, exterior openings such as doorways and loading docks lead to the active portion of the building containing waste, and floodwater may enter the building if the first level floor elevation is less than 4917 ft (still water level + ½ wave height). Therefore, all the buildings listed in Table 1 are exposed to potential floodwater infiltration.

The buildings are constructed of reinforced concrete. Previous analyses of floodwater forces on CPP-604 [3], CPP-1618 [3], and CPP-659 [4] showed that the foundation walls are strong enough to withstand hydrostatic and hydrodynamic forces. Therefore, the main concern is floodwater infiltration and the resulting hydrostatic force on tanks and ancillary piping, and whether the tanks and pipes will be damaged and allow hazardous waste to escape. It is only necessary to consider the exposed structures and show that the tanks and piping can withstand the hydrostatic pressure. In particular, it is necessary to check that external pressure on tank and pipes does not collapse the walls, and the buoyancy force does not cause the anchor bolts and pipe supports to fail.

Assumptions

1. In case the floodwater elevation is higher than the elevation of doorways or other openings, it is assumed that the building is exposed to floodwater infiltration [(a)].
2. The only pathway for water infiltration into a tank vault is at access hatches and pipe penetrations, which are assumed to be sealed and watertight [(b)].
3. The concrete foundation of the building is assumed to withstand hydrostatic and hydrodynamic forces, which is based on a previous analysis of floodwater forces on the PEWE and LET&D buildings [3].
4. Buoyancy force and external pressure on piping and pipe supports are negligible in comparison to those forces on large, empty tanks.
5. The liquid waste tanks are assumed to be empty and completely immersed in water since this leads to the maximum buoyancy force and pressure on the tank wall.
6. The tanks and piping are completely sealed and do not leak since they are regularly inspected.
7. Reduction of tank wall thickness due to corrosion is neglected since the stainless steel used to fabricate the tanks is very resistant to corrosion by nitric acid.
8. The anchor bolt (or rod) is assumed to be stainless steel type 304, and the strength of the bolt (or rod) is assumed to govern the capacity of an anchor [(c)].
9. In the event of a flood, it is assumed that the evaporation/separation/condensation operations in CPP-604 will be shut down and no steam or high temperature condensate will be present in the tanks.

[(a)] Sumps and steam jets in the cells and vaults can remove water infiltrating the building. Cells are accessible by doorways that are not watertight but are normally closed. Plugging the edges of doorways can significantly reduce the infiltration rate. In this analysis, no calculations are made of the infiltration rate through doorways or other openings.

[(b)] The access hatches at the CPP-604 storage tank vault (Drawings 103553), the CPP-604 feed tank vault (Drawing 162319), the CPP-641 vault (Drawing 111809) and the CPP-601 vault (Drawing 103064) are removable, tapered concrete plugs fitting into the tank vault concrete roof slab and designed to contain a watertight seal on all sides.

[(c)] High-strength stainless steel is commonly used for bolting material, and so the strength of the bolt is often larger than the strength assumed in the analysis.

Discussion

The tanks contained in storage vaults are not exposed to flooding since the access hatches and pipe penetrations are watertight. These tanks include the CPP-604 waste storage tanks (WM-100, WM-101, WM-102, WL-101, WL-102 and WL-150), the CPP-604 feed tanks (WL-132 and WL-133), the CPP-641 storage tanks (WL-103, WL-104 and WL-105), and the CPP-601 storage tanks (WH-100, WH-101, WG-100 and WG-101). The hatches are always closed except when performing maintenance in the vault, and all pipe penetrations are grouted and sealed to be watertight. Any water infiltration due to seepage at pipe penetrations and hatches is minor and readily removed by sumps and steam jets, as shown in a previous analysis of water seepage into CPP-604 [3]. Furthermore, it is necessary that the valve (PLV-YDB-28) on the vent line protruding from the CPP-641 tank vault (Drawing 111807) be closed during a flood.

The small tanks in the PWL collection system (WL-135, WL-136, WL-137, WL-138, WL-139, WL-142, and WL-144) have a capacity not exceeding 25 gallons and are adequately supported by the attached piping. Tank NCR-171 is located at CPP-659, which is not exposed to water infiltration as shown previously [4]. All the tanks in CPP-1618, except the bottoms tank (WLL-195), are above the floodwater elevation.

The tanks contained in the PEWE cells and the LET&D bottoms tank pit are exposed to flooding since they are accessible by doorways and other openings that are not watertight. Although doorways are normally closed, water infiltration into the cells is possible by seepage through the edge of doorways. Similarly, water infiltration into the bottoms tank pit is possible by seepage through the edge of the cover plate. Therefore it is necessary to evaluate these tanks in order to ensure that the anchorage is strong enough to prevent uplift and the tank wall is strong enough to resist collapse. The data used in the structural evaluation of the tanks are given in Tables 2-6.

List of Tanks

The capacity of each tank and the building in which it is located are given in Table 2 for all the tanks in the PEWE and LET&D systems listed in the RCRA Part B Permit Application, Volume 14, Section D-2c.

Table 2. Capacity of waste storage tanks.

Tank Identifier	Building	Capacity (gal.)
WM-100	CPP-604	18,400
WM-101	CPP-604	18,400
WM-102	CPP-604	18,400
WL-101	CPP-604	18,400
WL-102	CPP-604	18,400
WL-133	CPP-604	19,000
WL-132	CPP-604	4,700
WL-106	CPP-604	5,000
WL-107	CPP-604	5,000
WL-163	CPP-604	5,000
WL-103	CPP-641	5,000
WL-104	CPP-641	5,000
WL-105	CPP-641	5,000
WH-100	CPP-601	4,500
WH-101	CPP-601	4,500
WG-100	CPP-601	4,500
WG-101	CPP-601	4,500
WL-111	CPP-604	1,500
WL-129	CPP-604	1,000
WL-161	CPP-604	1,000
WL-300	CPP-604	250
WL-307	CPP-604	250
WL-301	CPP-604	180
WL-308	CPP-604	180
WL-131	CPP-604	66
WL-134	CPP-604	500
WL-108	CPP-604	70
WL-109	CPP-604	270
WL-135	CPP-649	10
WL-136	CPP-649	10
WL-137	CPP-649	25
WL-138	CPP-605	25
WL-139	CPP-605	10
WL-142	CPP-604	10
WL-144	CPP-604	25
WL-150	CPP-604	50
WLK-197	CPP-1618	270
WLL-170	CPP-1618	460
WLK-171	CPP-1618	460
WLL-195	CPP-1618	270
NCR-171	CPP-659	22,500

Depth of Tanks

The hydrostatic force will affect the large, empty tanks at maximum depth since the maximum hydrostatic pressure occurs at the lowest elevation. The depth of the tank below the floodwater elevation is given in Table 3 for the tanks in the PEWE and LET&D systems that are exposed to floodwater infiltration. The depth is measured to the floor of the PEWE evaporator and condenser cells or the floor of the LET&D bottoms tank pit.

Table 3.Depth of waste storage tanks.

Tank Identifier	Depth of tank below floodwater elevation (ft)	INEEL Drawing Number
WL-106	27	056692
WL-107	27	056692
WL-163	27	056692
WL-111	27	056692
WL-129	27	056692
WL-161	27	056692
WL-300	27	056692
WL-307	27	056692
WL-301	27	056692
WL-308	27	056692
WL-131	27	056692
WL-134	27	056692
WL-108	27	056692
WL-109	27	056692
WLL-195	5.7	347796

Weight of Tanks

The hydrostatic force of floodwater in the building will affect the large, empty tanks immersed in water since the buoyancy force is proportional to the volume of displaced water. The weight of the empty tank and the weight of contained water are given in Table 4 for the tanks in the PEWE and LET&D systems that are exposed to floodwater infiltration. The weight of contained water is calculated using the capacity given in Table 2.

Table 4. Weight of waste storage tanks.

Tank Identifier	Weight of empty tank (lb)	Weight of contained water (lb)	INEEL Drawing Number
WL-106	8300	41,700	098921
WL-107	8300	41,700	098921
WL-163	8400 (1)	41,700	056638
WL-111	4600 (1)	12,500	097880
WL-129	5320 (2)	8340	055920
WL-161	5320	8340	097722
WL-300	1150 (1)	2090	057231
WL-307	1150 (1)	2090	057231
WL-301	830 (1)	1500	055895
WL-308	830 (1)	1500	055895
WL-131	370 (1)	550	155074
WL-134	1100	4170	83-1529 (3)
WL-108	480 (1)	580	E-51-687-B (4)
WL-109	600 (1)	2250	098920
WLL-195	1500	2200	097672

(1) Approximate weight based on dimensions of shell and heads given in drawings; weight of piping and flanges is neglected.
(2) Weight of WL-129 assumed to be the same as weight of WL-161, since both tanks are similar flash columns.
(3) Vendor drawing from Mabe Industries.
(4) Vendor drawing from W. K. Mitchell & Co.

Diameter and Wall Thickness of Tanks

The hydrostatic force will affect the large, empty tanks at low elevation since the hoop stress in the tank wall is proportional to the tank diameter and the difference in external and internal pressure, and inversely proportional to the wall thickness. The tank diameter and the wall thickness are given in Table 5 for the tanks in the PEWE and LET&D systems that are exposed to floodwater infiltration.

Table 5.Diameter and wall thickness of waste storage tanks.

Tank Identifier	Tank Diameter (ft)	Wall Thickness (in.)	INEEL Drawing Number
WL-106	8	0.5	098921
WL-107	8	0.5	098921
WL-163	8	0.5	056638
WL-111	4.7 (1)	0.375 (2)	097880
WL-129	3	0.375	055920
WL-161	3	0.375	097722
WL-300	2 (3)	0.375	057231
WL-307	2 (3)	0.375	057231
WL-301	2.2	0.375	055895
WL-308	2.2	0.375	055895
WL-131	2	0.375	155074
WL-134	3.5	0.1875	83-1529 (4)
WL-108	2.5	0.375	E-51-687-B (5)
WL-109	3	0.25	098920
WLL-195	3	0.5	097673

(1) Equivalent diameter of rectangular tank cross-section.
(2) Wall thickness obtained from D. J. Henrikson, "Evaluation of PEW Tank VES-WL-111," CSS-94-003 (March 1994).
(3) Tank diameter is not given on the drawings, but is estimated to be 24 inches.
(4) Vendor drawing from Mabe Industries.
(5) Vendor drawing from W. K. Mitchell & Co.

Anchoring of Tanks

The tanks that are exposed to potential floodwater infiltration are anchored to prevent flotation. Descriptions of the tank support and anchorage are given in Table 6 for the tanks in the PEWE and LET&D systems that are exposed to floodwater infiltration. The anchoring details are given as the total number and size of bolts. It was necessary to determine the exact anchoring details for each tank in which these details are not given on the drawings but are present nonetheless.

Table 6. Anchoring of waste storage tanks.

Tank Identifier	Tank orientation and support	Anchoring details	INEEL Drawing Number
WL-106	Vertical, steel legs	4 – ¾ in. bolts [1]	098921
WL-107	Vertical, steel legs	4 – ¾ in. bolts [1]	098921
WL-163	Vertical, steel legs	4 – ¾ in. bolts [1]	056638
WL-111	Horizontal, steel legs	4 – 1 in. holes [2]	097880
WL-129	Vertical, steel brackets	2 – ¾ in. bolts	155072
WL-161	Vertical, steel brackets	4 – ¾ in. bolts	056079
WL-300	Vertical, steel brackets	2 – ¾ in. bolts	056079
WL-307	Vertical, steel brackets	2 – ¾ in. bolts	155072
WL-301	Vertical, steel brackets	4 – ¾ in. bolts	056079
WL-308	Vertical, steel brackets	4 – ¾ in. bolts	155072
WL-131	Horizontal, steel legs	4 – ½ in. bolts	155074
WL-134	Vertical, steel legs	4 – 7/8 in. bolts	83-1529 [3]
WL-108	Vertical, steel brackets	2 – 7/8 in. holes [2]	E-51-687-B [4]
WL-109	Vertical, steel brackets	2 – 7/8 in. holes [2]	098920
WLL-195	Horizontal, steel saddles	4 – 7/8 in. bolts	347796

[1] Anchoring details are not shown on the drawings, but photographs of the condensate cell show that the steel angles are welded to steel plates bolted to the concrete floor (see Attachment A). Drawing No. 158768 shows a typical anchorage, but the size of the bolts is not shown. Four ¾ in. diameter bolts are assumed, which is based on the weld size specified on Drawing No. 158768.

[2] Anchoring details are not shown on the drawings, which show instead the size of holes in each support. It is standard engineering practice to use anchor bolts in an oversized hole. It is assumed that a ¾ in. bolt is used in a 1 in. hole, and a 5/8 in. bolt is used in a 7/8 in. hole.

[3] Vendor drawing from Mabe Industries.

[4] Vendor drawing from W. K. Mitchell & Co.

Hydrostatic Forces on Tanks

Assuming the tanks are empty and immersed in water, the net uplift force on the tanks due to buoyancy is

$$P = W_{water} - W_{tank}$$

W_{water} Weight of displaced water from Table 4

W_{tank} Weight of empty tank from Table 4

The anchor bolts must have enough strength to withstand the uplift force tending to cause flotation of the tanks. The calculations of uplift force are given in Table 7 for the tanks in the PEWE and LET&D systems.

The tank walls must also have enough strength to withstand the hydrostatic forces tending to cause collapse of the tank walls. Assuming the tanks are empty and immersed in water, external pressure acts on the tank walls.

The hydrostatic pressure corresponding to the hydraulic head is

$$p = \gamma_{water} \times H = 62.4\,\text{lb/ft}^3 \times H$$

H Hydraulic head from Table 3

The calculations of hydrostatic pressure are given in Table 7 for the tanks in the PEWE and LET&D systems.

The tanks listed in Table 7 are fabricated according to ASME Section VIII Code with design pressures that include either full vacuum or 0.5 psia (15 in. H_20) in addition to internal pressure. Note that the hydrostatic pressure given in Table 7 is less than the external pressure resulting from either full vacuum or 0.5 psia.

The restraining force of anchor bolts is calculated using the resistance factor and nominal strength formula given in IBC-2000 Sections 1913.4 and 1913.5 [5]. The minimum yield strength of stainless steel bolts is 30,000 psi (ASTM 193 Grade B8 Class 1, type 304).

The strength of the various sizes and types of bolts used to anchor the tanks is

½ in. bolt: $\phi \times f_y \times A = 0.90 \times 30{,}000\ \text{psi} \times 0.142\ \text{in.}^2 = 3{,}830\ \text{lb}$

5/8 in. bolt: $\phi \times f_y \times A = 0.90 \times 30{,}000\ \text{psi} \times 0.226\ \text{in.}^2 = 6{,}100\ \text{lb}$

¾ in. bolt: $\phi \times f_y \times A = 0.90 \times 30{,}000\ \text{psi} \times 0.334\ \text{in.}^2 = 9{,}020\ \text{lb}$

7/8 in. bolt: $\phi \times f_y \times A = 0.90 \times 30{,}000\ \text{psi} \times 0.462\ \text{in.}^2 = 12{,}470\ \text{lb}$

The restraining force is equal to bolt strength × number of bolts. In case the restraining force exceeds the uplift force, the bolt can withstand the hydrostatic forces tending to cause flotation of the tanks.

The calculations of the restraining force at tank supports are given in Table 8 for the tanks in the PEWE and LET&D systems. These results demonstrate that all tanks contained in cells are adequately restrained from uplift due to buoyancy.

Table 7.Hydrostatic forces on waste storage tanks.

Tank Identifier	Uplift force on tank support (lb)	Hydrostatic pressure on tank (psi)
WL-106	33,400	11.7
WL-107	33,400	11.7
WL-163	33,300	11.7
WL-111	7900	11.7
WL-129	3020	11.7
WL-161	3020	11.7
WL-300	940	11.7
WL-307	940	11.7
WL-301	670	11.7
WL-308	670	11.7
WL-131	180	11.7
WL-134	3070	11.7
WL-108	100	11.7
WL-109	1650	11.7
WLL-195	700	2.5

Table 8. Restraining force at tank supports.

Tank Identifier	Uplift force on tank support (lb)	Restraining force at tank support (lb)	Adequate support (Yes/No)
WL-106	33,400	36,100	Yes
WL-107	33,400	36,100	Yes
WL-163	33,300	36,100	Yes
WL-111	7900	36,100	Yes
WL-129	3020	18,000	Yes
WL-161	3020	36,100	Yes
WL-300	940	18,000	Yes
WL-307	940	18,000	Yes
WL-301	670	36,100	Yes
WL-308	670	36,100	Yes
WL-131	180	15,300	Yes
WL-134	3070	49,900	Yes
WL-108	100	12,200	Yes
WL-109	1650	12,200	Yes
WLL-195	700	49,900	Yes

Conclusions

A structural evaluation was used to identify the capacity, dimensions, supports and anchorage of the liquid waste tanks in the PEWE and LET&D systems, and to show that the tanks are able to withstand hydrostatic forces resulting from the postulated 100-year flood. The tanks that are exposed to water infiltration are located in the PEWE evaporator and condenser cells and the LET&D bottoms tank pit. The analysis shows that the anchor bolts are able to withstand hydrostatic forces tending to cause flotation of the tanks. Moreover, the analysis shows that the tanks have enough strength to withstand hydrostatic forces that act on the tank walls. The structural capacity of the tanks, anchors, and foundation walls ensures that the connecting piping is not overstressed. Therefore the tanks and piping will not be damaged as a result of floodwater infiltration.

RCRA tanks that are located in concrete vaults are not exposed to water infiltration because the access hatches and pipe penetrations are watertight. The hatches are always closed except when performing maintenance in the vault, and all pipe penetrations are grouted and sealed to be watertight. Water transfers from the sumps are continually monitored, and if access hatches or pipe penetrations are found to be leaking, sealant or grout is reapplied in order to maintain a watertight vault. Therefore washout of hazardous waste from these tanks will be prevented.

Recommendations

The vent line protruding from the CPP-641 tank vault is the only pathway for water infiltration into the vaults. Therefore, it is necessary that the valve (PLV-YDB-28) on the vent line be closed during a flood.

References

1. K. N. Koslow and D. H. Van Haaften, *Flood Routing Analysis for a Failure of Mackay Dam*, EGG-EP-7184, June, 1986.
2. E. F. Brater and H. W. King, *Handbook of Hydraulics*, 6th Edition, McGraw-Hill, NY, 1976.
3. P. E. Murray, *Hydrodynamic and Structural Analyses of Flood Hazards at the PEWE and LET&D Buildings During a Peak Flow in the Big Lost River*, EDF-2613, May, 2001.
4. P. E. Murray, *Hydrodynamic and Structural Analyses of Flood Hazards at CPP-659 During a Peak Flow in the Big Lost River*, EDF-1747, January, 2001.
5. IBC-2000, *International Building Code*, International Code Council, 2000.

Attachments

A. Photographs of Condensate Collection Tanks.

Attachment A – Photographs of Condensate Collection Tanks

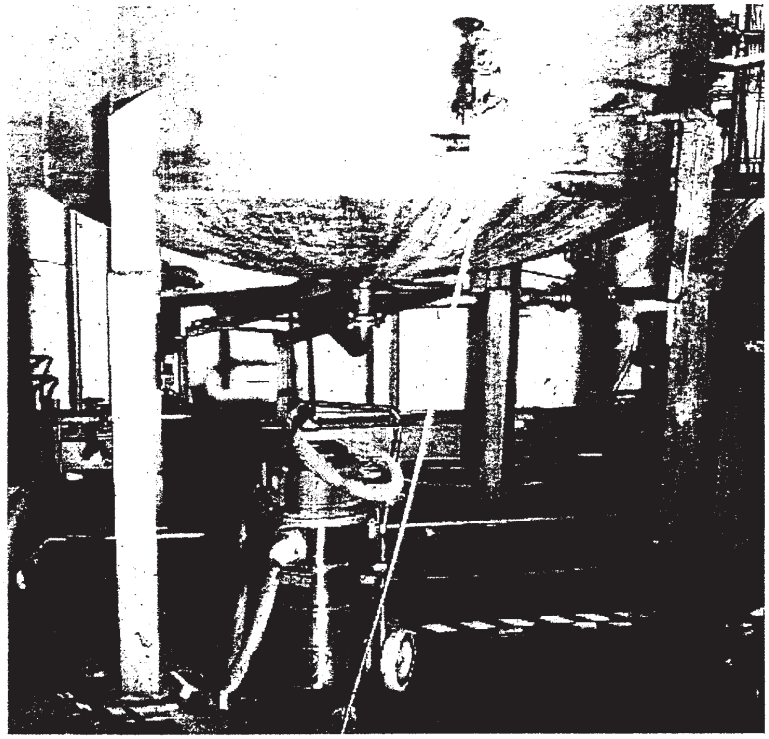

Tank WL-106; supports for tanks WL-107 and WL-163 are similar.

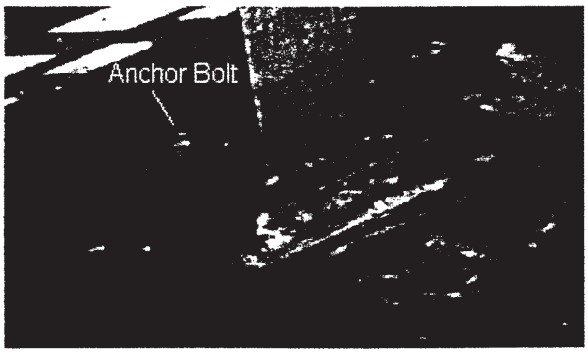

Tank anchorage for WL-106; WL-107 is similar.

Tank anchorage for WL-163; four bolts are used.

RCRA PERMIT

FOR THE

IDAHO NATIONAL LABORATORY

Volume 14
INTEC Liquid Waste Management System

Appendix IX

ETS Mercury Concentration Justification

Revision Date: April 12, 2011

JUSTIFICATION FOR A MERCURY FEED CONCENTRATION LIMIT OF 3000 PPM FOR ETS

A risk-based mercury (Hg) feed limit for ETS can be determined by evaluating the sampling results from NWCF ETS Offgas Emissions Inventory issued in February 2002 (INEEL/EXT-02-00198)[1]. These results showed that an ETS Hg feed concentration of 149 ppm resulted in an offgas Hg concentration of 39 ug/dscm (dry standard cubic meter) (Figure S-3 in reference 1) and an offgas Hg emission rate of 1.3E-5 g/s. The hazard quotient (HQ) calculated for this Hg emission rate at the off-site location of maximum impact was 7.56E-7 (pg. 80, reference 1). The mercury hazard accounted for 12% of the total ETS hazard index (HI) of 6.2E-6 from all contaminant emissions. The total HI for all contaminants was a very small fraction (2.48E-5) of the target HI of 0.25 typically used for RCRA combustion source risk assessments.

Mercury offgas emissions from the ETS will be a function of ETS process conditions, primarily temperature, redox chemistry, and waste feed rate. If these process conditions remain essentially the same, as they have since the time the emissions sampling was conducted, then Hg fractionations to offgas should remain relatively constant. Since process condition for the ETS have remained relatively unchanged, the Hg concentration in the offgas should be directly proportional to the Hg feed concentration. This also means that for a given waste feed rate, the Hg offgas emission rate will be directly proportional to the Hg feed concentration. For example, if the Hg feed concentration was increased from 149 ppm to 1490 ppm (factor of ten increase), then ETS emissions should increase from 1.3E-5 g/s to about 1.3E-4 g/s.

The human health and environmental impacts from ETS pollutant emissions were calculated using the models and equations in EPA's Human Health Risk Assessment Protocol for Hazardous Waste Combustion Facilities.[2] These models assume that downwind concentration and deposition rate are directly proportional to the pollutant's emission rate. Pollutant impacts (risk, hazard) are then calculated by multiplying the receptor concentration by a number of exposure scenario factors. This means that downwind impacts for a specific pollutant from a particular source are directly proportional to the emission rate of that pollutant (i.e., a factor of 10 increase in emissions will increase the calculated risk or hazard by a factor of 10).

Given these conditions, the new offgas emissions rate and resulting HQ for a proposed ETS Hg feed concentration limit of 3000 ppm can be estimated by multiplying the Hg emissions rate and HQ determined in the ETS offgas emissions inventory[1] by the ratio of the proposed Hg feed concentration limit (3000 ppm) to the feed concentration that existed during the offgas sampling (149 ppm):

New ETS emission rate = 1.3E-5 g/s x (3000 ppm/149 ppm) = 2.6E-04 g/s

and

New ETS HQ = 7.56E-7 x 3000 ppm/149 ppm = 1.5E-05

This is a factor 20.1 increase (3000 ppm/149 ppm) in the Hg emission rate and HQ but is still a very small fraction of the RCRA HI target criteria of 0.25. It should be noted that ETS Hg feed concentrations may often be less than the 3000 ppm limit, and, when this occurs, Hg emissions and hazard will decrease proportionately.

TOTAL MERCURY EMISSIONS AND HAZARD FROM ILWMS OPERATIONS

Table 1 lists the hazard quotients and total hazard index for all emitted pollutants from all emission sources within the INTEC Liquid Waste Management System (includes LET&D, PEWE, and ETS) as calculated in the ILWMS risk assessment[3]. The proposed 3000 ppm Hg ETS feed concentration does not significantly increase the total ETS hazard nor does it increase the total hazard ILWMS source emissions.

Table 1. Hazard quotients (HQs) and hazard index calculated for all ILWMS sources.

	Non-cancer Hazard Quotients/ Hazard Index				
Process	**Anions**	**Metals**	**SVOCs**	**VOCs**	**Total**
LET&D	6.6E-03	1.6E-03	8.2E-05	5.8E-07	8.3E-03
PEWE	2.0E-03	4.8E-04	2.5E-05	1.7E-07	2.5E-03
ETS	4.1E-07	7.6E-07[a] 1.5E-05[b]	3.9E-06	1.2E-08	6.5E-06
Total	**8.6E-03**	**2.1E-03**	**1.1E-04**	**7.7E-07**	**0.011**
				Target	**0.25**

a. Based on 149 ppm Hg feed concentration for ETS from reference 3.
b. New HQ estimated for 3000 ppm Hg feed limit for ETS.

COMPARISON TO NWCF MERCURY EMISSIONS

The Hg emissions measured from the New Waste Calcining Facility (NWCF) during the Phase IV offgas emission testing ranged from 1.1E-03 g/s (test 4) to 3.2E-03 g/s (tests 1-3)[4]. The estimated Hg emission rate from ETS at the proposed 3000 ppm Hg feed concentration limit is 2.6E-04 g/s or about 8 to 23% of the NWCF measured Hg emissions.

COMPARISON TO IDAHO DEQ TOXIC AIR POLLUTANT EMISSION LIMITS

The estimated ETS Hg emission rate at the 3000 ppm feed concentration (2.6E-04 g/s or 2.1E-3 lb/hr) is about 30% of the Idaho DEQ Toxic Air Pollutant Emission Limit (EL) for inorganic Hg emissions (7E-3 lb/hr) specified in Section 585 of IDAPA 58.01.01.

REFERENCES

1. Boardman, R.D., Lamb, K.M., Matejka, L.A., Nenni, J.A., NWCF Evaporator Tank System 2001 Offgas Emissions Inventory, INEEL/EXT-02-00198, February 2002.

2. Human Health Risk Assessment Protocol for Hazardous Waste Combustion Facilities, EPA530-D-98-001A, July 1998.

3. Human and Ecological Risk Assessment of Air Emissions from the INTEC Liquid Waste Management System, ICP/EXT-04-00399, May 2004.

RCRA PERMIT

FOR THE

IDAHO NATIONAL LABORATORY

Volume 14
INTEC Liquid Waste Management System

Appendix X

Pilot Plant Report for Treating Sodium Bearing Waste Surrogates Carbonate Flowsheet

(Document Number RT-ESTD-PMR-01)

Revision Date: April 12, 2011

Idaho Cleanup Project

Integrated Waste Treatment Unit

PROJECT NUMBER 28276

DOCUMENT NUMBER RT-ESTD-PMR-001

Revision 0

Pilot Plant Report for Treating Sodium-Bearing Waste Surrogates Carbonate Flowsheet

October 2006

Prepared for

CH2M-WG Idaho, LLC

by

THOR Treatment Technologies, LLC,

and

Washington Group International
7800 E. Union Ave., Suite 100
Denver, Colorado 80237

SBW PILOT PLANT TEST REPORT REVISION PAGE

Project Name:	Integrated Waste Treatment Unit	Document #:	RT-ESTD-PMR-001
Client:	CH2M-WG Idaho LLC	Latest Revision:	0
		Issue Date	10/12/06

Revision Signatures

Prepared by for [signature] 10/12/06 Arlin Olson Date	Approved by QA [signature] 10-12-06 Greg DiGregorio Date
Reviewed/Checked by [signature] 10-12-06 Brad Mason Date	Approved by Engineering Manager [signature] 10/12/06 William D. Kerley Date
Concurrence [signature] for 10/12/06 Alan Carvo by telecon Date	Approved by Testing Manager [signature] for KERyan 10/12/06 Kevin Ryan Date

Quality Level NA

Status	Rev. No.	Date	Prepared By	Pages	Description of Changes
Final	0	10/12/06	Arlin Olson	334	Original Issue

Quality affecting items addressed in this document include: NA

ABSTRACT

Approximately one million gallons of hazardous, radioactive, sodium-bearing liquid waste is currently stored in stainless-steel tanks at the Idaho Nuclear Technology and Engineering Center at the Idaho National Laboratory Site. Treatment and disposal of this waste is a top priority of the Department of Energy Idaho Operations Office. The Department of Energy has selected the THOR® steam reforming process as the means to treat and prepare this tank waste for disposal as remote-handled, transuranic waste at the Waste Isolation Pilot Plant in New Mexico.

Pilot plant testing of the THOR® steam reforming process was conducted at the Hazen Research facility in Golden, Colorado in a two-phase demonstration program. Phase 1 SBW carbonate testing (CP1) was performed during the period November 2005 through February 2006 and Phase 2 SBW carbonate testing (CP2) was during the period May 2006 through June 2006. During the CP1 and CP2 test program, approximately 7,900 gallons (~89,000 pounds) of simulated sodium-bearing waste were successfully processed into a dry, granular, solid product using a dual fluidized bed steam reforming system. A total of approximately 16,200 pounds of solid product was produced.

The simulated waste stream used in the testing program consisted of the principal chemical constituents found in the INL waste tanks including nitric acid, soluble metal nitrate salts, insoluble minerals, heavy metals, and radioactive surrogates. An organic constituent was also added to the waste stream in order to determine the organic destruction removal efficiency of the system.

Primary objectives of the testing program were to demonstrate that integrated operation of the treatment process confirms key design and operating parameters for the full-scale treatment process, and provides process off-gas data to support environmental permitting of the full-scale process. These test objectives were successfully accomplished.

EXECUTIVE SUMMARY

The THOR® fluidized bed steam reforming technology was selected by the Idaho Cleanup Project (ICP) to treat the approximately one million gallons of sodium-bearing waste (SBW) in storage at the Idaho Nuclear Technology and Engineering Center (INTEC) at the Idaho National Laboratory (INL) Site. The Integrated Waste Treatment Unit (IWTU) will house the processing system that will convert the SBW into a granular waste product suitable for disposal at the Waste Isolation Pilot Plant (WIPP), following regulatory approval.

Numerous bench-scale tests have been conducted over the last several years that have shown the THOR® steam reforming technology capable of processing non-radioactive liquid waste simulants into a solid waste form. Tests conducted at the STAR Center in Idaho Falls, Idaho, demonstrated the ability of the process to treat an SBW simulant. The shortcomings of these tests were two-fold. First, they did not combine all the major unit operations and equipment necessary for a complete processing system into a single integrated unit. Second, the small size of the fluidized beds used in the bench scale tests could not fully represent the operation of production scale units.

To demonstrate the integrated process and gather necessary technical data for IWTU design and operation, an engineering-scale pilot plant was needed. This was realized with the Engineering Scale Test Demonstration (ESTD) unit that was built and operated at the Hazen Research facility in Golden, Colorado. The ESTD is a one-tenth-scale version of the IWTU SBW treatment system that includes all unit operations present in the full-scale unit, excluding the product packaging equipment.

The ESTD was designed, constructed, and functionally tested between June and November 2005 using rigorous engineering and quality control practices, as described in the THOR® Treatment Technologies, LLC (TTT) Quality Assurance Plan, Project Quality Procedures, and Engineering Procedures. Rigor remained during testing operations with a robust system of operating documents and conduct of operations practices. A core team of technical professionals, the Joint Test Group (JTG), oversaw all testing activities and results. The JTG reviewed all test iterations and specified the details of each day's testing work, within the framework of the formal test plan and other controlling documents.

Scoping tests were conducted in December 2005 and January 2006. The scoping tests familiarized the operating and technical teams with process operations and established essential operating parameters for the follow-on production tests. Taken together, the production and scoping tests achieved a large number of specific test objectives, described in detail in Table 10-1. Key among these objectives was to:

- Establish target steady-state system operating conditions
- Demonstrate integrated operation of the entire SBW treatment process, including serial operation of the DMR and CRR
- Demonstrate and confirm long-term system operability with respect to process chemistry, material flows, mass and energy balance (MEB), equipment durability, and particle size control
- Establish key operating parameters for the full-scale IWTU process
- Obtain operational data to confirm IWTU design parameters
- Gather off-gas emissions data for purposes of environmental permitting

- Confirm solid product data for requesting Waste Isolation Pilot Plant (WIPP) transportation and disposal.

During January and February of 2006, a series of production run tests was completed. These were the Carbonate Phase 1 (CP1) tests. The CP1 test series consisted of a matrix of variable operating conditions that included feed composition, feed rate, DMR temperature, and CRR temperature. During the CP1 production tests, 5,450 gallons (~61,000 pounds) of SBW simulant were processed into ~11,500 pounds of granular solid product during 334 hours of "feed-on" operation. The key results from the CP1 tests are as follows:

- The safe, long-term operation of the process and key components was demonstrated.
- Emissions of potential pollutants were shown to be within regulatory limits.
- The solid products generated from the process were shown to meet the chemical and physical requirements for disposal at WIPP.
- Particle size control of the DMR bed was achieved for feed liquids that included undissolved solids (UDS).
- Technical data and operational parameters critical to the design of the full-scale IWTU process system were developed or confirmed and provided to the IWTU design team.

Following the completion of the CP1 tests, IWTU project management elected to conduct an additional series of tests to address some technical issues that remained or were identified during the scoping and CP1 tests. These issues were:

- Control of DMR bed particle size in the absence of UDS in the SBW simulant
- Further definition of the mercury removal performance of the granular activated carbon (GAC) unit
- Improved temperature control and oxidation efficiency in the CRR
- Evaluation of an improved DMR feed nozzle design
- Continued metallurgical evaluation of the sintered-metal filters used in the process.

In May and June 2006, eleven additional days of testing were accomplished at process conditions similar to those used during CP1. This test series, the Carbonate Phase 2 (CP2) tests, addressed the issues listed above and provided necessary additional information to the IWTU technical team. The CP2 tests processed an additional 2,450 gallons (~28,000 pounds) of SBW simulant into ~4,700 pounds of granular solid product during 164 hours of "feed-on" time. Process parameters and equipment operability considerations from the CP1 tests were reconfirmed, adequate particle size control in the DMR without UDS in the simulant feed or the addition of seed particles was demonstrated, and excellent control of CRR temperatures in an automatic control mode along with excellent oxidation efficiency was demonstrated. Gaseous emissions from the CP2 tests were, again, shown to be within regulatory limits.

The ESTD clearly demonstrated the capability of the integrated THOR® steam reforming process to convert SBW simulant in a variety of formulations, including heavy metals, UDS, and organic contaminants, into a granular solid product in a safe and efficient manner. Gaseous emissions from the process were found to be within regulatory limits and the solid products generated during the testing

displayed none of the characteristics that would preclude disposal at WIPP. Operational and design parameters critical to the development of the full-scale IWTU facility were either developed or confirmed and a number of lessons-learned necessary to enhance the design of the major IWTU unit operations were developed.

There were no recordable injuries during the entirety of the pilot plant construction, testing, and operation.

ACKNOWLEDGEMENTS

Many people contributed to the success of the sodium-bearing waste pilot plant program. Programmatic oversight was provided by Joel Case and Bill Owca from the Department of Energy Idaho Operations Office.

The THOR® Treatment Technologies, LLC, team provided the management, technical expertise, and administrative support for the project. The THOR® team consisted of Kathy Wolf, Kevin Ryan, Brad Mason, Brad Eldredge, Don Dustin, Greg DiGregorio, Dave Marudas, Bill Ingersoll, Phil Staats, Vishal Vora, Glynna Regan, Jim Desserich and Darcie Wiese. The THOR® team was augmented by key members of the management and technical staff of the Integrated Waste Treatment Unit Project of CH2M-WG Idaho, LLC (CWI), including Norm Boyter, Bill Kerley, Arlin Olson, Jim Law, Scott Roesener, John Tadlock, Jay Rumsey, Bob West, and Susan Harper. Nick Soelberg, Battelle Energy Alliance, at the Idaho National Laboratory, also provided technical support to the THOR® team.

The pilot plant facility was constructed and operated by Hazen Research, Inc., of Golden Colorado. Larry May, Harry Mudgett, and Steve Will managed the construction and operation of the pilot plant on a 24-hour per day, 7-day per week basis during test operations.

Manual sampling of off-gas emissions and operation of the continuous emissions monitoring system were performed by Air Pollution Testing, Inc., (APT) of Arvada, Colorado. Management and technical assistance were provided by Paul Ottenstein, Conrad VanDyke, and Clint Yeagley. John Yadon of Havlovick Engineering Services provided invaluable process control system support.

The authors wish to acknowledge and thank all individuals who contributed to the success of this program.

CONTENTS

ABSTRACT iii

EXECUTIVE SUMMARY iv

ACKNOWLEDGEMENTS vii

ACRONYMS xxi

1. INTRODUCTION 1-1

1.1 Background Information 1-1

1.2 Purpose and Scope of Testing 1-1

1.3 Overview of the Thor® Steam Reforming Process 1-2

1.4 Test Objectives 1-2

2. STEAM REFORMING SYSTEM DESCRIPTION 2-1

2.1 Process Flow Description 2-1

2.2 Additive and Process Streams 2-1

2.3 Liquid Simulant Preparation and Feed System 2-1

2.4 Fluidizing Gas System 2-3

2.5 Denitration and Mineralization Reformer 2-4

2.6 Product Receiver 2-7

2.7 High-Temperature Filter 2-9

2.8 Carbon Reduction Reformer 2-10

2.9 Off-Gas Cooler 2-13

2.10 Quencher/Scrubber System 2-13

2.11 Off-Gas Reheater 2-14

2.12 Process Baghouse Filter 2-14

2.13 Mercury Adsorber 2-15

2.14 Off-Gas Blowers 2-16

2.15 Process Data Acquisition And Control System 2-16

3. MEASUREMENTS, SAMPLE COLLECTION, AND SAMPLE ANALYSIS 3-1

3.1 Process Measurements 3-1

3.2 Continuous Process Monitoring System 3-1

3.3 Continuous Emissions Monitoring System 3-2

3.4 Periodic Manual Stack Gas Sampling 3-5

3.5 Periodic Process Liquids and Solids Sampling 3-5

3.6 Metallurgical Analysis 3-9

4. SIMULANT COMPOSITIONS 3-12

4.1 SBW Supernatant Solution 4-1

4.2 Undissolved Solids And Heavy Metals Simulants 4-4

4.3 Principal Organic Hazardous Constituent 4-14

5. TEST PROGRAM DESCRIPTION 5-1

5.1 Equipment Checkout and Functional Testing 5-1

5.2 Hydrogen/Oxygen Safety Test 5-2

5.3 Scoping Tests 5-2

5.4 Carbonate Phase 1 (CP1) Test 5-4

5.5 Carbonate Phase 2 (CP2) Test 5-6

6. QUALITY ASSURANCE/QUALITY CONTROL 6-1

7. TEST OBSERVATIONS AND RESULTS 7-1

7.1 Functional/Preparatory Tests 7-1

7.2 Hydrogen/Oxygen Safety Tests 7-2

7.3 Scoping Tests 7-3

7.4 Production Tests 7-16

7.4.1 Carbonate Phase 1 (CP1) Tests 7-16
7.4.2 CP1 Operating Conditions 7-26
7.4.3 Carbonate Phase 2 (CP2) Tests 7-26
7.4.4 CP2 Operating Conditions 7-35

7.5 System Performance 7-35

7.5.1 Fluidized Bed Performance 7-35
7.5.2 Fluidized Bed Particle Size Distribution 7-46
7.5.3 DMR Product Densities 7-56
7.5.4 Carbon Reductant Performance 7-63
7.5.5 Temperature Control of the DMR and the CRR 7-65
7.5.6 System Pressure Control and Performance 7-68
7.5.7 Filter (HTF and PBF) Performance 7-68
7.5.8 Data Acquisition and Control System Performance 7-71

7.6 Product Solids Composition Data 7-73

7.6.1 DMR/PR Bed Product 7-74
7.6.2 Fines (HTF Material) 7-81
7.6.3 PBF Solids 7-88
7.6.4 DMR Wall Scale 7-90

7.7 Process Gas And Stack Gas Measurements 7-93

7.7.1 DMR CPMS and Stack Cems Measurements 7-94
7.7.2 CPMS (DMR Process Gas) Data 7-97
7.7.3 CEMS (Stack Gas) Data 7-97
7.7.4 NO_X Destruction, CO, and THC Emissions 7-111
7.7.5 SO_2 Emissions 7-117
7.7.6 Manual Sample Train Measurements 7-118
7.7.7 Stack Gas Temperature, Moisture, and Flow Rate 7-118
7.7.8 Manual Sample Train Measurement Results 7-124
7.7.9 Mercury Control, Emission Measurements, and Spent Granular Activated Carbon Leachability 7-128
7.7.10 GAC Bed Thermal Event 7-144
7.7.11 VOC Emissions and POHC Destruction 7-145

7.8 Mass Balance 7-159

7.8.1 Methodology 7-159
7.8.2 Elemental Mass Balance Results 7-165

8. SOLID PRODUCT EVALUATION OF SUITABILITY FOR DISPOSAL 8-1

8.1 Primary Process Solids 8-1

8.1.1 Explosivity 8-1
8.1.2 Pyrophoricity 8-2
8.1.3 Ignitability 8-2
8.1.4 Reactivity 8-2
8.1.5 Detectable Liquids 8-4

9. METALLURGICAL ANALYSIS AND EVALUATION 9-1

10. COMPLETION OF TEST OBJECTIVES 10-1

11. CONCLUSIONS AND RECOMMENDATIONS 11-1

11.1 Lessons Learned 11-1

11.1.1 Integrated THOR® Process System 11-1
11.1.2 Waste Feed System 11-2
11.1.3 Denitration and Mineralization Reformer 11-4
11.1.4 High-Temperature Filter 11-9
11.1.5 Carbon Reduction Reformer 11-10
11.1.6 Off-Gas Cooler 11-12
11.1.7 Off-Gas System 11-13
11.1.8 Continuous Emissions Monitoring 11-15
11.1.9 Data Acquisition and Control System (DACS) 11-16

11.2 Conclusions 11-17

11.3 Recommended Path Forward 11-19

11.3.1 Testing Needs Prior To Integrated Process System Acceptance Test 11-19

12. REFERENCES 12-1

Appendix A—Summary of Data Validation Packages A-1

FIGURES

2-1. Denitration and Mineralization Reformer and High-temperature Filter 2-5

2-2. General Carbon Corporation "GC-CRB" 2-6

2-3. Representative Sample of DMR product material (20x) 2-8

2-4. Representative HTF product material (20x) taken during the CP1 Test 2-9

2-5. Carbon Reduction Reformer vessel top 2-10

2-6. Carbon Reduction Reformer vessel middle 2-11

2-7. Carbon Reduction Reformer vessel bottom 2-11

2-8. Hazen Process Baghouse Filter, Off-gas Blower, and Mercury Adsorber Systems 2-15

7-1. H_2-O_2 safety test data 7-2

7-2. Pilot Plant activities November 28 to December 7, 2005 7-5

7-3. Pilot Plant activities December 15 to 18, 2005 7-8

7-4. Pilot Plant activities December 19 to 22, 2005 7-10

7-5. Pilot Plant activities January 3 to 7, 2006 7-12

7-6. Pilot Plant activities January 8 to 13, 2006 7-14

7-7. Pilot Plant activities January 16 to January 21, 2006 7-17

7-8. Pilot Plant activities January 25 to February 1, 2006 7-20

7-9. Pilot Plant activities February 1 to 5, 2006 7-21

7-10. Pilot Plant activities February 7 to 10, 2006 7-25

7-11. Pilot Plant activities May 30 to June 9, 2006 7-33

7-12. DMR vessel temperatures and steam flow rate during steam boiler trips on June 4, 2006 7-41

7-13. Agglomerated bed material removed from the DMR vessel at the end of test CP2 7-42

7-14. Porous encrustations removed from the bottom of the DMR vessel at the end of test CP2 7-42

7-15. Comparison of superficial space velocities and twice minimum fluidizing velocity in the DMR bed during the CP2 test 7-43

7-16. Comparison between the CRR inlet SSV and twice the minimum fluidizing velocity in the CRR bed for the CP2 test 7-44

7-17. DMR Feed Nozzle insertion flanges layout 7-45

7-18. Functional Test: DMR average bed particle size 7-47

7-19. Scoping Tests 2 and 3: DMR average bed particle size 7-48

7-20. DMR average bed particle size January 8–13, 2006 7-50

7-21. CP1 Production Tests: DMR average bed particle size 7-51

7-22. Average DMR bed particle sizes during the CP2 test 7-53

7-23. Particle size distribution of DMR bed samples taken before and after seed particle addition 7-55

7-24. DMR solid product densities during the CP1 test 7-56

7-25. Cumulative mass of solids removed from the DMR during the CP2 test 7-57

7-26. Particle and bulk density of DMR bed samples during the CP2 test 7-57

7-27. Net PR product mass rate during CP2 test 7-58

7-28. HTF solids product mass rate during CP2 test 7-58

7-29. DMR bed turnover for Test CP2 7-60

7-30. Mass of solids elutriated from the CRR and captured in the PBF 7-61

7-31. Mass rate of solids collected in the PBF during CP2 test 7-61

7-32. Correlation of CP2 solids mixture density with mixing ratios 7-63

7-33. CRR outlet O_2 concentration and bed temperature during CP2 test 7-67

7-34. CRR outlet oxygen, stack THC, and CO concentrations during the CP2 test 7-67

7-35. Pressure rise on off-gas blowers during the CP1 test 7-69

7-36. Pressure rise on the gas blowers during the CP2 test 7-69

7-37. Damaged HTF filters at the end of the CP1 test 7-70

7-38. HTF pressure drop during the CP2 test 7-71

7-39. Micrograph of AGSCO alumina used as DMR starting bed 7-74

7-40. Micrograph of DMR solids produced during CP1 test P-4A-4 on February 2, 2006 7-75

7-41. Micrograph of DMR solids produced during the CP2 test on 6/5/06 7-75

7-42. Solids Analysis for CP1 test DMR and PR samples 7-77

7-43. Solids Analysis for CP2 test DMR and PR samples 7-79

7-44. Microphoto of PR Sample 2334 7-81

7-45. Solids Analysis for CP1 test HTF samples 7-83

7-46. Solids analysis for CP2 test HTF samples 7-85

7-47. Particle size distribution of HTF solids collected duringCP1 Test P-1, Sample No.. 1448 7-86

7-48. Particle size distribution of HTF sample collected during CP1 Test P-4A-3, Sample No. 1693 7-87

7-49. Particle size distribution of HTF sample collected during CP2 test on 6-4-06, Sample No. 2191 7-88

7-50. Chemical analysis of PBF solids produced during the CP1 Test 7-89

7-51. Chemical analysis of PBF solids produced during the CP2 test 7-91

7-52. Wall scale removed from the DMR cyclone downcomer on January 14, 2006 (Sample 1378) 7-92

7-53. DMR wall scale removed from the corrosion coupon rod after the end of CP2 test 7-92

7-54. Stack gas O_2 and CO levels compared to CRR outlet O_2 levels for CP1 7-111

7-55. Stack gas CO levels for different CRR bed temperatures 7-112

7-56. Stack gas O_2 and CO levels compared to CRR outlet O_2 levels for CP2 7-113

7-57. Stack gas O_2 and CO levels and CRR NO_X destruction for the CRR test conditions of CP2 7-113

7-58. System NO_X destruction compared to the DMR bed temperature for CP1 7-114

7-59. DMR, system, and CRR NO_X destruction compared to the DMR H_2 levels for CP1 7-115

7-60. DMR, system, and CRR NO_X destruction compared to the DMR H_2 levels for CP2 7-116

7-61. System NO_X destruction for medium and high simulant feedrates 7-117

7-62. Stack gas SO_2 concentrations compared to GAC Bed 3 temperature for CP1 and CP2 7-118

7-63. Hazardous metals (and surrogate) emission concentrations 7-127

7-64. ESTD GAC mercury adsorber 7-128

7-65. Hg concentrations in carbon bed samples from CP1 and CP2 7-135

7-66. Sulfur concentrations in spent carbon bed samplesfrom CP1 and CP2 7-136

7-67. Off-gas Hg concentrations during CP2 7-140

7-68. Hg removal efficiency by the carbon bed during CP1 and CP2 7-140

7-69. SO_4 in spent carbon samples from CP1 and CP2 7-141

7-70. Concentrations of trace off-gas elements sorbed on spent carbon from CP1 and CP2 7-142

7-71. Spent carbon Hg leachability results for CP1 and CP2 7-142

7-72. Total organic emissions at different CRR temperatures compared to CRR outlet O_2 concentrations 7-153

7-73. Elemental distribution of all discharges for CP1 7-171

7-74. Elemental distribution of solids discharges from DMR and HTF for CP1 7-172

7-75. Elemental distribution of all solids discharges for CP1 7-173

7-76. Elemental distribution of all discharges for CP2 7-179

7-77. Elemental distribution of solids discharges from DMR and HTF for CP2 7-180

7-78. Elemental distribution of all solids discharges for CP2 7-181

8-1. Effervescence of DMR Sample 1772 when mixed with water 8-3

TABLES

2-1. Mass and energy balance at CP1 Test baseline conditions 0.25 gpm SBW liquid feed, 640°C in DMR, 950°C in CRR 2-2

3-1. Analyzers used in the CPMS 3-3

3-2. Analyzers used in the APT CEMS 3-4

3-3. Off-gas manual sampling train schedule 3-6

3-4. CP2 stack gas particulate matter and hazardous metals concentrations and emission rates 3-7

3-5. Process liquids and solids sampling and analysis summary 3-7

3-6. Analytes requested in liquid and solid sample analyses 3-9

3-7. Corrosion coupons 3-10

4-1. Composition of non-radioactive simulants 4-1

4-2. Composition of baseline supernatant simulant solution (without heavy metals) 4-2

4-3. CP1 chemical analysis of baseline simulant solutions (without heavy metals) 4-3

4-4. Composition of the UDS Added to the Supernatant Solution 4-4

4-5. Production run UDS additions 4-6

4-6. Desired composition of the simulant solution (with heavy metal and radionuclide surrogates) 4-7

4-7. Chemical analysis of CP1 simulant solutions (with heavy metals) 4-8

4-8. Chemical analysis of CP2 simulant solutions (with heavy metals) 4-10

4-9. Reagent additions for CP1 production runs 5 and 6 with 120 g/L UDS 4-12

4-10. Chemical analysis of simulant solutions for CP1 Run 5 (with heavy metals, 120 g/L UDS) 4-12

4-11. Chemical analysis of 10% SBW simulant solutions for CP1 Run 6 (with heavy metals, 120 g/L UDS) 4-13

5-1. Scoping test conditions 5-3

5-2. CP1 production run test conditions 5-5

5-3. Carbonate Phase 2 test sequence 5-7

5-4. CP2 Off-gas measurements 5-8

5-5. CP2 DMR particle size control and CRR temperature control measures 5-9

6-1. Issued TTT non-conformance reports 6-2

6-2. Surveillances 6-6

6-3. Management assessments 6-7

7-1. Operating periods for scoping tests 7-4

7-2. Scoping test changes – November 28 to December 7, 2005 7-7

7-3. Scoping test changes – December 19 to 22, 2005 7-11

7-4. Scoping test changes – January 3 to 7, 2006 7-13

7-5. Scoping test changes – January 8 to 13, 2006 7-16

7-6. Operating periods for production tests 7-16

7-7. Production test changes – January 16 to 21, 2006 7-19

7-8. Summary of CP1 DMR operations 7-27

7-9. CP1 DMR gas flow rate and residence time 7-28

7-10. Summary of CP1 CRR operating parameters 7-29

7-11. Key CP1 off-gas system parameters 7-30

7-12. CP1 solid product rates 7-31

7-13. CP1 Steam Reformer process pressures and differential pressures 7-32

7-14. CP2 DMR flow rates 7-36

7-15. CP2 DMR temperatures 7-36

7-16. CP2 DMR and HTF pressures, differential pressures, and bed height 7-36

7-17. CP2 CRR flow rates 7-37

7-18. CP2 CRR and off-gas system temperatures 7-38

7-19. CP2 CRR pressures, differential pressures, and bed height 7-39

7-20. Bulk densities of CP2 test solid mixtures 7-62

7-21. Analysis of GC-CRB Carbon Reductant used in the DMR 7-64

7-22. Average composition of solids produced during the CP1 test 7-78

7-23. Average composition of DMR solids produced during the CP2 test 7-80

7-24. Microprobe composition of PR Sample 2334 7-81

7-25. Average composition of HTF solids produced during the CP1 test 7-82

7-26. Average composition of HTF solids produced during the CP2 test 7-84

7-27. Treatment of CP2 DMR wall scale solids 7-93

7-28. CP1 and CP2 stack emissions summary 7-95

7-29. CP1 DMR process gas dry composition 7-98

7-30. CP1 DMR process gas composition (wet basis) and NO_X destruction 7-100

7-31. CP2 DMR process gas dry composition 7-102

7-32. CP2 DMR process gas wet composition and NO_X destruction 7-103

7-33. CP1 stack gas dry composition 7-104

7-34. CP1 stack gas composition (wet basis), system NO_X destruction, and mass emission rates 7-105

7-35. CP2 stack gas dry composition for the manual sampling time periods 7-106

7-36. CP2 stack gas dry composition for the CRR test conditions 7-107

7-37. CP2 Stack gas wet composition and mass emission rates for the manual sampling time periods 7-108

7-38. CP2 stack gas composition (wet basis) for the CRR test conditions 7-109

7-39. CP1 operating conditions during emission test periods 7-119

7-40. CP2 operating conditions during emission test periods 7-120

7-41. CP1 stack temperature and flow-rate measurements 7-120

7-42. CP2 stack gas temperature and flow-rate measurements 7-121

7-43. CP1 stack gas particulate matter and metals concentrations and emission rates 7-125

7-44. CP2 stack gas PM and metals concentrations and emission rates 7-126

7-45. Carbon bed dimensions and operating conditions 7-129

7-46. Mercury analysis results for CP1 GAC bed activated carbon samples 7-131

7-47. Other analysis results for CP1 GAC bed activated carbon samples 7-132

7-48. Mercury analysis results for CP2 GAC bed activated carbon samples 7-133

7-49. Other analysis results for CP2 GAC bed activated carbon samples 7-134

7-50. CP1 stack gas mercury emission measurements 7-137

7-51. CP2 stack gas mercury emission measurements 7-138

7-52. Spent carbon TCLP leach results for CP1 7-143

7-53. Spent carbon TCLP leach results for CP2 7-143

7-54. CP1 stack gas VOC concentrations and emissions rates 7-147

7-55. CP1 stack gas SVOc concentrations and emission rates 7-149

7-56. CP1 stack gas Field GC (Method 0040) and TCO/GRAV concentrations and emission rates 7-151

7-57. CP1 stack gas dioxin and furan concentrations and emission rates 7-155

7-58. CP1 stack gas PCB concentrations 7-157

7-59. Summary of gaseous feed and discharge streams—method of flow rate quantification 7-161

7-60. Elemental Distribution and Mass Balance Closure for CP1 7-166

7-61. Elemental Distribution and Mass Balance Closure for CP1 7-168

7-62. GC-CRB coal analytical ash composition results 7-170

7-63. Elemental distribution and mass balance closure for CP2 7-175

7-64. Elemental Distribution and Mass Balance Closure for CP2 7-177

8-1. Summary of WIPP acceptability testing of SBW products 8-5

10-1. Testing program objectives, measurable parameters, and performance summary 10-2

ACRONYMS

APT	Air Pollution Testing, Inc.
ATG	autothermal gas
CAR	Corrective Action Report
CAS	Chemical Abstract Service
CCB	continuous calibration blank
CCV	continuous calibration verification
CEMS	Continuous Emissions Monitoring System
CFD	computation fluid dynamics
COT	cumulative operating time
CP	Carbonate Phase
CPMS	Continuous Process Monitoring System
CRR	Carbon Reduction Reformer
CWI	CH2M-WG Idaho, LLC
DACS	Data Acquisition and Control System
DCS	Distributed Control System
DMR	Denitration and Mineralization Reformer
DOE	U.S. Department of Energy
DR	deficiency report
DRE	destruction and removal efficiency
EPA	U.S. Environmental Protection Agency
ESS	Emergency Shutdown System
ESTD	Engineering-Scale Test Demonstration
FBSR	Fluidized Bed Steam Reforming
FG	fluidizing gas
FGC	Field Gas Chromatograph

GAC	granular activated carbon
GWI	general work instruction
HEPA	high-efficiency particulate air
HM	heavy metal
HMI	human-machine interface
HMPD	harmonic mass-mean particle diameter
HTF	High-temperature Filter
HWC	Hazardous Waste Combustor
I/O	input/output
ICB	initial calibration blank
ICP	Idaho Cleanup Project
ICV	initial calibration verification
ID	inside diameter
INL	Idaho National Laboratory
INTEC	Idaho Nuclear Technology and Engineering Center
IWTU	Integrated Waste Treatment Unit
JTG	Joint Test Group
MACT	Maximum Achievable Control Technology
MEB	mass and energy balance
MMPD	mass-mean particle diameter
MTEC	maximum theoretical emission concentration
MTZ	mass transfer zone
NAR	Nozzle Atomizing Ratio
NCR	non-conformance report
NGLW	newly-generated liquid waste
NWCF	New Waste Calcining Facility

OGB	Off-gas Blower
OGC	Off-gas Cooler
OHM	Ontario Hydro Method
PAC	Programmable Automation Controller
PBF	Process Baghouse Filter
PC	personal computer
PCB	polychlorinated biphenyls
PGF	Process Gas Filter
PM	particulate matter
POHC	principal organic hazardous constituent
PR	Product Receiver
PSD	product size distribution
PT	Pressure Transmitter
QA	quality assurance
QAPP	Quality Assurance Project Plan
QC	quality control
Q/S	Quencher/Scrubber
RH	remote-handled
RRF	relative response factor
RSD	relative standard deviation
RT	real time
SAM	Sample and Analysis Management
SAT	Site Acceptance Test
SBW	sodium-bearing waste
SOP	standard operating procedure
SRNL	Savannah River National Laboratory

SSV	Superficial Space Velocity
SVOC	semi-volatile organic compound
TCLP	Toxicity Characteristic Leaching Procedure
TCO	total chromatographable organic
TCO/Grav	total organic emissions
TFF	Tank Farm Facility
TGO	total gravimetric organic
THC	total hydrocarbon
TIC	tentatively identified compound
TOE	total organic emission
TRU	transuranic
TTT	THOR® Treatment Technologies, LLC
UDS	undissolved solids
VOC	volatile organic compound
WAC	waste acceptance criteria
WC	water column
WF	waste feed
WGI	Washington Group International
WIPP	Waste Isolation Pilot Plant

Pilot Plant Report for Treating Sodium-Bearing Waste Surrogates Carbonate Flowsheet

1. INTRODUCTION

1.1 Background Information

Sodium-bearing waste (SBW) is an acidic tank waste stored at the Idaho Nuclear Technology and Engineering Center (INTEC) at the Idaho National Laboratory (INL) Site. It consists primarily of waste from processing spent nuclear fuel, decontamination activities, and laboratory wastes. SBW contains high concentrations of nitric acid, alkali, and aluminum nitrates, with minor amounts of many inorganic compounds including radionuclides, mainly cesium and strontium.

The patented Thermal Organic Reduction (THOR®) steam reforming waste treatment technology has been selected as the technology of choice for treatment of the SBW for the Idaho Cleanup Project (ICP). The THOR® steam reforming process will convert the SBW into a dry, granular, solid product. SBW treatment will take place within the Integrated Waste Treatment Unit (IWTU), a new facility that will be located at INTEC.

1.2 Purpose and Scope of Testing

A pilot plant testing program using SBW simulants and the THOR® dual fluidizing bed steam reforming system was conducted. The primary purpose of the testing was to provide data to support the full-scale process system design, optimization, validation, permitting, and operational planning. Testing was performed at the Hazen Research, Inc. facility in Golden, Colorado, during the period November 2005 through February 2006 (Carbonate Phase 1 [CP1]). Following CP1 testing it was determined that a second phase of SBW carbonate testing (CP2) was needed. The second phase of testing was performed during the period May 2006 through June 2006.

A one-tenth scale (based on throughput) pilot plant of the IWTU production process was designed and constructed at Hazen Research using both existing and new equipment. A one tenth scale pilot plant was used because the operation of its key equipment items was determined to accurately reflect that of the full-scale plant, while still being of small enough scale to be economical to construct and operate, and had been previously used and successfully scaled up to full production scale at the Studsvik Processing Facility located in Erwin, TN.

Following construction of the pilot plant, the system was thoroughly tested through component and functional system tests. Following this, scoping tests were conducted to establish operating parameters for subsequent productions tests. The production tests operated the system at a wide variety of process conditions (e.g., reformer temperatures and liquid feed rates), during which numerous process off-gas samples were obtained to confirm compliance with Maximum Achievable Control Technology (MACT) and other emissions regulations, and solids samples were obtained to verify general suitability of the product materials for disposal at the Waste Isolation Pilot Plant (WIPP). During the scoping and two phases of production tests numerous specific test objectives were achieved (See Section 10).

This document describes the testing program and its results.

1.3 Overview of the Thor® Steam Reforming Process

SBW at the INL Site consists of radioactive, aqueous solutions with high concentrations of nitric acid, nitrates, alkali metals, aluminum, and a wide variety of other inorganic oxides. The THOR® steam reforming process destroys nitric acid, nitrates, and organic materials present in the SBW, and produces a dry, granular, solid product. The steam reforming process has been tested with smaller scale process equipment and shown to effectively handle, process, and immobilize the radionuclides, sodium, potassium, sulfate, chlorides, fluorides, and non-volatile heavy metals into a solid matrix [R1,2,3,4,5,6,7,8,9]. The process converts nitric acid, nitrates, and nitrites directly to nitrogen gas in the steam reformers. Any organic material in the SBW is converted to carbon dioxide and water vapor by a combination of steam reforming and oxidizing reactions. The THOR® process flow diagram for treatment of SBW is provided in Section 2.1.

The SBW tank waste feed is introduced into the first steam reformer, the Denitration and Mineralization Reformer (DMR). The bed particles in the steam reformer are fluidized by introduction of low-pressure superheated steam and a measured quantity of oxygen. The oxygen, present in the DMR in a sub-stoichiometric concentration, reacts with granular carbon that is metered into the DMR to create a chemically reducing environment and process energy. In the first steam reformer, liquids are evaporated; the vast majority of organics, nitric acid, nitrates, and nitrites are destroyed; and the reactive chemicals in the waste feed are converted to a solid waste product. The second reformer, the Carbon Reduction Reformer (CRR), serves to further reduce any NO_X gases from the first reformer and oxidize residual organics to carbon dioxide and water vapor. The gases (mainly carbon dioxide, nitrogen, and water vapor) from the process are filtered through sintered metal filters, baghouse filters, and a mercury adsorber. They are then vented to the atmosphere through a monitored stack.

1.4 Test Objectives

The principal, overall objectives of the SBW testing program [R10] were to:

- Establish target steady-state system operating conditions
- Demonstrate integrated operation of the entire SBW treatment process, including serial operation of the DMR and CRR
- Demonstrate and confirm long-term system operability with respect to process chemistry, material flows, mass and energy balance (MEB), equipment durability, and particle size control
- Establish key operating parameters for the full-scale IWTU process
- Obtain operational data to confirm IWTU design parameters
- Gather off-gas emissions data for purposes of environmental permitting
- Confirm solid product data for requesting WIPP transportation and disposal.

A complete listing of the test objectives and the level of achievement of these objectives is provided in Section 10.

2. STEAM REFORMING SYSTEM DESCRIPTION

2.1 Process Flow Description

The process flow description identifies each of the major THOR® system components employed for this test program. The major components include the Surrogate Liquid Waste Preparation and Feed System, the Fluidizing Gas (FG) Supply System, the DMR, the Product Receiver (PR), the High-temperature Filter (HTF), the CRR, the Off-gas Treatment System, and the Data Acquisition and Control System (DACS). These components are discussed below.

2.2 Additive and Process Streams

In addition to the major components of the THOR® system, the system included the additive and process streams used to treat the SBW simulant during the pilot scale testing. The scrubber system was bypassed (Stream 11 routed directly to the reheater) and the mercury adsorber was on line for the majority of the CP1 production tests (Stream 22a routed to stack via Stream 22b and the Off-gas Blower B407). Table 2-1 contains the data for most of the active streams in the process flow system for a specific feed condition for CP1. The table is based on a calculational model of the Mass and Energy Balance (MEB) for the system. It was updated to reflect actual operating conditions and stream flow rates and is expected to be correct to within 10%. The model conditions are considered baseline and represent the most common feed stream for the actual plant; specifically, SBW liquid (no significant Undissolved Solids [UDS]) fed at 0.25 gallons per minute (gpm), the DMR operating at 640ºC and the CRR operating at 950ºC. A stream name, stream number, pressure, temperature, and various flows are given for each stream. There are many unnumbered nitrogen streams in the process flow system; these streams are grouped together by unit operation. For example, most nitrogen flowing to the DMR, mostly line purges, is given the stream name DMR-N_2.

2.3 Liquid Simulant Preparation and Feed System

The liquid surrogate waste preparation and feed system included the following major components:

- A 1,600-gallon (gal) stainless-steel surrogate, Waste Holdup Tank with mixer (T-100)
- Surrogate Waste Feed Transfer Pump (P-100)
- Two parallel 500-gal plastic, surrogate waste feed tanks with mixers (T-101 A&B)
- Two surrogate waste feed tank recirculation pumps (P-101 A&B)
- Feed Solids Addition Mix Tank and Pump (T-102 and P-102)
- Principal Organic Hazardous Constituent (POHC) Tank and Pump (T-103 and P-205)
- Peristaltic surrogate waste feed pump, 0.10 to 0.40 gpm (P-200)
- Surrogate waste feed injectors (2), one in operation at a time.

Table 2-1. Mass and energy balance at CP1 Test baseline conditions 0.25 gpm SBW liquid feed, 640°C in DMR, 950°C in CRR.

Stream Summary	Mass Flowrates	P (psia)	T (C)	ACFM	SCFM	gpm	solid/ particulate (lb/hr)	lb/hr
Waste Feed	Stream 1	15.59	10	0.00	0.00	0.25	0.00	169.15
N_2	DMR-N_2	15.59	20	16.96	18.00	0.00	0.00	78.50
NAR	Stream 2	15.59	10	10.95	12.03	0.00	0.00	54.04
FG Water	Stream 39	15.59	20	0.00	0.00	0.26	0.00	96.06
FG N_2	Stream 41	15.59	20	0.00	0.00	0.00	0.00	0.00
FG O_2	Stream 40	15.59	20	1.60	1.69	0.00	0.00	8.44
FG	Stream 42 (39,40,41)	15.59	600	100.88	35.94	0.00	0.00	104.50
Bed	Stream 32	11.95	20	0.00	0.00	0.00	0.00	0.00
Charcoal	Stream 33	11.95	20	0.00	0.00	0.00	25.81	33.07
N_2	3-PN2	15.59	20	3.86	4.10	0.00	0.00	17.88
Additives	Stream 3 (32,33,PN2)	15.59	20	5.25	5.58	0.00	25.81	50.95
DMR Outlet Gas and Fine Solids	Stream 4	17.25	590	295.23	117.71	0.00	8.87	438.59
DMR Solid Bed Product	Stream 27	18.94	500	0.00	0.00	0.00	18.55	18.55
N_2	PF Backpulse and Product Purge	15.59	20	2.22	2.36	0.00	0.00	10.29
N_2	PF-N_2	15.59	20	0.40	0.42	0.00	0.00	1.83
PF Gas	Stream 5	14.12	590	369.18	120.49	0.00	0.01	441.86
PF Solid	Stream 28	14.12	320	0.00	0.00	0.00	8.86	8.86
Bed Media	Stream 34	11.95	20	0.00	0.00	0.00	0.60	0.60
Carbon	Stream 35	11.95	20	0.00	0.00	0.00	19.83	20.22
Clay	Stream 36	11.95	20	0.00	0.00	0.00	0.02	0.02
N_2	6-PN2	15.59	20	8.48	9.00	0.00	0.00	39.25
Additives	Stream 6 (34,35,36,PN2)	15.59	10	8.19	9.00	0.00	20.45	60.09
Oxygen/Air and Cooling Water/N_2	Stream 7/8/45	15.59	10	23.75	26.09	0.00	0.00	127.29
N_2	CRR-N_2	15.59	20	9.64	10.23	0.00	0.00	44.62
CRR Outlet Off-Gas	Stream 9	11.90	780	733.85	165.40	0.00	1.66	673.85
CRR Solid	Stream 29	12.90	950	0.00	0.00	0.00	0.00	0.00
OGC Quench Water/Atomizing Gas	Stream 10	16.90	10	16.80	20.00	0.41	0.00	296.94
OGC gas	Stream 11	11.90	185	500.34	259.23	0.00	1.66	970.79
N_2	OG-N_2	15.59	20	0.07	0.07	0.00	0.00	0.31
OG gas	Stream 22A	11.70	120	436.77	259.30	0.00	0.01	969.45
OG solid	Stream 31	11.90	120	0.00	0.00	0.00	1.65	1.65
Hg Adsorber Outlet	Stream 22C	11.79	125	438.93	259.30	0.00	0.01	969.45
Stack	Stream 24	12.15	120	420.54	259.30	0.00	0.01	969.45

All of the equipment items listed above, as well as the interconnecting piping, valves, and instruments, were resistant to nitric acid corrosion.

The Waste Holdup Tank (T-100) was used to make up and mix the surrogate waste feed liquids prior to addition of UDS or heavy metals. The holdup tank was provided with a mixer capable of maintaining the liquids well-mixed and providing agitation required to mix and dissolve solid reagents. The transfer pump (P-100) was used to help mix the surrogate feed solution and transfer the waste surrogate solutions from the holdup tank to one of the two Waste Feed Tanks (T-101 A or B), as needed. If UDS and/or heavy metals were to be included in the feed solution for a particular test, they were pre-mixed in the Feed Solids Addition Mix Tank (T-102). The resulting slurry was then combined with the surrogate waste solution in the waste feed tanks. Both feed tanks were equipped with mixers and recirculation pumps to ensure that the UDS remained suspended in the solution.

The feed solution in each of the Waste Feed Tanks was continually recirculated to maintain the UDS in suspension. Valves were provided to allow either pump to recirculate or transfer to either tank so that the solution could be recirculated even if one of the pumps required maintenance.

A peristaltic feed pump (P-200) was used to draw off a small portion of the contents of the feed tank recirculation loop and continuously meter the liquid surrogate into the DMR through one of two atomizing feed nozzles, only one of which was operated at a time. A standby waste feed pump was provided as a backup in the event of a failure of the primary feed pump. A coriolis type mass flow meter was used to measure and record the density and mass injection rate of the surrogate feed into the DMR. An auxiliary organic liquid metering pump (P-205) and tank (T-103) were used to meter the POHC into the process feed line at a rate of approximately 0.33 kilograms per hour (kg/hr) so that the Destruction and Removal Efficiency (DRE) of the POHC, chosen to be conservatively representative of the organics present in the actual SBW, could be determined during a portion of the test program.

2.4 Fluidizing Gas System

A mixture of steam and oxygen was used to fluidize the DMR during normal operations. Steam reacted with carbon in the bed to produce a small quantity of carbon monoxide and hydrogen that reduced nitrates in the waste feed stream to nitrogen gas. Oxygen also reacted with the carbon and hydrogen to generate process heat and carbon dioxide and water vapor. The actual sequence of reactions is more extensive and is described in other reports [R8]. During startup, the system was fluidized with nitrogen or a mixture of nitrogen and oxygen.

A steam generator (H-104) was used to provide the steam for the FG. The steam generator was capable of providing up to 500 pounds per hour (lb/hr) of low-pressure steam; however, typically only 70 to 200 lb/hr were required during the SBW tests. The steam generator was equipped with an automatic temperature controller, an isolation ball valve, and a pressure regulator valve.

The FG flowed through two electric superheaters in series (H-105 A and B) to increase the gas temperature to ~600°C before the steam and oxygen mixture was introduced into the FG distributor located at the bottom of the DMR. The superheaters also were used to heat nitrogen as the fluidizing gas during the DMR preheating (heat-up) operation. The major heat load for the superheater occurred during the initial heat-up of the reformers to the initial operating temperature because no external fluidized bed vessel heaters were provided. During initial startup and preheating of the DMR, the superheaters were capable of heating the fluidizing nitrogen to 700°C.

The combined power rating for both superheaters was 70 kW (35 kW each, 480 VAC, 3-phase). The superheaters were provided with a stainless-steel shell and Inconel heating elements. The steam and

oxygen supply lines included isolation ball valves to provide positive manual oxygen and steam isolation. The FG system downstream of the superheaters was fabricated from stainless steel to prevent corrosion from the steam/oxygen mixture at the high temperatures used in the FG system.

Automated control valves and flowmeters were used to control and monitor the amounts of oxygen and steam fed to the DMR during simulant treatment operations. During the CP1 test, the operator set the desired FG flow rate, and the control system automatically adjusted the steam flow rate (subtracting the fluidizing oxygen flow rate) to maintain a constant total flowrate in the bottom of the DMR.

The CP1 test results had shown that the oxygen concentration in the fluidizing gas could become excessively high during process upsets. Hence, the fluidizing gas control scheme was changed for the CP2 test to allow use of a constant steam flow rate in the fluidizing gas. The operator would set the desired fluidizing steam flow rate and the control system automatically maintained this flow rate.

The Superficial Space Velocity (SSV) given by the FG flowrate was controlled within an operator-selected range that always exceeded the minimum fluidizing velocity for the bed average particle size. The minimum fluidizing velocity was determined using the Wen and Yu correlation [R11] that accounted for the operating temperature and pressure, the FG composition, the bed particle density, and the average particle size.

2.5 Denitration and Mineralization Reformer

The DMR (T-200) was a fluidized bed vessel designed to operate in an autothermal steam reforming mode to evaporate water; reduce nitrates to nitrogen; volatilize and reform organics; convert alkali and alkaline earth metals into non-agglomerating solid products; and capture sulfur, fluoride, chloride, and phosphate compounds in the solid product. Non-volatile heavy metals, other metals, and the non-radioactive radionuclide surrogates (i.e., cerium and cesium) were also captured in the solid product.

The DMR was an existing 15-in. inside diameter by 96-in. high, carbon steel, refractory-lined vessel. The top 23-in. of the vessel expanded to 21-in. in diameter. The DMR was insulated with 4.5-in. each of Kasto-Lite-22 and Lo-Abraid refractory for a total refractory thickness of 9-in. A new bottom section for the DMR was fabricated to provide ports for the fluidizing nozzles, solids removal auger, and auxiliary FG nozzle. This new section was also insulated with Kasto-Lite-22 and Lo-Abraid refractories. Figure 2-1 is a photograph of the DMR (to the left).

The DMR vessel was modified to provide continuous, metered, solid additive injection of particulate carbon reductant and recycled bed material or other solid additives (if desired). Solid additives were introduced into the DMR through two independent solid feeders. The feeders discharged into a small chamber bounded by two valves that operated sequentially to form a lock hopper or shotpot. A nitrogen gas purge on the hopper discharge pipe excluded atmospheric air from the process and provided some of the motive force needed to inject the lightweight carbon reductant into the DMR bed. An automatically controlled vibratory feeder with a weight scale was used to monitor and control the feed rate of carbon reductant into the DMR. Figure 2-2 shows the carbon used in the DMR. The system was calibrated for the specific carbon reductant used, and the Data Acquisition and Controls System (DACS) controlled the carbon reductant feed rate at the desired value. The second solids feeder was a manually controlled auger that was used to add recycled bed material or other solid additives to the DMR.

Figure 2-1. Denitration and Mineralization Reformer and High-temperature Filter.

Figure 2-2. General Carbon Corporation "GC-CRB."

As solid product was generated, it accumulated in the DMR bed and was periodically removed to maintain a fluidized bed depth of approximately 36 to 42 in. The DMR vessel included a bottom solids removal auger for periodic batch draining of solid product materials to control the bed level within a 4-in. to 6-in. band. A nitrogen jet below the auger transferred the hot bed solids pneumatically to the product receiver vessel. A manually operated, pneumatically actuated, full port, rotating disk valve installed on the outlet of the auger assembly isolated the solids transfer system nitrogen jet eductor from the bottom of the DMR. Grab samples of the DMR bed material were acquired periodically through a sample line and valves located on the side of the vessel.

The DMR was connected to the Emergency Shutdown System (ESS) for the facility. Upon activation of the ESS or on loss of power to the process control system, the flow of fluidizing steam and oxygen to the DMR was switched to 100% nitrogen. A limiting flow orifice controlled the flowrate of the nitrogen if the ESS were ever activated.

A pair of two gas atomizing liquid feed nozzles was installed to introduce the SBW simulant liquid/slurry into the DMR fluidized bed reactor as an atomized droplet spray via a feed port on the side of the vessel. Only one feed nozzle was in use at any time. Valves were provided to allow easy switching from one nozzle to the other during operation. The feed nozzle that was not in use was purged to prevent bed solids from entering the nozzle orifices and plugging them. The atomizing gas flowed through an annulus to atomize the feed liquid into appropriately sized droplets for reaction in the DMR bed. The flow rate of the atomizing gas was set and automatically controlled with an integrated mass flow

meter/controller. Usually air was used as the atomizing gas; however, pure nitrogen and a mixture of air and nitrogen were also used as the atomizing gas at different times during the tests.

The oxygen introduced via the atomizing nozzle and FG distributor generated heat within the DMR by reacting with the added carbon reductant and with the carbon monoxide and hydrogen produced in the bed by the steam reforming reactions. Oxygen flow was adjusted to maintain the DMR temperature within the desired range, typically 600°C to 670°C, for production of a sodium carbonate-based product. Several thermocouples were used to monitor temperatures throughout the DMR. Typically, the DMR bed temperature was maintained within ± 10°C of the desired setpoint by automatically controlling the fluidizing oxygen flow rate. Typical residence time of the gas in the DMR was 2.0 to 2.5 seconds.

The DMR operated in a strongly reducing mode in order to ensure nearly complete conversion of nitrates directly to nitrogen gas, although a small oxidizing zone existed in the immediate vicinity of the point of oxygen injection into the vessel. The DMR operated at a slight positive pressure (typically 2 to 4 pounds per square inch gauge [psig]) because of backpressure from the CRR FG distributors and the CRR fluidized bed pressure drop. The DMR flanges and nozzle connections incorporated qualified gaskets and flanges in order to prevent leakage of process gases to the building area. Prior to operation, and after any shutdown for system maintenance, the entire pilot plant system was pressure tested to verify leak tightness.

The DMR, its FG lines, and its process gas outlet line were well insulated to minimize heat losses. Multiple thermocouples and pressure differential transmitters were used to provide real-time operating data. The differential pressure transmitters (PTs) were equipped with nitrogen purge lines to prevent moisture condensation in the sensing lines and plugging of the sensing lines with bed solids. The DACS provided remote readouts and trending for the thermocouples and differential pressure transmitters so that bed temperatures and pressure drops could be monitored continuously.

The DMR was provided with an external cyclone to help retain the solid bed particles within the vessel. When operating properly, the cyclone returned an estimated 90% of the particulates elutriated from the DMR back to the bed. Solids collected from the cyclone were returned directly to the bed of the DMR through an internal return line downcomer that extended into the DMR bed. Three nitrogen pulsejets were used to keep the downcomer clear from plugging. The 21-in. diameter disengagement section of the DMR also served to reduce the gas velocity and aid in the reduction of particulate material carried over to the cyclone.

2.6 Product Receiver

The PR (T-201) was used to collect high-temperature, granular bed product solids pneumatically transferred from the DMR. The PR was a vertical, cylindrical filter vessel, 12-in. in diameter with a conical bottom. It was fitted with four sintered metal, candlestick filters on a metal tube sheet. A manually actuated nitrogen gas pulse-back manifold was used to clean the filter elements when on-line or off-line. An automated pulse back system was not required because the PR filter was normally not on-line and was used only to receive occasional solids transfers from the DMR. When the fluidized bed height increased above ~42-in. in the DMR, operators would batch transfer a quantity of the bed media to the PR. A differential pressure gage, with sensing ports in the vessel and in the off-gas line downstream of the vessel, was used to determine the pressure drop across the filters and, in turn, alert the operator that the filters needed to be cleaned. External electrical heaters (H-201) were provided to maintain the filter elements and the vessel above ~120°C during operation to prevent condensation.

The outlet of the PR vented to the freeboard of the DMR so that gases removed from the solid auger were reintroduced to the DMR. Hence, the PR operated at the same pressure as the freeboard of the

DMR. The PR was provided with a product draining system incorporating a single high-temperature, manually-operated, full-port ball valve and 5-gallon stainless-steel metal collection vessels for periodic batch draining of product material. The product collection vessels provided residence time for the product solids to cool before being bagged, labeled, and placed into standard carbon steel 55-gal drums for storage. The drain valve and collection vessels were designed to contain solids with temperatures of up to 400°C. The collection vessels were provided with a nitrogen purge to displace process gases from the filter to ensure that moisture did not condense in the collection vessel, drain port, or valve. Periodic grab samples were taken of the cooled solids in the collection vessel prior to the solids being placed into the carbon steel drums for storage.

During liquid feed processing operations, the inorganic components in the feed stream surrogates formed granular product solids that accumulated in the DMR. As described above, these accumulated solids were transferred periodically to the PR for collection and packaging into drums. Figure 2-3 shows a 20-power enlargement of representative DMR product material. The option to recycle some of the bed product particles back into the DMR to maintain the required particle size range in the DMR was incorporated into the operating philosophy of the test program. An off-line vibratory screen was provided for the separation of the larger particles from the smaller granules in the cooled solids. If required, the different size fractions of the bed product could be returned on a semi-continuous basis to the DMR bed through the solids additive auger feeder and airlock. During CP2, solids larger than 12-mesh (primarily carbon) were removed from the PR solids and returned to the DMR during this test. The recycled carbon was returned on a semi-continuous basis to the DMR bed through the carbon feed hopper, vibratory feeder, and airlock.

Figure 2-3. Representative Sample of DMR product material (20x).

2.7 High-Temperature Filter

The HTF is shown on the right in Figure 2-1. The HTF (T-202) was a filter vessel that received the process gases and entrained fines from the DMR. The purpose of the HTF was to remove and collect the finely divided solids—predominately sodium carbonate product material and carbon reductant fines—elutriated from the DMR. Figure 2-4 shows a 20-power enlargement of representative HTF product material.

Figure 2-4. Representative HTF product material (20x) taken during the CP1 Test.

The HTF was a 24-in. diameter, vertical, cylindrical filter vessel modified to accommodate eighteen 3 to 5-micron, sintered metal or silicon carbide, candlestick filters. An automated nitrogen gas pulse-back manifold with four nitrogen pulse-back valves was used to clean the filter elements while they were on-line. The difference between two PTs, with sensing ports in the vessel and in the gas outlet line downstream of the vessel, gave the pressure drop across the filters. When the pressure drop exceeded the setpoint, the DACS automatically actuated the pulse-back function. External electrical heaters (H-202) were provided to maintain the filter elements and filter vessel at 400°C during operation.

The HTF incorporated a product solids drain and collection system similar to that described for the PR. The system consisted of a single, high-temperature, manually-operated, full-port ball valve with 5-gal metal collection vessels for periodic batch draining of product material. The product collection vessels provided residence time for the fine product solids to cool before being bagged, labeled, and placed into standard carbon steel 55-gal drums for storage. The collection vessels were designed to contain up to 10 psig, as the pressure in the HTF was typically between 1 and 3 psig during normal operation. The drain valve and collection vessel were designed to contain solids with temperatures of up to 400°C. The collection vessels were provided with a nitrogen purge to displace process gases from the filter to ensure that moisture did not condense in the collection vessel, drain port, or valve. Periodic samples were taken from the cooled collection vessel solids prior to being placed into the carbon steel drums for storage.

2.8 Carbon Reduction Reformer

The CRR (T-300) was a fluidized bed vessel operated in series with the DMR. The hot process gas from the DMR was filtered through the HTF, which removed essentially all of the product solids and carbon fines elutriated from the DMR. The filtered DMR process gas then consisted mainly of water vapor, nitrogen, carbon dioxide, carbon monoxide, hydrogen, methane and other short-chain organics, and small amounts of acidic gases such as hydrochloric acid and sulfur dioxide. This process gas mixture was introduced at the bottom of the CRR and fluidized the bed media. An oxygen/air mixture was injected through a second set of gas distributors positioned above the CRR FG distributors. The oxygen/air injection distributors created an oxidizing steam reforming environment in the upper section of the fluidized bed and in the CRR freeboard. A second set of auxiliary oxygen injectors located above the bed during CP1 and high in-bed during CP2 was used to inject additional oxygen into the CRR freeboard to fully react any carbon monoxide that might be generated from the steam reforming of carbon fines in the freeboard area. The CRR fully oxidized the hydrogen, carbon monoxide, and organics from the DMR, converting them to carbon dioxide and water and generating heat in the process.

The CRR was an existing, carbon steel, refractory-lined, fluidized bed vessel modified to provide for initial and periodic batch injections of bed media, supplemental carbon, and a solid phase mineralizing additive such as clay. The initial bed media consisted of alumina beads with a mean particle size of approximately 1,000 microns for CP1 and 400 microns for CP2. The pre existing portion of the CRR had a 24-in. inside diameter (ID), was 175 in. high, and was lined with Kasto-Lite-22 and Lo-Abraid refractory. A 3.5-in. thick liner, made from Ultragreen 45 refractory reduced the inside diameter in the bottom 30 in. of the CRR to 17 in. Figure 2-5, Figure 2-6, and Figure 2-7 show the top, middle and bottom views of the CRR.

Figure 2-5. Carbon Reduction Reformer vessel top.

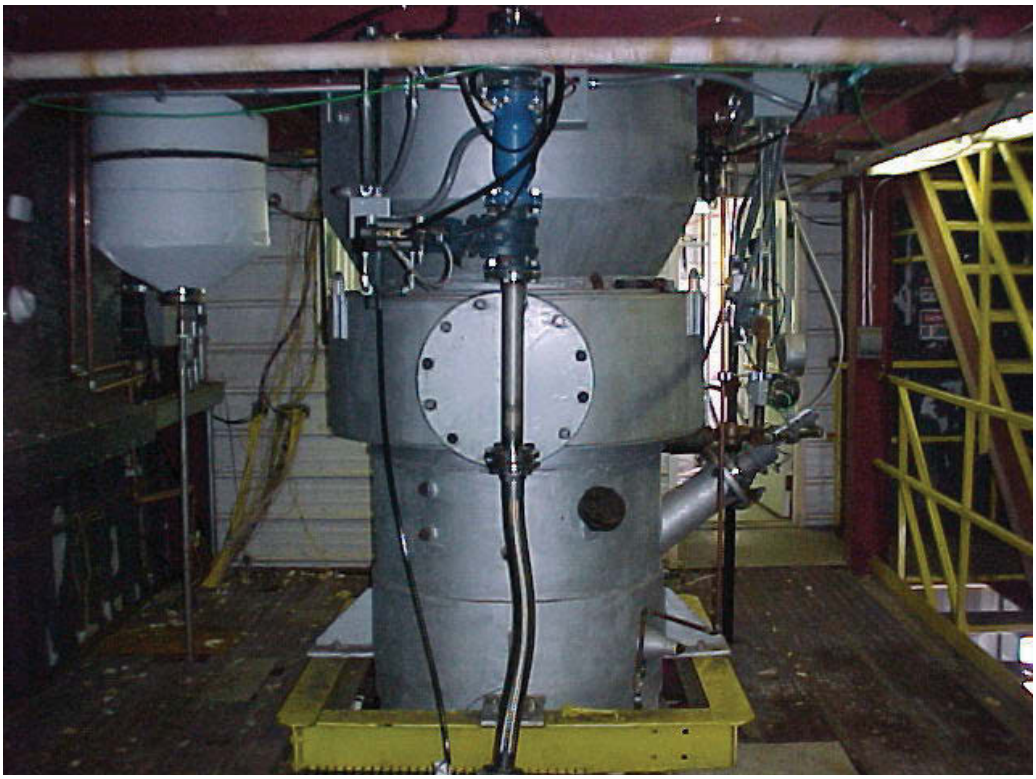

Figure 2-6. Carbon Reduction Reformer vessel middle.

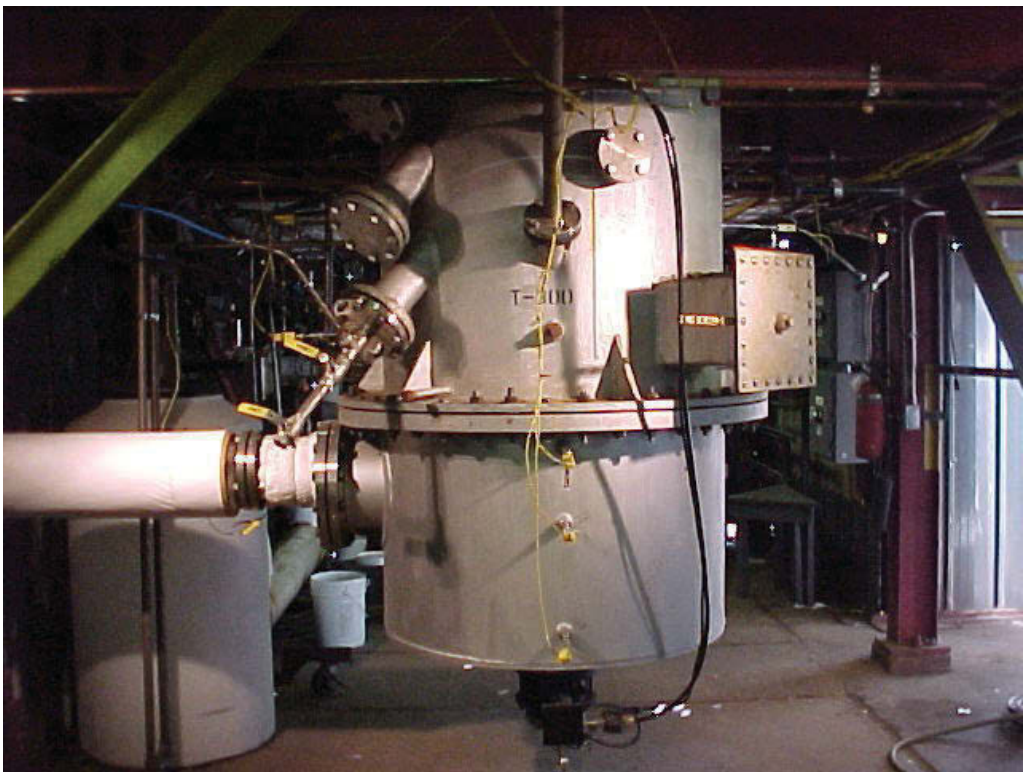

Figure 2-7. Carbon Reduction Reformer vessel bottom.

A new bottom section for the CRR was fabricated to have ports for the FG distributor, thermocouples, and differential pressure probes. The inside diameter of the new section was 17-in. and it was lined with Kasto-Lite-22 and Ultragreen-45 refractory. The new section also was provided with a high-temperature-rated, pneumatically-actuated, full-port, rotating-disk valve, and a nitrogen purge to allow the bed to be drained as needed to adjust the operating bed level or at the end of a process run. The only solids introduced into the CRR were bed media to replace bed media lost to attrition and elutriation, supplemental carbon that was converted in large part to carbon dioxide, and the mineralizing additive, which was added to combine with any sodium carbonate product carried over from the HTF to prevent it from melting and agglomerating the bed media.

Carbon was introduced into the CRR through a vibratory feeder, while the mineralizing additive was introduced through a motor-driven auger feeder or was added by a manual batch addition to the airlock chamber. A third feed hopper was provided that could be used to add or replenish bed media. All three feeders discharged solids into a small airlock chamber bounded by two valves that operated sequentially to form a lock hopper or shot pot. A nitrogen gas purge on the hopper discharge pipe excluded atmospheric air from the process and provided some of the motive force needed to inject the solids into the CRR. The carbon feeder was calibrated for the specific carbon reductant used, and the DACS controlled the carbon feed rate at the desired value. The CRR bed level was operated at a height of 26 to 36 in.

For the CP1 test, two gas distributors were installed in the CRR bed, and one was installed above the bed. The lowest distributor consisted of a three-point injector nozzle to provide uniform fluidization of the bed using the filtered process gas from the DMR. The middle, in-bed oxygen distributor consisted of a single distributor pipe above the FG distributor for injection of oxygen/air into the bed. A third inlet, above the level of the bed, was used to introduce additional oxygen into the vessel to ensure complete oxidation of carbon monoxide to carbon dioxide. The oxygen flow rate to the in-bed oxygen distributor was automatically controlled to maintain the CRR bed temperature within ± 10°C of the bed temperature setpoint. The oxygen flow above the bed was automatically controlled during operation to maintain a set outlet oxygen concentration in the CRR off-gas, typically 2% to 10% by volume. Typical gas residence time in the CRR was 2.5–3.0 seconds.

The configuration of the CRR oxygen distributor was modified for the CP2 test. The upper autothermal gas (ATG) nozzles were above the distributor in the upper portion of the CRR bed or in the "splash zone" (the interface between the fluidized bed and freeboard region of the CRR) depending on the bed depth in the CRR. The oxygen/nitrogen mixtures and flowrates to the lower two sets of ATG nozzles were automatically controlled by the DACS to maintain the desired CRR bed temperature. The oxygen/nitrogen mixture and flow to the upper nozzle set was controlled to achieve the desired level of oxygen in the CRR off-gas, and hence the required destruction of CO and total hydrocarbons (THCs).

The CRR bed temperature was maintained at approximately 850 to 1,050°C by adjusting the in-bed oxygen distributor flow rate. A ratio controller added air to the oxygen to maintain a desired nitrogen concentration (typically 25 or 50% depending on the test) in the in-bed oxygen/air distributor to help maintain the oxygen input jets cooler than they would be with 100% oxygen.

The oxygen input rate to the above-bed oxygen distributor was automatically controlled by the DACS to maintain the desired excess oxygen concentration in the CRR process outlet gas, which in turn, controlled the CO level in the process off-gas stream. The operator utilized the human machine interface (HMI) to set the desired excess oxygen level and the DACS automatically adjusted oxygen input to the upper distributor to maintain the desired oxygen level in the CRR off-gas.

During start-up, the initial energy for heating up the CRR was provided by hot nitrogen from the DMR FG superheaters without any bed material in the DMR or CRR. When the temperature in the CRR was above 125°C, the bed media was added to the CRR, and heat-up continued using the FG superheaters. In order to fully heat up the CRR in as short a time as possible, a natural gas fired burner was inserted into the CRR near the top of the bed. This supplemental heating capability was not used during process operations. Once the CRR bed temperature was above about 350°C, a wood-based carbon was added to the bed to provide a fuel source in the CRR and a small (~5 scfm) oxygen flow was initiated in the in-bed oxygen distributor. When the CRR bed temperature reached ~550°C, petroleum coke was used instead of the wood-based carbon, and the bed heat-up continued until the desired bed temperature was reached. As the CRR bed temperature increased, the amount of gas required to fluidize the bed decreased and the operators would reduce the flow manually as needed to maintain the desired SSV in the CRR. At any time after the CRR bed temperature was above ~850°C, the FG flow was reduced and bed material was added to the DMR. Once the bed material had been added to the DMR, the FG flow was again increased. The heat-up of both reformers continued until the desired operating temperatures were reached in both.

To decrease the CRR temperature slowly over a period of time, the carbon feed rate and oxygen injection rate to the CRR were reduced. To provide a faster temperature response in the CRR, water could be injected directly into the CRR bed through a manually controlled service water injector in the bed. Manual flow control valves and a rotameter were provided to monitor the service water flow to the CRR. During operations, the bottom zone of the CRR fluidized bed (below the oxygen/air distributors) operated under strongly reducing conditions to facilitate additional NO_X conversion. Above the in-bed oxygen/air distributor(s), the CRR operated in an oxidizing mode to convert carbon monoxide, hydrogen, and organics from the DMR to carbon dioxide and water vapor.

The pilot plant had an emergency shutdown capability that could isolate the oxygen and gas flow to the CRR upon activation of an emergency shutdown signal or upon loss of power to the plant. The oxygen and air supplies also were provided with emergency isolation manual ball valves to provide positive isolation of oxygen from the process. Nitrogen purges were provided to prevent plugging of the in-bed nozzles during these shutdowns.

2.9 Off-Gas Cooler

The Off-gas Cooler (OGC) (T-400) consisted of a direct contact, deionized water spray, air-atomizing nozzle inserted into a 24-in. diameter × 96-in. tall vessel downstream of the CRR. The OGC was designed to reduce the temperature of the CRR product gas to as low as 130 to 180°C in a fraction of a second. The water supply was provided with an automated flow control valve that could maintain the off-gas temperature typically within a 130 to 180°C range. The flow rate of cooling water was automatically controlled by the DACS, but the flow rate of atomizing air was controlled manually. Thermocouples, with readouts on the DACS, were placed upstream and downstream of the OGC. The downstream thermocouple indication automatically controlled the flow of water to the OGC via the DACS.

2.10 Quencher/Scrubber System

The off-gas from the CRR could be directed to a Quencher/Scrubber (Q/S) system for purposes of removing acid gases from the CRR process gas stream. However, early in the test program, the Joint Test Group (JTG), which monitored and controlled testing activities, determined that the Q/S system was not needed during the SBW testing because acid gas formation from SBW feed was very low. Consequently,

all SBW scoping and production run tests were performed without the use of the Q/S system. A description of the Q/S system is included here for completeness.

The Q/S system consisted of existing venturi and packed bed scrubbers at the Hazen facility. A new pad-type mist eliminator was installed at the top (downstream side) of the packed bed scrubber. The scrubbers could be used to remove any acid gases from the off-gas, neutralizing them by injection of sodium hydroxide solution to yield sodium salts (e.g., NaCl and Na_2SO_4). The rate of NaOH injection could be controlled by an automated system that monitored the pH of the scrubber solution and added NaOH to maintain a preset solution pH.

The venturi scrubber (T-401) could be operated so as to concentrate the scrubber solution from 20% to 25% by weight of dissolved and suspended solids to minimize the amount of solution generated. A recirculation pump was provided to recirculate the neutralizing solution through the scrubber. In order to concentrate the scrubber solution, the venturi scrubber could be operated at the saturation temperature at the system pressure. The spent scrubber solution, if generated, would have been placed into plastic drums and stored.

The packed bed scrubber (T-402) was also intended to be operated at the saturation temperature and system pressure, preventing water vapor in the off-gas from condensing in the packed bed. An external electric heater was provided to heat the scrub solution to the desired operating temperature for the packed bed scrubber system. A recirculation pump was provided to recirculate the packed bed scrubber solution. The rate of NaOH injection into the packed bed scrubber could be controlled by an automated system that monitored the pH of the scrubber solution and added NaOH to maintain a preset solution pH. The mist eliminator at the outlet of the packed bed was provided to capture and remove any mist carryover from the scrubbers.

A NaOH addition capability was provided to both scrubber units to allow for independent pH control. Two pH meters provided the means to continuously monitor scrubber pH. Two caustic addition pumps were provided to meter caustic on a continuous basis at variable rates into the two scrubbers, as required.

A scrubber by-pass line was installed from a point immediately downstream of the OGC to the inlet of the off-gas reheater. Bypassed gases passed through the reheater and entered the inlet of the Process Baghouse Filter (PBF). During all the scoping and production runs (CP1 and CP2) the process was operated with the Q/S system off-line.

2.11 Off-Gas Reheater

The off-gas exiting the OGC was saturated with water vapor (up to 70 vol%). To prevent moisture from condensing and damaging downstream off-gas equipment, an electric reheater (H 403) was used to raise the off-gas temperature to well above the dew point. This reheater raised the off-gas temperature from ~95°C from a minimum of 120°C to a maximum of 190°C. The 480VAC/3-phase reheater was rated at 25kW. A silicon-controlled rectifier was used to maintain the reheater at the desired power level and to prevent excessive temperature buildup in the heater elements.

2.12 Process Baghouse Filter

The PBF (T-406) was installed downstream of the Off-gas Reheater. Figure 2-8 shows the process baghouse filter, one of three off-gas blowers, and the mercury adsorber. The purpose of the PBF was to remove and collect any fine solids elutriated from the CRR during processing.

Figure 2-8. Hazen Process Baghouse Filter, Off-gas Blower, and Mercury Adsorber Systems.

The PBF was a vertical, rectangular vessel designed to hold high-temperature-rated, bag-type filter elements. The filter bags were Teflon-coated fiberglass felt rated for 250°C. An automated instrument air pulse-back manifold was used to clean the filter elements with the filters on-line. The difference between two PTs, with sensing ports in the vessel inlet and in the gas outlet line downstream of the vessel, gave the pressure drop across the filters. When the pressure drop exceeded the setpoint, the DACS automatically actuated the pulse-back function.

External electrical heaters (H-406) were installed to maintain the filter elements and vessel above the gas dew point to prevent moisture condensation on the filter media during normal operations and during start-up and shutdown periods. The PBF was provided with a product draining system using a full-port ball valve and a sealed canister with a 5-gal capacity.

2.13 Mercury Adsorber

A sulfur-impregnated Granular Activated Carbon (GAC) bed (T-408) was provided in the off gas system downstream of the PBF. The purpose of the GAC bed was to remove elemental mercury from the gas stream during processing. The GAC unit was a three-stage bed with sampling capability downstream of Stage 1 and downstream of Stage 2. Additional mercury analyses were performed in the stack as part of the total metals analysis in the stack emissions off-gas monitoring system. Thermocouples and temperature alarms were incorporated into the design of the GAC adsorber to identify transient temperature excursions that might occur. A high temperature alarm would invoke an emergency shutdown of the process and trigger the emergency shutdown system, which would purge the GAC vessel with nitrogen from high pressure nitrogen gas bottles. External electrical heaters (H-408, -409, and -410) were installed to maintain the GAC vessel above the gas dew point to prevent moisture condensation on the GAC media during all periods of operation.

For the CP2 test, The GAC unit was modified to provide additional gas sampling capability upstream of the entire unit, as well as between each of the three stages.

2.14 Off-Gas Blowers

Three Off-gas Blowers (OGBs) (B-404, B-407 and B-409) provided airflow and process vacuum for the DMR, HTF, CRR, and the downstream off-gas treatment equipment. The three OGBs were located upstream of the PBF, downstream of the PBF, and downstream of the GAC bed. Multiple OGBs were required to minimize the vacuum in the PBF and the mercury adsorber, as well as to provide the necessary gas flow rate. The freeboard vacuum of the CRR was maintained at -10 to -30 in. water column (WC). The off-gas was discharged through a monitored exhaust stack in compliance with State of Colorado environmental laws.

2.15 Process Data Acquisition And Control System

The test system Data Acquisition and Controls System (DACS) used National Instruments Programmable Automation Controllers (PACs) for control and data acquisition. The PAC architecture is a combination of LabView software, Fieldpoint Controllers, and I/O Modules. LabView software was utilized to monitor and control operations of the process from two or more human-machine interfaces (HMIs) running on Personal Computers (PCs) located in a control room adjoining the process equipment area. Additional PCs were available for monitoring only (no control allowed) from three remote locations. The Fieldpoint Controllers contained real-time (RT) programs that ran independently of any PC. These RT programs ran the primary control algorithms for the process. The Fieldpoint I/O Modules were the means of acquiring signals from and transmitting signals to field devices and sensors to be used in the DACS.

The process control functions included automatic and/or manual control of the following primary process loops:

- Superheater #2 Temperature Control
- DMR Fluidizing Temperature Control
- DMR Bed Fluidizing Flow
- DMR Temperature Control
- DMR Simulant Feed Control
- DMR Atomizing Control
- DMR H_2 Control
- DMR Carbon Feedrate Control
- DMR Shotpot Control
- Cyclone Timer Control
- HTF Temperature Control
- HTF Blowdown Timer Control

- CRR Temperature Control
- CRR O_2 Control
- CRR N_2 Control
- CRR Shotpot Control
- CRR Carbon Feedrate Control
- OGC Temperature Control
- Reheater Temperature Control
- PBF Temperature Control
- PBF Blowdown Timer Control
- GAC Temperature Control
- Blower Control.

The HMIs for the system showed the status of components, provided a control interface for the operators, and displayed readings from all the instrumentation in numerical and graphical trend form. In addition, the HMI performed NO_X destruction calculations and displayed the calculated results on the HMI.

The data acquisition system utilized National Instrument's proprietary Citadel database for electronically archiving data as it was monitored. Each day, data was transformed from the Citadel database to an SQL database where it could be exported to an Excel spreadsheet for analysis. Each record in the database included the tag name for the data-point, the description, the value, the units, and a time-stamp.

3. MEASUREMENTS, SAMPLE COLLECTION, AND SAMPLE ANALYSIS

3.1 Process Measurements

Key process data were recorded during the scoping and production runs. Many other parameters and calculations, including the CEMS data, were automatically logged. Additional parameters, such as purge-gas flow rates, measured using rotameters, were logged manually.

Process data logged by the DACS database was done according to appropriate deadband settings. A deadband is the minimum percentage of a given range by which a measured value must vary in order for the DCS to register a change. For example, if a DACS channel reading pressure is ranged 0-100 PSI and the channel "update" deadband is set to 1%, then the pressure from the device must vary by at least 1 PSI in order for the DACS to realize a change of value.

The two main deadbands that control logging resolution were as follows:

- Update deadband. This parameter dictated the threshold that a value must change by before a new value is registered in the tag engine for update on the HMI.
- Logging deadband. This parameter dictated the threshold that a value must change by before it is actually logged in the Citadel database.

The deadband setting that was of most concern was the logging deadband. In this DACS, the update deadbands were always set equal to or smaller than the logging deadbands. This allowed the DACS to update sensor/device values at least as frequently as it logged those values.

Process data that were not electronically logged by the DACS system was recorded manually on operator data sheets. Manual control of certain process parameters was also done according to operator discretion and the test plan. The measured data are provided in subsequent sections of the report.

3.2 Continuous Process Monitoring System

Continuous monitoring of process gas streams and gaseous emissions provided real-time off-gas composition measurements for process control, safety, air emissions measurements, and mass balance calculations such as NO_X destruction determinations. Continuous process gas measurements were made at the outlet of the HTF and immediately downstream of the CRR. The concentrations of the individual gas stream components were logged into the DACS.

At the outlet of the HTF downstream of the DMR, the continuous process monitoring system (CPMS) monitored for O_2, CO_2, CO, NO, NO_2, NO_X, H_2, and total hydrocarbons (THC). The THC, carbon monoxide, and hydrogen measurements provided an indication of the extent of reducing conditions existing in the DMR. Measurements of nitrogen oxides indicated the extent of nitrate conversion to nitrogen gas in the DMR. The amount of carbon reductant added to the DMR to maintain adequate reducing conditions was controlled by monitoring the hydrogen concentration in the DMR process outlet gas.

At the second CPMS location, downstream of the CRR, O_2 was the only gaseous constituent measured. Output from the oxygen analyzer controlled the amount of excess oxygen in the CRR and was used to determine if an adequate oxidizing environment existed in the CRR to ensure oxidation of carbon monoxide.

Table 3-1 identifies the types of analyzers and their relevant analytical capabilities used at the two sampling locations. The analyzers listed in Table 3-1 were used in conjunction with sample conditioning equipment that included sample probes, heated sample lines running from the sample point to the instrument location, filters, condensers, pumps, manifolds, and calibration gases. The analyzers were calibrated with calibration gases typically before, during, and after each series of tests. The actual calibration frequency was determined by consideration of the calibration error and calibration drift that the CPMS incurred during each test, as well as consideration of when the analyzers needed to be on-line for key test periods. The entire suite of process gas analyzers was typically calibrated at least once per operating day. The CPMS data were adjusted for calibration error, drift, linearity, interferences, or bias, as necessary, following the test.

3.3 Continuous Emissions Monitoring System

The continuous emissions monitoring system (CEMS) was used to generate emissions data to be used for environmental permitting and risk assessment activities. The CEMS sampling ports were located at the inlet of the carbon bed and in the exhaust stack immediately downstream of Blower B-409. The CEMS monitored for CO_2, CO, O_2, NO, NO_2, total NO_X, SO_2, THC, and Hg. The Hg CEMS was provided for CP2 (it was not used during CP1) by ADA Technologies, Inc., and was operated by Hazen personnel. The other CEMS, which contained all the other instruments, was provided and operated by Air Pollution Testing, Inc. (APT). All activities associated with the operation of the CEMS were in accordance with the appropriate, applicable Environmental Protection Agency (EPA) Methods. Table 3-2 lists the specific analytes of interest, the reference EPA method, and the specifications for the instruments used in the APT CEMS.

Sulfur dioxide (SO_2) was measured at the stack sample location along with the other gas species for both CP1 and CP2. SO_2 was also measured during two short CP2 periods upstream of the mercury adsorber, after testing indicated that the carbon bed tended to release small amounts of SO_2, which added to the process SO_2 that was measured at the stack. The S measured upstream of the carbon bed did not include any SO_2 that evolved from the carbon bed, providing a more direct measurement of the process SO_2 emissions during those time periods.

The Hg CEMS was separate from the other CEMS and was used only during CP2. An inadvertent bypass of off-gas around the carbon bed during CP1 resulted in stack gas Hg concentrations higher than would have occurred, had all the off-gas passed through the carbon bed when Hg was included in the simulant feed. This Hg contaminated piping and equipment downstream of the carbon bed during CP1. The Hg CEMS was used during CP2 to determine if continued Hg emissions from the residual contamination were: (a) significantly higher than the HWC MACT standard for Hg such that the test would not be able to demonstrate MACT Standard compliance, and (b) high enough that continued operation might exceed the state of Colorado emission limit for the test program of 10 lb total Hg.

The Hg CEMS included a sample probe, particulate filter, thermo-electric gas cooler to condense moisture from the sample gas, a sample pump, and the analyzer. The analyzer was an Ohio Lumex RA 915+ atomic absorption unit with Zeeman correction. The full-scale range was 0–7,200 $\mu g/m^3$. This analyzer was rangeable down to about 0–100 $\mu g/m^3$. The analyzer detection limit was about 10 $\mu g/m^3$ or higher. This sensitivity was sufficient for the test objectives, but was not sensitive enough to use the Hg CEMS to determine reliably if the stack Hg levels were within HWC MACT limits.

Table 3-1. Analyzers used in the CPMS.

Gas Species	Instrument	Detection Principle	Range	Acceptance Limits (% of Full Scale)				Reference Method
				Calibration	Drift	Linearity	Bias	
HTF Outlet:								
CO	CAI*, Model 100	NDIR	0–10%	5	10	2	—	40 CFR 60 App. A Method 10
CO_2	Nova, Model 4230	NDIR	0–100%	2	3	4	5	40 CFR 60 App. A Method 3A
**NO, NO_2, NO_X	CAI*, Model 400CLD	Chemiluminescence	0–3000 ppm	2	3	4	5	40 CFR 60 App. A Method 7E
**NO, NO_2, NO_X	TECO Model 42C	Chemiluminescence	0–500 through 0–5,000 ppm	2	3	4	5	40 CFR 60 App. A Method 7E
H_2	Nova, Model 4230	Thermal conductivity	0–20%	—	—	—	—	—
THC	TECO***, Model 51	FID	0–10,000 ppm	5	3	—	—	40 CFR 60 App. A Method 25A
O_2	Horiba PMA 200	Paramagnetic	0–2% 0–25%	2	3	4	5	40 CFR 60 App. A Method 3A
CRR Outlet:								
In situ O_2	Teledyne 9060UH-HT	Zirconium oxide	0–25%, 0–100%	2	3	4	5	40 CFR 60 App. A Method 3A

Two CO_2/H_2 monitors were used. Each of these monitors measured CO_2 and internally performed a pre-calibrated correction for the interference from CO_2 on the H_2 measurement.

*California Analytical Instruments, Inc.
**Two NO_X monitors were used. The TECO was on loan form Air Pollution Testing.
***Thermo Electron Corporation

FID = Flame ionization detection
NDIR = Nondispersive Infrared

Table 3-2. Analyzers used in the APT CEMS.

Gas Species	Instrument	Detection Principle	Range	Acceptance Limits (% of Full Scale)				Reference Method
				Calibration	Drift	Linearity	Bias	
CO	TECO Model 48H	Gas Filter Correlation IR	0–100 through 0–500 ppm,	5	10	2	—	40 CFR 60 App. A Method 10
CO_2	Servomex Series 1400	NDIR	0–25%	2	3	4	5	40 CFR 60 App. A Method 3A
NO, NO_2, NO_X	TECO Model 42C	Chemilumi-nescence	0–500 through 0–5,000 ppm	2	3	4	5	40 CFR 60 App. A Method 7E
SO_2	Western Research Model 721M	UV	0–10 through 0–1,000 ppm	2	3	—	5	40 CFR 60 App. A Method 6C
THC	JUM Model VE-7	FID	0–20 through 0–10000 ppm	5	—	—	—	40 CFR 60 App. A Method 25A
O_2	Servomex Series 1400	Para-magnetic	0–25%	2	3	4	5	40 CFR 60 App. A Method 3A

3.4 Periodic Manual Stack Gas Sampling

Supplemental sample points were provided in the off-gas line for the purpose of obtaining manual samples for subsequent off-site analysis. These sampling stations were used to collect process grab samples in order to support the environmental permitting process, risk assessment development, and the design of the GAC mercury adsorber for the full-scale treatment facility. Manually obtained gas samples were analyzed for metals, particulate matter, hydrochloric acid, chlorine, dioxins, furans, polychlorinated biphenyls, volatile organic constituents, semi-volatile organic constituents, and total organics. As part of these methods, the gas flow rates (velocity traverses), carbon dioxide, oxygen, and moisture content of the exhaust gases were also determined. In each case, an appropriate EPA Method was used to acquire, analyze, and report the result of those analyses.

The schedule of manual sampling for CP1 is shown in Table 3-3. The scope of manual gas sampling during CP2, shown in Table 3-4, was more limited, consistent with the CP2 test objectives.

The primary location of the sampling stations was in the vertical exhaust stack immediately downstream of Blower B-409. A seven-foot straight section of duct was provided between the nearest upstream flow disturbance (elbow) and the first of three pairs of sample ports. The three pairs of ports were separated by a distance of about 28 in., slightly greater than four duct diameters. Three sample locations were provided so that multiple sample acquisition events could be performed simultaneously. The sampling ports consisted of 2-in. diameter pipe nipples welded to the 6-in. diameter exhaust stack. These sampling ports were capped when not in use. The manual stack gas sampling ports were in addition to the ports utilized for the CEMS instrumental analyses described in Section 3.3.

Manual sampling (for Hg only) was also performed at the outlet of the mercury adsorber Stages 1 and 2 during CP1, and at the outlet of all three carbon bed stages during CP2. The purpose of these additional samples was to determine the effectiveness of each stage of the GAC adsorber to remove mercury from the gas stream. The metals analysis samples taken from the stack sampling ports also determined the mercury concentration.

Isokinetic and extractive samples taken at all locations were collected in impingers, filters, absorbents, and Tedlar bags for subsequent laboratory analysis. Sample acquisition was performed in accordance with the appropriate EPA Method by APT. Sample analyses were performed by Severn Trent Laboratories. All samples withdrawn from the process were carefully collected, individually packaged, recorded, and archived. Chain of custody documentation was prepared for all samples taken for environmental permitting purposes.

3.5 Periodic Process Liquids and Solids Sampling

Samples of process additives, including the waste feed simulant solutions, and the solid products from the PR, HTF, and PBF were collected and analyzed during each operational test phase. Solid product sampling and analyses were performed for mass balance purposes and to establish the acceptability of the material for ultimate disposal at WIPP. Solid products were also analyzed for physical and chemical properties such as particle size distribution, particle density, bulk density, mineralogy, and individual chemical constituents.

The chemical characteristics of the material generated by this pilot plant testing are expected to be similar to those of the IWTU facility when treating actual SBW. As such, a determination of whether or not the pilot plant product exhibited the characteristics that would preclude its acceptability at WIPP was relevant. Such analysis would also provide data that would eventually support the development of Acceptable Knowledge/Process Knowledge characterization information with respect to the IWTU waste.

Table 3-3. Off-gas manual sampling train schedule.

		Analyte									
									Total Organics		
Production Test Number	Planned Duration, hr	Hg GAC #1	Hg GAC #2	Metals	PM/ ($HCl+Cl_2$)	Dioxins/ Furans/ PCBs	VOCs	SVOCs	Field Gas Chromatograph (FGC)	Total Chromatographable Organics/Gravimetric (TCO/Grav)	Total Trains
		EPA 29	EPA 29	EPA 29	EPA 5/26A	EPA 0023A	EPA 0031	EPA 0010	EPA 0040	EPA 0010	
1	36			1	1		1	1	1	1	6
2A	24			1	1						2
3B	24	1	1	1	1						4
4A-1	24	1	1	1	1	1	1	1	1	1	9
4A-2	24	1	1	1	1	1	1	1	1	1	9
4A-3	24	1	1	1	1	2*	2*	2*	2*	2*	14
4A-4	24	1	1	1	1	1	1	1	1	1	9
4A-5	24	1	1	1	1	1	1	1	1	1	9
4A-6	24	1	1	1	1	1	1	1	1	1	9
5	24	1	1	1	1						4
6	24	1	1	1	1						4
	Total trains	9	9	11	11	7	8	8	8	8	79

* Due to a process upset, these sample trains were repeated on the following day of operation.
Hence, duplicate runs are indicated.

Table 3-4. CP2 stack gas particulate matter and hazardous metals concentrations and emission rates.

			Sample Location			
			Carbon Bed Outlet			
			1	2	3	Stack
Date	Test Period	Test	OHM	OHM	OHM	Method 29
1-Jun-06	1550-1910	1	x	x	x	x
3-Jun-06	1150-1550	2	x	x	x	x
5-Jun-06	1110-1440	3	x	x	x	x
6-Jun-06	1040-1415	4	x	x	x	x
7-Jun-06	0950-1310	5	x	x	x	x
7-Jun-06	1745-2110	6	x	x	x	x

OHM (Ontario Hydro Method)

(cp2 off-gas emissions aug 8.xls) scope of manual tests

It was expected that the product would not meet Toxicity Characteristic Leaching Procedure (TCLP) standards due to the presence of certain heavy metals that would likely not be immobilized by the carbonate-based product solid matrix. Although it is not necessary to meet TCLP standards to dispose of waste at WIPP, it was necessary to demonstrate that the solid products (material from the PR and HTF), did not exhibit other characteristically hazardous properties such as corrosivity, explosivity, reactivity, ignitability, or pyrophoricity. It is also necessary to demonstrate that the product contains no detectable liquids, which can be formed in the steam reformer process only if the product is deliquescent. Corrosivity is not an issue for the SBW solid product because WIPP considers non-liquid products to be non-corrosive by definition. (See *Remote-Handled Transuranic Waste Acceptance Criteria for the Waste Isolation Pilot Plant*, [R12]).

Table 3-5 presents a summary of the liquid and solid sampling and analyses performed for this test program that is representative, but not all-inclusive. Examples of liquid and solid sampling that are not in Table 3-5 include several samples that were obtained and were not scheduled, other laboratories that were employed, and some different analytical methods that were employed for special situations.

Table 3-5. Process liquids and solids sampling and analysis summary.

Sample Location	Sample Frequency	Analytical Laboratory	Analyses/Data Required
SBW Surrogate Solution	Once every makeup batch or as requested	Hazen Lab	Batch volume, concentration of each constituent in Table 3-6, %UDS if used
DMR Startup Bed Material	Bulk material and at beginning of each test	Hazen Lab	Concentration of each constituent in Table 3-6
DMR Carbon Additive	Bulk material and beginning of each test, at end, and composite of material fed	Hazen Lab	Ash constituents including constituents in Table 3-6.

Table 3-5. (continued).

Sample Location	Sample Frequency	Analytical Laboratory	Analyses/Data Required
DMR Active Bed Sample	Once every 4 hours or as requested	Hazen Lab, Chilworth Lab	Each event: total mass, particle size distribution (PSD), bulk density, particle density, wt% carbon. From Chilworth: reactivity, ignitability, pyrophoricity, explosivity, deliquescence. As Requested: wt% of each constituent in Table 3-6.
PR Solids Product	Once every 8 hours during scoping tests and once per day or as requested during production runs	Hazen Lab, Chilworth Lab	Each event: total mass, particle size distribution (PSD), bulk density, particle density. From Chilworth: reactivity, ignitability, pyrophoricity, explosivity, deliquescence. As Requested: wt% of each constituent in Table 3-6.
HTF Solids Product	Once every 8 hours during scoping tests and once per day or as requested during production runs	Hazen Lab, Chilworth Lab	Each drain: total mass. From Chilworth: reactivity, ignitability, pyrophoricity, explosivity, deliquescence. As Requested: Malvern PSD, bulk density, particle density, wt% of each constituent in Table 3-6.
CRR Starting Bed Material	Bulk material and at beginning of each test	Hazen lab	As Requested: Concentration of each constituent in Table 3-6
CRR Carbon Additive	Bulk material and beginning of each test, at end, and composite of material fed	Hazen Lab	As Requested: Analyze for ash constituents including constituents in Table 3-6.
CRR Mineralizing Additive	Bulk material and beginning of each test, at end, and composite of material fed	Hazen Lab	As Requested: Analyze for constituents in Table 3-6.
CRR Active Bed Sample	Every 8 hours or as requested	Hazen Lab	Each Drain: total mass, PSD, bulk density, particle density, wt% of each component in Table 3-6.
PBF Solids Product	Once every 8 hours or as requested during production runs	Hazen Lab, Chilworth Lab	Each Drain: total mass. From Chilworth: reactivity, ignitability, pyrophoricity, explosivity, deliquescence. As Requested: Malvern PSD, bulk density, particle density, wt% of each constituent in Table 3-6.
GAC Filter Media (Each of Three Stages, Multiple Samples from Each Stage)	At end of each test sequence/program	Hazen Lab	Mercury, sulfur, and chlorine content and mercury TCLP
CPMS and CEMS Condensates	Daily or as requested	Hazen Lab	pH, nitrate, nitrite, sulfate, NH_4^+, CN^-, Hg, TIC, TOC
CPMS carbon filter media	Weekly	Hazen Lab	Chloride, nitrate, nitrite, sulfate, HCN, NH_3, TGA or proximate analysis

Table 3-6. Analytes requested in liquid and solid sample analyses.

Cations	Cations	Anions	Other
Al	As[1]	Cl	Total C
B	Ce	F	
Ca	Cr[1]	NO_3	
Fe	Cs	PO_4	
K	Hg[1]	SO_4	
Mg	Ni	CO_3	
Mn	Pb[1]		
Na	Zn		
Si			
Zr			

Notes:
1 As, Cr, Hg, and Pb are RCRA heavy metals

The majority of the analyses were performed at an on-site laboratory at Hazen Research, Inc. Duplicate analyses of process solid grab samples, where needed to confirm WIPP acceptability, were performed by an independent, off-site laboratory (Chilworth Lab). Chain of custody documentation was prepared for all samples that were transferred to an off-site laboratory for analysis.

Results and discussion of the analyses of the samples obtained are presented in Section 7.

3.6 Metallurgical Analysis

The THOR® process utilizes moderate temperature thermal treatment to convert sodium-bearing liquid wastes into carbonate-rich solid products. Operation of the treatment equipment subjects the materials of construction to potentially corrosive environments. In order to verify the most suitable materials of construction and to determine acceptable corrosion allowances for the selected metal alloys for the full-scale production plant, it was necessary to install coupons of selected metal alloys into the process equipment for the duration of the test program. The coupons were subjected to thermal and chemical environments typical of the IWTU process operating conditions. Upon completion of the test program, the coupons, along with certain process equipment components (specifically, the HTF elements) were destructively examined to determine the extent of corrosion or wear. Corrosion mechanisms were identified and corrosion rates estimated.

Table 3-7 provides a list of metal coupons that were installed in each selected part of the process system for both the CP1 and CP2 demonstrations. Specific locations and the number of coupons at each location were identified. Prior to installing the coupons in the process equipment, each coupon was measured. Two coupons of each material were installed in the equipment prior to the start of the CP1 operations where one coupon was to be archived for future comparison with post-test coupons for the CP1 demonstration. At least one coupon of each metal was installed in the CP2 demonstration to serve as a confirmatory check on the corrosion that occurred during the shorter duration CP2 demonstration. The CP1 demonstration ran for a substantial period of time such that corrosion mechanisms and rates could be reliably determined. Material certificates of analysis were archived for all coupons. Coupons included a full penetration weld. In addition to coupons fabricated from candidate HTF filter materials, actual filter elements were fabricated from selected alloys or ceramics and installed in the HTF during testing.

Table 3-7. Corrosion coupons.

Process Location	Qty for CP1	Qty for CP2	Alloy
DMR – In bed above liquid waste feed injector	2	1	Haynes 556
	2	1	Haynes HR-160
	2	1	Inconel 230
	2	1	316L SS
DMR – Freeboard above bed	2	1	Haynes 556
	2	1	Haynes HR-160
	2	1	Inconel 230
	2	1	316L SS
		1	Inconel 601 – wire
		1	Inconel 617 – wire
		1	Inconel 625 – wire
		1	Haynes 556 – wire
		1	Haynes HR-160 – wire
		1	Alloy X – wire
		1	Alloy 693 – wire
HTF – On dirty side of filters suspended from inlet diffuser	2	1	Haynes 556
	2	1	Haynes HR-160
	2	1	Inconel 230
		1	316L SS
HTF Filter media:			Microfiltrex/Porvair
Sintered metal	2		Inconel 601 –Metal Fiber
Nominal 3-5 micron	2		Alloy VDM – Metal Fiber
		9	316L SS – Metal Powder
	2		Mott/Bekaert
	2		Inconel 601 – Metal Fiber
			Alloy HR – Metal Fiber
	2		Pall
			Inconel 601 – Metal Fiber
		5	Alloy X – Metal Powder
		4	Silicon Carbide - Ceramic

Table 3-7. (continued).

Process Location	Qty for CP1	Qty for CP2	Alloy
CRR – In bed above process FG distributors	2	1	Haynes 556
	2	1	Haynes HR-160
	2	1	Inconel 230
CRR – In bed above air/oxygen distributors	2	1	Haynes 556
	2	1	Haynes HR-160
	2	1	Inconel 230
CRR – Freeboard above bed	2	1	Haynes 556
	2	1	Haynes HR-160
	2	1	Inconel 230
QS – Submerged in tank	2		Hastelloy C-22
	2		Hastelloy C-276
	2		Hastelloy C-2000
	2		AL6XN
PBF – On upstream side of filters	2	2	316L SS
	2	2	317 SS
	2	2	AL6XN
		1	C-2000
		1	C-276
		1	C-22
PBF – Filter Element			Microfiltrex/Porvair
	2	2	Inconel 601 –Metal Fiber
PBF – Downstream side of filters		1	316L SS
		1	317 SS
		1	AL6XN
		1	C-2000
		1	C-276
		1	C-22

Upon completion of the test program the coupons were removed from the process equipment and shipped to a qualified metallurgical lab, Savannah River National Laboratory (SRNL), for analysis. Each coupon was measured and visually inspected by the lab. One of the two coupons of each material in each process location was destructively examined to identify the corrosion mechanism and extent of corrosion. An estimate of the extent of corrosion and corrosion rate was made for each coupon examined. A second metallurgical professional independently examined the results of the analyses and evaluations.

Two sets of corrosion coupons were prepared and evaluated, one set exposed during the CP1 operations and a second confirmatory set during the CP2 operations.

The detailed Metallurgical Plan GWI 1.5 provides details on the metallurgical evaluation plan for the corrosion coupons for both the CP1 and CP2 tests. Results of the metallurgical evaluation of the CP1 and CP2 corrosion coupons are discussed in Section 9.

4. SIMULANT COMPOSITIONS

Aqueous solutions of various metal salts in combination with organic constituents were prepared for use in the pilot plant test program. The non-radioactive simulants used are listed in Table 4-1.

Table 4-1. Composition of non-radioactive simulants.

Simulant Number	Composition
1	Baseline SBW supernatant solution to simulate the composition of actual SBW liquid decanted from the INL waste tanks.
2	Baseline SBW solution plus a quantity of UDS simulating fully mixed SBW slurry.
3	Fully mixed SBW slurry, plus the addition of selected heavy metals and radionuclide surrogates.
4	Fully mixed SBW slurry, plus selected heavy metals/radionuclide surrogates, plus one POHC.
5	Fully mixed SBW slurry (with heavy metals and radionuclide surrogates) but with a higher UDS loading, simulating a worst-case UDS concentration.
6	Very dilute SBW solution (including heavy metals and radionuclide surrogates) with a high UDS loading to simulate a water washdown of INL waste tanks to remove residual UDS sludge once the majority of the SBW liquid has been removed.
7	Baseline SBW supernatant solution plus selected heavy metals/radionuclide surrogates to simulate the composition of actual SBW liquid decanted from the INL waste tanks.

CP-1 testing used Simulants 1-6 while CP-2 testing used Simulants 1 and 7 only. Testing accomplished with Simulant 4 represented, as closely as is feasible in a pilot plant setting, the worst-case composition of the combined INL SBW liquid waste streams, with nominal UDS. Simulants 5 and 6 represented worst-case UDS loadings, and were intended to challenge the operability of the liquid feed and atomization system of the DMR. Simulant 7 represents the INL waste tank supernates, which will be the majority of the tank waste that will be processed through the IWTU.

The type and concentration of the components of the supernatant solution, the UDS, the appropriate heavy metals, and POHCs were derived from INEEL/EXT-2000-01378, “Feed Composition for the Sodium-Bearing Waste Treatment Process,” Revision 4, June 2004 [R13]. The composition of Tanks WM-187, -188, and -189 was considered in arriving at a baseline composition of the individual components of the feed materials. The compositions of the various components of the different types of feed liquids are discussed in the following sections.

4.1 SBW Supernatant Solution

Scoping Tests S-2 through S-8, and CP-1 Production Tests P-1 and P-2A used the surrogate materials and concentrations identified in the Table 4-2 baseline supernatant solution simulant. In most cases, the concentration value shown in the table represents the worst-case (highest) concentration found in the three tanks of interest or in the projected newly-generated liquid waste (NGLW) that is separate from the waste currently stored in WM-187, -188, and -189. For iron and manganese, which may have a beneficial catalytic effect on the process, the lowest concentration of the three tanks was used. The threshold concentration value used to determine whether cationic or anionic species were to be included in the formulation was 10-2 M. Species that were more dilute than 10-2 M were considered minor contributors and were not included in the baseline formulation. Neither surrogates for radionuclides nor heavy or toxic metals were included in the formulation of the baseline supernatant solution. The

concentration of the various constituents is given in both moles per liter (moles/L) and in parts per million (ppm) (by weight) assuming a specific gravity of the solution of 1.3. For the CP2 test, the concentration of phosphate was decreased to 0.005 moles/L to better reflect the concentration of phosphate in the SBW at the INL.

Table 4-2. Composition of baseline supernatant simulant solution (without heavy metals).

		CP1		CP2	
Component	Reagent	Conc. (moles/l)	Conc. (ppm)	Conc. (moles/l)	Conc. (ppm)
Acid	HNO_3 (See Nitrate)	3.06		3.06	
Aluminum	$Al(NO_3)_3 \cdot 9H_2O$	0.719	14,900	0.719	14,900
Boron	H_3BO_3	0.0217	180	0.0217	180
Calcium	$Ca(NO_3)_2 \cdot 4H_2O$	0.0731	2,250	0.0731	2,250
Iron	$Fe(NO_3)_3 \cdot 9H_2O$	0.0217	932	0.0217	932
Magnesium	$Mg(NO_3)_2 \cdot 6H_2O$	0.0257	480	0.0257	480
Manganese	$Mn(NO_3)_2$ (50 wt% sol'n, ρ=1.54)	0.0152	642	0.0152	642
Potassium	KNO_3	0.225	6,770	0.225	6,770
Sodium	$NaNO_3$	2.20	38,900	2.20	38,900
Anions in Solution					
Chloride	NaCl	0.0334	912	0.0334	912
Fluoride	HF (28.9 M sol'n)	0.0506	740	0.0506	740
Nitrate	HNO_3 (69 wt% sol'n, ρ=1.41)	7.53	359,000	7.53	359,000
Phosphate	$Na_3PO_4 \cdot 12H_2O$	0.0138	1,000	0.005	362
Sulfate	Na_2SO_4	0.107	8,070	0.107	8,070

Four batches of simulant were made for the scoping tests and ten for the production tests. Eight batches were made for the CP-1 testing and two batches were made for the CP-2 testing. The batches were produced using the procedure defined in Attachment A of OI 1.3, "Sodium Bearing Waste Pilot Plant Normal Operations" [R14].

Table 4-3 provides the as-analyzed chemical makeup of the SBW supernatant solution surrogates (without heavy metals) used in the CP1 and CP2 test programs. Samples of the feed solutions were acquired in accordance with OI 1.5, "Sodium-Bearing Waste Pilot Plant Solids and Liquid Sampling" [R15]. Several of the sample results exceeded the target composition by >20%. Since the elements that have discrepancies with the target are minor components of the simulant there is little effect to the process chemistry. The composition is reasonably close to actual SBW and representative of how SBW will be processed through the IWTU and how elements will interact and flow through the plant. The actual concentration of the feed is important to mass balance and the analytical results were used except where there was reason to use another concentration (see Section 7.8).

Table 4-3. CP1 chemical analysis of baseline simulant solutions (without heavy metals).

		CP1 Batch #1	CP1 Batch #2	CP1 Batch #3	CP1 Batch #4	CP1 Batch #5	CP1 Batch #6	CP1 Batch #10	CP1 Batch #14	CP2-1 TK100	CP2-2 TK 100
Batch Date		11/15/2005	11/16/2005	12/5/2005	1/6/2006	1/16/2006	1/22/2006	1/31/2006	2/3/2006	5/15/2006	6/3/2006
Batch Volume		26.4 gal	449.1 gal	1500 gal	1175 gal	1500 gal	1500 gal	1500 gal	1500 gal	1500 gal	1500 gal
Specific Gravity		N/A	N/A	N/A	1.31	1.32	1.34	1.32	1.3	1.34	1.34
Component	Desired Concentration (g/l)	Conc. (g/l)	Conc. (g/l)	Conc. (g/l)	Conc. (g/l)	Conc. (g/l)	Conc. (g/l)	Conc. (g/l)	Conc. (g/l)	Conc. (g/l)	Conc. (g/l)
Cations in Solution											
Acid as HNO3	195	190.00	190.00	167.00	161.00	162.00	174.00	162.00	151.00	144[1]	147[1]
Aluminum	19.4	11.40[1]	11.40[1]	18.00	20.80	17.70	18.50	17.40	16.90	21.9	21.1
Boron	0.235	0.23	0.23	0.21	0.19	0.22	0.11[2]	0.26	0.25	0.224	0.244
Calcium	2.93	3.23	3.23	3.43	2.87	2.73	2.94	2.64	2.59	3.14	3.17
Iron	1.21	1.27	1.27	1.55[1]	1.24	1.22	1.41	0.99	1.12	1.35	1.27
Magnesium	0.625	0.87[1]	0.87[1]	0.92[1]	0.76[1]	0.72	0.84[1]	0.62	0.60	0.764[1]	0.586
Manganese	0.835	0.73	0.73	1.30[2]	0.81	0.67	0.84	0.79	0.68	0.858	1.44[2]
Potassium	8.81	N/M	N/M	8.91	8.43	8.17	8.83	8.86	8.42	10.2	10.7[1]
Sodium	50.6	52.30	52.30	44.70	49.30	46.60	51.50	48.80	45.50	56.7	56.4
Anions in Solution											
Chloride	1.19	2.02[2]	2.02[2]	1.60[1]	1.76[1]	1.63[1]	2.01[2]	1.69[1]	1.72[1]	2.00[2]	2.03[2]
Fluoride	0.961	0.05[2]	0.05[2]	0.85	N/M	N/M	0.95	0.79	0.72	0.85	0.97
Nitrate	467	456.00	456.00	459.00	469.00	487.00	440.00	472.00	430.00	529	521
Phosphate	CP-1 = 1.31 CP-2 = 0.475	1.42	1.42	1.17	1.20	1.27	1.24	1.28	1.35	0.504	0.503
Sulfate	10.5	11.90	N/A	10.70	9.38	10.70	10.60	11.10	12.00	12.1	11.2

Notes:

1. Composition varies from the target by greater than 20%.
2. Composition varies from the target by greater than 50%.

N/A = Not Available
N/M = Not Measured

4.2 Undissolved Solids And Heavy Metals Simulants

The purpose of adding UDS to the feed mixture was to establish whether or not a slurry with the composition of a fully-mixed waste tank, specifically WM-187, that contains the majority of the UDS, can be accommodated by the design of the feed system and feed nozzle, and whether the system can process the feed simulant containing the UDS.

The composition of the UDS added to the supernatant solution to produce a combined supernate/UDS feed slurry is shown in Table 4-4. The third column of the table shows the concentration of the particular component in question; whereas, the fourth column shows the concentration of the reagent containing that component, e.g., the dry mixture of UDS consisted of 40.6 wt% $Zr(HPO_4)_2$, which resulted in a zirconium concentration in the mixture of 13.1 wt% and a phosphate concentration (as PO_4^{-3}) of 27.2 wt%.

Table 4-4. Composition of the UDS Added to the Supernatant Solution.

Component	Reagent	Component Concentration (wt%)	Reagent Conc. (wt%)
Aluminum	$Al_2O_3 \cdot 2SiO_2$ (kaolin)	2.2	8.9
Iron	Fe_2SiO_4	2.6	4.7
Silicon	Amorphous Silica	24.3*	22.9
	Ground Quartz		22.9
Zirconium	$Zr(HPO_4)_2$	13.1	40.6
Phosphate		27.2	

* Percentage shown includes the silicon contribution from both the kaolin and iron silicate

The particle size distribution of the UDS used for the test program matched that of the UDS in the INL waste tanks, i.e., 1-100 microns with a mean particle size of 10 microns. However, the zirconium phosphate received for use in the test program had a sizable (<5%) fraction of particles that exceeded 600 microns in size, which led to the following:

- A batch of UDS-bearing feed with the improper size distribution zirconium phosphate was made up. The processing of this surrogate batch led to plugging of the small (1/4 in.) tubing feed lines from the makeup feed tanks to the DMR and the waste feed injector. Processing of this batch of feed was successfully completed with installation of filters/strainers on the feed lines to remove oversize particles.

- The zirconium phosphate was sieved through a 30-mesh screen (595 micron) to separate the oversize particles from the feed.

- A second batch of UDS-bearing feed was made up where a portion of the zirconium phosphate used during makeup process was from the oversize portion of the screened zirconium phosphate. This led to a repeat of the plugging problems. This batch of feed was wet-sieved to remove the oversized zirconium particles and used in later testing.

The target concentration of UDS in the feed slurry was 93 grams per liter (g/L), which represented the expected UDS concentration found in Tank WM-187 if well mixed, which in turn, represented the worst case expected UDS loading in well mixed Tanks WM-187, -188, and -189. However, 14% of the mass of the UDS is water of hydration. Therefore, the net amount of insoluble materials with no waters of hydration to be added to the supernatant solution was 80 g/L. As the testing progressed, calcined kaolin clay was replaced by hydrated clay as the calcined clay was suspected of contributing to undesirable reactions in the DMR. When this change was made, the UDS from the clay was increased to meet the 93 g/L target stated above.

Batches of simulant solutions with 80 g/L unhydrated (93 g/L hydrated) UDS were generated using the procedure defined in Attachment C of OI 1.3, "Sodium Bearing Waste Pilot Plant Normal Operations" [R14]. To facilitate mixing and transfer of the UDS, four batches of UDS laden material were mixed in a small batch tank and then transferred to the feed tank.

Table 4-5 shows the as-added UDS content of the feed for the CP1 UDS production runs P-2A through P-4A-6.

CP1 production run P-2A involved the use of SBW with the addition of UDS only, without heavy metals and POHC. CP1 production runs P-3B through P-4A-6 included the addition of UDS and heavy metals, POHC, and radionuclide surrogates to the feed slurry. The reason for excluding these materials from scoping tests, CP1 production test P-1, and CP2 test DMR-1 was that a significant portion of the testing program could be accomplished without the added burden of industrial hygiene, waste disposal, and off-gas monitoring requirements attendant to using these hazardous materials. The additional metal salts included in the supernate/UDS/ heavy metal feed materials were derived from INEEL/EXT-2000-01378, Revision 4 [R13].

Chromium, arsenic, lead, mercury, nickel, cerium, cesium, and zinc were the selected metal salts added to the feed mixture for the heavy metal mixture (note that only chromium, arsenic, lead, and mercury are RCRA-listed heavy metals), and, in the case of these metals, the 10-2M threshold criterion was not considered. Beryllium, cadmium, silver, and selenium were not included in the heavy metal additive mix because of one or more of the following:

1. They have an extremely low concentration in the SBW tanks.

2. Their presence in the feed mixture would impose engineering controls and industrial hygiene requirements not available or feasible at the pilot plant facility.

3. Their chemistry in the DMR parallels, and was represented by, similar elements that were included in the feed mixture (e.g. cadmium was not include because it is chemically similar to zinc.).

Cerium was included in the mix as a surrogate for actinides expected to be present in the SBW tanks. Non-radioactive cesium was added to represent radioactive cesium isotopes known to be constituents in SBW. The expected concentrations of these two elements in the SBW tanks was very low (10^{-6} to 10^{-5} M), so their concentrations in the surrogate feed mixture were increased by a factor of 1,000 during CP1 and 100 during CP2 to increase their detectability in the solid products generated by the process.

Table 4-5. Production run UDS additions.

Component	Reagent	Reagent Conc. (wt %)	Reagent Weight Needed (kg)	Batch # 5A [1] Reagent Weight Added (kg)	Batch # 7 Reagent Weight Added (kg)	Batch # 8 Reagent Weight Added (kg)	Batch # 9 Reagent Weight Added (kg)	Batch # 11 Reagent Weight Added (kg)	Batch # 12 Reagent Weight Added (kg)	Batch # 13 Reagent Weight Added (kg)	Batch # 15 Reagent Weight Added (kg)
Aluminum	$Al_2O_3 \cdot 2SiO_2$ (kaolin)	8.9	12.8	11.3	12.8	12.8	12.8	12.8	12.8	12.8	12.8
Iron	Fe_2SiO_4	4.7	6.8	6.0	6.8	6.8	6.8	6.8	6.8	6.8	6.8
Silicon	Amorphous Silica	22.9	32.8	29.1	32.8	32.8	32.8	32.8	32.8	32.8	32.8
	Ground Quartz	22.9	32.8	29.1	32.8	32.8	32.8	32.8	32.8	32.8	32.8
Zirconium Phosphate	$Zr(HPO_4)_2$	40.6	58.4	51.8	58.4	58.4	58.4	58.4	58.4	58.4	58.4

Notes:

1. Batch 5A based on a 1600 liter final batch.
2. All UDS weights based on an 1800 liter final batch, except where noted.

Tests in which heavy metals and radionuclide simulants were used employed a supernatant solution similar to that shown in Table 4-2, but with additional cations included. Table 4-6 shows the target composition of the supernatant solution that included the heavy metal and radionuclide surrogates. Table 4-7 and Table 4-8 show the analytical composition of heavy metal batches from CP1 and CP2 testing respectively. Several of the sample results exceeded the target composition by >20%. Since the elements that have discrepancies with the target are minor components of the simulant there is little effect to the process chemistry. The composition is reasonably close to actual SBW and representative of how SBW will be processed through the IWTU, and how elements will interact and flow through the plant. The actual concentration of the feed is important to mass balance and the analytical results were used except where there was reason to use another concentration (see Section 7.8).

Table 4-6. Desired composition of the simulant solution (with heavy metal and radionuclide surrogates).

		CP-1		CP-2	
Component	Reagent	Concentration (M/l)	Concentration (ppm)	Concentration (M/l)	Concentration (ppm)
Cations in Solution					
Acid	HNO_3 (See Nitrate)	2.88		2.88	
Aluminum	$Al(NO_3)_3 \cdot 9H_2O$	0.719	14,900	0.719	14,900
Arsenic	$H_3AsO_4 \cdot 0.5H_2O$	0.000492	28.4	0	0
Boron	H_3BO_3	0.0217	180	0.0217	180
Calcium	$Ca(NO_3)_2 \cdot 4H_2O$	0.0731	2,250	0.0731	2,250
Cerium	$Ce(NO_3)_3 \cdot 6H_2O$	0.0483	5,210	0.00483	521
Cesium	$CsNO_3$	0.0353	3,610	0.00353	361
Chromium	$Cr(NO_3)_3 \cdot 9H_2O$	0.00569	228	0.00569	228
Iron	$Fe(NO_3)_3 \cdot 9H_2O$	0.0217	932	0.0217	932
Lead	$Pb(NO_3)_2$	0.00134	214	0.00134	214
Magnesium	$Mg(NO_3)_2 \cdot 6H_2O$	0.0257	480	0.0257	480
Manganese	$Mn(NO_3)_2$ (50 wt% sol'n, ρ=1.54)	0.0152	642	0.0152	642
Mercury	$Hg(NO_3)_2 \cdot 2H_2O$	0.00713	1,100	0.00713	1,100
Nickel	$Ni(NO_3)_2 \cdot 6H_2O$	0.00255	115	0.00255	115
Potassium	KNO_3	0.225	6,670	0.225	6,670
Sodium	$NaNO_3$	2.20	38,900	2.20	38,900
Zinc	$Zn(NO_3)_2 \cdot 6H_2O$	0.00498	250	0.008	402
Anions in Solution					
Chloride	NaCl	0.0334	912	0.0334	912
Fluoride	HF (28.9 M sol'n)	0.0506	740	0.0506	740
Nitrate	HNO_3 (69 wt% sol'n, ρ=1.41)	7.59	362,000	7.59	362,000
Phosphate	$Na_3PO_4 \cdot 12H_2O$	0.0138	1,000	0.005	362
Sulfate	Na_2SO_4	0.107	8,070	0.107	8,070

Table 4-7. Chemical analysis of CP1 simulant solutions (with heavy metals).

	Batch #7 T-101B	Batch #8 T-101A	Batch #9 T-101B	Batch #11 T-101A	Batch #12 T-101A	Batch #13 T-101B	Batch #15 T-101A
Test	P3B	P-4A1	P-4A2	P-4A3	P-4A4	P-4A5	P-4A6
Batch Date	1/28/2006	1/29/2006	1/30/2006	2/1/2006	2/2/2006	2/3/2006	2/4/2006
Batch Volume	1,800 liters	1,800 liters	1,800 liters	1,800 liters	1,800 liters	1,800 liters	1,800 liters
Batch Specific Gravity	1.37	1.38	1.39	1.37	1.35	1.37	1.33

Component	Desired Concentration (g/l)	Conc. (g/l)	Conc. (g/l)	Conc. (g/l)	Conc. (g/l)	Conc. (g/l)	Conc. (g/l)	Conc. (g/l)
Cations in Solution								
Acid	181	159.00	160.00	163.00	154.00	149.00	152.00	138.00
Aluminum	19.4	17.00	17.40	17.70	17.90	19.90	19.70	18.40
Arsenic	28.4 ppmw	24.00 ppmw	19.50 ppmw	21.50 ppmw	298.00 ppmw[2,3]	41.80 ppmw[1]	22.90 ppmw	24.60 ppmw
Boron	0.235	0.27	0.25	0.24	0.23	0.16	0.18	0.28
Calcium	2.93	2.82	2.80	2.91	2.59	2.62	2.67	2.54
Cerium	6.77	4.22	4.04	4.42	3.08[2]	2.07[2]	4.01	4.11
Cesium	4.69	6.47[1]	6.40[1]	6.60[1]	4.06	2.86	6.07[1]	6.09[1]
Chromium	0.296	0.23	0.24	0.25	0.23	0.11[2]	0.22	0.23
Iron	1.21	2.63[2]	2.84[2]	3.57[2]	3.63[2]	1.63[1]	2.34[2]	2.65[2]
Lead	0.278	0.26	0.26	0.26	0.25	0.24	0.26	0.24
Magnesium	0.625	0.69	0.75	0.78[1]	0.63	0.68	0.67	0.63
Manganese	0.835	0.73	0.76	0.77	0.73	0.73	0.73	0.61
Mercury	1,059 ppmw	1,280 ppmw[1]	1,300 ppmw[1]	1,320 ppmw[1]	1,390 ppmw[1]	1,320 ppmw[1]	1,310 ppmw[1]	1,340 ppmw[1]
Nickel	0.15	0.16	0.17	0.17	0.16	0.15	0.15	0.16
Potassium	8.8	8.82	9.45	9.11	8.78	8.45	8.81	7.73
Sodium	50.6	47.40	49.40	48.90	46.40	45.80	45.90	42.70
Silicon	19.4	19.20	20.00	20.30	20.10	17.70	21.20	20.90
Zinc	0.326	0.32	0.30	0.32	0.30	0.30	0.32	0.35
Zirconium	10.5	6.17	3.17[2]	6.53	7.81	3.91[2]	5.48	4.92[2]

Table 4-7. (continued).

Component	Desired Concentration (g/l)	Conc. (g/l)	Conc. (g/l)	Conc. (g/l)	Conc. (g/l)	Conc. (g/l)	Conc. (g/l)	Conc. (g/l)
Anions in Solution								
Chloride	1.18	0.72	0.79	0.84	1.10	1.15	1.21	1.07
Fluoride	0.961	0.84	0.83	0.89	0.78	0.72	0.75	0.60
Nitrate	471	526.00	475.00	473.00	462.00	463.00	462.00	382.00
Phosphate	23.07	17.50	20.30	23.40	27.50	15.70	21.20	28.50[1]
Sulfate	10.3	10.28	10.35	10.70	10.28	10.30	N/A	9.46

Notes:

1. Composition varies from the target by greater than 20%.
2. Composition varies from the target by greater than 50%.
3. Batch #11 arsenic high due to incorrect addition of arsenic acid during batch makeup (900 ml added instead of 90 ml).

N/A = Not Available

Table 4-8. Chemical analysis of CP2 simulant solutions (with heavy metals).

		CP2-M1 TK 101B	CP2-M2 TK 101A	CP2-M3 TK 101B	CP2-M4 TK 101A
Batch Date		6/3/2006	6/4/2006	6/5/2006	6/6/2006
Batch Volume		1800 liters	1800 liters	1800 liters	1800 liters
Batch Specific Gravity		1.35	1.36	1.36	1.36
Component	Desired Concentration (g/l)	Conc. (g/l)	Conc. (g/l)	Conc. (g/l)	Conc. (g/l)
Cations in Solution					
Acid	181	149	144	145	144
Aluminum	19.4	21.6	21.7	21.1	21.6
Arsenic	0	N/M	N/M	N/M	N/M
Boron	0.235	0.225	0.257	0.229	0.238
Calcium	2.93	3.03	3.09	3.23	3.03
Cerium	0.677	0.519[1]	0.508[1]	0.491[1]	0.507[1]
Cesium	0.469	0.402	0.417	0.420	0.426
Chromium	0.296	0.252	0.244	0.240	0.245
Iron	1.21	1.29	1.30	1.33	1.30
Lead	0.278	0.242	0.256	0.265	0.266
Magnesium	0.625	0.773[1]	0.609	0.603	0.570
Manganese	0.835	0.808	1.38[2]	1.37[2]	1.40[2]
Mercury	1059 ppmw	1111 ppmw	1103 ppmw	1103 ppmw	1118 ppmw
Nickel	0.15	0.141	0.146	0.145	0.148
Potassium	8.8	10.2	10.1	10.1	10.3
Sodium	50.6	52.9	53.5	55.5	58.0
Silicon	0	N/M	N/M	N/M	N/M
Zinc	0.523	0.522	0.524	0.523	0.522
Zirconium	0	N/M	N/M	N/M	N/M
Anions in Solution					
Chloride	1.18	1.43[1]	1.48[1]	1.54[1]	1.47[1]
Fluoride	0.961	0.93	0.93	0.92	0.94
Nitrate	471	524	488	545	544
Phosphate	0.475	0.562	0.572[1]	0.582[1]	0.572[1]
Sulfate	10.3	10.9	11.0	12.1	11.6

Notes:

1. Composition varies from the target by greater than 20%.
2. Composition varies from the target by greater than 50%.

N/A = Not Available

For the CP2 test it was decided, as written in the test plan, to modify the composition of the heavy metal SBW simulant. The following changes were made to the heavy metal surrogate target concentrations:

- The cesium and cerium target concentrations were reduced by a factor of 10. The concentrations used during CP1 testing were a factor of 1000 greater than the concentrations in of actual SBW for detectability. However, CP1 testing indicated that cesium and cerium would be detectable at a concentration 10x less than was used.
- Arsenic was not added to the heavy metal surrogate during CP2 testing. CP1 testing showed that the arsenic is captured in the solid product and not released in the process off-gas. Arsenic is not expected to influence DMR bed particle size since it is only present at very low concentrations and due to the industrial hygiene challenges associated with arsenic it was decided not to include arsenic in the surrogate.
- The phosphate target concentration was reduced from 0.138 M to 0.005 M to better reflect the concentration of the SBW at the INL.
- The zinc target concentration was increased to 0.008 M to represent the total concentration of zinc plus cadmium in the SBW on a mass basis rather than on a molar basis. Zinc and cadmium are chemically similar and therefore can be used to determine the fate of cadmium, which is a concern to industrial hygiene in the IWTU.

Batches of simulant solutions with heavy metal and radionuclide surrogates were generated using the procedures defined in Attachments B and C of OI 1.3, “Sodium Bearing Waste Pilot Plant Normal Operations” [R14]. Table 4-7 and Table 4-8 provide the desired and as-analyzed chemical makeup of the SBW supernatant solution simulants (with heavy metals) used in the CP1 and CP2 tests respectfully.

CP1 Production Test P-5 was run at a higher UDS loading to represent a more concentrated INL tank slurry, i.e., one in which some of the solution is decanted from the tank, but where the remaining solids and liquids are fully mixed. In this case, the concentration of UDS was 120 g/L unhydrated (140 g/L hydrated), a 50% increase over the UDS composition of Tank WM-187. This surrogate was produced in the same manner as the UDS and heavy metal additions above, with the exception that the higher level of UDS was added in a total of six additions instead of four. Table 4-9 and Table 4-10 show the UDS additions and SBW simulant analyses for CP1 Production Test P-5.

Production Test P-6 was conducted at the 120-g/L level of UDS unhydrated (140 g/L hydrated), but with a supernatant solution at only 10% of the concentration of that expected in Tank WM 187. This test simulated a concentrated UDS sludge being rinsed out of the tank with a dilute supernate solution or with water. This surrogate was produced using Attachments C and F of OI 1.3, “Sodium Bearing Waste Pilot Plant Normal Operations” [R14]; Table 4-9 and Table 4-11 show the UDS additions and SBW simulant analyses for Test P-6.

Table 4-9. Reagent additions for CP1 production runs 5 and 6 with 120 g/L UDS.

				Batch #16	Batch #17
				2/5/2006	2/10/2006
				CP-1 Test P-5	CP-1 Test P-6
Component	Reagent	Reagent Conc. (wt %)	Reagent Weight Needed (kg)	Reagent Weight Added (kg)	Reagent Weight Added (kg)
Aluminum	$Al_2O_3 \cdot 2SiO_2$ (kaolin)	13.4	19.2	19.2	19.2
Iron	Fe_2SiO_4	7.0	10.2	10.2	10.2
Silicon	Amorphous Silica	34.4	49.2	49.2	49.2
	Ground Quartz	34.4	49.2	49.2	49.2
Zirconium Phosphate	$Zr(HPO_4)_2$	60.9	87.6	87.6	87.6

Table 4-10. Chemical analysis of simulant solutions for CP1 Run 5 (with heavy metals, 120 g/L UDS).

		Batch #16 T-101A			
Batch Date		2/5/2006			
Batch Volume		1800 liters			
Batch Specific Gravity		1.36			
Component	Desired Concentration (g/L)	Conc. (g/L)	Component	Desired Concentration (g/L)	Conc. (g/L)
Cations in Solution					
Acid	181	140.00[1]	Magnesium	0.625	0.63
Aluminum	19.4	18.90	Manganese	0.835	0.61[1]
Arsenic	28.4 ppmw	24.30 ppmw	Mercury	1059 ppmw	1400.00 ppmw[1]
Boron	0.235	0.19	Nickel	0.15	0.16
Calcium	2.93	2.48	Potassium	8.8	7.70
Cerium	6.77	6.23	Silicon		29.90[2]
Cesium	4.69	4.45	Sodium	50.6	41.30
Chromium	0.296	0.23[1]	Zinc	0.326	0.33
Iron	1.21	3.01[2]	Zirconium		8.98[2]
Lead	0.278	0.25			
Anions in Solution					
Chloride	1.18	1.06	Phosphate	1.31	25.80[2]
Fluoride	0.961	0.61[1]	Sulfate	10.3	10.60
Nitrate	471	411.00			

Notes:

1. Composition varies from the target by greater than 20%.
2. Composition varies from the target by greater than 50%.

Table 4-11. Chemical analysis of 10% SBW simulant solutions for CP1 Run 6 (with heavy metals, 120 g/L UDS).

		Batch # 17			
Batch Volume		1800 liters			
Batch Specific Gravity		1.12			
Component	Desired Concentration (g/L)	Conc. (g/L)	Component	Desired Concentration (g/L)	Conc. (g/L)
Cations in Solution					
Acid	18.1	12[1]	Magnesium	0.0626	0.067
Aluminum	1.94	14.8[2]	Manganese	0.0835	0.056[1]
Arsenic	2.84 ppmw	0.45 ppmw	Mercury	105.9 ppmw	87.2 ppmw
Boron	0.0235	<0.06	Nickel	0.015	0.022[1]
Calcium	0.293	0.224[1]	Potassium	0.88	0.571[1]
Cerium	0.677	0.538[1]	Silicon	19.44	11.5[1]
Cesium	0.469	0.123[2]	Sodium	5.06	3.49[1]
Chromium	0.0296	0.022[1]	Zinc	0.0326	0.034
Iron	0.121	0.314[2]	Zirconium	0.12	0.67[2]
Lead	0.0278	0.022[1]			
Anions in Solution					
Chloride	0.118	0.1	Phosphate	0.131	6.32[2]
Fluoride	0.0961	0.09	Sulfate	1.03	0.79[1]
Nitrate	47.1	114[2]			

Notes:

1. Composition varies from the target by greater than 20%.
2. Composition varies from the target by greater than 50%.

The POHC chosen for the DRE phase of the testing was monochlorobenzene, a Class 1 POHC from the Dayton List. The POHC selection was based on criteria recommended in reference and guidance documents [R16, 17, 18, 19].

Monochlorobenzene was selected as the best POHC for the pilot-scale tests, as it is a liquid at room temperature and ranked 20th on the thermal stability index ($TSLoO_2$, Thermal Stability Low O_2). The thermal stability ranking is based on the temperature required to destroy at least 99% of the compound in 2 seconds at the test conditions (T99(2)). The T99(2) for monochlorobenzene is 990°C, higher than any other organic species identified in SBW sample analyses except for benzene (1,150°C). As a chlorinated aromatic compound, monochlorobenzene is a conservatively representative organic simulant, which is chemically similar to the very small quantity of difficult-to-destroy compounds detected in the SBW. Small quantities of oxygenated compounds like phthalates and nitrated compounds like nitrobenzene have been detected in the SBW, but these compounds tend to be easier to destroy in thermal processes according to their relative thermal stability rankings.

4.3 Principal Organic Hazardous Constituent

CP1 Production Tests P-4A-1 through P-4A-6 incorporated the metered injection of a POHC into the feed line from the liquid waste feed tank (T-101-A or T-101-B) to the DMR. The POHC injection rate was at a much higher concentration in the total simulant feed than the combined total of all potential organics in the actual SBW, in order to achieve detection limits needed to provide data on organic DRE in the steam reforming process. The POHC was metered into the feed stream rather than mixed with the remainder of the feed slurry so that a very accurate measurement could be made of the amount fed to the DMR for purposes of determining the DRE.

5. TEST PROGRAM DESCRIPTION

The overall test program was conducted in four discreet phases: (1) equipment checkout and functional testing, (2) the hydrogen/oxygen safety test, (3) scoping tests, and (4) production tests. The first three phases of testing were performed in order to complete all preparations necessary for the conduct of the production runs. The production tests were performed in two phases, noted as Carbonate Phase 1 (CP1) and Carbonate Phase 2 (CP2).

5.1 Equipment Checkout and Functional Testing

The primary purpose of equipment checkout and functional testing was to verify that all hardware was correctly installed and that the individual components operated properly and safely. The checkout tests verified the readiness of all systems, equipment, safety shutdowns, interlocks, and instrument calibrations.

Checkout testing was conducted in accordance with General Work Instruction (GWI) 1.3, "Pre Start and Checkout of Pilot Plant Equipment" [R20]. GWI 1.3 included pre-developed checklists for the testing of each piece of equipment, as determined by the testing management team. Each piece of equipment was tested to a predetermined set of parameters that were listed on each testing checklist. In addition to the testing of each individual piece of equipment, the entire system was pressure tested to ensure that piping and vessels would perform per their design requirements and that the system would be free of leaks. All results were documented on the appropriate forms, reviewed, approved and filed for future reference.

In addition to functional testing, specific items of equipment, such as pressure gauges, feeders, flow meters, and thermocouples, were calibrated to verify input–to-output performance. Some equipment was received with manufacturer's calibrations and others were calibrated on-site in accordance with GWI 1.2, "Calibration and Control of In-Process Instruments" [R21].

Functional tests and calibrations were used to verify many functions, such as superheater temperature, system flow capacities, valve timing and orientation, feeder speed control for solid additives, waste feed flow rates, cooling water control, blower performance, and DMR auger operation.

Functional testing and calibration allowed for the performance of logic checks assuring that the output of all equipment was coordinated with the DACS that was required to operate the pilot plant in an automated mode. This activity was important, as automatic control of the pilot plant functions allowed for more consistent responses of the operating system, such as the coordination of the DMR and CRR temperature controls as related to the input of oxygen, steam, or carbon.

Emergency shutdown tests were performed, overall system performance was determined, and operating limits were set for process temperatures, flows, and additive addition rates. Operating procedures were validated and updated as required.

The implementation of the requirements of GWI 1.3 and GWI 1.2 ensured the proper manual and automated operation of all equipment to achieve consistent and reproducible results. At the completion of the checkout and functional tests, the integrated DMR/CRR process system was ready for the next phase of testing.

5.2 Hydrogen/Oxygen Safety Test

Following the completion of the pilot plant test plan, a question was raised as to whether potentially explosive mixtures of hydrogen and oxygen could accumulate in the DMR. In the water gas reaction, carbon and steam react to form hydrogen and carbon monoxide. This reaction can be significant at temperatures below the auto-ignition temperature of hydrogen in air, which can range from 400–650ºC, depending on conditions. If the reaction rate of hydrogen with oxygen in the DMR process gas were low, it was thought that hydrogen and oxygen might both accumulate in the DMR process gas, which could lead to a rapid uncontrolled reaction (deflagration) in the presence of an ignition source.

A series of tests were conducted in which the temperature of the DMR was varied between 500ºC and 650ºC, the expected range of DMR startup and normal operating temperatures. At each temperature, steam, carbon, and oxygen were introduced into the DMR, and the concentrations of hydrogen, oxygen, carbon monoxide, and carbon dioxide in the DMR off-gas were monitored as a function of time. The results of the hydrogen/oxygen safety test are discussed in Section 7.2. The tests demonstrated that hydrogen and oxygen are not present in quantities above 1% at the same time in the DMR, and that the concentration of hydrogen and oxygen are safely and passively limited by thermodynamics.

5.3 Scoping Tests

At the completion of the hydrogen/oxygen test, a series of scoping tests was performed in order to establish the limitations of the integrated DMR/CRR system and determine the range of test parameters that would be evaluated in the production run tests. The primary purposes of the scoping tests were: (1) to verify proper integrated system operation; (2) to optimize the waste feed injection rate and atomizing gas rate to produce minimal fines carryover and to control particle size in the DMR; (3) to select an acceptable carbon reductant for use in the DMR and to optimize the carbon feed rate to maximize nitrate destruction, minimize generation of gaseous NO_X, and minimize the quantity of residual carbon in the final product solids; (4) to establish the effective range of liquid waste feed rates that can be accommodated by the system, while still achieving target emissions goals; and (5) to confirm various other target operating conditions for the production runs.

The initial conditions describing the anticipated process parameters for the scoping tests were first defined in the pilot plant testing sequence document [R22]. Prior to the start of the tests defined in the sequencing document, considerable effort was expended in adjusting key operating parameters, operating with different bed media and additives, and tuning the process control system. Once the system was determined to be functional within the desired ranges of operating conditions, a total of eight discreet scoping tests were conducted.

Initial operating experience with the process parameters shown in the sequence document led to subsequent changes in those parameters, which in turn, resulted in revisions to the sequence document. The actual conditions under which the eight structured scoping tests were conducted are shown in Table 5-1. In all cases, the feed material to the DMR was either water or the SBW supernatant solution without heavy metals or radionuclide surrogates. No UDS or POHCs were employed during the scoping tests. Neither the quencher/scrubber (Q/S) system nor the GAC Hg adsorber was used during any of the scoping tests. Two different types of feed nozzles were evaluated during the scoping tests designated as the E-1 and M-1 nozzles.

Table 5-1. Scoping test conditions.

Test Number	Feed	Feed Rate (gal/min)	Feed Nozzle	DMR Startup Bed Media	DMR Carbon Reductant	DMR Additive	DMR Temp (ºC)	CRR Bed Media	CRR Carbon	CRR Additive	CRR Temp (ºC)
S-1	Water	0.1	E-1	Alumina	Berger Bros P-6	None	650	Alumina	DeSulco	Mulcoa	850
S-2	SBW[1]	0.1	E-1	Alumina	Berger Bros P-6	Metakaolin	600	Alumina	DeSulco	Mulcoa	1,050
S-3	SBW	0.25	E-1	Alumina	Berger Bros P-6	Mulcoa	640	Alumina	DeSulco	Mulcoa	1,050
S-4	SBW	0.2	E-1	Alumina	GC-CRB	Mulcoa	620	Alumina	DeSulco	Mulcoa	1,050
S-5	SBW	0.2	M-1	Alumina	GC-CRB	Mulcoa	650	Alumina	DeSulco	Mulcoa	850
S-6	SBW	0.2	E-1	Alumina	GC-CRB	Mulcoa	600	Alumina	DeSulco	Mulcoa	850
S-7	SBW	0.2	E-1	Alumina	GC-CRB	Mulcoa	670	Alumina	DeSulco	Mulcoa	850
S-8	SBW	0.3	E-1	Alumina	GC-CRB	Mulcoa	670	Alumina	DeSulco	Mulcoa	950

Notes:

1. SBW composition per Table 4-1, Composition of Baseline Simulant Solution (Without Heavy Metals)

Based on preliminary evaluations of DMR bed media and the observation that granular sodium carbonate was unsatisfactory as a start-up DMR bed media, alumina (AGSCO 46 and 80) was determined to be the best startup bed for the DMR and was used in all eight scoping tests. Both Berger Brothers P-6 carbon and General Carbon Corporation GC 4X6 mesh CRB granular, carbonized, non-activated carbon (GC-CRB coal) were evaluated as the carbon reductant in the DMR. The P-6 was chosen as the startup carbon for the DMR (and CRR) because of its low ignition temperature. The GC-CRB coal was chosen for routine DMR operation because of its low calcium content. A high calcium level in the carbon was found to be associated with an increased potential for bed defluidization. DeSulco petroleum coke was used as the supplemental fuel in the CRR. Calcined clay and hydrated clay evaluated as additives to prevent bed agglomeration in both the DMR and CRR during CP1. Aluminum hydroxide was evaluated during CP2 for the CRR.

5.4 Carbonate Phase 1 (CP1) Test

Once the scoping tests were completed and the operating parameters under which the DMR/CRR system could be expected to operate effectively were determined, the CP1 production tests were initiated. As was the case with the scoping tests, early results from the initial production run tests dictated changes in the proposed operating parameters for the subsequent tests.

The most significant change from the original test plan involved deletion of the tests using the Q/S system. Preliminary results from the stack gas sampling tests for chlorine and hydrochloric acid indicated a chloride level of less than 1 ppm in the stack, more than an order of magnitude less than the current MACT emission level standard of 21 ppm. This result was consistent with the results from previous SBW test programs. As a result of the low measured HCl concentrations in the stack, the six originally scheduled production run (CP1) tests with the Q/S system on line were deleted.

Other minor modifications incorporated into the revised test plan were adjustments to the DMR and CRR temperatures, changes in the estimated number of hours of operation for certain tests, and a re-ordering of some tests so as to affect more expeditious changeover in conditions from one test to the next. The matrix of test conditions for the CP1 production run tests actually performed is shown in Table 5-2.

The liquid feed to the DMR followed the sequence defined in the initial SBW test plan. Test P-1 used supernatant SBW solution without heavy metals, UDS, or POHC. Tests P-2A through P 4A-1 each incorporated a single change to the feed liquid to afford an opportunity to assess the impact of each change on both system operation and off-gas emissions. The water-cooled M 2 feed nozzles used in these tests were a new design that proved to be more successful than the previous designs. Tests P-1 through P-3B were performed at the nominal DMR and CRR operating temperatures of 670°C and 950°C, respectively. In Tests P-4A-1 through P-4A-4, the DMR and CRR were operated at various combinations of high and low temperature extremes. Tests P-4A-5 and P-4A-6 duplicated the low/low and high/high DMR and CRR temperature tests from P-4A-2 and P-4A-4, but with a higher feed rate of 0.35 gpm. The combinations of temperatures and feed rates were intended to bracket system operating condition ranges and to assist in the preparation of environmental operating permits for the full-scale IWTU processing system.

Table 5-2. CP1 production run test conditions.

Test Number	Feed	Feed Rate (gal/min)	Feed Nozzle	DMR Bed Media	DMR Carbon Reductant	DMR Additive	DMR Temp (ºC)	CRR Bed Media	CRR Carbon	CRR Additive	CRR Temp (ºC)
P-1	SBW[1]	0.25	E-1 (0.120" dia)	Product	GC-CRB	None	640	Alumina	DeSulco	Mulcoa clay	950
P-2A	SBW + 80 g/L UDS[2]	0.25	M-2 (0.120" dia)	Product	GC-CRB	None	640	Alumina	DeSulco	Mulcoa clay	950
P-3B	SBW[3] + 80 g/L UDS + Heavy Metals	0.25	M-2 (0.120" dia)	Product	GC-CRB	None	640	Alumina	DeSulco	Mulcoa clay	950
P-4A-1	SBW + 80 g/L UDS + Heavy Metals + POHC	0.25	M-2 (0.120" dia)	Product	GC-CRB	None	670	Alumina	DeSulco	Mulcoa clay	850
P-4A-2	SBW + 80 g/L UDS + Heavy Metals + POHC	0.25	M-2 (0.120" dia)	Product	GC-CRB	None	600	Alumina	DeSulco	Mulcoa clay	850
P-4A-3	SBW + 80 g/L UDS + Heavy Metals + POHC	0.25	M-2 (0.120" dia)	Product	GC-CRB	None	600	Alumina	DeSulco	Mulcoa clay	1,050
P-4A-4	SBW + 80 g/L UDS + Heavy Metals + POHC	0.25	M-2 (0.120" dia)	Product	GC-CRB	None	670	Alumina	DeSulco	Mulcoa clay	1,050
P-4A-5	SBW + 80 g/L UDS + Heavy Metals + POHC	0.35	M-2 (0.180" dia)	Product	GC-CRB	None	670	Alumina	DeSulco	Mulcoa clay	1,050
P-4A-6	SBW + 80 g/L UDS + Heavy Metals + POHC	0.35	M-2 (0.180" dia)	Product	GC-CRB	None	600	Alumina	DeSulco	Mulcoa clay	850
P-5	SBW + 120 g/L UDS + Heavy Metals	0.25	M-2 (0.180" dia)	Product	GC-CRB	None	640	Alumina	DeSulco	Mulcoa clay	950
P-6	10% SBW[3] + 120 g/L UDS + Heavy Metals	0.25	M-2 (0.180" dia)	Product	GC-CRB	$Al(NO_3)_3$	600	Alumina	DeSulco	Mulcoa clay	950

Notes:

1. SBW composition per Table 4-2, Composition of Baseline Simulant Solution (Without Heavy Metals).
2. UDS composition per Table 4-4, Composition of the UDS Added to the Supernatant Solution.
3. SBW composition per Table 4-6, Composition of Simulant Solution (With Heavy Metals and Radionuclide Surrogates).

Tests P-5 and P-6 were performed to evaluate the process at higher UDS loadings (120 g/L versus 80 g/L). In all previous tests with UDS, the UDS simulated a fully-mixed slurry originating in liquid waste tank WM-187, the INL tank having the highest average UDS concentration. Increasing the UDS loading to 120 g/L for Test P-5 was intended to simulate a condition where some of the solution is decanted from WM-187, but the remaining supernatant and UDS are fully mixed before being pumped to the DMR. Test P-6 simulated the condition where a UDS heel in a waste tank was re slurried with either dilute supernatant solution or water. In this case, the UDS concentration was also 120 g/L, but the concentration of the supernatant solution was only 10% of previous values.

5.5 Carbonate Phase 2 (CP2) Test

After the completion of the CP1 tests and an initial analysis of data, it was determined by project management that a second phase of production tests (CP2) was needed. This second phase of production tests was performed to provide additional confirmatory data in the following areas:

- Production testing of SBW feed without UDS raised concerns about the particle size of the product materials. The CP2 tests were to evaluate the usage of alumina grit and possibly a clay slurry to provide seed particles for maintaining particle size control in the DMR when SBW without UDS is processed.

- Confirm product mass and density when processing SBW without UDS. Test data were to provide input to the IWTU project team to develop a more reliable estimate of waste canister count when processing SBW without UDS. Mass and density estimates were to be performed for product material that had been screened to remove carbon particles, which were to be recycled back into the process.

- Evaluate modified operations of the CRR intended to reduce the formation of small agglomerates in the CRR bed and to optimize NO_X, THC, and CO destruction. The configuration modifications include relocation of existing oxygen distributors, provision of three oxygen input distributors, and use of aluminum hydroxide as the CRR additive to replace the granular clay used in the scoping and production tests.

- Evaluate the operation of the CRR at varying bed depths and autothermal gas distribution configurations.

- Evaluate the overall performance of the GAC bed and the performance of individual stages with an increased level of both instrumental and manual sampling.

The general conditions under which the CP2 tests were to be conducted are identified in Table 5-3, Carbonate Phase 2 Test Sequence. Table 5-4, Off-gas Measurements, identifies the off-gas sampling points and means of analysis for mercury, other metals, and other gaseous constituents. Table 5-5, DMR Particle Size Control and CRR Temperature Control Measures, details the conditions under which the DMR and CRR were to be operated in order to achieve the desired results as a function of elapsed testing time. The DMR particle size control measures are consistent with those shown in Table 5-3. The CRR temperature control measures reflect bed heights of 32–34 in., 29–31 in., 26–28 in., and 35–37 in. as well as the location and the composition of the autothermal gas mixture (relative O_2 and N_2 concentrations). The fourteen options for the autothermal gas mixture injection points include the lower and middle gas distributors alone and the combined lower and middle distributors where the middle distributor flow rate is modulated for purposes of temperature control. In these cases, the non-controlling (lower) distributor would be fed a constant, pre-set flow of the autothermal gas mixture.

Table 5-3. Carbonate Phase 2 test sequence.

Test Number	Test Day	Feed	Feed Rate (gal/min)	DMR Bed Media	DMR Carbon	DMR Additive	DMR Temp (ºC)	DMR Seed Material	CRR Bed Media	CRR Carbon	CRR Additive	CRR Temp (ºC)
Preheat	1	None	0	Alumina[3]	GC-CRB	None	Heat Up to 640	None	Alumina[5]	DeSulco[6]	None	Heat Up to 950
Preheat	2	None	0	Alumina[3]	GC-CRB	None	Heat Up to 640	None	Alumina[5]	DeSulco[6]	None	Heat Up to 950
CP2-1	3	SBW[1]	0.25	Carbonate Product & Alumina	GC-CRB	None	640	None	Alumina[5]	DeSulco[6]	Aluminum Hydroxide[7]	950
CP2-1	4	SBW[1]	0.25	Carbonate Product & Alumina	GC-CRB	None	640	None	Alumina[5]	DeSulco[6]	Aluminum Hydroxide[7]	950
CP2-1/ CP2-2	5	SBW[1,2]	0.25	Carbonate Product	GC-CRB	None	640	None	Alumina[5]	DeSulco[6]	Aluminum Hydroxide[7]	950
CP2-2	6	SBW[2]	0.25	Carbonate Product	GC-CRB	None	640	None	Alumina[5]	DeSulco[6]	Aluminum Hydroxide[7]	950
CP2-2	7	SBW[2]	0.25	Carbonate Product	GC-CRB	None	640	None	Alumina[5]	DeSulco[6]	Aluminum Hydroxide[7]	950
CP2-2	8	SBW[2]	0.25	Carbonate Product	GC-CRB	None	640	None	Alumina[5]	DeSulco[6]	Aluminum Hydroxide[7]	950
CP2-2	9	SBW[2]	0.25	Carbonate Product	GC-CRB	None	640	None	Alumina[5]	DeSulco[6]	Aluminum Hydroxide[7]	950
CP2-3[4]	10	SBW[2]	0.25	Carbonate Product	GC-CRB	None	640	None	Alumina[5]	DeSulco[6]	Aluminum Hydroxide[7]	950
CP2-4[4]	11	SBW[2]	0.25	Carbonate Product	GC-CRB	None	640	Alumina[4]	Alumina[5]	DeSulco[6]	Aluminum Hydroxide[7]	950

Notes:

1. SBW supernate per Table 4, SBW Test Plan, amended for CP2 testing as described in Section 3.5. No heavy metals for initial 60 hours of operation. No UDS.
2. SBW supernate per Table 6, SBW Test Plan, amended for CP2 testing as described in Section 3.5. No UDS.
3. AGSCO alumina, #46 and #80
4. AGSCO Alumina #150
5. AGSCO Alumina, #30 and #46
6. DeSulco 9005 petroleum coke.
7. MPSI Code 650 hydrated alumina, 85 micron.

Table 5-4. CP2 Off-gas measurements.

Test Number	Test Day	Off-Gas Measurements								
		GAC Stage 1 Outlet		GAC Stage 2 Outlet		GAC Stage 3 Outlet		Stack		
		Ontario Hydro	Hg CEMS[1]	Ontario Hydro	Hg CEMS[1]	Ontario Hydro	Hg CEMS[1]	Method 29	Hg CEMS[1]	CEMS[2]
Preheat	1								X	X
Preheat	2									X
CP2-1	3	X		X		X		X	X	X
CP2-1	4									X
CP2-1/CP2-2	5	X		X		X			X	X
CP2-2	6	X		X		X		X		X
CP2-2	7							X	X	X
CP2-2	8									X
CP2-2	9	X		X		X		X	X	X
CP2-3	10	X		X		X				X
CP2-4	11	X		X		X		X	X	X

Notes:

1. Continuous instrumental monitor specific for mercury.
2. Continuous emissions monitoring system for oxygen, carbon dioxide, carbon monoxide, nitrogen oxides, sulfur dioxide, and total hydrocarbons (THC).

Table 5-5. CP2 DMR particle size control and CRR temperature control measures.

Key Operating Parameter Modifications	Elapsed Time (Hours)														
	12	24	36	48	60	72	84	96	108	120	132	144	156	168	180
DMR PARTICLE SIZE CONTROL															
Dry Alumina Seed														↔	↔
SBW w/o Heavy Metals	↔	↔	↔	↔	↔	↔	↔								
SBW w/ Heavy Metals								↔	↔	↔	↔	↔	↔	↔	↔
CRR TEMPERATURE CONTROL															
32-34" CRR Bed Height	↔	↔	↔	↔	↔										
1 Mid 50/50 (O_2/N_2)	↔														
2 Mid 75/25		↔	↔												
3 Low 75/25				↔											
4 Low 50/50			↔												
5 Both/Mid 50/50					↔										
29-31" CRR Bed Height						↔	↔	↔							
6 Both/Mid 50/50						↔									
7 Mid50/50							↔								
8 Low 50/50								↔							
26-28" CRR Bed Height									↔	↔	↔	↔			
9 Low 50/50									↔						
10 Mid 50/50										↔					
11 Both/Mid 50/50											↔				
35-37" CRR Bed Height												↔	↔	↔	↔

Key Operating Parameter Modifications	Elapsed Time (Hours)														
	12	24	36	48	60	72	84	96	108	120	132	144	156	168	180
12 Both/Mid 50/50												↔	↔		
13 Mid 50/50													↔	↔	
14 Low 50/50														↔	↔
15 Mid 75/25															↔

6. QUALITY ASSURANCE/QUALITY CONTROL

The Quality Assurance Program implemented for the pilot plant testing program was in accordance with TTT Quality Assurance Plan, Project Quality Procedures, and the TTT Quality Assurance Project Plan, QAPP 1.1.[R23] These documents are based on ASME NQA-1 2000, Quality Assurance Requirements for Nuclear Facility Applications, DOE Order 414.1C Quality Assurance and 10 CFR 830.120. Personnel performing work at the pilot plant were trained to these documents and other implementing procedures and instructions to ensure that work was performed safely and in a consistent manner. Records for each individual were documented and maintained in the project training file.

The design and fabrication of the treatment system were conducted in a prescribed and controlled manner. The design documents for the system were generated in accordance to the THOR® engineering procedures and approved by the TTT Testing Manager, TTT Chief Engineer, and the TTT QA Manager. Numerous procedures and work instructions were generated for the project and were controlled through the TTT Document Program. Records resulting from the project activities are retained temporarily onsite at Hazen or in the TTT Document Control System. Upon completion of all records, they shall be turned over to TTT Records Management for storage, archival, and will be submitted to the client, as defined in the records submittal schedule. Archived records shall be maintained by WGI as defined in the TTT Final Disposition of Project Documents and Files procedure.

Items procured for the project followed the TTT and Hazen procurement procedures and processes. Receipt and inspection of these items were conducted at Hazen and logged upon receipt. During testing (CP1 and CP2) trained personnel performed verification of material, and 13 nonconforming items were identified, documented on a TTT Non-Conformance Report (NCR), dispositioned, and closed. Table 6-1 identifies the NCRs and the actions taken for closure. All NCRs issued for the project have been logged, validated, closed, and are kept in Washington Group International (WGI) records storage. One Deficiency Report (DR) for material control and two Corrective Action Reports (CARs) for design control of the waste feed nozzles and the hot spot that initiated in the mercury adsorber GAC bed were also issued. The CAR-004 for the GAC bed is still open pending final Root Cause Analysis. There were no impacts to the test results or operation of the facility.

To ensure that the operations conducted at the Hazen facility seven surveillances were performed as identified in Table 6-2. All issues identified have been closed. Six Management Assessments were also conducted as listed in Table 6-3 and are closed. The Hazen facility and project personnel were made aware of all issues identified in the surveillances and management assessments. There were no impacts to the overall operations and samples collected that would jeopardize the final results or inputs to the design of the IWTU.

Data generated for the program were documented on data sheets, in logbooks, and electronically by the Data Acquisition and Control System (DACS) managed with LabView 7.0 software. Logbooks were controlled through Document Control and were issued to technical personnel for the project. Personnel documented their observations and activities in the logbooks, and initialed and dated each entry. Various data sheets were also used throughout the project to capture operational information and results and were maintained in binders. Upon final use of these data sheets, they will be turned over to Records Management for storage, archival, and submittal to the client as defined in the approved submittal schedule.

Table 6-1. Issued TTT non-conformance reports.

NCR No.	Description	Actions	Status
NCR-THOR-001	Pressure gauge #7116-G200 Spirahelic (0-200 psi) – needle on gauge floats and currently reads 70 psi in the box.	Upon inspection, the package was marked "BAD" and the gauge was returned to the supplier.	Closed 9/9/05
NCR-THOR-002	The Stainless steel tank fabricated by Dairy Engineering was not welded to any defined welding procedures or directions in the sketch.	Welds evaluated buy a Certified Weld Inspector and found to be acceptable for the intended use.	Closed 10/12/05
NCR-THOR-003	Corrosion Coupons received at Hazen did not have dimensional measurement welding information as required in the procurement specifications.	Hazen performing dimensional measurements with a calibrated caliper. Welding requirements are being requested from the vendor.	Closed 12/0505
NCR-THOR-004	Waste Feed Nozzles were not concentric as required by the engineered drawings.	Returning to vendor for re-work.	Closed 10/14/05
NCR-THOR-005	Tank T-100 Waste Feed Tank was determined to be incompatible with the proposed mixture and molar content of the acidic material to be processed through the system	The tank was removed from the facility and a new stainless steel tank, compatible with the waste feed, has been ordered and be used for the process. No further actions are required.	Closed 11/16/05
NCR-THOR-006	Three areas on the DMR were identified as having cracked welds that subsequently leaked during the leak testing activity of the system performed on 11/10–11/11/05. The leaks were identified at 2 nozzle locations that are flanged off and on the DMR Sample Port.	Repairs were made to the flanged off nozzle locations that were not being used on the system by cutting out one nozzle and replacing it with a patch and the other cracked nozzle was ground down to clean metal and repaired. The cracked weld on the DMR Sample Port was ground down to clean metal and then repaired by a qualified welder. All welds were leak tested again and found to be acceptable.	Closed 11/16/05
NCR-THOR-007	Instrument #AE-700-004, California Analytical Model 400 CLD, NO_X Analyzer may have a leak in the pump and the ozone generator is not functioning properly.	The instrument was sent back to the supplier.	Closed 12/21/05

Table 6-1. (continued).

NCR No.	Description	Actions	Status
NCR-THOR-008	Monohydrate Mercuric Nitrate was specified on the Purchase Requisition PR-034. Dihydrate Mercuric Nitrate was listed on the Purchase Order and received at the plant. The Certificate of Analysis that was received from the vendor was conflicting as to the form shipped listing both Dihydrate and Monohydrate	Obtain a corrected Certificate of Analysis from the supplier. Make adjustments during batch make-up to allow for Dihydrate in lieu of Monohydrate. Certificate of Analysis was received and the material verified as Dihydrate.	Closed 2/07/06
NCR-THOR-009	The 1000 kg of Zirconium Phosphate $ZR(HPO_4)_2$ was requisitioned on PR-034 with the requirement for particle size from 0.5-100 microns with a median particle size of 10 microns. The size of the material that was received at the Pilot Plant contained product that was greater that the required <100 micron size limit. PO-034 did not indicate the requirement for the Zirconium Phosphate	The material was used as-is and screened from –28 to -40 mesh before use.	Closed 2/07/06
NCR-THOR-010	4 buckets containing 8 samples of waste product each were sent from Hazen Research to Chillworth Technology Inc. The Chain of Custody (COC) form associated with these samples did not list all samples accurately, and 1 sample was broken upon arrival, as notified by Chillworth. 1. Bucket 2, 1 of 2 Samples of 1667 PBF was received broken. 2. Bucket 3, The COC listed 3 Samples for 1774 PBF. Only 2 of these samples were received. Another sample not listed on the COC was labeled 1736 PBF. 3. Bucket 4, Samples labeled 1821PBF, 1822 HTF, & 1827 PR were received. The COC listed samples 1802 PR, 1803 PBF & 1805 HTF.	**Item 1**: Hazen Research will send Chillworth another sample from the same sampling event to replace the broken sample. Chillworth will return the contents of the broken sample back to Hazen for proper disposal. **Item 2**: Sample 1736 PBF is part of the same batch from the PBF and is acceptable for use with sample 1774 PBF. Hazen Research will properly correct a copy of the COC to reflect the proper identification of samples sent and forward it to Chillworth to ensure the correct sample and analysis are performed and to maintain the integrity of the sampling event. **Item 3**: The samples received by Chillworth 1821 PBF, 1822 HTF, and 1827 PR are from the same process batches, (4A-6-1 & 2). Guidance was provided to Chillworth to use these samples as received and Hazen will properly correct the copy of the COC to reflect the proper identification of samples sent to the laboratory and will be forwarded to Chillworth to ensure the integrity of the samples is maintained.	Closed 2/22/06

Table 6-1. (continued).

NCR No.	Description	Actions	Status
NCR-THOR-011	During the dismantlement of equipment after the initial test runs of the pilot plant were complete, it was identified that valve HV407-001 was in the opened position as opposed to being closed during part of the testing, which resulted in process off -gases, containing mercury, bypassing the mercury absorber and being vented to the environment via the stack.	**Item 1**: Complete evaluations of the actuator for valve HV407-001, correct the configuration of the valve relative to the actuator, and verify that the actuator and valve properly operate. The actuator 407-001 number ST-U22-SR-5 was listed in the purchase order as fail open and upon evaluation and verification from the supplier, item was identified that the actuator was actually shipped fail closed, thus causing the valve to open incorrectly. **Item 2:** Physically mark the valve to ensure that the disc is in the correct orientation. The valve will then be installed and the valve position and actuator alignment will be verified and pressure tested. **Item 3**: Evaluate the amount of off-gas mercury emitted up the stack. Evaluate this relative to Hazen's release limits and ensure any necessary reports are made to the regulator. Determine the impacts of the release on additional IWTU testing activities. **Item 4:** Perform configuration verification and pressure check on all off-gas system valves to ensure the installation is correct. For valves that are not clearly identifiable as to whether they are open or are closed, they shall be properly marked and verified.	Closed 5/2/06
NCR-THOR-012	Manual air samples collected for laboratory analysis using analytical methods EPA-0031, Sampling Method for Volatile Organic Compounds and EPA-0040, Sampling of Principal Organic Hazardous Constituents From Combustion Sources Using Tedlar Bags, for Test Runs 4A-5 and 4A-6 were inadvertently left on the APT laboratory sample receiving shelf and exceeded their holding times prior to shipment for analysis.	**Item 1**: Personnel will determine which samples were impacted to ensure the results are not inadvertently utilized. **Item 2**: Results of the data were evaluated and reported as exceeding holding times.	Closed 5/10/06

Table 6-1. (continued).

NCR No.	Description	Actions	Status
NCR-THOR-013	Ceramic Tips required for the CRR ATG nozzles were received with cracks. Inconel nozzles are to be glued into the ceramic tips. 12 tips have been received (20 ordered) 2 are acceptable 9 contain cracks (1 also is out of tolerance which has the ID bore out of round) 1 is out of dimensional tolerance (too large of ID bore and not centered)	Use the tips with cracks and glue in the nozzles. (high strength/temperature glue). Scrap the tips that are out of tolerance. The ceramic tips were glued in place and heat cycled in a muffle furnace without degradation.	Closed 5/19/06

Table 6-2. Surveillances.

Surveillance No.	Description	Issues	Status
THOR-05-05	PQP 5.1 – Instructions, Procedures, Drawings – Hazen Facility	None	Closed 10/05/05
THOR-05-06	Weld Inspection of Hazen Facility	None	Closed 10/14/05
THOR-05-07	EP 1.0 - Equipment, Drawings and Specifications – Preparation Review and Approval – Hazen Facility	None	Closed 10/18/05
THOR-05-09	Documentation and M&TE Hazen Facility	None	Closed 11/14/05
THOR-05-11	Document Control and Records	Logbooks were not completed with the initials of the individual documenting the days activities or signing and dating at the end of the day. Personnel went back and signed and verified entries and were retrained.	Closed 12/28/05
THOR-05-12	APT Air Sampling – Hazen Facility	None	Closed 2/06/06
THOR-06-03	APT Air Sampling - Hazen Facility Follow up	COCs did not physically accompany the samples from the project site to the Lab. Verification of the control of the samples were performed and found to be in control at the lab. Personnel were briefed on the error. No impact to the sample integrity.	Closed 6/7/06

Table 6-3. Management assessments.

Management Assessment No.	Description	Issues	Status
THOR-MA-001	Project Status	None	Closed 9/28/05
THOR-MA-002	Operator Aides and Procedures	Operator Aides were not properly posted. Corrected. APT procedures or paperwork was not On-Site. Corrected	Closed 1/24/06
THOR-MA-003	Completion and Adequacy of Forms	The replacement of TAG 8A corrosion Coupon was not properly documented. Corrected.	Closed 1/24/06
THOR-MA-004	APT Sampling	None	Closed 2/03/06
THOR-MA-005	Hazen Sampling	None	Closed 6/03/06
THOR-MA-006	TTT Pilot Plant Tests on SBW at Hazen Research	Personnel were not properly trained with respect to safety during the pre-start operations of the pilot plant. Actions were taken to train personnel prior to the start of operations and found acceptable.	Closed 11/28/05

The majority of the data collected for the testing and operations of the pilot plant were collected through the use of LabView 7.0. The data were automatically backed up daily to ensure no loss of information. The software was subjected to various tests to ensure that it functioned properly on the various computer systems. The General Work Instruction (GWI) 1.6, "LabView Developer Suite Software Qualification Plan," [R24] provided the testing, verification and validation of the system software used for the operations. The data collected by the system will be copied to electronic media, stored, archived, and submitted to the client.

Off-gas and solids sampling conducted during pilot plant testing was performed by trained and qualified personnel to prescribed procedures and methods as defined in the SBW Test Plan and the QAPP. Instrumentation used to capture data and perform measurements was calibrated in accordance with GWI 1.2, "Calibration and Control of In-Process Instrumentation" [R21]. Functional tests of these instruments and systems were performed prior to startup to ensure that the data generated would be acceptable and usable to meet the objectives of the tests.

Air Pollution Testing, Inc. (APT), the contractor hired to acquire these samples, collected samples for air emissions testing from the stack. APT also performed off-gas monitoring using the CEMS. All samples were drawn in compliance with the applicable EPA methods for each analyte.

Hazen personnel collected additional samples as described in Section 3.5. Samples shipped off site for analysis utilized a chain-of-custody form to ensure that they were not compromised and were under control through analysis at the specified laboratory. A validation of the off-gas sample analysis data was performed in accordance with applicable procedures. The results of the validation are summarized in Appendix A.

CONTENTS

7. TEST OBSERVATIONS AND RESULTS 7-1

7.1 Functional/Preparatory Tests 7-1

7.2 Hydrogen/Oxygen Safety Tests 7-2

7.3 Scoping Tests 7-3

7.4 Production Tests 7-16

7.4.1 Carbonate Phase 1 (CP1) Tests 7-16
7.4.2 CP1 Operating Conditions 7-26
7.4.3 Carbonate Phase 2 (CP2) Tests 7-26
7.4.4 CP2 Operating Conditions 7-35

7.5 System Performance 7-35

7.5.1 Fluidized Bed Performance 7-35
7.5.2 Fluidized Bed Particle Size Distribution 7-46
7.5.3 DMR Product Densities 7-56
7.5.4 Carbon Reductant Performance 7-63
7.5.5 Temperature Control of the DMR and the CRR 7-65
7.5.6 System Pressure Control and Performance 7-68
7.5.7 Filter (HTF and PBF) Performance 7-68
7.5.8 Data Acquisition and Control System Performance 7-71

7.6 Product Solids Composition Data 7-73

7.6.1 DMR/PR Bed Product 7-74
7.6.2 Fines (HTF Material) 7-81
7.6.3 PBF Solids 7-88
7.6.4 DMR Wall Scale 7-90

7.7 Process Gas And Stack Gas Measurements 7-93

7.7.1 DMR CPMS and Stack Cems Measurements 7-94
7.7.2 CPMS (DMR Process Gas) Data 7-97
7.7.3 CEMS (Stack Gas) Data 7-97
7.7.4 NO_X Destruction, CO, and THC Emissions 7-111
7.7.5 SO_2 Emissions 7-117
7.7.6 Manual Sample Train Measurements 7-118
7.7.7 Stack Gas Temperature, Moisture, and Flow Rate 7-118
7.7.8 Manual Sample Train Measurement Results 7-124
7.7.9 Mercury Control, Emission Measurements, and Spent Granular Activated Carbon Leachability 7-128
7.7.10 GAC Bed Thermal Event 7-144
7.7.11 VOC Emissions and POHC Destruction 7-145

7.8 Mass Balance 7-159

7.8.1 Methodology 7-159
7.8.2 Elemental Mass Balance Results 7-165

FIGURES

7-1. H_2-O_2 safety test data 7-2

7-2. Pilot Plant activities November 28 to December 7, 2005 7-5

7-3. Pilot Plant activities December 15 to 18, 2005 7-8

7-4. Pilot Plant activities December 19 to 22, 2005 7-10

7-5. Pilot Plant activities January 3 to 7, 2006 7-12

7-6. Pilot Plant activities January 8 to 13, 2006 7-14

7-7. Pilot Plant activities January 16 to January 21, 2006 7-17

7-8. Pilot Plant activities January 25 to February 1, 2006 7-20

7-9. Pilot Plant activities February 1 to 5, 2006 7-21

7-10. Pilot Plant activities February 7 to 10, 2006 7-25

7-11. Pilot Plant activities May 30 to June 9, 2006 7-33

7-12. DMR vessel temperatures and steam flow rate during steam boiler trips on June 4, 2006 7-41

7-13. Agglomerated bed material removed from the DMR vessel at the end of test CP2 7-42

7-14. Porous encrustations removed from the bottom of the DMR vessel at the end of test CP2 7-42

7-15. Comparison of superficial space velocities and twice minimum fluidizing velocity in the DMR bed during the CP2 test 7-43

7-16. Comparison between the CRR inlet SSV and twice the minimum fluidizing velocity in the CRR bed for the CP2 test 7-44

7-17. DMR Feed Nozzle insertion flanges layout 7-45

7-18. Functional Test: DMR average bed particle size 7-47

7-19. Scoping Tests 2 and 3: DMR average bed particle size 7-48

7-20. DMR average bed particle size January 8–13, 2006 7-50

7-21. CP1 Production Tests: DMR average bed particle size 7-51

7-22. Average DMR bed particle sizes during the CP2 test 7-53

7-23. Particle size distribution of DMR bed samples taken before and after seed particle addition 7-55

7-24. DMR solid product densities during the CP1 test 7-56

7-25. Cumulative mass of solids removed from the DMR during the CP2 test 7-57

7-26. Particle and bulk density of DMR bed samples during the CP2 test 7-57

7-27. Net PR product mass rate during CP2 test 7-58

7-28. HTF solids product mass rate during CP2 test 7-58

7-29. DMR bed turnover for Test CP2 7-60

7-30. Mass of solids elutriated from the CRR and captured in the PBF 7-61

7-31. Mass rate of solids collected in the PBF during CP2 test 7-61

7-32. Correlation of CP2 solids mixture density with mixing ratios 7-63

7-33. CRR outlet O_2 concentration and bed temperature during CP2 test 7-67

7-34. CRR outlet oxygen, stack THC, and CO concentrations during the CP2 test 7-67

7-35. Pressure rise on off-gas blowers during the CP1 test 7-69

7-36. Pressure rise on the gas blowers during the CP2 test 7-69

7-37. Damaged HTF filters at the end of the CP1 test 7-70

7-38. HTF pressure drop during the CP2 test 7-71

7-39. Micrograph of AGSCO alumina used as DMR starting bed 7-74

7-40. Micrograph of DMR solids produced during CP1 test P-4A-4 on February 2, 2006 7-75

7-41. Micrograph of DMR solids produced during the CP2 test on 6/5/06 7-75

7-42. Solids Analysis for CP1 test DMR and PR samples 7-77

7-43. Solids Analysis for CP2 test DMR and PR samples 7-79

7-44. Microphoto of PR Sample 2334 7-81

7-45. Solids Analysis for CP1 test HTF samples 7-83

7-46. Solids analysis for CP2 test HTF samples 7-85

7-47. Particle size distribution of HTF solids collected duringCP1 Test P-1, Sample No.. 1448 7-86

7-48. Particle size distribution of HTF sample collected during CP1 Test P-4A-3, Sample No. 1693 7-87

7-49. Particle size distribution of HTF sample collected during CP2 test on 6-4-06, Sample No. 2191 7-88

7-50. Chemical analysis of PBF solids produced during the CP1 Test 7-89

7-51. Chemical analysis of PBF solids produced during the CP2 test 7-91

7-52. Wall scale removed from the DMR cyclone downcomer on January 14, 2006 (Sample 1378) 7-92

7-53. DMR wall scale removed from the corrosion coupon rod after the end of CP2 test 7-92

7-54. Stack gas O_2 and CO levels compared to CRR outlet O_2 levels for CP1 7-111

7-55. Stack gas CO levels for different CRR bed temperatures 7-112

7-56. Stack gas O_2 and CO levels compared to CRR outlet O_2 levels for CP2 7-113

7-57. Stack gas O_2 and CO levels and CRR NO_X destruction for the CRR test conditions of CP2 7-113

7-58. Sy stem NO_X destruction compared to the DMR bed temperature for CP1 7-114

7-59. DMR, system, and CRR NO_X destruction compared to the DMR H_2 levels for CP1 7-115

7-60. DMR, system, and CRR NO_X destruction compared to the DMR H_2 levels for CP2 7-116

7-61. Sy stem NO_X destruction for medium and high simulant feedrates 7-117

7-62. Stack gas SO_2 concentrations compared to GAC Bed 3 temperature for CP1 and CP2 7-118

7-63. Hazardous metals (and surrogate) emission concentrations 7-127

7-64. ESTD GAC mercury adsorber 7-128

7-65. Hg concentrations in carbon bed samples from CP1 and CP2 7-135

7-66. Sulfur concentrations in spent carbon bed samplesfrom CP1 and CP2 7-136

7-67. Off-gas Hg concentrations during CP2 7-140

7-68. Hg removal efficiency by the carbon bed during CP1 and CP2 7-140

7-69. SO_4 in spent carbon samples from CP1 and CP2 7-141

7-70. Concentrations of trace off-gas elements sorbed on spent carbon from CP1 and CP2 7-142

7-71. Spent carbon Hg leachability results for CP1 and CP2 7-142

7-72. Total organic emissions at different CRR temperatures compared to CRR outlet O_2 concentrations 7-153

7-73. Elemental distribution of all discharges for CP1 7-171

7-74. Elemental distribution of solids discharges from DMR and HTF for CP1 7-172

7-75. Elemental distribution of all solids discharges for CP1 7-173

7-76. Elemental distribution of all discharges for CP2 7-179

7-77. Elemental distribution of solids discharges from DMR and HTF for CP2 7-180

7-78. Elemental distribution of all solids discharges for CP2 7-181

TABLES

7-1. Operating periods for scoping tests 7-4

7-2. Scoping test changes – November 28 to December 7, 2005 7-7

7-3. Scoping test changes – December 19 to 22, 2005 7-11

7-4. Scoping test changes – January 3 to 7, 2006 7-13

7-5. Scoping test changes – January 8 to 13, 2006 7-16

7-6. Operating periods for production tests 7-16

7-7. Production test changes – January 16 to 21, 2006 7-19

7-8. Summary of CP1 DMR operations 7-27

7-9. CP1 DMR gas flow rate and residence time 7-28

7-10. Summary of CP1 CRR operating parameters 7-29

7-11. Key CP1 off-gas system parameters 7-30

7-12. CP1 solid product rates 7-31

7-13. CP1 Steam Reformer process pressures and differential pressures 7-32

7-14. CP2 DMR flow rates 7-36

7-15. CP2 DMR temperatures 7-36

7-16. CP2 DMR and HTF pressures, differential pressures, and bed height 7-36

7-17. CP2 CRR flow rates 7-37

7-18. CP2 CRR and off-gas system temperatures 7-38

7-19. CP2 CRR pressures, differential pressures, and bed height 7-39

7-20. Bulk densities of CP2 test solid mixtures 7-62

7-21. Analysis of GC-CRB Carbon Reductant used in the DMR 7-64

7-22. Average composition of solids produced during the CP1 test 7-78

7-23. Average composition of DMR solids produced during the CP2 test 7-80

7-24. Microprobe composition of PR Sample 2334 7-81

7-25. Average composition of HTF solids produced during the CP1 test 7-82

7-26. Average composition of HTF solids produced during the CP2 test 7-84

7-27. Treatment of CP2 DMR wall scale solids 7-93

7-28. CP1 and CP2 stack emissions summary 7-95

7-29. CP1 DMR process gas dry composition 7-98

7-30. CP1 DMR process gas composition (wet basis) and NO_X destruction 7-100

7-31. CP2 DMR process gas dry composition 7-102

7-32. CP2 DMR process gas wet composition and NO_X destruction 7-103

7-33. CP1 stack gas dry composition 7-104

7-34. CP1 stack gas composition (wet basis), system NO_X destruction, and mass emission rates 7-105

7-35. CP2 stack gas dry composition for the manual sampling time periods 7-106

7-36. CP2 stack gas dry composition for the CRR test conditions 7-107

7-37. CP2 Stack gas wet composition and mass emission rates for the manual sampling time periods 7-108

7-38. CP2 stack gas composition (wet basis) for the CRR test conditions 7-109

7-39. CP1 operating conditions during emission test periods 7-119

7-40. CP2 operating conditions during emission test periods 7-120

7-41. CP1 stack temperature and flow-rate measurements 7-120

7-42. CP2 stack gas temperature and flow-rate measurements 7-121

7-43. CP1 stack gas particulate matter and metals concentrations and emission rates 7-125

7-44. CP2 stack gas PM and metals concentrations and emission rates 7-126

7-45. Carbon bed dimensions and operating conditions 7-129

7-46. Mercury analysis results for CP1 GAC bed activated carbon samples 7-131

7-47. Other analysis results for CP1 GAC bed activated carbon samples 7-132

7-48. Mercury analysis results for CP2 GAC bed activated carbon samples 7-133

7-49. Other analysis results for CP2 GAC bed activated carbon samples 7-134

7-50. CP1 stack gas mercury emission measurements 7-137

7-51. CP2 stack gas mercury emission measurements 7-138

7-52. Spent carbon TCLP leach results for CP1 7-143

7-53. Spent carbon TCLP leach results for CP2 7-143

7-54. CP1 stack gas VOC concentrations and emissions rates 7-147

7-55. CP1 stack gas SVOc concentrations and emission rates 7-149

7-56. CP1 stack gas Field GC (Method 0040) and TCO/GRAV concentrations and emission rates 7-151

7-57. CP1 stack gas dioxin and furan concentrations and emission rates 7-155

7-58. CP1 stack gas PCB concentrations 7-157

7-59. Summary of gaseous feed and discharge streams—method of flow rate quantification 7-161

7-60. Elemental Distribution and Mass Balance Closure for CP1 7-166

7-61. Elemental Distribution and Mass Balance Closure for CP1 7-168

7-62. GC-CRB coal analytical ash composition results 7-170

7-63. Elemental distribution and mass balance closure for CP2 7-175

7-64. Elemental Distribution and Mass Balance Closure for CP2 7-177

7. TEST OBSERVATIONS AND RESULTS

Pilot plant testing activities were initiated on November 15, 2005. These initial activities were focused on equipment checkout and functional testing. Scoping and production tests were performed from November 28, 2005 to June 8, 2006, with scheduled shutdowns for holidays, data evaluation, equipment maintenance, and system modification.

The hydrogen-oxygen safety test was performed on December 5–6, 2005, prior to the initiation of the scoping tests, to determine if hydrogen generation would occur at temperature conditions where hydrogen and oxygen would not react, thus creating the potential for hydrogen and oxygen to reach levels where a deflagration resulting in an unacceptable risk to the public or co located workers might occur.

The scoping tests, intended to provide and verify the baseline operating conditions for the production testing operations, started December 8 and were completed January 13. After a brief shutdown for maintenance operations, Carbonate Phase 1 (CP1) production testing operations were initiated on January 17, 2006, and were successfully completed February 10, 2006. Carbonate Phase 2 (CP2) production tests were initiated on May 31, 2006, and were completed on June 8, 2006.

7.1 Functional/Preparatory Tests

The primary purpose of equipment checkout and functional testing was to verify that all hardware was correctly installed and that the individual components operated properly and safely. Checkout testing was conducted in accordance with GWI 1.3, “Pre-Start and Checkout of Pilot Plant Equipment” [R20]. GWI 1.3 included pre developed checklists for the testing of each piece of equipment, as determined by the testing management team. Each piece of equipment was tested to a predetermined set of parameters that were listed on each testing checklist. In addition to the testing of each individual piece of equipment, the entire system was pressure tested to ensure that piping and vessels would perform per their design requirements and that the system would be free of leaks. All results were documented on the appropriate forms, reviewed, approved and filed for future reference.

In addition to functional testing, specific items of equipment, such as pressure gauges, feeders, flow meters, and thermocouples, were calibrated to verify input–to-output performance. Some equipment was received with manufacturer’s calibrations and others were calibrated on-site in accordance with GWI 1.2, “Calibration and Control of In-Process Instruments” [R21]. Instrument logic checks were performed assuring that the output of all equipment was coordinated with the Data Acquisition and Control System (DACS) that was required to operate the pilot plant in an automated mode. This activity was important, as automatic control of the pilot plant functions allowed for more consistent responses of the operating system, such as the coordination of the DMR and CRR temperature controls as related to the input of oxygen, steam, or carbon.

Emergency shutdown tests were performed, overall system performance was determined, and operating limits were set for process temperatures, flows, and additive addition rates. Operating procedures were validated and updated as required. At the completion of the checkout and functional tests, the integrated DMR/CRR process system was ready for the next phase of testing.

7.2 Hydrogen/Oxygen Safety Tests

The hydrogen/oxygen test was designed to show that hydrogen and oxygen could not coexist in the DMR at normal processing temperatures between 500°C and 650°C. The test varied bed temperature and steam, carbon, and oxygen flow rates to give different hydrogen and oxygen concentrations in the DMR process gas. The test was conducted during December 5–6, 2005. The results of this test are shown in Figure 7-1.

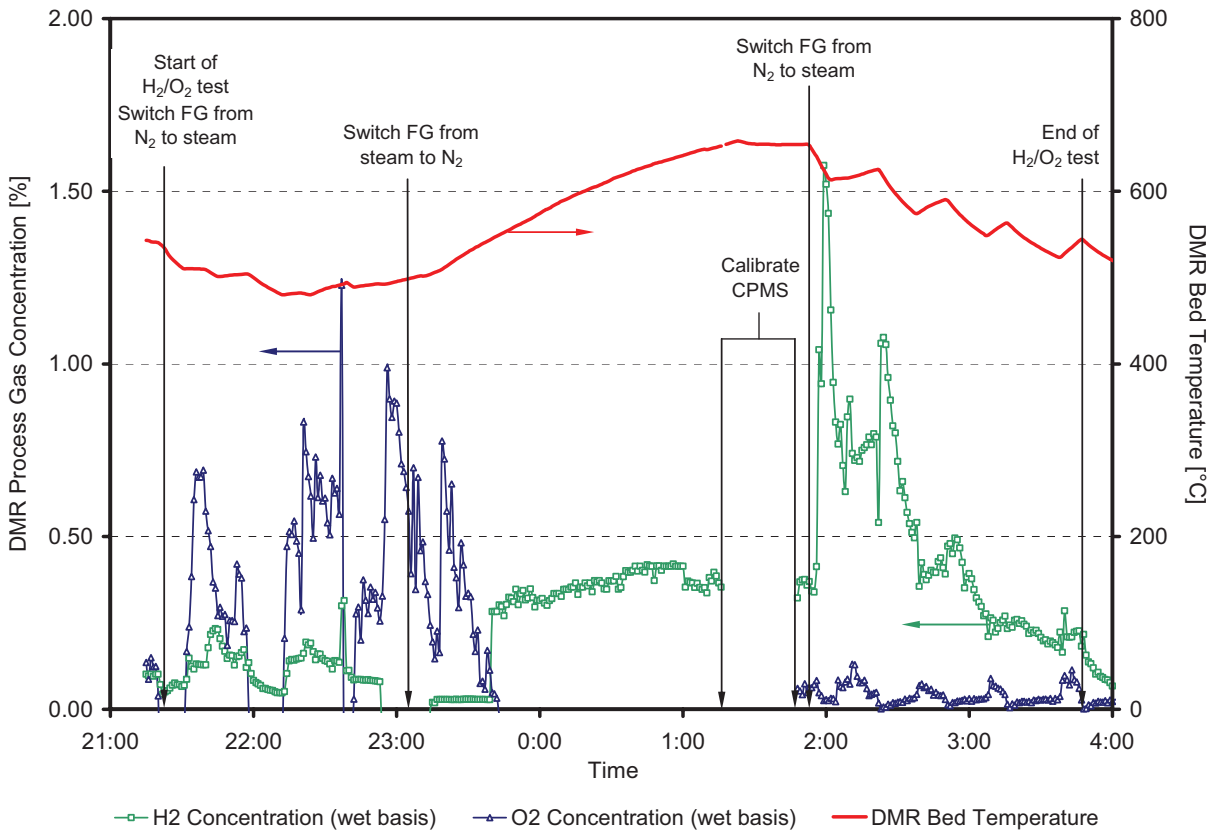

Figure 7-1. H_2-O_2 safety test data.

The test instrumentation used to measure hydrogen and oxygen concentrations are described in more detail in Table 3-1. The hydrogen analyzers were combined with carbon dioxide analyzers, which were used to correct for the known interferences on the hydrogen analyses from CO_2. The hydrogen analyzers used thermal conductivity detectors and had a range of 0–20% hydrogen by volume. The accuracy of the hydrogen analyzers was ± 2% of the full-scale reading. The oxygen analyzer used a paramagnetic detector with selectable full-scale ranges of 0–100% or 0–25% oxygen by volume. During the hydrogen/oxygen test, the 0–25% scale was used. The accuracy of the oxygen analyzer was ± 2% of the full-scale reading.

At the beginning of the test, the fluidizing gas (FG) was switched from nitrogen to steam at a bed temperature of approximately 540°C. The hydrogen concentration did not change significantly, indicating that insignificant steam reforming reactions were occurring in the DMR. The oxygen flow rate was periodically cycled off then back on to check for the presence of hydrogen. Hydrogen levels continued to

show no significant change. After about two hours, the fluidizing gas was switched back to nitrogen and the bed temperature was allowed to increase for the second part of the test.

During the second part of the test, the bed temperature was varied and the relative concentrations of hydrogen and oxygen were determined at the different temperatures. From Figure 7-1 it can be seen that the hydrogen concentrations were greatest at the highest bed temperature (~650°C) and decreased as the bed temperature went down. Below about 540°C, the hydrogen generation rate was essentially zero. The oxygen concentration during the entire second part of the test was not significantly different from zero.

The hydrogen/oxygen test demonstrated that significant hydrogen and oxygen concentrations are mutually exclusive over the wide temperature range tested. Below about 540°C, the production of hydrogen was very low and the hydrogen concentration was not significantly above zero. Above 520°C, up to and above 650°C, hydrogen and oxygen concentrations were mutually exclusive. For instance, if the DMR contained an excess of hydrogen, the free oxygen levels in the bed were near the oxygen monitor significance limit, i.e., 0.17 % oxygen on a wet basis. When the DMR contained excess oxygen, the free hydrogen levels in the bed were near the hydrogen monitor significance limits, i.e., 0.13 % hydrogen on a wet basis. The hydrogen/oxygen safety test is discussed in detail in, "Hydrogen Generation And Fate For The Sodium Bearing Waste Integrated Waste Treatment Unit" [R25].

7.3 Scoping Tests

The primary purpose of the scoping tests was to define the acceptable ranges of operating conditions for pilot plant operations. These operating conditions would be further evaluated in the production tests. The scoping tests were intended to accomplish the following:

- While feeding the SBW simulant solution, sequentially and separately operate the process using different feed rates of charcoal reductant to the DMR. Monitor H_2 generation rates and nitrate conversion efficiencies. The scoping tests included testing of two types of carbon in the DMR.
- Compare nitrate conversion efficiencies and charcoal fines carryover rates to the HTF. Change types of charcoal and feed rates as desired. Compare energy generation in the CRR for each type of charcoal used, if feasible.
- Confirm thermal performance and energy requirements for DMR and CRR while varying waste feed rate and establish the maximum sustainable waste feed rate.
- Confirm/establish operating parameters and additive usage rates for production run operations.
- Verify that DMR particle size control is achieved by adjusting waste feed nozzle atomizing gas rate ratio up to a maximum of 600.
- Confirm/establish operating parameters to produce desired average bed particle size and particle size distribution.
- Determine the need and rate for recycle of DMR bed solids to help maintain particle size control.
- Confirm capability to operate the CPMS in conjunction with the DMR and CRR.
- Evaluate critical operating conditions, e.g., throughput, excess oxygen, temperatures, etc., throughout the system.

- Initiate verification that the use of a mineralizing additive would prevent agglomeration in the CRR.
- Verify feed rates and confirm optimal locations for air/oxygen input to both the DMR and the CRR.
- Evaluate liquid waste feed nozzle(s) for accretion formation and plugging.

The actual scoping tests were performed to the conditions depicted in Table 5-1 of this document, using procedures that were updated and refined during system operational tests and the actual scoping tests by actions of the Joint Test Group (JTG). A specific document detailed the specific operating mode, which was followed during the scoping test operational period. [R22]

The liquid waste feed used in these tests was the baseline SBW simulant solution (except for Test S-1 where water was the only feed) without UDS, heavy metals, radionuclide surrogates, or POHCs.

The pilot plant scoping tests (including the hydrogen/oxygen safety tests) were initiated on December 5, 2005, and the scoping tests were successfully completed on January 13, 2006. However, the entire scoping test program was performed during five operating periods. Table 7-1 details the operating period and scoping tests performed therein.

Table 7-1. Operating periods for scoping tests.

Time Period	Scoping Tests Performed
November 15–23, 2005	Functional
November 28–December 7, 2005	H_2-O_2 Safety Test, S-1
December 15–18, 2005	S-1, S-2
December 19–22, 2005	S-3
January 3–7, 2006	S-3
January 8–13, 2006	S-4, 5, 6, 7, & 8

Figure 7-2 provides a timeline graphic for the period of November 28 through December 7, 2005.

This time period initialized actual fluidized bed operations. The initial bed addition to the DMR on November 28 was a dense sodium carbonate material. Following addition to the DMR, it was noticed that the overall DMR bed differential pressure and temperatures dropped off rapidly. This was coupled with a substantial increase in the inventory of material in the HTF and high pressure differential there. It was determined that the sodium carbonate had been rapidly ground to a powder by the fluidizing action of the DMR and high gas velocities through the cyclone, and had blown over into the HTF.

This issue with the sodium carbonate confirmed alumina, not sodium carbonate, as the DMR startup bed. It also confirmed that the filters in the HTF operated well, as no carbonate passed beyond the HTF. However, other improvements for future operations, such as adding new trending functions to the DACS, removing the flapper on the cyclone downcomer to prevent plugging with recycled fines, modifying the cyclone to reduce gas inlet velocities, and controlling the maximum wall temperature on the HTF to prevent product melting, were identified and implemented.

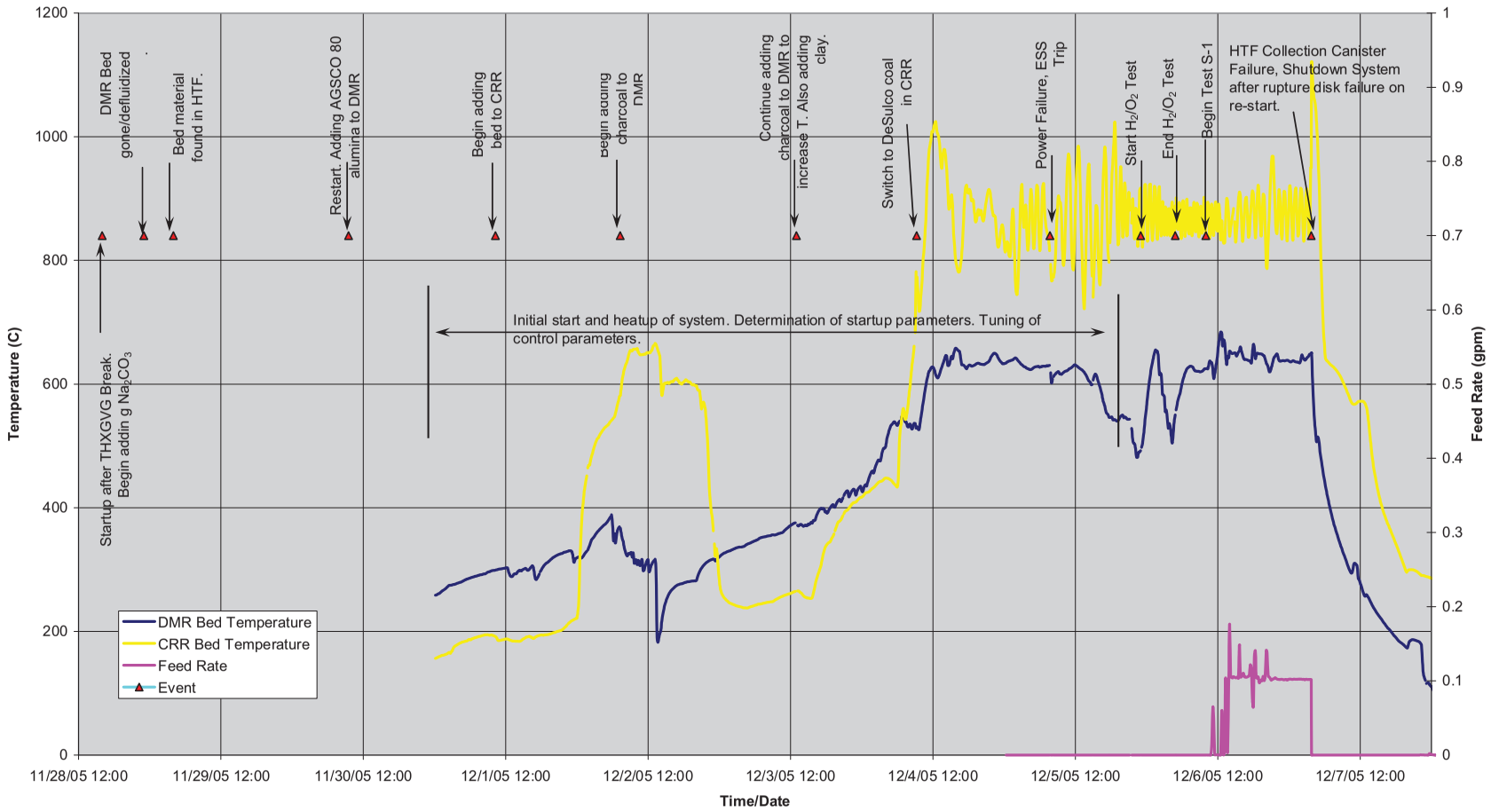

Figure 7-2. Pilot Plant activities November 28 to December 7, 2005.

A starting bed of AGSCO 80 alumina material was added to the DMR and heatup resumed of the DMR and CRR. But problems were experienced in getting enough heat into the DMR and the rest of the system in a timely manner. The JTG approved utilizing nitrogen/oxygen in the fluidizing gas and adding carbon to continue heat up of the DMR using carbon oxidation. This facilitated heatup of the CRR as well. The DMR was brought to an operating temperature of ~640°C with carbon oxidation (P-6 charcoal) as was the CRR operating at ~850°C with carbon oxidation (petroleum coke). Operating and technical personnel became familiar with coordinated operation of the reformers, especially the tuning and balancing of carbon and oxygen inputs to maintain stable operation.

As described above, the hydrogen/oxygen safety test was completed on December 5–6, 2006. Scoping Test S-1 using water feed was initiated on December 6 further confirming process chemistry and advancing understanding of process operation. The major unit operations and equipment items were functioning well. This activity demonstrated the basic operation of the feed injection system and the thermal capability of the DMR to evaporate water in the feed.

Early on the morning of December 7, while sampling solids from the HTF, a technician observed gas escaping from the sample container vent. He had placed the container isolation valve switch in the closed position, but had not verified the valve was actually in the closed position. He called his supervision and the TTT technical engineer, but before they arrived, he released the sample can from its lock, believing that the venting had ceased. Process gases and solids immediately flowed from the sample line. The major gas sources to the DMR were shut down and the team was successful in closing the isolation valve and reinstalling the sample container. Approximately 25 scfm nitrogen flow was then started to the DMR, but the DMR rupture disc released, which activated the ESS, completely shutting down the system. These events occurred over an approximately 20 minute period of time. Water was being fed to the system; no surrogate feed had been started. The technician was wearing all required PPE, including a respirator. No one was injured.

It is believed that the initial problem with the sample valve not closing was caused by an excessive buildup of solid material in the HTF, which was, in turn, caused by the bed level becoming too low in the DMR and bed material streaming out of the DMR via reverse flow through the cyclone downcomer. This is the same thing that happened with the sodium carbonate material. A contributing factor was that there was a restricted pressure probe in the DMR, which provided limited information on true bed level in the unit.

The release of the DMR rupture disc was caused by the reverse flow of solids from the CRR during the pressure reversal that plugged the CRR distributors and the attendant buildup of pressure in the system. It is believed that the CRR distributors were plugged when the venting of the HTF to the room caused the HTF to be at a lower pressure than the CRR, resulting in a back flow of bed material into the distributors.

It was determined that the system remain shut down while making system improvements. Table 7-2 summarizes improvements made to enhance the operational capability of the pilot plant during this period.

Figure 7-3 provides a timeline graphic for the operational period of December 15–18, 2005. A number of restart actions were completed and heatup of the system began again on December 15. Late in the day operations were temporarily suspended to remove restrictions from fluidizing gas distributor nozzles; re-heating began immediately after about 2 pounds of material were removed. System heatup and Test S-1 was completed the afternoon of December 17. Scoping Test S-2 using simulated SBW feed was then started.

Table 7-2. Scoping test changes – November 28 to December 7, 2005.

Change/Improvement Description	Reason
Changed size of charcoal in DMR from P3 to P6	To prevent plugging of the shot pot
Added thermocouples to the shell of the HTF, PR, PBF & GAC	To monitor the shell temperatures to prevent overheating and damage to heaters
Reconfigured inlet/outlet piping on flow meters	Minimum straight run dimensions must be maintained for proper instrument operation
Add water cleanout to OGC	Allow periodic method of flush and cleaning
Add a valve to the DMR to PR pipe	To allow to isolate for maintenance of the auger w/o opening the system to the DMR
Added cleanout rods to PTs and waste feed nozzles	To be able to clear the lines if plugging did occur
Added second superheater	To increase pilot plant capabilities for heat up and maintain temp
Added a steam trap to the steam line to the superheaters	To assure the steam service was as dry as possible
Added expansion joint to DMR fluidizing gas line	To allow for thermal expansion
Increased the size of the DMR cyclone inlet	To slow down the flow and allow larger particles to return to the DMR, thus reducing carryover
Lowered the DMR downcomer	To assure the bed media was returning deep enough and preventing siphoning of bed
Installed a pulser system to the DMR downcomer	To help keep the downcomer clear
Installed isolation valve between HTF off-gas line and CPMS analyzers.	Allow for periodic method of flush and cleaning
Added manually operated valve to bottom of HTF	To provide a valve that gives positive indication of position and will close better on solids

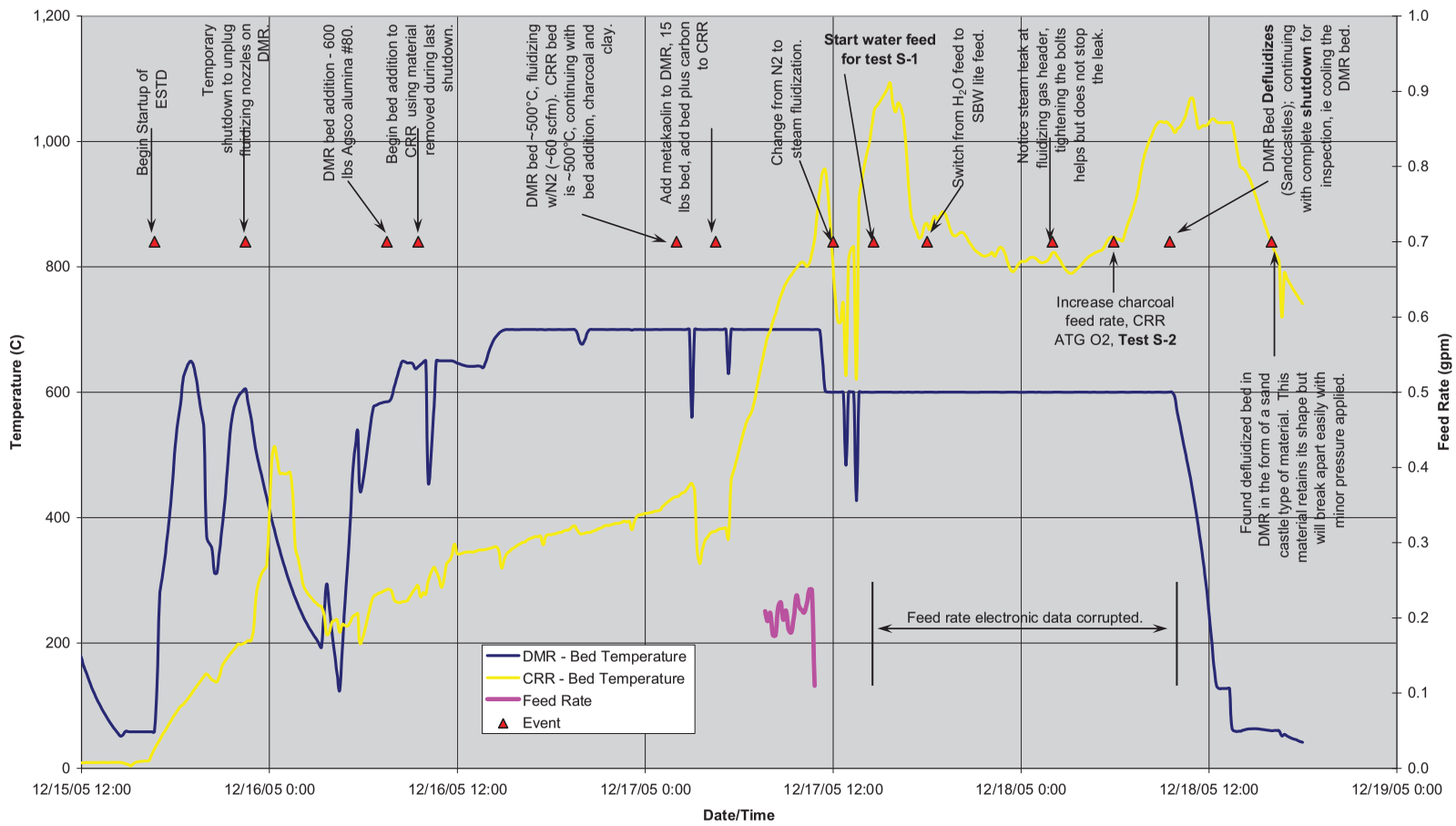

Figure 7-3. Pilot Plant activities December 15 to 18, 2005.

Significant leakage developed in two flanges on the fluidizing gas line to the DMR distributor, resulting in greatly reduced fluidizing steam and oxygen flow, after about 14 hours of operation with simulated SBW feed. At the same time, the temperatures in the DMR deviated, indicating that the bed was defluidized. The system was cooled down, the bed material was removed from the DMR, and the side port on the DMR vessel was removed for inspection of the vessel interior.

It was postulated that the flange leakage was due possibly to a combination of thermal and mechanical stress and the need for new high temperature gaskets was determined. Replacement gasket material for the key flanges on the fluidizing gas line was located and installed. High temperature steam with oxygen oxidizes low temperature gasket materials such as elastomers and graphite that can result in loosened bolts and cut gaskets.

It was found that a large fraction of the DMR bed had agglomerated into a “sandcastle” formation that was hard enough to cause the bed to defluidize during the inspection, but soft enough that it broke with gentle mechanical force. It was thought that the defluidization may have been caused by the uneven gas distribution in the bed caused by the FG distributor flange leak. This leak may have caused the bed solids close to the feed nozzle to become saturated with feed, leading to the defluidization event.

Figure 7-4 provides a timeline graphic for the period of December 19–22, 2005. The ESTD system was reassembled and heatup was initiated. Heatup was completed and simulant feed for Test S-3 was started ~0800 on December 21. At ~0900 indications of possible DMR bed defluidization were noted with the temperature and differential pressure data traces. Simulant feed was immediately stopped, as well as carbon and oxygen addition, and the fluidizing gas was switched from steam to nitrogen. Alumina was added to the DMR bed and the auger purge rate was increased to break up any “sandcastles” that may have formed in the bed. These actions resulted in recovery of normal bed temperature and differential pressure indications. Simulant feed was resumed at ~1150.

Operation of the ESTD system continued until ~1200 on December 22. Then, a routine system shutdown for the holidays was performed. The system operated quite well during this period; operation of the DMR at 0.25 gpm and 640ºC was amply demonstrated.

The bed from the DMR was removed by transferring it to the Product Receiver (PR) via auger and nitrogen jet eductor. The feed nozzles were removed from the DMR; small accretion buildup on E-1 nozzle was noted and some erosion on the plunger for the M-1 nozzle was noted. The DMR downcomer was plugged with “sandcastled” material, likely from same condition that caused the rest of the bed to sandcastle on December 21, before being cleared. Free flowing fine material was noted above the sandcastled material in the downcomer, indicating the cyclone was functioning until the downcomer plugged. The plugged downcomer resulted in no recycle of fines to the DMR and, hence, excessive carbon usage and material buildup in HTF. The material from the downcomer was removed.

Over the holiday break, the major portions of the system were disassembled and cleaned, and maintenance work was performed. Table 7-3 summarizes improvements made to enhance the operational capability of the pilot plant during this period.

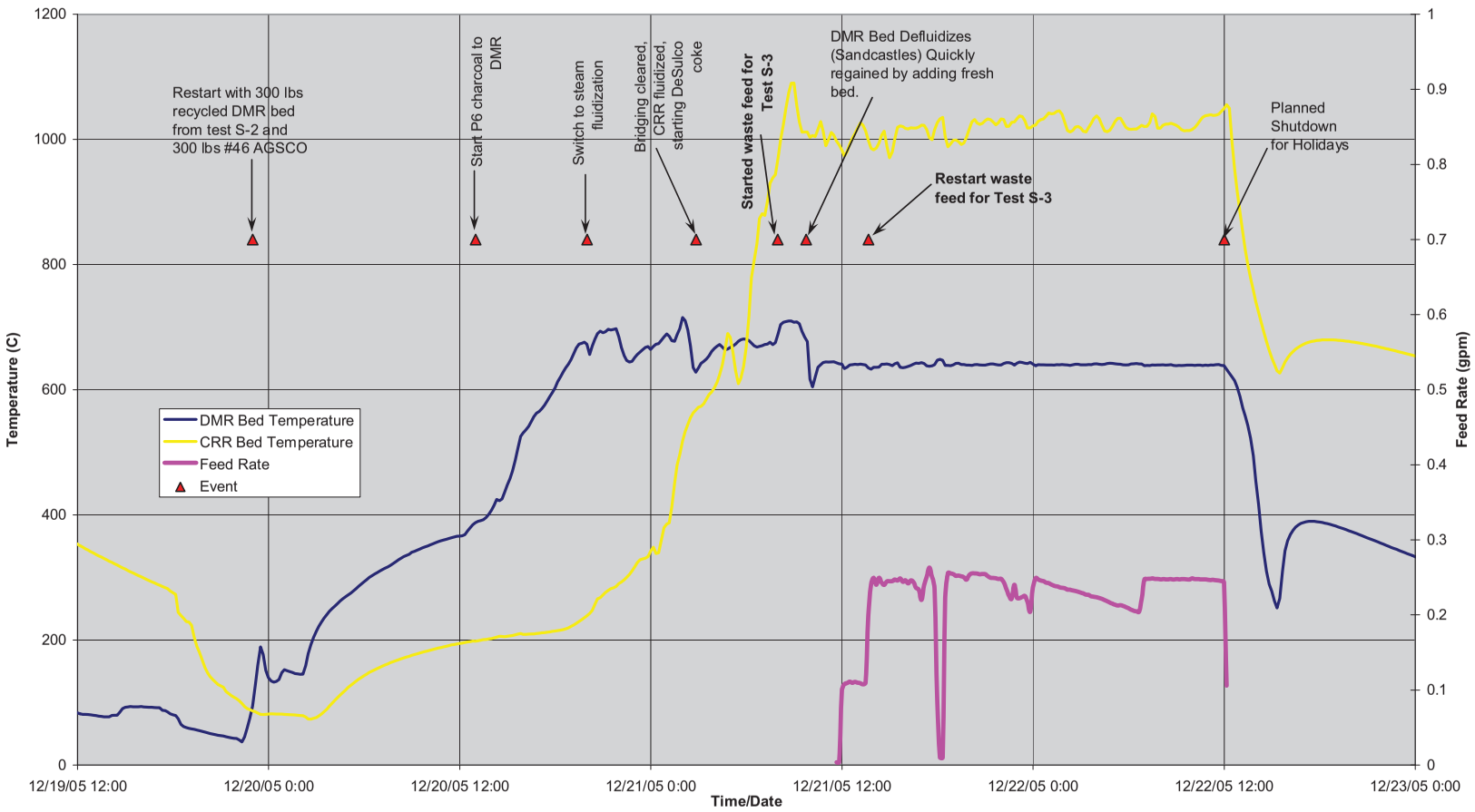

Figure 7-4. Pilot Plant activities December 19 to 22, 2005.

Table 7-3. Scoping test changes – December 19 to 22, 2005.

Change/Improvement Description	Reason
Plug 2 holes in DMR FG distributor	Increase FG velocity into DMR
Added ports to GAC inlet/outlet	Allows for more sample ports
Added N_2 purge to DMR auger, sample port, and PTs	To keep the lines from plugging
Installed high temp/corrosive environment pipe gaskets	Normal service gaskets leaked. Used Thermiculite gaskets
Replaced Ryton WF pump head with Kynar heads	Ryton did not hold up to corrosive waste feed

Figure 7-5 provides a timeline graphic for the period of January 3 to 7, 2006. Operations were resumed after the holiday break on January 3, with feed started on January 4. The CRR bed level was lowered to help decrease pressure fluctuations in the DMR freeboard. A higher bed level makes temperature control easier, but lower bed level minimizes back pressure spikes on the HTF and DMR and, in turn, improves cyclone operation and lessens fines carryover to HTF. It was postulated that this issue could be addressed by modifying the control scheme for the CRR bed temperature to allow a lower bed level.

On January 5, the DMR downcomer pulse jets were placed into service and the downcomer was cleared. The system operated until approximately midnight when the bed partially defluidized. The system was again cooled and disassembled to determine the cause of the defluidization. The investigation revealed a number of possible contributing factors:

- Simulant feed fluctuations due to feed line check valve pluggage and feed pump issues, resulting in bed temperature swings
- Shocking of bed fluidization dynamics due to downcomer clearing
- Build-up of material on opposite wall from feed nozzle
- High carbon levels in the bed resulting in a shift in the basic chemistry of the unit, possibly favoring “sticky” compounds.

Following the investigation and a set of conditions for system restart were adopted and reheating the system began. The main operating parameters were:

- Reduce feed rate from 0.25 to 0.20 gpm, while increasing NAR from ~250 to ~300
- Operate downcomer pulse jets to keep downcomer clear from the start of operations
- Automatically control DMR and CRR bed temperature with oxygen input rate
- Reduce CRR bed depth to ~26 in. to minimize back pressures surges on HTF and DMR.

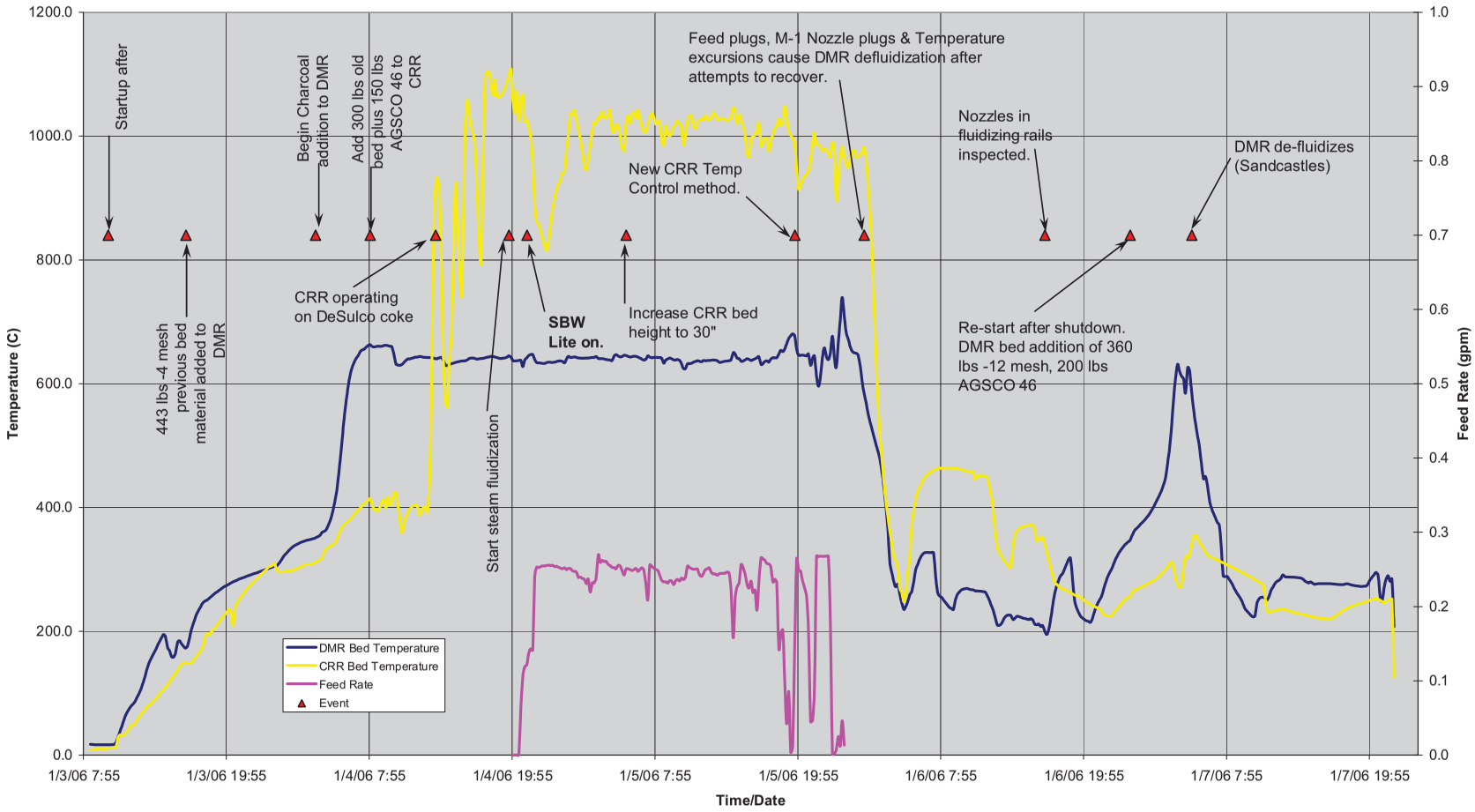

Figure 7-5. Pilot Plant activities January 3 to 7, 2006.

During heatup of the DMR bed, with charcoal and oxygen addition, but no steam or simulant feed, it was attempted to "tune" the automatic bed temperature controller, which controls oxygen flow to the DMR bed via the fluidizing gas distributors. Several large oscillations in oxygen addition rate during the tuning process were experienced, and simultaneously experienced a partial bed defluidization or "sandcastle." The system was cooled down, bed removed, and conditions investigated. The apparent cause was localized melting of certain low-melting calcium compounds due to high localized temperatures created by the reaction of carbon in the bed with the high transient oxygen levels. Micro-probe analyses of the apparent "glue" causing the bed particles to stick loosely together during this and previous "sandcastling" conditions consistently showed high levels of calcium. The P-6 charcoal is the source of at least two-thirds of the calcium in the bed. It was decided that a "buffer" additive was needed to tie-up the potential "bad actors" that are causing the sandcastling and to make the process less susceptible to physical or chemical perturbations. It was decided to add calcined Mulcoa clay to the bed to help tie up any low-melting eutectics that may have formed in the bed. It was also determined that GC-CRB carbon should be tried in place of the Berger Brothers P-6 charcoal, as it contains far less calcium.

Table 7-4 summarizes improvements made to enhance the operational capability of the pilot plant during this period.

Table 7-4. Scoping test changes – January 3 to 7, 2006.

Change/Improvement Description	Reason
DACS auto control for O_2 to CRR	Better control the CRR temperature
DACS to use CRR O_2 at outlet in control	Control of CEMS results
Continually adjust the DACS for auto control	To allow more consistent control of temperature, flow, pressures, etc..
Install snubbers on the DPTs	To level out the signals
Changed DMR carbon from charcoal to coal	To reduce sandcastling of the DMR bed

Figure 7-6 provides a timeline graphic for the period of January 8 to 13, 2006.

Muffle furnace tests of DMR bed material (removed from the DMR earlier in the day) were conducted. It was noted that the bed material, with no clay added, started to stick together at 640–650ºC. Just 5 wt% clay added to the bed material substantially mitigated "stickiness" (i.e., sandcastling potential) at 650ºC and 750ºC.

The broken-up bed material from the DMR was screened through a -12 mesh and reused in the DMR, along with ~10% Mulcoa clay, for resumption of the scoping tests. Heatup of the DMR and CRR was concluded and simulant feed to the DMR was started for Test S-4 at ~2200 on January 8. Test S-4 at 0.2 gpm, a DMR temperature of ~620ºC, and a CRR temperature of ~1050ºC was completed, and GC-CRB coal-based carbon was successfully used in the DMR, with ~5% clay added. No signs of bed agglomerations or sandcastling were observed during the test.

Test S-5 was initiated on January 10 at ~0500; the DMR temperature was increased to ~650ºC, with other process conditions unchanged. Operation remained good; both E-1 and M-1 feed nozzles were used, but intermittent restriction of both feed nozzles was experienced.

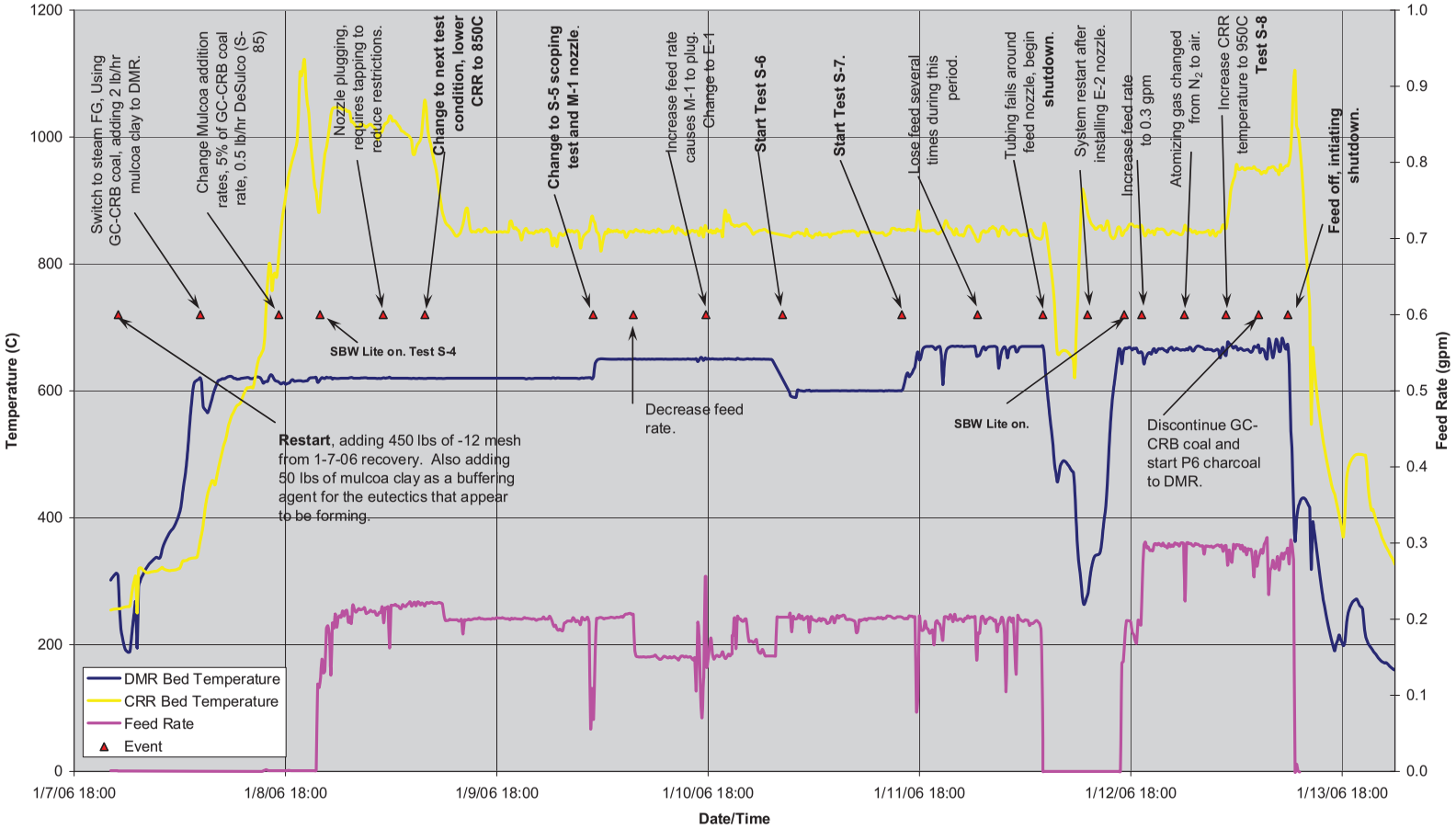

Figure 7-6. Pilot Plant activities January 8 to 13, 2006.

Scoping Test S-6 of was initiated early on January 11. A DMR bed temperature of ~590ºC was desired, but it did not appear that the Erwin coal was sufficiently reactive for this temperature. The practical minimum DMR operating temperature appears to be ~600ºC. No signs of bed agglomerations or sandcastling have been observed. The DMR bed particle size conditions were very good and the off-gas composition was as expected. Micro-probe analyses of product produced since restart showed much lower calcium on the surface of the bed particles and higher sulfur, both consistent with the reduction or tying up "bad actor" compounds. Periodic feed nozzle restrictions were experienced. A principal issue was determining the cause of the feed nozzle restrictions and doing what was necessary to eliminate it.

At ~1700 on January 11, Scoping Test S-7 was started; 0.2 gpm feed rate, a DMR temperature of ~670ºC, and a CRR temperature ~850ºC. Some DACS functions were lost on three separate occasions resulting in significant process upsets, e.g., loss of liquid feed, loss of atomizing nitrogen, high fluidizing gas flow rates, and accompanying high elutriation rates to HTF. The apparent cause was attempting to switch DACS recognition between two CPMS NO_X monitors when one of the units stopped working properly and the other was put on line. The system was rebooted and it corrected the problem. Process operation was suspended at ~0800 January 12 when the feed line failed. The apparent cause of failure was stress due to placement of a vibrator on the small feed tubing to help maintain consistent feed injection rates and repeated tapping of the feed nozzle flange to clear nozzle restrictions.

Enough DMR bed material was removed to allow removal of the feed nozzles for inspection. M-1 nozzle was completely plugged off with nozzle accretions. The E-1 nozzle had ~50% of the atomizing gas annulus plugged, resulting in a significant accretion on one side of the nozzle.

The backup E-1 was installed, along with improved nozzle purge capabilities. Bed was reloaded into the DMR and system heatup at commenced ~1300 January 12. Simulant feed was resumed to the DMR at ~1650 and increased to 0.3 gpm at ~1900; the system handled it well. Adding a small amount of nitrogen to the liquid feed does not seem to decrease plugging potential. There was little difference in plugging potential whether nitrogen or air was used as the atomizing gas. No plugging observed when feeding water only. The hypothesis was that partial vaporization and drying of the feed simulant inside the feed nozzle due to radiant and conductive heat transfer was occurring.

Scoping Test S-8 was initiated at ~0500 on January 13. The CRR temperature was increased to 950°C and the feed rate remained at ~0.3 gpm. The system was operated until ~1200, then a scheduled shutdown was initiated.

Solid material was found in CPMS/CEMS units that was causing intermittent sample flow issues. The material appears to be an ammonium carbonate. The off-gas sampling subcontractor was consulted to find ways to better configure the gas analysis system and condition the feed gas.

A cool down of the system was performed and the beds from the DMR and CRR were removed. Both beds were free flowing. An inspection of the inside of DMR noted a buildup of a brown scale on the internals of the DMR, e.g., walls, downcomer, corrosion coupons, and other hardware, but not on the feed nozzle. The scale was ~1/16 to 1/8 in. thick on walls, but heavier on the downcomer and corrosion coupons. The material did not cause sandcastling of DMR bed material and did dissolve in water. The scale was submitted for analysis and removed from the downcomer and corrosion coupons to the extent possible, but not from the walls to avoid damaging the refractory.

Table 7-5 summarizes improvements made to enhance the operational capability of the pilot plant during this period. These changes were implemented prior to initiating Production Tests on January 17.

Table 7-5. Scoping test changes – January 8 to 13, 2006.

Change/Improvement Description	Reason
Add PR overtemp controller	Assure PR heaters do not overheat the vessel
Install N_2 purge to waste feed nozzles when running	Make sure the nozzle not in use stays clear
Add a check valve to the waste feed system	Prevent backflow
Changed atomizing gas from N_2 to air in waste feed nozzle	Eliminate hot spots
Added water flush to waste feed nozzles	Maintenance item to periodically flush nozzles to prevent plugging
Add DP gauges to the DMR downcomer pulsers	Assure the downcomer pulsers are working
Add cooling water to the waste feed nozzles	Reduce plugging of waste feed in nozzles
Added additional filters to the CPMS	Dust from the HTF and ammonium carbonate formation in sample lines was restricting the instruments
Add a steam regulator	More consistent steam pressure

7.4 Production Tests

Production tests were performed in two phases. Phase 1 (CP1) was performed from January 16 to February 10, 2006. Phase 2 (CP2) was performed between May 15 and June 8, 2006. Sections 5.4 and 5.5 describe the scope of these tests. Each test was performed as required by the approved test plan and operating procedures. Data quality was subjectively assessed based on CPMS and CEMS monitors being lined out, liquid feed continued uninterrupted, all required liquid and solid samples were acquired, documentation of test conditions had been accomplished, and all scheduled manual stack gas sampling was completed and determined by the sampling contractor to be acceptable.

7.4.1 Carbonate Phase 1 (CP1) Tests

The CP1 tests were performed to the conditions depicted in Table 5-2 of this document. The CP1 test program was performed during three operational periods. Table 7-6 details the operating period and scoping tests performed therein.

Table 7-6. Operating periods for production tests.

Time Period	Production Tests Performed
January 16–21, 2006	P-1
January 25–February 5, 2006	P-2A, P-3B, P-4A-1, P-4A-2, P-4A-3, P-4A-4, P-4A-5, P-4A-6
February 7–10, 2006	P-4A-6 (completion), P-5, P-6

Figure 7-7 provides a timeline graphic for the period of January 16 to 21, 2006.

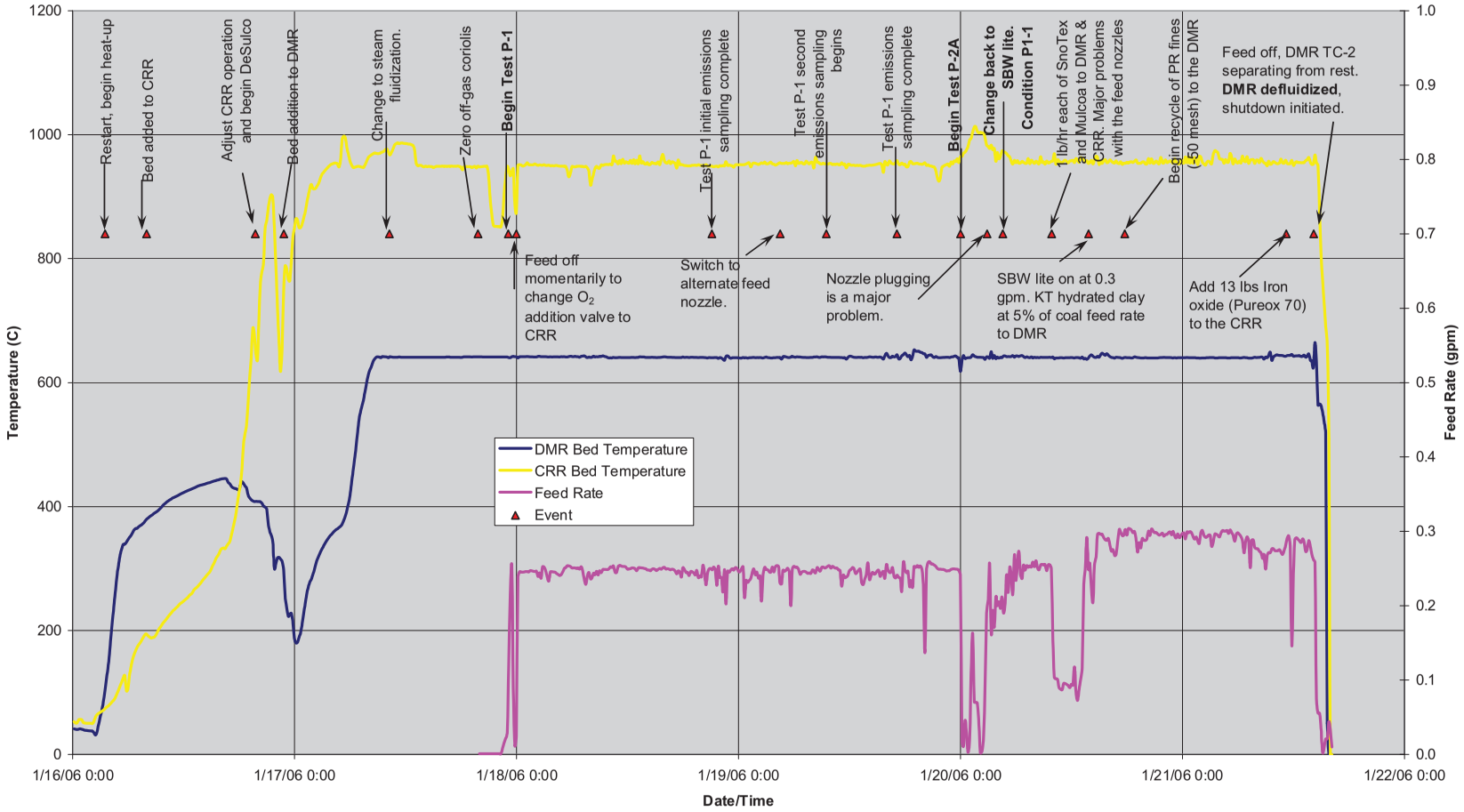

Figure 7-7. Pilot Plant activities January 16 to January 21, 2006.

Production Test P-1 was initiated on January 16, 2006, when the pilot plant transitioned from the scoping test conditions by implementing a DMR temperature at 640°C and a CRR temperature of 950°C. It was concluded by the JTG, after reviewing mineralogy results, that the Mulcoa clay was ineffective at tying up low melting point compounds to prevent deposition on the DMR hardware. It was decided to go to a more reactive clay, not fired, as the Mulcoa is. Snow Tex 45 clay at 5 wt% relative to DMR carbon usage will be added to the DMR.

The simulant feed rate was set to a nominal rate of 0.25 gpm using the E-1 nozzle beginning the test at ~2300 on January 17. The simulant feed nozzle experienced intermittent plugging throughout the test. Mechanical rodding of the feed tube combined with purges and water were used to clear the obstructions. Solid process samples of the HTF, PBF, DMR and CRR were collected at ~4 hr intervals beginning on January 18, 2006, at 1725 and continuing throughout the test. These samples were assayed for metals, carbonate, fluoride, and chloride. It was decided to continue with the organics sampling on the morning of January 19, 2006. Operating conditions were maintained throughout the night, which included several more nozzle plugging events.

More focus was being placed on the DMR bed particle size growth. The bed was becoming depleted in particles smaller than 50 mesh, so screening PR product material and recycling the minus 50 mesh fraction to the DMR to provide seed particles was instigated. The addition to the bed of some Mulcoa clay, with its large particle size range, which previous appeared to be a source of seed particles for bed growth, was reinstituted.

Required emissions sampling was successfully performed during the test period and sample quality was determined to be adequate to allow transition to test conditions for Production Test P-2.

Test P-1 ran for ~40.6 hours operating time and processed 609.3 gallons of feed solutions. Process operations generated 621.8 pounds of product from the PR, and 257.3 pounds of material recovered from the HTF.

Test P-2A was initiated about midnight on January 20. This test added UDS to the simulant feed. The feed nozzle quickly plugged and many different techniques were tried to establish and maintain feed flow, but were unable to get feed to flow for more than a few minutes through either nozzle. The system was returned to supernatant feed after about four hours, suspending production tests. The situation was evaluated and it was elected to design and build improved feed nozzles simultaneous with continuing to operate the process to work on DMR bed particle size control. Parts were obtained and two new waste feed injectors were fabricated. The simulant feed rate was increased to 0.32 gpm and feeding was much better at this rate, likely due to lower liquid residence time in the nozzle.

The process operated well for almost 24 hours on supernatant feed at a high average supernatant feed rate. DMR particle size control was successful by recycling product material less than 50 mesh in size. The E-2 feed nozzle performed well at the higher feed rate. Operations were suspended at ~1400 on January 21 when some of the temperature points low in the bed diverged from the rest and the bed defluidized. An investigation revealed that the metal sleeves around the two feed nozzles had worked their way loose and into the active bed, one about 7 inches and the other about 2 inches. This was probably caused by some combination of pushing the sleeves into the bed during nozzle installation, tapping on the nozzles to clear restrictions, and mechanical action of the bed. It is thought that the disruption of the DMR fluidization and atomization patterns caused by this resulted in bed defluidization. The metal sleeves likely also increased the rate of heat transfer into the feed nozzles, increasing the potential for feed vaporization and solidification inside the liquid tubes of the nozzles. The metal sleeves were replaced by an insulating material when the new feed nozzles were installed.

Table 7-7 lists changes to the system in this time period to enhance process operability.

Table 7-7. Production test changes – January 16 to 21, 2006.

Change/Improvement Description	Reason
Reconfigure T-101A/B to recirc independently	Better use of tanks to mix in one while utilizing the other
Modify waste feed nozzle design	To optimize performance and prevent plugging
Added additional thermocouples to DMR and CRR	To better monitor vessel temperatures
Added additional pressure transmitters to DMR and CRR	To better monitor the differential pressures between, and in, vessels
Switched to diaphragm pumps on waste feed system for UDS	Centrifugal pumps exhibited severe wear when pumping UDS
Install strainers on the waste feed line	Prevent plugging of the waste feed system

Figure 7-8 and Figure 7-9 provide a timeline graphic for the period of January 25 to February 5, 2006.

Production Test P-2A added ~80 grams/liter UDS to the SBW feed liquid to determine the impact of UDS on the liquid feed system operability. The process was started up and brought to the required test conditions at ~1245 on January 26. While no heavy metals were planned for this test, the GAC adsorber bed was placed in service and allowed to preheat prior to initiating the test.

Numerous brief (1 to 5 minutes) feed interruptions were experienced during the first few hours of feeding the SBW with UDS because of feed line plugging. These interruptions were determined to be due to oversized zirconium phosphate particles in the UDS. It was directed that inline Y-strainers with water backflush capability be added to the liquid feed system, and that future UDS batches be made up with pre-screened zirconium phosphate (30 mesh screen). The final strainer location was determined during operation over several hours. Operations continued to establish stable off-gas conditions to support emissions sampling.

Required emissions sampling was successfully performed during the test period and sample quality was determined to be adequate to allow transition to test conditions for Production Test P-3.

This test ran for 23.2 hours operating time and processed 348.2 gallons of feed solutions. Process operations generated 278.2 pounds of product from PR, and 477.6 pounds of material recovered from the HTF.

Production Test P-3B was started at ~1800 on January 27. This test investigated the impact on system performance of adding heavy metals to the SBW feed liquid and began the evaluation of GAC adsorber efficiency.

Periodic feed interruptions occurred, due to feed line plugging. Lines were flushed and feed tank recirculation rate increased, which stopped the feed interruptions. This occurred early in the test stabilization period and did not affect emissions sampling. The feed line plugging that resulted from the over-sized UDS material was solved by depleting the affected feed simulant and going to a new makeup with pre-screened UDS components.

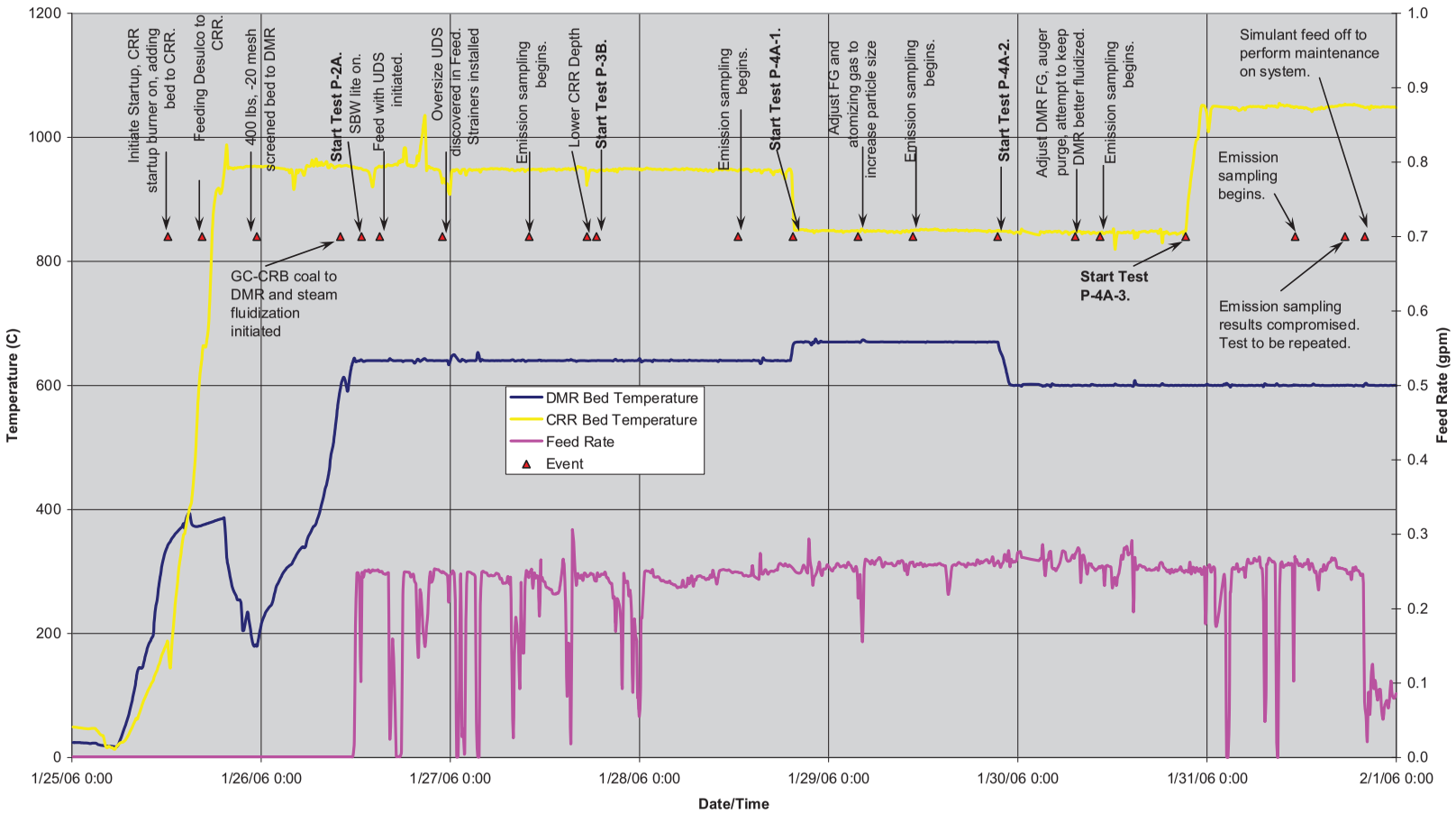

Figure 7-8. Pilot Plant activities January 25 to February 1, 2006.

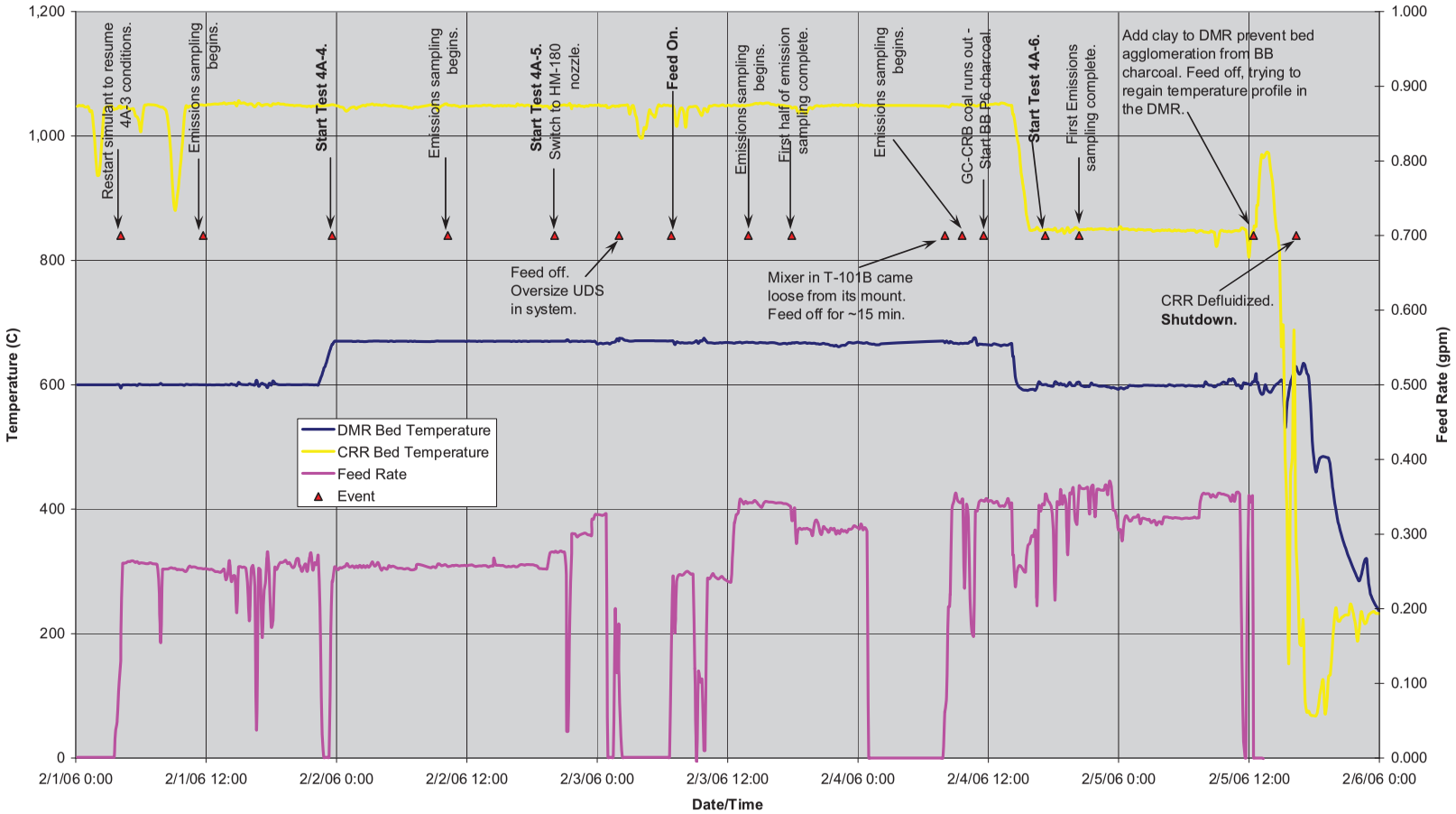

Figure 7-9. Pilot Plant activities February 1 to 5, 2006.

Required emissions sampling was successfully performed during the test period, and sample quality was determined to be adequate to allow transition of the process conditions to those required for test P-4A-1. The test ran for 23.8 hours operating time and processed 357.7 gallons of feed solutions. Process operations generated 263.3 pounds of product from the PR, and 394.8 pounds of material recovered from the HTF.

Production Test P-4A-1 was started at ~1930 on January 28, 2006, by increasing the DMR temperature from 640°C to 670°C, and lowering the CRR temperature from 950°C to 850°C. This test determined system performance with full feed at maximum DMR temperature and minimum CRR temperature.

Required emissions sampling was successfully performed during the test period and sample quality was determined to be adequate to allow transition to test conditions for P-4A-2. This test ran for 25.6 hours operating time and processed 383.7 gallons of feed solutions and 10.6 pounds of POHC. Process operations generated 135.3 pounds of product from the PR and 660.5 pounds of material recovered from the HTF.

Production Test P-4A-2 was started on January 29, 2006, by lowering the DMR temperature from 670°C to 600°C while maintaining the CRR temperature at 850°C. This test determined system performance with full feed at minimum DMR temperature and minimum CRR temperature. This test ran for 23.2 hours operating time and processed 347.4 gallons of feed solutions and 9.5 pounds of POHC. Process operations generated 379.2 pounds of product from the PR and 544.0 pounds of material recovered from the HTF. Required emissions sampling was successfully performed during the test period and sample quality was determined to be adequate to allow transition to test conditions for P-4A-3

Production Test P-4A-3 was started on January 30, 2006, by maintaining DMR temperature at 600°C and increasing the CRR temperature from 850°C to 1050°C. The simulant feed rate was maintained at a nominal rate of 0.25 gpm. This test determined system performance with full feed at minimum DMR temperature and maximum CRR temperature.

The process feed system experienced periods of plugging throughout the test cycle. This plugging was likely due to the UDS and mechanical pump head failures. Cleaning and/or replacement of the feed lines and reconfiguration of the feed pump heads resolved the plugging issues and operations continued.

During the air pollution sampling portion of this test period, a set of sampling trains was halted due to excessive moisture accumulation. The other organic trains sampling activities continued to completion. The decision was made to maintain the current test conditions and repeat the total organics test the following day.

Upon completion of the remaining samples, the system was put on idle (no feed/minimum gas flow) for the night to allow for maintenance on the feed system to eliminate sources of plugging. In the morning, feed and gas flows were restarted to achieve operating stability for testing. The remaining sampling activities were then completed. The single head masterflex pump was replaced with a triple head model during the period when feed was not flowing, which allows for a more consistent and even flow to the flow meter and feed nozzles.

The P-4A-3 test ran for 37.7 hours operating time and processed 566.0 gallons of feed solutions and 15.9 pounds of POHC. Process operations generated 366.4 pounds of product from the PR and 728.7 pounds of material recovered from the HTF.

Required emissions sampling was successfully performed during the test period and sample quality was determined to be adequate to allow transition to test conditions for P-4A-4.

Production Test P-4A-4 was started on February 1, 2006, by increasing DMR temperature at 670°C and maintaining the CRR temperature at 1,050°C. The simulant feed rate was maintained at a nominal rate of 0.25 gpm. This test determined system performance with full feed at maximum DMR temperature and maximum CRR temperature.

During this test the process feed system experienced a pump and feed tube failure. The tubing for the peristaltic pump heads failed on a regular basis. This was expected and spare tubing was obtained. Repairs were made and feed was restarted.

Required emissions sampling was successfully performed during the test period and sample quality was determined to be adequate to allow transition to test conditions for P-4A-5. This test ran for 19.9 hours operating time and processed 297.9 gallons of feed solutions and 8.9 pounds of POHC. The process operations generated 292.2 pounds of product from the PR and 300.5 pounds of material recovered from the HTF.

Production Test P-4A-5 was started on February 2, 2006, by maintaining DMR temperature at 670°C and maintaining the CRR temperature at 1,050°C. This test determined system performance with maximum feed rate at maximum DMR temperature and maximum CRR temperature.

The simulant feed rate was increased to a nominal rate of 0.35 gpm. The simulant feed nozzle was switched from the 0.12-in. diameter H-2 nozzle used on the previous test sequences to the 0.18-in. diameter M-2 nozzle to accommodate the higher feed rate. The simulant feed rate of 0.35 gpm could not be sustained throughout the test due to feed line pressure spikes exceeding 80 psi. A steady simulant feed rate of ~0.34 gpm was achieved.

The process feed system did experience a pump and feed tube failure. Repairs were made, and feed was restarted.

This test ran for 34.6 hours operating time and processed 639.4 gallons of feed solutions and 8.6 pounds of POHC. The process operations generated 550.9 pounds of product from the PR and 818.8 pounds of material recovered from the HTF. Required emissions sampling was successfully performed during the test period, and sample quality was determined to be adequate to allow transition to test conditions for P-4A-6.

Production Test P-4A-6 was started on February 4, 2006, by reducing DMR temperature to 600°C and reducing the CRR temperature to 850°C. This test determined system performance with maximum feed rate at minimum DMR temperature and minimum CRR temperature.

The simulant feed rate was maintained at a nominal rate of 0.35 gpm. The first half of the test was conducted using Berger Brothers P-6 charcoal as the carbon source for the DMR, as GC CRB was not available. CK-46 clay was added to the DMR to prevent bed agglomeration during usage of the P-6 charcoal. It was decided to "idle" the process after the first half of the emissions sampling, pending the arrival of more General Carbon material, which would allow better control of the DMR operation. On February 5, 2006, defluidization of the CRR resulted from mechanical problems with the CRR solids addition system. It was subsequently decided to shutdown the process for inspection of the DMR and CRR internals. Inspections were conducted on February 6 and 7, 2006. A small amount of bed material (~2 lb) in the CRR was agglomerated into relatively small pieces. The underside of the in-bed oxygen distributor appeared to be burned/eroded at the end, but was suitable for continued use. There were no

large agglomerates in the DMR bed although there was a significant (about 2.5 cm thick × 20 cm high) "bathtub ring" of sandcastled material on the walls of the DMR vessel about the level of the feed nozzles. It is possible the high FG flows used attempt to refluidize the CRR broke up the agglomerated DMR bed material. The atomizing gas tube on one of the feed nozzles was replaced, as it was significantly eroded. The rest of the DMR internal hardware looked good.

Re-start took place later on February 7, 2006, using General Carbon as the DMR carbon source. Figure 7-10 provides a timeline graphic for the period of February 7 to 10, 2006. It was determined that the use of P-6 charcoal during the inorganic emissions sampling would have no material affect on the emissions sampling/results. However, completion of emissions sampling for Test P-4A-6 had to be completed after restart of the system.

Some problems were encountered in getting the CRR to fully fluidize during restart. There appeared to be a light "crust" on the top of the bed. To address this, ~200 lb of media were drained out of bed and new media added. Test P-4A-6 was resumed at ~0200 on February 8. Emissions organic sampling was completed at ~1800.

The test ran for 35.6 hours operating time and processed 688.2 gallons of feed solutions and 11.4 pounds of POHC. Process operations generated 851.1 pounds of product from the PR and 1122.0 pounds of material recovered from the HTF.

Production Test P-5 was started on February 8, 2006. No POHC was added for this test. This test added ~120 g/L UDS to the SBW feed liquid to determine the impact of high UDS on system operability. This test simulates high UDS concentration in the SBW tanks.

Near the end of the test period, operators experienced difficulty in transferring product from the DMR to the PR. Subsequent investigation (at the end of the tests) indicated the some of the bed material was bridged over above the DMR auger screw. The balance of the DMR bed remained well fluidized, and DMR bed level was controlled by removing material via the bed sample port. General process operation remained good.

This test ran for 23.9 hours operating time and processed 357.9 gallons of feed solutions. Process operations generated 411.8 pounds of product from the DMR and the PR and 467.9 pounds of material recovered from the HTF.

Required emissions sampling was successfully performed during the test period and sample quality was determined to be adequate to allow transition of the process conditions to those required for Test P-6.

Production Test P-6 was started at ~0030 on February 10, 2006. No POHC was added for this test. This test determined the impact of high UDS loading and dilute SBW on system operability. This test simulated UDS clean-out from SBW tanks with water.

The GAC adsorber bed was in service for this test. DMR bed level was controlled by using the bed sample port. General process operation remained good.

This test ran for 12.2 hours operating time and processed 182.5 gallons of feed solutions. Process operations generated 137.3 pounds of product from the DMR and the PR and 173.9 pounds of material recovered from the HTF. Required emissions sampling was successfully performed during the test period and sample quality was determined to be adequate for analysis. Completion of Production Test P-6 ended the operating portion of the testing program. A controlled shutdown of the process was initiated at approximately 1300 of February 10, 2006.

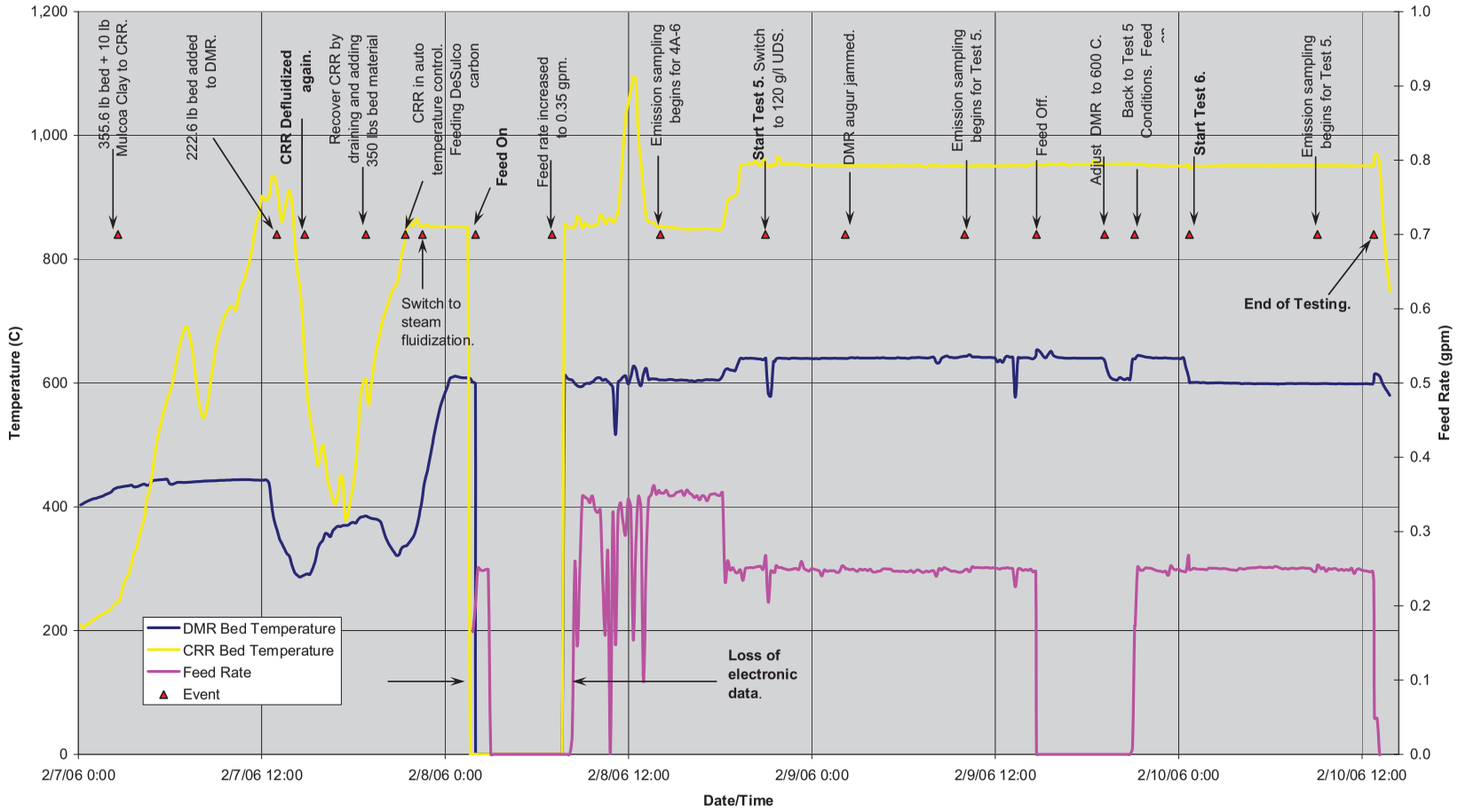

Figure 7-10. Pilot Plant activities February 7 to 10, 2006.

7.4.2 CP1 Operating Conditions

Test CP1 included 12 production runs, which varied simulant feed composition, simulant feed flow rate, DMR operating temperature, CRR operating temperatures, and process additive. The desired process setpoints for CP1 may be found in Section 5. The achieved operating condition for each CP1 test condition may be found in Table 7-8 through Table 7-13.

7.4.3 Carbonate Phase 2 (CP2) Tests

The CP2 tests were performed to the conditions depicted in Tables 5-3, 5-4 and 5-5 of this document. The CP2 test program was started initially on May 15, but a thermal event in the granular activated carbon bed mercury adsorber precluded complete performance of CP2 at that time. New granular activated carbon was ordered, and the bed repaired/enhanced with instrumentation before CP2 was re-initiated on May 30. Figure 7-11 provides a timeline graphic for the period of May 30 to June 9, 2006.

The granular activated carbon thermal event is documented in detail in Joint Test Group Action Form No. 07 [R26].

CP2 Preheat (May 30 and 31, 2006)

Heatup of the process system began with superheated N_2 and the CRR auxilliary burner operating, but with the GAC bed bypassed; a lesson learned from May 16. An alumina starting bed (574 lb) was added to the CRR to maintain the heatup rate at ~100°C/hr. An initial 50/50 mixture of AGSCO 46 and AGSCO 80 was added to the DMR to achieve a bed height of 36 inches. With the DMR at 310°C the fluidizing gas was switched from N_2 to steam and P6 carbon addition began. Heatup continued with the process set in automatic mode. Upon completion of the heatup of the CRR, the GAC bed was valved on-line and as the GAC bed was heated up it was noticed that the #3 GAC bed experienced a sharp rise in temperature that leveled off at ~150°C.

Heatup of the process continued with process parameters set for Test Condition #1. The SBW surrogate (no metals/UDS/POHC) feedrate of 0.25 gpm was established at ~0430 on June 1; with the DMR bed temperature at 640°C and the CRR bed temperature at 950°C. The CRR ATG mixture was set at 50% O_2 and 50% N_2. The CRR bed height was operated at ~33 inches. With conditions stabilized, manual off-gas sampling was initiated at the stack using EPA Method 29 for total metals and at the GAC Stages 1, 2, and 3 using the Ontario Hydro Method for Hg speciation. The process configuration was changed to CRR Condition #2 by adjusting the ATG mixture to a 75/25 ratio with the successful completion of sampling.

The process configuration was changed to Condition #4 with an ATG mixture of 50/50 in the lower flow nozzle on June 2. Condition #4 continued for ~10 hours prior to switching the configuration to Condition #3. The ATG mixture was set at 75/25 in the lower flow nozzle.

Table 7-8. Summary of CP1 DMR operations.

Test Start		Finish	COT Duration (hr)	Simulant feed rate (gpm)	DMR fluidizing steam rate (lb/hr)	DMR fluidizing O_2 rate (scfm)	Atomizing air rate (scfm)	Coal feed rate (lb/hr)	DMR clay feed rate (lb/hr)	DMR fluidized bed density (gm/cc)	DMR bed T (°C) (12" E)	DMR freeboard T (°C) (92" S)	DMR outlet T (°C)	DMR freeboard P (psig)
				FT-200-001	FT-104-001	FTCV-104-002	FTCV-200-003	WDT-204-001	—	PDT-200-001	TT-200-003 TT-2	00-010 TT-2	00-011	PT-200-005
P1	1/17/2006 23:02	1/19/2006 17:09	40.6	0.243	84.7	2.4	11.2	28.6	0.74	0.75	641	565	540	2.9
P1-1	1/19/2006 17:09	1/21/2006 13:36	35.0	0.242	85.0	3.1	10.7	30.6	2.23	0.87	641	545	525	3.0
P2	1/26/2006 12:45	1/27/2006 18:30	23.2	0.207	68.8	2.6	11.3	29.9	0.22	1.05	640	570	547	2.3
P3B	1/27/2006 19:20	1/28/2006 19:10	23.9	0.234	55.0	2.7	10.0	34.0	0.00	0.87	640	595	567	2.2
P4A1	1/28/2006 19:10	1/29/2006 21:26	25.6	0.256	43.5	3.4	8.3	33.6	0.00	0.89	669	619	588	1.7
P4A2	1/29/2006 21:26	1/30/2006 21:05	23.2	0.260	54.5	1.6	7.0	32.9	0.00	0.81	601	542	515	1.6
P4A3 1/	30/2006 21:05	2/1/2006 22:18	37.7	0.244	59.6	2.7	7.4	21.7	0.00	0.94	600	523	494	1.4
P4A4	2/1/2006 22:18	2/2/2006 19:23	19.9	0.246	38.9	3.3	7.6	30.3	0.00	0.92	668	595	562	1.6
P4A5	2/2/2006 19:23	2/4/2006 14:15	34.6	0.285	40.2	3.0	9.7	32.8	0.00	0.83	668	597	560	1.5
P4A6	2/4/2006 14:15	2/8/2006 18:15	35.6	0.306	52.0	2.6	10.6	31.9	0.03	0.76	601	545	518	1.8
P5 2/	8/2006 18:15	2/10/2006 0:42	23.9	0.198	47.0	3.3	8.0	32.6	0.00	0.72	637	565	522	1.8
P6	2/10/2006 0:42	2/10/2006 12:46	12.2	0.250	55.4	7.9	8.0	39.7	0.00	0.75	599	551	517	1.9
Linear averages (total COT)			335.2	0.248	57.1	3.2	9.1	31.5	—	0.85	634	568	538	2.0

Notes:

1. COT = Continuous operating time, and indicates the cumulative time when simulant feed was on. The COT time is often less than the total time span between each test condition start and stop times.
2. The fluidized bed density is the bed density dP (PDT-200-001) divided by 12 inches, the distance between the bed density pressure ports.
3. Ambient barometric pressure averaged about 12.2 psia.

[gas comp and nox destruct aug 1.xls]DMR table

Table 7-9. CP1 DMR gas flow rate and residence time.

Test	NO3 in feed (g/L)	Water in feed (g/L)	H+ in feed (g/L)	Total water from feed (scfm)	Water from fluidizing steam (scfm)	Water from coal (scfm)	Total water (scfm)	Fluidizing O_2 (scfm)	O_2 from atomizing air (scfm)	O_2 from NO_3 decomposition (scfm)	O_2 from coal (scfm)	Total O_2 input (total CO_2 in off-gas) (scfm)	Portion of purge N_2 entering upstream of HTF (scfm)	N_2 from NO_3 (scfm)	Shot-pot and HTF pulse N_2 (scfm)	Total N_2 (scfm)	Total DMR off-gas flow rate (scfm)	Total DMR off-gas flow rate (acf m)	DMR Bed Height,in DMR bedheight	DMR bed superficial gas residence time (seconds)	DMR freeboard gas residence time (seconds)	Total DMR gas residence time (seconds)
P1 487		740	2.59	33.3	30.4	1.8	65.5	2.4	2.3	9.2	0.2	14.1										
P1-1 487		739	2.59	33.2	30.4	1.9	65.6	3.0	2.2	9.2	0.2	14.7	21.9	3.1	1.6	26.6	106	296	42.0	0.87	1.3	2.2
P2 458		757	2.47	29.2	24.5	1.9	55.6	2.6	2.4	7.3	0.2	12.4	22.3	3.1	1.6	27.0	107	291	40.5	0.85	1.4	2.3
P3B	510	707	2.52	30.7	19.7	1.8	52.2	2.7	2.1	9.4	0.1	14.4	26.3	2.4	1.6 30.	4 98		287	37.7	0.80	1.5	2.3
P4A1	475	751	2.56	35.7	15.6	2.0	53.4	3.5	1.7	9.5	0.2	14.9	27.1	3.1	1.6 31.	8 98		300	39.7	0.81	1.4	2.2
P4A2	473	755	2.61	36.3	19.5	2.2	58.1	1.8	1.5	9.6	0.2	12.9	25.1	3.2	1.6 29.	9 98		317	36.6	0.71	1.4	2.1
P4A3	462	791	2.46	31.0	20.6	1.4	53.0	2.5	1.4	7.3	0.1	11.2	22.8	3.2	1.6 27.	6 99		293	40.1	0.84	1.4	2.2
P4A4	463	748	2.38	34.0	13.9	1.9	49.9	3.5	1.6	8.9	0.2	13.9	24.9	2.4	1.6 28.	9 93		274	39.6	0.89	1.5	2.4
P4A5	462	795	2.43	35.7	14.6	2.1	52.4	2.9	2.0	8.9	0.2	13.9	23.6	3.0	1.6 28.	1 92		292	40.6	0.85	1.4	2.2
P4A6	382	819	2.21	40.3	19.2	2.1	61.6	2.4	2.0	8.0	0.2	12.5	25.3	3.0	1.6 29.	9 96		308	39.6	0.79	1.3	2.1
P5 444		750	2.21	27.4	16.8	2.1	46.3	3.3	1.7	6.8	0.2	12.0	24.2	2.7	1.6	28.5	103	301	39.2	0.80	1.4	2.2
P6	114	966	0.19	43.5	19.9	2.5	65.9	7.9	1.7	2.2	0.2	12.0	25.2	2.3	1.6 29.	0 87		264	38.8	0.90	1.6	2.5
Avgs 435		777	2.27	34.2	20.4	2.0	56.6	3.2	1.9	8.0	0.2	13.3	23.5	0.7	1.6	25.9	104	306	37.9	0.76	1.4	2.1
													24.4	2.7	1.6	28.6	99	294	39.4	0.82	1.4	2.2

Notes:

1. The feed composition data are from the lab analysis values for the batch(es) that were being feed during the time of each test condition.
2. The H_2O from simulant feed is calculated from the simulant feedrate, the amounts of H_2O and H+ in the simulant.
3. Total molar H_2O in the DMR off-gas = fluidizing steam + H_2O from simulant feed + H_2O in the coal + 0.5 times the H in the coal. The total H_2O is not reduced for the amount of H_2 formed, so represents a total H_2O + H_2 flow rate.
4. The average coal composition was (wet basis as measured):

Samples 1321, 1881	Moisture, %	8	Nitrogen, %	1
Average Erwin	Ash, %	8	Oxygen, %*	3
ULTIMATE (As Received)	Sulfur, %	0	Hg, ppm	0
11 Jan, 14 Jan 06	Carbon, %	78	As, ppm	0
	Hydrogen, %	1	Total, %	100

5. Total molar O_2 in the off-gas is assumed to be zero, a good assumption for normal operation when, on a wet basis, the O_2 in the DMR off-gas is under 0.1 volume %.
6. Total molar CO2 in the off-gas is calculated assuming that coal feed reacts with any free O, producing CO2. Amounts of CO and THC are assumed to be negligible, since CO and THC are typically each less than 5% of the CO2 on a molar basis.
7. Sources of O are the fluidizing O_2, the atomizing air, nitrate in the simulant, O in the coal, and release of O by H_2O when it converts to H_2. Oxygen formation equations on a molar (volumetric) basis are:
   - O_2 from atomizing air = 0.79 × atomizing air flow rate
   - O_2 from nitrate in feed = 1.5 moles O_2 per mole NO_3 according to: $2NaNO_3 + 2.5C = Na_2CO_3 + 1.5\ CO_2 + N_2$
   - O_2 from H_2O = 0.5 O_2 per mole H_2O according to: $H_2O = H_2 + 0.5O_2$
8. Calculation of O_2 from H_2O decomposition is iterative and results in only 0.5% CO_2 per 1% H_2. CO_2 from H_2O decomposition is typically less than 5% of the total CO_2, and so is not included in this calculation for simplicity.
9. Total molar N_2 in the DMR off-gas = 60% of the total purge N_2 + 0.79 x atomizing air + shotpot and HTF pulse N_2 + N_2 from NO_3 assuming $2NO_3 = N_2 + 3O_2$. Only about 60% of the total purge N_2 is estimated to pass through the DMR and HTF; the other 40% of the total purge N_2 enters the system downstream of the HTF, and is added to the CRR gas flow rate for total system flow rate calculation.
10. HTF and PBF pulse N_2, and product receiver N_2, are not included in total N_2 calculation. The mass balance calculations are not valid for time periods of filter pulsing or product receiving.
11. The DMR off-gas flow rate is calculated based on the DMR input feedstreams, making several simplifying assumptions and calculations to account for H_2O, H_2, N_2, NO_X, CO_2, CO, THC, and O_2 in the off-gas.
12. Total molar DMR off-gas determined using the above calculations = $(H_2O + H_2) + N_2 + CO_2$. Levels of NO_X, CO, and THC are considered negligible because they typically total less than 1 volume % of the total DMR off-gas (wet basis).
13. The superficial gas residence time in the DMR bed is the residence time of gas in the empty volume of the bed. This residence time was calculated using the DMR outlet gas flow rate, although the actual gas volumetric flow rate in the bed varies depending on height in the bed (above or below the feed nozzle and purges) and on reactions occurring in the bed that affect the gas. The bed volume was calculated using the average bed height above the distributor.
14. The DMR volumes used for the gas residence time were calculated using the following dimensions:

Item	ID (in.)	L (in.)	V (ft^3)	
DMR bed section	15	60	6.1	
Distributor section	15	5	0.5	
Bed volume above distributor, for avg bed height	15	39.4	4.0	The bed superficial gas residence time is adjusted for the bed height for each test condition.
Conical section from 15 to 21 in. ID in 13 in.			1.9	V_{cone} = 1/3 pi r^2 h
Freeboard section	21	23	2.4	Vexpansion = 1/3 pi/4 h/(D-d)(D3 - d3)
Total vessel volume above distributor	—	—	10.9	
Gas space (above bed + cone + freeboard)			6.4	The freeboard gas residence time is adjusted for the bed height for each test condition.

[gas comp and nox destruct aug 1.xls]DMR res T

Table 7-10. Summary of CP1 CRR operating parameters.

Test	COT duration (hr)	CRR coke feed rate (lb/hr)	CRR Clay (lb/hr)	CRR bed sample rate (lb/hr)	CRR fluidizing O_2 flow rate (scfm)	CRR fluidizing air flow rate (scfm)	CRR overbed O_2 flow rate (scfm)	CRR shot pot N_2 (scfm)	CRR cooling/ leak water rate (gpm)		CRR outlet gas flow rate		CRR off-gas O_2 (wet %)	CRR Bed T (°C) (8" S)	CRR free-board gas T (°C) (54" SE)	CRR free-board gas T (°C) (150" NE)	CRR outlet gas T (°C)	CRR free-board P (psig)	CRR bed height (in.)	CRR bed superficial gas res. time	CRR freeboard gas res. time	Total CRR gas res. time
		WT-302-001	Calc Calc		FT-300-001	FTCV-300-002	FI-300-012	Estimate	gpm	scfm	scfm acf	m AT	-300-001	TT-300-002	TT-300-008	TT-300-011	TT-300-016	PT-300-004	PDI-300-002	sec	sec	sec
P1	40.6	19.5	0.44	0.32	9.2	4.3	7.3	0.1	0.19	34	192	995	3.9 951		943	828 800		-0.45	42.8	0.34	2.6	2.9
P1-1	35.0	24.0	0.57	0.33	6.3	2.9	8.6	0.1	0.19	34	190	982	3.6 959		958	872 842		-0.31	30.7	0.25	2.7	2.9
P2	23.2	34.8	1.27	4.67	13.3	6.1	10.1	0.1	0.19	34	194	993	4.2 950		953	862 839		-0.26	24.3	0.19	2.7	2.9
P3B	23.9	36.1	0.60	0.21	15.6	7.2	13.0	0.1	0.19	34	197	1,019	6.0 947		961	907 887		-0.25	18.4	0.14	2.7	2.8
P4A1	25.6	29.3	0.62	0.28	13.5	6.2	13.0	0.1	0.19	34	193	926	7.1 850		870	830 807		-0.31	18.9	0.16	3.0	3.1
P4A2	23.2	26.3	0.39	0.16	16.5	7.6	16.5	0.1	0.19	34	196	929	10.0 846		859	816 796		-0.26	18.4	0.16	2.9	3.1
P4A3 37.	7	42.7	0.73	0.14	14.2	7.4	16.8	0.1	0.19	34	190	1,089	5.2	1,040	1,090	1,028	991	-0.32	19.5	0.14	2.5	2.7
P4A4	19.9	35.6	0.50	0.23	15.2	9.1	13.3	0.1	0.19	34	190	1,089	6.0 1,	048	1,090	1,046 1,	009	-0.31	20.0	0.15	2.5	2.6
P4A5	34.6	34.8	0.46	0.28	14.2	8.5	13.8	0.1	0.19	34	194	1,095	6.0 1,	048	1,080	1,072 1,	029	-0.23	16.9	0.12	2.5	2.6
P4A6	35.6	24.1	1.37	0.08	12.0	8.5	14.3	0.1	0.19	34	197	907	8.5 860		822	828 801		-0.29	21.8	0.19	3.0	3.2
P5	23.9	18.6	1.05	0.21	8.7	8.7	9.4	0.1	0.19	34	180	894	7.9 951		908	828 795		-0.35	26.3	0.23	3.0	3.2
P6	12.2	20.0	0.74	0.00	9.9	9.9	8.8	0.1	0.19	34	197	908	8.0 951		825	848 813		-0.27	25.9	0.23	3.0	3.2
Averages (total COT)	335.2	28.8	0.73	0.58	12.4	7.2	12.1	0.1	0.19	34	192	986	6.4 950		946	897 868		-0.30	23.7	0.19	2.8	2.9

Notes:

1. The total CRR outlet gas volumetric flow rate was calculated by summing the total calculated DMR off-gas flow rate with the input flow rates of fluidizing O_2, fluidizing air, freeboard O_2, CRR shotpot, evaporated cooling/leak water, and the remainder of the purge N_2 not assumed to have entered the process upstream of the HTF.
2. The freeboard O_2 flow rate was not electronically recorded. The flow rate was periodically recorded on round sheets. The flow rate used here is an average of the flow rates recorded for the APT sample times.
3. The cooling water was not recorded, and leaked even when it was thought to be off. The total cooling/leak water rate is an average for the test determined so that the total calculated moisture content in the stack gas agreed with the average stack gas moisture content that was measured during the APT manual sample times.
4. Most of the CRR input O_2 is converted to CO2, without any change in the volumetric gas flow rate.
5. The trace levels of H_2, CO, and THC in the DMR off-gas are converted in the CRR to mainly CO_2 and H_2O. The change in volumetric flow rate from these conversions are not included in the total CRR off-gas flow rate calculations, since the total concentrations of these species are typically around 1% (wet basis) in the DMR off-gas.
6. The superficial gas residence time in the CRR bed is the residence time of gas in the empty volume of the bed. This residence time was calculated using the CRR outlet gas flow rate, less the volumetric flow rate of the overbed O_2, although the actual gas volumetric flow rate in the bed varies depending on height in the bed (above or below the ATG nozzles) and on reactions occuring in the bed that affect the gas. The bed volume was calculated using the average bed height above the distributor for each test condition.
7. The DMR volumes used for the gas residence time were calculated using the following dimensions:

Item	ID (in.)	L (in.)	V (ft^3)
CRR bed section	17	60	7.9
Distributor section	17	11.2	1.5
Bed volume above distributor, for avg bed height	17	23.7	3.1
Conical section from 15 to 21 in. ID in 13 in.	—	—	2.5
Freeboard section	24	138.4	36.2
Total vessel volume above distributor	—	—	48.1
Gas space (above bed + cone + freeboard)	—	—	43.5

The bed superficial gas residence time is adjusted for the bed height for each test condition.

$V_{cone} = 1/3\ pi\ r^2\ h$, and $V_{expansion} = 1/3\ pi/4\ h/(D-d)(D^3 - d^3)$

The freeboard gas residence time is adjusted for the bed height for each test condition.

[gas comp and nox destruct aug 1.xls]CRR table

Table 7-11. Key CP1 off-gas system parameters.

Test Sta	rt	Finish	COT Duration (hr)	OGC atomizing air (scfm)	OGC Cooling H_2O (gpm)	OGC Cooling H_2O (scfm)	OGC Outlet T (°C)	PBF Outlet T (°C)	GAC Bed 1 T (°C)	GAC Bed 2 T (°C)	GAC Bed 3 T (°C)	Stack T (°C)	Calc stack gas flow rate (wscfm)	Stack gas flow rate (scfm)	Ratio, meas/ calc stack gas flow rate (scfm)
				FIT-400-001	FT-400-002	Calc	TT-400-001	TT-406-010	TT-408-001	TT-408-002	TT-408-003	TT-500-001	Calc	FT-500-001	Calc
P1	1/17/2006 23:02	1/19/2006 17:09	40.6	20 0.36		64	179	138	Bypassed			115	276	262	0.95
P1-1	1/19/2006 17:09	1/21/2006 13:36	35.0 21		0.40	71	180	147	Bypassed			122	281	260	0.93
P2	1/26/2006 12:45	1/27/2006 18:30	23.2	19 0.48		85	180	147	Bypassed			135	298	283	0.95
P3B	1/27/2006 19:20	1/28/2006 19:10	23.9	18	0.55	98 180		142 128		133 141		128	314	299	0.95
P4A1	1/28/2006 19:10	1/29/2006 21:26	25.6	18	0.45	79 180		140 126		131 139		123	290	273	0.94
P4A2	1/29/2006 21:26	1/30/2006 21:05	23.2	18	0.47	74 180		142 128		133 139		125	286	288	1.01
P4A3	1/30/2006 21:05	2/1/2006 22:18	37.7	17	0.58	103 180		148 133		139 146		131	310	278	0.90
P4A4	2/1/2006 22:18	2/2/2006 19:23	19.9	21	0.58	98 180		149 133		139 147		131	308	275	0.89
P4A5	2/2/2006 19:23	2/4/2006 14:15	34.6	21	0.61	108 180		143 128		133 139		126	323	294	0.91
P4A6	2/4/2006 14:15	2/8/2006 18:15	35.6	20	0.41	73 182		138 126		131 136		125	292	270	0.92
P5	2/8/2006 18:15	2/10/2006 0:42	23.9	21	0.31	55 185		132 121		123 126		114	256	244	0.96
P6	2/10/2006 0:42	2/10/2006 12:46	12.2	22	0.34	61 185		138 119		121 126		114	281	253	0.90
Averages (total COT)			335.2	20	0.46	81 181		142 127		131 138		124	293	273	0.93

[gas comp and nox destruct aug 1.xls]off-gas table

Table 7-12. CP1 solid product rates.

Test Start		Finish	COT duration (hr)	DMR product (lb/hr)	HTF product (lb/hr)	PBF product (lb/hr)	Total product (lb/hr)	DMR product: HTF fines ratio	Total lb product per gallon stimulant (lb/gal)
P1	1/17/2006 23:02	1/19/2006 17:09	40.6	15	7	1.2	23.2	2.30	1.6
P1-1	1/19/2006 17:09	1/21/2006 13:36	35.0	10	10	2.2	21.9	0.95	1.5
P2	1/26/2006 12:45	1/27/2006 18:30	23.2	12	19	2.6	33.1	0.64	2.7
P3B	1/27/2006 19:20	1/28/2006 19:10	23.9	11	17	0.5	28.1	0.67	2.0
P4A1	1/28/2006 19:10	1/29/2006 21:26	25.6	5.3	26	2.6	33.8	0.21	2.2
P4A2	1/29/2006 21:26	1/30/2006 21:05	23.2	16	23	1.4	41.3	0.70	2.6
P4A3 1/30/2	006 21:05	2/1/2006 22:18	37.7	10	14	0.9	25.3	0.70	1.7
P4A4	2/1/2006 22:18	2/2/2006 19:23	19.9	18	15	0.4	33.7	1.20	2.3
P4A5	2/2/2006 19:23	2/4/2006 14:15	34.6	16	24	0.5	40.1	0.67	2.3
P4A6	2/4/2006 14:15	2/8/2006 18:15	35.6	21	31	3.1	55.3	0.66	3.0
P5 2/8/20	06 18:15	2/10/2006 0:42	23.9	22	20	1.1	42.7	1.12	3.6
P6	2/10/2006 0:42	2/10/2006 12:46	12.2	11	14	0.0	25.5	0.79	1.7
		Averages (total COT)	335.2	14	18	1.4	33.7	0.88	2.3

Notes:

1. The product includes residual unreacted coal and petroleum coke, but does not inclue the small amount of OGC solids.

[gas comp and nox destruct aug 1.xls]Product rates

Table 7-13. CP1 Steam Reformer process pressures and differential pressures.

			dP ("WC)					Pressure					
			DMR distributor	DMR cyclone HTF		CRR distributor PBF		DMR Freeboard P (psig)	CRR Freeboard P (psia)	DMR Bed Height (in.)	DMR Bed Density dP ("WC)	CRR Bed Height (in.)	CRR Bed Density dP ("WC)
Test Sta	rt	Finish	PDI-200-004	PDI-200-003	PDI-202-001	PDI-300-004	PDI-406-001	PT-200-005	PT-300-004	DMR bed height	PDT-200-001	PDI-300-002	PDI-300-001
P1	1/17/2006 23:02	1/19/2006 17:09	36.3	5.44	24.9 20.9		3.4	2.94 11.	7 42.0		9.0	42.8	20.2
P1-1	1/19/2006 17:09	1/21/2006 13:36	39.6	6.79	29.9 20.0		3.5	2.98 11.	9 40.5		10.4	30.7	17.2
P2	1/26/2006 12:45	1/27/2006 18:30	29.8	3.41	27.0 17.0		4.1	2.33 11.	9 37.7		12.6	24.3	13.2
P3B	1/27/2006 19:20	1/28/2006 19:10	21.4	3.92	28.1 16.2		3.9	2.16 12.	0 39.7		10.5	18.4	11.3
P4A1	1/28/2006 19:10	1/29/2006 21:26	18.4	3.74	18.4 15.7		3.9	1.72 11.	9 36.6		10.7	18.9	11.3
P4A2	1/29/2006 21:26	1/30/2006 21:05	19.3	2.12	14.9 15.6		4.1	1.59 11.	9 40.1		9.7	18.4	11.5
P4A3	1/30/2006 21:05	2/1/2006 22:18	21.4	1.20	14.0 14.5		4.0	1.42 11.	9 39.6		11.2	19.5	11.5
P4A4	2/1/2006 22:18	2/2/2006 19:23	17.2	0.77	15.8 15.3		4.0	1.56 11.	9 40.6		11.1	20.0	12.2
P4A5	2/2/2006 19:23	2/4/2006 14:15	16.5	1.06	14.9 15.1		3.9	1.50 12.	0 39.6		10.0	16.9	10.5
P4A6	2/4/2006 14:15	2/8/2006 18:15	19.5	0.96	19.5 17.0		4.1	1.85 11.	9 39.2		9.1	21.8	12.9
P5 2/8/2006	18:15	2/10/20060:42	17.7	0.25	16.0 15.6		3.8	1.76 11.9		38.8 8.7		26.3	16.4
P6	2/10/2006 0:42	2/10/2006 12:46	32.6	0.23	15.8 17.3		3.6	1.86 11.9		37.9 9.0		25.9	16.7

[pressure summary july 27.xls]Press. Tab.

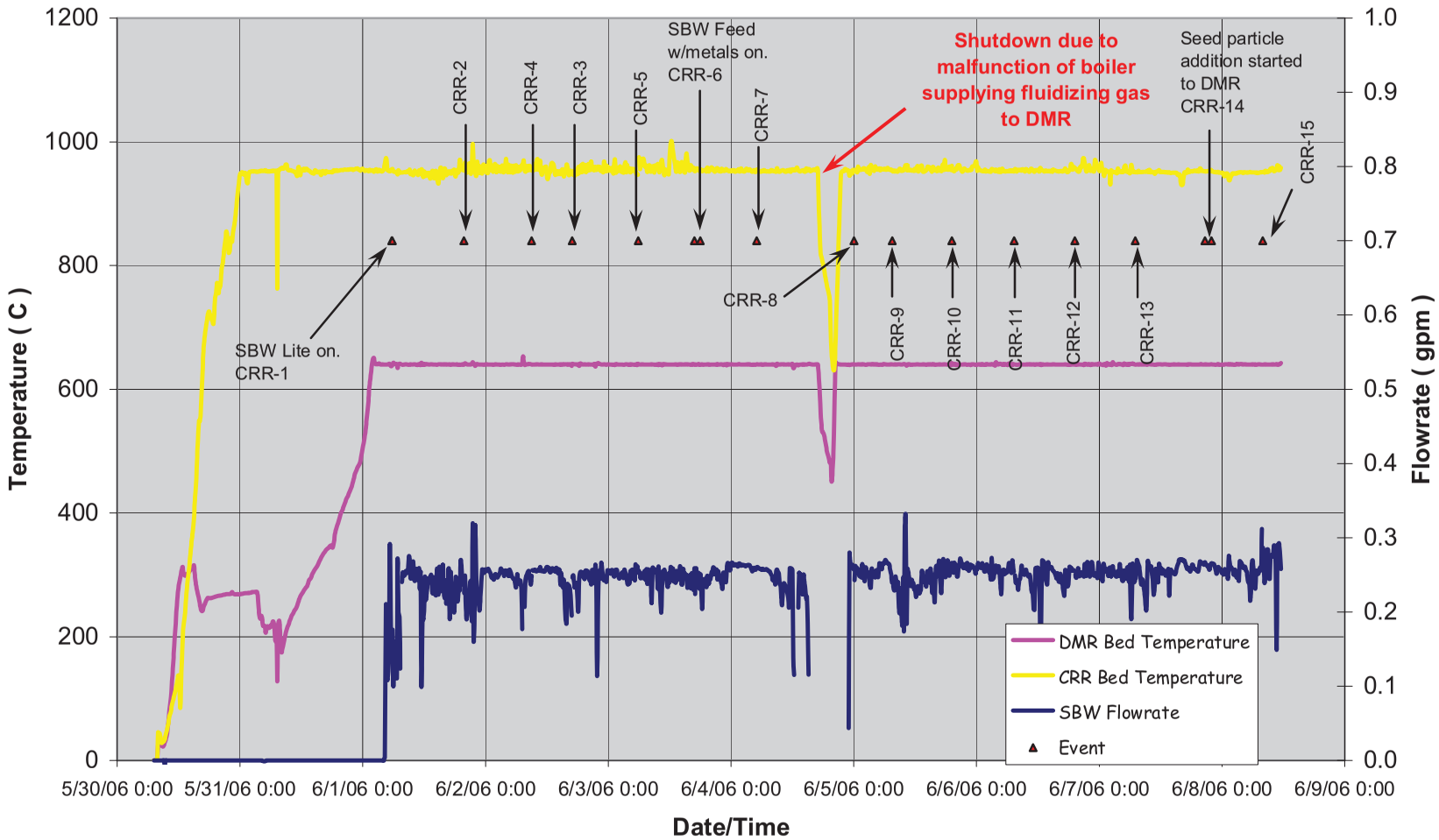

Figure 7-11. Pilot Plant activities May 30 to June 9, 2006.

The process configuration was changed to Condition #5 with the ATG mixture set at 50/50 in the lower/middle flow nozzle on June 3. The feed rate continued at ~0.25 gpm with SBW (no metals, UDS, or POHC). The DMR bed particle size measured at MMPD ~430µm and HMPD ~220µm. APT began manual off-gas sampling at the stack under these conditions using EPA Method 29 for total metals and at the GAC Stages 1, 2, and 3 using the Ontario Hydro Method for Hg speciation. The first traverse was completed when NO_X levels increased to ~1500 ppm causing APT to pause the sampling event. Carbon addition to the DMR was increased to lower the NO_X level. APT resumed sampling as the NO_X level decreased below 1000 ppm. With the successful completion of sampling, the process configuration was changed to CRR Condition #6 by adjusting the ATG mixture to a 50/50 ratio through the lower/middle flow nozzles. The CRR bed height was decreased from 32–34 to 29–31 inches. Feedrate remained at ~0.25 gpm. Heavy metals were added to the feed makeup of SBW surrogate (no UDS, no POHC), thereby transitioning to Test 3 for the DMR.

At 0500 on June 4, the process configuration was changed to CRR Condition #7. An ATG gas mixture of 50/50 was retained with input flow adjusted to the middle bed nozzle only. A DACS network upset caused a steam fluidization update failure and the steam boiler tripped off ceasing steam flow the process. Corrective actions to reboot the system and restore the steam boiler averted a system shutdown. Manual off-gas sampling at the stack using EPA Method 29 for total metals and at the GAC Stages 1, 2, and 3 using the Ontario Hydro Method for Hg speciation was initiated after conditions stabilized. However, the steam boiler continued to trip off resulting in partial clogging of the fluidizing gas distribution pipes. Process operations were suspended and a shutdown of the system was instigated. Manual sampling of the off-gas was suspended as well. The fluidizing gas distributors were cleaned and process heatup was initiated at ~2000.

The process configuration was changed to Condition #8 at midnight on June 5 with the ATG mixture set to 50/50 utilizing the lower flow nozzle. The DMR HMPD was measured at 130µm. The atomizing air flow was decreased from 5 to 4 scfm to increase particle size. The process configuration was changed at ~0715 to CRR Condition #9 by lowering the CRR bed height from 29–31 to 26–28 inches. The ATG mixture remains at 50/50 with the lower flow gas nozzle. The atomizing air flow was increased from 4 to 6 scfm. Manual off-gas sampling at the stack using EPA Method 29 for total metals and at the GAC Stages 1, 2, and 3 using the Ontario Hydro Method for Hg speciation was initiated at these conditions. The HTF catch increased and appeared light to dark tan, microscopic examination indicated the fines were larger in size than previous samples and were likely from the DMR bed. The product to fines ratio dropped from a ratio of 20:1 to 2:1. It appears that some restriction of the DMR downcomer caused this. The cyclone downcomer pulse jets were manually cycled to clear the downcomer obstruction. The process configuration was changed to Condition #10 by adjusting the ATG mixture to a 50/50 ratio through the middle flow nozzle upon successful completion of sampling.

The process configuration was changed to Condition #11 at 0710 on June 6 by setting the ATG mixture at 50/50 utilizing the middle and lower gas flow nozzles with the middle nozzles controlling. The product to fines ratio returned to the previous level of ~20:1. Manual off-gas sampling at the stack began at ~1040 using EPA Method 29 for total metals and at the GAC Stages 1, 2, and 3 using the Ontario Hydro Method for Hg speciation. A continuous SO_2 sampling probe was installed at the GAC off-gas stream inlet to determine if SO_2 generation was occurring in the GAC. The process configuration was changed to Condition #12 by adjusting the ATG mixture to a 50/50 ratio through both the middle and lower flow nozzles with the successful completion of sampling. The CRR bed height was increased to 36 inches with the addition of a 50/50 mixture of AGSCO 30/46. CRR Condition #12 operated for ~12 hours.

The process configuration was changed to CRR Condition #13 at 0705 on June 7. The ATG mixture was set at 50% O_2 and 50% N_2 utilizing the middle flow nozzle. Manual off-gas sampling at the stack at 0950 using EPA Method 29 for total metals and at the GAC Stages 1, 2, and 3 using EPA Method Ontario Hydro for Hg speciation was initiated after conditions stabilized.

A second set of manual off-gas samples were collected at the stack using EPA Method 29 for total metals and at the GAC Stages 1, 2, and 3 using the Ontario Hydro Method for Hg speciation for Condition #13. The process configuration was changed to Condition #14 at 2146 by adjusting the ATG mixture to a 50/50 ratio through lower flow nozzles upon successful completion of sampling. It was decided to begin adding alumina seed particles to the DMR to test the affects on particle size, even though the mean particle size had not reached 400 microns. 92 micron alumina seed particles at ~3 lb/hr was added and continued through the end of CP2. Condition #14 operated throughout the night.

The process configuration was changed to Condition #15 at 0710 on June 8 by adjusting the ATG mixture to 75/25 on both the mid and upper flow nozzles. Condition #15 operated until a planned shutdown of the process was initiated at ~1300. A run of train blank manual off-gas samples were obtained to close out the sampling events for CP2.

7.4.4 CP2 Operating Conditions

The CP2 tests consisted of three tests for the DMR and 15 tests for the CRR. The first DMR test used SBW supernate simulant feed to the DMR without heavy metals. The second and third test condition used SBW supernate simulant feed to the DMR with heavy metals. The third test added alumina seed particles to the DMR to determine the effect on the process if alumina seed particle addition were required for particle size control. The 15 CRR tests varied CRR oxygen feed locations (low, middle, or both), CRR oxygen feed composition (75% O_2/25% N_2 or 50%O_2/50%N_2), CRR bed height, and CRR carbon composition (high or low). The desired process setpoints for CP2 may be found in Section 5. The achieved operating condition for each CP2 test condition may be found in Table 7-14 through Table 7-19.

7.5 System Performance

7.5.1 Fluidized Bed Performance

The performance of the THOR® dual fluidized bed system depends on several different subsystems that must work together in a robust and integrated manner. These subsystems include the fluidizing gas supply, the fluidized bed gas distributors, the feed nozzles, and product removal. The operation of each of these subsystems influences the operation of the others and in particular the fluidized bed particle size distribution and solids carryover. The performance of each of these subsystems during the tests will be discussed in turn.

7.5.1.1 Fluidizing Gas Supply. The fluidizing gas (FG) supply worked very well during the CP1 SBW test, especially after the system was set up to automatically control the steam flow based on the desired total DMR fluidizing gas flow rate. During the CP1 test the FG oxygen flow rate was subtracted from the total gas flow rate to give the setpoint for the steam FG flow rate. This procedure resulted in a fairly constant FG flow, even when the FG oxygen flow rate changed significantly because of temperature control requirements of the DMR. The FG flow rate generally was high enough to give SSV of 1 fps or more. The fluidizing gas supply also worked very well during the CP2 test. For this test, the steam flow was changed to be controlled based either on the total FG flow rate (as was used during the CP1 test) or to maintain a constant steam flow rate. Constant steam flow control was used exclusively during the CP2 test. Because the minimum fluidizing velocity was generally less than 0.2 fps, the bed was very well fluidized. Even when the DMR bed particle size approached 1000 µm during the scoping tests, the FG supply system was capable of delivering sufficient gas flow to ensure that the SSV was generally at least twice the minimum fluidizing velocity.

Table 7-14. CP2 DMR flow rates.

Test Feed		Start	Finish	COT duration (hours)	Simulant DMR FT-200-001 (gpm)	coal WDT-204-001 (lb/hr)	DMR clay Calc (lb/hr)	DMR fluidizing steam FT-104-001 (lb/hr)	DMR fluidizing O_2 FTCV-104-002 (scfm)	DMR atomizing gas FTCV-200-003 (scfm)	DMR product Calc (lb/hr)	HTF product Calc (lb/hr)	PR:HTF ratio Calc —
DMR-1	SBW Lite	6/1/2006 5:46	6/3/2006 18:00	58.5	0.24	32.3	0	62.0	2.3	7.84	29.2	1.8	16.3
DMR-2	SBW w/HM	6/3/2006 18:00	6/7/2006 21:46	90.2	0.25	39.9	0	69.7	2.2	5.97	31.4	2.3	13.7
DMR-3	SBW w/HM + alumina	6/7/2006 21:46	6/8/2006 13:00	15.1	0.26	43.9	2.8	69.8	2.1	5.87	40.0	0.9	43.8
Total hours, average flow rates				163.8	0.25	38.7	—	67.2	2.2	6.56	33.5	1.7	24.6

[summary tables.xls]DMR Flows

Table 7-15. CP2 DMR temperatures.

Test Feed		Start	Finish	COT duration (hours)	DMR - bed temperature (6" NW) TT-200-002 (°C)	DMR - bed temperature (24" E) TT-200-006 (°C)	DMR - freeboard temperature (92" S) TT-200-010 (°C)	DMR - outlet gas temperature TT-200-011 (°C)	HTF outlet gas temperature TT-202-005 (°C)
DMR-1	SBW Lite	6/1/2006 5:46	6/3/2006 18:00	58.5	640	638	583	537	398
DMR-2	SBW w/HM	6/3/2006 18:00	6/7/2006 21:46	90.2	642	640	591	546	408
DMR-3	SBW w/HM + clay	6/7/2006 21:46	6/8/2006 13:00	15.1	642	639	585	538	403
Total hours, average temperatures				163.8	641	639	586	540	403

[summary tables.xls]DMR Temps

Table 7-16. CP2 DMR and HTF pressures, differential pressures, and bed height.

Test Feed		Start	Finish	DP (inches water) DMR distributor PDI-200-004	DMR cyclone PDI -200-003	HTF -202-001	Pressure (psig) DMR freeboard PT-200-005	DMR Bed Height (in.) DMR bedheight	DMR bed specific gravity PDT-200-001
DMR-1	SBW Lite	6/1/2006 5:46	6/3/2006 18:00	29	0.16	18	2.2	41.7	1.05
DMR-2	SBW w/HM	6/3/2006 18:00	6/7/2006 21:46	33	0.38	24	2.3	40.7	0.80
DMR-3	SBW w/HM + clay	6/7/2006 21:46	6/8/2006 13:00	35	-0.50	24	2.7	40.0	0.82
Averages				32	0.01	22	2.4	40.8	0.89

[summary tables.xls]DMR Press

Table 7-17. CP2 CRR flow rates.

Test Sta	rt	Finish	COT duration (hours)	CRR - Lower ATG O_2 FT-300-018 (scfm)	CRR - Lower ATG N_2 FT-300-019 (scfm)	CRR Middle ATG O_2 FT-300-001 (scfm)	CRR - Middle ATG N_2 FT-300-002 (scfm)	CRR Upper ATG O_2 FT-300-016 (scfm)	CRR - Upper ATG N_2 FT-300-017 (scfm)	CRR sample rate Calc (lb/hr)	PBF product rate Calc (lb/hr)	OGC atomizing air FIT-400-001 (scfm)	OGC water FT-400-002 (gpm)	N_2 purge FT-600-001 (scfm)	CRR petroleum coke WDT-302-001 (lb/hr)	CRR aluminum hydroxide Calc (lb/hr)
CRR-1	6/1/2006 5:46	6/1/2006 19:47	13.6	0.0	0.0	6.4	6.4 10.2		10.2	0.38	3.2	18.2 0.36		43.0	27.0	0.48
CRR-2	6/1/2006 19:47	6/2/2006 9:00	12.3	0.0	0.0	5.2	1.7 8.9		8.9	0.34	3.4	18.8 0.36		45.2	25.2	0.49
CRR-3	6/2/2006 16:57	6/3/2006 5:52	12.6	3.5	1.2	0.0	0.1 10.4		10.3	0.55	3.2	17.8 0.40		45.0	26.3	0.52
CRR-4	6/2/2006 9:00	6/2/2006 16:57	7.9	2.9	2.9	0.0	0.0 9.7		7.9	0.51	3.7	17.2 0.38		43.0	24.6	0.50
CRR-5	6/3/2006 5:52	6/3/2006 16:50	11.0	1.7	1.7	2.2	2.2 9.8		9.8	7.05	3.3	17.1 0.41		43.6	29.1	0.46
CRR-6	6/3/2006 16:50	6/4/2006 5:00	12.2	1.1	1.1	2.5	2.5 10.3		10.3	0.41	3.8	19.0 0.41		44.6	25.0	0.49
CRR-7	6/4/2006 5:00	6/5/2006 0:03	10.0	0.0	0.0	4.2	4.2 10.3		10.3	0.14	3.0	21.3 0.35		45.3	24.1	0.75
CRR-8	6/5/2006 0:03	6/5/2006 7:30	7.5	3.0	3.0	0.0	0.1 12.2		12.2	5.49	3.1	21.8 0.40		46.3	25.3	0.53
CRR-9	6/5/2006 7:30	6/5/2006 19:10	11.2	3.3	3.3	0.0	0.0 12.3		12.3	0.36	2.9	19.9 0.40		44.1	24.4	0.49
CRR-10	6/5/2006 19:10	6/6/2006 7:21	12.2	0.0	0.0	2.7	2.7 15.2		15.2	0.16	4.6	21.0 0.44		44.9	25.9	0.49
CRR-11	6/6/2006 7:21	6/6/2006 19:12	11.9	1.8	1.8	3.2	3.2 14.5		14.5	0.44	3.1	18.4 0.44		44.1	25.2	0.51
CRR-12	6/6/2006 19:12	6/7/2006 7:03	11.7	2.1	2.1	3.8	3.8 11.8		11.8	0.42	3.7	20.3 0.43		46.2	22.5	0.51
CRR-13	6/7/2006 7:03	6/7/2006 21:55	14.9	0.0	0.0	7.1 7.1		11.1	11.1	0.65	1.8 18.6		0.42	43.1	24	0.50
CRR-14	6/7/2006 21:55	6/8/2006 7:56	9.3	10.8	10.8	0.0 0.1		6.9	7.0	0.50	1.5 20.4		0.41	44.7	22	0.54
CRR-15	6/8/2006 7:56	6/8/2006 13:00	5.7	0.0	0.0	4.0 1.3		12.4	4.1	0.00	1.9 19.6		0.38	43.2	20	0.35
		Averages (Total COT)	163.8	2.0	1.9	2.7	2.4 11.1		10.4	1.16	3.1	19.3 0.40		44.4	24.7	0.51

Notes:

1. CRR-7 Averages do not include the time the process was down.

[summary tables.xls]CRR Flows

Table 7-18. CP2 CRR and off-gas system temperatures.

Test Sta	rt	Finish	COT Duration (hours)	CRR bed (8" W) TT-300-003 (°C)	CRR free-board (54" SE) TT-300-008 (°C)	CRR freeboard (150" NE) TT-300-011 (°C)	CRR outlet gas TT-300-016 (°C)	OGC outlet gas TT-400-001 (°C)	PBF outlet gas TT-406-010 (°C)	GAC Bed 1 TT-408-001 (°C)	GAC Bed 2 TT-408-002 (°C)	GAC Bed 3 TT-408-003 (°C)	Stack T TT-500-001 (°C)
CRR-1	6/1/2006 5:46	6/1/2006 19:47	13.6	951 942		825 773		172 135		126 128		143 131	
CRR-2	6/1/2006 19:47	6/2/2006 9:00	12.3	960 951		846 789		169 132		121 120		130 120	
CRR-3	6/2/2006 16:57	6/3/2006 5:52	12.6	957 951		863 809		170 135		125 126		138 127	
CRR-4	6/2/2006 9:00	6/2/2006 16:57	7.9	956 949		855 799		170 137		127 125		132 122	
CRR-5	6/3/2006 5:52	6/3/2006 16:50	11.0	962 955		872 818		170 137		127 121		128 120	
CRR-6	6/3/2006 16:50	6/4/2006 5:00	12.2	954 946		871 817		170 138		128 126		136 126	
CRR-7	6/4/2006 5:00	6/5/2006 0:03	10.0	954 939		853 798		170 135		121 122		131 120	
CRR-8	6/5/2006 0:03	6/5/2006 7:30	7.5	955 945		859 804		170 136		123 120		132 123	
CRR-9	6/5/2006 7:30	6/5/2006 19:10	11.2	955 948		870 818		170 139		128 124		130 121	
CRR-10	6/5/2006 19:10	6/6/2006 7:21	12.2	960 951		886 836		170 140		130 130		141 130	
CRR-11	6/6/2006 7:21	6/6/2006 19:12	11.9	958 945		881 833		170 141		131 129		138 129	
CRR-12	6/6/2006 19:12	6/7/2006 7:03	11.7	959 946		872 821		170 139		129 129		142 132	
CRR-13	6/7/2006 7:03	6/7/2006 21:55	14.9	951 938		858 809		170 140		129 129		138 128	
CRR-14	6/7/2006 21:55	6/8/2006 7:56	9.3	949 934		852 802		170 138		127 126		138 128	
CRR-15	6/8/2006 7:56	6/8/2006 13:00	5.7	954 939		854 802		170 138		127 126		136 126	
		Averages (Total COT)	163.8	956 945		861 809		170 137		127 126		135 126	

Notes:

1. CRR-7 Averages do not include the time the process was down

[summary tables.xls]CRR Temps

Table 7-19. CP2 CRR pressures, differential pressures, and bed height.

			DP (inches water)		Pressure (psia)	CRR bed height (in.)	CRR Bed specific gravity
			CRR distributor	PBF	CRR freeboard		
Test Start		Finish	PDI-300-004	PDI-406-001 PT-3	00-004 PD	I-300-002	PDI-300-001
CRR-1	6/1/2006 5:46	6/1/2006 19:47	15	4.6	11.7	39	1.5
CRR-2	6/1/2006 19:47	6/2/2006 9:00	15	4.5	11.8	39	1.5
CRR-3	6/2/2006 16:57	6/3/2006 5:52	16	4.6	11.8	38	1.5
CRR-4	6/2/2006 9:00	6/2/2006 16:57	15	4.7	11.8	39	1.5
CRR-5	6/3/2006 5:52	6/3/2006 16:50	16	4.7	11.7	38	1.5
CRR-6	6/3/2006 16:50	6/4/2006 5:00	16	4.8	11.8	32	1.4
CRR-7	6/4/2006 5:00	6/5/2006 0:03	13	4.8	11.7	31	1.4
CRR-8	6/5/2006 0:03	6/5/2006 7:30	15	6.0	11.8	31	1.4
CRR-9	6/5/2006 7:30	6/5/2006 19:10	14	6.2	11.7	26	1.3
CRR-10	6/5/2006 19:10	6/6/2006 7:21	15	5.3	11.8	26	1.3
CRR-11	6/6/2006 7:21	6/6/2006 19:12	15	5.4	11.8	24	1.3
CRR-12	6/6/2006 19:12	6/7/2006 7:03	16	5.1	11.8	45	1.6
CRR-13	6/7/2006 7:03	6/7/2006 21:55	17	5.0	11.8	50	1.8
CRR-14	6/7/2006 21:55	6/8/2006 7:56	17	4.8	11.8	47	1.7
CRR-15	6/8/2006 7:56	6/8/2006 13:00	17	4.9	11.7	47	1.8
		Averages	16	5.0	11.8	37	1.5

Notes:

1. CRR-7 Averages do not include the time the process was down.

[summary tables.xls]CRR Press

During startup and shutdown, the fluidizing gas was nitrogen, which was controlled manually. This system also performed very well, even though it was sometimes a challenge to make the change from nitrogen to steam and vice versa because the controls for the two were in different locations and the procedure calls for increasing one while decreasing the other. Having separate nitrogen and steam FG systems allowed the operators to use the FG nitrogen to supply additional fluidizing gas flow when needed for process heating or upsets.

The fluidizing gas supply for the CRR was the gas that exited the DMR and, therefore, was not independently controlled; however, the gas flow to the CRR was generally high enough that the CRR was well fluidized. The exception to this situation was during the initial startups. When both the DMR and CRR beds were in place, the flow through the DMR had to be kept low enough to not elutriate the DMR bed media, which was sufficient to keep the CRR fluidized during normal operations, but not sufficient to keep the CRR fluidized during heat-up periods. Once the DMR bed temperature became hot enough, the CRR would finally fluidize, but this would increase the time required for startup heating. This situation was resolved by adding the CRR bed first, using sufficient gas flow to fluidize the CRR. Upon reaching the desired CRR temperature (which reduced the amount of gas needed for fluidizing the CRR and allowed the use of carbon to maintain the CRR bed temperature), bed was added to the DMR bed and heat-up was continued.

During the CP2 test, the steam boiler experienced several trips on June 4 due to the low steam flow and warmer temperatures experienced during this test. The first trip occurred at 1154. The boiler controls were reset and steam flow was restored at 1200 but feed flow was not restored until 1303. The second trip occurred at 1419. Again, the boiler was reset and steam was restarted at 1425. Feed was not shut off during this second boiler trip. The third boiler trip occurred about 1507. The feed was also shut off at 1507 when the second steam boiler trip occurred. Steam flow was restored at 1542. The loss of steam during this last two boiler trips caused the fluidizing gas distributors to become partially plugged. This plugging caused the flow rate through the two FG distributors to be significantly different as measured by the FG orifice flowmeters; at 1600 PDI-200-11A read 2-in. WC while PDI-200-11B read 24-in. WC. Previous to the boiler trips, these gages read within 1-in. WC of each other.

Once the FG flow maldistribution occurred, it was very difficult to bring the flows back into balance because the lower flow rate on one rail tended to form a less-well fluidized area around the deficient rail, and would perpetuate the maldistribution. Because of the maldistribution of the fluidizing gas, the JTG decided to shut the system down and clean the distributors. The shutdown occurred at 1702. The distributors were cleaned and the system was put back into service at 2300. The cause of the boiler trips was determined to be due to the overcapacity of the boiler system for this application. A steam vent line was opened and left open for the remainder of the run to provide additional load for the boiler. This prevented any further boiler trips for the rest of the test. Figure 7-12 shows the DMR vessel temperature and steam flow rates for June 4, 2006. The loss of steam flow and the resultant change in vessel temperatures can clearly be seen from this graph. The fluidizing gas system was modified after CP2 to add backup nitrogen flow to prevent defluidization should the steam boiler trip off again.

7.5.1.2 Fluidizing Gas Distributors. The DMR used a twin-rail perforated pipe distributor, and the CRR used a single three-hole large orifice distributor for both the CP1 and CP2 tests. The CRR distributor worked well during the test program, providing sufficient pressure drop to evenly fluidize the CRR bed.

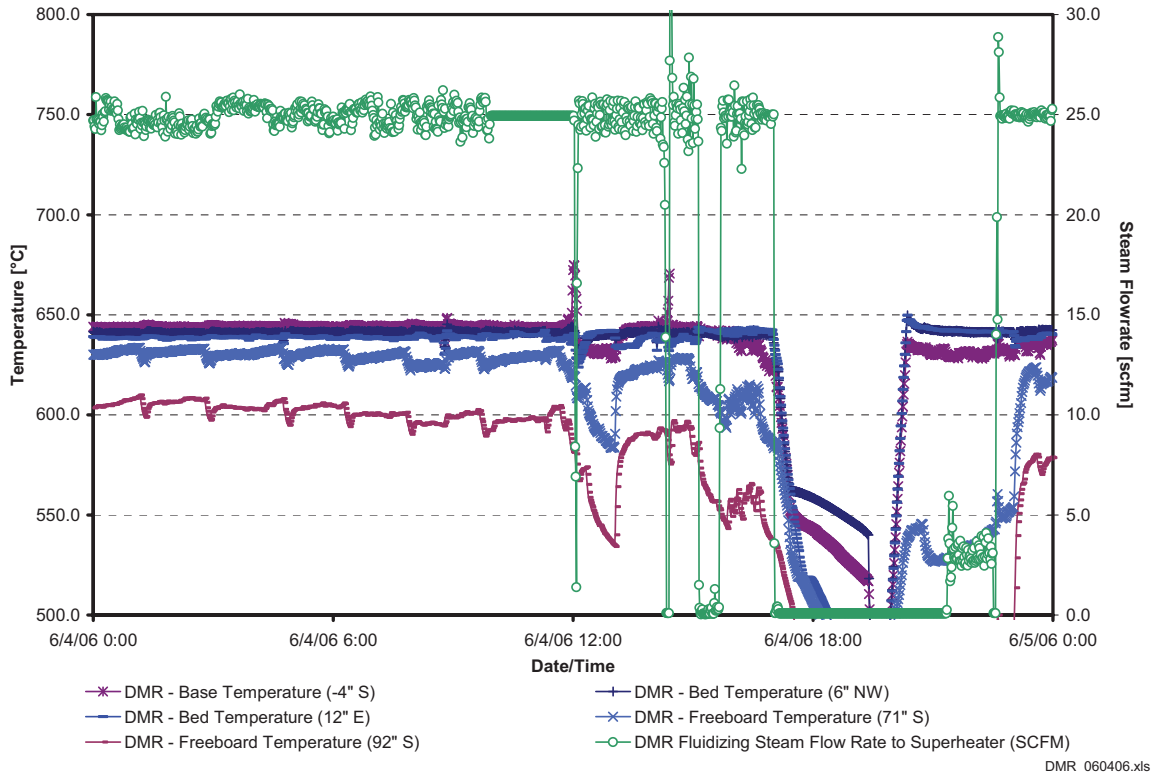

Figure 7-12. DMR vessel temperatures and steam flow rate during steam boiler trips on June 4, 2006.

The DMR twin-rail distributor worked well when the bed was well fluidized, but if there were any restrictions or impediments to the gas flow, it tended to favor flow through one rail or the other. This situation was especially pronounced when the total FG flow rate was low—at an SSV of less than 1 fps. Once a FG flow imbalance occurred, it was difficult to bring the flows back into balance because the lower flow rate on one rail tended to form a less-well fluidized area around the deficient rail and would perpetuate the imbalance. Increasing the total FG flow rate was the usual remedy to this situation, although this procedure would also tend to increase the elutriation rate from the DMR. On several occasions, it was observed that draining down the bed level in the DMR via the bottom auger would cause the imbalance to switch to the other rail or cease altogether, probably as a result of disturbing or moving the solids around the distributor rails. This flow imbalance probably only affected the lower 6–12 inches of the bed because, above this level, gross circulation patterns in the bed (i.e., "gulf streaming") is much more important for maintaining the uniformity of the bed media composition and temperature than the gas distribution pattern.

The distributors used for the CP1 test were reused for the CP2 test with one modification: two of the holes in the distributors (one in each rail) were welded closed to provide additional pressure drop through the distributor at the lower gas flow rates used during the CP2 test. After the CP2 test was terminated, approximately 15–20 lb of agglomerated bed material was discovered just above the south FG distributor (see Figure 7-13). It is probable that this agglomerated material was a direct contributor to the maldistribution observed in the distributor rail flow rates. Additionally, 3-in. diameter pieces of porous encrustations were found in the bottom of the fluidized bed (see Figure 7-14). It is thought that these encrustations formed when the steam boiler tripped during the CP2 test and the FG steam flow rate went to zero. Even though the steam flow rate was zero, the oxygen was still flowing into the bed. The reaction of oxygen with carbon in the poorly fluidized area around the distributors probably caused localized hot spots and formation of these porous encrustations.

Figure 7-13. Agglomerated bed material removed from the DMR vessel at the end of test CP2.

Figure 7-14. Porous encrustations removed from the bottom of the DMR vessel at the end of test CP2. The curved piece at the bottom left fit the outside diameter of the fluidizing rails.

7.5.1.3 Superficial Space Velocities. An objectives of the CP2 test was to determine an acceptable range of fluidizing velocities for the DMR and CRR. This was to be accomplished by determining DMR and CRR particle size distributions, bed temperature spreads, and bed product general appearance as a function of fluidizing velocities.

It is generally accepted that a fluidized bed is well mixed if the superficial space velocity (SSV) is at least twice the minimum fluidizing velocity. The SSV at the DMR distributors during the CP2 test ranged from 0.72–1.39 fps with an average SSV of 0.99 fps. This was well in excess of twice minimum fluidizing velocity required to adequately fluidize the bed (see Figure 7-15). This figure also shows the small spread in the DMR bed temperatures indicating that the bed was well fluidized during CP2.

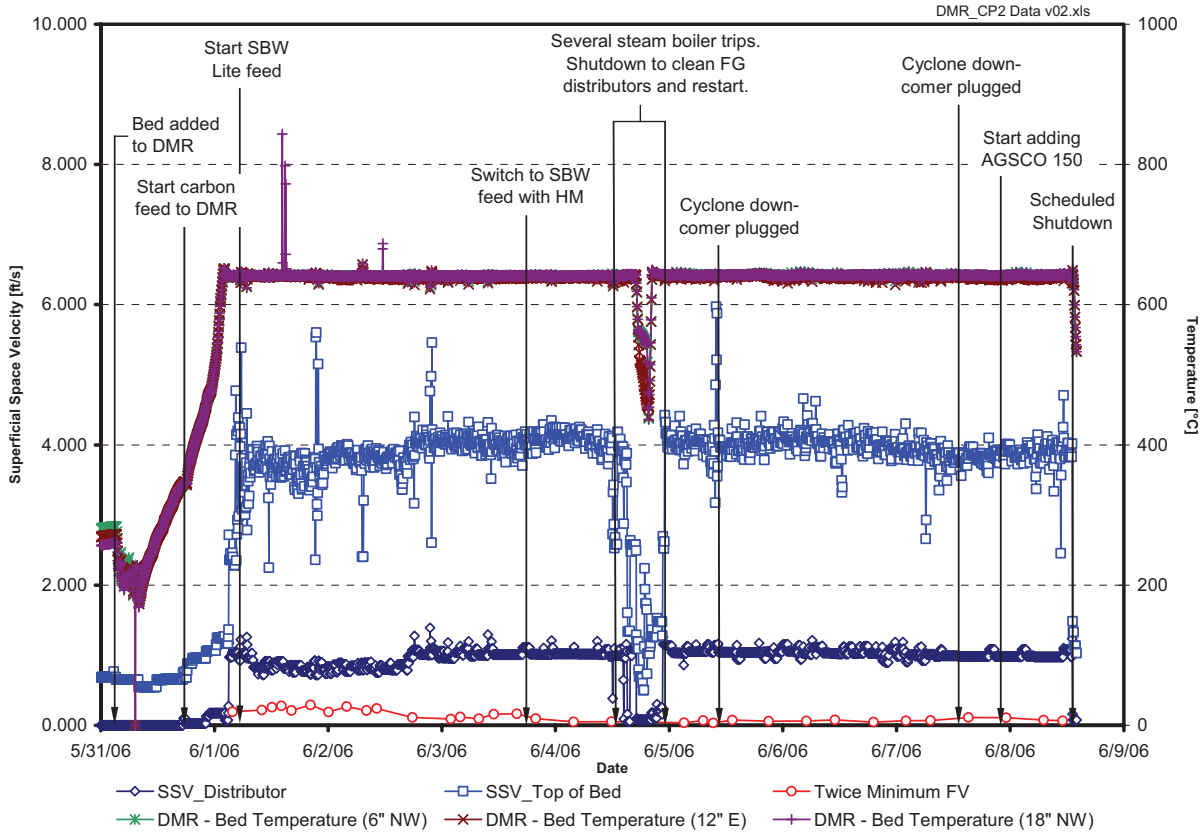

Figure 7-15. Comparison of superficial space velocities and twice minimum fluidizing velocity in the DMR bed during the CP2 test.

The axial range of temperature readings in the bed (very small) show that the DMR was well fluidized during this test. The SSV at the CRR inlet ranged from 2.24–8.36 fps and averaged 5.86 fps. As in the DMR, the axial range of bed temperature readings in the CRR showed that the bed was well fluidized. Figure 7-16 shows the comparison between the CRR inlet SSV and twice the minimum fluidizing velocity for the CRR bed material.

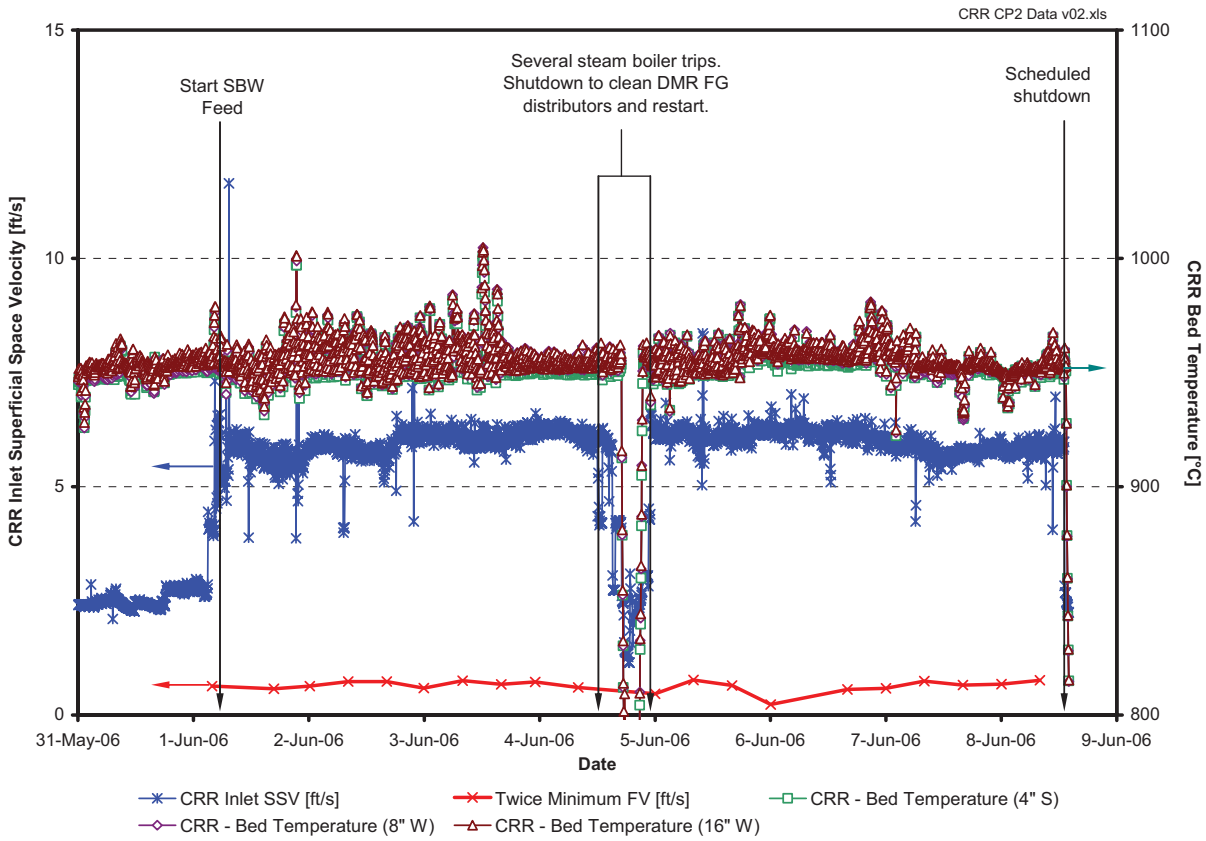

Figure 7-16. Comparison between the CRR inlet SSV and twice the minimum fluidizing velocity in the CRR bed for the CP2 test.

7.5.1.4 DMR Liquid Feed Nozzle Performance. Four different designs were used for the liquid feed nozzles during the CP1 Scoping and Production tests. These different designs were designated E-1, E-2, M-1, and M-2. Another similar nozzle design, designated M-3, was used for the CP2 test. All the feed nozzles were two fluid atomizing nozzles, although the M-2 nozzles used a second atomizing gas flow to help atomize the feed and keep the nozzle cool. The nozzles were inserted into the bed through the flanged connectors shown in Figure 7-17. All the nozzles were tested prior to installation to make sure that proper atomization of the feed could be achieved, and a qualitative determination was made on how well the nozzles atomized feed material at various air atomization ratios and feed rates.

The initial operation during the scoping test used the E-1 nozzle. The nozzle worked very well with water feed, showing no operational problems. Shortly after the beginning of Scoping Test S-4 on January 8, the E-1 liquid feed nozzle started to show signs of plugging, indicated by increased back-pressure on both the liquid and atomizing air, as well as a decreased feed rate. Gentle tapping on the feed nozzle seemed to help the problem with the pressures falling rapidly and the flow rate increasing; however, the cycle would then repeat and would require tapping on the nozzle every 5–15 minutes to clear the plug. This plugging continued through the first five scoping tests. Flushing with water and blowing out the nozzle with nitrogen seemed to help for a short time, but nothing was as successful as gentle tapping on the nozzle, as needed. Both the E 1 and M-1 nozzles experienced this plugging, although the M-1 nozzle eventually plugged so solidly that it could no longer be used, and the rest of the tests were performed using the E 1 nozzle.

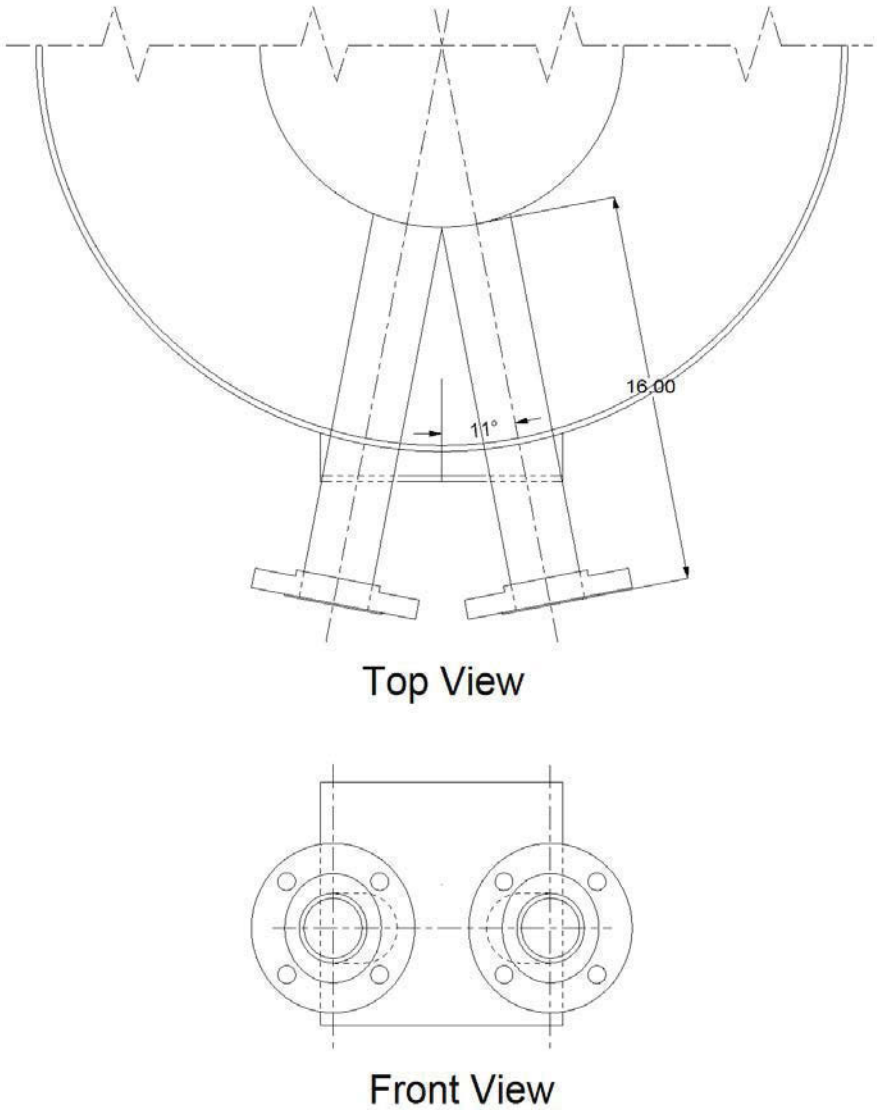

Figure 7-17. DMR Feed Nozzle insertion flanges layout.

The cause of the nozzle plugging was evaluated by switching from SBW simulant feed to deionized water feed for a period, and observing the behavior of the nozzle back pressures. After the feed was switched to water, the pressure on both the gas and liquid side gradually decreased to baseline levels. Switching back to SBW feed caused the pressures to increase once again until the nozzle plugged. From this observation it was concluded that the cause of the nozzle plugging was the heating and partial evaporation of feed while it was still in the nozzle, causing dissolved solids in the feed to precipitate out of solution and cause the pressure in the nozzle to increase until it plugged. The E-1 nozzles were modified to add a cooling jacket (resulting in the E-2 nozzle design) around the outside of the atomizing air tube which reduced, but did not eliminate, the plugging problem.

The second CP1 production test (P-2A) added UDS to the base SBW solution to test its effect on the DMR operation. Almost immediately after switching to the feed solution containing the UDS plugging occurred in the E-2 feed nozzle and it could not be cleared with gentle tapping on the nozzle. Attempts to clear the plugs continued for several hours before the feed was switched back to the base

SBW solution without UDS. When this switch to baseline SBW feed (without UDS) was made, the nozzle plugging was greatly reduced.

At the time it was assumed that the nozzle plugging was due to heating and precipitation of feed solution solids in the nozzle tip and that additional nozzle cooling was needed to prevent this plugging. Accordingly, P-2 was suspended until two new tri-axial nozzles (M-2 nozzles) with additional feed cooling could be fabricated and installed. It was later learned, however, that the main cause of plugging with the UDS was oversized $Zr(HPO_4)_2$ granules in the UDS solids.

7.5.1.5 Product Removal. The DMR product removal system functioned well during both the CP1 and CP2 tests. The major problems that were experienced in removing bed from the DMR generally had more to do with the operation of the DMR than with the product removal system (i.e., when the bed agglomerated and prevented product from being removed from the DMR). The major operational problem with the bed removal system was plugging of the auger or the auger screen. The auger screen cleanout tool on the auger screen was useful for cleaning out the screen when it plugged, but plugs inside the auger itself were more difficult to clear. Two procedures used to clear the auger when it restricted; (1) run the auger in reverse for several seconds, or (2) to quickly close and then open the isolation valve on the inlet to the Product Receiver while the eductor was operating. Both these procedures would tend to move the solids that were plugging the auger and allow solids to flow again. The operators also found that hammering on the auger body and valve would help to break up bridging solids in the auger screen or outlet. On one occasion, the auger screen plugged solid with large chunks of agglomerated bed material. In this case it was necessary to remove the cleanout cover to rod out the auger screen to allow the solids to flow through. There also were several instances when the plug valve on the outlet of the auger would stick open or closed. Generally this could be fixed by rapping on the valve body with a hammer.

Solids removal from the CRR during CP1 and CP2 was generally straightforward, although there were a couple instances where the solids bridged in the CRR drain cone and could not be removed. In both these cases, adding solids to the top of the CRR bed caused the bridged material to break up and allow solids to be drained. During the CP2 test, the solids were easily removed from the CRR.

7.5.2 Fluidized Bed Particle Size Distribution

One of the most important parameters for successful operation of a fluidized bed process is the particle size distribution. If the bed particles are too small, they are rapidly elutriated from the bed, causing the bed level to decrease. If the particles become too large, the bed will defluidize. Both of these processes can occur rapidly if the bed particle size changes too much. The effect of reduction in particle size was demonstrated in the early functional tests, when the soft sodium carbonate starting bed in the DMR broke up rapidly and was largely elutriated to the HTF. The bed particles used in the CRR were very attrition-resistant, and particle size control was not an important factor in operating the CRR. In the DMR, bed particle size control was a major factor in the success of the process, especially because the particle size could change due to feed deposition on the bed particles and bed particle attrition.

There were three distinct particle size distribution (PSD) histories for the DMR CP1 tests – the Functional Tests, the Scoping Tests, and the Production Tests. The Functional Tests took place November 28 through December 5, 2005. Scoping tests took place from December 7, 2005 through January 13, 2006. The CP1 Production Tests took place from January 17 through February 10, 2006. These different histories are shown graphically in Figure 7-18 through Figure 7-21 in the following sections. These graphs show the average (Harmonic Mean) particle size of “active” bed samples that were taken from the DMR sample port.

7.5.2.1 Functional Test. The Functional Test (see Figure 7-18 depicts the DMR PSD history from November 30 through December 8, 2005. This test was designed to allow functional testing of all the ESTD systems during operation and enable control system tuning of automated control loops. The bed material used in the DMR for these tests was AGSCO 80 alumina with an initial particle size of approximately 147 µm. After the bed was added to the DMR, the average particle size increased slightly over several days because of the smaller fractions being elutriated from the bed.

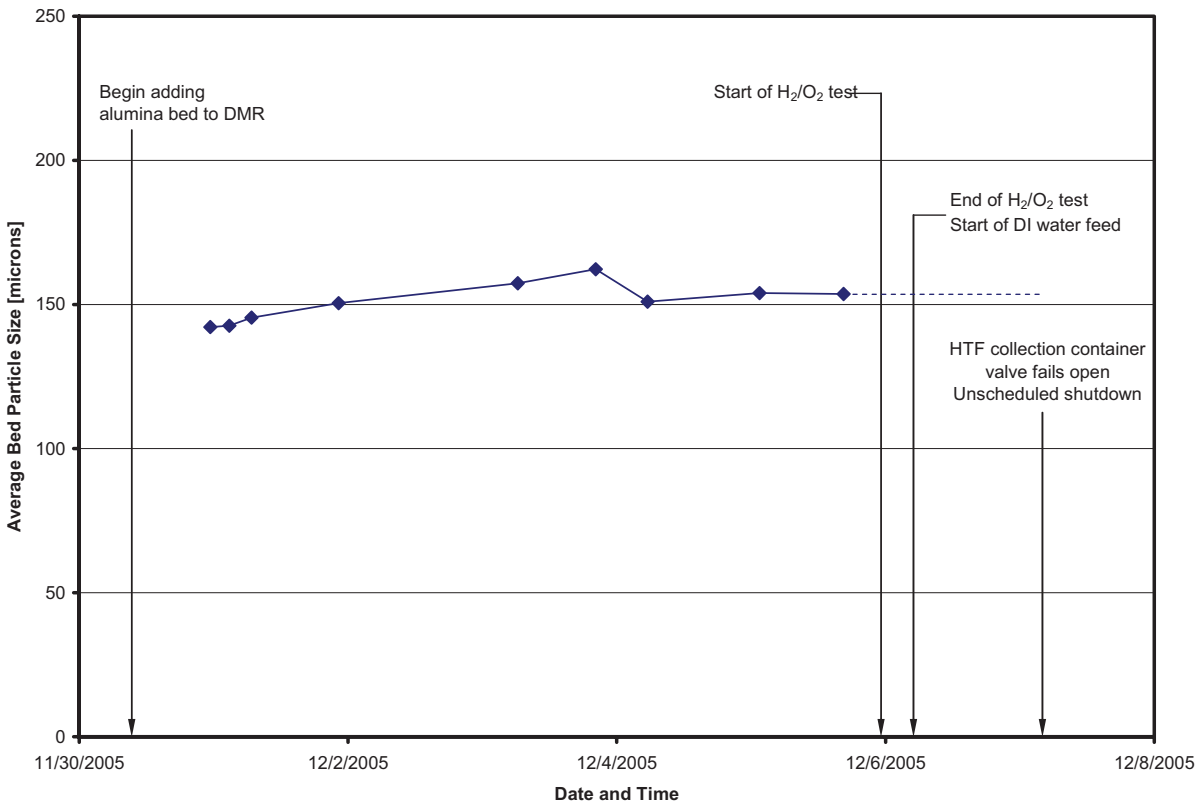

Figure 7-18. Functional Test: DMR average bed particle size.

7.5.2.2 Scoping Test 1. Deionized water feed was used to test the DMR feed system, initiating CP1 Scoping Test 1. On December 7, the HTF collection container failed open while a sample of the HTF solids was being taken. A restricted FG distributor created sufficient back-pressure that, during an attempted restart, the rupture disk on the DMR burst, causing the emergency shutdown system to activate. It was decided to keep the system shut down to perform system upgrades and required maintenance.

7.5.2.3 Scoping Tests 2 and 3. The CP1 Scoping Tests 2 and 3 were performed December 17, 2005 through January 6, 2006, with a break from December 22 through January 3 (see Figure 7-19). The system was configured for operation and heatup on December 15, but simulated SBW feed was not started until December 17. The carbon reductant used for this test was Berger Brothers wood-based P-6 carbon. Both tests used simulated SBW feed solution that did not include any undissolved solids, heavy metal compounds, or POHC.

A leak developed in the FG distributor flange after about 14 hours of operation with simulated SBW feed. At the same time, the temperatures in the DMR deviated, indicating that the bed was defluidized on the morning of December 18.

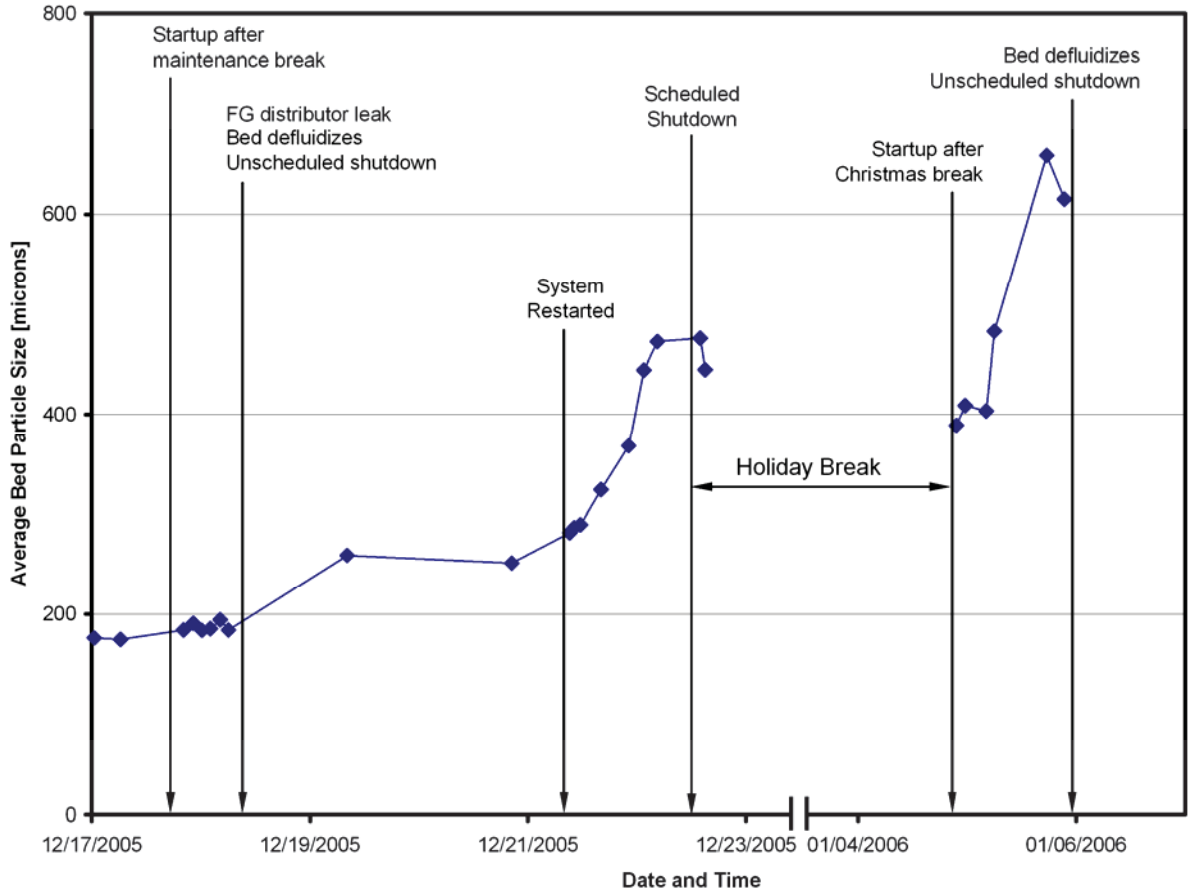

Figure 7-19. Scoping Tests 2 and 3: DMR average bed particle size.

It was found that a large fraction of the DMR bed had formed into an agglomerate ("sandcastle") formation that was hard enough to cause the bed to defluidize, but soft enough that it broke with gentle mechanical pressure. The cause of the leak in the FG distributor was determined to be a failure of the flange gaskets at the high temperatures in the FG system. At the time, it was thought that the defluidization may have been caused by the uneven gas distribution in the bed caused by the FG distributor flange leak. It was postulated that this leak may have caused the bed solids close to the feed nozzle to become saturated with feed, leading to the defluidization event. The insulation around the FG system flanges was removed, and the gaskets replaced with gaskets that were suitable for the high temperature and chemical composition (steam and oxygen) of FG. Four of the FG distributor rail orifices (two on each rail) were welded shut to increase the velocity of the FG into the bed. Testing to this point had indicated that the fluidizing gas flow rate in the DMR did not need to be as high as originally anticipated in the design.

The system was placed back into operation on December 21 and tests continued until the COT had reached 40 hours on December 22 when a scheduled shutdown for the holiday break was initiated. Another deviation in the bed temperatures was observed during operations on December 21, indicating partial defluidization of the DMR bed, but rapid response by the operators to shut off feed and increase nitrogen purges in the bed quickly brought these temperatures back in line, and feed was restarted after about 2 hours. This situation indicated that the previous conclusion that maldistribution of the FG caused the bed defluidization was incorrect. The average DMR bed particle size during this period of operation increased from 281 to 444 µm during 29.75 hours of operating time.

Over the holiday break, the system was disassembled, cleaned and maintenance work was performed. The cyclone downcomer was found to be plugged, and was cleaned. The system was reassembled and pressure tested.

Operations were resumed after the holiday break on January 3, 2006, with feed started on January 4. During the heatup, the particle size decreased slightly to 389 µm, but rapid growth in particle size soon resumed when feed was restarted, with the average particle size reaching 658 µm after just 19.8 hours of operation. After almost 20 hours of operation, operators observed another deviation in the DMR bed temperatures and decrease in total bed pressure drop indicating defluidization of the bed. Chemical analysis of the defluidized DMR bed material showed it to have relatively high amounts of calcium, especially at the interface between agglomerated particles. (See C. M. Jantzen letter report to B. Mason, SRNL-PSE-2006-00044, Rev. 1, "Characterization of Hazen Pilot Scale Demonstration Waste Form Products, Agglomerates, and Scale," March 20, 2006 [R27].) The source of this calcium was the ash from the Berger Brothers wood-based charcoal used as a reducing agent in the DMR. As a result of this finding, the JTG decided to use GC-CRB calcined coal as the reducing agent in the DMR and also to add calcined mullite to the bed to help tie up any low-melting eutectics that may have formed in the bed. The broken up bed material from the DMR was screened through a 12 mesh screen and the smaller fraction reused in the DMR for the scoping tests which started on January 8.

7.5.2.4 Scoping Tests 4 through 8. Until the beginning of the Scoping Test 4 on January 8, 2006, the CRR bed temperature had been controlled by varying the carbon feedrate to the CRR and using the in-bed oxygen distributor to maintain the outlet oxygen concentration in the CRR off-gas. However, because there was about a 20 minute lag between the time when carbon was fed to the CRR and a change in the CRR bed temperature was observed, this method resulted in the CRR bed temperature control being ± 50°C to 100°C from the desired setpoint. The operation of the CRR was modified to use the in-bed oxygen flow rate to control the bed temperature, which is the same operating method used in the DMR. At the same time, the over-bed oxygen flow was used to control the CRR outlet off-gas oxygen concentration. Both of these were set up to be controlled automatically. The carbon feedrate was controlled manually at a fixed rate that maintained a constant bed height in the CRR. This method of CRR bed level and oxygen control worked very well to control temperature and bed level in the CRR at stable, consistent levels.

Scoping Test 4 began on January 8, 2006 using GC-CRB coal in the DMR as the carbon reductant and adding calcined mullite to the bed to tie up any eutectics that may still be present in the bed media. Shortly after the beginning of Scoping Test 4 on January 8, the liquid feed nozzle started to show signs of plugging—i.e., increased back-pressure on both the liquid and atomizing air feeds to the nozzle and decreased feedrate. Gentle tapping on the feed nozzle seemed to help the problem, with the pressures falling rapidly and the flow rate increasing. However, the cycle would then repeat and would require tapping on the nozzle every 5–15 minutes to clear the plug. This continued throughout Scoping Tests 4–8. Flushing with water and blowing out the nozzle with nitrogen seemed to help for a short time, but nothing was as successful as gentle tapping on the nozzle as needed. Both the E-1 and M-1 nozzles experienced this plugging, although the M-1 nozzle eventually plugged so completely that it could no longer be used, and the rest of these scoping tests were performed using the E-1 nozzle.

The test conditions for the scoping tests are shown in Table 5-1. The tests proceeded on schedule through the middle of Scoping Test 5 when the tubing to the feed nozzle cracked, causing a small leak of the feed solution. The system was shutdown, the bed was drained from the DMR, and the feed nozzle removed, repaired, and re-installed. The system restarted after a 9.25 hour break. The apparent cause of the crack was installation of a pneumatic vibrator on the feed line to prevent plugging of the feed nozzle. The high-frequency vibration caused metal fatigue in the tubing where it entered a swaged fitting. This metal fatigue eventually caused the tube to crack through.

The cause of the nozzle plugging was evaluated by switching to deionized water feed for a period and observing the behavior of the nozzle back pressures. After the feed was switched to water, the pressure on both the gas and liquid size gradually decreased to baseline levels. Switching back to SBW feed caused the pressures to increase once again until the nozzle plugged. From this observation it was concluded that the cause of the nozzle plugging was the heating and partial evaporation of feed while it was still in the nozzle. This caused dissolved solids in the feed to precipitate out of solution, causing the pressure in the nozzle to increase until it plugged. The E-1 nozzles were subsequently modified to add a cooling jacket around the outside of the atomizing air tube, which reduced, but did not eliminate, the plugging problem.

The scoping tests were finished on January 13, 2006 when a scheduled shutdown was initiated. During the scoping test, the average particle size in the DMR was generally 250–450 µm (see Figure 7-20). Note that two average particle sizes are shown in this figure, one with the as received data and the other with the greater than 8 mesh fraction removed. The GC-CRB calcined coal was generally found in the greater than 8 mesh fraction of the bed material. This carbon skewed the results of the particle size distribution analysis, especially when there was a large amount of carbon in the bed (e.g., the sample at 0800 on January 9). Removal of the greater than 8 mesh fraction gave a better indication of the carbonate bed product particle size history for these tests.

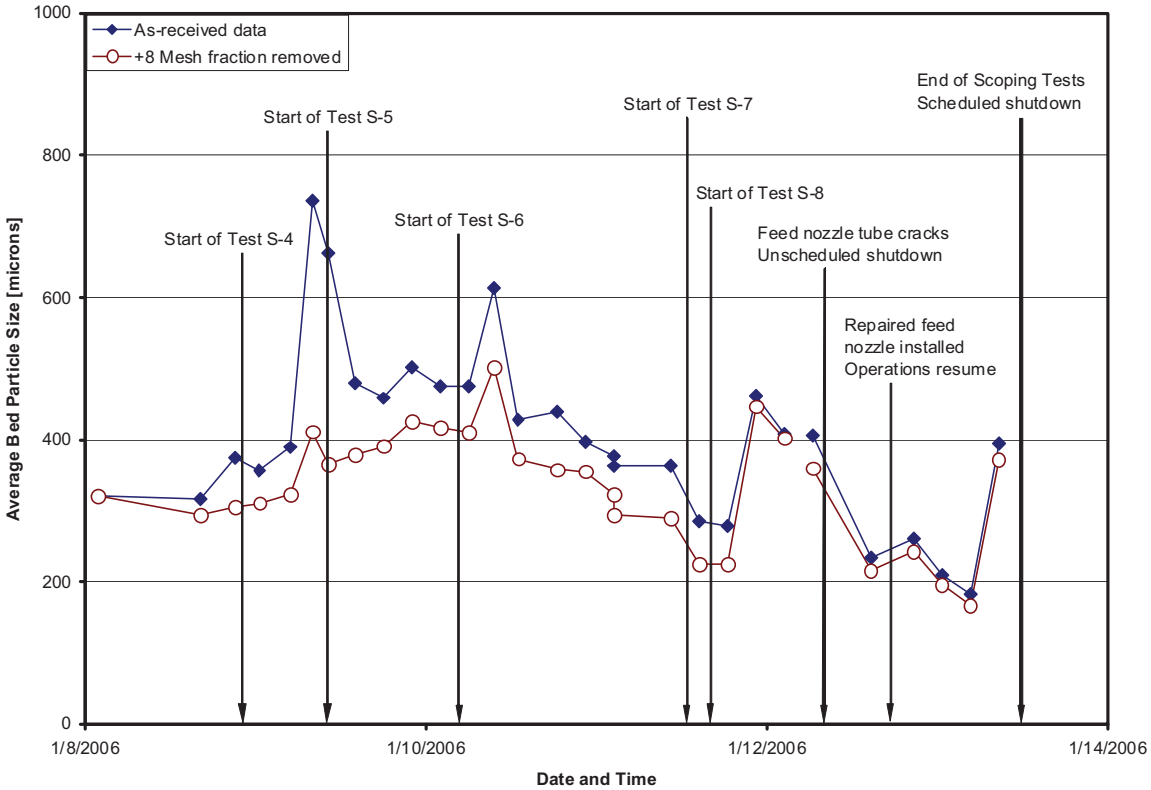

Figure 7-20. DMR average bed particle size January 8–13, 2006.

7.5.2.5 CP1 Production Tests. The CP1 production tests started on January 17, 2006, and continued with two brief shutdown periods until February 10. The test conditions used for the production tests are discussed in Section 5.4.

No mullite or clay was added to the DMR during Production Test P-1. As can be seen in Figure 7-21, the particle size increased rapidly and continually until the end of this test (which was the start of Test P-2). Therefore, at the end of P-1, the DMR bed level was drained down to 32 in. and 62.5 lb of PR bed material that had been screened to -50 mesh (297 µm) was added to the bed along with 2 lb of Snow Tex clay. This caused the average bed particle size to decrease from 936 to 724 µm at the end of P-1 and beginning of P-2. As with the scoping tests, the average bed product particle size shown for the production tests are all with the greater than 8 mesh coal fraction removed.

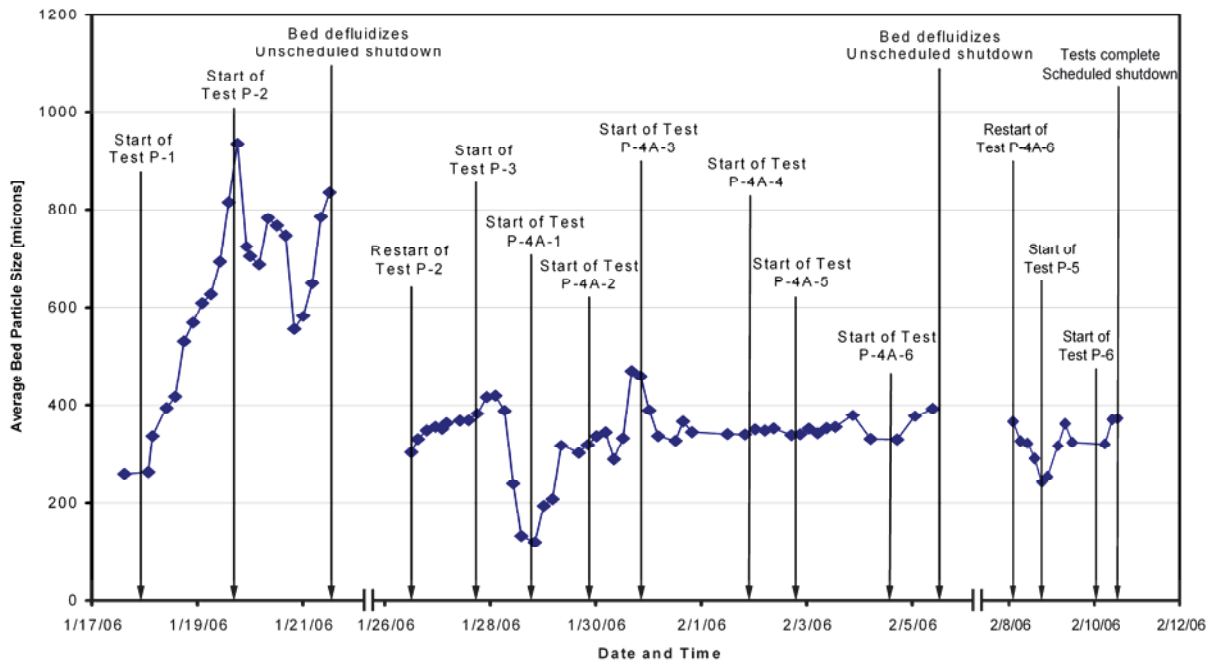

Figure 7-21. CP1 Production Tests: DMR average bed particle size.

Production Test P-2 added UDS to the base SBW solution to test its effect on the DMR operation. Test P-2 resumed on January 26 after a shutdown to replace the WF nozzles. The bed used for this continuation of P-2 was PR product that was screened to less than 20 mesh (~841 µm). Mulcoa clay was added to the DMR during heat-up, but not during operation with SBW feed. After about 2 hours of operation, the feed was switched to SBW solution that contained UDS. Again nozzle plugging started after feed with UDS resumed. These large solids were determined by chemical analysis to be $Zr(HPO_4)_2$. The $Zr(HPO_4)_2$ had been specified to have a particle size of less than 100 µm, but the material obtained did not meet this specification. The batch of feed currently in use was discarded and future batches of SBW feed with UDS were made up with $Zr(HPO_4)_2$ that had been prescreened to remove this oversize material before it was mixed into the feed solution. The average particle size in the DMR remained relatively constant during this portion of the test, varying between 302 and 382 µm.

Test P-3B used SBW solution with UDS and heavy metals to test the DMR performance with these compounds. The operation of the DMR was fairly smooth during this test with relatively minor feed system plugging that was quickly cleared. The average particle size increased slightly at the beginning of

the test and then fell dramatically after 0630 on January 28. It is unknown what caused this decrease in the average particle size; however, it is possible that the introduction of heavy metals in the feed may have caused the particle size to drop.

Test P-4A-1 included POHC and the SBW solution with UDS and heavy metals that were mixed with the base SBW solution. The temperature in the DMR was also increased to 670°C for this test. The average particle size increased during the beginning of this test and then stabilized at about 350 µm. With a few exceptions, the average particle size remained at this value for the remainder of the production tests, regardless of the feedrate, DMR operating temperature, or feed concentration used. It is probable that kaolin clay in the UDS that were added to the base SBW solution kept the particle size from growing too large. Analysis of the particle size distribution samples also shows that carbon from the reductant was a significant fraction of the larger screen sizes, which probably kept the particle size from becoming too small.

During P-4A-5, a batch of feed was made up inadvertently with the oversize $Zr(HPO_4)_2$ that had been screened out of the bulk $Zr(HPO_4)_2$ material. Feed supply system restrictions occurred again and resulted in a 10.75 hour shutdown while the feed system was taken apart, cleaned, and serviced. During this shutdown, the DMR was idled with no feed, and the nozzles were purged to keep them from plugging. At the end of P-4A-5, the supply of GC-CRB coal ran out. Because there was a significant amount of kaolin in the UDS added to the SBW feed, the JTG decided to go back to using Berger Brothers wood-based carbon as the reductant in the DMR. The last 8.8 hours of P-4A-5 used the Berger Brothers carbon in the DMR.

Shortly after the start of P-4A-6, the FG oxygen flow rate started to oscillate dramatically because of the low temperature and high liquid feedrate. Attempts to retune the temperature control loop were not successful in reducing the flow oscillations; therefore, the decision was made to run the DMR bed temperature control loop in manual mode. This test continued to use Berger Brothers charcoal in the DMR. After 5 hours into this test (for a total of 18.8 hours using charcoal) the DMR bed thermocouples diverged and the bed pressure drop started to fall indicating that the bed was starting to defluidize. Attempts to break up any potential agglomerates in the bed by increasing the total FG flow rate and nitrogen purges were not successful. Thus, the JTG decided to keep the bed on standby using the FG superheaters to maintain the bed temperature until additional GC-CRB calcined coal could be obtained. It is likely that using the Berger Brothers carbon, with its high calcium ash, caused the bed to defluidize, as had happened previously during the scoping tests. There were no large agglomerates in the DMR bed although there was a significant (about 2.5 cm thick × 20 cm high) ring of agglomerated bed material on the walls of the DMR vessel about the level of the feed nozzles. It is possible that this material adhered to the walls and was part of a larger mass of agglomerated bed material that was broken up by the high fluidizing gas and nitrogen purge flows used in attempting to refluidize the DMR and CRR. At 1620 the CRR also showed signs of defluidization after the DMR FG velocities were reduced to minimize product particle attrition in the DMR. Subsequently, the DMR bed was removed from the vessel to enable higher FG flows to help refluidize the CRR. In spite of using FG flows as high as 100 scfm, the CRR could not recover and the shift engineers decided to remove the bed from the CRR to determine the cause of the defluidization.

When the CRR bed was removed, it was observed that the CRR cooling water nozzle was injecting about 560 ml/min of water into the bed through a leaking valve on the rotameter. The cooling water flow was greatly in excess of the energy production rate that the CRR was capable of, and it appears that the build up of water in the bed caused the CRR to defluidize. The system was shut down until the GC-CRB calcined coal could be obtained for use in the DMR. During the shutdown, while waiting for the shipment of GC-CRB coal to arrive, both the DMR and CRR systems were disassembled and inspected, and needed

maintenance was performed. After the calcined coal had arrived, the system was restarted and P-4A-6 was resumed. The average particle size during this test declined slightly.

CP1 Test P-5 was started following the conclusion of P-4A-6 and continued for 30.45 hours. At the end of P-5, it appeared that the bottom of the DMR vessel was obstructed because the bed could not be transferred from the DMR to the PR with the auger and eductor, although the DMR bed remained well fluidized throughout the subsequent test. As during P-4A-6, the bed could not be drained from the bottom of the DMR during this test. Instead, the bed was removed using the DMR bed sample line.

CP1 Test P-6 was started at the conclusion of P-5 and continued for 12.07 hours. The DMR average bed particle size increased slightly during this test, but this particle size increase appeared to be due to increased carbon carryover in the upper particle size analysis sieves. The bed media could not be drained from the bottom of the DMR during or after this test.

7.5.2.6 CP2 Production Tests. During the first CP1 production test (P1), the particle size increased to over 800 µm when using SBW feed without undissolved solids (UDS). (See Figure 7-21). Therefore, one of the test objectives of test CP2 was to demonstrate particle size control of the DMR bed particles when feeding SBW without undissolved solids (UDS). Test CP2 was very successful in demonstrating particle size control as shown in Figure 7-22.

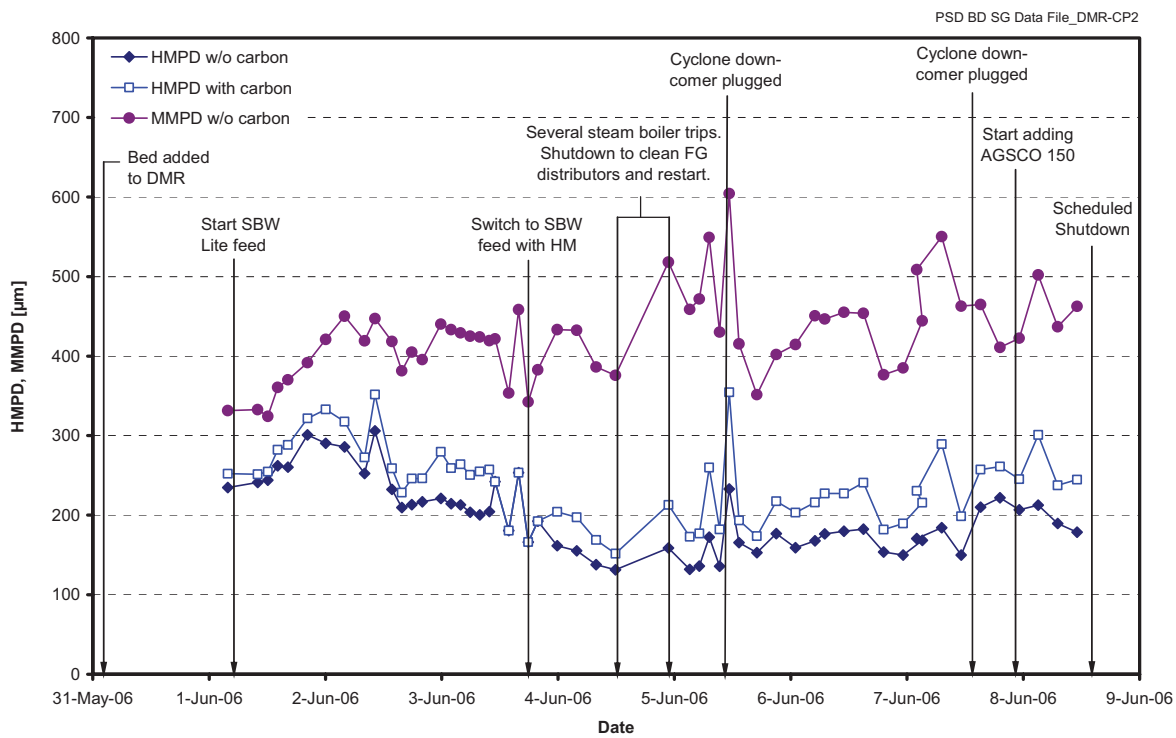

Figure 7-22. Average DMR bed particle sizes during the CP2 test.

Three different average particle sizes are shown in Figure 7-22. The Harmonic Mean Particle Diameter (HMPD) is the average particle size that has the same ratio of surface area to volume as the all the particles in the bed and is calculated from:

$$HMPD = \frac{1}{\sum_{i=1}^{N} \frac{x_i}{d_i}}$$

where

x_i	=	mass fraction of particles caught on sieve *i* (dimensionless)
d_i	=	average size of particles caught on sieve *i* (µm)
N	=	number of sieve screens.

Since the drag force on the particles in a fluidized bed is a function of the particles surface area and the weight of the particles is a function of the particle volume, the HMPD is the appropriate average particle size for calculating the minimum fluidizing velocity in a fluidized bed (the velocity where the drag force equals the weight of the bed particles and the particles are neutrally buoyant or fluidized).

The Mass Mean Particle Diameter (MMPD) is the mass average particle size calculated by:

$$MMPD = \sum_{i=1}^{N} x_i d_i \quad .$$

The MMPD has no physical significance but is often reported as an average particle size.

The particle size distribution of the DMR bed material was measured using standard 8-in. diameter sieve trays in a Ro-Tap testing sieve shaker machine. The HMPD for the DMR bed particles was calculated two ways – the first using all the data from all the sieve screens and the second mathematically removed the mass of particles from the top two screens in the stack (4 and 8 mesh). The carbon particles in the bed samples were generally much larger than the bed particles and were primarily collected on these top two sieve screens. Mathematical removal of the material on these two screens gave a more representative value for the DMR bed particles average particle size. Both the HMPD and MMPD were calculated without using the values from the top two screens (w/o carbon). The HMPD using all the screens (with carbon) was also calculated and is shown in Figure 7-22 for comparison.

From Figure 7-22, it can be seen that the average particle size was very uniform for all of the CP2 test. The starting bed was a 50/50 mixture of two different sizes of alumina particles (AGSCO 46 and AGSCO 80) with an average particle size of 235 µm. The average particle size increased to just over 300µm before dropping to about 150 µm and remaining there for almost the rest of the test. In only two instances did the particle size start to increase rapidly as was observed during the CP1 test: when the cyclone downcomer restricted on June 5 and 7. The downcomer restrictions led to a vastly increased amount of solids going over from the DMR vessel to the HTF. Since these solids were primarily the smaller size fractions in the bed, loss of these particles caused the average bed size to increase dramatically after each downcomer restriction event.

Another factor that seemed to have an effect on the average particle size was the addition of heavy metals (HMs) to the SBW feed solution. Immediately after the addition of heavy metals, the average particle size decreased from about 200 to 150 µm. This confirms the observation in the CP1 test that the addition of HMs to the SBW feed seemed to cause a slight decrease in the average particle size.

One of the methods that was to be used to control the particle size during the CP2 test was the addition of small seed particles to the bed. Two seed particle materials were procured for use during the CP2 test: alumina grit with an average particle size of 82 µm (AGSCO 180) and alumina grit with an average particle size of 92 µm (AGSCO 150). Although the average particle size did not grow uncontrollably during CP2 as it did during CP1, the decision was made to add seed particles to the DMR to see if they would have any effect on the average particle size. Figure 7-23 shows that after addition of the seed particles, the average bed size decreased slightly. Figure 7-23 shows the particle size distribution for the four DMR bed samples just before the seed particle additions (sample numbers 2307, 2315, 2318, and 2325) compared to the size distribution for the four DMR bed samples after the seed particle addition (sample numbers 2332, 2342, 2347, and 2359). As would be expected, the seed particles show up primarily in the size fraction between 75 and 150 µm. Interestingly, the less than 600 and greater than 300 µm size fraction also increased after seed particle addition. It is unknown if this increase was related to the seed particle addition.

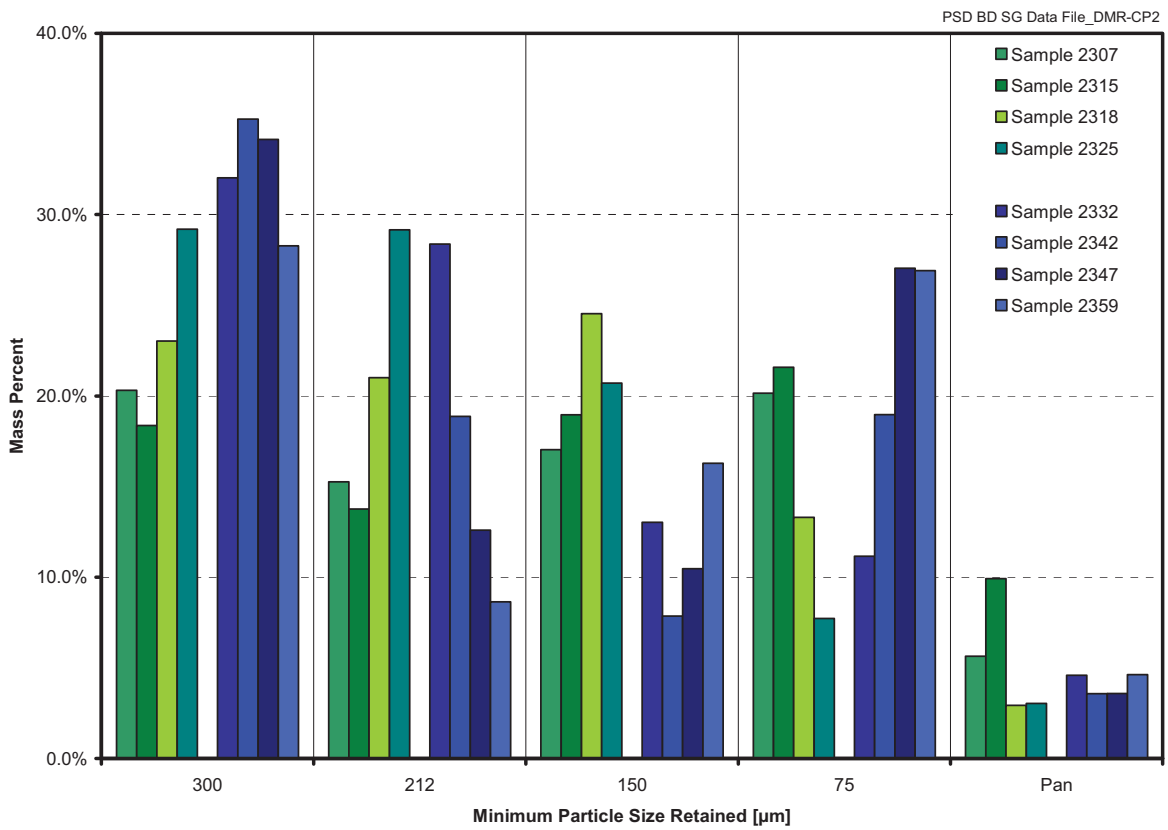

Figure 7-23. Particle size distribution of DMR bed samples taken before and after seed particle addition.

7.5.3 DMR Product Densities

The density of the solids produced in the DMR during CP1 is shown in Figure 7-24. Both the bulk density and particle densities are shown in the graph. Although there was significant variability in the particle density, it averaged 1.9 g/cm^3. The bulk density was also somewhat variable, but averaged 1.06 g/cm^3. Based on these values, the average voidage was 0.44.

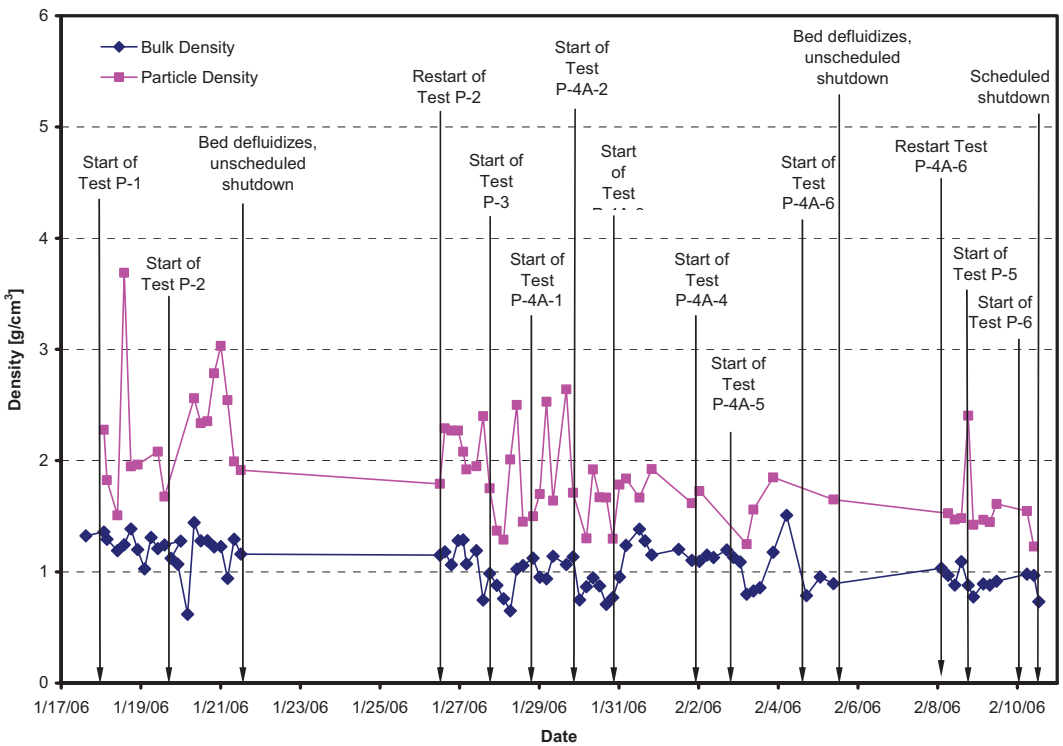

Figure 7-24. DMR solid product densities during the CP1 test.

One of the main objectives for the CP2 test was to confirm the product volume and density when processing simulant feed without UDS. This would provide data to support development of a more reliable estimate of IWTU waste canister count. Measurements were made of the mass and density of the solid products removed from the DMR during CP2 to meet this objective. The mass of solids removed from the DMR is shown in Figure 7-25. The bulk density and particle density of the DMR bed samples is shown in Figure 7-26. Figure 7-27 shows the solids rate in the PR and Figure 7-28 shows the solids rate in the HTF.

The total net mass of material produced in the DMR was the total sum of the net PR solids, the DMR bed samples and the HTF solids minus the starting bed mass. The net PR solids were 4,072.1 lb, the DMR bed samples mass was 253.3 lb and the HTF solids were 364.9 lb. The DMR starting bed mass was 500 lb. This gives a total net mass of DMR solids of 4,190.3 lb. The volume of SBW feed that was processed during the test was 2,497.0 gallons, giving a feed production factor of 1.678 lb solids/gallon feed. The total cumulative operating time (COT) was 164.5 hours, which gives an average feedrate of 0.2503 gpm – remarkably close to the desired feedrate of 0.250 gpm.

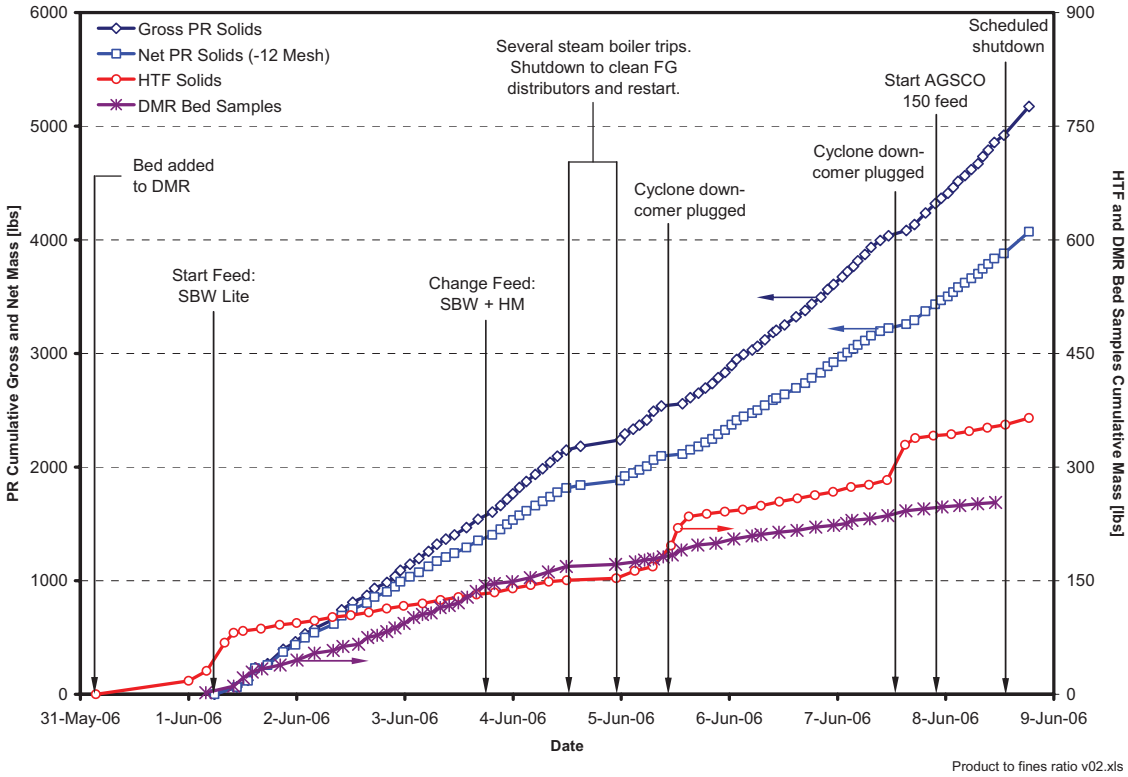

Figure 7-25. Cumulative mass of solids removed from the DMR during the CP2 test.

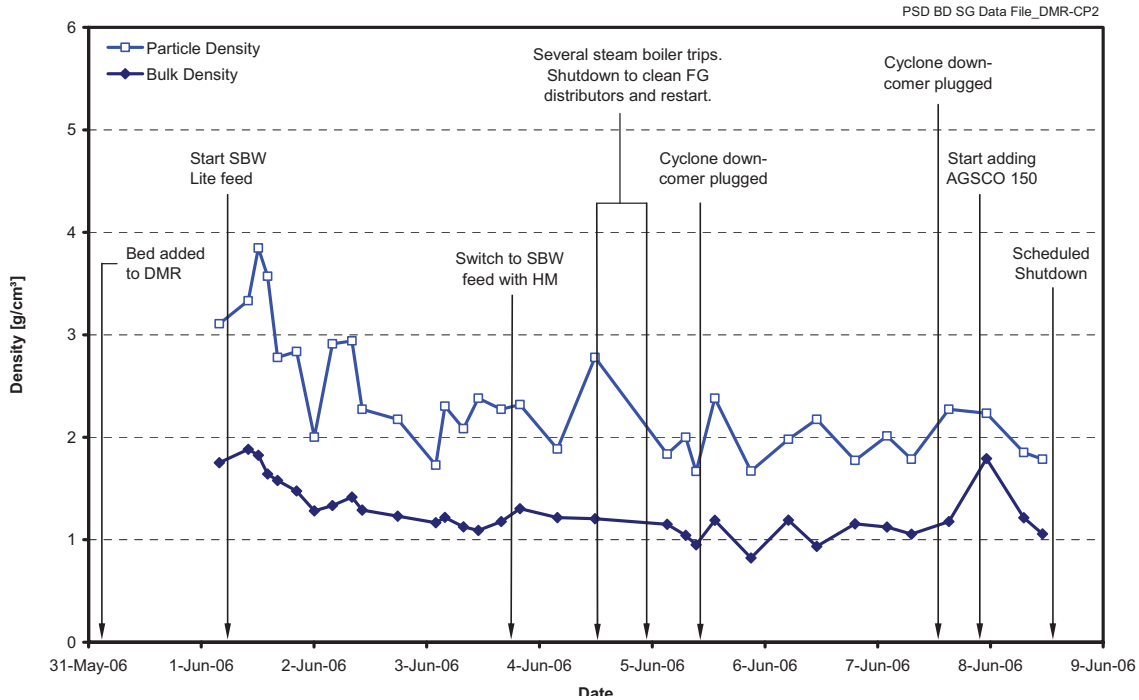

Figure 7-26. Particle and bulk density of DMR bed samples during the CP2 test.

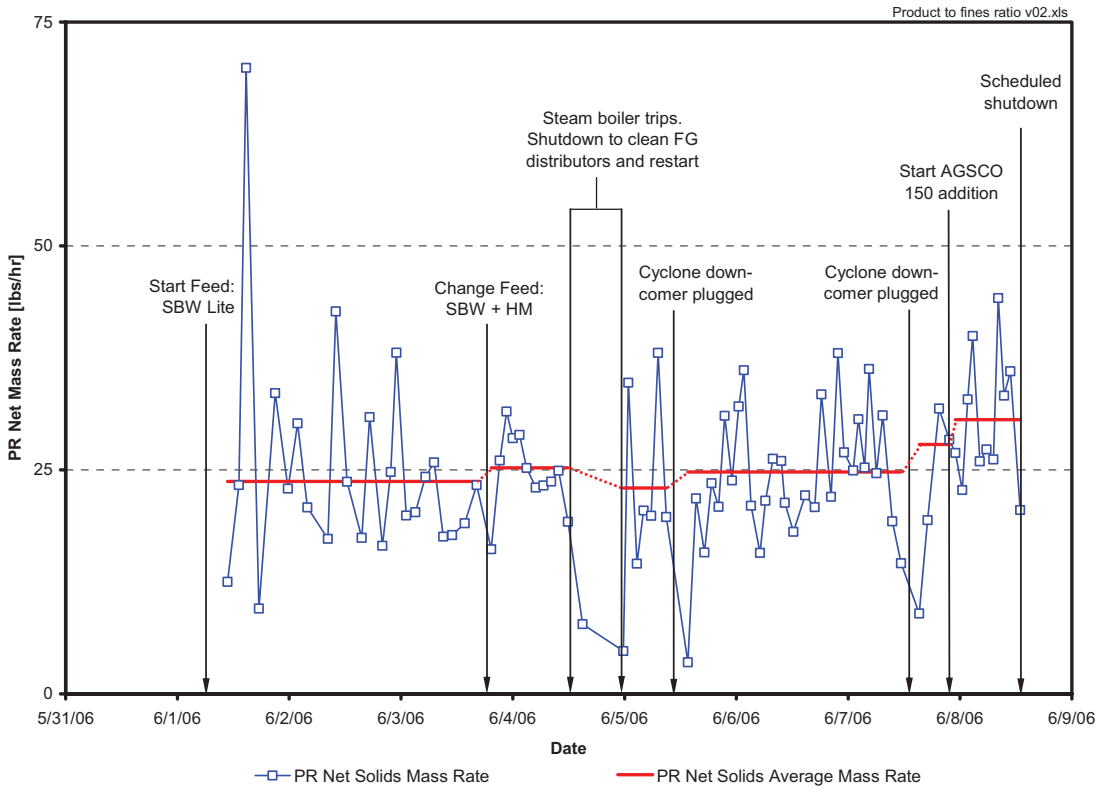

Figure 7-27. Net PR product mass rate during CP2 test.

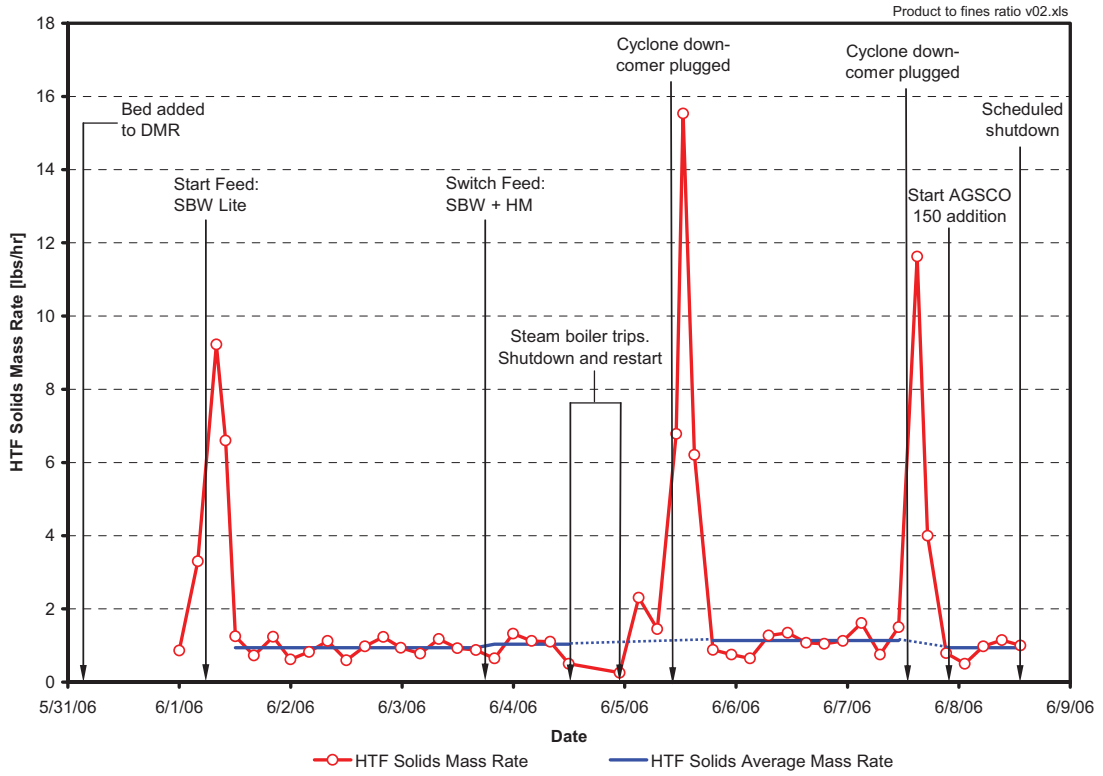

Figure 7-28. HTF solids product mass rate during CP2 test.

The net solids production rate in the PR is shown in Figure 7-27. The average PR solids production rate varied during the run from 23.0 to 30.6 lb/hr while the net PR solids average mass production rate was 25.9 lb/hr over the entire run. The average net production rate was significantly higher after AGSCO 150 seed particle addition started. This indicates that the majority of the seed particles was collected in the bed material and did not elutriate from the bed.

The solids production rate in the HTF is shown in Figure 7-28. The HTF solids production rate ranged from 0.26 to 15.5 lb/hr, with the highest rates observed when the cyclone downcomer restricted. However, excluding the times when the cyclone downcomer plugged, the HTF production rate averaged 1.0 lb/hr. The high HTF solids rates during periods when the downcomer restricted is very evident in Figure 7-28. The HTF average solids production rate did not change after seed particle addition, showing that this material primarily remained in the bed.

The bed turnover is defined as the percentage of the starting bed material that has been replaced by product solids. Bed turnover is calculated as follows:

$$TO(t) = \left[1 - \exp\left(\frac{-M_p(t)}{M_{SB}}\right)\right] \times 100\%$$

where

$M_p(t)$ = net mass of product solids at time t (lbs)

M_{SB} = mass of active starting bed (lbs)

$TO(t)$ = bed turnover at time t (%).

In the DMR, approximately 100–150 lb of the starting bed material collects in the cone and auger below the fluidizing gas distributors. Hence this material is not available as part of the active starting bed. Pressure measurements from the DMR show that the active starting bed mass at the beginning of the test was approximately 415 lb. Using this value for the starting bed mass, the bed turnover is shown in Figure 7-29. Test CP2 achieved 95% bed turnover after approximately 53 hours of cumulative operating time and 99% bed turnover after 90 hours of operation.

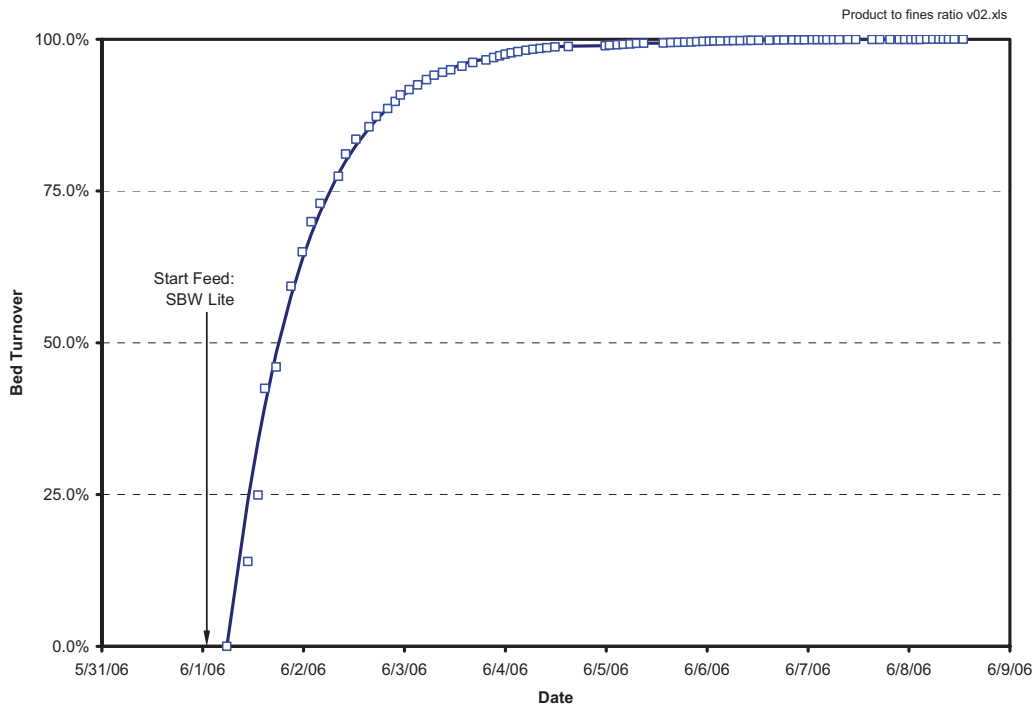

Figure 7-29. DMR bed turnover for Test CP2.

In addition to the solids produced in the DMR, carbon fines and attritted bed material in the CRR elutriate from the bed and are captured in the PBF. The mass of solids captured in the PBF is shown in Figure 7-30. Approximately 588.4 lb of solids were collected from the PBF by the end of the test. The mass rate of solids collected in the PBF ranged from 0.3 to 5.5 lb/hr while the mass rate over the entire run averaged 2.9 lb/hr (Figure 7-31). The PBF mass rate at the end of the test was significantly lower than the rate at the beginning. This was due to the use of a lower bed inventory of carbon in the CRR at the end of the test resulting in higher CRR outlet gas oxygen concentrations and less carbon fines carryover to the PBF.

As shown in Figure 7-26, the density of the DMR bed solids did not change substantially during the run once the bed had reached 95% turnover. Measurements were performed after the end of the test to determine the bulk density of mixtures of PR solids, HTF solids and PBF solids. The results of these measurements are shown in Table 7-20. Based on the relative amounts of solids produced during the CP2 test, the ratio of PR/PBF/HTF solids was 11.85/1.61/1.0.

A linear regression model of the bulk density data was derived based on the data in Table 7-20 (see Figure 7-32). In equation form, this model is

$$Bulk\ Density_{Mixture} = 62.63 + 12.27\left(\frac{PR}{HTF}\right) - 1.345\left(\frac{PR}{HTF}\right)^2 + 0.0403\left(\frac{PR}{HTF}\right)^3 - 74.03\left(\frac{PBF}{PR}\right)$$

where

PR = mass of DMR product solids

HTF = mass of solids captured in the HTF

PBF = mass of solids captured in the PBF.

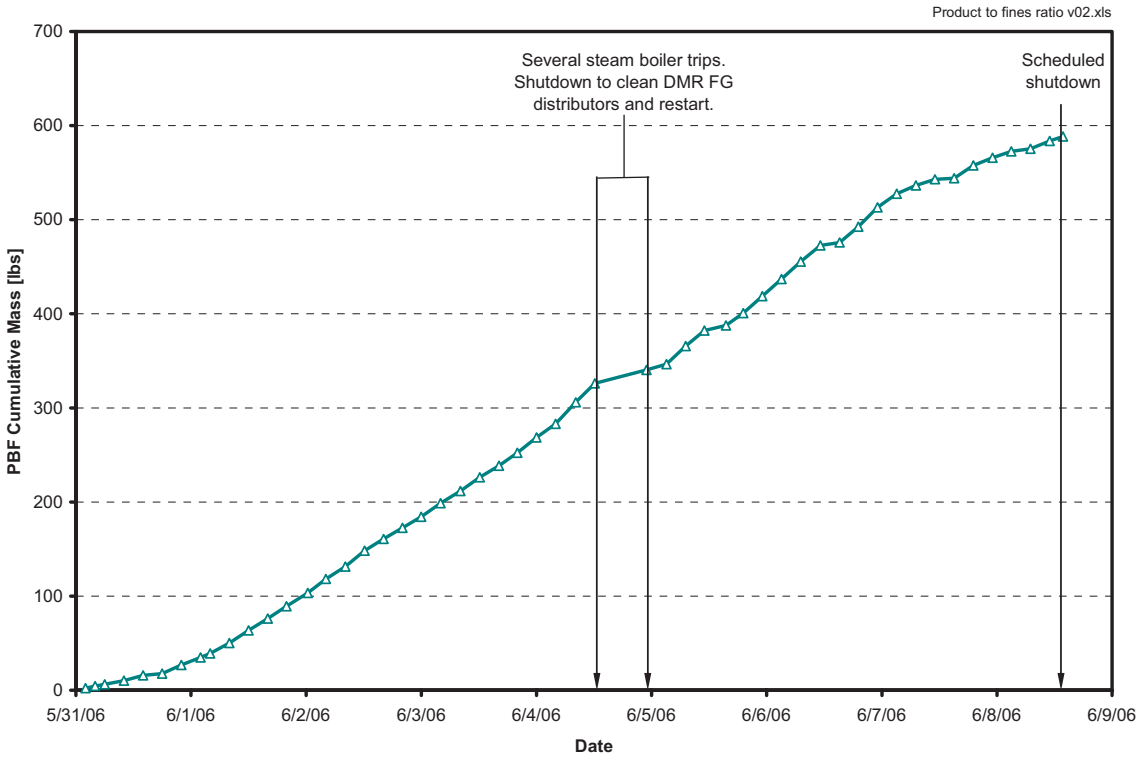

Figure 7-30. Mass of solids elutriated from the CRR and captured in the PBF.

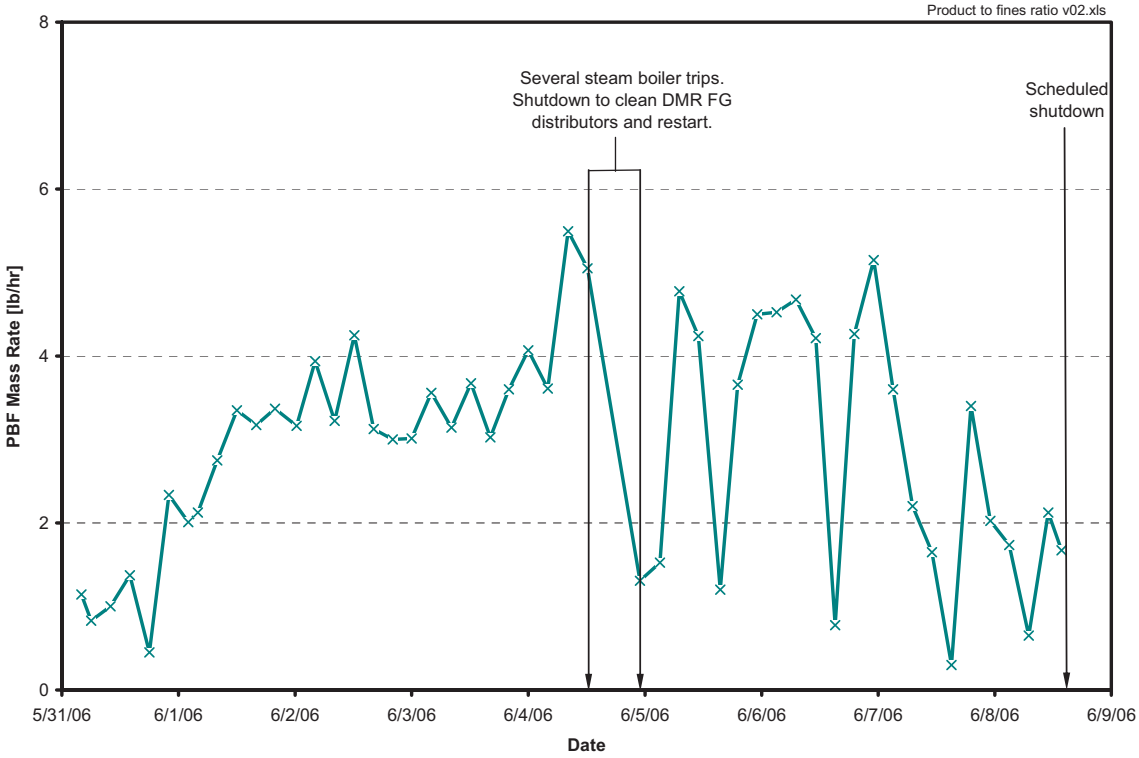

Figure 7-31. Mass rate of solids collected in the PBF during CP2 test.

Table 7-20. Bulk densities of CP2 test solid mixtures.

Sample	S or U[1]	Target Ratio			Actual Ratio			Mixture Bulk Density			
								Loose Packed			
		PR	HTF	PBF	PR	HTF	PBF	g/cm^3	lb/ft^3	g/cm^3	lb/ft^3
1	S	20	1	5	20.00	1	5.00	0.871	54.35	1.177	73.44
2	S	10	1	2.5	10.00	1	2.50	0.875	54.60	1.137	70.95
3	S	5	1	1.25	4.50	1	1.25	0.850	53.04	1.118	69.76
4	S	2	1	0.5	2.00	1	0.50	0.813	50.72	1.029	64.21
5	S	1	1	0.25	1.00	1	0.25	0.759	47.34	1.039	64.85
6	U	25	1	6.25	25.14	1	6.21	0.860	53.66	1.108	69.15
7	U	12.5	1	3.125	12.52	1	3.09	0.870	54.31	1.145	71.47
8	U	6.25	1	1.563	6.25	1	1.54	0.882	55.04	1.179	73.58
9	U	2.5	1	0.625	2.50	1	0.625	0.785	48.97	1.102	68.78
10	U	1.25	1	0.313	1.25	1	0.313	0.760	47.40	1.091	68.10
11	S	20	1	2	20.00	1	2.00	1.106	68.99	1.365	85.17
12	S	10	1	1	10.00	1	1.00	1.122	70.01	1.352	84.35
13	S	5	1	0.5	5.00	1	0.50	1.033	64.48	1.276	79.61
14	S	2	1	0.2	2.00	1	0.20	0.864	53.91	1.189	74.19
15	S	1	1	0.1	1.00	1	0.10	0.760	47.42	1.158	72.26
16	S	20	1	0	20.00	1	0.00	1.324	82.62	1.488	92.83
17	S	10	1	0	10.00	1	0.00	1.300	81.10	1.547	96.54
18	S	5	1	0	5.00	1	0.00	1.201	74.97	1.560	97.36
19	S	2	1	0	2.00	1	0.00	1.047	65.33	1.434	89.49
20	S	1	1	0	1.00	1	0.00	0.878	54.76	1.202	75.02
PBF								0.283	17.66	0.378	23.59
HTF								0.595	37.13	0.763	47.61
PR (S)	S							1.310	81.74	1.440	89.86
PR (U)	U							0.908	56.66	0.955	59.59

Notes:

1. S = screened PR, U = unscreened PR.

All samples obtained: 6/6/2006: PR: 09:40 (S), 01:37 (U), HTF: 07:00, 11:05, 15:05, PBF: 07:05.

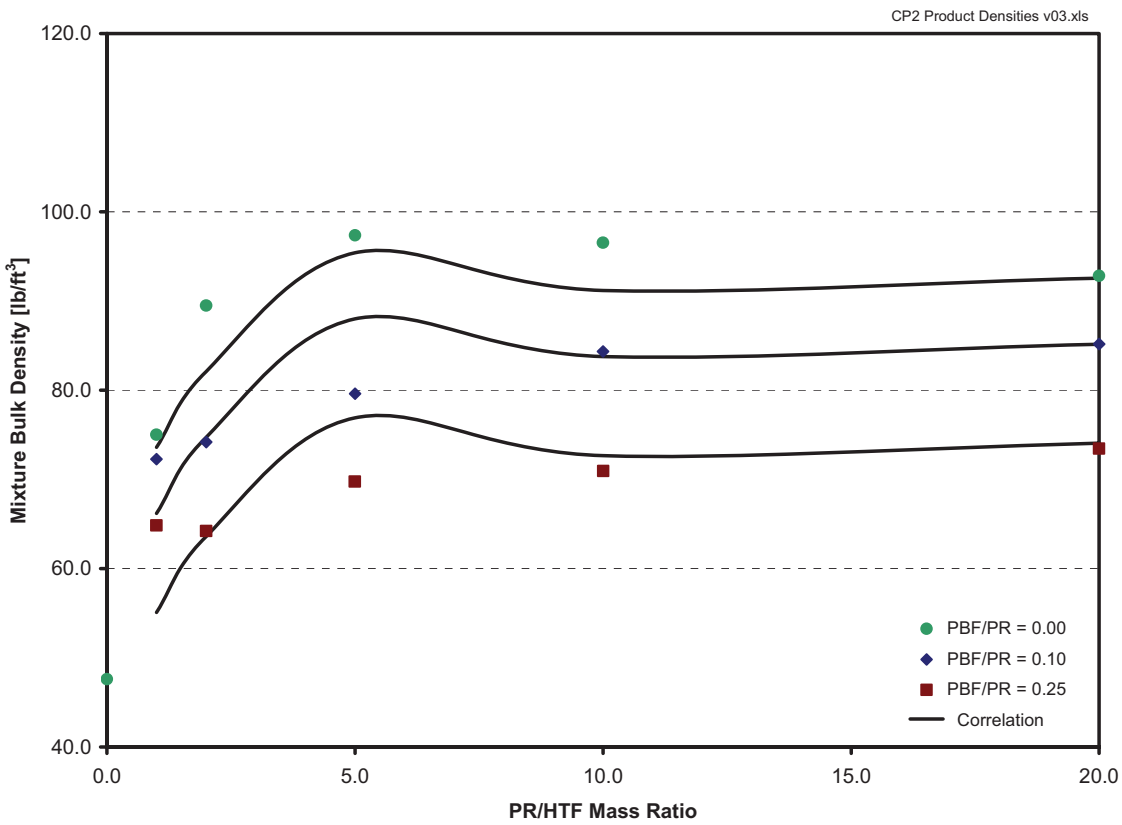

Figure 7-32. Correlation of CP2 solids mixture density with mixing ratios.

The Coefficient of Determination (R2) for this model is 0.783. Using this model for the ratio of solids produced during the CP2 test gives a mixture density of 80.2 lb/ft³. Based on this value, the total volume of the solids produced during the CP2 test would be approximately 65.8 ft³ if mixed together. The total volume of feed processed during the test was 2497.0 gallons = 333.8 ft³. This gives a volume reduction factor of 5.04 ft³ liquid feed per cubic foot of solids produced.

7.5.4 Carbon Reductant Performance

Two different types of carbon reductant were used in the DMR: Berger Brothers P6 wood-based charcoal and GC-CRB coal. The analyses for these two types of carbon are shown in Table 7-21.

In previous work, analyses of the carbon reductants had shown that the Berger Brothers charcoal ash is high in calcium while the GC-CRB calcined coal ash is high in silicon. (See C. M. Jantzen, J. C. Marra, J. M. Pareizs, "Analysis of Raw Materials for Fluidized Bed Steam Reforming [FBSR]," SRNL-ITB-2004-0004, June 30, 2004 [R28].) Neither are favorable compounds to have in a high-temperature fluidized bed, since both are capable of forming low-melting eutectics that can cause the bed to defluidize. However, both the Berger Brothers charcoal and GC-CRB carbon had been shown in previous work to be satisfactory for use in the THOR® process.

As can be seen in Table 7-21, there is significant variation in the amount of ash in the GC-CRB carbon and in the chemical analysis of this ash. In particular, the silicon content of the ash varies from 51.3 to 37.8% on an oxide basis. During the CP2 test, the only source of silicon in the DMR bed product was from the GC-CRB reductant.

Table 7-21. Analysis of GC-CRB Carbon Reductant used in the DMR.

Ultimate Analysis							
Sample Type	BB P6	BB P6	GC-CRB	GC-CRB	GC-CRB	GC-CRB	GC-CRB
Number 1	023	1089	*	1321	1881	2005	2172
Test CP1	CP1		CP1	CP1	CP1	CP2	CP2
Date 12/	12/05	12/17/05		1/11/06	2/14/06	5/16/06	6/4/06
Moisture	4.23 4.	20	7.48	7.80 8.	11	6.20 7.	25
Ash	6.18 6.	67	8.60	9.22 7.	72	5.51 7.	91
Carbon	78.22 76	.89	77.72	77.31 79	.42	85.03 83	.91
Hydrogen	4.57 2.	50	2.04	1.64 1.	35	1.79 1.	11
Nitrogen	0.48 0.	48	1.01	0.88 0.	72	0.86 0.	76
Oxygen (by difference)	6.30 9.	24	2.97	2.97 2.	31	0.21	<0.01
Sulfur	0.02 0.	02	0.18	0.18 0.	37	0.40 0.	40
Ash elemental analysis, weight % oxide basis							
Sample Type	BB P6	BB P6	GC-CRB	GC-CRB	GC-CRB	GC-CRB	GC-CRB
Number	1023	1089 *	1	321	1881	2005	2172
Al_2O_3	0.70%	1.20% 11	.82% 15	.96%	14.86%		
CaO 77	.50%	65.90%	18.80%	12.30%	23.40%		
Fe_2O_3 0.	66%	1.50%	11.22%	6.89%	6.70%		
K_2O 4.	12%	4.62%	0.85%	2.15%	0.56%		
MgO 2.	32%	1.82%	2.70%	2.50%	1.23%		
Na_2O 0.	54%	0.41%	0.69%	0.96%	0.94%		
P_2O_5 1.	19%	1.06%	0.28%	0.65%	0.20%		
SO_3 0.	56%	0.60%	11.10%	5.34%	11.40%		
SiO_2 6.	28%	15.82%	39.32%	51.29%	37.81%		
TiO_2 <0.	01%	<0.01%	0.59%	0.60%	0.64%		
Total 93	.87%	92.93%	97.37%	98.64%	97.74%		

The experience gained from the completed scoping and production tests showed that the GC CRB calcined coal was a better reductant than the Berger Brothers charcoal. The calcium in the charcoal formed compounds in the bed that tended to cause the bed to defluidize. Even when the SBW feed contained UDS, which had a high percentage of kaolin (as during Tests P-4A-5 and P4A-6), the calcium compounds appeared to cause defluidization.

The Berger Brothers P6 charcoal was more reactive than the GC-CRB calcined coal and was used during startup to heat the bed until it was hot enough for the coal-based carbon to react; the higher reactivity also caused the carbon usage for the charcoal to be less than the coal. Another advantage was that the charcoal contained slightly less sulfur than the GC-CRB coal. But these advantages did not

outweigh the greater disadvantage that the charcoal tended to make the DMR bed defluidize because of high calcium content in the ash. The Berger Brothers P6 charcoal appears to be an excellent material for process startup and heating to operating temperature, but not as the normal carbon reductant.

The carbon used in the CRR was Superior Graphite Desulco 9005 desulfurized petroleum coke. This material was 99.99% carbon, 0.01% ash and 0.009% sulfur [R29]. This material worked very well in the CRR, although it would not start reacting until the bed temperature was at least 550°C. As in the DMR, Berger Brothers P6 charcoal coal was used for startup heating until the bed was capable of sustaining the reaction with Desulco.

7.5.5 Temperature Control of the DMR and the CRR

In the original design basis [R30] for the ESTD, control of the bed temperature in the DMR was to be accomplished by controlling the amount of air in the feed atomizing gas and using a small (2–5 vol%) amount of oxygen in the fluidizing gas. The initial MEB for the project, however, underestimated the heat losses from the DMR. Because of this, the temperature control method originally specified in the design basis was not adequate and had to be changed during the CP1 tests. Instead of using a small baseline oxygen flow, the bulk of the oxygen needed to provide the temperature control in the DMR was supplied in the fluidizing gas and the atomizing gas was changed to 100% air. Performing this change meant that, during the CP1 test, the fraction of oxygen in the fluidizing gas could be as high as 70%, although generally it was in the 15–30% range. These changes required a larger flow indicator/controller for the FG oxygen; however, because the flow controller for the feed atomizing nitrogen was no longer needed, it was possible to reuse this flow indicator/controller for the FG oxygen flow rate.

Using the FG oxygen flow rate to control the DMR bed temperature proved very successful, with the temperature generally controlled within ± 5°C of the desired setpoint. The exception to this was when the DMR bed temperature was low (600°C) and the liquid feedrate was high (0.35 gpm). At these conditions, automatic control of the bed temperature resulted in unacceptable oscillations in the oxygen flow rate, and required the operators to run the oxygen manually which resulted in wider DMR bed temperature variations. A change in the DMR fluidizing gas flow control scheme was made for the CP2 test.

The steam flow rate was held constant during the CP2 test while the oxygen was varied to control the bed temperature. This resulted in less variation of the oxygen concentration in the fluidizing gas and did not significantly affect the SSV in the bottom part of the DMR bed. This control method was very successful in maintaining a constant bed temperature in the DMR. The only problem that occurred using this method was when the steam boiler tripped and caused the steam flow rate to drop to zero.

The original CRR bed temperature control method used during CP1 was to vary the carbon feed rate as needed to control bed temperature. Because there was about a 20 minute lag between the time when carbon was fed to the CRR and when a change in the CRR bed temperature was observed, this method resulted in the CRR bed temperature control being ± 50 to 100°C of the desired setpoint. The operation of the CRR during CP1 was modified to the same method of temperature control used in the DMR, i.e., use the in-bed oxygen flow rate to control the bed temperature. At the same time, the above-bed oxygen flow was used to control the CRR outlet off-gas oxygen concentration. Both of these flow rates were controlled automatically. The carbon feed rate was controlled manually at a fixed rate that maintained a constant bed height in the CRR. Using this control method, the CRR bed temperature was controlled generally within ± 10°C of the desired setpoint. This same control scheme was used during the CP2 test, although the in-bed oxygen injection locations were varied during the test (see below).

There were occasions when the CRR bed temperature could not be controlled using the in-bed oxygen flow alone. During these periods, it was necessary to use cooling water to control the CRR bed temperature. The response to the cooling water was rapid, and very low water flow rates (~100–200 ml/min) were usually sufficient to control the bed temperature. The one problem that was experienced with this cooling system during CP1 was that the rotameter valve would not close completely. A block valve was installed to prevent inadvertent addition of cooling water to the CRR, but on at least one occasion the block valve was left open (during Test P-4A-6), and may have contributed to a defluidization of the CRR. The cooling water rotameter was oversized, which made control of the water flow rate difficult; however, because the rotameter was seldom used, this did not seem to be a major problem for the process.

The CRR temperature control was modified for CP2 testing by adding two additional levels of ATG nozzles and flow ratio controllers for O_2 and N_2 control. It was intended to confirm CO, THC, and NO_X emission levels that could be permitted for the IWTU. These changes were also intended to reduce temperature variations in the CRR that caused formation of small agglomerates during previous operations.

An extensive test sequence matrix was developed to meet this test objective. The test sequence was modified as testing progressed to take advantage of information gained during the testing. The test sequence matrix is shown in Table 5-5.

Figure 7-33 shows the bed temperature and outlet O_2 concentration in the CRR for the CP2 test with the various test conditions indicated. During the first part of the test, the outlet O_2 concentration of at least 4% (wet basis) could not be achieved. This was primarily due to the high carbon concentration in the bed which reacted with the oxygen even when the bed level was below the upper ATG nozzle. This also made bed temperature control difficult. The operation of the CRR evolved during the test as more experience was gained. By the end of the test the CRR operation was much smoother than at the beginning. The optimum operating mode used a bed depth of 35–37 inches, a low carbon concentration in the bed (enabling more excess O_2 while still maintaining bed temperature control), the middle and upper ATG nozzles on automatic control, and only purge gas flow in the lower ATG nozzles. This achieved a typical outlet oxygen concentration of 2–4% (wet basis).

Figure 7-34 shows the CO and THC stack gas concentrations along with the CRR outlet O_2 concentration during the test. Higher stack CO and slightly higher stack THC levels occurred when the CRR outlet O_2 concentration was below the 4% (wet basis) target value. Both the THC and CO concentrations were inversely proportional to the CRR outlet oxygen concentration. Thus, the best way to reduce THC and CO emissions was to maintain a higher CRR outlet O_2 concentration. The CO and THC concentrations also were related to the amount of carbon in the CRR bed. During the last CRR test conditions when the bed carbon inventory was low, the CO and THC concentrations were lower than what had been observed for the previous test conditions.

In automatic mode, ratio controllers were used to set the flow rate of N_2 to the CRR ATG nozzles, using the O_2 flow as the process variable. Once tuned, the nitrogen ratio controllers seemed to function well. During the CRR tests, however, it was seen that the amount of O_2 required to meet the desired above-bed O_2 concentration was frequently beyond the full-scale range of the O_2 meter for the upper ATG nozzle, FT-300-016. When this occurred, the N_2 was controlled using the full-scale reading of FT-300-016 instead of the true amount of O_2 being fed. This issue can be eliminated by installing a flowmeter with a wider range for the O_2 flow.

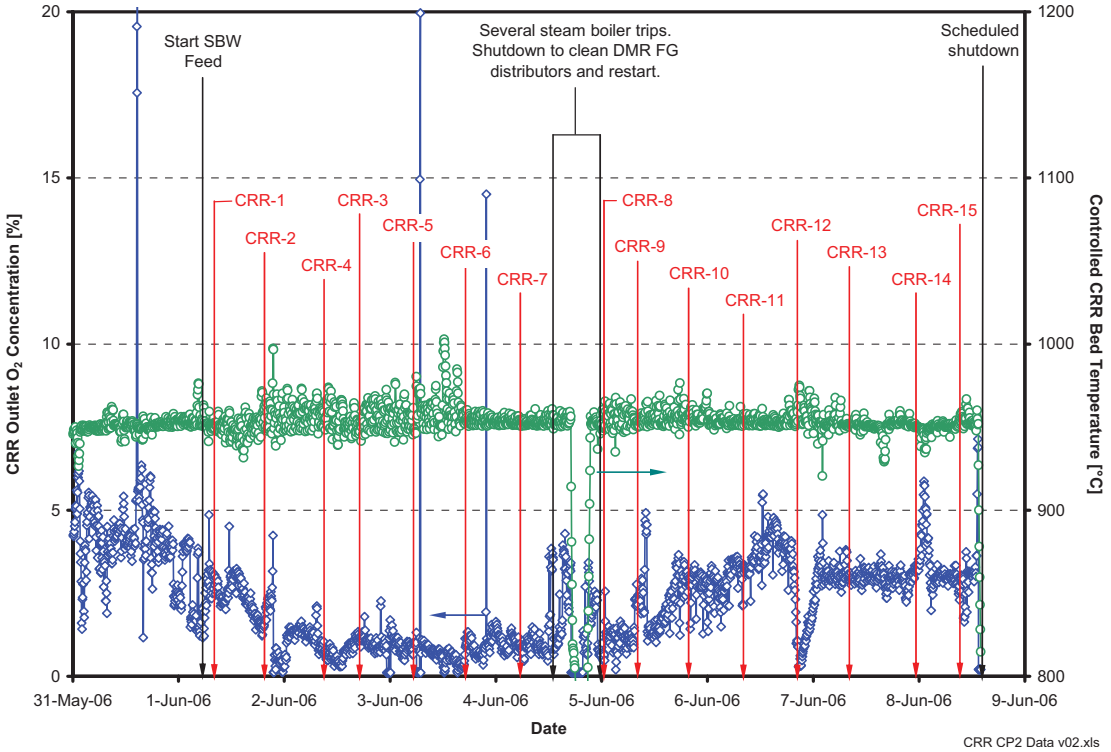

Figure 7-33. CRR outlet O_2 concentration and bed temperature during CP2 test.

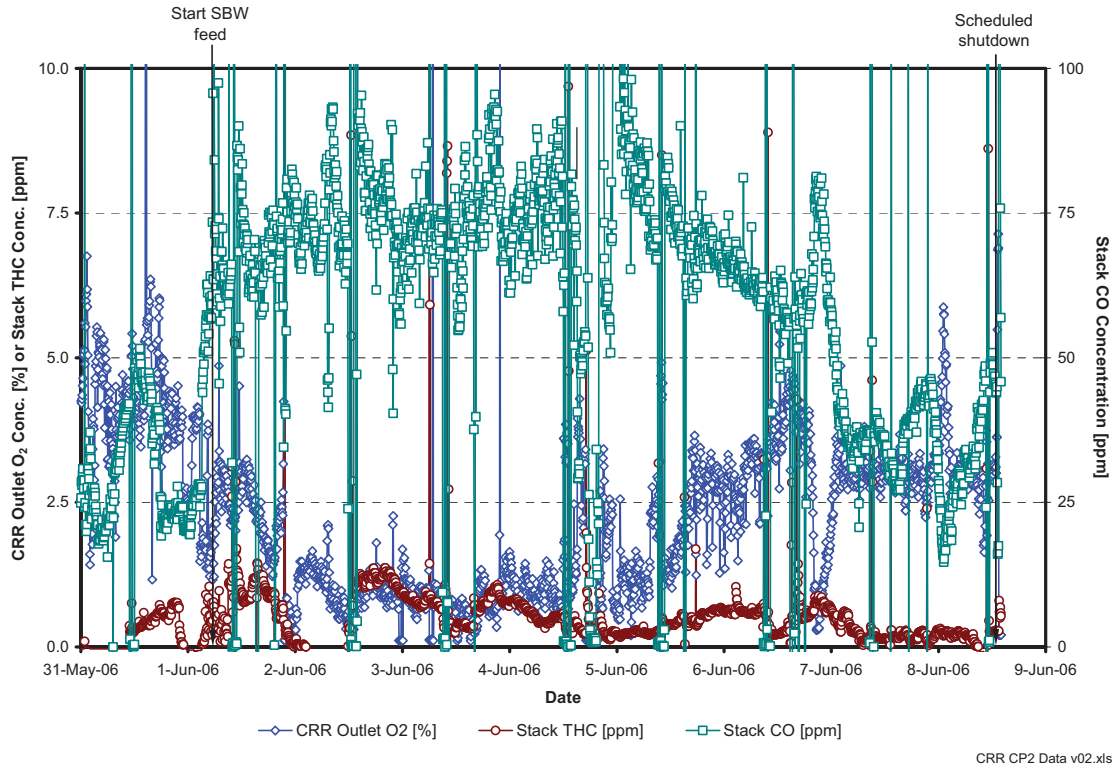

Figure 7-34. CRR outlet oxygen, stack THC, and CO concentrations during the CP2 test.

Modifications were made so that the CRR temperature control loop, TIC 300, would not be too reactive to major temperature upsets. Attempts to rate-limit the PID control signal were not very successful because the system would take too long to recover from a major temperature upset (such as a bed drain) and would produce exaggerated overshoot. It was found that a lead/lag term helped to control the CRR temperature much more acceptably than in previous testing.

7.5.6 System Pressure Control and Performance

System pressure control was provided by three off-gas blowers (B-404, B-407 and B-409). Blowers B-404 and B-409 were the primary off-gas blowers and both were used during the entire testing program. Blower B-407 was used to increase the system pressure drop when GAC bed was online or when higher pressure drop was desired in the system than could be provided by B 404 and B-409 alone.

The blowers were designed to operate with automatic pressure control; however, due to work priorities, the control loops were never tuned for the CP1 test. In all of the CP1 runs they were operated in manual. Since the off-gas flows were generally very stable, this resulted in stable pressure control also. The blowers were each capable of providing 20-in. WC pressure rise at 1000 acfm. Generally, they were operated to give 5–10-in. WC pressure rise. Operation of the blowers was satisfactory during all the tests, as exemplified by the data in the time period shown in Figure 7-35.

For the CP2 test, the blowers were tuned and were operated in automatic control mode. The automatically controlled pressure rise across the blowers was very smooth for the CP2 test (see Figure 7-36).

7.5.7 Filter (HTF and PBF) Performance

The two process filters operated very well during the CP1 and CP2 tests. The HTF initially had some plugging due to the large quantity of fine sodium carbonate particles that elutriated from the DMR due to excessive particle grinding action in the DMR during the first start-up operations. Repetitive on-line and off-line gas pulse backs cleared the elements. No additional caking problems were noted in the HTF for the duration of the test program, which appeared to operate reliably with only on-line pulse back cleaning.

The PBF had a few problems with condensation in the fines collection container attached to the bottom of the filter cone early on in the tests. However, once the PBF drain purge was configured to flow dry nitrogen through the container and the filter heaters were maintained on line, these condensation problems were eliminated. After these modifications, the PBF worked flawlessly.

After the CP1 test was complete, the HTF filter was disassembled to examine the filter internals and filter elements to determine how they performed during the test. The ceramic seals, venturi block, and pulse cleaning system all worked well. During visual inspection at the end of the test, one filter element had a blistered cover and one had some radial cracking. Previous inspections of the CRR inlet piping on December 30, 2005, showed that solids were passing through the HTF. The post-test inspection on February 12, 2006, revealed a layer of fine particulate almost 1 inch thick on top of the HTF filter holddown block and tubesheet indicating that one of more of the filter elements had failed or had been losing efficiency and allowing some fine solids to bypass the filter. During maintenance activities after the end of the CP1 test, all of the HTF filters were determined to have suffered failure (see Figure 7-37). This failure was the most likely reason for the large amount of solids found on top of the holddown block at the end of the CP1 test. The filter elements used during the CP1 test were of the sintered metal fiber type. This type of filter element has a lower permanent pressure drop, than sintered powder filter elements, but the post test examination showed that they were not suitable for use in this application.

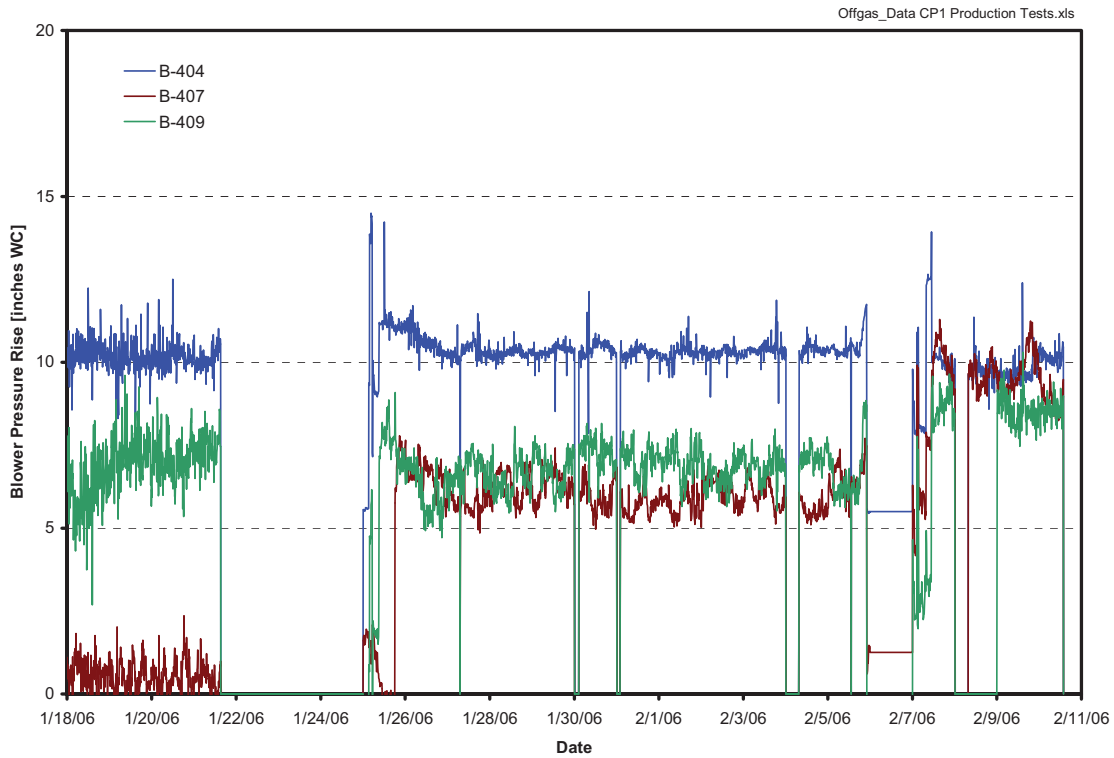

Figure 7-35. Pressure rise on off-gas blowers during the CP1 test.

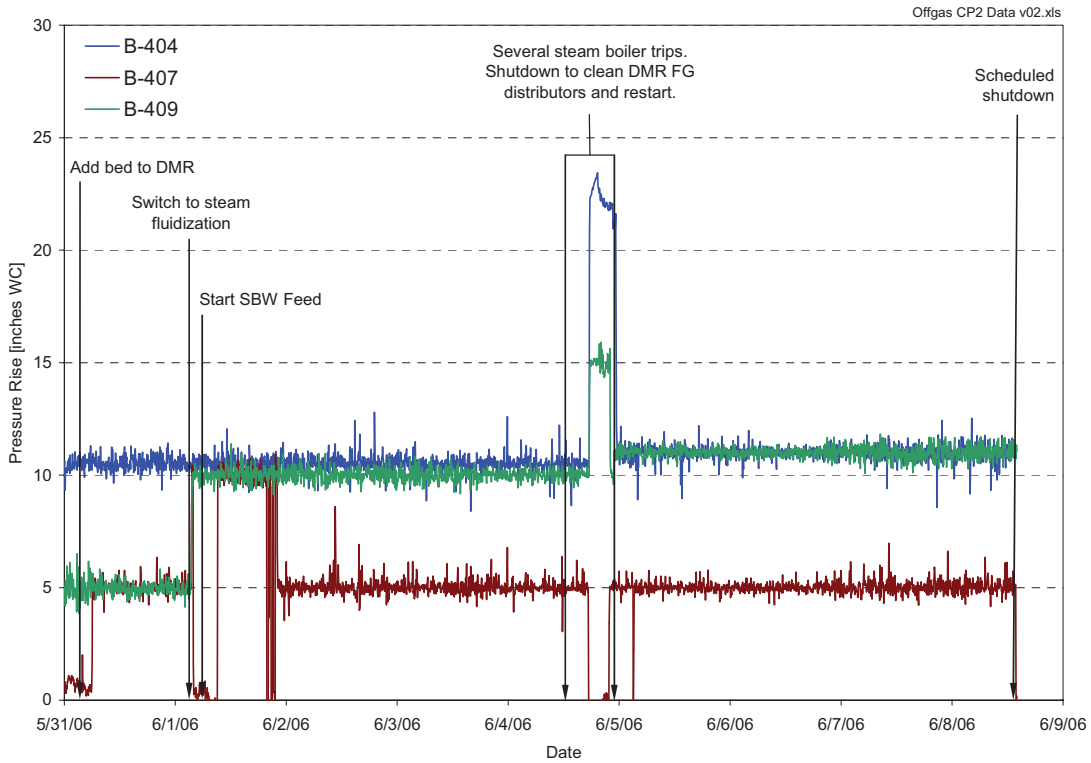

Figure 7-36. Pressure rise on the gas blowers during the CP2 test.

Figure 7-37. Damaged HTF filters at the end of the CP1 test.

For the CP2 test, all of the HTF filter elements were replaced: 14 with sintered metal powder filters and 4 with alumina-coated silicon carbide similar to the type used at the Studsvik® treatment facility in Erwin, TN. Two different metal alloys were used for the sintered metal powder elements: 316L stainless steel and Hastelloy. Although these elements have higher pressure drop than the sintered metal fiber elements used in CP1, they are also more robust. These filters performed very well during the CP2 test. No solids were observed on top of the filter holddown block as had been observed at the end of the CP1 test. The permanent pressure drop across the filters increased during the CP2 test, but eventually leveled out at about 20-in. WC (see Figure 7-38).

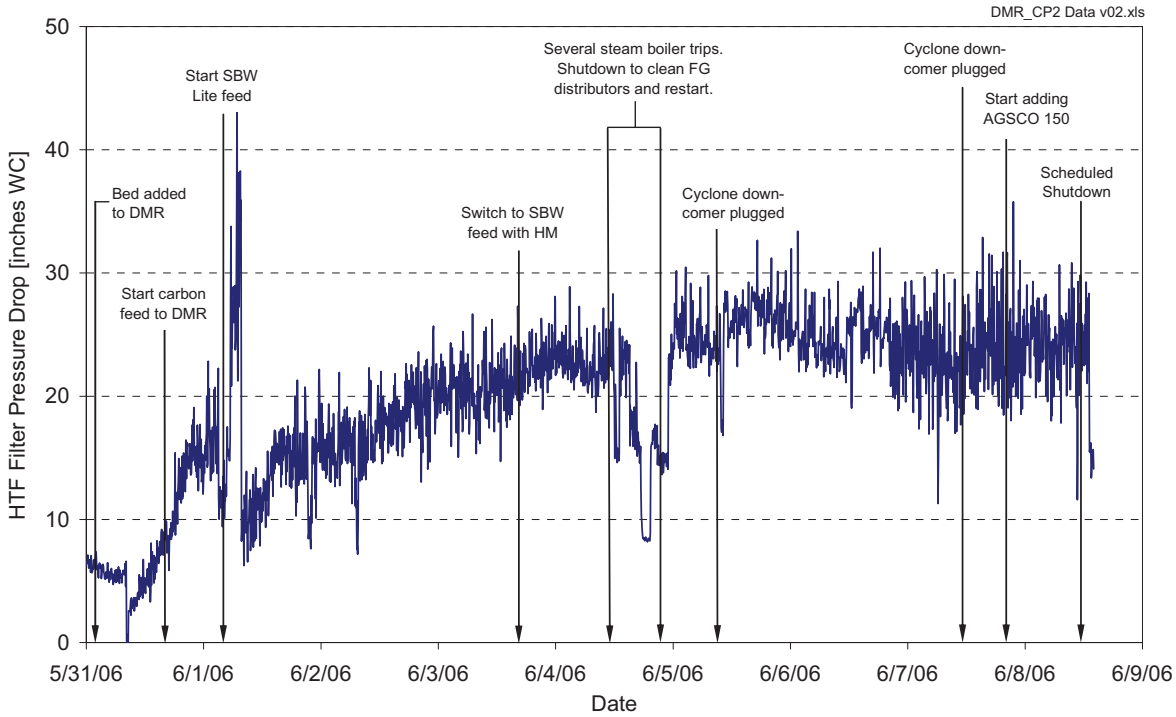

Figure 7-38. HTF pressure drop during the CP2 test.

7.5.8 Data Acquisition and Control System Performance

The Data Acquisition and Control System (DACS) performance for the SBW Pilot Plant process was frequently modified and refined as a result of troubleshooting during the functional and scoping test runs. This is typical of pilot plant scoping operations, as changes and modifications to the physical system and process are ongoing. Because of these constant modifications, the DACS was not as reliable in the scoping tests as it was for the production testing. This section documents the performance of the DACS when it was at its final stage during the production test runs, summarizing the following five key performance items:

- Automated control loops
- Modifying DACS configuration files and logic
- DACS error handling
- DMR shot pot valve instability
- DACS Citadel Database file size.

7.5.8.1 Automated Control Loops. Control loops in the context of this pilot plant testing are defined as device-sensor process loops, where the device controls a process parameter, which is measured by a sensor, based on a desired set point entered at the HMI by an operator. A device is a mechanism for controlling process parameters, such as a valve or pump. A sensor is an instrument for measuring process parameters, such as a thermocouple or pressure transducer.

There were approximately 25 control loops that could be automatically or manually controlled from the HMI. Nearly 20 of these control loops were typically set in automatic mode. Each of these loops required some amount of "tuning," that is, setting the control parameters such that the device controlled the process parameter very near the set point, even when a minor upset in the process occurred. A couple of these loops were difficult to tune and required more advanced control parameters than the others. One such control loop was the CRR temperature control. The temperature, which was controlled by oxygen flow into the CRR bed, was relatively slow to react to the oxygen injection. This made the loop difficult to fine tune with standard control parameters; therefore, advanced control parameters were added. With the additional tuning capability, this particular loop controlled quite well. One other loop seemed susceptible to a certain change in process parameters. This was the DMR temperature control. The DMR temperature control typically controlled extremely well; however, towards the end of CP1 production tests when liquid feed rate was increased to 0.3–0.35 gpm, and the DMR bed was drained below a certain height, the control would start to oscillate. At lower liquid feed rates (typically 0.25 gpm) the controller did not have any problems during bed drains or any other disturbances in the process.

During CP2 testing, it was determined that the CRR startup burner was affecting other thermocouples on the controller that it was plugged into. This is believed to be due to a grounding problem through the dual head element of the thermocouple for the startup burner, TT-300-009. This issue was resolved by unplugging TT-300-009 from the startup burner control unit and seeing that the other thermocouples on the 202 Temperature Module were working properly.

7.5.8.2 Modifying DACS Configuration Files and Logic. During early scoping tests, there were occasional problems associated with the frequent changing and updating of the DACS configuration files and logic while running a test. Because of these issues, the architecture of the DACS was modified, which greatly improved the reliability of the system, even when changes were made to the configuration files or logic. It was, however, still considered best not to modify the DACS system during production testing if at all possible.

Every attempt was made to not modify the DACS system during CP2 testing by the following steps that were taken:

- The programs running on the Fieldpoint network modules were modified to not stop on error.
- Frequent changing of the DACS configuration files and logic during a test was avoided as much as possible.
- Visiting any of the Fieldpoint controllers within the LabView user interface was avoided if at all possible.

These practices helped to make the system more stable than it had been in previous testing.

During CP1 and CP2 testing, it was noticed that the LabView software could begin developing problems after running for very long periods of time. This is quite common for virtually any program being run in a Microsoft Windows operating system. For longer periods of testing, it might be necessary to perform routine maintenance activities on the DACS every ten to fourteen days. Such maintenance activities would consist of systematically archiving databases, rebooting computers, and rebooting controllers to keep the DACS system stable.

7.5.8.3 DACS Error Handling. Another issue addressed during scoping tests was error handling in the DACS logic. During CP1, the error handling initially was not as robust as it should have been. This was evident when some of the real-time programs (logic) would stop running because of an error while

reading or writing the required data. The error would have to be manually cleared and the real-time program restarted. Depending on the real-time program, this could result in a significant disturbance to the process. During CP1 testing, much of the error handling was modified, which greatly improved the overall performance of the system. Given more time, however, error handling would be a high priority in working towards a highly reliable system.

During CP2 testing, there was one major network disruption where the entire 201 Controller was offline for approximately one minute during testing. A stop-on-error condition in the programming caused one of the real-time programs to shut down, leaving the steam valve open at the last known setting. This was resolved by removing the corresponding stop-on-error condition from the programming, and for the remainder of the testing this event did not repeat itself. The cause of the disruption is not yet understood, but it is believed to be a network issue rather than an issue with the programming or the hardware.

7.5.8.4 DMR Shot Pot Valves Instability. One performance issue that was evident during CP1 testing was a minor instability in the DMR carbon feed interlocked airlock valves. Once every day or two, and sometimes more frequently, the upper and lower shot pot valves would be open at the same time just for an instant. This literally defied logic because each valve was interlocked with the other valve's closed limit switch. According to the logic, the upper shot pot valve could not be open unless the lower shot pot valve was closed and vice versa. After extensive investigations into the logic, it was determined the problem might have been with the physical Fieldpoint I/O hardware, but this could not be tested during production runs without significantly upsetting the system.

In preparations for CP2 testing, system improvements were made in the operation of the DMR and CRR shotpots. After extensive investigation, the DMR/CRR shotpot programming was altered to be more robust and to handle network disruptions. In addition, the relays were stepped down from 120 VAC to 24 VDC as this was determined to be the cause of network disruptions knocking the control modules offline. During CP2 testing, the shot pots performed well and exhibited no misfiring from the DCS. The few times that puffing was observed from the shot pots, it was due to the vent plugging up with carbon dust.

7.5.8.5 DACS Citadel Database File Size. The final key performance item in this section relates to the file size of the DACS Citadel Database. When the Citadel Database grew to 500+ MB the control personal computers would begin to slow down noticeably. This slowdown was especially evident when navigating between HMI Trend Screens. The trends acquired their data from the database, so trend problems were typically a warning that the database was growing to large. The course of action was to archive all databases soon after they exceeded 400 MB. The database file size was routinely monitored and archived when necessary to avoid this issue.

In preparation for CP2 testing, daily data downloading, archiving, and charting functionality was developed so that it was possible to receive and archive data on a daily basis. In addition, nitrate destruction calculations were run as a stand-alone HMI on each of the database computers. The results of these nitrate destruction calculations were logged into the database in real-time along with the measured data.

7.6 Product Solids Composition Data

Solid products were collected from the PR, the HTF, and the PBF in both the CP1 and CP2 tests. Accumulated DMR bed product solids were routinely transferred to the PR to maintain an acceptable DMR operating bed level. Smaller diameter material (fines) were elutriated from the DMR and collected in the HTF. The cyclone recycled intermediate sized particles internally in the DMR to help minimize carryover of fines to the HTF. Material collected by the PBF consisted of fines that elutriated from the CRR bed.

7.6.1 DMR/PR Bed Product

The properties of the material collected in the PR in both the CP1 and CP2 test were essentially the same as those of DMR bed samples, except with reduced carbon content. In both tests, the starting DMR bed material was white aluminum oxide supplied by AGSCO Corp. The particle specific gravity of AGSCO alumina was 3.95 g/cm^3, and the loose pack bulk density was 1.87 g/cm^3. The material appeared white as a bulk material to the naked eye, but appeared translucent when viewed at ~20–30x under a microscope (see Figure 7-39). The individual particles were angular in nature, and resembled broken pieces of glass. Two different sizes of alumina particles were mixed to serve as the start-up bed in the DMR – AGSCO 80 (with an average particle size of 165 microns) and AGSCO 46 (with an average particle size of 356 microns) were mixed on a 50/50 weight basis. The average particle size of the mixture was approximately 250 microns.

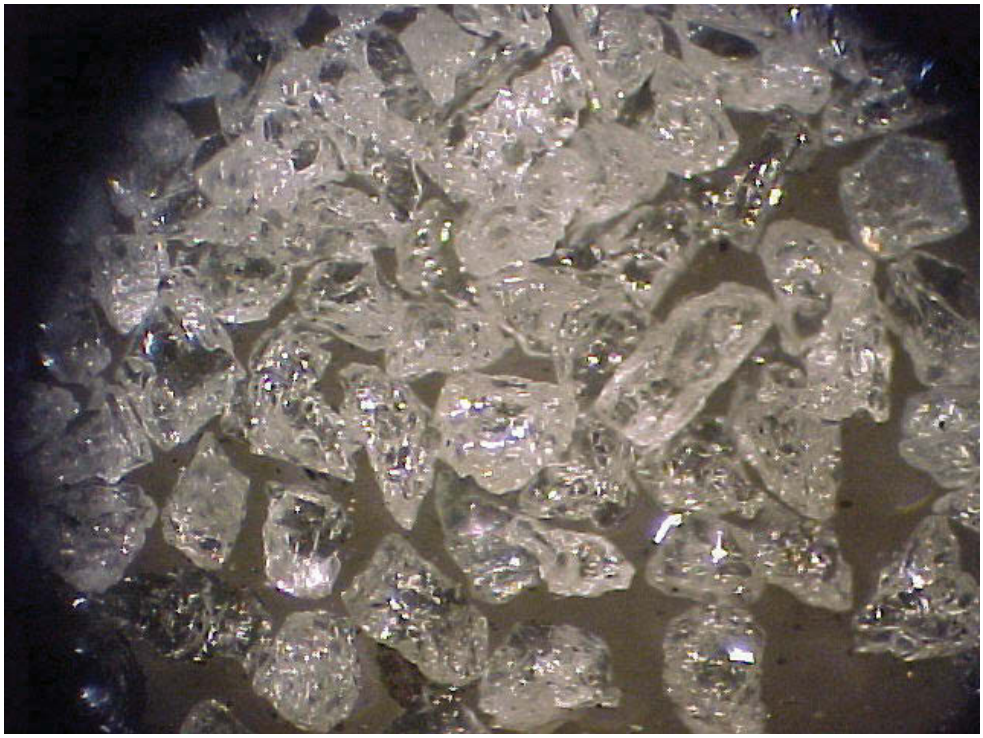

Figure 7-39. Micrograph of AGSCO alumina used as DMR starting bed.

As the test program progressed, the appearance of the solid DMR and PR product changed due to deposition of solids from the feed. The color of the material changed from clear white to brown or dark tan and the particle shape changed to spheroidal with small spheroidal inclusions, or lumps (see Figure 7-40 and Figure 7-41). The appearance of the DMR product was similar to particles produced from previous testing at the STAR center. [R8]. In addition to the solids produced by feed deposition on the bed particles, the DMR and PR samples also contained carbon particles from the solid reductant added to the DMR vessel.

Figure 7-40. Micrograph of DMR solids produced during CP1 test P-4A-4 on February 2, 2006.

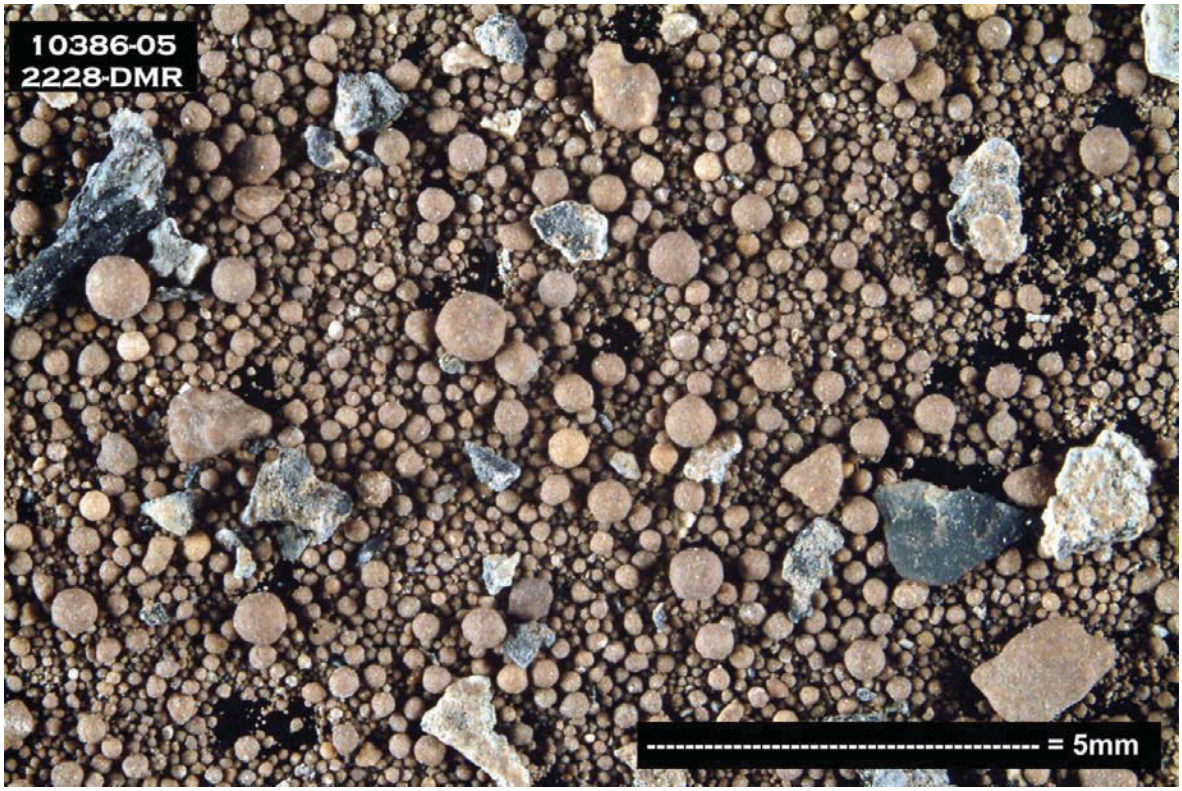

Figure 7-41. Micrograph of DMR solids produced during the CP2 test on 6/5/06.

7.6.1.1 CP1 Test Solids Analysis. Samples from the CP1 DMR bed and PR solids were submitted for chemical analysis. The results of these analyses are shown in Figure 7-42. This figure shows the evolution of the solids elemental composition as a function of time during the CP1 test. The oxygen content of the solids was estimated from a charge balance on the individual samples. The original analyses also included total carbon in the samples. The values shown in Table 7-22 have been renormalized on a carbon free basis.

Figure 7-42 shows that the sodium content of the DMR solids peaked during CP1 test P-2 and then declined as UDS, HM, and minor constituents were added to the feed. The nitrates in the solid product averaged 0.19%, however, the average for the last six production tests (P-4A-1 through P-6) was approximately 0.012%. The aluminum content of the solids was relatively constant over time. The silicon and phosphate content of the solids increased steadily after the addition of UDS to the feed started during test P-3. In general, the solids analysis tracks the composition of the SBW feed during test CP1 as expected.

The average composition of the solids produced during the CP1 test is shown in Table 7-22 compared to the theoretical composition from a thermodynamic computation performed with HSC Chemistry 5.11. (See "Outokumpu HSC Chemistry® for Windows," Chemical reaction and equilibrium software with extensive thermochemical database, version 5.11, copyright © 1974–2002 by Outokumpu Reasearch Oy, 2002 [R31].) A comparison of the measured composition to the theoretical values based on thermodynamic equilibrium can give an estimate of the relative importance of reaction rate kinetic limitations on the process.

The measured values show fair agreement between the P-4A test compositions with the theoretical values for the same time period, showing that the reactions in the DMR are not kinetically limited. The major differences between the measured and calculated values are for carbonate, sodium, oxygen and phosphate. Phosphate, oxygen, and sulfate are higher than expected while carbonate is much lower than expected. Since oxygen is calculated from a charge balance, a low carbonate value would naturally give a higher oxygen value.

There are several reasons for the differences between the measured and theoretical values. The theoretical values are based on the target feed makeup concentrations shown in Table 4-6; not the actual measured feed composition. Additionally, the theoretical values are all calculated for operations at 640°C while actual temperatures in the DMR ranged from 600 to 670°C. Perhaps most importantly, the calculations were based on an average hydrogen concentration of 1% (wet basis) in the process gas. The actual hydrogen concentration ranged from approximately 0.2 to 1.5% during the CP1 P-4A production tests. It also is probable that the variation in the GC-CRB reductant composition resulted in some of the observed variation in the sulfate solids composition since the calculations were based on an average reductant composition.

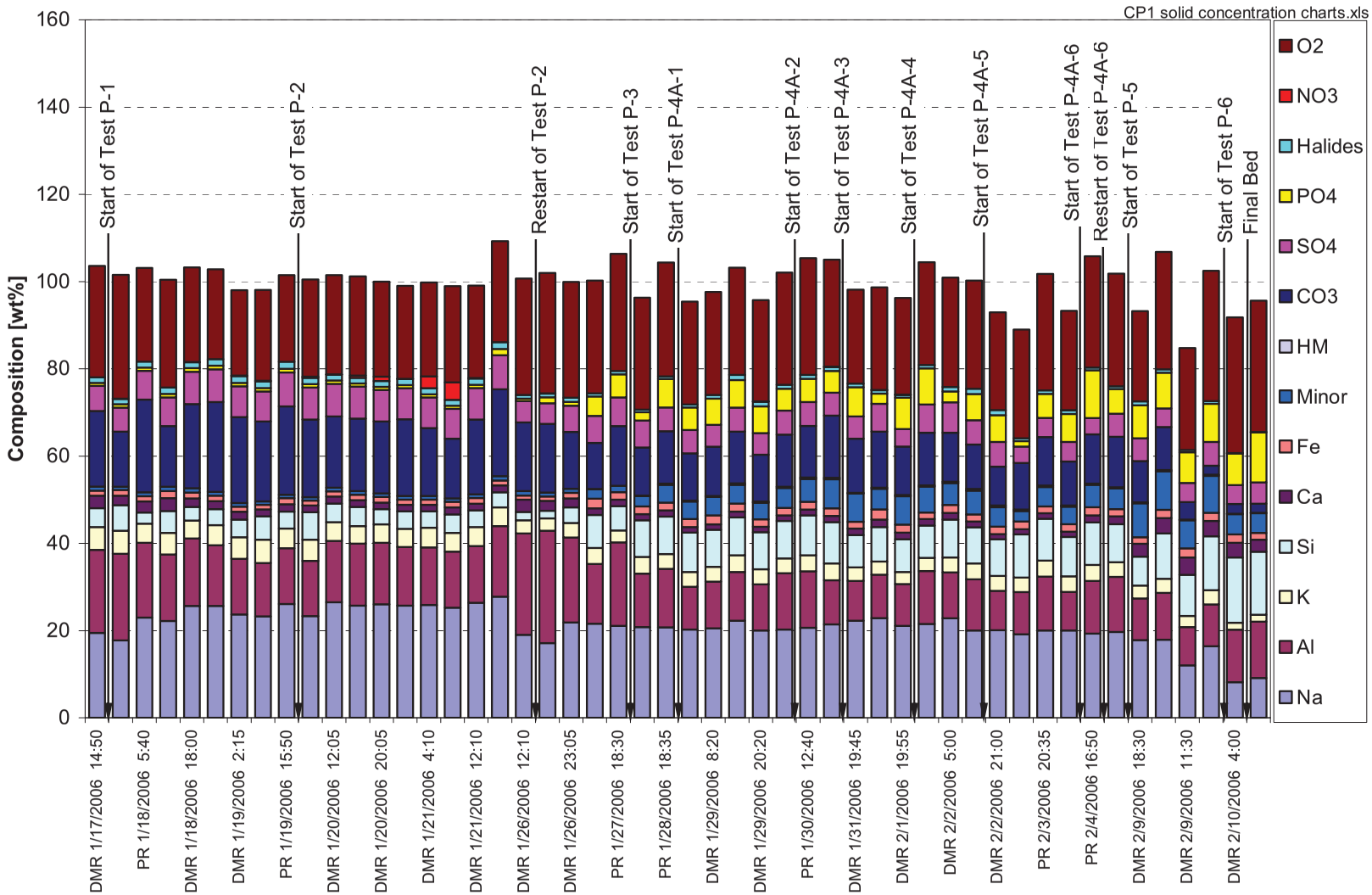

Figure 7-42. Solids Analysis for CP1 test DMR and PR samples.

The Minor series includes the minor metal constituents: B, Ce, Cs, Mg, Mn, Ni, Zn, and Zr. The HM series includes the RCRA heavy metals: As, Cr, Hg, and Pb. The Halides series includes the Cl and F.

Table 7-22. Average composition of solids produced during the CP1 test.

Component	Average Composition (wt%)		
	Entire Test	P-4A-1 through P-4A-6	Theoretical (HSC Chemistry)
Al 13	.17	10.83	11.63
Ca 1.	857	1.392	1.301
CO_3 13	.04	11.38	21.88
Fe 1.	556	1.781	0.556
HM 0.	146	0.297	0.187
K 3.	704	3.419	3.558
Minor 3.	219	4.842	4.191
Na 21	.14	20.75	23.14
Si 6.	910	8.650	8.647
Halides 1.	004	0.867	0.867
NO_3 0.	191	0.015	0.000
O_2 24	.20	24.26	17.99
PO_4 3.	864	5.672	2.556
SO_4 5.	885	5.211	3.500

HSC DMR Products CP1.xls

7.6.1.2 CP2 Test Solids Analysis. Samples from the CP2 DMR bed and PR solids also were submitted for chemical analysis; the results of these analyses are shown in Figure 7-43. The oxygen content of the solids was estimated from a charge balance on the individual samples. The original analyses also included total carbon in the samples. The values shown in Table 7-23 have been renormalized on a carbon-free basis.

The DMR product that was removed from the product receiver during the CP2 Test was screened to remove oversize particles (primarily carbon). The screen size that was used to make this separation was 12 mesh (1,680 microns). The average carbon content of the unscreened solids removed from the PR was 24.6 wt% while the average carbon content in screened product was 10.2 wt%.

Figure 7-43 clearly shows the transition from an alumina starting bed to a sodium carbonate bed. After the bed reached greater than 95% turnover on June 3, 2006, the composition remained relatively constant until the AGSCO seed particles were added on June 7, 2006. There were essentially no nitrates in the solids, with the nitrate content of the solids averaging less than 0.02% over the entire test. The sum of the component mass fractions for most of the samples range between 105–115%, especially for those later in the test after bed turnover reached >95%.

Table 7-23 shows the average composition of solids produced during the CP2 test compared to the theoretical composition from a thermodynamic computation performed with HSC Chemistry 5.11. The measured values after 95% bed turnover show good agreement with the theoretical values. As with the solids produced from the CP1 test, the good agreement between the theoretical and measured values shows that the reactions in the DMR during CP2 were not kinetically limited.

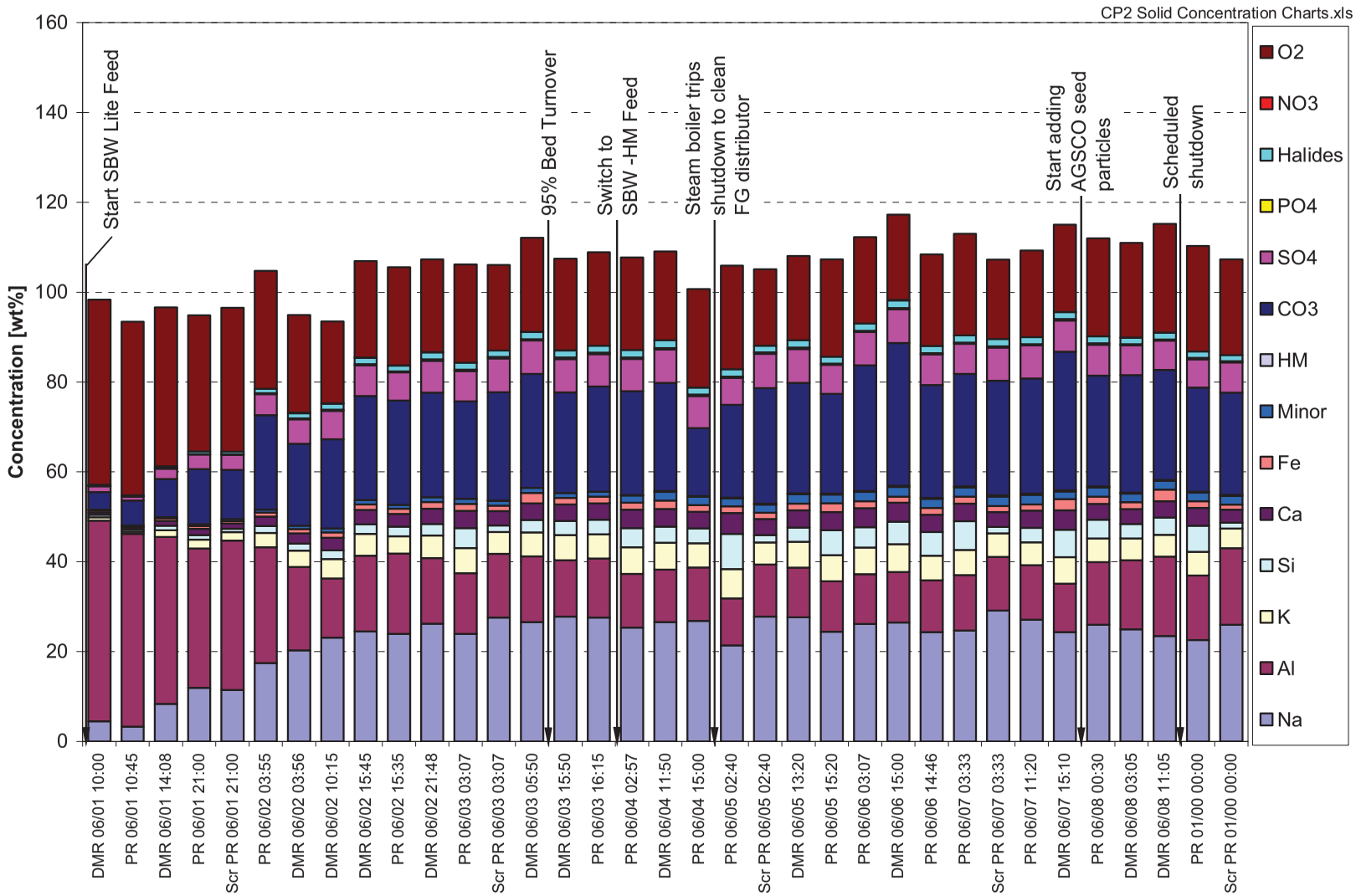

Figure 7-43. Solids Analysis for CP2 test DMR and PR samples.

The Minor series includes the minor metal constituents: B, Ce, Cs, Mg, Mn, Ni, Zn, and Zr. The HM series includes the RCRA heavy metals: As, Cr, Hg, and Pb. The Halides series includes the Cl and F.

Table 7-23. Average composition of DMR solids produced during the CP2 test.

Component	Average Composition (wt%)		
	Entire Test	After 95% Bed Turnover	Theoretical (HSC Chemistry)
Al 17	.23	12.61	12.60
Ca 3.	204	3.815	1.563
Fe 1.	380	1.610	0.669
HM 0.	127	0.210	0.207
K 4.	647	5.496	4.285
Minor 1.	394	1.850	4.127
Na 22	.68	25.74	26.14
Si 3.	155	4.099	4.924
CO_3 21	.57	24.48	23.59
Halides 1.	353	1.569	1.044
NO_3 0.	019	0.010	0.000
O_2 22	.94	20.64	14.84
PO_4 0.	251	0.284	2.314
SO_4 6.	197	7.017	3.695

HSC DMR Products CP2.xls

The major differences between the measured and calculated values are for calcium, minor components, oxygen, and phosphate. Calculations were based on the target feed compositon instead of actual analytical values and an average hydrogen concentration of 1% (wet basis). Phosphate is low, probably as a result of the difficulty in dissolving $Zr(HPO_4)_2$ in the samples prior to analysis which also resulted in a lower than expected value for Zr (and hence, for the minor species). It also is probable that the variation in the CG-CRG reductant composition resulted in some of the observed variation in the sulfate solids composition since the calculations were based on an average reductant composition.

Mineralogical analysis of CP2 sample No. 2334 was conducted by Hazen after the conclusion of the test. (See Hazen Memo from Bob Johnson to Harry Mudget, "Microprobe and XRD analysis of Sample No. 2334-PR, Hazen Project No. 10386-05," dated August 11, 2006 [R32].) Microprobe and XRD analysis of this sample was conducted because this was a "typical" sample of product solids from the DMR/PR during this test.

The sample was alkaline when slurried in water and evolved CO_2 when acidified. A polished section of the sample was prepared for microprobe analysis. The x-ray diffraction pattern indicated major gregoryite $(Na_2,K_2,Ca)CO_3$ and sodium aluminate $(NaAlO_2)$ and possibly minor amounts of cerianite (CeO_2) and sylvite (KCl). These observed mineral species are consistent with the theoretical composition of the CP2 test solids predicted by HSC Chemistry for the target feed composition used during this test. A microprobe photo of PR sample is shown in Figure 7-44. The composition of the light gray matrix is variable, but generally in Al, Na, and Ca. Analyses of four typical spots in the gray matrix of different pellets is shown in Table 7-24, but are not labeled in the photo. The whitest inclusions in the samples like "a" and "b" are high in Ce and Al. Lower concentrations of Ce are found in the light gray circular bands. The light gray inclusions like "c", "d," and "e" are relatively high in Ca and Si. No particles of KCl could be found with the microprobe although there was an indication of it in the XRD pattern.

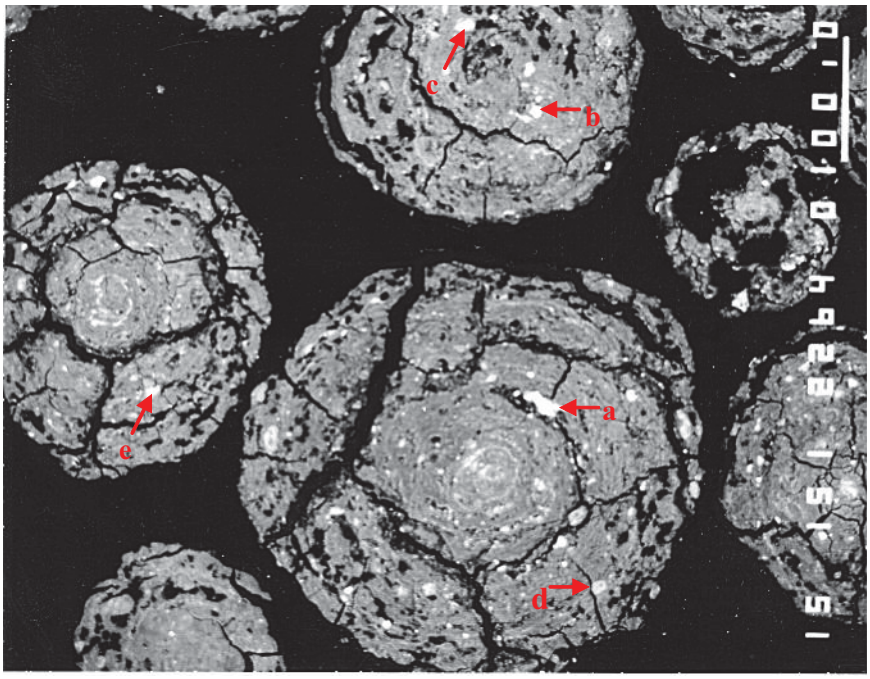

White Bar = 100 μm 150 ×

Figure 7-44. Microphoto of PR Sample 2334.

Table 7-24. Microprobe composition of PR Sample 2334.

Spots	Weight (%)									
	Na K		Al	Ca	Si	Mn	Fe	S	P	Ce
m_1 1	5	2	27	8	6			1.0		
m_2	13 2		28	10	3	2		1.2		
m_3	8 2		28	13	3	5		0.6		
m_4	3 2		30	8	5	5 4		0.7		
a	2		23 6		3	4	3		2	2
b			15 7		3	6	3		3	4
c	3		6	42	11				1.1	
d	4 1		9	36	10			1	.8	
e	4 1		4	44	11			0	.8	

7.6.2 Fines (HTF Material)

The HTF product material from both the CP1 and CP2 tests was quite fine and had the consistency of talc or flour. The color of the HTF fines was predominantly a lighter tan, but at times was a dark gray color. Higher carbon levels in the DMR resulted in darker solids collected in the HTF. There was a significant difference in the rate of solids collected in the HTF between the CP1 and CP2 test. The most likely cause of the difference between the tests was the performance of the DMR cyclone (see Section 7.6.2.3)

7.6.2.1 CP1 Test Solids Analysis. The composition of the HTF solids produced during the CP1 test is shown in Table 7-25 and Figure 7-45. These values are all renormalized on a carbon-free basis. The average carbon content of the CP1 HTF solids was 17.5%; although it ranged from a low of 2.5 to a high of 58.7%. Table 7-25 also compares the HTF solids composition to the composition of solids produced in the DMR over the same time period. The HTF solids had lower concentrations of Al, Fe, HM, and CO_3, while having higher concentrations of the Minor species (B, Ce, Cs, Mg, Mn, Ni, Zn, and Zr), K, Si, Cl, F, NO_3 and PO_4 when compared to solids from the DMR. Relative agreement within about ±20% should be considered good agreement, considering potential sampling and analytical differences when comparing analyses of somewhat different materials; except that when the concentrations are low, such as for HM and NO_3, larger relative differences are likely. The enrichment of K, many of the minor elements, some of the HMs, Si (as silica fume), halides, and PO_4 in the HTF solids is consistent with the known higher volatility of these species, especially when present at lower concentrations when the amount material can be proportionately more significant.

Table 7-25. Average composition of HTF solids produced during the CP1 test.

Component	Average Composition (wt%)			Relative Difference P-4A-1 through P-4A-6 HTF/DMR
	HTF Solids Entire Test	HTF Solids P-4A-1 through P-4A-6	DMR Bed Solids P-4A-1 through P-4A-6	
Al 9.	194	7.944	10.83	-26.65%
Ca 2.	055	1.533	1.392	10.15%
Fe 1.	413	1.375	1.781	-22.77%
HM 0.	145	0.217	0.297	-27.02%
K 4.	308	3.962	3.419	15.9%
Minor 5.	424	6.870	4.842	41.88%
Na 20	.27	20.20	20.75	-2.67%
Si 9.	447	10.77	8.650	24.53%
CO_3 11	.630	8.625	11.376	-24.18%
Halides 1.	450	1.451	0.867	67.34%
NO_3 0.	068	0.077	0.015	402.84%
O_2 22	.85	23.61	24.26	-2.65%
PO_4 6.	553	7.728	5.672	36.25%
SO_4 5.	316	4.835	5.211	-7.21%

CP1 solid concentration charts.xls

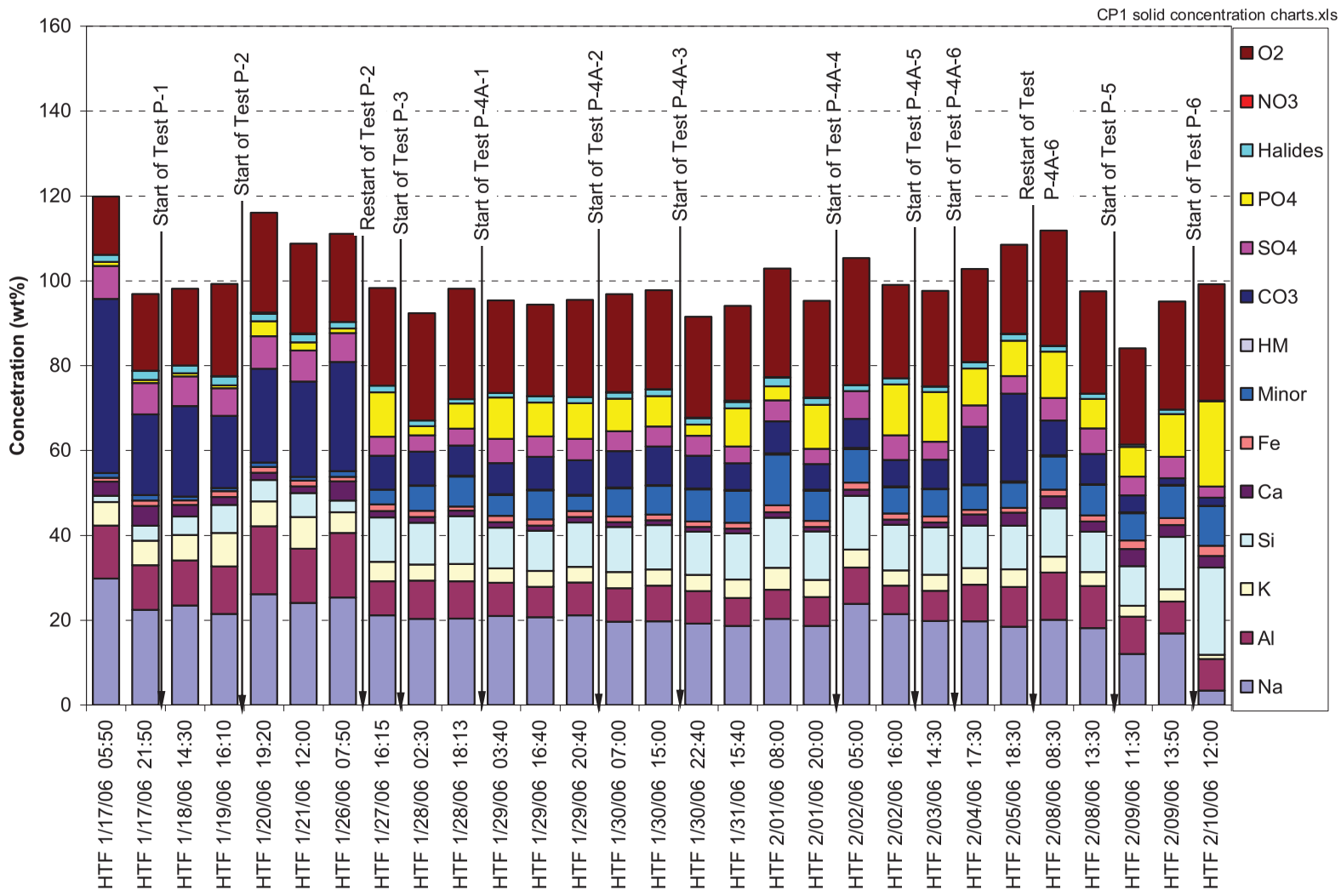

Figure 7-45. Solids Analysis for CP1 test HTF samples.

The Minor series includes the minor metal constituents: B, Ce, Cs, Mg, Mn, Ni, Zn, and Zr. The HM series includes the RCRA heavy metals: As, Cr, Hg, and Pb. The Halides series includes the Cl and F.

7.6.2.2 CP2 Test Solids Analysis. The composition of the HTF solids produced during the CP2 test is shown in Table 7-26 and Figure 7-46. These values are all renormalized on a carbon-free basis. The average carbon content of the CP2 HTF solids was 6.89%; and ranged from a low of 3.75% to a high of 15.1%. Table 7-26 also compares the HTF solids composition to the composition of solids produced in the DMR over the same time period. The HTF solids had lower concentrations of Al, Ca, Fe, Si, and O_2, while having higher concentrations of heavy metals (Cr, Hg, and Pb) Cl, F, NO_3, PO_4 and SO_4 when compared to solids from the DMR.

Table 7-26. Average composition of HTF solids produced during the CP2 test.

Component	Average Composition (wt%)			Relative Difference P-4A-1 through P-4A-6 HTF/DMR
	HTF Solids Entire Test	HTF Solids 95% Bed Turnover	DMR Bed Solids 95% Turnover	
Al 12	.62	11.85	12.61	-6.02%
Ca 3.	111	3.193	3.815	-16.31%
Fe 1.	062	1.176	1.610	-26.97%
HM 0.	207	0.269	0.210	28.04%
K 5.	153	5.330	5.496	-3.01%
Minor 1.	550	1.829	1.850	-1.11%
Na 26	.90	27.86	25.74	8.24%
Si 1.	565	1.500	4.099	-63.41%
CO_3 24	.40	23.69	24.48	-3.23%
Halides 2.	344	2.122	1.569	35.24%
NO_3 0.	064	0.035	0.010	256.59%
O_2 17	.26	17.28	20.64	-16.29%
PO_4 0.	316	0.325	0.284	14.28%
SO_4 7.	736	7.795	7.017	11.09%

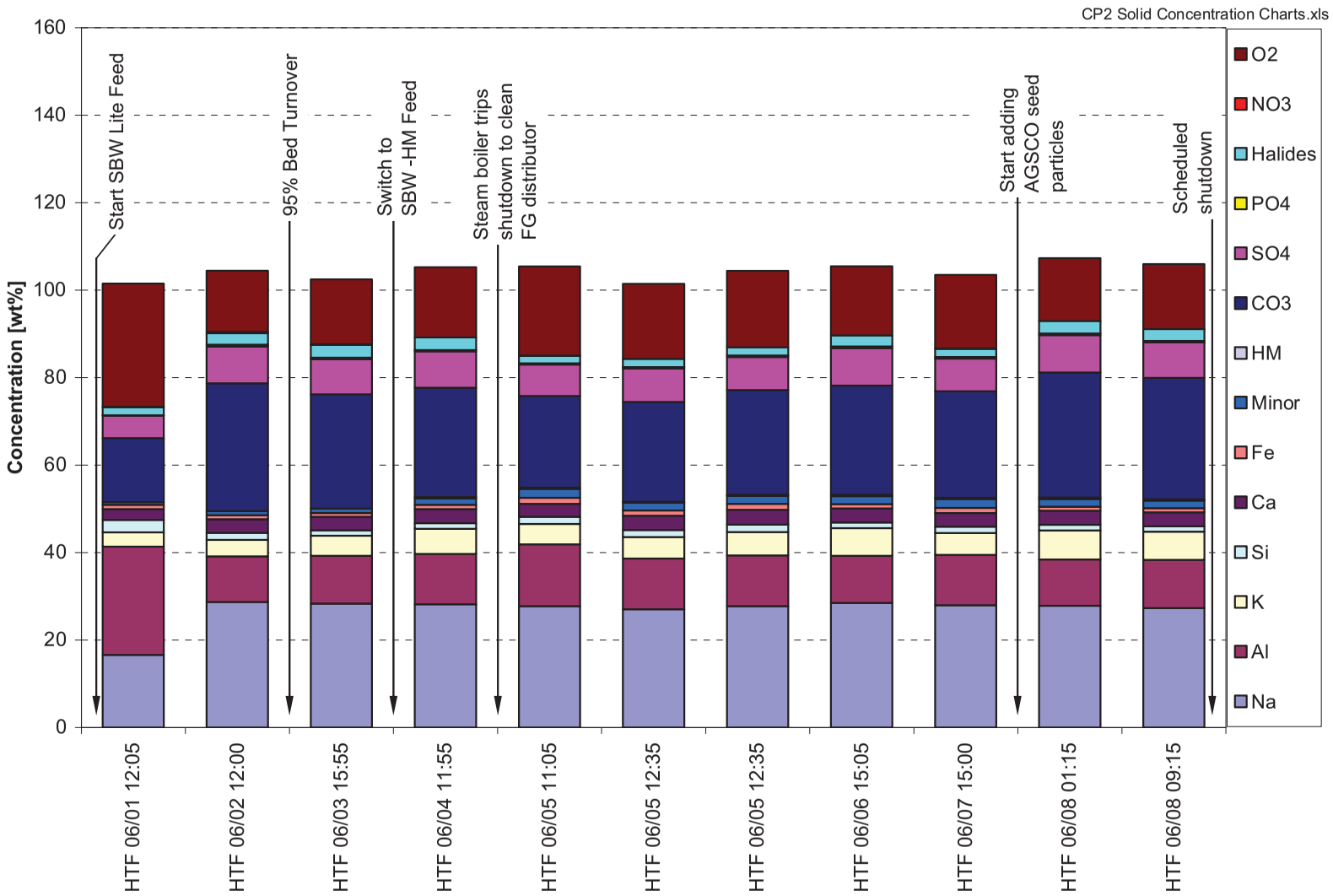

Figure 7-46. Solids analysis for CP2 test HTF samples.

The Minor series includes the minor metal constituents: B, Ce, Cs, Mg, Mn, Ni, Zn, and Zr. The HM series includes the RCRA heavy metals: As, Cr, Hg, and Pb. The Halides series includes the Cl and F.

As with the CP1 HTF solids, agreement within about ±20% should be regarded as good, considering potential sampling and analytical differences when comparing analyses of somewhat different materials; except that when the concentrations are low, such as for metals and NO_3, larger relative differences are likely. Species with expected higher volatilities were generally enriched in the HTF fines compared to the DMR product. Al, which is less volatile than most other elements and is also a component of the attrition-resistant starting alumina bed, is slightly depleted in the HTF fines in both CP1 and CP2. Assuming representative sample analyses, the Si in CP2 appears to partition more to the DMR product compared to CP1; but analytical variations, especially for more difficult-to-dissolve species like Si, may have also caused such apparent variations in partitioning between the DMR product and HTF fines.

7.6.2.3 HTF Solids Particle Size Analysis. The particle size distribution of the HTF solids showed significant variation between the CP1 and CP2 tests. The CP1 HTF solids had a larger average particle size and wider size distribution than the solids collected during the CP2 test.

CP1 Test

The particle size distribution of the HTF solids collected during CP1 test P-1 is shown in Figure 7-47. A laser diffraction spectrometer (Malvern Mastersizer) was used to measure the particle size distribution of this material using methanol as the dispersant. The HMPD of the HTF solids was 2.10 microns while the MMPD was 56.2 microns. The midpoint of the cumulative mass fraction undersize curve occurs at 27.7 microns. The wide PSD and large difference in the average particle sizes are evidence that a large fraction of the material captured in the HTF was nominally bed material that should have been retained in the DMR. This indicates that the DMR cyclone was not working well during this test, most likely due to partial plugging of the cyclone downcomer.

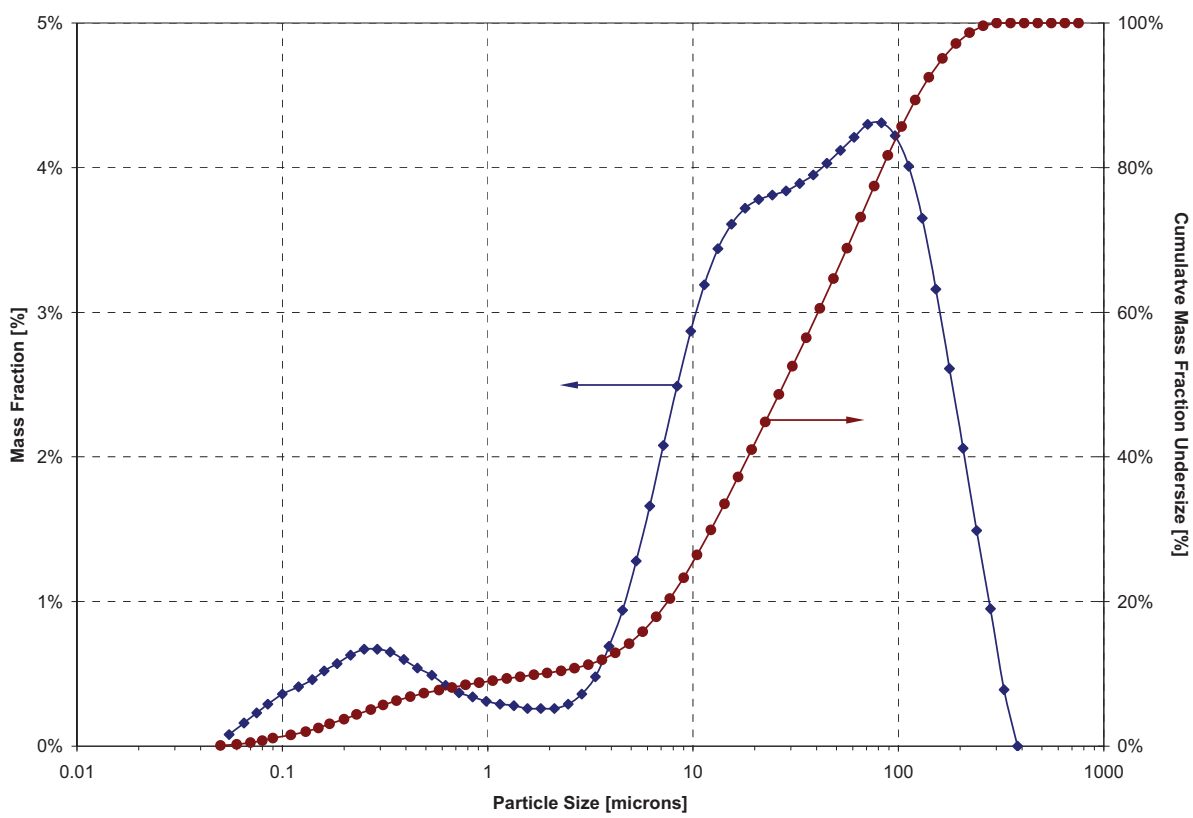

Figure 7-47. Particle size distribution of HTF solids collected duringCP1 Test P-1, Sample No. 1448.

Figure 7-48 shows the particle size distribution of solids collected during CP1 test P-4A-3. The HMPD of these solids is 1.84 microns, the MMPD 39.0 microns and the midpoint of the cumulative mass fraction undersize curve occurs at 22.6 microns. As with the sample taken during CP1 test P1, the wide distribution and variation in the average particle sizes also show that the DMR cyclone was not working well during this part of the CP1 test.

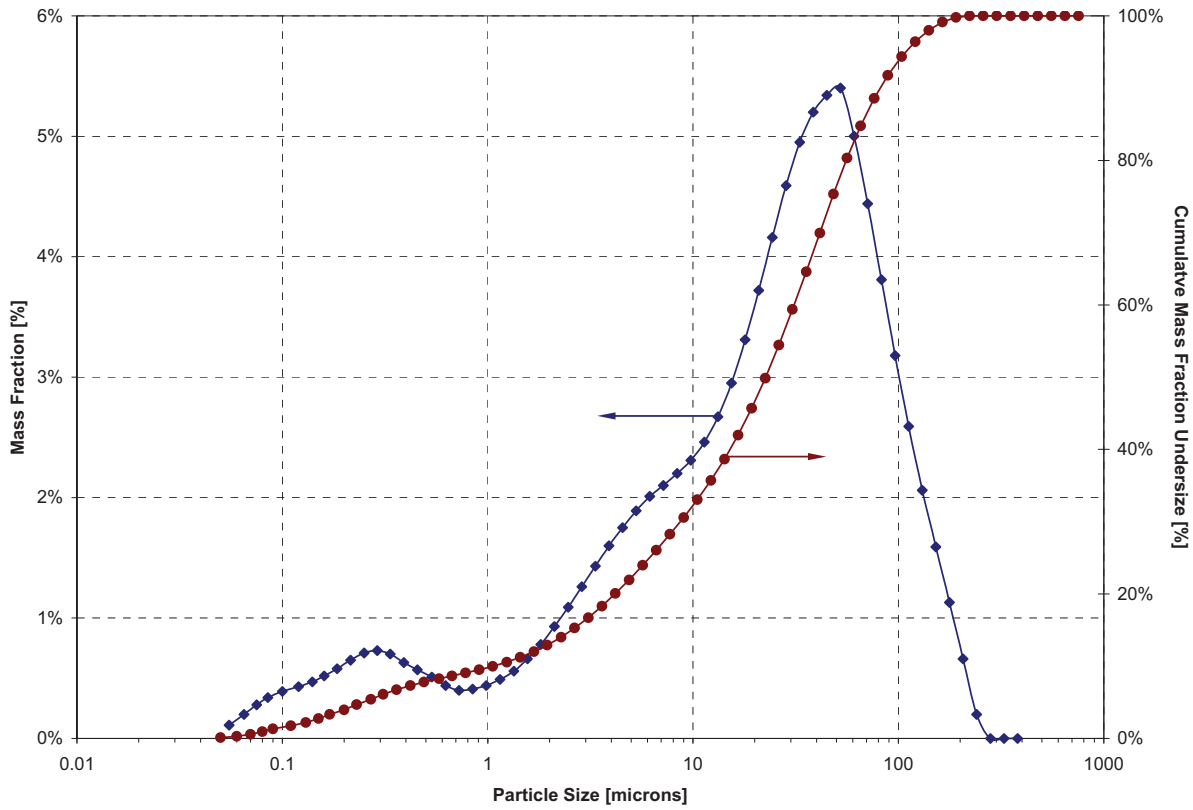

Figure 7-48. Particle size distribution of HTF sample collected during CP1 Test P-4A-3, Sample No. 1693.

CP2 Test

The particle size distribution of the HTF solids collected during the CP2 test is shown in Figure 7-49. This sample was taken June 4, 2006, at 1155 after the DMR bed had reached 95% bed turnover. The HMPD of the HTF solids was 2.75 microns while the MMPD was 18.2 microns. The midpoint of the cumulative mass fraction undersize curve occurs at 9.12 microns. This graph shows that the cyclone was much more effective at capturing particles elutriated from the DMR during the CP2 test. The most likely reason for the improved performance was modified operation of the cyclone downcomer pulse jets. The timer interval for the pulse jets was reduced from 60 to 30 seconds and the operators performed manual pulse cleaning of the cyclone downcomer more frequently during the CP2 test.

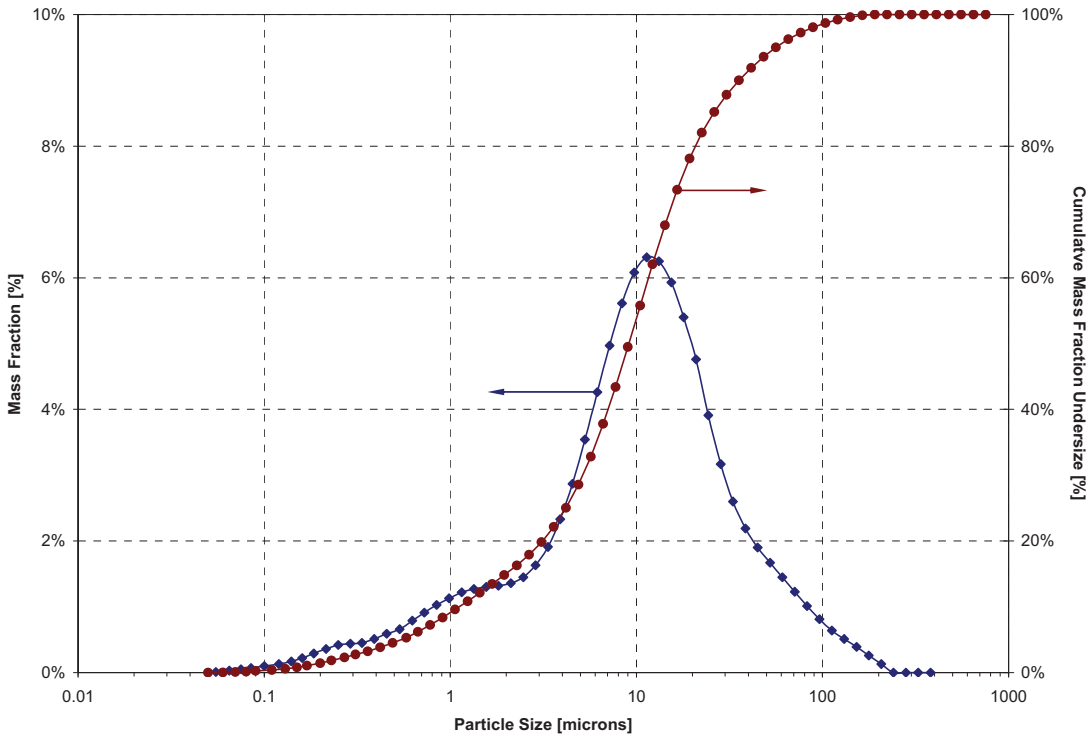

Figure 7-49. Particle size distribution of HTF sample collected during CP2 test on 6-4-06, Sample No. 2191.

7.6.3 PBF Solids

The PBF solids produced during both CP1 and CP2 test were quite fine with a consistency of talc or flour. They were predominately carbon fines that had been elutriated from the CRR and were quite dark in color. A small amount of SO4 was detected in the PBF samples for both tests. This sulfate is probably due to oxidation of sulfur contained in the Desulco carbon added to the CRR. With the high surface area of fine particles, and high carbon concentration, the PBF fines from both CP1 and CP2 tended to be enriched in Hg; but the mass of the PBF fines was small enough that the amount of Hg that partitioned to the PBF, like the amounts of Hg that partitioned to the DMR product and HTF fines, was small compared to the amount captured in the GAC bed.

7.6.3.1 CP1 Test Pbf Solids Analysis. The PBF solids composition reflected the composition of the CRR bed material that was in the CRR during the CP1 test. The CRR bed material during CP1 was sintered bauxite which contained Fe_2O_3, SiO_2, TiO_2 and Al_2O_3, along with DeSulco carbon.

Figure 7-50 shows the composition of PBF solids produced during the CP1 test. The carbon concentration in the PBF solids for the entire test averaged 84.2%. The last sample, taken February 10, 2006, shows significant amounts of Na and K in the solids analysis. This indicates that when this sample was taken, the HTF filters had failed (see Section 7.1.10) which allowed solids from the HTF to enter the CRR and be carried through the CRR to the PBF.

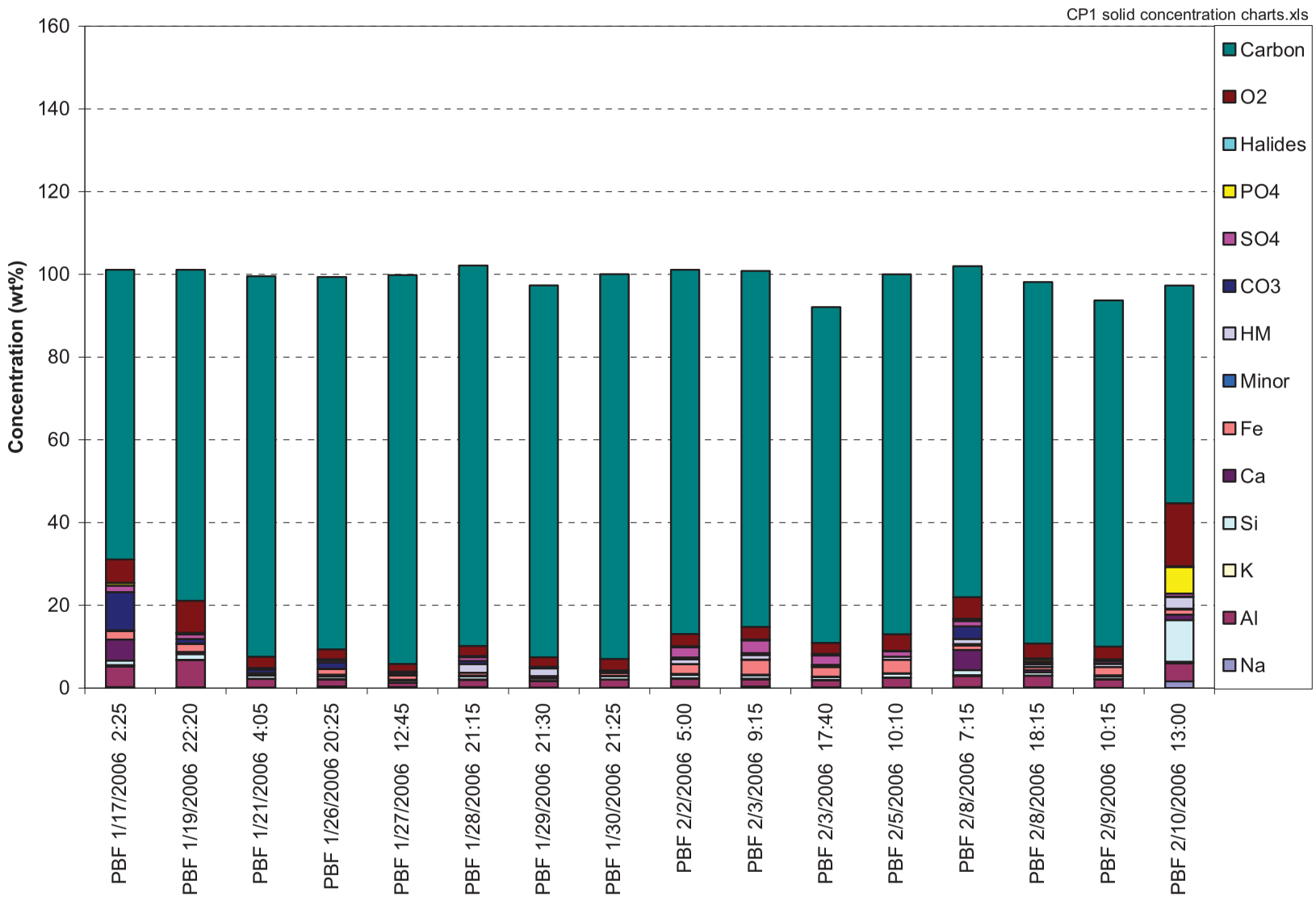

Figure 7-50. Chemical analysis of PBF solids produced during the CP1 Test.

7.6.3.2 CP2 Test PBF Solids Analysis. The PBF solids composition during the CP2 test was primarily alumina and carbon (see Figure 7-51). The carbon concentration in the PBF solids for the entire test averaged 78.9%. After the bed height in the CRR was increased to 36 inches and the carbon inventory in the CRR bed was reduced (resulting in higher CRR outlet O_2 concentrations), the alumina concentration in the PBF samples increased from an average of 4.6% to 18.2%. The carbon concentration during the first part of the test (before the CRR bed height was increased) averaged 89.6%, while the carbon concentration averaged 57.7% after the CRR bed height was increased.

7.6.4 DMR Wall Scale

During both the CP1 and CP2 tests inspections of the DMR vessel revealed a thin scale deposit on the walls of the DMR vessel. The wall scale was observed during CP1 on January 14, 2006 after the conclusion of the scoping tests when the vessel was opened for a post run inspection and on January 21 after the P-1 shutdown. Wall scale was again observed after the CP2 scheduled shutdown when the DMR was opened for post-run inspection. Figure 7-52 and Figure 7-53 show typical examples of the wall scale on DMR internal surfaces.

The wall scale in the CP1 test was generally 1-6 mm thick. Scanning electron microscope (SEM) analyses performed by Hazen indicated that the January 14, 2006 cyclone downcomer scale (sample number 1378) was made up mainly of sodium, potassium, calcium, aluminum, and sulfur with minor amounts of silicon, potassium and iron. X-ray diffraction (XRD) also revealed the presence of sodium aluminate in this sample (Seee Hazen Memo from Bob Johnson to Larry May, "Summary of Samples Analyzed from Pilot Plant Operations," dated May 5, 2006 [R33].) Further XRD analysis showed that this sample contained $Na_2Mg(CO_3)_2$ (Eitelite), $Na_2(CO_3)\bullet H_2O$ (thermonatrite), $K_3Na(SO_4)_2$ (aphthitalite), $Al(OH)_3$ (bayerite), $NaAlSiO_4$ (nepheline), and Al_2SiO_5 (kyanite) [R27].

Samples of the wall scale were submitted to Hazen and sent to SRNL for analysis (Sample No.1511). The SEM analysis by Hazen showed that this wall scale contained relatively high levels of alkalis and sulfates [R33]. The DMR reductant was switched to GC-CRB calcined coal after January 8, 2006 which led to increased sulfate in the DMR solids. A low-melting ternary eutectic mixture (Na_2CO_3-K_2CO_3-Na_2SO_4) was identified as the probable source of the "glue" in this wall scale material. The use of calcined mullite clay as a DMR bed feed additive seemed to exacerbate the formation of this scale by reacting in the bed to form Al_2SiO_5 (kyanite) and a aluminosilicate glass [R27]. Increasing the reducing conditions in the DMR (higher H_2 concentrations), stopping of the use of mullite clay bed additive after January 21, and the addition of UDS in the DMR feed on January 28 all seemed to contribute to cessation of wall scale formation in the DMR for the rest of the CP1 test.

After the CP2 production test was concluded, a thin (1–6 mm) wall scale deposit was discovered in the DMR on the inside metal and refractory surfaces. The CP2 wall scale was similar in appearance to the CP1 wall scale. The CP2 test did not use bed additives in the DMR and did not have UDS in the SBW feed. An approximate calculation showed that the mass of the CP2 wall scale was 15 to 30 pounds.

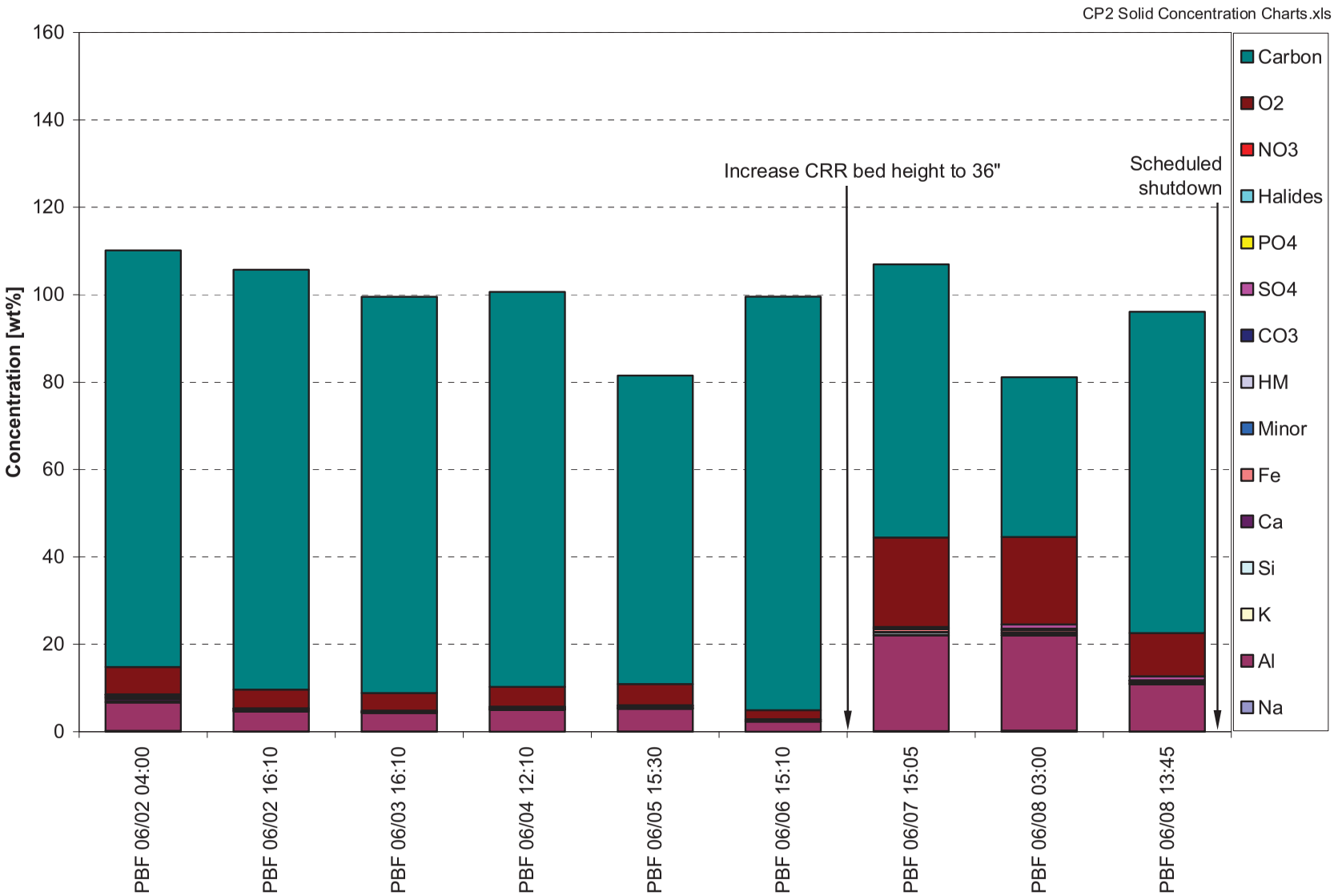

Figure 7-51. Chemical analysis of PBF solids produced during the CP2 test.

Figure 7-52. Wall scale removed from the DMR cyclone downcomer on January 14, 2006 (Sample 1378).

Figure 7-53. DMR wall scale removed from the corrosion coupon rod after the end of CP2 test.

Microprobe and XRD analysis by Hazen show that the CP2 wall scale (sample #2376) is comprised mainly of sodium aluminate and sodium carbonate (bed type solids), and a Ca-Mg-Si mineral similar to merwinite, with an amorphous low-melting point eutectic binder of high sulfate content [Reference: Hazen Memo from Bob Johnson to Harry Mudget, "Sample 2376 Bark, Hazen Project 1-386-05" dated July 21, 2006] [RL]. This analysis also indicates that the wall scale likely formed from residual ash constituents of the GC-CRB calcine coal; in particular, the sulfate, calcium, and silicate in the coal ash. Approximately 97% of the silicate, 31% of the sulfate, and 54% of the calcium in the DMR product comes from coal ash residues. The sulfate in the SBW and most of the sulfate released into the DMR from the coal ash appears to readily combine with the SBW alkali metals and form higher melting sulfates in the majority of the product. However, a small amount of the sulfate from the coal ash combines with other coal ash constituents, calcium and silicates to form low melting eutectics that tend to slowly accumulate or stick to the internal refractory and metal surfaces of the DMR. The presence of the small quantity of sticky sulfates and calcium silicates on the wall surfaces attracts other fine solids in the bed to form a layer matrix of carbonates, aluminates, and calcium silicates that produces a gradual slow build up of the wall scale over time.

The scale was readily dissolvable in hot water and in nitric acid as shown in Table 7-27. The treatment time for these samples was 20 minutes. A simple wash of water and then nitric acid was used to remove the scale from the inside surfaces of the DMR.

Table 7-27. Treatment of CP2 DMR wall scale solids.

Sample Treatment	Initial Weight (g)	Final Weight (g) %	loss
Cold H_2O 9.99		3.316	66.8%
Hot H_2O 10.1	2	3.309	67.3%
1 M HNO_3 9.98		1.506	84.9%
3 M HNO_3 10.0	4	1.498	85.1%

The mechanism of the CP2 DMR wall scale formation is being evaluated and analytical testing is still being performed on the deposits. A separate detailed report will be prepared and issued that will address the mechanism for development of the wall scale in the DMR.

7.7 Process Gas And Stack Gas Measurements

Process gas and stack gas measurements were made at the outlet of the High-Temperature Filter (HTF), at the outlet of the CRR, at selected locations in the carbon bed, and at the stack. Measurements that were made include:

- HTF outlet—DMR process gas composition
- CRR outlet—CRR process gas oxygen concentration
- CP1 GAC bed—Hg manual sampling at the outlet of Beds 1 and 2
- CP2 GAC bed—Hg manual sampling at the outlet of Beds 1, 2, and 3; continuous SO_2 monitoring at the inlet of Bed 1
- Stack—Continuous monitoring and manual sampling.

The scope of the stack measurements was more extensive during CP1 to perform the full scope of gaseous, metals, particulate, acid gas, and organics measurements specified in the test plan. The stack gas Hg measurements from CP1 were contaminated with elevated Hg levels because a portion of the stack gas bypassed the GAC bed due to an incorrect valve actuator configuration. The CP1 stack Hg measurements were not valid for use in determining GAC bed performance and representative Hg emissions.

The stack gas manual sampling was less extensive during CP2, limited to metals and particulate sampling. The GAC bed measurements were more extensive during CP2, because of the increased focus on determining the performance of the GAC bed and Hg stack gas emissions. The CP2 measurements included continuous stack gas Hg monitoring to determine levels of residual contamination left from the CP1 stack gas GAC bed bypass and to determine the order of-magnitude of the Hg concentration in the stack gas.

The process gas and stack gas measurement results are summarized in Table 7-28. Measurement detail is provided in the following subsections.

7.7.1 DMR CPMS and Stack CEMS Measurements

The continuous process monitoring system (CPMS) monitored the DMR outlet composition downstream of the HTF. The continuous emissions monitoring system (CEMS) monitored the stack gas composition downstream of all of the ESTD equipment. These data were available for the operators to use in setting and maintaining operating conditions. These data were also recorded using the DACS and are included in the electronically logged data for the tests.

The CPMS and CEMS were operated, calibrated and maintained according to the test plan, quality assurance plan, and operating procedures. The CPMS and CEMS data were provided and logged on a dry, moisture-free basis (except for the stack gas THC measurement, which was performed on a wet basis), because the sample conditioning systems condense and remove the moisture in the gas (along with filtering any particulate matter and condensed aerosols) to provide sample gas conditioning necessary to protect the gas analyzers from fouling and damage. The CPMS NO_X measurement was made on both a dry basis and also diluted with air to provide excess O_2 during analysis to prevent passivation of the catalytic NO_X converter.

The dry-basis CPMS and CEMS data were normalized to a wet basis in order to perform mass balance calculations such as NO_X destruction and mass balance closure calculations. The CPMS NO_X values were also normalized to correct for the air dilution used in this analysis.

All of the CPMS data was corrected for dilution, calibration error, and drift, which were measured and documented during periodic CPMS and CEMS calibrations. Only the CEMS data obtained during each of the manual sampling periods were corrected for calibration error and drift. These CPMS and CEMS data corrections were performed even when the calibration error and drift were within acceptance limits.

Table 7-28. CP1 and CP2 stack emissions summary.

Test	Average stack gas composition, wet									
	O_2 (%)	CO_2 (%)	NO (ppm)	NO_2 (ppm)	NO_X (ppm)	CO (ppm)	THC (ppm)	SO_2 (ppm)	N_2 (%)	H_2O (%)
CP1 4.	8	9.4	444	17	455	18	<0.2	25	27.9	57.9
CP2 4.	0	8.9	228	2	233	31 0.	3	31	37.7	49.5
Avg 4.	4	9.1	336	10	344	25 0.	2	28	32.8	53.7

Test	Average mass emission rate of key species (lb/hr)					Stack gas NO_X MTEC (ppm)	System NO_X removal efficiency (%)
	NO_X (NO_2)	CO THC		SO_2	HCl+Cl_2 (ppm as HCl)		
CP1 0.	92	0.023	<0.0004	0.077	0.0065	22,822	98.0
CP2 0.	46	0.037	0.0005	0.085	—	21,739	98.9
Avg 0.	69	0.030	0.0005	0.081	0.0065	22,281	98.5

Test	Concentrations of HWC-MACT regulated species, dry (@7% O_2)								
	Dioxins and furans (ng/dcsm TEQ)	CO (ppm)	THC (ppm)	HCl+Cl_2 (ppm as HCl [Method 26])	PM (mg/ dscm [Method 26])	Semivolatile metals (µg/dscm [Method 29])			
						Cd Zn		Pb	Total
CP1 0.	011	23	<0.2	4.6	0.91	0.08	5.1	0.25	5.5
CP2 —		26	0.4	—	0.38	0.046	3.7	0.15	3.9
Average 0.	011	24	0.2	4.6	0.64	0.064	4.4	0.20	4.7
HWC MACT standard for new facilities	0.11 10	0	10	23	3.4	—	—	—	10
Measured value, % of MACT limit	9.7%	22.6% 2.	4% 20	.1%	26.7%	—	—	—	55%

Test	Concentrations of HWC-MACT regulated species (dry, @7% O_2)				POHC destruction and removal efficiency (% [Method 0031])
	Low volatility metals (µg/dscm [Method 29])				
	As Be		Cr	Total	
CP1 0.	15	0.077	2.65	2.7	99.9997
CP2 0.	09	0.046	0.33	0.5	—
Average 0.	12	0.061	1.49	1.6	99.9997
HWC MACT standard for new facilities	— — —			23	99.99
Measured value, % of MACT limit	— — —			7.0%	almost 100x better

Table 7-28. (continued).

VOC emission summary - Method 0031	
Detected VOCs:	µg/dscm
Dichlorodifluoromethane (Freon 12)	**17.6**
Methylene chloride	**9.1**
Naphthalene	**5.1**
1,2,3-Trichlorobenzene	**4.8**
1,2,4-Trichlorobenzene	**4.6**
Summed VOCs:	µg/dscm
Non-detected Constituents, µg/dscm	147
Non-detected Constituents, lb/hr	6.7E-05
Detected Constituents, µg/dscm	**29**
Detected Constituents, lb/hr	**1.3E-05**
All Constituents, µg/dscm	**166**
All Constituents, lb/hr	**7.6E-05**

SVOC emission summary - Method 0010	
Detected SVOCs:	µg/dscm
Di-n-butyl phthalate	**19.6**
N-Nitro sodimethylamine	**6.4**
SVOC mass rates and summed SVOCs	
Di-n-butyl phthalate, lb/hr	**3.7E-05**
N-Nitro sodimethylamine, lb/hr	**1.3E-05**
Total nondetected SVOC concentration, µg/dscm	535
Total nondetected SVOC emission rate, lb/hr	9.8E-04
All SVOC concentration, µg/dscm	**557**
All SVOC emission rate, lb/hr	**1.0E-03**

PCB emission summary - Method 23	
Total PCB Congener Concentrations, ng/dscm	**10.6**
Dioxin-like Coplaner PCB Concentrations, ng/dscm	11.2

Total Organics Analysis for Risk Assessment - Method 0010	
Field GC summary	
Total Tedlar bag and condensate results, µg/dscm	**10,136**
TCO/GRAV results	
Total TCO/GRAV conncentration, µg/dscm	**7,400**

Notes:

1. **Bolded** values are detected values, or sums of detected and nondetected (reporting limit) values; values that are **not bolded** are reporting limit values, or sums of reporting limit values.
2. Total Detected Constituent values may not equal the sum of the values of individual detected species, because detection limit values have been included in the total values of detected species, but excluded from the Total Detected Constituent values.
3. The total PCB Congener Concentrations represents the sum of PCBs measured in total isomer groups, which is a separate categorization of PCB compounds from those PCBs classified as dioxin-like coplanar PCBs.
4. The reported values are averaged over the stack sampling test periods, not the entire duration of the test series.
5. HWC MACT = Hazardous Waste Combustor Maximum Achievable Control Technology standards.

[cp1 off-gas emissions and nox destruct aug 5.xls]Emissions summary

7.7.2 CPMS (DMR Process Gas) Data

The DMR process gas composition, DMR NO_X destruction, and other key data are shown in Table 7-29 and Table 7-30 (for CP1) and Table 7-31 and Table 7-32 (for CP2). The DMR process gas data are summarized as follows:

- The DMR outlet gas moisture content ranged between 50–60 volume % for most of CP1 and all of CP2. The wet-basis total O_2, CO_2, H_2, CO, THC, and NO_X concentrations typically ranged between 40–50% of the dry basis, as-measured values. The balance of the dry-basis process gas composition was primarily N_2.

- Water was the major DMR process gas constituent. The other DMR process gas components, in order of decreasing concentration, were N_2, CO_2, H_2, and NO_X, with trace levels (typically less than 0.5%) of O_2 and THC (reported as CH_4).

- The DMR operates in a stoichiometrically reducing condition to cause the nitric acid and metal nitrates in the simulant feed to convert to water, metal carbonates, and N_2. Wet basis H_2 levels typically ranged between 0–2% so that conditions were suitable to reduce NO_X levels from the typical Maximum Theoretical Emission Concentration (MTEC) at the DMR outlet of about 55,000–75,000 ppm (wet basis, depending on the simulant feed rate and other conditions) to typically 1,000–8,000 ppm (wet basis) for most of the test durations.

- The DMR outlet O_2 levels typically ranged between about 0–1% (wet basis). During periods when the DMR bed contained a lower coal inventory, the hydrogen level would drop significantly before the oxygen concentration would show a significant increase.

Along with H_2, the CO and THC indicate the degree of reducing stoichiometry in the DMR. CO typically ranged between 0.1–1.5% (wet basis). THC typically ranged between about 300–3,000 ppm (wet basis).

7.7.3 CEMS (Stack Gas) Data

The CRR was operated to oxidize the H_2, CO, and THC in the DMR process gas to convert these constituents to CO_2 and H_2O and meet air emission regulations for CO and hydrocarbon emissions. The stack gas compositions are reported on dry and wet bases for CP1 and CP2 in Table 7-33 through Table 7-38. Two tables each for dry and wet CP2 stack gas compositions show: (a) the compositions for the manual sample periods, used to determine emission rates for comparison to regulatory limits, and (b) the compositions for the 15 different CRR operating condition tests.

Water was the major stack gas off-gas constituent, ranging between 46–63%. The other stack components, in order of decreasing concentrations, were N_2, CO_2, and O_2, with ppm levels of NO_X, CO, and THC (reported as propane for direct comparison to air emission limits).

Table 7-29. CP1 DMR process gas dry composition.

			DMR process gas composition (dry basis)						
			O_2 (%)	CO_2 (%)	H_2 (%)	NO_X (ppm)	CO (ppm)	THC (ppm)	N_2 (%)
Date Test	Period	Test	AT-700-001-O_2	Avg AT-700-002A and B CO_2	Avg AT-700-002A and B H_2	AT-700-004-NO_X	AT-700-003-CO	AT-700-005-THC	By Difference
18-Jan-06	1730–2107	1, day 1	-0.08	26.0 2.45		10,756	0.41	1,414	70.0
19-Jan-06	1000–1330	1, day 2	0.31	23.9 2.32		12,896	0.81	4,280	70.9
27-Jan-06	1000–1310	2A	0.95	21.9	3.02 7,192		0.58	5,034	72.3
28-Jan-06	1230–1640	3B	0.21	22.5	2.17 7,853		0.54	4,893	73.3
29-Jan-06	1040–1426, 1600–1930	4A-1 -0.59		24.6	2.97	9,609	0.63	5,344	70.9
30-Jan-06	1025–1415, 1620–1950	4A-2 0.47		20.2	1.20	6,277	0.48	5,348	76.5
31-Jan-06	1110–1525	4A-3, day 1	0.94	22.0 0.68		2,984	0.32	4,784	75.2
1-Feb-06	1015–1335, 1600–2020	4A-3, day 2	0.57	22.7	0.66	7,351	0.48	5,646	74.3
2-Feb-06	1015–1340, 1450–1810	4A-4 0.11		33.9	3.40	11,182	0.64	6,540	60.1
3 Feb 06	1355–1720	4A-5, day 1	1.34	29.8 2.16		9,684	1.36	5,381	63.8
4-Feb-06	0935–1351	4A-5, day 2	0.40	27.3 4.36		9,700	1.12	6,256	65.3
4-Feb-06	1805–2205	4A-6, day 1	1.18 25.6		0.61	8,913		5,377	71.2
8-Feb-06	1400–1722	4A-6, day 2	0.45	30.1 2.79		8,293	1.12	4,209	64.3

Table 7-29. (continued).

			DMR process gas composition (dry basis)						
			O_2 (%)	CO_2 (%)	H_2 (%)	NO_X (ppm)	CO (ppm)	THC (ppm)	N_2 (%)
Date Test	Period	Test	AT-700-001-O_2	Avg AT-700-002A and B CO_2	Avg AT-700-002A and B H_2	AT-700-004-NO_X	AT-700-003-CO	AT-700-005-THC	By Difference
9-Feb-06	1000–1415	5	0.35	20.9	1.01	7,959	0.57	1,591	76.2
10-Feb-06	0905–1241	6	1.97	23.1	-0.33	10,465	4.13	692	70.0
Averages —		—	0.57	25.0	1.96	8,741	0.94	4,453	70.3

Notes:

1. All CPMS analyses were made on a dry basis.
2. All dry basis values were corrected for zero and span calibration error, even when the calibration error and drift values were within acceptance limits.
3. Two analyzers, each with separately logged data, measured the CPMS CO_2 and H_2 concentrations. These duplicate data were averaged for final reporting.
4. Two analyzers were used to measure the NO_X concentrations, but data from only one of the NO_X analyzers at a time was logged, so there is only a single set of recorded NO_X data. Total NO_X was the only recorded value (NO and NO_2 were not recorded). The recorded NO_X data was adjusted for the zero calibration error and the combined span error and air dilution using the calibration data for the analyzer that was being logged at the time.
5. CPMS data was not valid during certain time periods. Invalid CPMS data has been deleted. These time periods included (a) times when the CPMS was off-line for calibrations or maintenance, (b) times when there was some sort of CPMS malfunction such as insufficient sample gas pressure or flowrate, or analyzer malfunction, and (c) when DMR product was being drained and product eductor N_2 was vented into the DMR freeboard. In some cases that has resulted in no valid data for some time periods (such as for CO during 4A-6 day 1.
6. Occasionally the data for only a single analyzer was invalid for some time periods if only that analyzer was malfunctioning, or if, for the NO_X analyzer, the NO_X dilution ratio deviated from the setpoint value of 4:1.
7. Some values, even after calibration correction, can be slightly negative. These values are not normalized to zero, to avoid biasing averages that include these values.
8. The dry basis $\%N_2$ is calculated by difference, 100 - sum of measured species.

[corr cpms - cems july 29.xls]CMPS dry corr summary

Table 7-30. CP1 DMR process gas composition (wet basis) and NO_X destruction.

			DMR process gas composition (wet basis)											
			O_2 (wet %)	CO_2 (wet %)	H_2 (wet %)	NO_X, (ppm wet)	CO (ppm wet)	THC (ppm wet)	H_2O (wet %)	N_2 (wet %)	Total (wet %)	DMR NO_X METC (ppm wet)	DMR NO_X destruction (%)	CRR NO_X destruction (%)
Date	Test Period	Test	AT-700-001-O_2	Avg AT-700-002A and B CO_2	Avg AT-700-002A and B H_2	AT-700-004-NO_X	AT-700-003-CO	AT-700-005-THC	Calc	Calc	Calc	Calc	Calc	Calc
18-Jan-06	1730–2107	1, day 1	-0.03	10.0	0.95	4,158	0.16	547	61.3	25.1	98.1	60,515	93.1	52.5
19-Jan-06	1000–1330	1, day 2	0.12	9.5	0.92	5,138	0.32	1,705	60.2	26.4	98.1	58,193	91.3	46.3
27-Jan-06	1000–1310	2A	0.42	9.8	1.34	3,206	0.26	2,244	55.4	31.3	99.1	57,071	94.3	81.1
28-Jan-06	1230–1640	3B	0.10	10.7	1.03	3,731	0.26	2,325	52.5	31.8	97.0	69,424	94.6	80.1
29-Jan-06	1040–1426, 1600–1930	4A-1	-0.27	11.2	1.35	4,378	0.29	2,435	54.4	30.5	98.1	68,064	93.5	89.9
30-Jan-06	1025–1415, 1620–1950	4A-2	0.20	8.5	0.50	2,631	0.20	2,242	58.1	29.6	97.5	60,165	95.3	72.4
31-Jan-06	1110–1525	4A-3, day 1	0.39	9.2	0.29	1,249	0.13	2,003	58.1	28.9	97.4	61,562	98.0	-43.0
1-Feb-06	1015–1335, 1600–2020	4A-3, day 2	0.25	10.1	0.30	3,275	0.21	2,515	55.5	30.5	97.4	61,561	95.1	62.4
2-Feb-06	1015–1340, 1450–1810	4A-4	0.05	15.5	1.56	5,122	0.29	2,995	54.2	30.6	103.1	66,701	92.3	71.8
3 Feb 06	1355–1720	4A-5, day 1	0.59	13.2	0.95	4,278	0.60	2,377	55.8	27.6	99.5	65,276	94.0	47.7
4-Feb-06	0935–1351	4A-5, day 2	0.18	12.3	1.97	4,385	0.50	2,828	54.8	30.3	100.8	72,796	94.2	65.7

Table 7-30. (continued).

Date	Test Period	Test	DMR process gas composition (wet basis) O_2 (wet %)	CO_2 (wet %)	H_2 (wet %)	NO_X, (ppm wet)	CO (ppm wet)	THC (ppm wet)	H_2O (wet %)	N_2 (wet %)	Total (wet %)	DMR NO_X METC (ppm wet)	DMR NO_X destruction (%)	CRR NO_X destruction (%)
			AT-700-001-O_2	Avg AT-700-002A and B CO_2	Avg AT-700-002A and B H_2	AT-700-004-NO_X	AT-700-003-CO	AT-700-005-THC	Calc	Calc	Calc	Calc	Calc	Calc
4-Feb-06	1805-2205	4A-6, day 1	0.48	10.4	0.25	3,640		2,196	59.2	27.5	98.4	60,323	94.3	20.8
8-Feb-06	1400-1722	4A-6, day 2	0.17	11.2	1.04	3,084	0.41	1,565	62.8	23.7	99.8	56,469	93.7	87.6
9-Feb-06	1000-1415	5	0.16	9.6	0.47	3,663	0.26	732	54.0	30.5	95.5	62,315	94.2	86.2
10-Feb-06	0905-1241	6	0.71	8.3	-0.12	3,771	1.49	249	64.0	24.5	99.2	15,403	75.5	41.4
Averages		—	0.24	10.6	0.85	3,714	0.38	1,931	57.3	28.6	98.6	59,722	92.9	57.5

Notes:

1. The corrected, dry-basis CPMS data was adjusted to wet basis to better reflect the actual process gas concentrations.
2. The wet-basis adjustment calculation was made by first calculating the DMR process gas flow rate, and then the moisture content of the DMR process gas, based on the input flowrates. Then the dry basis values were normalized to wet-basis values by multiplying by the factor (1-%moisture/100).
3. Unlike the dry basis N_2 values, which were determined by difference of the measured gas species from 100%, the wet basis N_2 values were independently calculated like the wet basis H_2O concentration was - using the input N_2 flowrates and the calculated DMR outlet process gas flowrate.
4. Some values, even after calibration correction, can be slightly negative. These values are not normalized to zero, to avoid biasing averages that include these values.
5. The DMR and CRR NO_X destruction were calculated by a NOx mass balance. The DMR NOx destruction was calculated using the input flowrate of nitrate in the feed to calculate the NO_X Maximum Theoretical Emission Concentration (MTEC) at the DMR outlet based on the equation $2NO_3 = 2NO_2 + O_2$. The CRR NO_X destruction was calculated by a NO_X mass balance across the CRR.
6. The CRR NO_X desctruction may be negative (NO_X formation in the CPR) under some conditions such as occurred on January 31, 2006. During this time the DMR H_2 level was low and the CRR freeboard O_2 flow rate was at its highest.
7. Data that is not valid, for time periods during which there were process upsets such as DMR bed drains, or periods when the CPMS was undergoing maintenance or calibrations, has been deleted. In some cases that has resulted in no valid data for some time periods (such as for CO during 4A6 day 1.

[corr cpms - cems july 29.xls]CPMS wet corr summary

Table 7-31. CP2 DMR process gas dry composition.

				DMR process gas composition (dry basis)						
				O_2 (%)	CO_2 (%)	H_2 (%)	NO_X (ppm)	CO (ppm)	THC (ppm)	N_2 (%)
Test F	eed	Start	Finish	AT-700-001-O_2	Avg AT-700-002A and B CO_2	Avg AT-700-002A and B H_2	AT-700-004-NO_X	AT-700-003-CO	AT-700-005-THC	by diff
DMR-1	SBW Lite	6/1/2006 5:46	6/3/2006 18:00	1.11	25.6	1.61	9,071	0.48	9,623	69.4
DMR-2	SBW w/HM	6/3/2006 18:00	6/7/2006 21:46	0.88	26.3	2.42	8,903	0.48	8,303	68.2
DMR-3	SBW w/HM + clay	6/7/2006 21:46	6/8/2006 13:00	1.04	25.8	2.17	16,430	0.46	16,041	67.3
			Averages	1.01	25.9	2.07	11,468	0.47	11,322	68.3

Notes:

1. All CPMS analyses were made on a dry basis.
2. All dry basis values were corrected for zero and span calibration error, even when the calibration error and drift values were within acceptance limits.
3. Two analyzers, each with separately logged data, measured the CPMS CO_2 and H_2 concentrations. These duplicate data were averaged for final reporting.
4. Two analyzers were used to measure the NO_X concentrations, but data from only one of the NO_X analyzers at a time was logged, so there is only a single set of recorded NO_X data. Total NO_X was the only recorded value (NO and NO_2 were not recorded). The recorded NO_X data was adjusted for the zero calibration error and the combined span error and air dilution using the calibration data for the analyzer that was being logged at the time.
5. CPMS data was not valid during certain time periods. Invalid CPMS data has been deleted. These time periods included (a) times when the CPMS was off-line for calibrations or maintenance, (b) times when there was some sort of CPMS malfunction such as insufficient sample gas pressure or flow rate, or (c) analyzer malfunction. There were many time periods when DMR product was being drained and product eductor N_2 was vented into the DMR freeboard. The CPMS data for these time periods has not been deleted for the CP2 test.
6. Occasionally the data for only a single analyzer was invalid for some time periods if only that analyzer was malfunctioning, or if, for the NO_X analyzer, the NO_X dilution ratio deviated from the setpoint value of 4:1.
7. Some values, even after calibration correction, can be slightly negative. These values are not normalized to zero, to avoid biasing averages that include these values.
8. The dry basis $\%N_2$ is calculated by difference, 100 - sum of measured species.

[cp-2 cmps cal data aug 3.xls]CPMS dry sum

Table 7-32. CP2 DMR process gas wet composition and NO_X destruction.

				DMR process gas composition (wet basis)									NO_X METC at DMR outlet (ppm wet)	DMR NO_X destruction (%)
				O_2 (wet %)	CO_2 (wet %)	H_2 (wet %)	NO_X (ppm wet)	CO (ppm wet)	THC (ppm wet)	H_2O (wet %)	N_2 (wet %)	Total (wet %)		
Test F	eed	Start	Finish	AT-700-001-O_2	Avg AT-700-002A and B CO_2	Avg AT-700-002A and B H_2	AT-700-004-NO_X	AT-700-003-CO	AT-700-005-THC	Calc	Calc	Calc		Calc
DMR-1	SBW Lite	6/1/2006 5:46	6/3/2006 18:00	0.51	11.5	0.72	4,078	0.21	381	54.8	31.3	99.4	67,042	93.9
DMR-2	SBW w/HM	6/3/2006 18:00	6/7/2006 21:46	0.30	12.4	1.18	4,067	0.22	568	56.7	30.8	102.0	63,540	93.4
DMR-3	SBW w/HM + clay	6/7/2006 21:46	6/8/2006 13:00	0.20	11.9	0.99	7,156	0.21	542	57.8	29.3	101.1	64,876	88.9
Averages				0.34	12.0	0.97	5,100	0.22	497	56.4	30.5	100.8	65,153	92.0

Notes:

1. The corrected, dry-basis CPMS data was adjusted to wet basis to better reflect the actual process gas concentrations.
2. The wet-basis adjustment calculation was made by first calculating the DMR off-gas flowrate, and then the moisture content of the DMR process gas, based on the input flowrates. Then the dry basis values were normalized to wet-basis values by multiplying by the factor (1-%moisture/100).
3. Unlike the dry basis N_2 values, which were determined by difference of the measured gas species from 100%, the wet basis N_2 values were independently calculated like the wet basis H_2O concentration was - using the input N_2 flow rates and the calculated DMR outlet process gas flow rate.
4. Some values, even after calibration correction, can be slightly negative. These values are not normalized to zero, to avoid biasing averages that include these values.
5. The DMR and CRR NO_X destruction were calculated by a NO_X mass balance. The DMR NO_X destruction was calculated using the input flow rate of nitrate in the feed to calculate the NO_X Maximum Theoretical Emission Concentration (MTEC) at the DMR outlet based on the equation $2NO_3 = 2NO_2 + O_2$. The CRR NO_X destruction was calculated by a NO_X mass balance across the CRR.
6. Data that is not valid, for time periods during which there were process upsets such as DMR bed drains, or periods when the CPMS was undergoing maintenance or calibrations, has been deleted.

cp-2 cmps cal data aug 3.xls]CPMS wet sum

Table 7-33. CP1 stack gas dry composition.

			Stack gas composition (dry basis)											Average $\%O_2$ in input gas	7% O_2 correction factor	Concentration of regulated species, dry (@7% O_2)		
			O_2 (%)	CO_2 (%)	NO (ppm)	NO_2 (ppm)	NO_X (ppm)	CO (ppm)	THC (ppm)	SO_2 (ppm)	$HCl+Cl_2$ (ppm as HCl)	N_2 (%)	Total (%)			CO (ppm)	THC (ppm)	$HCl+Cl_2$ (ppm as HCl)
Date Test	Period	Test	CEM	CEM	CEM		CEM	CEM		CEM	CEM	M26A	by diff	Calc	Calc	Calc		CEM	CEM	M26
18-Jan-06	1730–2107	1, day 1	10.5	17.7	1,863	126	1,988	22	<0.4	35	0.9	71.8	100.0		37.2	0.52	11	<0.2	0.5
19-Jan-06	1000–1330	1, day 2	10.0	17.1	2,465	170	2,637	25	<0.4	31	—	72.9	100.0		36.9	0.52	13	<0.2	—
27-Jan-06	1000–1310	2A	9.2	25.0	433	3	433	62	<0.5	373	0.9	65.8	100.0		38.8	0.47	29	<0.2	0.4
28-Jan-06	1230–1640	3B	12.2	24.1	565	-1	562	45	<0.5	68	0.9	63.7	100.0		42.6	0.46	21	<0.2	0.4
29-Jan-06	1040–1426, 1600–1930	4A-1 15.4		23.1	357	-5	351	63	<0.5	50	10.8	61.4	100.0		45.4	0.47	29	<0.2	5.1
30-Jan-06	1025–1415, 1620–1950	4A-2 17.7		21.1	462	8	460	64	<0.5	51	18.9	61.1	100.0		43.6	0.54	34	<0.3	10.2
31-Jan-06	1110–1525	4A-3 day 1	9.4	22.4	1,175	45	1,221	16	<0.5	77	—	68.1	100.0		46.3	0.38	6	<0.2	—
1-Feb-06	1015–1335, 1600–2020	4A-3 day 2	10.7	28.9	1,110	25	1,127	24	<0.5	75	13.0	60.5	100.0		46.4	0.39	9	<0.2	5.1
2-Feb-06	1015–1340, 1450–1810	4A-4 10.2		28.5	1,069	41	1,106	19	<0.5	38	13.0	61.2	100.0		40.9	0.46	9	<0.2	5.9
3 Feb 06	1355–1720	4A-5 day 1	9.1	32.3	1,528	45	1,568	20	<0.5	70	11.7	58.7	100.0		42.5	0.42	8	<0.2	4.9
4-Feb-06	0935–1351	4A-5 day 2	8.9	30.5	1,153	19	1,168	17	<0.6	41	—	60.6	100.0		38.6	0.47	8	<0.3	—
4-Feb-06	1805–2205	4A-6 day 1	12.0	18.8	393	0	389	85	<0.5	2	11.9	69.2	100.0		36.7	0.57	48	<0.3	6.7
8-Feb-06	1400–1722	4A-6 day 2	9.6	15.5	337	4	336	61	<0.5	8	—	74.9	100.0		36.6	0.52	32	<0.2	—
9-Feb-06	1000–1415	5	12.5	17.5	617	1	503	39	<0.4	6	11.0	70.0	100.0		32.5	0.70	28	<0.3	7.7
10-Feb-06	0905–1241	6	12.1	18.7	1,990	82	2,077	83	<0.4	6	6.3	69.2	100.0		34.0	0.64	53	<0.3	4.0
		Averages	11.3	22.7	1,034	38	1,062	43	<0.5	62	9.0	66.0	100.0		39.9	0.50	23	<0.2	4.6

Notes:

1. The stack gas THC was typically not detected. The estimated detection limit of the analyzer, at 0.2 ppm (wet basis), was used when the average THC level was less than the detection limit.
2. All stack CEMS data has been corrected for applicable span drift and calibration error.
3. The 7% O_2 correction factor is 14/(E - Y), were E is the average O_2 content of all input air, O_2, and N_2, and Y = measured O_2 concentration in the stack gas, on a dry basis (FR 55[82], 17918, April 27, 1990, and 40 CFR 264.343). The oxygen contents of the simulant feed and of the coal and petroleum coke are not included in this calculation, making the calculation of E conservatively low.
4. The average O_2 content if all input air, O_2, and N_2 was determined based on these input flows:
   (a) Air: simulant feed atomizing air, ATG air, and OGC atomizing air.
   (b) N_2: Total purge N_2, shot pot N_2, HTF and PBF pulse N_2, and ATG nozzle purge N_2
   (c) O_2: DMR fluidizing O_2, ATG O_2, and freeboard O_2.
5. The HCl and Cl_2 results from all test conditions were validated by CWI. No data qualifiers were required based on this data validation.
6. The N_2 concentration is determined by difference.

[cp1 off-gas emissions and nox destruct aug 5.xls]Stack dry CEM

Table 7-34. CP1 stack gas composition (wet basis), system NO_X destruction, and mass emission rates.

			Stack gas composition (wet)											Mass emission rate of key species (lb/hr)					Stack gas NO_X MTEC (ppm)
			O_2 (%)	CO_2 (%)	NO (ppm)	NO_2 (ppm)	NO_X (ppm)	CO (ppm)	THC (ppm)	SO_2 (ppm)	N_2 (%)	H_2O (%)	Total (%)	NO_X (as NO_2)	CO	THC	SO_2	$HCl+Cl_2$ (ppm as HCl)	
Date Test	Period	Test	CEM	CEM	CEM	CEM	CEM	CEM	CEM	CEM	Diff	Trains	Calc	CEM	CEM	CEM	CEM	M26	CEM
18-Jan-06 1730–2107		1, day 1	4.9	8.2	865	58	923	10	<0.2	16	33.3	53.6	100.0	1.48	0.010	<0.0003	0.036	0.00061	26,624
19-Jan-06	1000–1330	1, day 2	4.8	8.2	1,181	82	1,264	12	<0.2	15	34.9	52.1	100.0	2.25	0.013	<0.0004	0.036	—	23,962
27-Jan-06 1000–1310		2A	3.6	9.7	168	1	168	24	<0.2	145	25.6	61.2	100.0	0.38	0.033	<0.0004	0.462	0.00078	18,522
28-Jan-06 1230–1640		3B	5.3	10.5	246	-1	245	20	<0.2	30	27.7	56.5	100.0	0.62	0.031	<0.0005	0.105	0.00064	17,691
29-Jan-06 1040–1426, 1600–1930		4A-1	6.6	9.9	153	-2	151	27	<0.2	21	26.4	57.0	100.0	0.30	0.033	<0.0004	0.059	0.0074	22,760
30-Jan-06 1025–1415, 1620–1950		4A-2	7.6	9.1	198	3	197	27	<0.2	22	26.2	57.1	100.0	0.43	0.036	<0.0004	0.065	0.015	20,576
31-Jan-06	1110–1525	4A-3, day 1	3.5	8.2	432	17	449	6	<0.2	28	25.0	63.2	100.0	1.05	0.009	<0.0004	0.092	—	18,909
1-Feb-06 1015–1335, 1600–2020		4A-3, day 2	4.0	10.8	416	9	423	9	<0.2	28	22.7	62.5	100.0	0.98	0.013	<0.0004	0.091	0.0091	18,467
2-Feb-06 1015–1340, 1450–1810		4A-4	4.0	11.0	413	16	428	7	<0.2	15	23.7	61.3	100.0	0.94	0.010	<0.0004	0.045	0.0089	20,220
3 Feb 06	1355–1720	4A-5, day 1	3.4	12.2	577	17	592	7	<0.2	26	22.2	62.2	100.0	1.40	0.011	<0.0005	0.087	0.0084	23,849
4-Feb-06 0935–1351		4A-5, day 2	3.2	11.0	417	7	422	6	<0.2	15	21.9	63.9	100.0	1.04	0.009	<0.0005	0.050	—	22,035
4-Feb-06 1805–2205		4A-6, day 1	4.8	7.6	158	0	157	34	<0.2	1	27.9	59.7	100.0	0.31	0.040	<0.0008	0.002	0.0075	29,380
8-Feb-06 1400–1722		4A-6, day 2	4.0	6.5	142	2	141	25	<0.2	3	31.5	58.0	100.0	0.27	0.030	<0.0004	0.009	—	32,098
9-Feb-06 1000–1415		5	6.4	8.9	315	0	257	20	<0.2	3	35.7	49.0	100.0	0.47	0.023	<0.0004	0.008	0.0083	23,410
10-Feb-06 0905–1241		6	5.9	9.1	971	40	1,013	41	<0.2	3	33.8	51.2	100.0	1.86	0.045	<0.0004	0.008	0.0045	23,831
Averages 4.8				9.4	444	17	455	18	<0.2	25	27.9	57.9	100.0	0.92	0.023	<0.0004	0.077	0.00647	22,822

Notes:

1. The stack gas THC was typically not detected. The estimated analyzer detection limit, at 0.2 ppm (wet basis), was used when the average THC level was less than the detection limit.
2. All stack CEMS data has been corrected for applicable span drift and calibration error.
3. MTEC = Maximum Theoretical Emission Concentration, calculated from the feedrate of NO_3 and the stack gas flowrate.
4. The S balance has not been adjusted for the amount, if any, of SO_2 that may have evolved from the S-impregnated carbon bed.

Average S and Cl emission rates, lb/hr	0.039	0.00629
Average simulant feedrate, gpm	0.29	
Target feed S and Cl concentration, gm/L	3.4	1.2
Average S and Cl feedrate, lb/hr	0.49	0.17
Average system removal efficiency, %	84.4	96.2

Table 7-35. CP2 stack gas dry composition for the manual sampling time periods.

			Stack gas composition (dry basis)													Concentration of regulated species, dry (@7% O_2)	
			O_2 (%)	CO_2 (%)	NO (ppm)	NO_2 (ppm)	NO_X (ppm)	CO (ppm)	THC (ppm)	SO_2 (ppm)	N_2 (%)	Total (%)	Carbon bed inlet SO_2 (ppm)	Avg %O_2 in input gas	7% O_2 correction factor	CO (ppm)	THC (ppm)
Date Test	Period	Test	CEM	CEM	CEM	CEM	CEM	CEM	CEM	CEM	by diff	—	CEM	—	—	—	—
1-Jun-06	1550–1910	1	7.5	17.0	384	10	398	70	1.1	108	75.5	100.0	—	21.8	0.98	68	1.0
3-Jun-06	1150–1550	2	5.6	18.8	511	3	522	71	0.3	19	75.5	100.0	—	20.7	0.93	66	0.3
5-Jun-06	1110–1440	3	7.9	17.1	227	-2	231	77	0.5	23	75.0	100.0	—	20.8	1.08	83	0.5
6-Jun-06	1040–1415	4	9.5	17.2	564	25	595	62	0.3	52	73.2	100.0	—	23.2	1.02	63	0.3
7-Jun-06	0950–1310	5	8.9	17.1	460	-6	466	39	0.2	62	74.1	100.0	—	22.7	1.01	39	0.2
7-Jun-06	1030–1305	5	Carbon bed inlet/outlet triplicate tests						—	62	—	—	41	—	—	—	—
7-Jun-06	1745–2110	6	8.5	17.9	560	-2	563	45	0.2	84	73.6	100.0	—	22.7	0.99	44	0.2
7-Jun-06	1745–2120	6	Carbon bed inlet/outlet triplicate tests						—	85	—	—	42	—	—	—	—
Averages			8.0	17.5	451	5	463	60	0.5	58	74.5	100.0	41	22.0	1.00	61	0.4
HWC MACT standard																100	10
Average emission, % of MACT standard																61%	4%

Notes:

1. All stack CEMS data has been corrected for applicable span drift and calibration error.
2. The 7% O_2 correction factor is 14/(E - Y), where E is the average O_2 content of all input air, O_2, and N_2, and Y = measured O_2 concentration in the off-gas, on a dry basis (FR 55[82], 17918, April 27, 1990, and 40 CFR 264.343). The oxygen contents of the simulant feed and of the coal and petroleum coke are not included in this calculation, making the calculation of E conservatively low.
3. The average O_2 content of all input air, O_2, and N_2 was determined based on the following input flows:
   (a) Air: simulant feed atomizing air, OGC atomizing air, and about 16 scfm total air inleakage (probably at the ID fans).
   (b) N_2: Total purge N_2, shot pot N_2, CRR ATG N_2, and HT and PBF pulse N_2 (the total unlogged N_2 flowrate was estimated at 4 scfm).
   (c) O_2: DMR fluidizing O_2 and CRR ATG O_2.
4. The N_2 concentration is determined by difference.

[cp2 off-gas emissions aug 8.xls]Stack dry CEM

Table 7-36. CP2 stack gas dry composition for the CRR test conditions.

Test Sta	rt	Finish	COT duration (hrs)	Dry stack composition									CRR outlet O_2 (wet %)
				O_2 (%)	CO_2 (%)	NO (ppm)	NO_2 (ppm)	NO_X (ppm)	CO (ppm)	THC (ppm [wet basis])	SO_2 (ppm)	N_2 (%)	
				AT-500-001	AT-500-002	AT-500-003	AT-500-004	AT-500-005	AT-500-006	AT-500-007	AT-500-008	FT-400-002	AT-300-001
CRR-1	6/1/2006 5:46	6/1/2006 19:47	13.6	7.9	17.0	468	125	599	68	0.8	113	75.1	2.4
CRR-2	6/1/2006 19:47	6/2/2006 9:00	12.3	6.9	17.3	736	75	816	72	-0.1	30	75.8	1.2
CRR-3	6/2/2006 16:57	6/3/2006 5:52	12.6	6.6	18.4	744	35	784	73	1.0	56	75.0	1.0
CRR-4	6/2/2006 9:00	6/2/2006 16:57	7.9	6.4	17.8	1,311	8	1,329	78	0.2	32	75.8	0.7
CRR-5	6/3/2006 5:52	6/3/2006 16:50	11.0	5.6	17.1	573	15	593	81	0.6	27	77.3	0.9
CRR-6	6/3/2006 16:50	6/4/2006 5:00	12.2	6.3	17.8	569	20	594	76	0.8	46	75.9	1.0
CRR-7	6/4/2006 5:00	6/5/2006 0:03	10.0	7.1	17.7	158	0	160	85	0.4	37	75.1	0.9
CRR-8	6/5/2006 0:03	6/5/2006 7:30	7.5	7.1	17.9	248	3	252	88	0.2	30	75.1	1.1
CRR-9	6/5/2006 7:30	6/5/2006 19:10	11.2	7.1	14.5	467	25	496	66	0.5	38	78.4	2.2
CRR-10	6/5/2006 19:10	6/6/2006 7:21	12.2	8.4	17.8	536	26	565	67	0.6	68	73.7	2.8
CRR-11	6/6/2006 7:21	6/6/2006 19:12	11.9	9.2	17.5	633	34	671	59	0.4	61	73.3	3.7
CRR-12	6/6/2006 19:12	6/7/2006 7:03	11.7	8.0	17.7	745	40	788	52	0.5	252	74.3	2.4
CRR-13	6/7/2006 7:03	6/7/2006 21:55	14.9	8.4	17.2	708	7	719	37	0.2	66	74.4	3.0
CRR-14	6/7/2006 21:55	6/8/2006 7:56	9.3	8.9	17.2	1,426	18	1,452	29	0.2	69	73.9	3.3
CRR-15	6/8/2006 7:56	6/8/2006 13:00	5.7	9.1	18.9	472	3	478	42	0.1	56	72.0	2.9
Averages (Total COT)			163.8	7.5	17.4	653	29	686	65	0.4	66	75.0	2.0

Notes:

1. CRR-7 Averages do not include the time the process was down.
2. These stack CEMS data have not been corrected for calibration error. In most cases, no correction is necessary because the drift and calibration error is within acceptance limits.
3. The N_2 concentration is determined by difference.

[gas comp and nox destruct aug 1.xls]DMR res T

Table 7-37. CP2 Stack gas wet composition and mass emission rates for the manual sampling time periods.

			Stack gas composition (wet)											Carbon bed inlet SO_2 (ppm)	Mass emission rate of key species (lb/hr)							Stack gas NO_X MTEC (ppm)	System NO_X removal efficiency (%)
			O_2 (%)	CO_2 (%)	NO (ppm)	NO_2 (ppm)	NO_X (ppm)	CO (ppm)	THC (ppm)	SO_2 (ppm)	N_2 (%)	H_2O (%)	Total (%)		NO_X (as NO_2)	CO	THC	Stack SO_2	Carbon bed inlet SO_2	SO_2 from carbon bed	$HCl+Cl_2$ (ppm as HCl)		
Date	Test Period	Test	CEM	CEM	CEM	CEM	CEM	CEM	CEM	CEM	—	Trains	—	CEM	CEM	CEM	CEM	CEM	CEM	—	—	—	—
1-Jun	1550–1910	1	4.0	9.1	205	5	212	37	0.6	58	40.4	46.6	100.0	—	0.40	0.043	0.0004	0.150	—	—	—	22,847	99.1
3-Jun	1150–1550	2	2.8	9.2	250	2	255	34	0.1	9	36.9	51.2	100.0	—	0.52	0.043	0.0006	0.026	—	—	—	20,860	98.8
5-Jun	1110–1440	3	4.0	8.7	115	-1	117	39	0.2	12	38.1	49.2	100.0	—	0.23	0.047	0.0009	0.032	—	—	—	20,806	99.4
6-Jun	1040–1415	4	4.8	8.7	284	13	300	31	0.2	26	36.9	49.2	100.0	—	0.62	0.039	0.0005	0.075	—	—	—	21,154	98.6
7-Jun	0950–1310	5	4.5	8.6	232	-3	235	20	0.2	31	37.3	49.6	100.0	—	0.47	0.024	0.0003	0.088	—	—	—	22,650	99.0
7-Jun	1030–1305	5	Carbon bed inlet and outlet triplicate tests						—	31	—	49.6	—	20	—	—	—	0.087	0.057	0.030	—	—	—
7-Jun	1745–2110	6	4.2	8.9	279	-1	281	22	0.2	42	36.7	50.1	100.0	—	0.54	0.026	0.0003	0.111	—	—	—	23,392	98.8
7-Jun	1745–2120	6	Carbon bed inlet and outlet triplicate tests						—	43	—	50.1	—	21	—	—	—	0.114	0.056	0.057	—	—	—
Averages			4.0	8.9	228	2	233	31	0.3	31	37.7	49.5	20.7		0.46	0.037	0.0005	0.085	0.057	0.044	—	21,952	98.9

Notes:

1. The stack gas THC was typically detected, but at levels near the estimated detection limit of the analyzer, at 0.2 ppm (wet basis).
2. All stack CEMS data has been corrected for applicable span drift and calibration error.
3. MTEC = Maximum Theoretical Emission Concentration, calculated from the feedrate of NO_3 and the stack gas flowrate.
4. The S balance data includes the calculation of the S system removal efficiency based on the total stack SO_2 emission rate and based on measurements of the process SO_2 emission upstream of the carbon bed. The difference in the SO_2 emission represents the amount S that evolved from the S-impregnated carbon bed during the test period.

Average S and Cl emission rates, lb/hr	0.043	0.029	0.022	—
Average stimulant feedrate, gpm	0.25			
Target feed S and Cl concentration, gm/L	3.4		—	—
Average S and Cl feedrate, lb/hr	0.49		—	—
Average system removal efficiency, %	91.3%	94.2%	—	—

[cp2 off-gas emissions july 25.xls]Stack wet CEM

Table 7-38. CP2 stack gas composition (wet basis) for the CRR test conditions.

Test Sta	rt	Finish	COT duration (hrs)	Wet stack gas composition										NO_X METC (ppm wet)	System NO_X destruction (%)	CRR NO_X destruction (%)
				O_2 (%)	CO_2 (%)	NO (ppm)	NO_2 (ppm)	NO_X (ppm)	CO (ppm)	THC (ppm)	SO_2 (ppm)	H_2O (%)	N_2 (%)			
				AT-500-001	AT-500-002	AT-500-003	AT-500-004	AT-500-005	AT-500-006	AT-500-007	AT-500-008	— —				
CRR-1	6/1/2006 5:46	6/1/2006 19:47	13.6	4.0	8.6	236 63		303 34		0.8	57	49.5	37.9	24,513	98.7	86.9
CRR-2	6/1/2006 19:47	6/2/2006 9:00	12.3	3.5	8.7	372 38		412 36		-0.1	15	49.5	38.3	26,324	98.4	76.1
CRR-3	6/2/2006 16:57	6/3/2006 5:52	12.6	3.3	9.3	376 17		396 37		1.0	28	49.5	37.9	26,812	98.5	73.5
CRR-4	6/2/2006 9:00	6/2/2006 16:57	7.9	3.2	9.0 662		4	671	40	0.2	16	49.5	38.3	27,047	97.5	63.7
CRR-5	6/3/2006 5:52	6/3/2006 16:50	11.0	2.9	8.6 289		8	300	41	0.6	14	49.5	39.0	26,416	98.8	76.5
CRR-6	6/3/2006 16:50	6/4/2006 5:00	12.2	3.2	9.0	288 10		300 38		0.8	23	49.5	38.3	25,820	98.8	80.0
CRR-7	6/4/2006 5:00	6/5/2006 0:03	10.0	3.6	9.0	80 0		81	43	0.4	19	49.5	37.9	24,941	99.7	95.3
CRR-8	6/5/2006 0:03	6/5/2006 7:30	7.5	3.6	9.0	125 1		127	44	0.2	15	49.5	37.9	25,455	99.5	92.5
CRR-9	6/5/2006 7:30	6/5/2006 19:10	11.2	3.6	7.3	236 13		250 33		0.5	19	49.5	39.6	24,263	98.9	73.8
CRR-10	6/5/2006 19:10	6/6/2006 7:21	12.2	4.3	9.0	271 13		286 34		0.6	35	49.5	37.2	25,121	98.9	75.1
CRR-11	6/6/2006 7:21	6/6/2006 19:12	11.9	4.7	8.8	320 17		339 30		0.4	31	49.5	37.0	23,911	98.6	73.2
CRR-12	6/6/2006 19:12	6/7/2006 7:03	11.7	4.0	8.9	376 20		398 26		0.5	127	49.5	37.5	24,971	98.4	81.2
CRR-13	6/7/2006 7:03	6/7/2006 21:55	14.9	4.2	8.7 358		3	363	19	0.2	33	49.5	37.6	25,778	98.6	75.7
CRR-14	6/7/2006 21:55	6/8/2006 7:56	9.3	4.5	8.7 720		9	733	15	0.2	35	49.5	37.3	25,405	97.1	71.3
CRR-15	6/8/2006 7:56	6/8/2006 13:00	5.7	4.6	9.5 239		1	241	21	0.1	28	49.5	36.4	28,543	99.1	92.3
Averages (Total COT)			163.8	3.8	8.8	330 15		347 33		0.4	33	49.5	37.9	25,688	98.6	79.1

Notes:

1. CRR-7 Averages do not include the time the process was down.
2. These stack CEMS data have not been corrected for calibration error. In most cases, no correction is necessary because the drift and calibration error is within acceptance limits.
3. The N_2 concentration is determined by difference.

[gas comp and nox destruct aug 1.xls]DMR res T

This page is intentionally left blank.

7.7.4 NO_X Destruction, CO, and THC Emissions

The DMR and the CRR work together to destroy NO_X, CO, and hydrocarbon emissions. Stack concentrations of THC typically ranged from non-detectable at a detection limit of about 0.2 ppm up to about 0.6 ppm (reported as propane), regardless of system operating condition. THC levels ranged well under 10% of the Hazardous Waste Combustor (HWC) Maximum Achieveable Control Technology (MACT) standard of 10 ppm (dry @ 7% O_2) for new facilities. NO_X and CO levels were more variable and have been compared with various operating conditions to show how well they correlate with operating conditions that can be readily monitored and controlled.

The CP1 test condition average wet basis stack CO and O_2 levels are compared to the CRR outlet O_2 concentration (also wet basis) in Figure 7-54. A relationship between the stack O_2 and the CRR outlet O_2 is evident and expected, since the stack O_2 concentration results from the sum of O_2 in the CRR outlet gas and the O_2 added to the process in the air used to atomize the cooling water in the OGC. Stack CO levels did not correlate well with the CRR outlet O_2 levels during CP1, because other factors, mainly the CRR temperature, CRR bed height, and CRR carbon inventory, could have also affected the stack CO levels. While a correlation between the stack CO and CRR outlet O_2 levels is likely, this correlation appears to be affected by other factors.

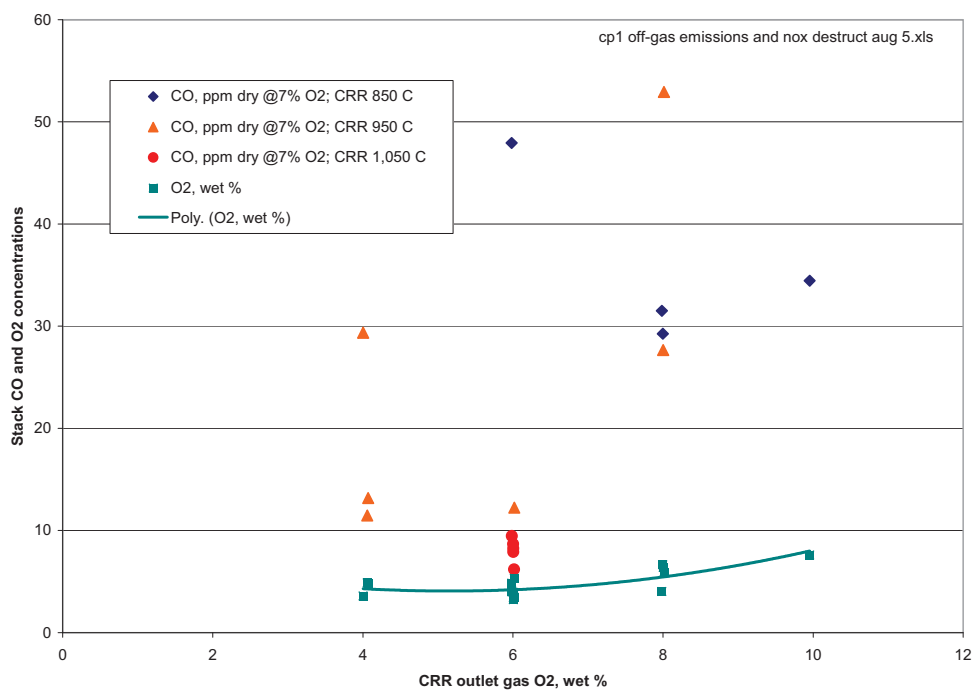

Figure 7-54. Stack gas O_2 and CO levels compared to CRR outlet O_2 levels for CP1.

Figure 7-55 shows that during CP1 the stack gas CO levels decreased with increasing CRR bed temperature. Some data scatter exists in these and other test-condition-average concentrations because of other factors (such as the CRR outlet O_2, CRR bed height, and CRR bed carbon inventory). The CRR freeboard temperature might also affect these concentrations, but was not controlled independently from the CRR bed temperature. The CRR freeboard temperatures were monitored at several locations, along with the CRR outlet gas temperature. The gas temperature tended to decrease as the gas flowed up through the freeboard and out of the CRR, but the gas temperature near the bed was very close to the bed temperature.

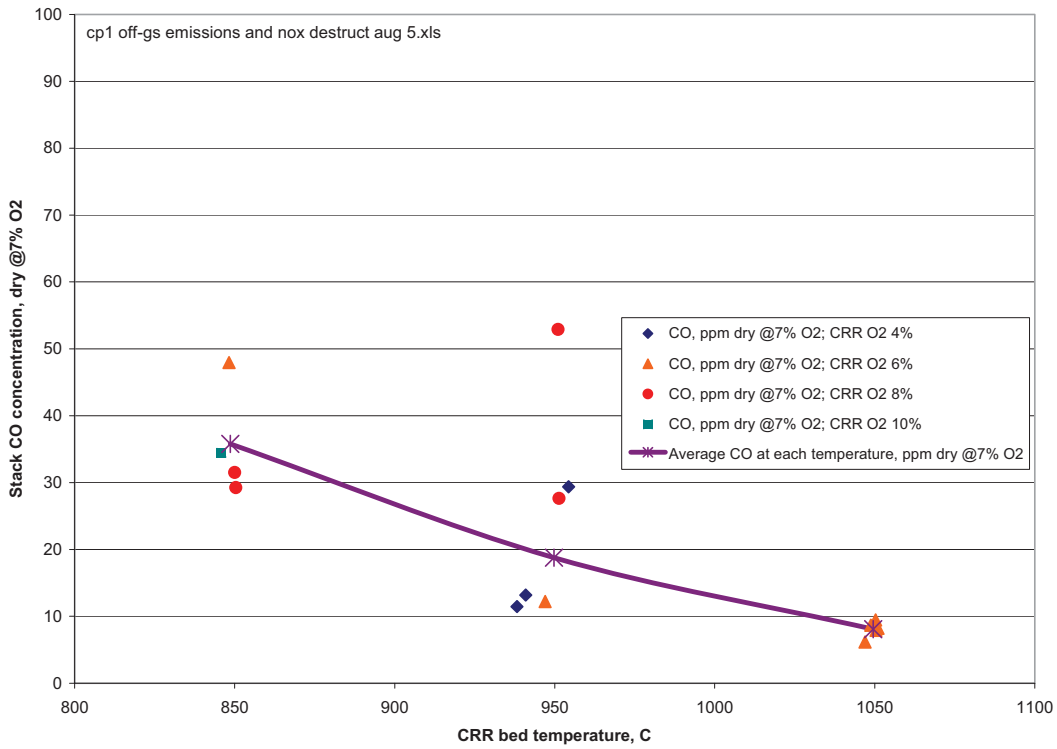

Figure 7-55. Stack gas CO levels for different CRR bed temperatures.

Figure 7-56 shows CO measurements for the 15 different CRR test conditions of CP2. During CP2, the CRR temperature was held relatively constant, normally ranging within ±10°C of 950°C. During CP1 the stack CO averaged 23 ppm (dry, corrected to 7% O_2) and the stack THC was nondetectable at a detection limit of 0.2 ppm. During CP2, the stack CO and THC averaged 61 ppm and 0.4 ppm respectively (dry, corrected to 7% O_2).

Both CO and THC trended higher during CP2 than in CP1, because the ATG gas configuration was changed and the overbed oxygen injection that existed in CP1 was eliminated. With this configuration, ATG O_2 was available in the bed or near the surface of the bed for reaction with carbon in the bed. This forced the level of excess O_2 to be lower than during CP1, because to much O_2 resulted in too much exothermic oxidation of the carbon in the bed, causing the CRR bed temperature to exceed the setpoint. The CRR automatic temperature control lowered the ATG O_2 flow rate to the level necessary to avoid temperature excursions above the setpoint. This caused more reducing conditions in the CRR bed, achieved higher NO_X destruction in the CRR in addition the NO_X destruction achieved in the DMR, but caused the CRR outlet O_2 concentration to be less than the test target O_2 concentration of 4% (wet basis) for most of the test. This resulted in the higher CO and THC in CP2 compared to CP1. The relationship between CRR outlet O_2 and stack CO and THC is more evident with the more constant CRR temperatures during CP2. Both the stack THC and CO concentrations varied inversely with the CRR outlet oxygen concentration. Thus, the best way to reduce THC and CO emissions under the CRR operating conditions of CP1 was to maintain a higher CRR outlet O_2 concentration.

The CO and THC concentrations during CP2 were also related to the amount of carbon in the CRR bed. During the last CRR test conditions of CP2 when the bed carbon inventory was low, the CO and THC concentrations were lower than what had been observed for the previous test conditions, as shown in Figure 7-57.

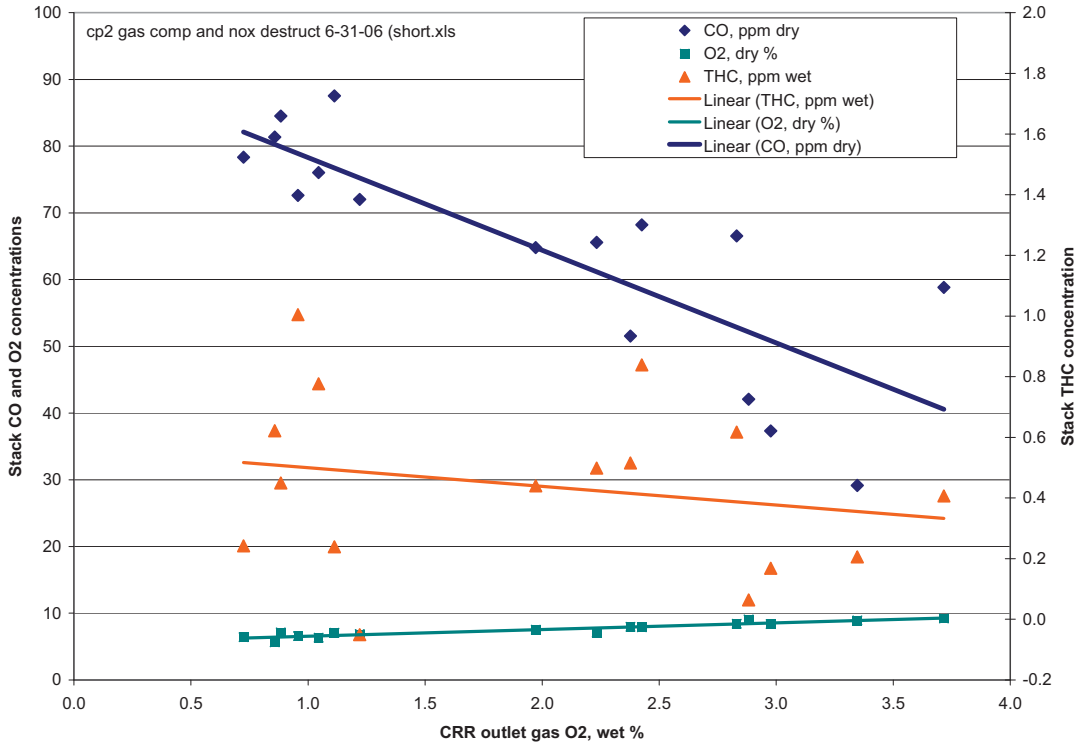

Figure 7-56. Stack gas O_2 and CO levels compared to CRR outlet O_2 levels for CP2.

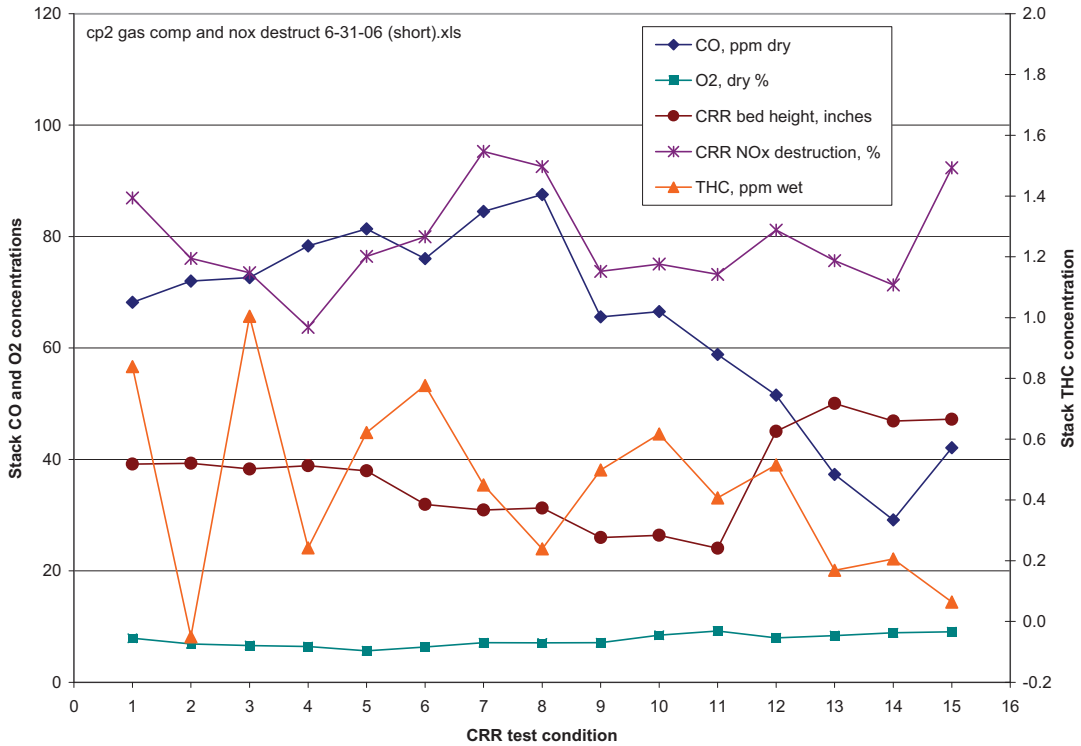

Figure 7-57. Stack gas O_2 and CO levels and CRR NO_X destruction for the CRR test conditions of CP2.

CO levels measured during the stack emission manual sampling time periods tended to vary according to CRR operating conditions, but CO levels averaged below 30% (for CP1) and below 90% (for CP2) of the HWC MACT standard for CO of 100 ppm (dry at 7% O_2) for new facilities.

Figure 7-58 also shows how the CRR NO_X destruction averaged for the different CRR test conditions. The CRR NO_X destruction averaged between about 65–95%. The CRR NO_X destruction tended to be highest when the stack CO was also high (during CRR-7 and CRR-8), but the CRR NO_X destruction was also high near the test end, after the CRR bed height was raised, and the CRR carbon inventory lowered, allowing higher CRR excess O_2 and lower stack CO levels (CRR-12 through CRR-15). The best overall operating condition for CP2 appears to be near the test end, when the bed height was raised, the CRR bed inventory of carbon was lowered, outlet O_2 nearly reached the test setpoint of 4% (wet basis), CO levels averaged lowest, and CRR NO_X destruction was still relatively high at 70–90%.

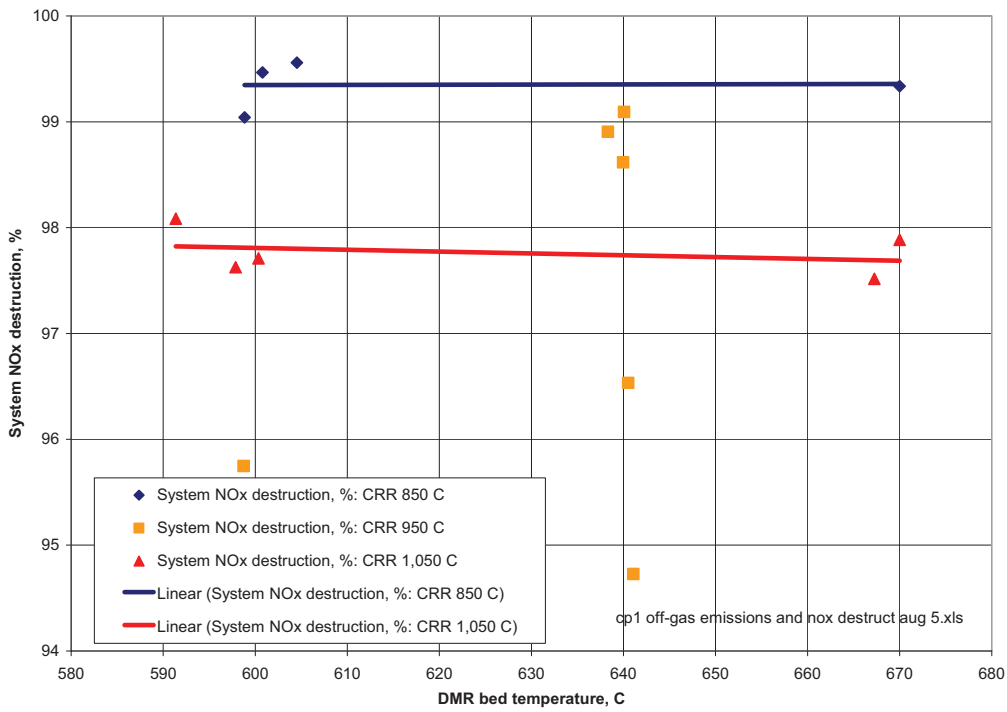

Figure 7-58. System NO_X destruction compared to the DMR bed temperature for CP1.

System NO_X destruction for CP1 is compared to the DMR bed temperature in Figure 7-58. System NO_X destruction is the degree to which the nitrates in the simulant feed are destroyed (converted primarily to N_2) in the complete system consisting of the DMR, the CRR, and downstream equipment. NO_X destruction, even when charted separately by CRR bed temperature, does not appear to depend on the DMR operating temperature for the tested conditions. Other factors such as DMR H_2 levels and CRR operating conditions can also affect system NO_X destruction.

The CP1 DMR, total system, and CRR NO_X destruction are compared to the DMR H_2 levels in Figure 7-59. When the DMR H_2 level approaches zero, stoichiometric conditions can be insufficient for nitrate destruction in the DMR, resulting in low NO_X destruction in the DMR (and possibly other undesired conditions such as incomplete carbonation of the solid DMR product). The degree of CRR NO_X destruction also varies with DMR process gas H_2 levels, although data scatter exists, caused by the various DMR and CRR process variations for different CP1 test conditions. Considering DMR, CRR, and

total system NO_X destruction, the most stable and highest NO_X destruction tended to occur when the wet basis DMR H_2 levels ranged above 1%. When the DMR H_2 concentration exceeded 1% (wet), then the DMR NOx destruction exceeded 92%; The CRR NO_X destruction exceeded 50%; and the total system NO_X destruction exceeded 98%. A reasonable operating range for the DMR H_2 level based on these test results might be 1% +0.5% (wet basis), to ensure adequate NO_X destruction without excessive coal in the DMR product. This finding is consistent with results from prior steam reforming tests conducted by the Idaho National Laboratory (INL).

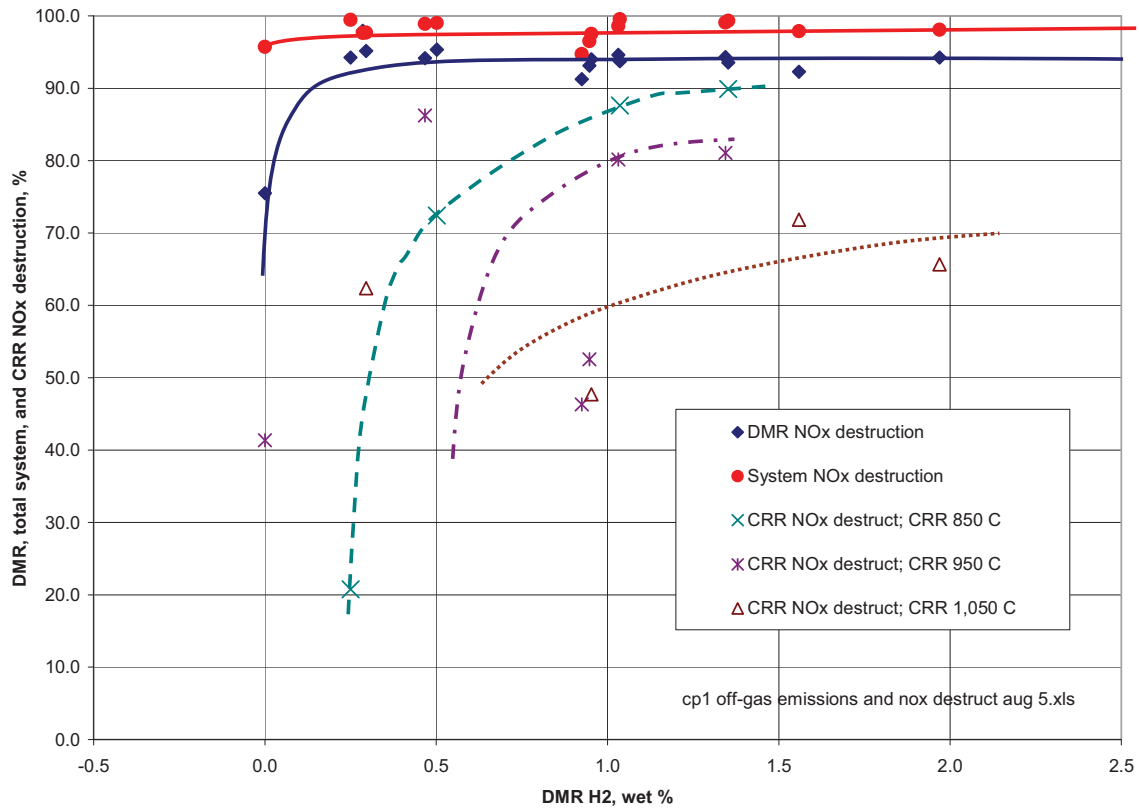

Figure 7-59. DMR, system, and CRR NO_X destruction compared to the DMR H_2 levels for CP1.

The CRR was operated in an oxidizing mode to oxidize H_2, CO, and hydrocarbons from the DMR, but additional NO_X destruction in addition to that achieved in the DMR was typically observed. The level of NO_X destruction in the CRR varied depending on operating conditions and the input levels of NO_X from the DMR process gas. This has also been observed in prior steam reforming tests performed by the INL, and occurs because equilibrium NO_X concentrations at conditions in the DMR and CRR are typically lower than the NO_X concentrations that exit the DMR. NO_X reduction reactions in both the DMR and CRR do not reach chemical equilibrium because of kinetic limitations. The gas residence time in the CRR and the higher CRR temperatures continue to provide NO_X destruction downstream of the DMR, as long as the CRR operating temperature and excess O_2 are not so high the chemical equilibrium shifts to higher NO_X concentrations. The degree of NO_X destruction in the CRR also depends on other parameters including local and overall carbon-oxygen stoichiometry and gas speciation in the CRR.

Figure 7-60 shows system NO_X destruction for the CP2 tests. During CP2, the DMR was held at relatively constant conditions except for H_2 levels that varied according to variations in the coal inventory in the DMR bed. The operation of the CRR was modified by varying the locations of ATG O_2 and N_2 injection in an effort to optimize CRR performance to reduce further reduce stack NO_X emissions. NO_X

destruction during CP2 averaged 98.9%, when the CRR was operated with the modified ATG O_2 injection and more reduced stoichiometry, compared to 98% during CP1 when freeboard O_2 injection was used to control higher CRR outlet gas O_2 levels. With more reducing CRR conditions during CP2, the stack gas CO levels averaged 61 ppm (dry @ 7% O_2), about three times higher than the CP1 average CO concentration of 23 ppm (dry @ 7% O_2).

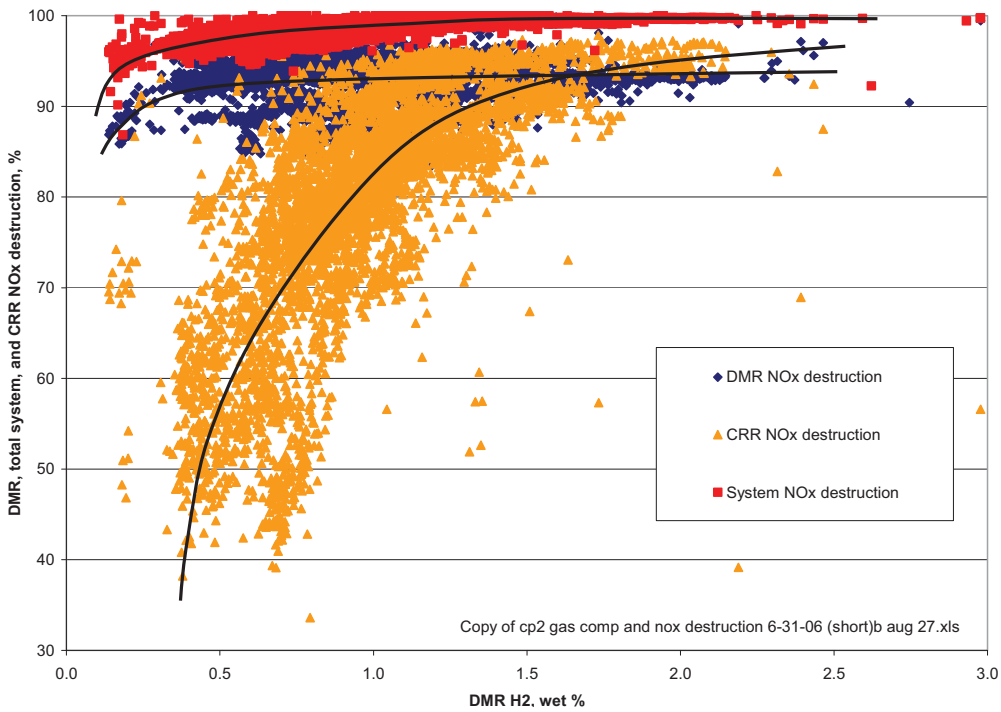

Figure 7-60. DMR, system, and CRR NO_X destruction compared to the DMR H_2 levels for CP2.

System NO_X destruction for the range of medium and high simulant feed rates is shown in Figure 7-61. Slightly higher NO_X destruction was observed for the higher simulant feedrates, but this was because of the higher NO_X METC that resulted from the higher feedrates. The greater difference between the NO_X METC value and the equilibrium NO_X levels for higher simulant feed rates resulted in slightly higher NO_X destruction.

Like the stack CO and THC, several factors including DMR and CRR operating temperatures, CRR excess O_2, and CRR bed height and carbon inventory in the bed can affect the stack NO_X levels. These parameters were varied during CP1 and to a lesser extent in CP2, but they are not always independent, so the responses in the CO, THC, or NO_X concentrations were not always clear or as expected following an operating condition change.

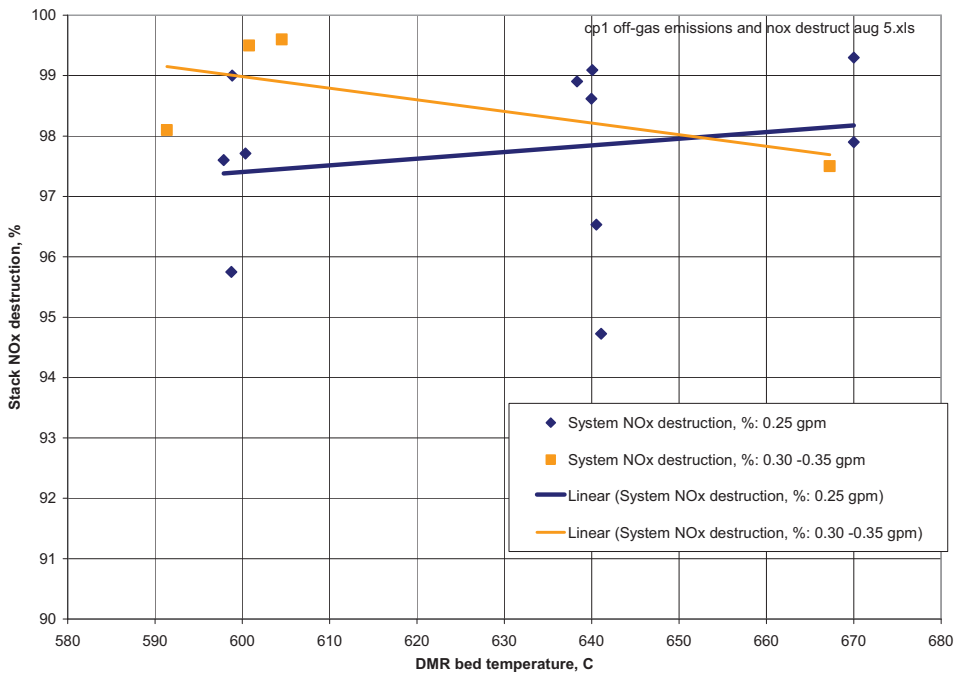

Figure 7-61. System NO_X destruction for medium and high simulant feedrates.

7.7.5 SO_2 Emissions

Stack gas SO_2 was continuously monitored during CP1 and CP2. SO_2 concentrations were occasionally higher than were observed in the prior INL steam reforming tests, which had indicated that both the carbonate and mineralized products from SBW testing efficiently captured SO_4 that was in the simulant feed. Figure 7-62 shows the SO_2 concentrations for CP1 and CP2, when the process gas flowed through the GAC bed. The highest stack gas SO_2 levels during these times occurred when the GAC Bed 3 was at its highest temperatures. SO_2 measurements made during CP2 at the inlet of the GAC bed determined SO_2 emissions directly from the simulant feed, and confirmed that some of the stack gas SO_2 was not from SO_4 in the feed; it was from S evolved from the sulfur-impregnated GAC bed, especially when the GAC bed was at its highest temperatures, and even though these temperatures were well within the design operating range of the GAC bed.

SO_2 levels during CP1 eventually decreased to 1–3 ppm, near the analyzer detection limit, and similar to levels determined in the INL steam reforming tests. These low levels occurred after the GAC bed had been on-line for at least 200 hours, and was apparently releasing less, if any, S after the early high-temperature operation.

The average system removal efficiency for S in the CP1 test, based on an average stack SO_2 concentration of 25 ppm (wet basis), without subtracting any estimated amount of SO_2 thought to come from the GAC bed, was about 84%. Near the end of CP1, when the stack gas SO_2 levels decreased to 1–3 ppm, the calculated system removal efficiency for S increased to over 98–99%, without accounting for any portion of the stack SO_2 levels that that may have evolved from the GAC bed during that time.

The average system removal efficiency for S in the CP2 test, without accounting for S evolved from the GAC bed, was 91%. The CP2 system removal efficiency for S, accounting for S evolved from the GAC bed, was 94%.

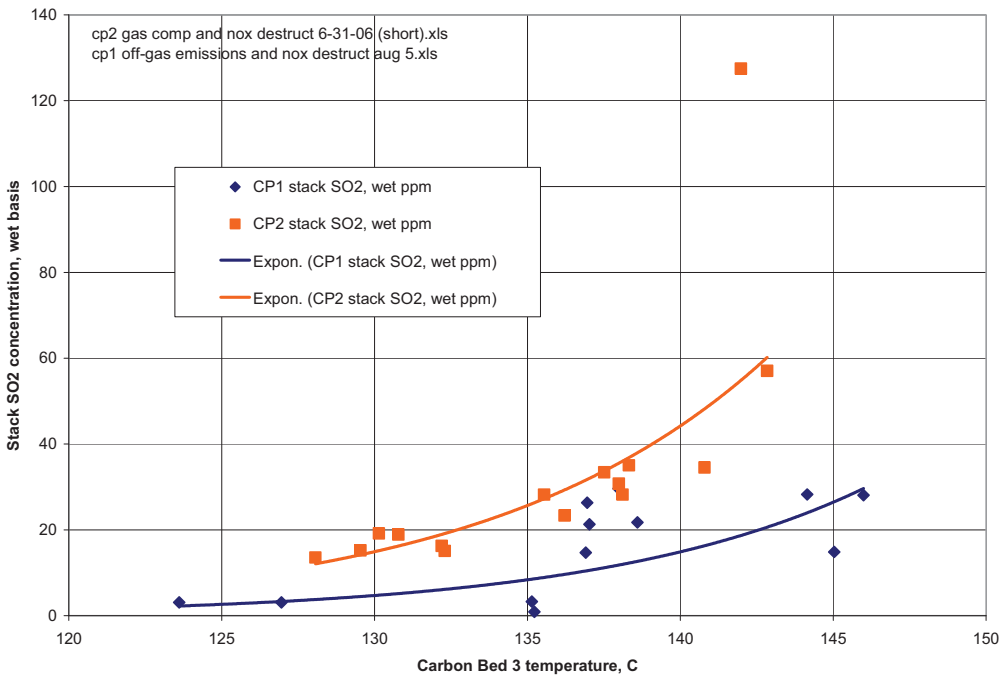

Figure 7-62. Stack gas SO_2 concentrations compared to GAC Bed 3 temperature for CP1 and CP2.

7.7.6 Manual Sample Train Measurements

Manual sampling trains were performed to measure the concentrations and emissions of various pollutant species that were not continuously monitored during CP1 and CP2. These sample trains were performed as simultaneously as practical during specified 3–4 hour sample periods in each test condition. Process operating conditions were held constant (to the degree that was practical) during these sample times. Operating conditions during these sample periods were generally the most stable and controlled conditions of each test condition. Table 7-39 and Table 7-40 show summaries of key operating conditions during the stack manual sample periods for CP1 and CP2.

A validation was performed on stack sample analysis data generated by the sample train measurements during CP1. The data were validated in accordance with the applicable procedures for performing analytical method data validation, the SBW Test Plan [R10], and Quality Assurance Project Plan 1.1 (QAPP) [R21]. A summary of the data validation is included as Appendix A to this document. The complete set of data validation reports is available from the authors of this report if needed.

7.7.7 Stack Gas Temperature, Moisture, and Flow Rate

All of the isokinetic sampling trains measured not only the pollutant species for which the train was configured, but also stack gas temperature, flow rate, and moisture content. The stack gas moisture content has been tabulated with the CEMS wet basis compositions. The stack gas temperature and flow rate measurements are compared with the process temperature and flow rate measurements in Table 7-41 and Table 7-42 for CP1 and CP2. Good agreement generally within ± 5%, was achieved for the installed process temperature sensors and stack gas flowmeter compared to the subcontractor stack gas measurements.

The manual sampling activities during the CP1 tests are summarized below.

Table 7-39. CP1 operating conditions during emission test periods.

				DMR					CRR						
				Simulant feedrate	DM Bed Temp (12" E)	DMR Freeboard Temp (92" S)	Cyclone outlet gas Temp	HTF outlet Temp	CRR Bed Temp (8" S)	CRR Freeboard Temp (54" SE)	CRR Freeboard Temp (150' NE)	CRR outlet gas O_2	OGC outlet gas T	Reheater outlet gas T,	Carbon bed 3 T
				(gpm)	(°C) (	°C) (	°C) (	°C) (	°C) (	°C) (	°C)	(wet %)	(°C) (	°C) (	°C)
Date Test	Period	Test	Test condition summary	FT-200-001	TT-200-003	TT-200-010	TT-200-011	TT-202-005	TT-300-002	TT-300-008	TT-300-011	AT-300-001	TT-400-001	TT-403-001	TT-408 -003
18-Jan-06	1730–2107	1, day 1	Baseline, nominal feedrate and temps, no heavy metals or UDS	0.244	641	572	546	421	950	938	826	4.1	180	184	Off-line
19-Jan-06	1000–1330	1, day 2		0.244	641	543	524	412	951	941	839	4.1	180	184	Off-line
27-Jan-06	1000–1310	2A	Nominal feedrate and temps, include UDS but no heavy metals	0.234	640	583	557	423	948	954	887	4.0	180	170	Off-line
28-Jan-06	1230–1640	3B	Nominal feedrate and temps, include UDS and heavy metals	0.248	640	616	586	440	947	954	904	6.0	180	175	138
29-Jan-06	1040–1426, 1600–1930	4A-1	Nominal feedrate, high DMR temp, low CRR temp, include UDS and heavy metals	0.260	670	611	577	436	850	872	829	8.0	180	175	137
30-Jan-06	1025–1415, 1620–1950	4A-2	Nominal feedrate, low DMR temp, low CRR temp, include UDS and heavy metals	0.255	599	540	516	401	846	862	822	10.0	180	175	139
31-Jan-06	1110–1525	4A-3, day 1	Nominal feedrate, low DMR temp, high CRR temp, include UDS and heavy metals	0.252	598	533	509	391	1,047	1,097	1,044	6.0	180	175	144
1-Feb-06	1015–1335, 1600–2020	4A-3, day 2		0.244	600	534	510	394	1,050	1,100	1,058	6.0	180	175	146
2-Feb-06	1015–1340, 1450–1810	4A-4	Nominal feedrate, high DMR temp, high CRR temp, include UDS and heavy metals	0.258	670	602	570	437	1,049	1,091	1,050	6.0	180	172	145
3 Feb 06	1355–1720	4A-5, day 1	High feedrate, high DMR temp, high CRR temp, include UDS and heavy metals	0.342	667	615	587	458	1,051	1,093	1,107	6.0	180	175	137
4-Feb-06	0935–1351	4A-5, day 2		0.305	591	611	579	445	1,050	1,070	1,098	6.0	180	171	137
4-Feb-06	1805–2205	4A-6, day 1	High feedrate, low DMR temp, low CRR temp, include UDS and heavy metals	0.333	601	553	528	416	848	832	884	6.0	180	171	135
8-Feb-06	1400–1722	4A-6, day 2		0.350	605	564	539	426	850	842	803	8.0	185	167	135
9-Feb-06	1000–1415	5	Nominal feedrate and temps, include heavy metals and 50% extra UDS	0.249	638	579	543	421	951	910	838	8.0	184	181	127
10-Feb-06	0905–1241	6	Nominal feedrate, low DMR temp, nominal CRR temp, simulant diluted to 10%, but with 50% extra UDS	0.249	599	553	519	438	951	763	850	8.0	185	191	124
			Averages	0.287	619	572	542	425	983	978	970	6.7	182	175	137

[cp1 off-gas emissions and nox destruct aug 5.xls]Production Test Overview

Table 7-40. CP2 operating conditions during emission test periods.

				DMR					CRR					
Date Test	period	Test	Feed	Simulant feed rate (gpm)	DMR bed temp. (6" E) (°C)	DMR free board temp. (92" S) (°C)	DMR outlet gas temp (°C)	HTF outlet temp (°C)	CRR bed temp. (8" S) (°C)	CRR freeboard temp. (54" SE) (°C)	CRR freeboard temp. (150" NE) (°C)	CRR outlet gas O_2 (wet %)	OGC outlet gas temp (°C)	Carbon Bed 3 Temp (°C)
				FT-200-001	TT-200-002	TT-200-010	TT-200-011	TT-202-005	TT-300-003	TT-300-008	TT-300-011	AT-300-001	TT-400-001	TT-408-003
1-Jun-06	1550–1910	1	Lite	0.230	641	568	519	381	953	945	834	1.8	165	143
3-Jun-06	1150–1550	2	Lite	0.248	641	601	557	414	968	960	877	0.51	170	128
5-Jun-06	1110–1440	3	Metals & rad surr	0.238	642	587	540	403	954	949	872	1.5	170	130
6-Jun-06	1040–1415	4	Metals & rad surr	0.241	642	591	545	406	958	946	882	3.9	170	137
7-Jun-06	0950–1310	5	Metals & rad surr	0.252	642	592	543	408	951	938	858	3.0	170	136
7-Jun-06	1745–2110	6	Metals & rad surr	0.262	641	586	540	404	953	940	860	2.9	170	140
			Averages	0.245	642	588	541	403	956	946	864	2.3	169	136

[cp2 off-gas emissions aug 8.xls]CP2 Overview

Table 7-41. CP1 stack temperature and flow-rate measurements.

			Average stack gas temperature (°C)				Average stack gas flow rate		
Date Test	period	Test	From DACS	From manual sampling	DACS % difference from reference method	From DACS (lb/min)	From manual sampling (lb/min)	From manual sampling (scfm)	DACS % difference from reference method
			TT-500-1	—	—	FT-500-000	— — —		
18-Jan-06	1730–2107	1, day 1	114	112	2.0%	15.2	14.1	226	8.0%
19-Jan-06	1000–1330	1, day 2	118	116	2.0%	16.0	15.7	250	2.0%
27-Jan-06	1000–1310	2A	139	135	2.9%	19.5	19.0	311	2.4%
28-Jan-06	1230–1640	3B	126	124	1.3%	19.2	20.3	344	-5.6%
29-Jan-06	1040–1426, 1600–1930	4A-1 121		119	2.3%	17.9	17.5	280	2.1%
30-Jan-06	1025–1415, 1620–1950	4A-2 126		122	3.2%	18.9	21.2	305	-10.8%
31-Jan-06	1110–1525	4A-3, day 1	130	129	0.5%	19.2	19.6	328	-2.3%
1-Feb-06	1015–1335, 1600–2020	4A-3, day 2	132	130	1.7%	19.6	19.9	325	-1.6%
2-Feb-06	1015–1340, 1450–1810	4A-4 130		128	1.6%	18.8	19.2	313	-1.9%
3 Feb 06	1355–1720	4A-5, day 1	127	124	2.3%	20.6	21.4	352	-4.0%
4-Feb-06	0935–1351	4A-5, day 2	126	129	-2.7%	19.8	21.0	340	-5.4%
4-Feb-06	1805–2205	4A-6, day 1	122	124	-1.4%	18.0	16.6	279	8.3%
8-Feb-06	1400–1722	4A-6, day 2	126	129	-2.7%	17.7	16.2	268	9.5%
9-Feb-06	1000–1415	5	115	112	2.6%	16.4	16.7	262	-2.0%
10-Feb-06	0905–1241	6	112	110	1.3%	15.8	16.4	256	-3.7%
Averages 124				123	1.1%	18.2	18.3	296	-0.3%

Notes:
1. Standard temperature is 70 °F, and standard pressure is 1 atm.
2. The stack gas pressure used to convert the FT-500 units to scfm is 12.1 psig.

[cp1 off-gas emissions and nox destruct aug 5.xls]Off-gas T, Q

Table 7-42. CP2 stack gas temperature and flow-rate measurements.

			Average stack gas temperature (°C)			Average stack gas flow rate			
			From DACS	From manual sampling	DACS % difference from reference method	From DACS (lb/min)	From manual sampling (lb/min)	From manual sampling (wscfm)	DACS % difference from reference method
Date Test	period	Test	TT-500-1	—	—	FT-500-000	— — —		
1-Jun-06 1550	0–1910	1	133	124	7.7%	16.2	17.0	263	-4.5%
3-Jun-06 1150	0–1550	2	119	120	-0.5%	16.7	18.2	287	-7.9%
5-Jun-06 1110	0–1440	3	121	115	5.6%	16.7	17.6	277	-5.2%
6-Jun-06 1040	0–1415	4	128	124	3.0%	17.4	18.3	288	-5.2%
7-Jun-06 0950	0–1310	5	127	119	6.5%	16.9	17.9	282	-5.7%
7-Jun-06 1745	5–2110	6	129	124	4.4%	17.3	17.1	268	1.5%
Averages			126	121	4.5%	16.9	17.7	277	-4.5%

Notes:

1. Standard temperature is 70°F, and standard pressure is 1 atm.
2. The test periods were defined by the start and stop times of the manual sample trains. The sample trains were all started and stopped at the same times.
3. The stack gas pressure used to convert the FT-500 units to scfm is 12.1 psig.

[cp2 off-gas emissions aug 8.xls]Offgas T, Q

7.7.7.1 Production Test P-1. The feed solution for P-1 consisted only of the SBW supernatant solution without heavy metals, as described in Table 4-1. The only potential source of organics in the stack stream was the carbon added to both the DMR and the CRR. Because it was necessary to know the baseline contribution of the carbons to the concentration of organics in the stack, separate trains for EPA Method 0010 (for both gravimetric and gas chromatographic fractions and for total SVOCs), Method 0031 for VOCs, and Method 0040 for the FGC fractions were employed. In addition, a Method 29 train was used to determine metals emissions, and a combined Method 5/Method26A train was used to determine Particulate Matter (PM) and hydrochloric acid/chlorine gas, respectively. Because there were no heavy metals added to the feed stream, sampling trains within the GAC adsorber were not used. The Method 0023A train was similarly not used because there was no POHC added to the feed stream.

Manual off-gas sampling took place at five separate locations in the stack. Sampling that required traverse measurements were performed using one of three sets of sampling ports. Each set of ports consisted of two 2-in. diameter pipe nipples welded to the stack at right angles to each other. A 12-point traverse was accomplished along one axis across the diameter of the stack, followed by a second 12-point traverse 90 degrees from the axis of the first traverse. The combined volume of gas from all traverse points for a given sampling event were passed through filters, impingers, or absorbents depending on the particular EPA Method being used. Two other sample ports were used to obtain non-isokinetic samples for EPA Methods 0031 and 0040.

Two additional non-isokinetic sample ports were located downstream of GAC Beds 1 and 2. These ports were used only for the determination of mercury in the off-gas at the outlets of GAC Beds 1 and 2, and not for purposes of providing regulatorily driven emissions data.

A significant preliminary result obtained from the manual sampling of stack gas emissions from P-1 was the level of chlorine emissions. An estimate of total chlorine (in the form of HCl and Cl_2) was 0.8 ppm, which was less than the current HWC MACT standard for chlorine of 21 ppm. Based in part on this finding, the JTG decided to delete test runs that would utilize the Q/S system. All production tests were accomplished with the Q/S system off-line. The concurrence of the CWI Engineering Manager and Project Manager was obtained for this decision.

7.7.7.2 Production Test P-2A. The feed stream for P-2A consisted of the same supernatant solution as used in P-1, but with the addition of UDS. The only difference in the composition of the gas stream that could be attributed to the UDS would be in the metals concentration and the particulate loading; hence, the only sample trains used in P-2A were the Method 29 and Method 5/26A trains. The relative percent difference for comparable stack gas parameters was less than 1%, and no adverse sampling anomalies were noted for this test.

7.7.7.3 Production Test P-3B. In P-3B, minor metals were added to the supernatant solution. Sample trains for Method 29 and Method 5/26A were run to determine if the addition of the minor metals affected the stack gas concentrations of those metals. In addition, Ontario Hydro Method sample trains for the determination of mercury across the GAC adsorber were used. No other sampling anomalies were noted.

7.7.7.4 Production Test P-4A-1. In P-4A-1 (and in all of the tests in series 4A), the full complement of supernatant solution, heavy metals, UDS, and a POHC comprised the feed stream; consequently, the full suite of nine different sample trains was used in order to obtain a complete profile of the off-gas composition. The sampling was completed during a single shift. All measured stack gas parameters had a relative percent difference of less than 4%, and all isokinetic sample trains were within the 90–110% range of acceptability. One anomaly occurred during the conduct of the Method 0010

SVOC train. A kink in the cooling water line may have subjected the XAD-2 absorbent module to slightly higher temperatures than allowed for as long as 30 minutes out of the 210 minute total sampling time. Since the module outlet temperature never exceeded ambient temperatures, this temperature deviation was determined to not have a significant impact on the SVOC measurement.

7.7.7.5 Production Test P-4A-2. The full suite of nine sample trains was run for Test P-4A-2. Sampling occurred without incident. Isokinetic runs were accomplished within the 90–110% allowable range, and comparable stack gas parameters had a relative percent difference of less than about 2%.

7.7.7.6 Production Test P-4A-3. P-4A-3 was begun on January 31, but was suspended and run again on February 1. Due to a higher than expected moisture content in the stack gas, the water collecting impingers filled up prematurely on the Method 0010 and Method 0023A trains. As a consequence, two of the three traverses were outside the 90–110% isokinetic range. Samples from these trains were discarded and the test period was repeated on the following day. The metals and particulate trains were run first on the following day with the organic sampling trains repeated that afternoon. Intermittent feed interruptions during the sampling times resulted in all three organic sampling trains being outside of the 90–110% isokinetic range. Corrections to the train results due to these deviations were made according to the quality assurance plan. For the nine trains run on February 1, the relative percent difference in measured stack gas parameters was less than 2%. Other than the problems noted above, no other sampling interruptions occurred.

7.7.7.7 Production Test P-4A-4. Sampling for P-4A-4 was accomplished without incident and was completed within an eight hour time period. All isokinetic runs were within the 90–110% range, and comparable stack gas parameters had a relative percent difference of less than about 2%. No sampling anomalies were noted.

7.7.7.8 Production Test P-4A-5. P-4A-5 required several hours of adjusting feed rates and gas flow rates to achieve steady-state conditions at a high feed rate of 0.35 gpm. Consequently, stack gas sampling was initiated late in the shift and was continued on the following day. Sampling was completed without incident. All isokinetic runs were within the 90–110% range, and the relative percent difference of comparable stack gas parameters was within 4%.

7.7.7.9 Production Test P-4A-6. P-4A-6 was initiated on February 4, at which time the first four manual sampling runs were conducted. Due to a number of operational problems, including exhaustion of the supply of GC CRB coal and a desire to inspect both the DMR and CRR beds, the system was shut down until February 7. Once the system was heated back up to temperature and had achieved steady state conditions (on February 8), the remaining stack sampling took place without incident. All isokinetic runs were accomplished within the 90–110% allowable range, and the relative percent difference of measured stack gas parameters was less than 3%.

7.7.7.10 Production Test P-5. The liquid feed for P-5 consisted of only supernatant solution, UDS, and heavy metals, so manual sampling of the stack gas for organic constituents was not conducted. Sampling was conducted only for particulate matter, chlorides, metals in the stack, and mercury in the GAC adsorber. Both the Method 5/26A and Method 29 trains were within the 90–110% isokinetic range, and the relative percent difference of comparable stack parameters was less than 2%. All stack emissions samples were collected over a 4-hour period.

7.7.7.11 Production Test P-6. The liquid feed for P-6 had the same constituents as in P-5, although in different concentrations, so the same four sample trains were used. The sampling began at 0905 on February 10, and was noted on the draft daily summary sheet. Operator logs indicate that sampling was

completed at 1242. The isokinetic sampling rate was within the 90–110% range and the relative percent difference of comparable stack gas parameters was less than 7%.

7.7.8 Manual Sample Train Measurement Results

All stack gas emissions were within applicable regulatory limits such as the HWC MACT standards.

7.7.8.1 HCL and CL_2. Emissions of HCl and Cl_2 were measured during CP1 (but not during CP2) and are shown on Table 7-33. Combined HCl and Cl_2 levels (reported at total HCl) averaged about 20% of the HWC MACT standard of 21 ppm (dry @ 7% O_2) for new facilities. Total HCl/Cl_2 averaged about 0.6 ppmv (dry, corrected to 7% O_2) during tests P-1, P-2, and P-3 when the POHC was not spiked and no chlorinated organics were in the feed. Total HCl/Cl2 during tests when the POHC was spiked averaged about 8 ppmv (dry, 7% O_2). Cl_2 was not detected at the detection limit of about 0.05 ppmv, as was expected for this type of process.

The POHC increased the stack HCl level, as was expected, but still the total HCl/Cl_2 for the tests in which the POHC was spiked was about 30% of the HWC MACT limit. The total feedrate of Cl from the POHC during these tests was higher than the expected Cl feedrate from trace organics in the actual SBW, so HCl/Cl_2 emissions from the IWTU should be less than 8 ppmv, if all else is equal. The IWTU has the option of HCl/Cl_2 compliance based on the concentration standard, or based on risk assessment, as also allowed by MACT, without HCl control such as wet scrubbing.

7.7.8.2 PM and Non-Mercury Hazardous Metals. Table 7-43 and Table 7-44 shows stack gas particulate matter (PM) and metal concentrations and emission rates for CP1 and CP2. Particulate matter concentrations averaged below 30% of the HWC MACT standard of 3.4 mg/dscm (dry @ 7% O_2) for new facilities.

The Hazen test system is not HEPA filtered. HEPA filtration in the IWTU is expected to significantly lower these levels, probably to levels below currently available detection limits using standard methods.

Hazardous metals that were included in the simulant feed were Pb, As, and Cr. Zn was used as a surrogate for Cd, which is a hazardous metal known to be in the SBW, but which was excluded from the testing because its industrial hygiene concerns exceeded the value of including it. Other hazardous metals including Cd, As, and Be were included in the stack sample analysis to confirm detection limits and to determine if unknown levels of these metals were in the simulant feed. Cd was detected in only one sample at a level within the range of detetability. Zn, Pb, and Cr were all detected in all sample trains. As and Be were not detected in any sample trains.

The concentration of total semivolatile metals (Cd + Pb + Zn [surrogate]) averaged about 55% of the HWC MACT standard of 10 µg/dscm (dry @ 7% O_2) for new facilities. The concentration of total low volatile metals (As + Be + Cr) averaged about 12% of the HWC MACT standard of 23 µg/dscm (dry @ 7% O_2) for new facilities. The Hazen test system is not HEPA filtered. HEPA filtration in the IWTU will probably lower these emission levels.

System removal efficiencies were calculated using the stack gas mass emission rates for hazardous metals and the input feedrates of those metals. System removal efficiencies for Zn, Pb, As, and Cr ranged between 99.99% and 99.9999%. HEPA filtration in the IWTU might increase these removal efficiencies if the stack gas detection limits can be lowered when testing the IWTU stack gas for metals that were not detected in the stack gas during the Hazen testing.

Table 7-43. CP1 stack gas particulate matter and metals concentrations and emission rates.

			Concentrations, dry (@7% O_2)									Mass emission rates (lb/hr)						
			PM (mg/dscm)	Semivolatile metals (µg/dscm)				Low volatility metals (µg/dscm) Metals				PM						
				Cd Zn		Pb	Total	As	Be	Cr	Total		Cd Zn		Pb	As	Be	Cr
Date Test	Period	Test	M26A	M29 M29		M29 M29 M29 M29				M29	M29	M26A	M29	M29 M29 M29 M29 M29				
18-Jan-06 1730–2107		1, day 1	0.27	0.130	**7.3**	**0.60**	**8.1**	0.264 0.129		**1.68**	**2.1**	2.1E-04 9.6E-08		**5.3E-06**	**4.4E-07**	2.0E-07 9.6E-08		**1.2E-06**
19-Jan-06	1000–1330	1, day 2	—	— —		— —		— —		— —		—	—	—	— — — —	—		
27-Jan-06 1000–1310		2A	0.25	0.118	**4.1**	**0.54**	**4.7**	0.239 0.118		**1.52**	**1.63**	2.1E-04 9.6E-08		**3.9E-06**	**4.4E-07**	2.0E-07 9.6E-08		**1.2E-06**
28-Jan-06 1230–1640		3B	0.65	0.055	**3.2**	**0.25**	**3.5**	0.111 0.055		**0.71**	**0.76**	8.1E-04 6.0E-08		**3.3E-06**	**2.8E-07**	1.2E-07 6.0E-08		**7.7E-07**
29-Jan-06 1040–1426, 1600–1930		4A-1 0.35		0.059	**3.5**	**0.10**	**3.7**	0.117 0.059		**0.34**	**0.40**	3.4E-04 5.8E-08		**3.4E-06**	**1.0E-07**	1.1E-07 5.8E-08		**3.3E-07**
30-Jan-06 1025–1415, 1620–1950		4A-2 0.76		0.069	**4.4**	**0.12**	**4.6**	0.136 0.069		**0.39**	**0.46**	7.2E-04 5.8E-08		**4.1E-06**	**1.0E-07**	1.1E-07 5.8E-08		**3.3E-07**
31-Jan-06	1110–1525	4A-3, day 1	—	— —		— —		— —		— —		—	—	—	— — — —	—		
1-Feb-06 1015–1335, 1600–2020		4A-3, day 2	0.82	0.090	**9.9**	**0.11**	**10.1**	0.096 0.049		**0.38**	**0.43**	9.5E-04 1.0E-07		**4.2E-06**	**1.3E-07**	1.1E-07 5.5E-08		**4.3E-07**
2-Feb-06 1015–1340, 1450–1810		4A-4 1.46		0.057	**3.5**	**0.13**	**3.7**	0.112 0.057		**0.66**	**0.72**	1.4E-03 5.5E-08		**3.4E-06**	**1.2E-07**	1.1E-07 5.5E-08		**6.4E-07**
3 Feb 06	1355–1720	4A-5, day 1	0.32	**0.087**	**4.6**	**0.22**	**4.9**	0.102 0.050		**13.50**	**13.55**	3.5E-04	**9.2E-08**	**5.0E-06**	**2.3E-07**	1.1E-07 5.3E-08		**1.4E-05**
4-Feb-06	0935–1351	4A-5, day 2	—	— —		— —		— —		— —		—	—	—	— — — —	—		
4-Feb-06 1805–2205		4A-6, day 1	3.23	0.074	**4.8**	**0.13**	**5.0**	0.155 0.079		**2.39**	**2.47**	2.3E-03 5.5E-08		**3.5E-06**	**9.8E-08**	1.2E-07 5.9E-08		**1.8E-06**
8-Feb-06	1400–1722	4A-6, day 2	—	— —		— —		— —		— —		—	—	—	— — — —	—		
9-Feb-06 1000–1415		5	0.91	0.091	**4.6**	**0.16**	**4.9**	0.192 0.098		**2.96**	**3.06**	6.2E-04 5.5E-08		**3.2E-06**	**9.8E-08**	1.2E-07 5.9E-08		**1.8E-06**
10-Feb-06 0905–1241		6	0.96	0.081	**6.7**	**0.36**	**7.1**	0.161 0.081		**4.57**	**4.66**	7.1E-04 6.1E-08		**5.0E-06**	**2.7E-07**	1.2E-07 6.1E-08		**3.4E-06**
Averages 0.91				0.083	**5.1**	**0.25**	**5.5**	0.153 0.077		**2.65**	**2.75**	7.8E-04 7.1E-08		**4.0E-06**	**2.1E-07**	1.3E-07 6.4E-08		**2.4E-06**

Notes:

1. Detected values,and sums of detected and nondetected values, are **bolded**. Detection limits are use for metals that are not detected, and reported in **non-bolded** values.
2. Occasional detects in blank trains have not been subtracted from the reported stack values.
3. All metals trains were validated. Data validation confirmed that As is a non-detect.
4. Cd was not spiked in the feed. Zn was used as a surrogate for Cd. For conservatism, Total SVM includes Cd, Pb, and Zn, since Cd was not spiked into the feed but was still detected in 1 sample train.

Average simulant feedrate, gpm	0.29					
Target feed metals concentration, gm/L	0	0	0.28	0.037	0	0.30
Average metals feedrate, lb/hr	0	0.047	0.040	0.0053	0	0.043
Average system removal efficiency, %	—	**99.991**	**99.9995**	**99.998**	—	**99.994**

Table 7-44. CP2 stack gas PM and metals concentrations and emission rates.

					Concentrations, dry (@7% O_2)											Mass emission rates (lb/hr)								
						Semivolatile metals (µg/dscm)				Low volatility metals (µg/dscm)				Radionuclide surrogates (µg/dscm)			Metals						Radionuclides surrogates	
Date Test	Period	Test	Feed	Sample train isokinetic rate (%)	PM (mg/ dscm)	Cd Zn		Pb	Total	As	Be	Cr	Total	Ce	Cs	PM	Cd	Zn Pb As			Be	Cr	Ce	Cs
					M29	M29	M29 M29		M29 M29 M29			M29 M29 M29			M29	M29	M29 M29		M29 M29 M29 M29				M29	M29
1-Jun-06	1550–1910	1	Lite	81.7	2.60	0.132	28.2	3.09	31.4 0.26	0.132		2.60 2.	99 0.66		0.66	1.4E-03	**7.1E-08**	**1.5E-05**	**1.6E-06**	1.4E-07 7.1E-08		**1.4E-06**	1.4E-07 1.4E-07	
3-Jun-06	1150–1550	2	Lite	95.0	1.30	0.108	3.1	0.35	3.6	0.21 0.108		0.79 1.	11 0.53		0.53	7.3E-03	**6.1E-08**	**1.8E-06**	**2.0E-07**	1.2E-07 6.1E-08		**4.4E-07**	1.4E-07 1.4E-07	
5-Jun-06	1110–1440	3	Metals & rad surr	95.9	0.74	0.124	10.5	0.42	11.0 0.24	0.124		0.87 1.24		0.62 0.61		3.6E-04	6.0E-08	**5.1E-06**	**2.0E-07**	1.2E-07 6.0E-08		**4.4E-07**	1.4E-07 1.4E-07	
6-Jun-06	1040–1415	4	Metals & rad surr	99.5	0.83	0.110	8.7	0.25	9.0	0.22 0.110		0.71 1.04		0.59 0.54		4.4E-04	5.8E-08	**4.6E-06**	**1.3E-07**	1.1E-07 5.8E-08		**3.8E-07**	1.4E-07 1.4E-07	
7-Jun-06	0950–1310	5	Metals & rad surr	99.1	0.88	0.111	8.0	0.56	8.7	0.22 0.111		0.80 1.13		0.58 0.55		4.6E-04	5.8E-08	**4.2E-06**	**2.9E-07**	1.1E-07 5.8E-08		**4.2E-07**	1.4E-07 1.4E-07	
7-Jun-06	1745–2110	6	Metals & rad surr	102.7	1.34	0.111	9.2	0.29	9.6	0.22 0.111		0.93 1.26		0.56 0.55		6.8E-04	5.6E-08	**4.7E-06**	**1.5E-07**	1.1E-07 5.6E-08		**4.7E-07**	1.4E-07 1.4E-07	
Averages				95.6	0.95	0.114	9.1	0.38	9.6	0.224	0.114	0.83	1.17	0.59	0.56	—	—	—	—	—	—	—	—	—
HWC MACT standard, new facilities					3.4	—	—	—	10	—	—	—	23	—	—	—	—	—	—	—	—	—	—	—
Avg meas value, % of MACT std					27.9%	—	—	—	96%	—	—	—	5.1%	—	—	—	—	—	—	—	—	—	—	—
Average measured value (not incl Lite)					—	—	—	—	—	—	—	—	—	—	—	4.8E-04	5.8E-08	**4.6E-06**	**1.9E-07**	1.1E-07	5.8E-08	**4.3E-07**	1.4E-07	1.4E-07
Average simulant feedrate, gpm					—	—	—	—	—	—	—	—	—	—	—	—	0.245							
Analytical feed metals concentration, gm/L					—	—	—	—	—	—	—	—	—	—	—	—	0	0.52	.026	0	0	0.25	0.511	0.415
Average metals feedrate, lb/hr					—	—	—	—	—	—	—	—	—	—	—	—	0	0.064	0.031	0	0	0.030	0.063	0.051
Average system removal efficiency, %					—	—	—	—	—	—	—	—	—	—	—	—	—	**99.9928**	**99.9994**	—	—	**99.9986**	99.9998	99.9997

Notes:

1. Detected values, and sums of detected and nondetected values, are **bolded**. Detection limits are use for metals that are not detected, and reported in **non-bolded** values.
2. Occasional detects in blank trains have not been subtracted from the reported stack values.
3. The first two tests were performed with Lite simulant feed containing no added hazardous metals or radionuclide surrogates. Those tests are stack gas blank tests and represent complete system blanks for hazardous metals and radionuclide surrogate emissions. Those blank values are not included in emissions averaging calculations, and have not been subtracted from the reported metals and radionuclide surrogate emission values.
4. The test 1 M29 train had only 81.7% isokinetic rate, outside the acceptance limit of 90–110%. At this lower sampling rate, the measurement of particulate matter and particle-bound metals may be biased high by the ratio of 1-%iso/100. The metals emission data were not adjusted for this potential bias, since this test was a system blank - no hazardous metals or radionuclide surrogates were included in the simulant feed.
5. Cd, As, and Be were not spiked in the feed. Zn was used as a surrogate for Cd. For conservatism, total SVM includes Cd, Pb, and Zn, since Cd was not spiked into the feed but was still detected in 1 sample train.

[cp2 off-gas emissions aug 8.xls]Metals - PM conc

The primary mechanisms for evolution of PM, hazardous metals and radionuclides to the stack gas are:

- Elutriation as solid particulate matter from the DMR, passing through the HTF as PM, and then downstream carryover either as PM or after volatilization in the CRR. Even if the PM volatilizes in the CRR, it is likely to condense as it cools in the OGC, enabling capture in the PBF. Amounts that pass through the filtration steps (the HTF and the PBF) will probably pass through CRR and the GAC bed with low capture efficiency and will exit the stack.

- Volatilization in the DMR, allowing pass-through the HTF as a gas. If the species volatilized in the DMR, then it might remain volatilized, or condense and then re-volatilize, in the CRR. However, the OGC cools the hot off-gas to about 180°C, and volatile metals will tend to re condense upon cooling to this temperature. If the metals remain a gas even after passing through the OGC, or if they exist as very small particles, they might pass through the PBF and GAC bed and exit the stack.

Figure 7-63 shows how the hazardous metals emissions during CP1 relate to the DMR bed temperature, which would drive the volatilization of heavy metals and radionuclides. Except for the rising trendline for Cr (which probably results from contamination from stainless steel used in the system), no relationship is apparent between the DMR bed temperature and heavy metals in stack gas. This is because, at the relatively moderate DMR temperatures compared to traditional incinerator temperatures, most metals and metal species (not including Hg) exhibit low volatility.

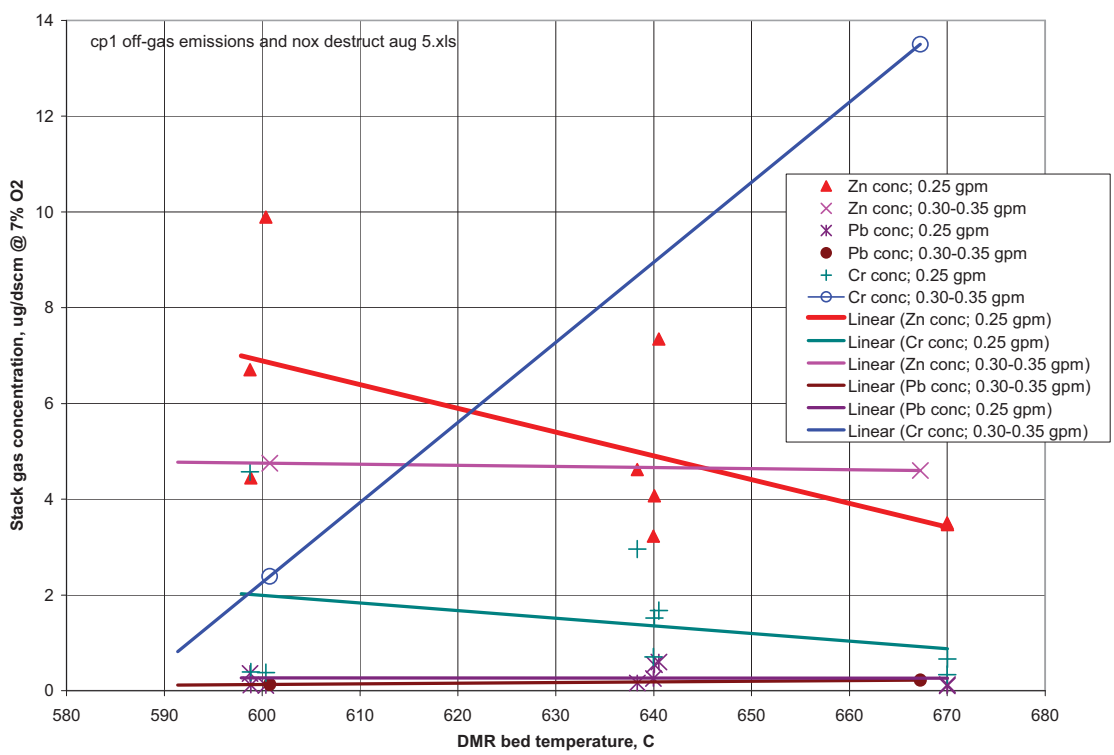

Figure 7-63. Hazardous metals (and surrogate) emission concentrations.

Cs and Ce were not detected in any of the stack samples. Cs and Ce system removal efficiencies are consistent with the ~4–6 nine or better removal efficiency found for the other metals spiked into the feed. HEPA filtration would likely increase these removal efficiencies, if more sensitive stack gas measurements for Cs and Ce can be made.

7.7.9 Mercury Control, Emission Measurements, and Spent Granular Activated Carbon Leachability

Mercury emissions were controlled using a 3-stage packed bed of sulfur-impregnated granular activated carbon (GAC or SGAC) shown in Figure 7-64. This carbon bed was designed according to "Design of the ESTD Mercury Adsorption Activated Carbon Bed Vessel." [R35] The dimensions and operating conditions of the GAC bed during CP1 and CP2 are shown in Table 7-45.

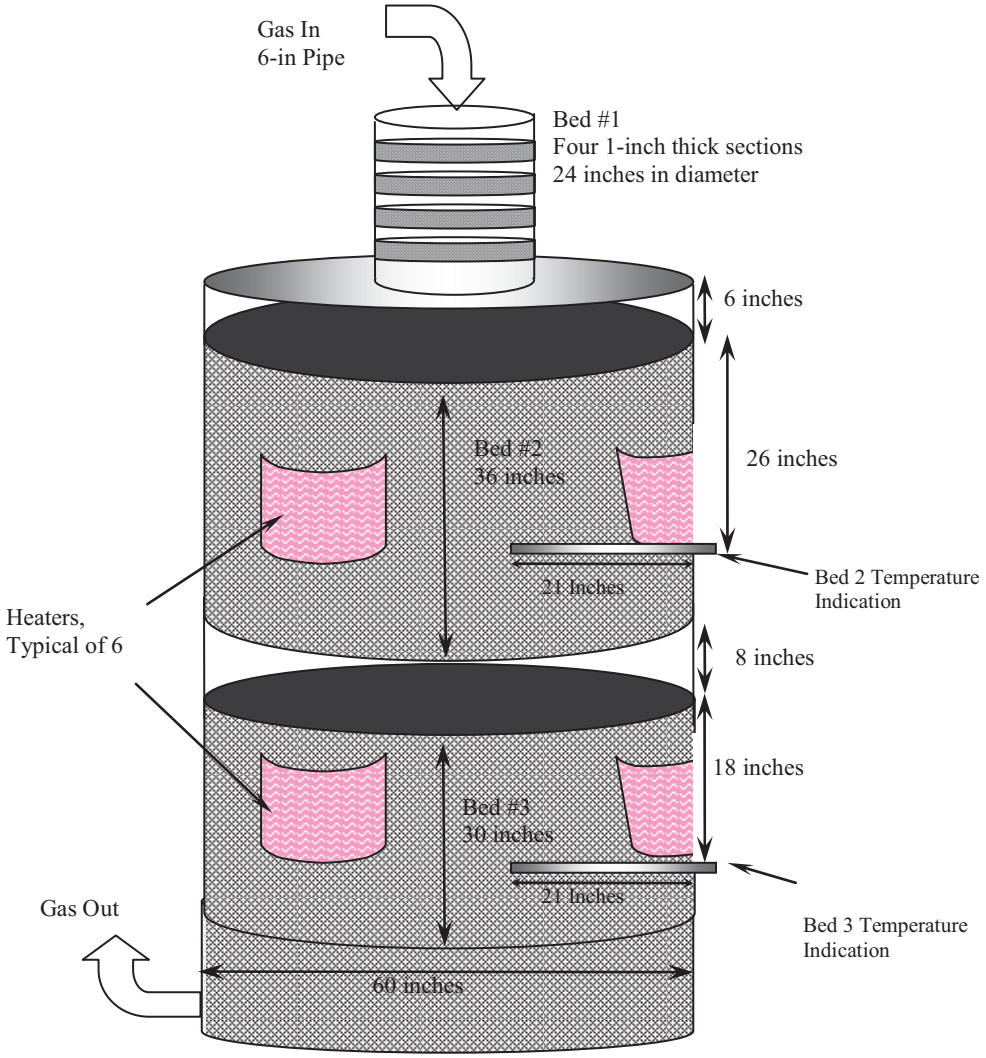

Figure 7-64. ESTD GAC Mercury Adsorber.

Table 7-45. Carbon bed dimensions and operating conditions.

Design parameters and operating conditions	Bed 1	Bed 2	Bed 3	Totals/ averages
CP1				
Stack gas flow rate, wscfm (EPA 1A/2 during manual sample periods)	296			
GAC bed gas temperature, C (TT-408-001, 2, 3 for 15 CRR tests)	127	131	138	132
GAC bed inlet pressure, psia (PT-407-001 from CP1)	11.99			
GAC bed outlet pressure, psia (PT-408-001 from CP1)	11.82			
Bed pressure drop, in. H_2O —		—	—	4.7
Mersorb mass, lb, (installed)	52.5	2,031	1,692	3,776
Stack gas flow rate, acfm	493	499	507	500
Bed diameter, ft	2.0	5.0	5.0	—
Bed superficial velocity, f/s	2.6	0.42	—	—
Bed depth, inches	5.9	36.4	30	72.3
Bed residence time, seconds	0.19	7.2	5.8	13.2
CP2				
Stack gas flow rate, wscfm (EPA 1A/2 during manual sample periods)	277			
GAC bed gas temperature, C (TT-408-001, 2, 3 for 15 CRR tests)	127	126	135	129
GAC bed inlet pressure, psia (PT-407-001 from CP1)	11.99			
GAC bed outlet pressure, psia (PT-408-001 from CP1)	11.82			
Bed pressure drop, in. H_2O —		—	—	4.7
Mersorb mass, lb, (installed)	52.4	2,047	1,719	3,818
Stack gas flow rate, acfm	462	460	472	465
Bed diameter, ft	2.0	5.0	5.0	—
Bed superficial velocity, f/s	2.5	0.39	0.40	—
Bed depth, inches	5.9	36.4	30	72.3
Bed residence time, seconds	0.20	7.8	6.2	14.2

Notes:

1. The stack gas flow rate, temperature, and pressure values are averages of measurements made during the CP1 and CP2 manual sample times.

[Hazen carbon bed CP1-CP2 results aug 8.xls]Report Table

Bed 1 was sized to be small enough to demonstrate Hg loading capacity on the carbon within a reasonable minimum test operating time of about 100 hours. Bed 1 breakthrough was expected early in the test, due to its shallow depth (4–6 in.) and small diameter (2 ft). The residence time in Bed 1 was only 0.2 seconds, considerably less than the 1–10 second range found necessary to achieve efficient Hg capture. While this bed is designed to reach breakthrough and sorption capacity, it is not intended for efficient Hg capture. Bed 1 was separated into four layers by separating screens that ensured that bed media from different depths could be separately sampled for analysis after a test.

Beds 2 and 3 were sized to provide gas velocity, bed depth, and residence time for efficient Hg sorption. Bed 2 was 5-ft diameter and 36 in. deep, and sized for a nominal 5 second residence time.

Bed 3 was sized to provide a total nominal residence time for all three beds of at least 10 seconds. Bed 3 is identical to Bed 2, except that there was room for the bed depth to be only 30 inches instead of the initially planned 36 inches.

No gas distributors were considered necessary in the design because the carbon bed vendor advised that the pressure drop of the carbon bed itself is normally high enough to cause the gas to relatively evenly distribute in the plenum spaces at the inlet and outlet of a carbon bed. A gas inlet baffle was installed at the outlet of Bed 1 to prevent impingement of the inlet gas at the high Bed 1 exit gas velocity on the carbon at the top of Bed 2. The Bed 3 outlet gas was also slightly baffled by a down-facing elbow in the outlet gas pipe.

7.7.9.1 Mercury Control and Emission Measurements. Table 7-46, Table 7-47, Table 7-48, and Table 7-49 show Hg analysis results of spent GAC samples collected during and following CP1 and following CP2.

Figure 7-65 shows the carbon bed Hg concentrations. Hg concentrations in Bed 1 samples after the CP1 test approached vendor-recommended Hg loading capacities of about 20 wt% of the virgin GAC. The Bed 1 carbon did not reach maximum design Hg concentrations during CP2, even though the Hg feed time during CP2 was about 90 hours, close to the target of 100 hours used in designing Bed 1. About 37% of the Hg that was fed during CP2 (about 17 lb) was captured in Bed 1.

The samples collected during CP1 show that as the test progressed, the Bed 2 and 3 Hg concentrations began to increase. This increase occurred as the Hg concentration increased in Bed 1 over time, causing some of the Hg that would have sorbed in Bed 1 and the top of Bed 2 to pass through Bed 1 and be sorbed in the lower volume of Bed 2 and in Bed 3.

These concentration results provide some bounding data on the mass transfer zone (MTZ), which is the zone of active Hg sorption as the Hg-laden gas enters the carbon bed. Theoretically, this zone progresses over time through the depth of the bed. At the start of operations, this zone is at the front of the bed. As the carbon at the front face of the bed approaches saturation, more Hg passes through that carbon and is sorbed by carbon further downstream in the bed. Over time, the MTZ progresses through the carbon bed, leaving behind carbon that approaches the saturation concentration. Carbon that is downstream of the MTZ absorbs little if any Hg, because the Hg has already been sorbed in the MTZ. Carbon in the bed appreciably downstream of the MTZ remains essentially free of Hg until the MTZ reaches the depth of that carbon.

The depth of the MTZ depends on how long it takes for almost all of the Hg in the gas phase to sorb into the carbon. This, in turn, depends on operating conditions of the carbon bed that define Hg mass transfer to the carbon, but not the carbon capacity for Hg sorption. The carbon capacity for Hg sorption defines how fast the carbon in the MTZ reaches saturation, and defines how fast the MTZ progresses through the carbon bed.

Several prior studies, and vendor experience, have indicated that the MTZ for the sorption of most gas species on activated carbon typically ranges a few inches thick. The ESTD carbon bed operation has not been configured to rigorously determine the MTZ for Hg sorption under the conditions of the test, but the depth of the MTZ can be estimated and bounded by the test results.

Table 7-46. Mercury analysis results for CP1 GAC bed activated carbon samples

Sample I.D.	Sample Description	Date	Time	COT	Hg conc., ppmw as measured: Digest 1	Digest 2	Digest 3	Total	Hg conc., virgin GAC basis (wt %)	Hg in 1st digestion (%)	Sample port depth (in.)	Cumul. gas superficial res. time (sec)	Mass of GAC rep. by sample (lb)	Differential Hg mass (lb)	Cumul. Hg removal efficiency (%)
Mersorb 3AT	As-Received GAC			0	0.83	0.09	0.06	0.98	0.000098	84.7%	—	0	—	—	—
1786	GAC bed 2 upper port	2/3/2006	0:20	136	1.48	0.12	0.04	1.64	0.000164	90.2%	29	4.72	—	—	—
1787	GAC bed 2 lower port	2/3/2006	0:20	136	0.64	0.10	0.03	0.77	0.000077	83.1%	41	7.08	—	—	—
1789	GAC bed 3 lower port	2/3/2006	0:20	136	0.75	0.07	0.02	0.84	0.000084	89.3%	70	12.78	—	—	—
1859	GAC bed 2 upper port	2/9/2006	19:00	229	7.97	0.42	0.05	8.44	0.000844	94.4%	29	4.72	—	—	—
1860	GAC bed 2 lower port	2/9/2006	19:00	229	0.50	0.10	0.05	0.65	0.000065	76.9%	41	7.08	—	—	—
1862	GAC bed 3 lower port	2/9/2006	19:00	229	0.51	0.12	0.04	0.67	0.000067	76.1%	70	12.78	—	—	—
Post-test samples															
1886	GAC bed 1, screen 1	2/15/2006	Post	247	168,000	5,800	146	173,946	22.0	96.6%	1.5	0.048	—	—	—
1887	GAC bed 1, screen 2	2/15/2006	Post	247	173,000	6,940	173	180,113	19.3	96.1%	3.0	0.095	—	—	—
1888	GAC bed 1, screen 3	2/15/2006	Post	247	157,000	4,370	126	161,496	18.9	97.2%	4.5	0.143	—	—	—
1889	GAC bed 1, screen 4	2/15/2006	Post	247	154,000	4,870	128	158,998	15.6	96.9%	6.0	0.191	—	—	—
Avg Bed 1 conc./total Hg in Bed 1		—		163,000		5,495	143	168,638	18.9	—	6.0	0.191	52.5	9.9	26.5
—	GAC bed 2 top 3 inches	—			—	—	—	—	—	—	—	0.78	143.0	27.1	—
1891	GAC bed 2 upper port	2/16/2006	Post	247	130,000	4,820	132	134,952	15.6	96.3%	29	4.72	1,488	0.26	—
1892	GAC bed 2 lower port	2/15/2006	Post	247	64.7	3.13	0.31	68	0.0068	95.0%	41	7.08	401	0.027	—
Avg Bed 2 conc./total Hg in Bed 2		—			—	—	—	—	—	—	42	7.27	2,031	27.4	99.4
1893	GAC bed 3 upper port	2/16/2006	Post	247	166	7.29	0.40	174	0.0174	95.6%	58	10.42	1,241	0.216	—
1894	GAC bed 3 lower port	2/15/2006	Post	247	10.4	0.47	0.21	11	0.0011	93.9%	70	12.78	451	0.005	—
Avg Bed 3 conc/total Hg in Bed 3		—			—	—	—	—	—	—	—		1,692	0.221	—
Avgs/totals for all 3 beds		—			—	—	—	—	—	90.8%	—		3,776	37.5	—

Notes:

1. Mercury Digestion Procedure:
   a) Samples were digested as normal for carbons and/or other organic containing solids. (Tall test tubes, 5 ml HNO_3, 5 ml HCl, block digestor, 110°F for 7 hours with frequent vortexing).
   b) Samples and solutions were allowed to settle overnight. Solutions were carefully decanted to 100 ml vol flasks. A rinse of 20 ml DI was added to tubes and allowed to settle again. Rinses were decanted and added to original flasks, brought to volume, shaken, and a portion poured into vials for analysis.
   c) Second digestion: Remaining residue was then re-digested for 2 hours. Decanted and rinsed as described in step 2.
   d) Third digestion: Remaining residue was re-digested for 2 hours. Entire contents of tubes and subsequent rinses were transferred to flasks.
   Notes and comments regarding procedure:
   - Some "floating" and suspended fine residues were transferred to flasks in digestions 1 and 2. This could not be avoided.
   - Approximately 3 ml of rinse solution was left in tubes after digestions 1 and 2, and were carried over to digestions 2 and 3, respectively.
   - "Normal" procedure involves rinsing digestion tubes 3 times. This was not done for digestions 1 and 2.
2. Only the final post-test data are used for mass balance calculations. The analyses of GAC samples collected on February 5 and February 9, before the test end, are not used for mass balance calculations.
3. The Hg and S concentrations are converted to an Hg-free, virgin GAC basis. For simplicity, no other corrections for S loss, S conversion to SO_4, or moisture change were made.
4. The post-test GAC bed 2 upper port sample (Number 1891) is an outlier, considering prior sample analyses from this location, and so is not included in calculations. Using this analysis causes the amount of Hg collected in Bed 2 to be impossibly high, compared to the amount of Hg fed. The Bed 2 upper port Hg concentration is assumed to be equal to the Bed 3 concentration upper port for mass balance calculations.
5. The Bed 1 reached breakthrough, so some Hg certainly passed through Bed 1 into Bed 2. Assume that the top 2.5 inches of Bed 2 has the same Hg concentration as Bed 1. Assume that the mass of GAC represented by Bed 2 upper port is the GAC in Bed 2 above the upper port, less the top 2.5 inches. The mass of GAC represented by the Bed 3 upper port is estimated to be the mass of GAC between that sample location and the top of the bed. The mass of GAC represented by the Bed 2 and 3 lower ports is assumed to be the GAC below the upper port to the bottom of the bed.
6. The GAC Bed 1 and 2 estimated Hg removal efficiencies were calculated using the mass of Hg captured in each of the 3 GAC beds, assuming 100% cumulative Hg capture in all 3 beds. This is a reasonably good assumption for calculating the Bed 1 and Bed 2 Hg removal efficiencies.
7. The total bed Hg and S average concentrations were calculated using weighted averages for each of the 3 beds.

[Hazen carbon bed CP1-CP2 results aug 8.xls]CP1 GAC Hg analyses

Table 7-47. Other analysis results for CP1 GAC bed activated carbon samples.

Sample I.D.	Sample Description	Date	Total S (wt %)	S normalized to Hg-free basis (%)	S loss (%)	S remaining (lb)	SO_4 (%)	S conversion to SO_4 (%)	Cl (%)	F (%)	NO_2 (ppm)	NO_3 (ppm)	PO_4 (%)
Mersorb 3AT	As-Received GAC		11.4	11.4 0		430	1.0	2.8	0.01	0.022	<1	14	0.082
1786	GAC bed 2 upper port	2/5/2006	11.7	11.7	-2.6 —		11.8	33.6	<0.01	0.012	<1	<1	0.062
1787	GAC bed 2 lower port	2/5/2006	9.5	9.5	16.8 —		9.2	32.4	0.03	0.009	<1	<1	0.055
1789	GAC bed 3 lower port	2/5/2006	7.9	7.9	30.7 —		12.0	50.6	0.01	0.005	<1	<1	0.058
1859	GAC bed 2 upper port	2/9/2006	10.9	10.9	4.4 —		12.8	39.1	0.03	0.011	<1	<1	0.059
1860	GAC bed 2 lower port	2/9/2006	8.9	8.9 22.1		—	9.9	37.2	0.07	0.015	<1	8	0.053
1862	GAC bed 3 lower port	2/9/2006	7.5	7.5 34.1		—	12.1	53.7	0.02	0.007	<1	1	0.059
Post-test samples													
1886	GAC bed 1, screen 1	2/15/2006	7.9	9.6	15.7 —		13.2	55.4	interference	0.017	<1	<1	0.062
1887	GAC bed 1, screen 2	2/15/2006	7.9	9.6	15.4 —		12.4	52.3	interference	0.012	<1	<1	0.034
1888	GAC bed 1, screen 3	2/15/2006	9.1	10.8	5.1 —		11.5	42.3	interference	0.011	<1	<1	0.052
1889	GAC bed 1, screen 4	2/15/2006	9.8	11.6	-2.0 —		11.6	39.5	interference	0.011	<1	<1	0.062
Avg Bed 1 conc./total Hg in Bed 1		—	8.7 10.4		8.5	5.47	12.2	47.4 —		0.013	<1	<1	0.05
1891	GAC bed 2 upper port	2/16/2006	9.2	10.6	6.8	— 13.6		49.3	interference	0.009	<1	<1	0.051
1892	GAC bed 2 lower port	2/15/2006	10.0	10.0	12.3 —		11.1	37.0	<0.01	0.013	<1	<1	0.058
Avg Bed 2 conc./total Hg in Bed 2		—	9.6 10.3		9.5	209	12.4	43.2	<0.01	0.01	<1	<1	0.05
1893	GAC bed 3 upper port	2/16/2006	11.7	11.7	-2.6 —		12.6	35.9	interference	0.012	<1	<1	0.083
1894	GAC bed 3 lower port	2/15/2006	8.3	8.3 27.6		—	4.1	16.4	0.11	0.009	<1	2	0.064
Avg Bed 3 conc/total Hg in Bed 3		—	10.0 10.0 12.5			169	8.3	26.2 0.11		0.011	<1	2	0.074
Weighted Averages/totals for all 3 beds			9.8 10.2 10.8			384	10.5	35.6 0.055		0.011	<1	1	0.063

Notes:

1. The analyses of GAC samples collected on February 5 and February 9, before the test end, are not used for mass balance calculations.
2. The post-test GAC bed 2 upper port sample (Number 1891) seems to be an outlier, considering prior sample analyses from this location, and so is not included in calculations. Using this analysis causes the amount of Hg collected in Bed 2 to be impossibly high, compared to the amount of Hg fed. The Bed 2 upper port Hg concentration is assumed to be equal to the Bed 3 concentration upper port for mass balance calculations.
3. The S content in the GAC Bed 3 lower port sample appears to be an outlier since this S content is inexplicably, significantly lower than the S content in any other GAC samples. This S content is excluded from the S content averaging and totaling calculations.

[Hazen carbon bed CP1-CP2 results aug 8.xls]CP1 GAC S, other analyses

Table 7-48. Mercury analysis results for CP2 GAC bed activated carbon samples.

Sample I.D.	Sample Description Date		COT	Hg conc. (ppmw as measured) Digest 1	Digest 2	Digest 3	Total	Hg conc., virgin GAC basis (wt %)	Hg in 1st digestion (%)	Sample port depth (in.)	Cumul. gas superficial res. tim (sec)	Mass of GAC rep. by sample (lb)	Differential Hg mass (lb)	Cumul. Hg removal efficiency (%)
2377 Mersorb,	batch MER063Ht/01	6/21/2006	0	1.32	—	—	1.32	0.000132	—	—	0	—	—	—
2366	GAC BED 1, screen 1	6/19/2006	90	112,000	34	2.5	112,037	12.6	99.97%	1.5	0.051	—	—	—
2367	GAC BED 1, screen 2	6/19/2006	90	103,000	—	—	103,000	11.5	—	3.0	0.102	—	—	—
2368	GAC BED 1, screen 3	6/19/2006	90	107,000	—	—	107,000	12.0	—	4.5	0.153	—	—	—
2369	GAC BED 1, screen 4	6/19/2006	90	98,000	—	—	98,000	10.9	—	6.0	0.204	—	—	—
Avg Bed 1 conc./total Hg in Bed 1		—	105,000		34.4	2.5	105,009	11.7	—	6.0	0.204	52.4	6.2	36.6
2374	GAC BED 2, top surface	6/20/2006	90	57,700	30	2	57,732	6.1	99.9%	6.5	0.31	170.6	10.5	—
2370	GAC BED 2, Upper	6/20/2006	90	41	—	—	41	0.0041	—	29	5.11	1,592	0.06	—
2371	GAC BED 2, Lower	6/20/2006	90	69	—	—	69	0.0069	—	41	7.66	398	0.027	—
Avg Bed 2 conc./total Hg in Bed 2		—		—	—	—	—	—	—	42	7.88	2,161	10.5	99.3
2375	GAC BED 3, top surface	6/20/2006	90	42	1.4	1.3	45	0.0045	93.8%	43	8.09	191.0	0.009	
2372	GAC BED 3, Upper	6/20/2006	90	49	—	—	49	0.0049	—	58	11.29	1,070	0.052	—
2373	GAC BED 3, Lower	6/20/2006	90	155	—	—	155	0.0155	—	70	13.85	458	0.071	—
Avg Bed 3 conc/total Hg in Bed 3		—		—	—	—	—	—	—	—		1,719	0.123	—
Avgs/totals for all 3 beds		—		—	—	—	—	—	97.9%	—		3,932	16.8	—

Notes:

1. Mercury Digestion Procedure:
   a) Samples were digested as normal for carbons and/or other organic containing solids. (Tall test tubes, 5 ml HNO_3, 5 ml HCL, block digestor, 110°F for 7 hours with frequent vortexing).
   b) Samples and solutions were allowed to settle overnight. Solutions were carefully decanted to 100 ml vol flasks. A rinse of 20 ml DI was added to tubes and allowed to settle again. Rinses were decanted and added to original flasks, brought to volume, shaken, and a portion poured into vials for analysis.
   c) Second digestion: For selected samples, remaining residue was then re-digested for 2 hours. Decanted and rinsed as described in step 2.
   d) Third digestion: For selected samples, remaining residue was re-digested for 2 hours. Entire contents of tubes and subsequent rinses were transferred to flasks.
   Notes and comments regarding procedure:
   - Some "floating" and suspended fine residues were transferred to flasks in digestions 1 and 2. This could not be avoided.
   - Approximately 3 ml of rinse solution was left in tubes after digestions 1 and 2, and were carried over to digestions 2 and 3, respectively.
   - "Normal" procedure involves rinsing digestion tubes 3 times. This was not done for digestions 1 and 2.
2. Selected samples were triple-digested as a quality check of the digestion procedure. Test results show that almost all (94-100%) of the Hg that was digested was digested was digestd in the first digestion, so no corrections were made to samples that did not receive the triple digestion.
3. The Hg and S concentrations are converted to an Hg-free, virgin GAC basis. For simplicity, no other corrections for S loss, S conversion to SO_4, or moisture change were made.
4. The Bed 1 reached breakthrough, so some Hg certainly passed through Bed 1 into Bed 2. Assume that the Bed 2 and Bed 3 top samples represent the top 3 inches of that bed. Assume that the mass of GAC represented by Bed 2 and Bed 3 upper ports is each bed above the upper port, less the top 3 inches. The mass of GAC represented by the Bed 2 and 3 lower ports is assumed to be the GAC below the upper port to the bottom of the bed.
5. The GAC Bed 1 and 2 estimated Hg removal efficiencies were calculated using the mass of Hg captured in each of the 3 GAC beds, assuming 100% cumulative Hg capture in all 3 beds. This is a reasonably good assumption for calculating the Bed 1 and Bed 2
6. The total bed Hg and S average concentrations were calculated using weighted averages for each of the 3 beds.

[Hazen carbon bed CP1-CP2 results aug 8.xls]CP2 GAC Hg analyses

Table 7-49. Other analysis results for CP2 GAC bed activated carbon samples.

Sample I.D.	Sample Description	Date	Total S (wt %)	S normalized to Hg-free basis (%)	S loss (%)	S remaining (lb)	SO_4 (%)	S conversion to SO_4 (%)	Cl (%)	F (%)	NO_2 (ppm)	NO_3 (ppm)	PO_4 (%)
2377 Mersorb,	batch MER063Ht/01	6/21/2006	15.4	15.4 0.0%		582	1.58	3.4	<0.01 0.002		<10	<10	0.108
2366	GAC BED 1, screen 1	6/19/2006	10.9	12.3 20.3		—	8.65	26.5	0.06 0.005		<10	<10	0.10
2367	GAC BED 1, screen 2	6/19/2006	12.5	13.9	9.5	—	7.11	19.0	— —		— — —		
2368	GAC BED 1, screen 3	6/19/2006	11.5	12.9	16.4	—	7.00	20.3	— —		— — —		
2369	GAC BED 1, screen 4	6/19/2006	11.6	12.9	16.5	—	7.07	20.3	— —		— — —		
Avg Bed 1 conc./total Hg in Bed 1		—	11.6 13.0		15.7	6.81	7.5	21.5	0.06 0.005		<10	<10	0.095
2374	GAC BED 2, top surface	6/20/2006	11.0	11.7 24.2		—	7.63	23.1	<0.01 0.007		<10	<10	0.095
2370	GAC BED 2, Upper	6/20/2006	12.7	12.7	17.5	—	7.35	19.3	— —		— — —		
2371	GAC BED 2, Lower	6/20/2006	13.6	13.6	11.7	—	6.19	15.2	— —		— — —		
Avg Bed 2 conc./total Hg in Bed 2		—	13.2 12.7		17.8	274	7.1	17.2	<0.01 0.01		<10	<10	0.095
2375	GAC BED 3, top surface	6/20/2006	13.8	13.8	10.4		7.32	17.7 <0.01		0.004	<10	<10	0.088
2372	GAC BED 3, Upper	6/20/2006	12.2	12.2	20.8	—	5.78	15.8	— —		— —		NA
2373	GAC BED 3, Lower	6/20/2006	12.4	12.4	19.5	—	5.35	14.4	— —		— —		NA
Avg Bed 3 conc/total Hg in Bed 3		—	12.2 12.8		16.9	220	6.2	15.8	<0.01 0.004		<10	<10	0.088
Avgs/totals for all 3 beds		—	—	12.7 14.0		500	6.7	16.7	<0.01 0.006		<10	<10	0.092

[Hazen carbon bed CP1-CP2 results aug 8.xls]CP2 GAC S, other analyses

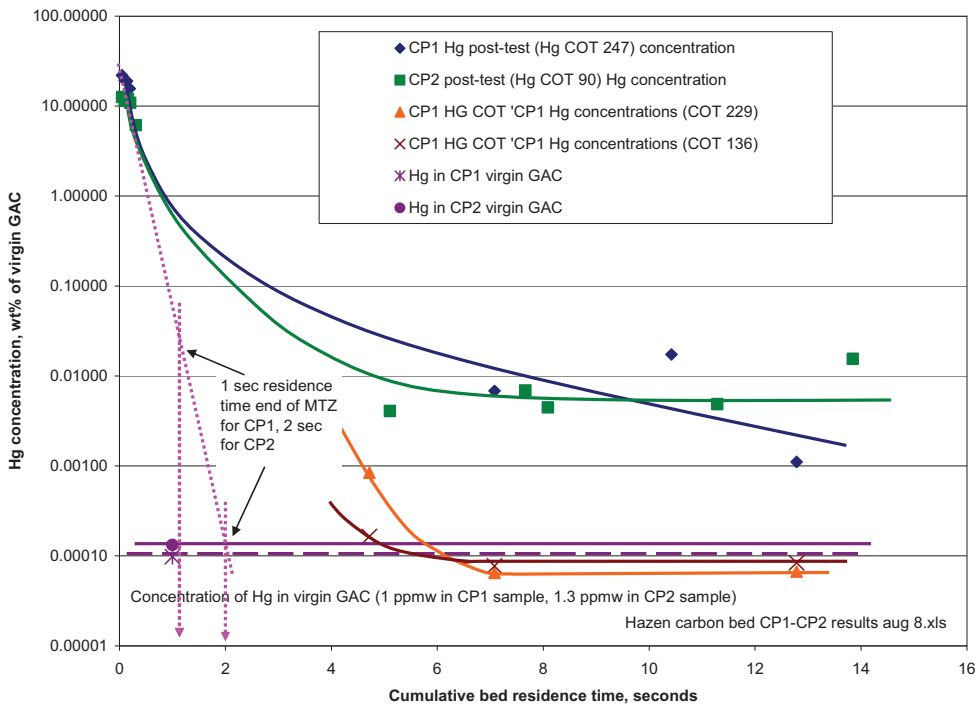

Figure 7-65. Hg concentrations in carbon bed samples from CP1 and CP2.

Post-test Hg concentrations decreased logarithmically after Bed 1, decreasing from levels that were (at almost 20 wt% loading) 200,000 times higher than the baseline Hg level in the virgin GAC of 1 ppmw. After a residence time of about 13 seconds, as the off-gas passed through almost the entire depth of the GAC bed, almost no Hg was left to sorb into the bed media. The Hg concentration in the spent GAC had decreased by up to 20,000x, to about a factor of 10 higher than the virgin GAC Hg level.

The CP1 and CP2 tests were not configured to enable an accurate determination of the mass transfer zone. Additional samples in Bed 2 during those tests would be necessary to determine the MTZ. But the bounding limit for the MTZ can be estimated by drawing the lines shown in Figure 7-65 through the measured concentrations in Bed 1 down to the "baseline" levels represented by the relatively flat concentrations in Beds 2 and 3. The bounding MTZ for CP1 corresponded to about a 1 second residence time, or about 5 inches. The bounding MTZ for CP2 corresponded to about a 2 second residence time, or about 10 inches. The actual MTZ was probably less than 5 inches for the CP1 and CP2 test conditions.

The GAC is sulfur-impregnated to enable chemisorption of elemental Hg, forming solid-phase and very nonvolatile HgS, the synthetic analog of naturally occurring cinnabar. Figure 7-66 shows that the spent carbon had lost a portion of the sulfur mass, an average of 11% in CP1 and 14% in CP2. The higher sulfur mass loss in CP2 may have been due to a higher initial S concentration of 15 wt% of the virgin carbon, versus 11 wt% of the virgin carbon in CP1.

Table 7-50 and Table 7-51 show the results of the Hg emission measurements made during CP2 at the outlet of each of the GAC bed stages and at the stack. After the CP1 test was completed, it was found that a portion of the off-gas had bypassed through the bypass piping around the carbon bed, due to an incorrectly configured valve actuator, and was not treated by the carbon bed to remove Hg. The CP1 stack gas was contaminated with this Hg, resulting in higher than expected Hg emissions. The CP1 stack gas Hg emissions do not represent levels of Hg that are expected in the off-gas following fixed bed carbon sorption treatment.

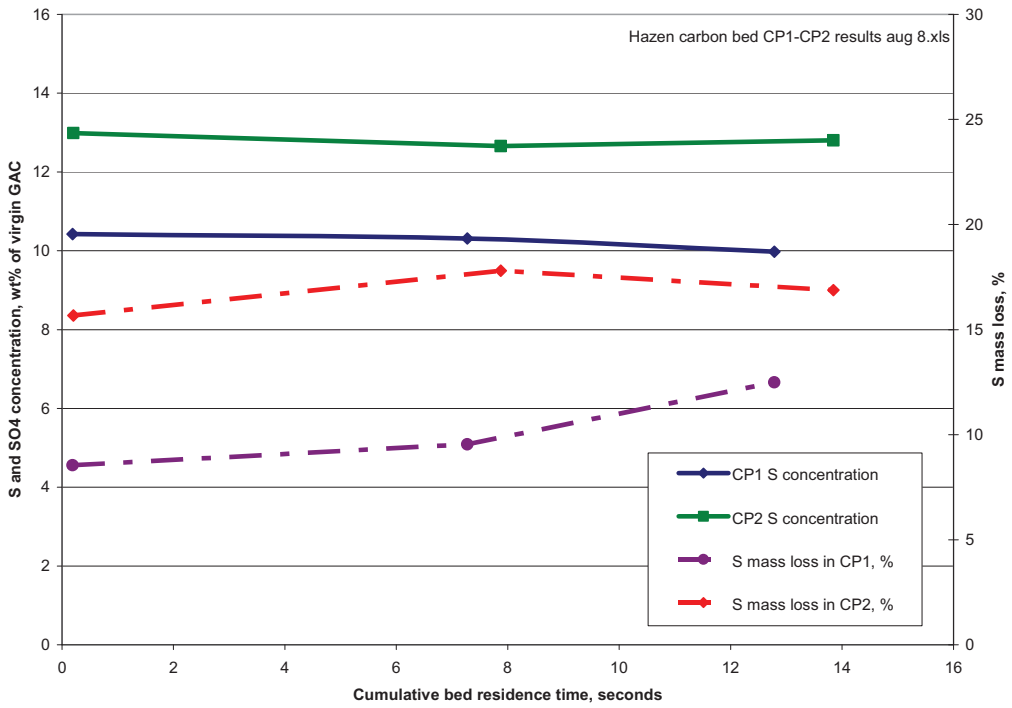

Figure 7-66. Sulfur concentrations in spent carbon bed samplesfrom CP1 and CP2.

Table 7-50. CP1 stack gas mercury emission measurements.

				Carbon bed 1 outlet						Carbon bed 2 outlet						Stack			
				OHM 1						OHM 2						M29 uncorrected for stack contamination			
				Hg Conc (µg/dscm [dry, 7% O_2])						Hg conc. (µg/dscm [dry, 7% O_2])						Hg con. (µg/dscm [dry, 7% O_2])			
Date Test	Period	Test	Hg feed COT at test end (hr)	Particle bound	Oxidized	Elemental	Total	Elemental Hg (% of total)	Hg SRE (%)	Particle bound	Oxidized	Elemental	Total	Elemental Hg (% of total)	Hg SRE (%)	Particle bound	Oxid. + elem	Total	Hg SRE (%)
18-Jan-06	1730–2107	1, day 1	0	—	—	—	—	—	—	—	—	—	—	—	—	0.01	3.41	3.42	—
19-Jan-06	1000–1330	1, day 2	0	—	—	—	—	—	—	—	—	—	—	—	—	—	—	—	—
27-Jan-06	1000–1310	2A	0.0	—	—	—	—	—	—	—	—	—	—	—	—	0.01	1.63	1.63	—
28-Jan-06	1230–1640	3B	16.5	0.45	388	9,971	10,360	96%	96%	0.38	12	3.6	16	23%	99.994%	0.01	1.63	1.63	99.9993%
29-Jan-06	1040–1426, 1600–1930	4A-1 38.2		24	30,438	4,408	34,870	13%	86%	1.10	12 3.5		16	21%	99.993%	30	10,876 10,906		95.5
30-Jan-06	1025–1415, 1620–1950	4A-2 62.0		945	52,479	8,397	61,820	14%	75%		12.1 3.8		16	24%	99.993%	29	5,311	5,340	98.7%
31-Jan-06	1110–1525	4A-3, day 1		— —		—	—	—	—	—	—	—	—	—	—	—	—	—	
1-Feb-06	1015–1335, 1600–2020	4A-3, day 2	101.0	3,726	78,719	8,397	90,841	9%	63%	0.39	12.1	3.6	16	22%	99.993%	45	23,480	23,524	90.3%
2-Feb-06	1015–1340, 1450–1810	4A-4 125.0		6,822	115,454	15,744	138,020	11%	43%	2.99	12.1 4.0		19	21%	99.992%	51	5,932	5,983	97.5%
3 Feb 06	1355–1720	4A-5, day 1	147.0	3,883	68,223	14,169	86,276	16%	64%	1.00	14.2	4.3	19	22%	99.992%	278	45,072	45,349	81.3%
4-Feb-06	0935–1351	4A-5, day 2		— —		—	—	—	—	—	—	—	—	—	—	—	—	—	
4-Feb-06	1805–2205	4A-6, day 1	176.0	2,414	131,198	27,289	160,901	17%	34%	131.20	4,600.0	3.6	4,735	0%	98%	2,061	35,879	37,941	84.4%
8-Feb-06	1400–1722	4A-6, day 2	224.0	—	—	—	—	—	—	—	—	—	—	—	—	—	—	—	
9-Feb-06	1000–1415	5	224.0	289	493	22,041	22,823	97%	91%	0.63	11.5	3.6	16	23%	99.994%	4	1,062	1,065	99.6%
10-Feb-06	0905–1241	6	247.0	997	15,744	17,843	34,584	52%	0%	0.01	0.0	3.5	3	99%	0%	3	580	583	95.6%
			Averages	2,122	54,793	14,251	71,166	36.1%	61.2%	17	521 3.7		540	28.5%	99.8%	227	11,882 11,882		93.6%

Notes:

1. MTEC = Maximum Theoretical Inlet Concentration, based on the simulant feedrate, the simulant Hg concentration, and the off-gas flow rate (which, at the carbon bed, is equal to the stack gas flow rate).
2. The Hg MTEC at the inlet to the carbon bed was calculated using the Hg concentration in the simulant feed, the simulant feedrate, the stack gas flow rate, and the 7% O_2 correction. This MTEC does not account for any small amounts of Hg that partition to the solid products. Some Hg partitions to the OGC effluent and the PBF fines, but the mass balance shows that the amount of Hg that partitions to these effluents is small compared to the total input Hg.

Hg in simulant feed, P6, gm/L:	1.81	Avg sim. feedrate, gpm:	0.248	Stack gas flow rate, dscfm:	125
Hg in simulant feed, P3-P5, gm/L:	0.098	HG MTEC, P3-P5, µg/dscm:	483,741	Hg MTEC, P3-P5, µg/dscm @ 7% O_2:	242,878
Stack gas rate, dscm/min:	3.53	HG MTEC, P6, µg/dscm:	26,192	Hg MTEC, P6, µg/dscm @ 7% O_2:	13,150

3. SRE = System Removal Efficiency, which is (1-Hg conc./Hg MTEC) × 100%
4. OHM = Ontario Hydro Method, used to better speciate elemental and oxidized Hg at the carbon bed sample locations.
5. Tests 1 and 2A were stack gas blank tests, when no Hg was in the simulant feed. Detected Hg levels during these tests is presumed to be from contamination.

[cp2 off-gas emissions aug 8.xls]offgas Hg control

Table 7-51. CP2 stack gas mercury emission measurements.

Date Test	Period	Test	Hg feed COT at test end (hr)	Carbon bed 1 outlet						Carbon bed 2 outlet						Carbon bed 3 outlet							Stack			Stack			
				OHM 1						OHM 2						OHM 3							M29 uncorrected for stack contamination			M29 corrected for stack contamination			
				Hg Conc (µg/dscm [dry, 7% O_2])				Elemental Hg (% of total)	Hg SRE (%)	Hg Conc. (µg/dscm [dry, 7% O_2])				Elemental Hg (% of total)	Hg SRE (%)	Isokinetic rate (%)	Hg Conc. (µg/dscm [dry, 7% O_2])				Elemental Hg (% of total)	Hg SRE (%)	Hg Con (µg/dscm [dry, 7% O_2])			Hg Conc (µg/dscm [dry, 7% O_2])			Hg SRE (%)
				Particle bound	Oxidized	Elem ental	Total			Particle bound	Oxidized	Elemental	Total				Partical bound	Oxidized	Elemental	Total			Particle bound	Oxid. + elem.	Total	Particle bound	Oxid. + elem.	Total	
1-Jun-06	1550–1910	1	0	2.3	7,300	112	7,414	—	—	3.0	1.5	5.0	9.5	—	—	—	0.3	1.5	7.2	8.9	—	—	0.64	36	37	—	—	—	—
3-Jun-06	1150–1550	2	0	9.4	361	1,180	1,551	—	—	4.0	1.9	3.3	9.3	—	—	—	0.4	0.9	2.5	3.7	—	—	0.73	13	14	—	—	—	—
5-Jun-06	1110–1440	3	35.2	5.2	139,522	46,341	185,868	25%	48%	10.0	2.2	3.3	15.5	21.5%	99.996%	95.5	0.6	3.9	1.9	6.5	29%	99.9982%	0.68	15	16	-0.05	2.16	2.1	99.9994%
6-Jun-06	1040–1415	4	58.8	2.2	125,225	45,545	170,773	27%	52%	3.0	3.5	3.3	9.8	34.1%	99.997%	98.3	0.3	1.3	1.6	3.1	50%	99.9991%	1.91	19	21	1.18	5.91	7.1	99.9983%
7-Jun-06	0950–1310	5	81.7	14.0	22,890	2,220	25,124	9%	93%	3.2	87,589	27,778	115,371	24.1%	68%	98.4	0.3	1.2	1.5	3.0	51%	99.9992%	1.89	14	16	1.16	0.81	2.0	99.9998%
7-Jun-06	1745–2110	6	89.7	6.6	191,788	49,345	241,140	20%	32%	13.4	13,068	2,249	15,331	14.7%	96%	102.1	4.8	1.5	2.1	8.4	25%	99.9976%	1.84	20	21	1.11	6.49	7.6	99.9982%
Averages				7	119,856	35,863	155,726	20%	56%	7.4	25,166	7,508	32,682	23.6%	91%	98.6	1.5	2.0	1.8	5.3	39%	99.9985%	1.58	17	19	0.85	3.84	4.7	99.9989%
HWC MACT standard, µg/dscm (dry, 7% O_2)				—	—	—	—	—	—	—	—	—	—	—	—	—	—	—	—	8.1	—	—	—	—	8.1	—	—	8.1	—
Average measured value, % of MACT standard				—	—	—	—	—	—	—	—	—	—	—	—	—	—	—	—	65%	—	—	—	—	229%	—	—	58%	—

Notes:

1. MTEC = Maximum Theoretical Inlet Concentration, based on the simulant feedrate, the simulant Hg concentration, and the off-gas flow rate (which, at the carbon bed, is equal to the stack gas flow rate).
2. The Hg MTEC at the inlet to the carbon bed was calculated using the Hg concentration in the simulant feed, the simulant feedrate, the stack gas flow rate, and the 7% O_2 correction. This MTEC does not account for any small amounts of Hg that partition to the solid products. Some Hg partitions to the OGC effluent and the PBF fines, but the mass balance shows that the amount of Hg that partitions to these effluents is small compared to the total input Hg.

Hg in simulant feed, gm/L:	1.51	Avg sim. feedrate, gpm:	0.245	Stack gas flow rate, dscfm:	140
Stack gas rate, dscm/min:	3.96	HG MTEC, µg/dscm:	355,382	Hg MTEC, µg/dscm @ 7% O_2:	356,289

3. SRE = System Removal Efficiency, which is (1-Hg conc./Hg MTEC) × 100%
4. OHM = Ontario Hydro Method, used to better speciate elemental and oxidized Hg at the carbon bed sample locations.
5. Tests 1 and 2 were stack gas blank tests, when no Hg was in the simulant feed. Detected Hg levels during these tests is presumed to be from stack contamination.
6. The stack Method 29 samples were contaminated by residual Hg in the process from when the carbon bed was bypassed in CP1, allowing the equipment downstream of the carbon bed (the off-gas ducting, valves, blowers, and stack) to become contaminated by Hg. The stack gas Method 29 Hg results for test days when no Hg was fed into the process show that the Hg contamination could have been a significant, but possibly decreasing, portion of the stack Hg measured when Hg was fed to the process.
7. Averages shown above include only Tests 3-6, which are those tests during which Hg was fed to the process.
8. For comparison, the stack gas Hg levels were corrected for blank contamination using the measured Hg values from Test 2.

[cp2 off-gas emissions aug 8.xls]offgas Hg control

The incorrectly configured valve actuator was corrected prior to CP2. In addition, a blind was installed in the bypass to ensure against off-gas bypass flow around the carbon bed. Some residual contamination remained in the stack from the CP1 test. A continuous Hg monitor was operated during CP2 to determine instantaneous stack gas Hg levels. This analyzer was not sufficiently sensitive to demonstrate HWC MACT compliance, but it indicated that initially high levels of Hg contamination in the equipment were reduced to a range of 0–40 μg/dscm, providing some confidence that the Hg testing could go forward without: (a) discharging amounts of Hg that could approach the Hazen project Hg emission limit of 10 lb, and (b) excessively high levels of Hg in the stack that would invalidate stack gas Hg measurements at the stack location.

Additional actions taken to confirm blank Hg levels, and to ensure the highest quality Hg measurements that were practical, were: (a) Hg sampling was performed at the outlet of all three GAC beds; the Hg measurements made at the outlet of Bed 3 were essentially equivalent to those performed at the stack, but were subject to far less potential Hg contamination, and (b) Hg train measurements were made after the start of CP2, but before Hg and other hazardous metals and radionuclide surrogates were added to the simulant feed, to establish off-gas blank levels of Hg.

Two stack gas blank tests were performed prior to Hg feeding. The results of these blank tests confirmed: (a) residual Hg stack contamination from CP1, and (b) lower, but detectable levels of blank levels of Hg even at the outlet of GAC Bed 3.

The Hg emission results from both the GAC Bed 3 outlet (uncorrected for any blank Hg levels) and from the stack (corrected for blank stack contamination) are in reasonably close agreement, with average values of 5.3 and 4.7 μg/dscm (@ 7% O_2) respectively. These values are about 58–65% of the HWC MACT limit for Hg of 8.1 μg/dscm (@ 7% O_2). If the GAC Bed 3 outlet sample location were also corrected for the blank Hg level measured prior to Hg feeding, then the corrected Hg concentration at this location would be lowered to 1.6 μg/dscm (@ 7% O_2).The Hg sorption performance of the 3-stage GAC bed during CP2 is shown in Figure 7-67. Bed 1 was designed with a very short residence time and only 4 inches deep, so that it could approach Hg saturation within a reasonable test duration in order to evaluate the Hg sorption capacity of the GAC under the test operating conditions. The blank (COT = 0) Hg levels at the outlet of Bed 1 indicate Hg contamination at this location from the CP1 test. By the first Hg test that ended at about COT 35, the off-gas Hg levels at the outlet of Bed 1 had reached almost 190,000 μg/dscm (@ 7% O_2). Considering the Hg Maximum Theoretical Emission Concentration at the inlet to the GAC bed of almost 360,000 μg/dscm (@ 7% O_2), this bed was still capturing about 50% of the Hg. Through the remainder of the test, the Bed 1 outlet Hg level varied from test to test but gradually increased to over 240,000 μg/dscm (@ 7% O_2), indicating a continuing control efficiency of over 30%. This shows that the Bed 1 in fact did not reach its Hg sorption capacity during the test.

Figure 7-68 shows carbon bed Hg removal efficiencies for both CP1 and CP2 calculated two different ways. The first method calculates the removal efficiency by comparing the total Hg measured in the off-gas at the outlet of each of the three carbon bed stages (the first two in CP1, since no Hg measurements were made at the outlet of Bed 3 in CP1) and the stack. The stack Hg removal efficiency calculated for CP1 is not included in this figure, since the stack gas samples from CP1 were contaminated with Hg that had bypassed the carbon bed, resulting in an invalid indication of stack gas Hg levels downstream of the carbon bed, and an invalid indication of the carbon bed Hg removal efficiency. The second method of calculating the Hg removal efficiency for Beds 1 and 2 uses the mass of Hg captured in each bed, compared to the total Hg captured in all three beds, based on the analysis of the samples collected at discrete sample locations.

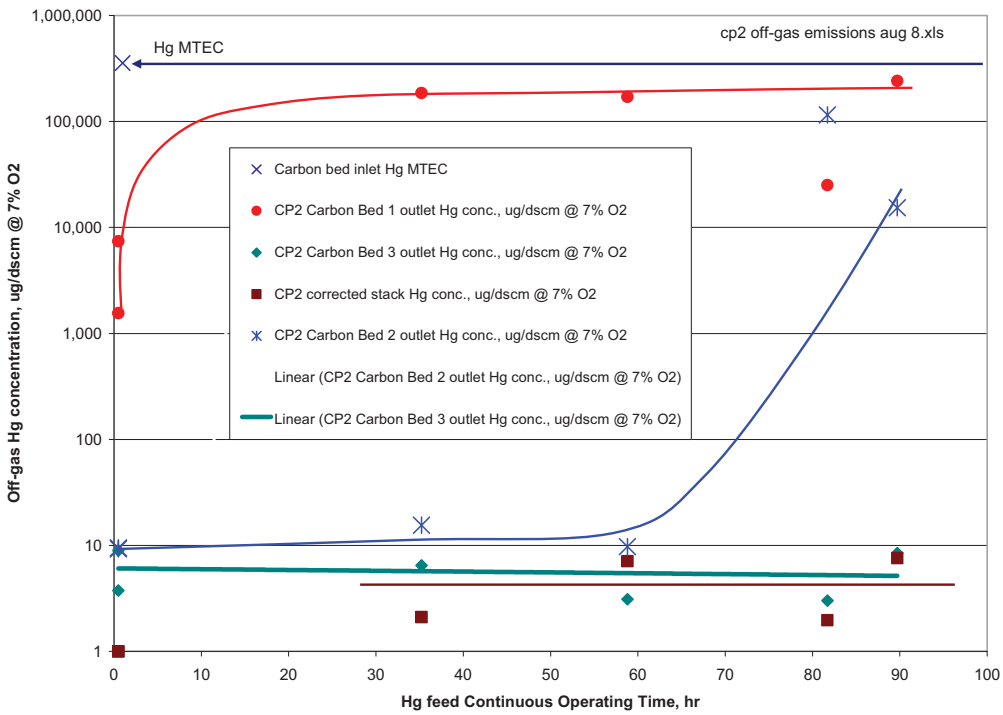

Figure 7-67. Off-gas Hg concentrations during CP2.

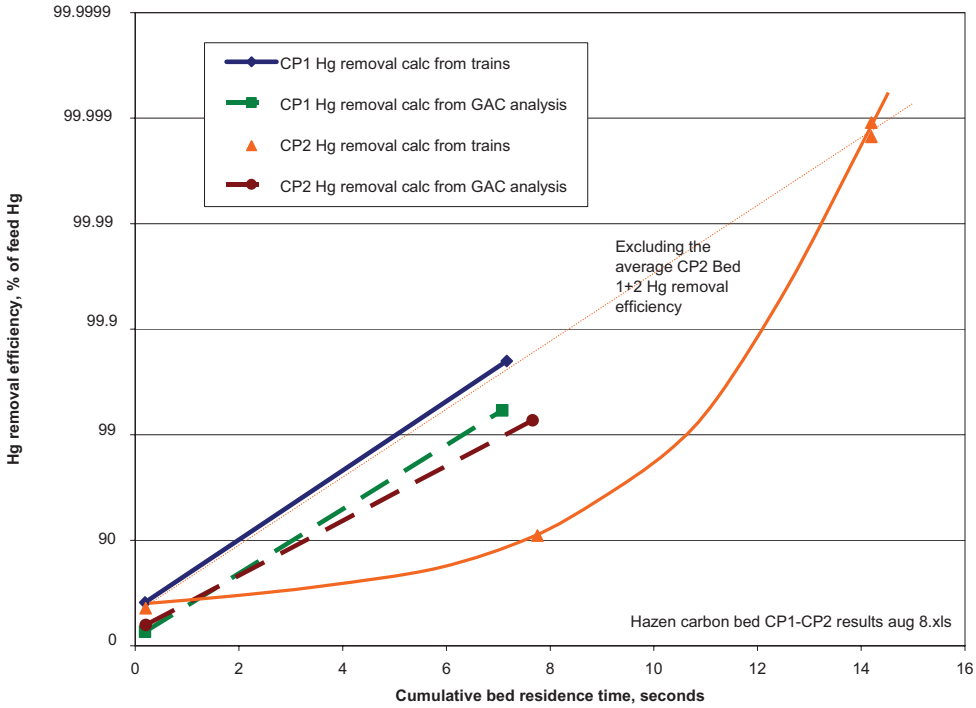

Figure 7-68. Hg removal efficiency by the carbon bed during CP1 and CP2.

The carbon bed Hg removal efficiency results based on the test-average stack gas analyses and post-test spent carbon analyses trend reasonably well. This figure shows that high stack gas Hg removal efficiencies can be achieved with appropriately designed GAC beds with sufficient residence times.

The CP2 Bed 3 outlet and corrected stack Hg measurements indicate that the cumulative 3-bed sorption efficiency was steady at almost 99.9999% during the entire test duration.

7.7.9.2 Spent Granular Activated Carbon Leachability. The concentrations of Hg, S, SO4, Cl, F, nitrite, nitrate, and PO4 sorbed on the carbon are tabulated in Section 7.9.9.1. That section also discusses the Hg sorption performance of the carbon, and the retention of S, which is critical for efficient elemental Hg sorption, on the carbon. Figure 7-69 shows the concentrations of SO4 in spent carbon compared to SO4 concentrations in virgin carbon. A portion of the S impregnated on the carbon converted to SO4 during the tests. NUCON International, the carbon vendor, reports that SO4 performs as well or better than elemental S for aiding in the chemisorption of elemental Hg on the carbon.

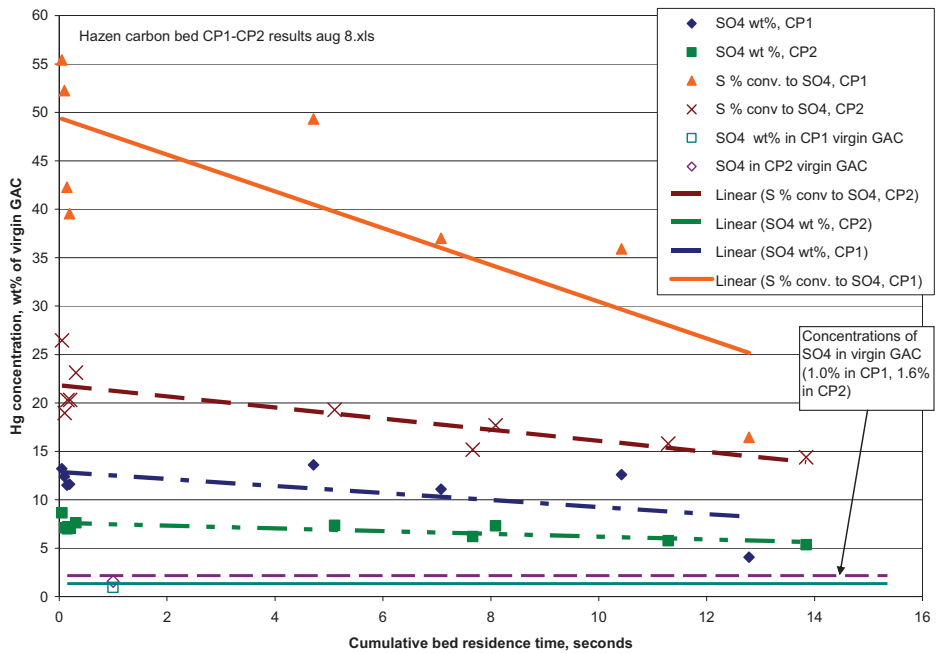

Figure 7-69. SO_4 in spent carbon samples from CP1 and CP2.

Figure 7-70 shows that levels of Cl, F, and PO4 remained very low or nondetectable during the tests. Nitrate and nitrite were also almost all nondetects, or were present at levels of 10 ppmw (0.001 wt%) or less. These low concentrations should have little affect on the disposability of the spent carbon.

Sorbed Hg, sometimes approaching 20 wt% of the original weight of the carbon, presents a significant disposability issue since Hg is a hazardous metal. Figure 7-71 and Table 7-52 and Table 7-53, show Toxicity Characteristic Leachability Procedure (TCLP, EPA Method 1311) test results for Hg leachability. Samples of spent carbon that contained Hg at concentrations below about 200 ppmw (0.02 wt%) generally passed TCLP limits. These carbon samples retained about 99.9% or more of the sorbed Hg. Samples that contained over about 60,000 ppmw (6 wt%) Hg generally exceeded the TCLP limits for Hg concentration in the leachate, although these samples still generally retained 98–99.9% of the sorbed Hg. The percentage of Hg that leached tended to increase as the concentration of Hg in the spent carbon increased.

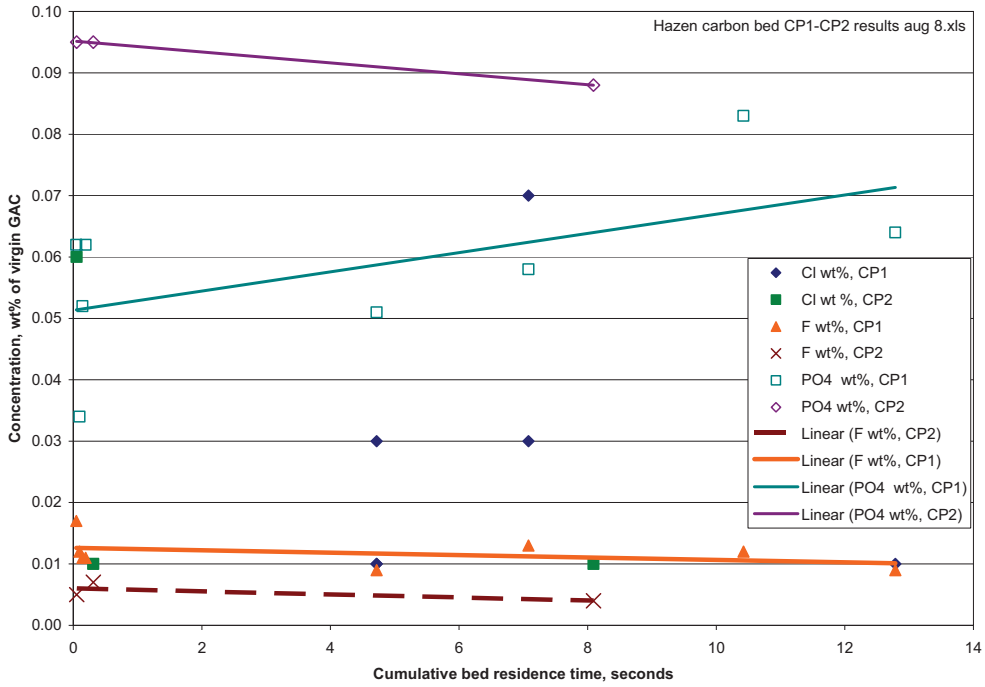

Figure 7-70. Concentrations of trace off-gas elements sorbed on spent carbon from CP1 and CP2.

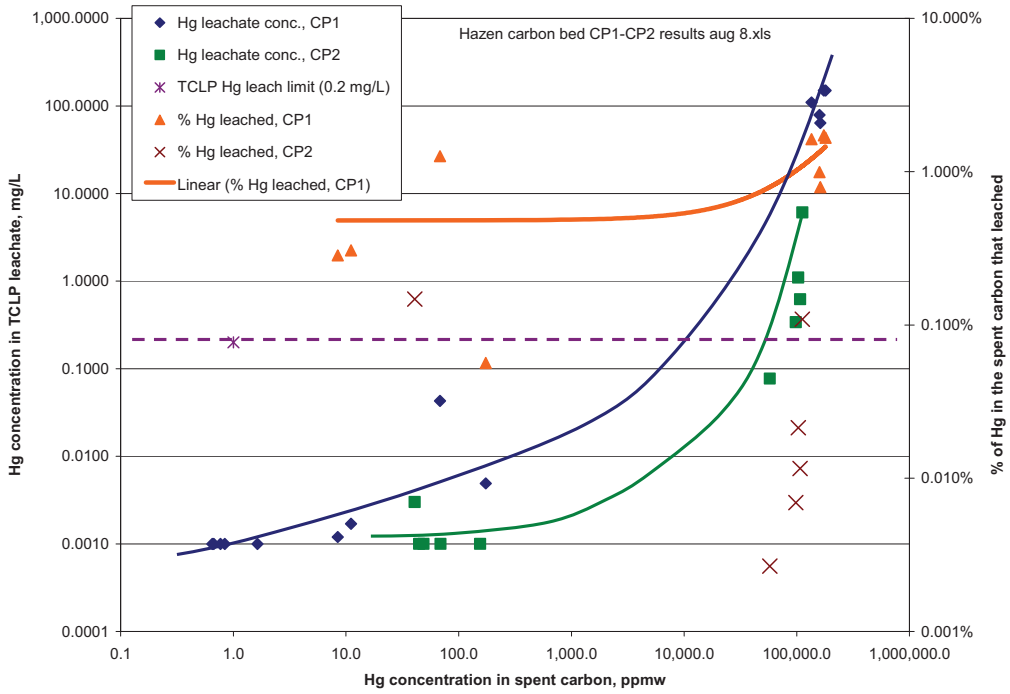

Figure 7-71. Spent carbon Hg leachability results for CP1 and CP2.

Table 7-52. Spent carbon TCLP leach results for CP1.

Sample I.D.	Sample Description	Date	Total Hg (ppmw)	TCLP Leachate Hg (mg/L)	TCLP Leachate Hg leached (%)
Mersorb 3AT	As-Received Activated Carbon		0.98	—	—
1786	GAC bed 2 upper port	2/5/2006	1.64	0.0010	—
1787	GAC bed 2 lower port	2/5/2006	0.77	0.0010	—
1789	GAC bed 3 lower port	2/5/2006	0.84	0.0010	—
1859	GAC bed 2 upper port	2/9/2006	8.44	**0.0012**	**0.28%**
1860	GAC bed 2 lower port	2/9/2006	0.65	0.0010	—
1862	GAC bed 3 lower port	2/9/2006	0.67	0.0010	—
1886	GAC bed 1, screen 1	2/15/2006	173,946	**150**	**1.72%**
1887	GAC bed 1, screen 2	2/15/2006	180,113	**150**	**1.67%**
1888	GAC bed 1, screen 3	2/15/2006	161,496	**64**	**0.79%**
1889	GAC bed 1, screen 4	2/15/2006	158,998	**79**	**0.99%**
1891	GAC bed 2 upper port	2/16/2006	134,952	**110**	**1.63%**
1892	GAC bed 2 lower port	2/15/2006	68	**0.043**	**1.26%**
1893	GAC bed 3 upper port	2/16/2006	174	**0.0049**	**0.06%**
1894	GAC bed 3 lower port	2/15/2006	11	**0.0017**	**0.31%**

Notes:

1. **Bolded** leachate concentration values indicate detected results. **Unbolded** values indicate no detectable Hg.
2. Detection limit values were not used in leach calculations because they could bias the results.

[Hazen carbon bed CP1-CP2 results aug 8.xls]CP1 Hg leach

Table 7-53. Spent carbon TCLP leach results for CP2.

Sample I.D.	Sample Description	Date	Total Hg (ppmw)	TCLP Leachate Hg (mg/L)	TCLP Leachate Hg leached (%)
2377 Mersorb,	batch MER063Ht/01	6/21/2006	1.32	—	—
2366	GAC BED 1, screen 1	6/19/2006	112,037	**6.1**	**0.11%**
2367	GAC BED 1, screen 2	6/19/2006	103,000	**1.1**	**0.02%**
2368	GAC BED 1, screen 3	6/19/2006	107,000	**0.62**	**0.01%**
2369	GAC BED 1, screen 4	6/19/2006	98,000	**0.34**	**0.01%**
2374	GAC BED 2, top surface	6/20/2006	57,732	**0.077**	**0.003%**
2370	GAC BED 2, Upper	6/20/2006	41	**0.0030**	0.15%
2371	GAC BED 2, Lower	6/20/2006	69	0.0010	—
2375	GAC BED 3, top surface	6/20/2006	45	0.0010	—
2372	GAC BED 3, Upper	6/20/2006	49	0.0010	—
2373	GAC BED 3, Lower	6/20/2006	155	0.0010	—

Notes:

1. **Bolded** leachate concentration values indicate detected results. **Unbolded** values indicate no detectable Hg.
2. Detection limit values were not used in leach calculations because they could bias the results.

[Hazen carbon bed CP1-CP2 results aug 8.xls]CP2 Hg leach

A few samples of spent carbon contained Hg in concentrations between 200–60,000 ppm, because of the high affinity of the carbon for Hg. When a layer of carbon was exposed to Hg, it tended to sorb Hg until it reached Hg concentrations over 60,000 ppm. Only then did that layer allow Hg to pass on through to the next layer of carbon. This is consistent with the Mass Transfer Zone theory of Hg sorption, but results in carbon near the front of a carbon bed that is loaded with higher Hg concentrations that may fail leachability tests, while carbon near the back of the carbon bed may contain very little Hg and can easily pass leachability tests.

The Hg TCLP results show that even though the spent carbon retained almost all of the sorbed Hg, the small fraction of Hg that leaches was large enough to cause the TCLP test results to exceed the TCLP limit for Hg.

7.7.10 GAC Bed Thermal Event

The GAC bed was valved on-line during the entire ESTD start-up period beginning on May 15. During the heat-up a “hot spot” formed in the top of the third bed. The term “hot spot” is used to describe an area in the GAC bed that increased in temperature up due to exothermic sorption of gas species, or from exothermic reactions between sorbed or gaseous species and the activated carbon. Sorption of many gas species onto activated carbon is an exothermic process. When the rate of heat generation due to sorption exceeds the rate of convective and conductive cooling, then the GAC bed temperature can rise. Temperature increases typically occur only in a portion or “spots” in a GAC bed, where sorption rates or gas temperatures are are high, or where low gas velocities or gas maldistribution result in low convective cooling rates.

When the hot spot occurred during the CP2 startup, and local temperatures near the wall at the top of Bed 3 rose sharply above 200°C, the process emergency shutdown system was activated. The GAC bed was isolated, and a cool, inert nitrogen purge introduced to the GAC bed as a result of the shutdown system activation. The start-up of the ESTD CP2 test was terminated and the GAC bed temperature event was investigated and evaluated prior to restart of the CP2 demonstration. Exothermic reactions ceased at the time, or shortly after, the nitrogen purge started. The cooldown required several hours for heat to transfer from the hot spots to the nitrogen gas, and progress through the depth of the GAC bed until the GAC bed again approached ambient temperature.

The startup time for a GAC bed is a time when, as the gas starts to flow through the GAC bed and change compositions, heat and mass transfer can cause bed heatup (or cool-down). The ESTD GAC bed had been started up several times and operated over extended periods with good temperature control during the CP1 prior to the thermal event, and again during CP2 after the event. An investigation has focused on differences between the successful GAC bed start-ups and the subject start-up that experienced the thermal event. The principal difference that occurred during this startup was that the GAC bed was online with gas flow through bed during initial heating and startup of the CRR. During the CRR startup, the gas composition varies as the natural gas-fired startup burner is started, and oxygen, charcoal, and petroleum coke are added. Oxidation in the CRR is initially slow and incomplete until the CRR temperature exceeds 700°C. During this heatup time, the gas that entered the GAC bed was changing in composition and heating up, and carried levels of incompletely oxidized hydrocarbon species.

The events that lead up to this thermal event have been identified and appear to be related to conditions that occurred during the CRR heatup. The test data, and supporting data from NUCON International, the GAC vendor, suggest that temperature increase followed a fairly typical sequence that is common in process startups. The GAC bed media was initially heated through sorption of water (and possibly organic species from the CRR startup natural gas-fired burner) in the gas stream. When localized “hot spots” were heated enough from heat of sorption of gas species, then exothermic reactions between

sorbed hydrocarbons (from the startup burner) and oxygen in the gas stream perhaps further heated those hot spots, eventually to a temperature high enough that some of the carbon in the heated area began to oxidize.

This hypothesis, which is supported by data and activated carbon industry experience, is being evaluated in detail, with additional sample analysis, by TTT and Nucon International. Evaluations shortly after the event led to this hypothesis and identified corrective actions that were implemented for the successful restart and completion of the CP2 test (See Hazen CP2 Granular Activated Carbon (GAC) Bed Over-temperature Condition Joint Test Group Action Form No. 7, Washington Group International, May 17, 2006[R26].)

Recommendations for engineered and administrative controls for safe GAC bed design and operation for the IWTU will be prepared from the results of the still-ongoing evaluations and analyses of this thermal event. TTT is working with NUCON and supporting organizations to complete this evaluation. The engineered and administrative controls will include the following components:

- Bed design for appropriate gas velocity and residence time, adequate gas flow distribution to ensure an adequate and distributed gas flow for even convective cooling and gas species adsorption evenly across the entire bed cross section area

- Automatic and continous monitoring of both bed temperatures and CO, which is the industry standard for sensing hot spots

- Corrective actions, including incoming gas temperature, flowrate, and composition control, to respond to indications of hot spot formation before the GAC bed reaches temperatures that exceed limits for the GAC bed

- Additional corrective actions, including automatic waste feed cutoff, GAC bed bypass, and GAC bed inert gas purging, in the event that GAC bed high and high high temperature limits are approached.

Implementing the first steps will normally provide adequate temperature control during startup and operation, even when, as by design, gas species sorb onto the GAC bed and release heat. Appropriate implementation of the first steps will prevent the need to implement the last steps. The last steps will ensure against environmental releases, permit violations, equipment damage, and worker and public hazards in the event that unusual circumstances are not controlled by the first steps.

7.7.11 VOC Emissions and POHC Destruction

Table 7-54 shows the VOC emission measurement results from CP1. Monochlorobenzene, a chlorinated, aromatic Class 1 VOC, was the POHC. No monochlorobenzene was detected in any of the 6 tests when it was spiked in the feed and measured for in the off-gas. The POHC DRE for 4 of the 6 tests was >99.9997% using the off-gas detection limit values, almost 2 orders of magnitude better than the HWC MACT limit of 99.99%. The Method 0031 samples for 2 test conditions exceeded their hold times prior to analysis and so are flagged. Including the detection limit data for these two tests, the POHC DRE was >99.998%, ten times lower than for the other 4 tests, but still almost ten times higher than the MACT limit.

No VOCs on the Standard 0031 VOC analysis list were detected in any of the tests, except for: (a) Freon 12 or methylene chloride in one or more runs from P-1, P-4A3, and P-4A4, and (b) various tentatively identified compounds (TICs) that were not included in the standard VOC target list, but which

were sporadically detected and tentatively identified and estimated from GC/MS peaks. The amounts of all TICs were near or below detection limits. The appearance of a few TICs, and the occurrance of a few low surrogate recoveries, are common in Method 0031 measurements.

7.7.11.1 SVOC Emissions. Table 7-55 shows the CP1 SVOC emission measurement results. No SVOCs were detected, except for one in all tests (Di-n-butyl phthalate) and one other one (N-Nitrosodimethylamine) in 4A-3. Both detects were at low levels, near the detection limit.

7.7.11.2 Total Organic Emissions. Table 7-56 shows the results of the CP1 Total Organic Emission (TOE) measurements using a Field Gas Chromatograph (EPA Method 0040) and Total Chromatographable Organics (TCO)/Gravimetrically Determined Organics (Grav). Hydrocarbons in the C1 to C7 range and larger hydrocarbons were detected, but not speciated using these methods.

The 0040 Field Gas Chromatograph results averaged around 2 mg/dscm C1-C7 compounds for tests without the POHC spike, and about 10 mg/dscm with the POHC spike. These values are consistent with the stack gas THC and the 0031 results if the C1-C7 compounds detected in the 0040 analyses are halogenated, multiple-bonded, or partially oxidized species that are too volatile to have been detected in the 0031 analysis. Halogenated, multiple-bonded, and partially oxidized species are not well detected using the THC CEM, and they are often found in off-gas from thermal processes. They might result from the POHC spike, even when the POHC itself is efficiently destroyed.

The 0040 results range about 10x lower than the 0040 results from the Idaho National Laboratory New Waste Calcining Facility (NWCF), based on emission inventory measurements.
(See Boardman, R. D., L. J. Young, N. R. Soelberg, M. L. Abbott, and D. V. Croson, "Summary of NWCF Calciner Emissions Inventory Data," INEEL/EXT-99-1190, November 1999 [R26].)

The TCO/Grav results showed detectable total SVOCs ranging around 1–13 mg/dscm. This range is about 10x to 100x lower than the TCO/Grav range measured in the NWCF calciner emission inventory tests. (See Young, L. J., N. R. Soelberg, B. H. O'Brien, R. D. Boardman, L. A. Matejka, M. L. Abbott, and G. R. Hassel, "NWCF Calciner Emissions Inventory – Final Report for Test Series 1, 2, and 3," INEEL/EXT-2000-00114, January 2000 [R37].)

Figure 7-72 shows that, while there is considerable scatter in the TOE measurements due in part to different CRR temperatures, the TOE concentrations decrease with increasing CRR outlet O_2 concentrations, as expected.

7.7.11.3 Dioxin and Furan Emissions. Table 7-57 shows the CP1 stack gas dioxin measurements. No dioxins or furans were detected above their reporting limits. Using detection limit values, the dioxin results range about 0.01 to 0.02 ng/dscm corrected to 7% O_2. This is less than 10–20% of the HWC MACT limit of 0.11 ng/dscm (dry @ 7% O_2) for new facilities.

7.7.11.4 PCB Emissions.Table 7-58 shows the stack gas PCB measurements made during CP1. PCBs totaled about 5–10 ng/dscm, corrected to 7% O_2. Most PCB congeners were not detected. These levels are 10–100 times lower than were found in the NWCF offgas.

Dioxin-like coplanar PCBs were not detected at detection limits of about 0.5 to 1 ng/dscm.

Table 7-54. CP1 stack gas VOC concentrations and emissions rates.

Test	1, day 1	1, day 2	2A	3B	4A-1	4A-2	4A-3, day 1	4A-3, day 2	4A-4	4A-5 day 1	4A-5 day 2	4A-6, day 1	4A-6, day 2	5	6
Date	18-Jan	19-Jan	27-Jan	28-Jan	29-Jan	30-Jan	31-Jan	1-Feb	2-Feb	3-Feb	4-Feb	4-Feb	8-Feb	9-Feb	10-Feb
Test Period	—	1003–1240	—	—	1040–1426	1025–1415	1110–1525	—	1450–1810	—	0935–1351	—	1400–1722	—	—
Total sample duration, min	—	112	—	—	120	120	120	—	120	—	120	—	120	—	—
Total sample volume, dry standard liters	—	48.8	—	—	50.1	50.4 49.3		—	50.5	—	51.3	—	48.9	—	—
VOC species concentrations, µg/dscm															
2-Butanone —		<,R 16.7	—	—	<,R 16.3	<,R 20.5	<,R 20.9	<,R 20.8	<,R 20.4	—	<,R 20.1		<,R 16.7	—	—
Monochlorobenzene —		< 4.0	—	—	< 3.9	< 4.7	< 4.8	< 4.8	< 4.7	—	<,R 4.6	—	<,R 3.9	—	—
Dibromochloromethane —		< 4.0	—	—	< 3.9	< 4.7	< 4.8	< 4.8	< 4.7	—	<,R 4.6	—	<,R 3.9	—	—
1,2-Dibromo 3-Chloropropane	—	<,R 7.9	—	—	<,R 7.7	<,R 9.4	<,R 9.6	<,R 9.5	<,R 9.3	—	<,R 9.2	—	<,R 7.9	—	—
1,2-Dibromoethane (ethylene dibromide)	—	< 4.0	—	—	< 3.9	< 4.7	< 4.8	< 4.8	< 4.7	—	<,R 4.6	—	<,R 3.9	—	—
Dibromomethane (methylene bromide)	—	< 4.0	—	—	< 3.9	< 4.7	< 4.8	< 4.8	< 4.7	—	<,R 4.6	—	<,R 3.9	—	—
1,2-Dichlorobenzene —		< 4.0	—	—	< 3.9	< 4.7	< 4.8	< 4.8	< 4.7	—	<,R 4.6	—	<,R 3.9	—	—
1,3-Dichlorobenzene —		< 4.0	—	—	< 3.9	< 4.7	< 4.8	< 4.8	< 4.7	—	<,R 4.6	—	<,R 3.9	—	—
1,4-Dichlorobenzene —		< 4.0	—	—	< 3.9	< 4.7	< 4.8	< 4.8	< 4.7	—	<,R 4.6	—	<,R 3.9	—	—
Dichlorodifluoromethane (Freon 12)	—	< **97.6**	—	—	< 4.7	< 6.4	< 6.5	< 6.5	< **6.5**	—	<,R **6.5**	—	<,R **6.0**	—	—
1,1-Dichloroethane —		< 4.0	—	—	< 3.9	< 4.7	< 4.8	< 4.8	< 4.7	—	<,R 4.6	—	<,R 3.9	—	—
1,2-Dichloroethane (ethylene dichloride)	—	< 4.0	—	—	< 3.9	< 4.7	< 4.8	< 4.8	< 4.7	—	<,R 4.6	—	<,R 3.9	—	—
1,1-Dichloroethylene —		< 4.0	—	—	< 3.9	< 4.7	< 4.8	< 4.8	< 4.7	—	<,R 4.6	—	<,R 3.9	—	—
1,2-Dichloropropane —		< 4.0	—	—	< 3.9	< 4.7	< 4.8	< 4.8	< 4.7	—	<,R 4.6	—	<,R 3.9	—	—
Ethylbenzene —		< 4.0	—	—	< 3.9	< 4.7	< 4.8	< 4.8	< 4.7	—	<,R 4.6	—	<,R 3.9	—	—
Hexachloro-1,3-butadiene (perchlorobutadiene)	—	< 4.8	—	—	< 4.7	< 6.4	< 6.5	< 6.5	< 6.4	—	<,R 6.3	—	<,R 4.8	—	—
Methylene chloride	—	< **13.1**	—	—	< 4.7	< 6.4	< 6.5	< **6.8**	< **7.1**	—	<,R **20.8**	—	<,R **7.0**	—	—
Naphthalene —		< 4.0	—	—	< 3.9	< 4.7	< 4.8	< 4.8	< 4.7	—	<,R **9.2**	—	<,R 4.8	—	—
1,1,1,2-Tetrachloroethane —		< 4.0	—	—	< 3.9	< 4.7	< 4.8	< 4.8	< 4.7	—	<,R 4.6	—	<,R 3.9	—	—
1,1,2,2-Tetrachloroethane —		< 4.0	—	—	< 3.9	< 4.7	< 4.8	< 4.8	< 4.7	—	<,R 4.6	—	<,R 3.9	—	—
1,2,3-Trichlorobenzene —		< 4.0	—	—	< 3.9	< 4.7	< 4.8	< 4.8	< 4.7	—	<,R 6.8	—	<,R **4.7**	—	—
1,2,4-Trichlorobenzene —		< 4.0	—	—	< 3.9	< 4.7	< 4.8	< 4.8	< 4.7	—	<,R 6.1	—	<,R **4.3**	—	—
1,1,1-Trichloroethane —		< 4.0	—	—	< 3.9	< 4.7	< 4.8	< 4.8	< 4.7	—	<,R 4.6	—	<,R 3.9	—	—
1,1,2-Trichloroethane —		< 4.0	—	—	< 3.9	< 4.7	< 4.8	< 4.8	< 4.7	—	<,R 4.6	—	<,R 3.9	—	—
1,2,3-Trichloropropane —		< 4.0	—	—	< 3.9	< 4.7	< 4.8	< 4.8	< 4.7	—	<,R 4.6	—	<,R 3.9	—	—
1,3,5-Trimethylbenzene —		< 4.0	—	—	< 3.9	< 4.7	< 4.8	< 4.8	< 4.7	—	<,R 4.6	—	<,R 3.9	—	—
m- and p-Xylene	—	< 7.0	—	—	< 6.8	< 7.7	< 7.8	< 7.8	< 7.6	—	<,R 7.5	—	<,R 7.0	—	—
o-Xylene —		< 4.0	—	—	< 3.9	< 4.7	< 4.8	< 4.8	< 4.7	—	<,R 4.6	—	<,R 3.9	—	—

Table 7-54. (continued).

Test	1, day 1	1, day 2	2A	3B	4A-1	4A-2	4A-3, day 1	4A-3, day 2	4A-4	4A-5 day 1	4A-5 day 2	4A-6, day 1	4A-6, day 2	5	6
Date	18-Jan	19-Jan	27-Jan	28-Jan	29-Jan	30-Jan	31-Jan	1-Feb	2-Feb	3-Feb	4-Feb	4-Feb	8-Feb	9-Feb	10-Feb
Test Period	—	1003–1240	—	—	1040–1426	1025–1415	1110–1525	—	1450–1810	—	0935–1351	—	1400–1722	—	—
Summary															
Non-detected Constituents, µg/dscm	—	< 131	—	—	< 130	< 1.6E+02	< 163	< 162	< 158	—	<,R 142	—	<,R 129	—	—
Non-detected Constituents, lb/hr	—	< 5.9E-05	—	—	< 5.7E-05	< 7.4E-05	< 7.5E-05	< 7.8E-05	< 7.3E-05	—	<,R 6.6E-05	—	<,R 5.5E-05	—	—
Detected Constituents, µg/dscm	—	< **103**	—	—	—	—	—	< **0.77**	< **2.4**	—	<,R **31**	—	<,R **9.5**	—	—
Detected Constituents, lb/hr	—	< **4.7E-05**	—	—	—	—	—	< **3.7E-07**	< **1.1E-06**	—	<,R **1.4E-05**	—	<,R **4.1E-06**	—	—
All Constituents, µg/dscm	—	< **234**	—	—	< 130	< 1.6E+02	< 163	< **163**	< **160**	—	<,R **180**	—	<,R **138**	—	—
All Constituents, lb/hr	—	< **1.1E-04**	—	—	< 5.7E-05	< 7.4E-05	< 7.5E-05	< **7.9E-05**	< **7.4E-05**	—	<,R **8.4E-05**	—	<,R **5.9E-05**	—	—
Monochlorobenzene feedrate, lb/hr	—	0.00	—	—	0.73	0.73	0.74	0.74	0.73	0.72	<,R 0.73	0.74	<,R 0.73	—	—
Monochlorobenzene emission rate, lb/hr	—	< 1.8E-06	—	—	< 1.7E-06	< 2.2E-06	< 2.2E-06	< 2.3E-06	< 2.2E-06	—	<,R 2.1E-06	—	<,R 1.7E-06	—	—
Monochlorobenzene destruction efficiency, %	—	—	—	—	> 99.9998	> 99.9997	> 99.9997	> 99.9997	> 99.9997	—	>, R 99.9997	—	>, R 99.9998	—	—

Notes:

1. Each 0031 test consisted of triplicate runs. Each run include 3 sorbent tubes per EPA 0031. The two TENAX tubes from each run were analyzed together; the Anasorb tube was analyzed separately. A single composite condensate sample, representing the total condensate collected for all 3 runs, was analyzed. The reported value for each analyte is the sum of the mass of the analyte detected in 6 tube analyses, 2 per run, and 1 condensate analysis.
2. Each 0031 run was performed for nominally 40 minutes, and collected ~20 L at a sample rate of ~0.5 L/min, per the "Slow-VOST" method of extending the sample time without increasing the sample volume.
3. If there were no detects in any analyses of a 3-run test, then the reported value is the sum of the analytical reporting limits with a "<" sign. If there was a detect in any of the analyses in a 3-run test, then the reported value is **bolded**. This value is the sum of the detected values and the reporting limit values for any analyses in which the analyte was not detected, and is shown with a "<" sign, unless there was a detected value in all analyses in the test. Destruction efficiency results reported using "<" emissions data are greater than (">") the reported value.
4. The total concentration and emission rate for all analytes is shown as **bolded** and without a "<" sign, even though a significant portion of the total reported values is the sum of non-detect values.
5. No blank values, even if detected, have been subtracted from the stack sample values.
6. Data validation was performed by Tetra Tech, under subcontract to the test program, on Method 0031 samples from the Test Conditions 4A-1, 4A-2, 4A-3, and 4A-4. The off-gas sample Anasorb tube analyses generally had low recoveries of sampling surrogates and internal standards, causing all of the reported values to be flagged as estimated or rejected. This has been noted in other test programs and may be due to NO_X levels in the off-gas that were high enough to interfere with the analysis of those surrogates. Since the Anasorb tube is a backup for the 2 Tenax tubes, and the Tenax tube and condensate analyses generally had good surrogate and internal standard recoveries, the flags on the Anasorb tube results have not been propagated to the test total values that include the Anasorb, Tenax, and condensate analyses.
7. The non-detect 2-butanone and 1,2-dibromo-3-chloropropane results have all been R flagged because the initial or continuing calibrations were below the relative response factor (RRF) for those compounds.
8. The VOC data from Test Conditions 4A-5 and 4A-6 are R (Rejected) flagged because these samples exceeded the hold time limits. These data are still reported here for comparison and completeness. The results from these 2 test conditions are generally consistent with the results for the other test conditions.

[cp1 off-gas emissions and nox destruct aug 5.xls]VOC

Table 7-55. CP1 stack gas SVOc concentrations and emission rates.

Test	1, day 1	1, day 2	2A	3B	4A-1	4A-2	4A-3, day 1	4A-3, day 2	4A-4	4A-5 day 1	4A-5 day 2	4A-6, day 1	4A-6, day 2	5	6
Date	18-Jan	19-Jan	27-Jan	28-Jan	29-Jan	30-Jan	31-Jan	1-Feb	2-Feb	3-Feb	4-Feb	4-Feb	8-Feb	9-Feb	10-Feb
Test Period	—	1000–1330	—	—	1040–1426	1025–1415	1110–1525	—	1450–1810	—	0935–1351	—	1400–1722	—	—
Train sample duration, min	—	180	—	—	180	180	180	—	180	—	180	—	180	—	—
Train sample volume, dscm	—	1.38	—	—	2.522	2.570	2.763	—	1.513	—	1.566	—	1.523	—	—
SVOC species concentrations, µg/dscm															
Disulfoton	—	< 36.2	—	—	< 19.8	< 19.5	< 18.1	—	< 33.0	—	< 31.9	—	< 32.8	—	—
4-Bromophenyl phenyl ether	—	< 7.2	—	—	< 4.0	< 3.9	< 3.6	—	< 6.6	—	< 6.4	—	< 6.6	—	—
4-Chloro-3-methylphenol	—	< 36.2	—	—	< 19.8	< 19.5	< 18.1	—	< 33.0	—	< 31.9	—	< 32.8	—	—
2-Chloronaphthalene	—	< 7.2	—	—	< 4.0	< 3.9	< 3.6	—	< 6.6	—	< 6.4	—	< 6.6	—	—
2-Chlorophenol	—	< 7.2	—	—	< 4.0	< 3.9	< 3.6	—	< 6.6	—	< 6.4	—	< 6.6	—	—
4-Chlorophenyl phenyl ether	—	< 7.2	—	—	< 4.0	< 3.9	< 3.6	—	< 6.6	—	< 6.4	—	< 6.6	—	—
Dibenz(a,h)anthracene	—	< 7.2	—	—	< 4.0	< 3.9	< 3.6	—	< 6.6	—	< 6.4	—	< 6.6	—	—
Di-n-butyl phthalate	—	U **28.3**	—	—	U **9.9**	U **18.3**	U **12.7**	— U	**17.2**	— U	**37.7**	— U	**13.1**	—	—
3,3'-Dichlorobenzidine	—	< 7.2	—	—	< 4.0	< 3.9	< 3.6	—	< 6.6	—	< 6.4	—	< 6.6	—	—
2,4-Dichlorophenol	—	< 7.2	—	—	< 4.0	< 3.9	< 3.6	—	< 6.6	—	< 6.4	—	< 6.6	—	—
Diethyl phthalate	—	< 7.2	—	—	< 4.0	< 3.9	< 3.6	—	< 6.6	—	< 6.4	—	< 6.6	—	—
2,4-Dimethylphenol	—	< 7.2	—	—	< 4.0	< 3.9	< 3.6	—	< 6.6	—	< 6.4	—	< 6.6	—	—
Dimethyl phthalate	—	< 7.2	—	—	<,UJ 4.0	<,UJ 3.9	<,UJ 3.6	—	< 6.6	—	< 6.4	—	< 6.6	—	—
1,3-Dinitrobenzene		< 7.2	—	—	< 4.0	< 3.9	< 3.6	—	< 6.6	—	< 6.4	—	< 6.6	—	—
2,4-Dinitrophenol	—	< 36.2	—	—	< 19.8	< 19.5	< 18.1	—	< 33.0	—	< 31.9	—	< 32.8	—	—
2,4-Dinitrotoluene	—	< 7.2	—	—	< 4.0	< 3.9	< 3.6	—	< 6.6	—	< 6.4	—	< 6.6		—
2,6-Dinitrotoluene	—	< 7.2	—	—	< 4.0	< 3.9	< 3.6	—	< 6.6	—	< 6.4	—	< 6.6	—	—
Di-n-octyl phthalate	—	< 7.2	—	—	< 4.0	< 3.9	< 3.6	—	< 6.6	—	< 6.4	—	< 6.6	—	—
Fluoranthene	—	< 7.2	—	—	< 4.0	< 3.9	< 3.6	—	< 6.6	—	< 6.4	—	< 6.6	—	—
Fluorene	—	< 7.2	—	—	< 4.0	< 3.9	< 3.6	—	< 6.6	—	< 6.4	—	< 6.6	—	—
Hexachlorobenzene	—	< 7.2	—	—	< 4.0	< 3.9	< 3.6	—	< 6.6	—	< 6.4	—	< 6.6	—	—
Hexachlorocyclopentadiene	—	<,R 36.2	—	—	<,UJ 19.8	< 19.5	<,UJ 18.1	—	<,UJ 33.0	—	<,UJ 31.9	—	<,UJ 32.8	—	—
Hexachloroethane	—	< 7.2	—	—	< 4.0	< 3.9	< 3.6	—	< 6.6	—	< 6.4	—	< 6.6	—	—
Indeno(1,2,3-cd)pyrene	—	< 7.2	—	—	< 4.0	< 3.9	< 3.6	—	< 6.6	—	< 6.4	—	< 6.6	—	—
Isophorone	—	< 7.2	—	—	< 4.0	< 3.9	< 3.6	—	< 6.6	—	< 6.4	—	< 6.6	—	—
2-Methylphenol	—	< 14.5	—	—	< 7.9	< 7.8	< 7.2	—	< 13.2	—	< 12.8	—	< 13.1	—	—
3-Methylphenol	—	< 36.2	—	—	< 19.8	< 19.5	< 18.1	—	< 33.0	—	< 31.9	—	< 32.8	—	—
4-Methylphenol	—	< 14.5	—	—	< 7.9	< 7.8	< 7.2	—	< 13.2	—	< 12.8	—	< 13.1	—	—
2-Nitroaniline	—	< 7.2	—	—	< 4.0	< 3.9	< 3.6	—	< 6.6	—	< 6.4	—	< 6.6	—	—

Table 7-55. (continued).

Test	1, day 1	1, day 2	2A	3B	4A-1	4A-2	4A-3, day 1	4A-3, day 2	4A-4	4A-5 day 1	4A-5 day 2	4A-6, day 1	4A-6, day 2	5	6
Date	18-Jan	19-Jan	27-Jan	28-Jan	29-Jan	30-Jan	31-Jan	1-Feb	2-Feb	3-Feb	4-Feb	4-Feb	8-Feb	9-Feb	10-Feb
Test Period	—	1000–1330	—	—	1040–1426	1025–1415	1110–1525	—	1450–1810	—	0935–1351	—	1400–1722	—	—
3-Nitroaniline	—	< 7.2	—	—	< 4.0	< 3.9	< 3.6	—	< 6.6	—	< 6.4	—	< 6.6	—	—
Nitrobenzene	—	< 7.2	—	—	< 4.0	< 3.9	< 3.6	—	< 6.6	—	< 6.4	—	< 6.6	—	—
2-Nitrophenol	—	< 36.2	—	—	< 19.8	< 19.5	< 18.1	—	< 33.0	—	< 31.9	—	< 32.8	—	—
N-Nitrosodi-n-butylamine	—	< 7.2	—	—	< 4.0	< 3.9	< 3.6	—	< 6.6	—	< 6.4	—	< 6.6	—	—
N-Nitrosodimethylamine	—	< 7.2	—	—	**8.7**	< 3.9	**5.1**	—	< 6.6	—	< 6.4	—	< 6.6	—	—
N-Nitrosodiphenylamine	—	< 7.2	—	—	< 4.0	< 3.9	< 3.6	—	< 6.6	—	< 6.4	—	< 6.6	—	—
N-Nitrosodi-n-propylamine	—	< 7.2	—	—	< 4.0	< 3.9	< 3.6	—	< 6.6	—	< 6.4	—	< 6.6	—	—
Pentachlorobenzene	—	< 7.2	—	—	< 4.0	< 3.9	< 3.6	—	< 6.6	—	< 6.4	—	< 6.6	—	—
Pentachloronitrobenzene	—	<,R 36.2	—	—	<,R 19.8	< 19.5	<,R 18.1	—	<,R 33.0	—	<,R 31.9	—	<,R 32.8	—	—
Pentachlorophenol	—	< 36.2	—	—	< 19.8	< 19.5	< 18.1	—	< 33.0	—	< 31.9	—	< 32.8	—	—
Phenanthrene	—	< 7.2	—	—	< 4.0	< 3.9	< 3.6	—	< 6.6	—	< 6.4	—	< 6.6	—	—
Phenol	—	<,UJ 36.2	—	—	<,UJ 19.8	<,UJ 19.5	<,UJ 18.1	—	<,UJ 33.0	—	<,UJ 31.9	—	<,UJ 32.8	—	—
1,2,4,5-Tetrachlorobenzene	—	< 7.2	—	—	< 4.0	< 3.9	< 3.6	—	< 6.6	—	< 6.4	—	< 6.6	—	—
2,3,4,6-Tetrachlorophenol	—	< 36.2	—	—	< 19.8	< 19.5	< 18.1	—	< 33.0	—	< 31.9	—	< 32.8	—	—
o-Toluidine	—	< 14.5	—	—	< 7.9	< 7.8	< 7.2	—	< 13.2	—	< 12.8	—	< 13.1	—	—
2,4,5-Trichlorophenol	—	< 7.2	—	—	< 4.0	< 3.9	< 3.6	—	< 6.6	—	< 6.4	—	< 6.6	—	—
2,4,6-Trichlorophenol	—	< 36.2	—	—	< 19.8	< 19.5	< 18.1	—	< 33.0	—	< 31.9	—	< 32.8	—	—
1,3,5-Trinitrobenzene	—	<,R 36.2	—	—	<,R 19.8	< 19.5	<,R 18.1	—	<,R 33.0	—	<,R 31.9	—	<,R 32.8	—	—
Summary															
Di-n-butyl phthalate, lb/hr	—	U **4.3E-05**	—	—	U **1.8E-05**	U **3.3E-05**	U **2.9E-05**	—	U **3.3E-05**	—	U **8.2E-05**	—	U **2.2E-05**	—	—
N-Nitrosodimethylamine, lb/hr		—	—	—	**1.5E-05**	**—**	**1.1E-05**	—	—	—	—	—	—	—	—
Total nondetected SVOCs, µg/dscm	—	< 7.0E+02	—	—	< 3.8E+02	< 3.8E+02	< 3.9E+02	—	< 6.4E+02	—	< 6.2E+02	—	< 6.4E+02	—	—
Total nondetected SVOCs, lb/hr	—	< 1.1E-03	—	—	< 6.7E-04	< 6.9E-04	< 7.9E-04	—	< 1.2E-03	—	< 1.4E-03	—	< 1.1E-03	—	—
All SVOC concentration, µg/dscm	—	< **7.3E+02**	—	—	< **4.0E+02**	< **4.0E+02**	< **4.1E+02**	—	< **6.6E+02**	—	< **6.6E+02**	—	< **6.5E+02**	—	—
All SVOC emission rate, lb/hr	—	< **1.1E-03**	—	—	< **7.1E-04**	< **7.2E-04**	< **8.3E-04**	—	< **1.3E-03**	—	< **1.4E-03**	—	< **1.1E-03**	—	—

Notes:

1. **Unbolded** values with "<" indicate reporting limits for those analytes that were not detected.
2. **Bolded** values are detected, or are sums of detected and nondetected (reporting limit) values. A "<" on a **bolded** value indicates summed detected and non-detected (reporting limit) values.
3. SVOC results for Test Conditions 1 and 4A-1 through 4A-6 were validated. Di-n-butylphthalate, detected at levels below the action level, were qualified with a "U". 1,3.5-dinitrobenzene and pentachloronitrobenzene, were R flagged because a continuing calibration was less than the relative response factor (RRF) limit. Hexachlorocyclopentadiene was UJ flagged (non-detect, estimate) because a continuing calibration exceeded the 20% difference quality control criterion (in some tests), and was R flagged due to low spike recoveries in other tests.

[cp1 off-gas emissions and nox destruct aug 5.xls]SVOC

Table 7-56. CP1 stack gas Field GC (Method 0040) and TCO/GRAV concentrations and emission rates.

Test	1, day 1	1, day 2	2A	3B	4A-1	4A-2	4A-3, day 1	4A-3, day 2	4A-4	4A-5 day 1	4A-5 day 2	4A-6, day 1	4A-6, day 2	5	6
Date	18-Jan	19-Jan	27-Jan	28-Jan	29-Jan	30-Jan	31-Jan	1-Feb	2-Feb	3-Feb	4-Feb	4-Feb	8-Feb	9-Feb	10-Feb
Test Period	—	1000–1330	—	—	1040–1426	1025–1415	1025–1415	—	1450–1810	—	0935–1351	—	1400–1722	—	—
Field GC results															
Train sample duration, min	—	30	—	—	50	50	50	—	50	—	45	—		—	—
Train sample volume, dscf	—	1.00	—	—	0.81	0.67	0.53	—	0.60	—	0.45	—		—	—
Tedlar Bag , ppmv															
C_1 compounds	—	**1.45**	— —		**0.89**	**1.13**	**1.57**	—	**1.09**	— R	**1.12**	— R	0.7	—	—
C_2 compounds	—	**0.51**	— —		**0.45**	**0.36**	**0.27**	—	**0.42**	— R	**0.51**	— R	1.0	—	—
C_3 compounds	—	**0.53**	— —		0.20	0.23	**0.24**	—	0.20	—	R **0.57**	— R	1.0	—	—
C_4 compounds	—	**0.47**	— —		0.20	0.20	**0.26**	—	**0.35**	— R	**0.33**	— R	1.0	—	—
C_5 compounds	—	**0.24**	— —		0.20	0.20	**0.42**	—	0.20	—	R 0.20	—	R 1.0	—	—
C_6 compounds	—	0.20	—	—	0.20	0.20	**0.26**	—	**0.21**	— R	0.20	—	R 1.0	—	—
C_7 compounds	—	**0.38**	— —		**0.23**	**0.44**	**2.14**	—	**1.45**	— R	**2.38**	— R	1.0	—	—
Condensate, µg/L															
C_4 compounds		1.0		UJ	1.0	1.0 UJ	1.0		UJ 1.0		R 1.0		R 1.0	—	—
C_5 compounds		1.0			1.0	1.0	1.0		1.0		R 1.0		R 1.0	—	—
C_6 compounds		1.0			1.0	**1.9**	**3.0**		**2.3**	R	**1.2**	R	**1.8**	— —	
C_7 compounds		1.0			1.0	1.0	1.0		1.0		R 1.0		R 1.0	—	—
Total Tedlar bag and condensate results, µg/dscm															
C_1 compounds (BP < 0°C)	—	**967**	— —		**594**	**754**	**1,047**	—	**727**	— R	**747**	— R	467	—	—
C_2 compounds (BP < 0°C)	—	**638**	— —		**563**	**450**	**338**	—	**525**	— R	**638**	— R	1,250	—	—
C_3 compounds (BP < 0°C)	—	**972**	— —		367	422	**440**	—	367	—	R **1,045**	— R	1,834	—	—
C_4 compounds (BP 0°C - 30°C)	—	**1,137**	— —		485	486	**631**	—	**848**	— R	**801**	— R	2,419	—	—
C_5 compounds (BP 30°C - 60°C)	—	**722**	— —		602	602	**1,263**	—	603	—	R 603	—	R 3,002	—	—
C_6 compounds (BP 60°C - 90°C)	—	718	—	—	719	721	**940**	—	**758**	— R	**721**	— R	**3,587**	— —	
C_7 compounds (BP 90°C - 98°C)	—	**1,585**	— —		**960**	**1,836**	**8,919**	—	**6,044**	— R	**9,920**	— R	4,169	—	—
Total		**6,739**			**4,289**	**5,270**	**13,579**		**9,872**		R **14,474**	R	**16,728**		

Table 7-56. (continued).

Test	1, day 1	1, day 2	2A	3B	4A-1	4A-2	4A-3, day 1	4A-3, day 2	4A-4	4A-5 day 1	4A-5 day 2	4A-6, day 1	4A-6, day 2	5	6
Date	18-Jan	19-Jan	27-Jan	28-Jan	29-Jan	30-Jan	31-Jan	1-Feb	2-Feb	3-Feb	4-Feb	4-Feb	8-Feb	9-Feb	10-Feb
Test Period	—	1000–1330	—	—	1040–1426	1025–1415	1025–1415	—	1450–1810	—	0935–1351	—	1400–1722	—	—
TCO/GRAV results															
Train sample duration, min	—	180	—	—	180	180	180	—	180	—	180	—	180	—	—
Train sample volume, dscm	—	1.37	—	—	2.52	2.55	2.37	—	1.53	—	1.54	—	1.49	—	—
Total Chromatographable Organics Emissions															
Total chromatographable organics, µg/dscm	—	**1,747**	— —		**795**	**981**	**2,066**	— J	**1,830**	— J	**908**	—	**1,206**	— —	
Total chromatographable organics, g/hr	—	**0.35**	— —		**0.16**	**0.21**	**0.42**	— J	**0.38**	— J	**0.19**	—	**0.23**	— —	
Ttotal chromatographable organics, lb/hr	—	**7.8E-04**	— —		**3.6E-04**	**4.6E-04**	**9.3E-04**	— J	**8.3E-04**	— J	**4.2E-04**	—	**5.0E-04**	— —	
Total Gravimetric Organics Emissions															
Total gravimetric organics, µg/dscm	—	**6,844**	— —		**3,975**	**8,632**	**4,216**	— J	**11,113**	— J	**4,607**	—	**2,880**	— —	
Total gravimetrics organics, g/hr	—	**1.38**	— —		**0.82**	**1.8**	**0.86**	— J	**2.28**	— J	**0.96**	—	**0.55**	— —	
Total gravimetric organics, lb/hr	—	**3.0E-03**	— —		**1.8E-03**	**4.1E-03**	**1.9E-03**	— J	**5.0E-03**	— J	**2.1E-03**	—	**1.2E-03**	— —	
Total TCO/GRAV conncentration, µg/dscm	—	**8,591**	— —		**4,770**	**9,613**	**6,282**	— J	**12,943**	— J	**5,515**	—	**4,086**	— —	

Notes:

1. **Bolded** values are detected values, or sums of detected and nondetected (reporting limit) values; values that are not **bolded** are reporting limit, or sums of reporting limit values.
2. Detected TCO and GRAV values in the method blank for the train blanks were subtracted from the train values. Some of the TCO trains had a significant train blank value, that has also been subtracted from the reported values.
3. The TCO/GRAV results from Test Conditions 1, 2A, 4A-1 through 4A-6 were validated by Tetra Tech under subcontract to the test program. No data qualifiers were applied based on this validation, except for J (estimate) flags applied to TCO and GRAV for Tests 4A-4 and 4A-5, for exceeding the 14-day hold time.
4. The Field GC data from Test Conditions 4A-5 and 4A-6 are R (Rejected) flagged because these samples exceeded the hold time limits. These data are still reported here for comparison and completeness. The results for these test conditions are generally consistent with the results of the other test conditions. The C_4 compound results for the condensate are flagged as UJ, because the continuing calibration exceeded the 10% difference QC criterion. These non-detects do not significantly contribute to the total C_4 results so the flag does not propagate to the total C_4 values.

[cp1 off-gas emissions and nox destruct aug 5.xls]FGC, TCO-GRAV

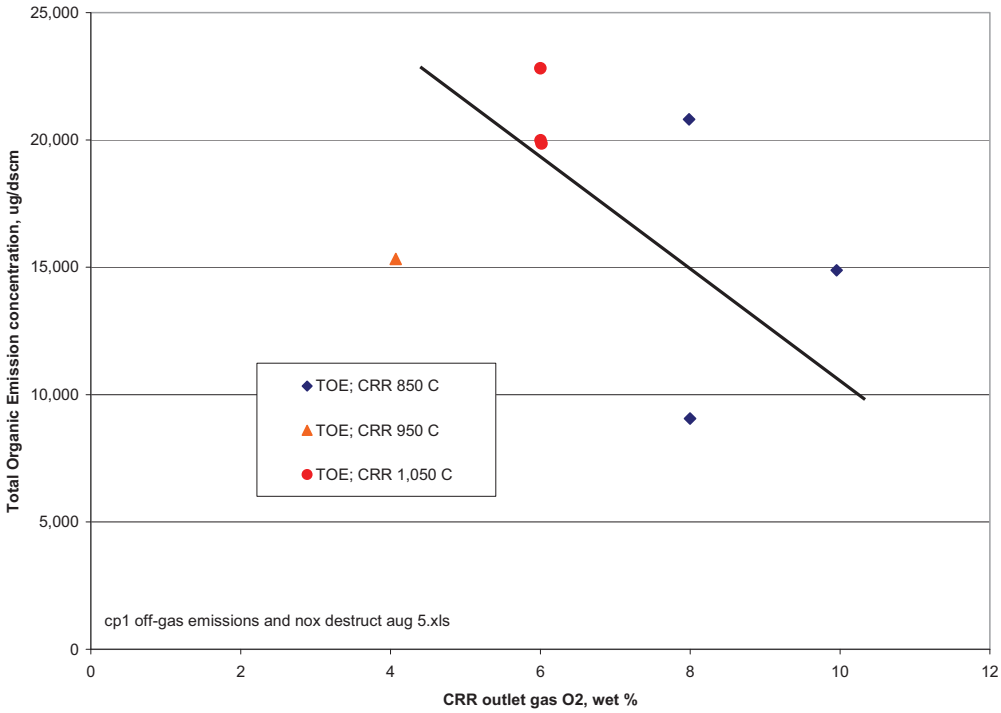

Figure 7-72. Total organic emissions at different CRR temperatures compared to CRR outlet O_2 concentrations.

This page is intentionally left blank.

Table 7-57. CP1 stack gas dioxin and furan concentrations and emission rates.

Test		1, day 1	1, day 2	2A	3B	4A-1	4A-2	4A-3, day 1	4A-3, day 2	4A-4	4A-5 day 1	4A-5 day 2	4A-6, day 1	4A-6, day 2	5	6
Date		18-Jan	19-Jan	27-Jan	28-Jan	29-Jan	30-Jan	31-Jan	1-Feb	2-Feb	3-Feb	4-Feb	4-Feb	8-Feb	9-Feb	10-Feb
Test Period		—	—	—	—	1040–1426	1025–1415	1025–1415	—	1450–1810	—	0935–1351	—	1400–1722	—	—
Train sample duration, min		—	—	—	—	180	180	180	—	180	—	180	—	180	—	—
Train sample volume, dscm		—	—	—	—	2.56	2.56	2.23	—	1.52	—	1.54	—	1.50	—	—
Concentrations, ng/dscm	*Relative toxicity*															
2,3,7,8-Cl4-Dibenzofuran	*0.1*	— —		—	—	0.005	0.005	0.007	—	0.008	—	0.008	—	0.007	—	—
2,3,7,8-Cl4-Dibenzo-p-dioxin	*1*	— —		—	—	0.004	0.003	0.004	—	0.006	—	0.006	—	0.006	—	—
1,2,3,7,8-Cl5-Dibenzofuran	*0.05*	— —		—	—	0.005	0.005	0.006	—	0.007	—	0.007	—	0.008	—	—
2,3,4,7,8-Cl5-Dibenzofuran	*0.500*	— —		—	—	0.005	0.005	0.006	—	0.007	—	0.007	—	0.008	—	—
1,2,3,7,8-Cl5-Dibenzo-p-dioxin	*0.500*	— —		—	—	0.013	0.011	0.016	—	0.018	—	0.017	—	0.021	—	—
1,2,3,4,7,8-Cl6-Dibenzofuran	*0.100*	— —		—	—	0.005	0.005	0.006	—	0.007	—	0.007	—	0.008	—	—
1,2,3,6,7,8-Cl6-Dibenzofuran	*0.1*	— —		—	—	0.005	0.005	0.005	—	0.006	—	0.006	—	0.007	—	—
2,3,4,6,7,8-Cl6-Dibenzofuran	*0.1*	— —		—	—	0.005	0.005	0.006	—	0.006	—	0.007	—	0.007	—	—
1,2,3,7,8,9-Cl6-Dibenzofuran	*0.1*	— —		—	—	0.006	0.006	0.007	—	0.007	—	0.008	—	0.009	—	—
1,2,3,4,7,8-Cl6-Dibenzo-p-dioxin	*0.1*	— —		—	—	0.008	0.008	0.009	—	0.012	—	0.011	—	0.012	—	—
1,2,3,6,7,8-Cl6-Dibenzo-p-dioxin	*0.1*	— —		—	—	0.007	0.006	0.007	—	0.010	—	0.009	—	0.010	—	—
1,2,3,7,8,9-Cl6-Dibenzo-p-dioxin	*0.1*	— —		—	—	0.007	0.007	0.008	—	0.010	—	0.009	—	0.010	—	—
1,2,3,4,6,7,8-Cl7-Dibenzofuran	*0.01*	— —		—	—	0.007	0.007	0.008	—	0.009	—	0.009	—	0.014	—	—
1,2,3,4,7,8,9-Cl7-Dibenzofuran	*0.01*	— —		—	—	0.009	0.009	0.010	—	0.012	—	0.012	—	0.019	—	—
1,2,3,4,6,7,8-Cl7-Dibenzo-p-dioxin	*0.01*	— —		—	—	0.018	0.015	0.014	—	0.023	—	0.021	—	0.022	—	—
1,2,3,4,6,7,8,9-Cl8-Dibenzofuran	*0.001*	— —		—	—	0.027	0.021	0.025	—	0.043	—	0.032	—	0.027	—	—
1,2,3,4,6,7,8,9-Cl8-dibenzo-p-dioxin	*0.001*	— —		—	—	0.017	0.015	0.021	—	0.030	—	0.025	—	0.025	—	—
Total		—	—	—	—	0.153	0.140	0.165	—	0.220	—	0.203	—	0.220	—	—
Concentrations in Toxicity Equivalents (ng/dscm, @ 7% O_2)																
2,3,7,8-Cl4-Dibenzofuran		—	—	—	—	2.6E-04	2.5E-04	2.6E-04	—	3.6E-04	—	3.7E-04	—	3.8E-04	—	—
2,3,7,8-Cl4-Dibenzo-p-dioxin		—	—	—	—	2.0E-03	1.7E-03	1.6E-03	—	2.6E-03	—	2.6E-03	—	2.9E-03	—	—
1,2,3,7,8-Cl5-Dibenzofuran		—	—	—	—	1.2E-04	1.5E-04	1.2E-04	—	1.7E-04	—	1.7E-04	—	2.1E-04	—	—
2,3,4,7,8-Cl5-Dibenzofuran		—	—	—	—	1.1E-03	1.5E-03	1.1E-03	—	1.7E-03	—	1.7E-03	—	2.1E-03	—	—
1,2,3,7,8-Cl5-Dibenzo-p-dioxin		—	—	—	—	3.0E-03	3.1E-03	3.0E-03	—	4.1E-03	—	4.1E-03	—	5.5E-03	—	—

Table 7-57. (continued).

Test	1, day 1	1, day 2	2A	3B	4A-1	4A-2	4A-3, day 1	4A-3, day 2	4A-4	4A-5 day 1	4A-5 day 2	4A-6, day 1	4A-6, day 2	5	6
Date	18-Jan	19-Jan	27-Jan	28-Jan	29-Jan	30-Jan	31-Jan	1-Feb	2-Feb	3-Feb	4-Feb	4-Feb	8-Feb	9-Feb	10-Feb
Test Period	—	—	—	—	1040–1426	1025–1415	1025–1415	—	1450–1810	—	0935–1351	—	1400–1722	—	—
1,2,3,4,7,8-Cl6-Dibenzofuran	—	—	—	—	2.6E-04	2.9E-04	2.4E-04	—	3.0E-04	—	3.3E-04	—	4.2E-04	—	—
1,2,3,6,7,8-Cl6-Dibenzofuran	—	—	—	—	2.2E-04	2.7E-04	2.0E-04	—	2.6E-04	—	2.9E-04	—	3.5E-04	—	—
2,3,4,6,7,8-Cl6-Dibenzofuran	—	—	—	—	2.4E-04	2.9E-04	2.4E-04	—	2.9E-04	—	3.3E-04	—	3.8E-04	—	—
1,2,3,7,8,9-Cl6-Dibenzofuran	—	—	—	—	2.8E-04	3.4E-04	2.7E-04	—	3.3E-04	—	3.7E-04	—	4.5E-04	—	—
1,2,3,4,7,8-Cl6-Dibenzo-p-dioxin	—	—	—	—	3.9E-04	4.2E-04	3.4E-04	—	5.4E-04	—	5.2E-04	—	6.2E-04	—	—
1,2,3,6,7,8-Cl6-Dibenzo-p-dioxin	—	—	—	—	3.1E-04	3.4E-04	2.7E-04	—	4.5E-04	—	4.3E-04	—	5.2E-04	—	—
1,2,3,7,8,9-Cl6-Dibenzo-p-dioxin	—	—	—	—	3.3E-04	3.6E-04	2.9E-04	—	4.5E-04	—	4.3E-04	—	5.2E-04	—	—
1,2,3,4,6,7,8-Cl7-Dibenzofuran	—	—	—	—	3.3E-05	3.6E-05	2.9E-05	—	4.2E-05	—	4.3E-05	—	7.3E-05	—	—
1,2,3,4,7,8,9-Cl7-Dibenzofuran	—	—	—	—	4.4E-05	4.8E-05	3.9E-05	—	5.7E-05	—	5.8E-05	—	9.7E-05	—	—
1,2,3,4,6,7,8-Cl7-Dibenzo-p-dioxin	—	—	—	—	8.6E-05	8.2E-05	5.4E-05	—	1.1E-04	—	1.0E-04	—	1.1E-04	—	—
1,2,3,4,6,7,8,9-Cl8-Dibenzofuran	—	—	—	—	1.2E-05	1.2E-05	9.4E-06	—	2.0E-05	—	1.5E-05	—	1.4E-05	—	—
1,2,3,4,6,7,8,9-Cl8-dibenzo-p-dioxin	—	—	—	—	7.9E-06	8.2E-06	7.8E-06	—	1.4E-05	—	1.2E-05	—	1.3E-05	—	—
Total	—	—	—	—	0.0087	0.0091	0.0080	—	0.012	—	0.012	—	0.015	—	—
% of the HWC MACT standard (0.11 ng/dscm)		—	—	—	7.9%	8.3%	7.3%	—	10.7%	—	10.8%	—	13.4%	—	—

Notes:

1. **Bolded** values are detected values; **non-bolded** values indicate non-detected levels reported at the reporting limit, or estimated levels detected below the reporting limit.
2. No dioxins or furans were detected in any samples above the reporting limit. All dioxin and furan levels, and the concentrations as percentages of the HWC MACT standard, are less than the reported values.
3. The dioxin and furan analysis data was validated by an outside validator (Tetra Tech, USA) under subcontract to the test program. No data qualifiers were identified by this data validation.

[cp1 off-gas emissions and nox destruct aug 5.xls]dioxins

Table 7-58. CP1 stack gas PCB concentrations.

Test	1, day 1	1, day 2	2A	3B	4A-1	4A-2	4A-3, day 1	4A-3, day 2	4A-4	4A-5 day 1	4A-5 day 2	4A-6, day 1	4A-6, day 2	5	6
Date	18-Jan	19-Jan	27-Jan	28-Jan	29-Jan	30-Jan	31-Jan	1-Feb	2-Feb	3-Feb	4-Feb	4-Feb	8-Feb	9-Feb	10-Feb
Test Period	—	—	—	—	1040–1426	1025–1415	1025–1415	—	1450–1810	—	0935–1351	—	1400–1722	—	—
Train sample duration, min	—	—	—	—	180	180	180	—	180	—	180	—	180	—	—
Train sample volume, dscm	—	—	—	—	2.56	2.56	2.23	—	1.52	—	1.54	—	1.50	—	—
Total PCB Congener Concentrations, ng/dscm															
Monochlorobiphenyl (total)	—	—	—	—	0.59	0.59	0.67	—	0.98	—	**1.10**	— 1.00		—	—
Dichlorobiphenyl (total)	—	—	—	—	**1.37**	**3.12**	**1.03**	— 0.	98	—	**4.40**	— 2.13		—	—
Trichlorobiphenyl (total)	—	—	—	—	**2.46**	**2.96**	**0.72**	— 0.	98	—	**2.07**	— 2.67		—	—
Tetrachlorobiphenyl (total)	—	—	—	—	0.59	**0.82**	0.67 —		0.98	—	0.97	—	1.00	—	—
Pentachlorobiphenyl (total)	—	—	—	—	0.59	0.59	0.67	—	0.98	—	0.97	—	1.00	—	—
Hexachlorobiphenyl (total)	—	—	—	—	0.59	0.59	0.67	—	0.98	—	0.97	—	1.00	—	—
Heptachlorobiphenyl (total)	—	—	—	—	0.59	0.59	0.67	—	0.98	—	0.97	—	1.00	—	—
Octachlorobiphenyl (total)	—	—	—	—	0.59	0.59	0.67	—	0.98	—	0.97	—	1.00	—	—
Nonachlorobiphenyl (total)	—	—	—	—	0.59	0.59	0.67	—	0.98	—	0.97	—	1.00	—	—
Decachlorobiphenyl (total)	—	—	—	—	0.59 0.59		0.67	— 0.98		—	0.97	—	1.00	—	—
Total —		—	—	—	**8.51**	**11.00**	**7.12**	— 9.	84	—	**14.38**	— 12.81		—	—
Dioxin-like Coplaner PCB Concentrations, ng/dscm															
3,4,4',5-Tetrachlorobiphenyl —		—	—	—	0.59	0.59	0.67	—	0.98	—	0.97	—	1.00	—	—
3,3',4,4'-Tetrachlorobiphenyl —		—	—	—	0.59	0.59	0.67	—	0.98	—	0.97	—	1.00	—	—
2',3,4,4',5-Pentachlorobiphenyl —		—	—	—	0.59	0.59	0.67	—	0.98	—	0.97	—	1.00	—	—
2,3',4,4',5-Pentachlorobiphenyl —		—	—	—	0.59	0.59	0.67	—	0.98	—	0.97	—	1.00	—	—
2,3,4,4',5-Pentachlorobiphenyl —		—	—	—	0.59	0.59	0.67	—	0.98	—	0.97	—	1.00	—	—
2,3,3',4,4'-Pentachlorobiphenyl —		—	—	—	0.59	0.59	0.67	—	0.98	—	0.97	—	1.00	—	—
3,3',4,4',5-Pentachlorobiphenyl —		—	—	—	0.59	0.59	0.67	—	0.98	—	0.97	—	1.00	—	—
2,3',4,4'5,5'-Hexachlorobiphenyl —		—	—	—	0.59	0.59	0.67	—	0.98	—	0.97	—	1.00	—	—
2,3,3',4,4',5-Hexachlorobiphenyl —		—	—	—	0.59	0.59	0.67	—	0.98	—	0.97	—	1.00	—	—
2,3,3',4,4',5'-Hexachlorobiphenyl —		—	—	—	0.59	0.59	0.67	—	0.98	—	0.97	—	1.00	—	—
3,3',4,4',5,5'-Hexachlorobiphenyl —		—	—	—	0.59	0.59	0.67	—	0.98	—	0.97	—	1.00	—	—
2,2',3,4,4',5,5'-Heptachlorobiphenyl —		—	—	—	0.59	0.59	0.67	—	0.98	—	0.97	—	1.00	—	—
2,2',3,3',4,4',5-Heptachlorobiphenyl —		—	—	—	0.59	0.59	0.67	—	0.98	—	0.97	—	1.00	—	—
2,3,3',4,4',5,5'-Heptachlorobiphenyl —		—	—	—	0.59	0.59	0.67	—	0.98	—	0.97	—	1.00	—	—
Total —		—	—	—	8.20	8.19	9.41	—	13.78	—	13.60	—	14.01	—	—

Notes:

1. **Bolded** values are detected values; **non-bolded** values indicate non-detected levels reported at the reporting limit, or estimated levels detected below the reporting limit.

[cp1 off-gas emissions and nox destruct aug 5.xls]PCBs

This page is intentionally left blank.

7.8 Mass Balance

An important indicator of the quality of data taken from these tests is the mass balance. The mass balance determines the amount of mass fed to the system and the amount removed and compares them to see if they balance. The mass balance is performed on both an overall and elemental basis. An overall balance showing a difference (or "closure") of less than 10% is considered acceptable and less than 5% is considered excellent. Test objective 41 was for a mass balance closure of less than 10% for major components (Al, Na, C, N, O and H_2O for both CP1 and CP2 and also Si for only CP1). Test Objective 42 was for a mass balance closure of less than 30% for minor components (all those not listed as major).

Overall and elemental mass balances have been calculated for CP-1 during the time period between P-2 and P-4A-6 (time between the second start-up and shut down during production testing, January 25, 2006, 1630 to February 5, 2006, 1905) and for CP-2 testing (May 30, 2006, 1457 to June 8, 2006, 1325). The overall balances for both CP1 and CP2 were excellent with differences of 0.8% and 2.4%, respectively. The elemental balance for major components met the test objectives for both CP1 and CP2. The elemental balance for minor components met the test objective for all components in CP2 and most components in CP1. The closure was greater than 30% for Ca and Ce in CP1.

7.8.1 Methodology

The methodology and assumptions used to develop the mass balances are described below. It provides the overall and elemental mass balance closures, and provides reasoning when some elements appear to be outside test objective closure values. Hazen Feed Logs, Hazen Product Logs, Hazen Operator Logs, Hazen Data Logs, DCS data, and analytical data were used to perform elemental mass balances for the pilot plant tests. In some cases data was unavailable and therefore had to be estimated. The methodology for calculating the elemental flows of each inlet and outlet stream as well as any assumptions made are described in this section.

The mass balances cover the time for CP1 during the time period between P-2 and P-4A-6 (time between the second start-up and shut down during production testing, January 25, 2006, 1630 to February 5, 2006, 1905) and for CP2 testing (May 30, 2006, 1457 to June 8, 2006, 1325). The mass balance for CP1 between the first production start-up and shut-down were not calculated since CP2 testing accomplished the same test objectives under conditions that are more representative of expected IWTU operation. The mass balance for CP1 between the third production start-up and shut-down were not calculated due to the short duration of the test period.

The mass balances cover the time from the addition of oxygen to the CRR for heating to the time oxygen is shut off just prior to the end of a test period. This time frame was chosen in order to account for the consumption of all carbon fed to the process. Prior to oxygen feed no reactions occur and therefore the gaseous inputs are all removed through the stack while having no impact on the solids. Once oxygen is fed it begins reacting with carbon and therefore affecting the carbon mass balance. During shutdown, once the oxygen is shut off and the process is switched to nitrogen fluidization, the carbon oxidation reactions are stopped and only nitrogen is sent out only through the stack. Thus the time when oxygen is not fed has no impact on the solid mass balance and since all gas inputs go directly to the stack this time may be discounted from the gaseous mass balance without affecting the over mass balance closure.

The following methodology explanation has been divided into two sections, solid/liquid and gaseous. Since different assumptions and methodologies were required for determination of the solids and gaseous flows, the methodology explanation has been separated into two sections.

7.8.1.1 Elemental Solid/Liquid Flows. Determining the elemental mass balance involves tracking several liquid and solid inlets and all solid and gaseous products. All solid and liquid flows are measured and have analytical results showing the elemental composition of the streams. The following is the methodology used for determining the total elemental mass for each stream.

Simulant feed rate was measured using flow meter FT-200-001. This flow meter measures all liquid feed flow to the DMR including both simulant feed and flush-water feed. The times when flush-water was being fed were determined from the operator logs and accounted for in the mass balance calculations.

Since the flush-water was deionized, the concentration was assumed to be 1000 g/L pure water. The analytical composition results for simulant feed varied substantially throughout the CP1 test so the sample most representative of the testing time period was used for the duration of each test period (e.g., for test P-4A-3 the analytical results for batch 11 were used for the concentration of the simulant feed). During CP2 testing, only SBW simulant without heavy metals and SBW simulant with heavy metals were fed to the DMR. Since the analytical results for each tank of SBW simulant without heavy metals did not vary much and the SBW simulant with heavy metals did not vary much, the average concentration for each type was used for the duration (as recorded in the operator log book) of that type of feed. The DCS flow was multiplied by the concentration of the feed to determine the total simulant feed to the DMR.

The total mass of coal, coke, clay, and other additives to the DMR and CRR were obtained from the Hazen feed logs. The total mass of each additive was multiplied by its elemental composition as given in sample results or from vendor data to determine the total elemental mass in each feed. During CP2 testing, particles from the PR that exceeded 12 mesh in size (primarily unburned carbon) were recycled back to the DMR with the feed coal. Since the composition of this recycled coal was not measured and several compositional measurements of the screened PR sample were made, it was determined to use the unscreened analytical results on the amount of PR product less than 12 mesh. Also, the amount of product greater than 12 mesh was subtracted from the carbon added to the DMR.

The composition of the PR, DMR, HTF, CRR, and PBF solids was analytically determined by the Hazen Analytical Laboratory. The Hazen results were then charge balanced assuming that any ion not associated with a carbonate, sulfate, phosphate, or halogen would be associated with an oxide anion. This mass of oxide was summed with the masses of species specifically analyzed for, to determine if the total mass of material in each sample summed to 100 wt%. With the oxide addition, the total mass of analytically determined species in almost all samples that had a carbon measurement summed to between 90–110%, which was considered to be an acceptable range considering reasonable sample representativeness and analytical error.

For those samples that did not have a direct carbon analysis, a carbon composition was calculated (by difference) to achieve ~100% mass balance for the sample. The required carbon composition to achieve mass balance in these samples was similar to the measured carbon in other samples and was therefore considered a good estimate for the carbon composition in samples for which the carbon content was not directly measured.

Seven samples (1 PR, 4 DMR, and 2 HTF) did not achieve a reasonable mass balance (between 90 and 110 percent of the mass accounted for) indicating that one or more of the elemental analyses were not accurate. It is typical to be provided some imprecise data when when several elemental analyses are performed. The reason for performing the individual sample balances is so that obvious problem analyses can be excluded. The seven samples that did not achieve sample mass balance were discarded and not used in the pilot plant mass balance determination. The overall affect of the loss of these few samples is

small as there were adequate numbers of similar samples to allow for the mass balance. In addition to the seven samples, all the CRR measurements for CP-2 testing and the last 6 PBF measurements from the CP-2 test (samples 2231, 2274, 2317, 2341, and 2363) did not achieve sample mass balance. The CRR measurements for CP-2 were used even though they only accounted for 70–80% of the total mass. It is believed that the aluminum was measured low and therefore the aluminum concentration in the CRR has been increased to achieve mass balance closure of the sample analytical result. Also, as stated above, the analytical results for the screened PR samples was used for determining mass balance.

7.8.1.2 Elemental Gaseous Flows. The elemental mass balances for oxygen, nitrogen, "water," carbon and sulfur, involves tracking many gaseous feeds and discharges. Most of the gaseous feeds and discharges are measured; however, there are a few significant gaseous streams that are not measured. The unmeasured masses had to be estimated. A summary of the gaseous feeds and discharges and how they were quantified is shown in Table 7-59. For most stream flow rates, the method of quantification was a minute-by-minute measurement by flowmeters, automatically logged by the Data Acquisition and Control System. Various methods were used for quantification of the unmeasured gaseous streams. These methods are discussed in detail in the following paragraphs.

Table 7-59. Summary of gaseous feed and discharge streams—method of flow rate quantification.

Component and Stream	Measured (Yes or No)	Estimation Method and Comments (if not measured)
DMR		
Fluidizing gas steam	Yes	
Fluidizing gas oxygen	Yes	
Fluidizing gas nitrogen	No	Flow rate obtained from operator logs
Nitrogen purges	Yes	
Carbon addition nitrogen transfer gas	No	Estimated based on carbon addition system design number of system cycles
Product transfer nitrogen	No	Estimated based on operator logs, system design of transfer line, and temperature changes in transfer line (an indication of a the presence of nitrogen transfer gas)
HTF		
Nitrogen purges	Yes	
Filter back-pulse nitrogen	No	Estimated based on back-pulse system design
CRR		
Auto-thermal gas oxygen	Partially	One oxygen stream was unmeasured during CP1, it was estimated based on operator logs of meter flow and downstream pressure
Auto-thermal gas nitrogen	Yes	
Nitrogen purges	Yes	
Carbon addition nitrogen transfer gas	No	Estimated based on carbon addition system design number of system cycles

Table 7-59. (continued).

Component and Stream	Measured (Yes or No)	Estimation Method and Comments (if not measured)
OGC		
Atomizing air	Yes	
Cooling water (liquid as opposed to gaseous feed)	Yes	
PBF		
Nitrogen purges	Yes	
Filter back-pulse nitrogen	No	This system seldom operated and the contribution was negligible
Mercury Adsorber		
Nitrogen purges	No	Estimated based on system design and on operator logs.
Stack		Concentrations and flow rates of minor constituents (NO_X, SO_2, CO, and THC were measured but were not significant to overall elemental mass balance).
Total	Yes	Also measured by separate instrumentation during off-gas sampling.
Oxygen	Yes	Determined using the measured % dry concentration and the stack N_2 flow rate calculated from all the process N_2 inputs, assuming that the only significant dry stack gas constituents were O_2, CO_2, and N_2.
Carbon dioxide	Yes	Determined using the measured % dry concentration and the stack N_2 flow rate calculated from all the process N_2 inputs, assuming that the only significant dry stack gas constituents were O_2, CO_2, and N_2.
Nitrogen	No	Calculated from all the process N_2 inputs by difference based on the assumption that nitrogen, oxygen and carbon dioxide are the only significant contributors to the % dry concentration.
Water	Occasionally	Estimated by difference from the total stack gas flow rate and the total calculated flow rate of O_2, CO_2, and N_2. The accuracy of this estimate was validated by comparison to (a) stack gas water flow rate determined from the sum of all process input water, and (b) the water concentration measured during manual stack gas sampling.
Sulfur dioxide	Yes	Measured % dry concentration and flow rate - not significant to overall stack flow, but significant to sulfur balance.
Exceptions/Leaks		
Unmonitored water to CRR (liquid as opposed to gaseous feed)	No	Estimated based on mass balances and on water measured in stack during off-gas testing, only affected CP1 – the leak rate was measured once during a shutdown condition.
Unmonitored air leak into off-gas blowers	No	Estimated based on mass balances and on total gas measured in stack during off-gas testing – only affected CP2.

Most of the nitrogen feeds were directly measured. The exceptions include the carbon addition transfer nitrogen, the product transfer nitrogen, the filter back-pulse nitrogen, the mercury adsorber purge nitrogen, the DMR fluidizing nitrogen, and the nitrogen associated with the blower leak during CP2. The product transfer nitrogen was estimated at 20 scfm when it was being used. The 20 scfm is based on design of the nitrogen transfer system and on the flows logged by the operators as read on a local flowmeter. The times at which the system was in use can be estimated from the minute-by-minute temperature profiles in the product transfer line – rapid cooling or heating indicates use of transfer nitrogen. Generally, the transfer nitrogen was used for 10 to 20 minutes during each transfer. The estimated transfers were added to the mass balance and the total off-gas flows were checked to confirm that the expected response was being seen.

The DMR fluidizing nitrogen flow rate was recorded in the operator logs. The recorded rates were added to the mass balance. Once again, the total off-gas flows were checked to confirm that the expected response was being seen.

The mercury adsorber purge flow during CP1, based on system design and operator logs, was negligible on average being less than 0.1% of the gaseous nitrogen fees. A design change between CP1 and CP2 resulted in a higher mercury adsorber purge flow. During CP2, the mercury adsorber purge as indicated on a local flowmeter and as logged about eight times a day, was constant at 2 scfm. Carbon transfers during both tests occurred at regular intervals, approximately once a minute through-out all testing, and were estimated based on system design and frequency of use to be only a small contribution – about 0.1% of the gaseous nitrogen feeds.

The filter back-pulse nitrogen was estimated to be about 5 scf per pulse cycle. Pulse cycles occurred at irregular intervals during testing, varying from a few times an hour to nearly continuous (30 to 60 times per hours). Thus, the nitrogen flow rate varied from being negligible up to 5 scfm.

The blower air leak was discovered during CP2 when it was found that the % moisture in the off-gas was lower than expected and that the mass flow rate was larger than expected. Subsequent investigation indicated that the oxygen and nitrogen appeared to be higher than expected, an indication of an air leak somewhere in the off-gas system. A comparison of temperature drops measured in CP1 and CP2 off-gas components indicated that there was a increased drop between the mercury absorber outlet and stack. Local investigation of the entire off-gas system found that there was an air leak into the system around the blower shaft for the blower between the mercury absorber and the stack, which confirmed the measured findings. Indications are that this air in-leakage was only significant during CP2 testing.

Most of the unmeasured nitrogen streams were estimated as a constant value for the entire CP2 test or as a few constant values for the CP1 test. The constant value included the nitrogen associated with the mercury adsorber purge, the carbon transfer nitrogen, and the air in-leakage nitrogen. The product transfer nitrogen and the DMR fluidizing nitrogen were not included as those values were specifically accounted for as discussed above. For CP2, the constant value was estimated to be 16 scfm. This value was chosen as it resulted in a minute-by-minute oxygen, carbon dioxide, and water composition that matched the measurements made during the six separate periods of off-gas testing performed by APT. In addition, the assumption of 16 scfm total unmeasured nitrogen resulted in a predicted water mass flow rate in the off-gas that matched that predicted based on summing the various water feeds to the system (fluidizing steam, water in the waste feed, and OGC cooling water). In other words, there were three separate methods used to determine that 16 scfm was a reasonable estimate of unmeasured nitrogen to the system.

A similar approach was used for CP1. However, test conditions were varied more widely during CP1 and a single nitrogen leak value was applied to each major test unit, instead of to the total test. The constant leakage nitrogen applied to each test varied between 0 and 5 scfm. The CP1 test values were lower because there was no blower air in-leakage during the CP1 test.

The discharge nitrogen was not measured. What was available on a minute-by-minute basis was the discharge mass flow rate and the percentage dry concentrations of carbon dioxide and oxygen (sulfur dioxide, total nitrogen oxides, and carbon monoxide were also measured but were only present at ppm levels). Given that over 99% of the dry components consisted of oxygen, carbon dioxide, and nitrogen, dry nitrogen was determined as follows:

$$\%\ \text{dry}\ N_2 = 100 - \%\ \text{dry}\ O_2 - \%\ \text{dry}\ CO_2 \quad .$$

Expected nitrogen mass flow rate was calculated from all the measured nitrogen feeds, including the nitrogen from nitrates in the waste feed and the nitrogen from the estimated unmeasured nitrogen. Knowing the mass flow rate of nitrogen expected in the off-gas and all the percentages for oxygen, carbon dioxide and nitrogen, the mass flow rate of oxygen and carbon dioxide were then calculated.

$$\text{Mass flow rate}\ O_2 = \left(\text{Mass flow rate}\ N_2 / \%\ \text{dry}\ N_2\right) \times \%\ \text{dry}\ O_2 \quad .$$

$$\text{Mass flow rate}\ CO_2 = \left(\text{Mass flow rate}\ N_2 / \%\ \text{dry}\ N_2\right) \times \%\ \text{dry}\ O_2 \quad .$$

Finally, given that over 99% of the total off-gas consisted of oxygen, carbon dioxide, nitrogen, and water, the water was calculated by subtracting the calculated mass flow rates of oxygen, carbon dioxide, and nitrogen from the measure total mass flow rate.

Mass flow rate H_2O – Total mass flow rate – Mass flow rate CO_2 – Mass flow rate O_2 – Mass flow rate N_2 .

The expected mass flow rate of water can also be calculated from the known feeds (steam, water in the waste feed, and OGC cooling water). This method of calculating water mass flow rate when compared to the above method of calculation resulted in an average minute-by-minute difference of less than 1%. Restated as an equation, the following was found:

W = minute-by-minute water estimated by summing all input water streams .

V = minute-by-minute water estimated by subtracting nitrogen, oxygen, and carbon dioxide from total flow .

Sum for entire test of {(V-W)/V)} <1% for CP2 .

There was one additional unknown flow that needed to be estimated to perform calculations during the CP1 test. It was found during off-gas sampling that the measured moisture and the total off-gas flow were both higher than expected based on known feeds. It was estimated that 20 to 50 scfm of extra water was present in the off gas. It was later found, during a shutdown, that the water spray used to cool the CRR during system startup while adjusting carbon feed rates had been left on during testing. The flow rate measured during the shutdown was equivalent to 28 scfm. Individual mass balances performed during each major test section of CP1 in order to match APT measured moisture percentages and total flows against calculated values resulted in water spray leak estimates of 28 to 49 scfm. The estimates of water spray leak, the 0 to 5 scfm estimates of unmeasured nitrogen, the estimates for fluidizing and

product transfer nitrogen, and the measured minute-by-minute flows were used to calculate the off-gas flows as discussed previously. Note that once again, the average minute-by-minute difference between the water calculated by adding all the known and estimated feeds was in excellent agreement (less than 2% difference) with the water calculated from the total all gas flows and the off-gas nitrogen, oxygen and carbon dioxide.

W = minute-by-minute water estimated by summing all input water streams.

V = minute-by-minute water estimated by subtracting nitrogen, oxygen, and carbon dioxide from total flow.

Sum for entire test of {(V-W)/V)} <2% for CP1.

7.8.2 Elemental Mass Balance Results

7.8.2.1 CP-1 Mass Balance. The elemental distribution and mass balance for the CP-1 test is shown in Table 7-60 and Table 7-61. The total mass balance closure is excellent with a difference of just 0.8% between feeds and discharges. The major gaseous components, including water, oxygen, nitrogen and carbon dioxide, account for 95% of the total mass. All the gaseous components show excellent mass balance closure with the greatest difference being just 3.4%. The solid components are judged based on the test objective of less than 10% difference between input and output mass for major components (Al, Na, C, and Si) and 30% for minor components. These mass balance closure objectives were achieved for all but two elements. No major components failed to meet the test objective of 10% closure. The minor components calcium and cerium both failed to meet the test objective of 30% closure. The calcium closure failure can be traced to the high variability in the coal composition. The cerium closure failure can be traced to inaccuracies in product analytical results. The overall excellence of the mass balance indicates that the measured masses of the product elements are reliable and that conclusions drawn on the fate of elements, based on these measurements, are valid.

A significant portion of the calcium fed to the steam reformer process is from the coal (over 50%). The ash content of the coal added to the DMR, as well as the elemental composition of the ash, vary significantly from batch to batch. Hazen performed four analyses for ash content in the coal. The ash content of the as received coal was 9.22%, 7.91%, 7.72%, and 5.51%, a variation of 60%. The coal is specified by the supplier to contain less than 5% ash. Also, the elemental composition of the ash is highly variable as shown by the three elemental analyses that were done on the ash (see Table 7-62). The elemental concentration of calcium in the coal ash varied by as much as 90%. Due to the high variability of the coal ash content and composition, there is a large uncertainty in how much calcium is added with the coal. This large uncertainty is the likely source of failure to meet the test objective mass balance closure of 30%. Note that a decrease in calcium added with the coal of just 2 pounds out of 72 pounds would have resulted in meeting the 30% criteria. The lesson learned from this information is that there is the potential for high variability in the DMR coal feed, that control of composition will be needed for the full scale process, and that it is desirable to more fully/frequently characterize the composition of the coal being fed to the test process. Since the problem with the silicon mass balance is likely due to the variability of the input coal composition, and since the failure to close at 30.5% is well within the expected variation of silicon in the feed coal, it is concluded that the product silicon masses are reliable and may be used to draw conclusion relative to the fate of silicon.

Table 7-60. Elemental Distribution and Mass Balance Closure for CP1.

2nd Start-up		Total (lb)	Al (lb)	As (lb)	B (lb)	Ca (lb)	Ce (lb)	Cs (lb)	Cr (lb)	Fe (lb)	Pb (lb)	Mg (lb)	Mn (lb)	Hg (lb)	Na (lb)	Ni (lb)	K (lb)
1/25/06 16:30 to 2/5/06 19:05																	
Feeds	DMR Starting Bed	400	56.7	0.00	0.00	8.82	0.00	0.00	0.00	4.86	0.00	3.43	1.95	0.00	73.7	0.00	14.3
	CRR Starting Bed	505	255	0.00	0.00	0.944	0.00	0.00	0.00	16.1	0.00	0.140	0.0674	0.00	0.343	0.00	0.197
	Simulant Feed	39798	508	2.64	6.46	75.5	134	90.2	5.76	77.4	6.19	19.2	20.0	44.1	1301	3.92	244
	DMR Coal	7317.00	41.8		72.1				32.1		7.17			3.54		5.49	
	DMR Clay	0.00	0.0		0.000				0.000							0.00	
	CRR Coke	9061.40											0.000408				
	CRR Clay	132.50	48.2		0.057				1.13		0.0639			0.0688		0.0550	
	CRR Carbo Ceramic	0.00	0.00						0.00								
	DMR Gas	26524															
	CRR Gas	42257															
	OGC Cooling Adds	90032															
	Purge N_2	50711															
	Unmonitored N_2 estimate	10678															
	Water Leak Estimate	22327															
	GAC Adds	1422															
	Total	301165.3	909	2.64	6.46	157.4	133.52	90.2	5.76	132	6.19	30.0	22.0	44.1	1379	3.92	264

Table 7-60. (continued).

2nd Start-up		Total (lb)	Al (lb)	As (lb)	B (lb)	Ca (lb)	Ce (lb)	Cs (lb)	Cr (lb)	Fe (lb)	Pb (lb)	Mg (lb)	Mn (lb)	Hg (lb)	Na (lb)	Ni (lb)	K (lb)
Outlet	DMR Solids	3104	345	0.756	2.05	38.7	Note 1	22.5	3.02	44.3	3.49	9.49	11.6	0.00862	534	2.20	89.8
	HTF Solids	4614	336	1.18	3.97	68.8	Note 1	54.6	2.72	55.2	3.40	13.3	12.4	0.0292	840	2.30	165
	CRR Solids	924	277	0.00482	0.00	1.27	0.0905	0.00122	0.201	15.30	0.00123	0.223	0.0991	0.00232	3.53	0.369	1.26
	PBF Solids	287	4.76	0.00765	0.01	0.584	0.0202	0.84	0.0391	3.56	0.0110	0.0612	0.0099	1.27	0.649	0.135	0.270
	OGC Solids	47.9	1.68	0.00023	0.00	0.103	0.0029	0.00	0.0101	0.82	0.0005	0.0057	0.0062	0.121	0.015	0.027	0.013
	GAC Final	37.5											37.5				
	Stack 289759												4.20				
	Total 298773		965	1.95	6.03	109	Note 1	78.0	5.99	119	6.91	23.1	24.2	43.2	1378	5.04	256
Produced																	
Reacted																	
Mass Balance		-2393	55.5	-0.692	-0.429	-48.0	Note 1	-12.2	0.235	-12.5	0.718	-6.87	2.19	-0.886	-0.958	1.12	-7.76

Notes:

1.Due to discrepencies in the analytical data for PR, DMR, and HTF solids the mass of Ce in the DMR and HTF was indeterminate. Based on results from the CP2 test it is expected that Ce would split the same as other metal species.

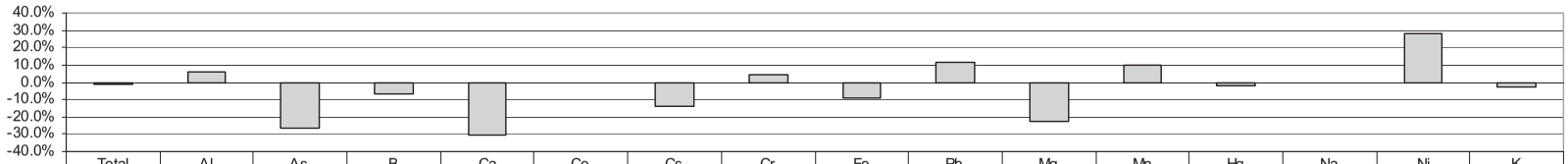

	Total	Al	As	B	Ca	Ce	Cs	Cr	Fe	Pb	Mg	Mn	Hg	Na	Ni	K
% Mass Imbalance	-0.8%	6.1%	-26.2%	-6.6%	-30.5%		-13.5%	4.1%	-9.5%	11.6%	-22.9%	10.0%	-2.0%	-0.1%	28.5%	-2.9%

Table 7-61. Elemental Distribution and Mass Balance Closure for CP1.

2nd Start-up		Si (lb)	Zn (lb)	Zr (lb)	Cl (lb)	F (lb)	PO_4 (lb)	H+ (lb)	H_2O (lb)	Nitrogen Sulfur NO_3 (lb)	N_2 (lb)	SO_4 (lb)	SO_2 (lb)	Carbon Carbon (lb)	CO_3 (lb)	CO_2 (lb)	O_2 (lb)
1/25/06 16:30 to 2/5/06 19:05																	
Feeds	DMR Starting Bed	11.1	0.00	0.00	3.03	1.29	2.39		0.201		21.8		62.7		60.9	77.6	
	CRR Starting Bed	0.00	0.00	0.00	0.00	0.00	0.511		0.00		0.00			0.225		231	
	Simulant Feed	541	7.66	149	48.7	21.8	604	70.9	22710	12825	284						
	DMR Coal	111				2.82		106	610	262	136		5881			21.0	
	DMR Clay	0.0														0.0	
	CRR Coke						26.3		2.72	14.0	6.79		8795			227	
	CRR Clay	16.6				0.195										61.5	
	CRR Carbo Ceramic	0.00														0.00	
	DMR Gas							13357		7425						5742	
	CRR Gas									6687						35570	
	OGC Cooling Adds							67166		17540						5327	
	Purge N_2									50711							
	Unmonitored N_2 estimate									10678							
	Water Leak Estimate							22327									
	GAC Adds											1422					
	Total 680		7.66	149	51.8	23.1	610	203.3	126172	131019304		1871	0.00	14739	61.2	0.00	47257

Table 7-61.(continued).

2nd Start-up		Si (lb)	Zn (lb)	Zr (lb)	Cl (lb)	F (lb)	PO_4 (lb)	H+ (lb)	H_2O (lb)	Nitrogen Sulfur NO_3 (lb)	N_2 (lb)	SO_4 (lb)	SO_2 (lb)	Carbon Carbon (lb)	CO_3 (lb)	CO_2 (lb)	O_2 (lb)
Outlet	DMR Solids	219	4.12	26.9	16.0	5.28	184		0.220		135		462		308	662	
	HTF Solids	426	4.53	119	42.6	17.0	327		2.50		198		474		400	949	
	CRR Solids	46.01	0.0664	0.2488	0.00	0.0514	1.23		0.00		0.19		217.9		0.513	305	
	PBF Solids	2.00	0.0227	0.0447	0.07	0.02	0.514		0.01		2.12		260		1.53	7.31	
	OGC Solids	0.49	0.0053	0.0000	0.01	0.01	0.005		0.00		0.01		43		0.000	2.35	
	GAC Final										1364						
	Stack			1.50					123658		93733		11.84			50858	19220
	Total	693	8.74	146	60.1	22.4	512	0.00	123658	2.72	93733	1699	11.8	1457	710	50858	21147
Produced								1817		2959		11.8		649		48197	10152
Reacted							203		13098		18.1		0.00	13282		37177	
Mass Balance		13.5	1.08	-2.64	8.32	-0.70	-97.7	0.00	-4331	2267.7		51.4		-726			915

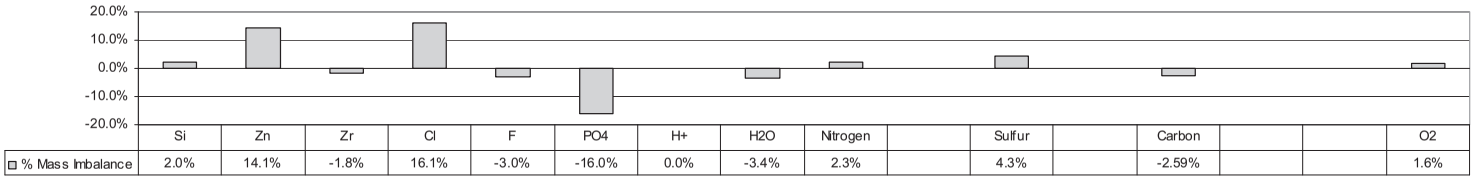

Table 7-62. GC-CRB coal analytical ash composition results.

	Sample ID			
	1321 1	881	Supersack	% Variation
SiO_2 51	.29%	37.81%	39.32%	36%
Al_2O_3 15	.96%	14.86%	11.82%	35%
TiO_2 0.	60%	0.64%	0.59%	8%
Fe_2O_3	6.89% 6.	70%	11.22% 67	%
CaO 12	.30%	23.40%	18.80%	90%
MgO 2.	50%	1.23%	2.70%	120%
Na_2O 0.	96%	0.94%	0.69%	39%
K_2O 2.	15%	0.56%	0.85%	284%
P_2O_5 0.	65%	0.20%	0.28%	225%
SO_3 5.	34%	11.40%	11.10%	113%
Total 98	.64%	97.74%	97.37%	1%

Due to unresolved inaccuracies in the analytical data for cerium in the PR/DMR/HTF the quantity of cerium in the PR/DMR/HTF is indeterminate for CP1. From the PR/DMR/HTF analytical results it appears that cerium is not measured very well in these products. All other component concentrations in the PR/DMR/HTF solids tend to follow a trend and reach a relatively steady-state concentration. Numerically, the percent standard deviation of the measured values for iron is 21% and for manganese is 23% but for cerium it is 65%. Percent deviations for metals during CP1, with the exception of cerium, ranged from 11% to 38%. The analytical inaccuracies associated with cerium means that the fate of cerium cannot be determined for the CP1 test. Fortunately, this scatter of data is not seen in the CP2 analytical results for cerium.

Figure 7-73 shows the elemental distribution for all component discharges, including gases. The gases, at 95% of discharges, tend to dominate the figure which is why only the solids are shown in Figure 7-74 and Figure 7-75.

The non-volatile components including heavy metals and radionuclide surrogates in the SBW simulant are incorporated into the solid product and are either transferred out the bottom of the DMR to the PRR as product or elutriated by the fluidizing gas as fines which are then filtered out in the HTF. A small portion of the fines pass through the HTF and into the CRR. These fines either build-up in the CRR or elutriate out to be collected in the OGC and PBF. During the second portion of the CP1 test, 60% of the solid product was elutriated to the HTF with the remaining 40% being transferred to the PRR as solid product (Figure 7-74). The majority of non-volatile components of the simulant feed tended to split with approximately 50%–70% percent being elutriated to the HTF and 30%-50% remaining in the DMR product. Zirconium, fluorine, and phosphate split with a higher fraction being elutriated to the HTF (>70%). Aluminum, chromium, and lead split with a lower fraction elutriated to the HTF (<50%). The aluminum elutriation is biased low by the alumina in the starting bed, which tended to split to the PRR. There is little difference between the overall solids split and the individual elemental splits.

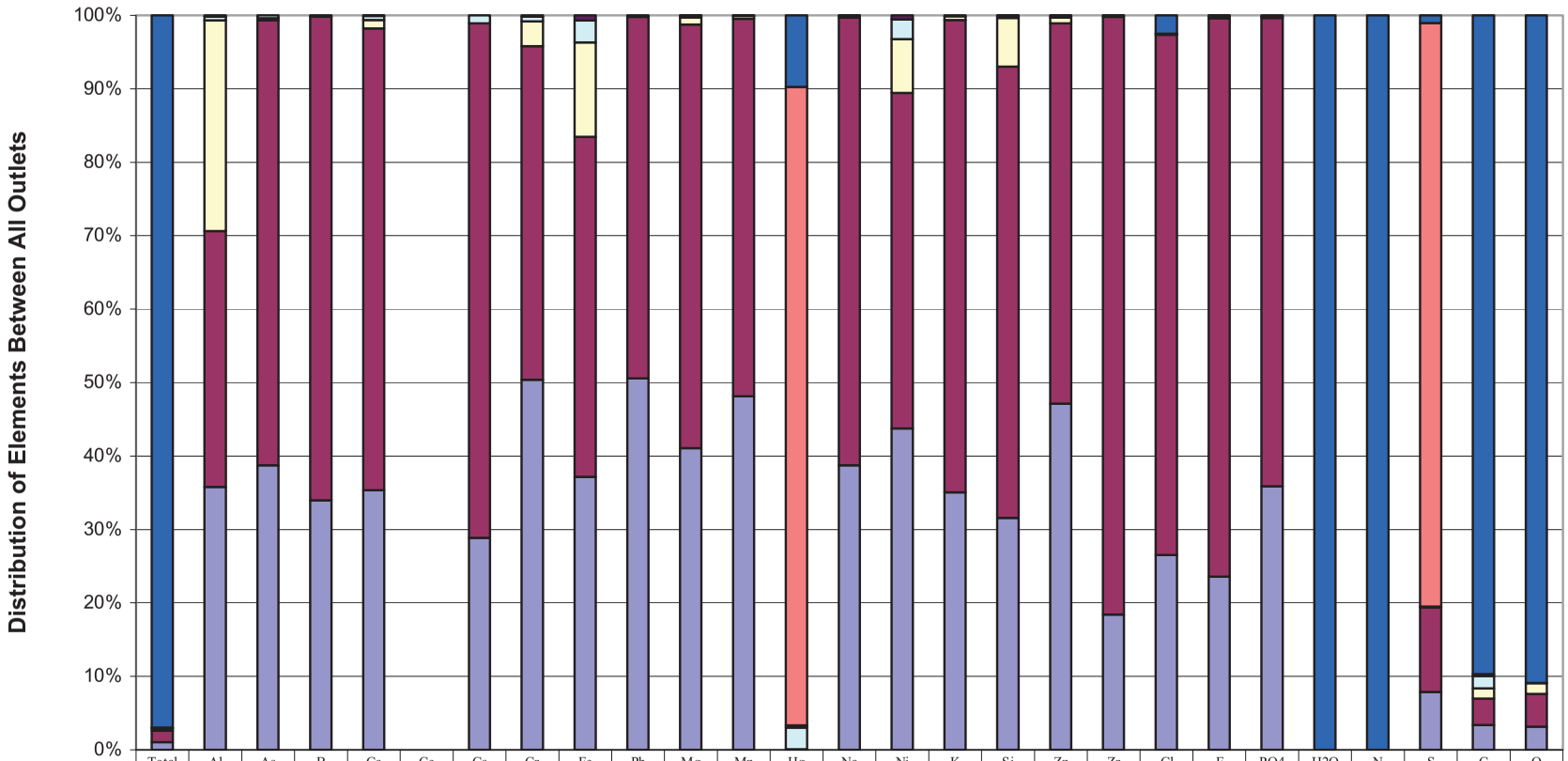

	Total	Al	As	B	Ca	Ce	Cs	Cr	Fe	Pb	Mg	Mn	Hg	Na	Ni	K	Si	Zn	Zr	Cl	F	PO4	H2O	N	S	C	O
Stack	97.0%	0.0%	0.0%	0.0%	0.0%		0.0%	0.0%	0.0%	0.0%	0.0%	0.0%	9.7%	0.0%	0.0%	0.0%	0.0%	0.0%	0.0%	2.5%	0.0%	0.0%	100.0%	100.0%	1.0%	89.7%	90.9%
GAC Final	0.0%	0.0%	0.0%	0.0%	0.0%		0.0%	0.0%	0.0%	0.0%	0.0%	0.0%	87.0%	0.0%	0.0%	0.0%	0.0%	0.0%	0.0%	0.0%	0.0%	0.0%	0.0%	0.0%	79.4%	0.0%	0.0%
OGC Solids	0.0%	0.2%	0.0%	0.0%	0.1%		0.0%	0.2%	0.7%	0.0%	0.0%	0.0%	0.3%	0.0%	0.5%	0.0%	0.1%	0.1%	0.0%	0.0%	0.0%	0.0%	0.0%	0.0%	0.0%	0.3%	0.0%
PBF Solids	0.1%	0.5%	0.4%	0.2%	0.5%		1.1%	0.7%	3.0%	0.2%	0.3%	0.0%	2.9%	0.0%	2.7%	0.1%	0.3%	0.3%	0.0%	0.1%	0.1%	0.1%	0.0%	0.0%	0.1%	1.7%	0.0%
CRR Solids	0.3%	28.7%	0.2%	0.0%	1.2%		0.0%	3.4%	12.8%	0.0%	1.0%	0.4%	0.0%	0.3%	7.3%	0.5%	6.6%	0.8%	0.2%	0.0%	0.2%	0.2%	0.0%	0.0%	0.0%	1.4%	1.4%
HTF Solids	1.5%	34.8%	60.6%	65.9%	62.9%		70.1%	45.4%	46.3%	49.2%	57.7%	51.4%	0.1%	60.9%	45.7%	64.3%	61.4%	51.8%	81.4%	70.8%	76.1%	63.8%	0.0%	0.0%	11.5%	3.6%	4.5%
DMR Solids	1.0%	35.8%	38.8%	34.0%	35.3%		28.8%	50.4%	37.2%	50.6%	41.1%	48.1%	0.0%	38.7%	43.7%	35.1%	31.6%	47.1%	18.4%	26.5%	23.6%	35.9%	0.0%	0.0%	7.9%	3.4%	3.1%

*Note - Ce not included due to discrepencies in the analytical results for PR, DMR, and HTF solids

Figure 7-73. Elemental distribution of all discharges for CP1.

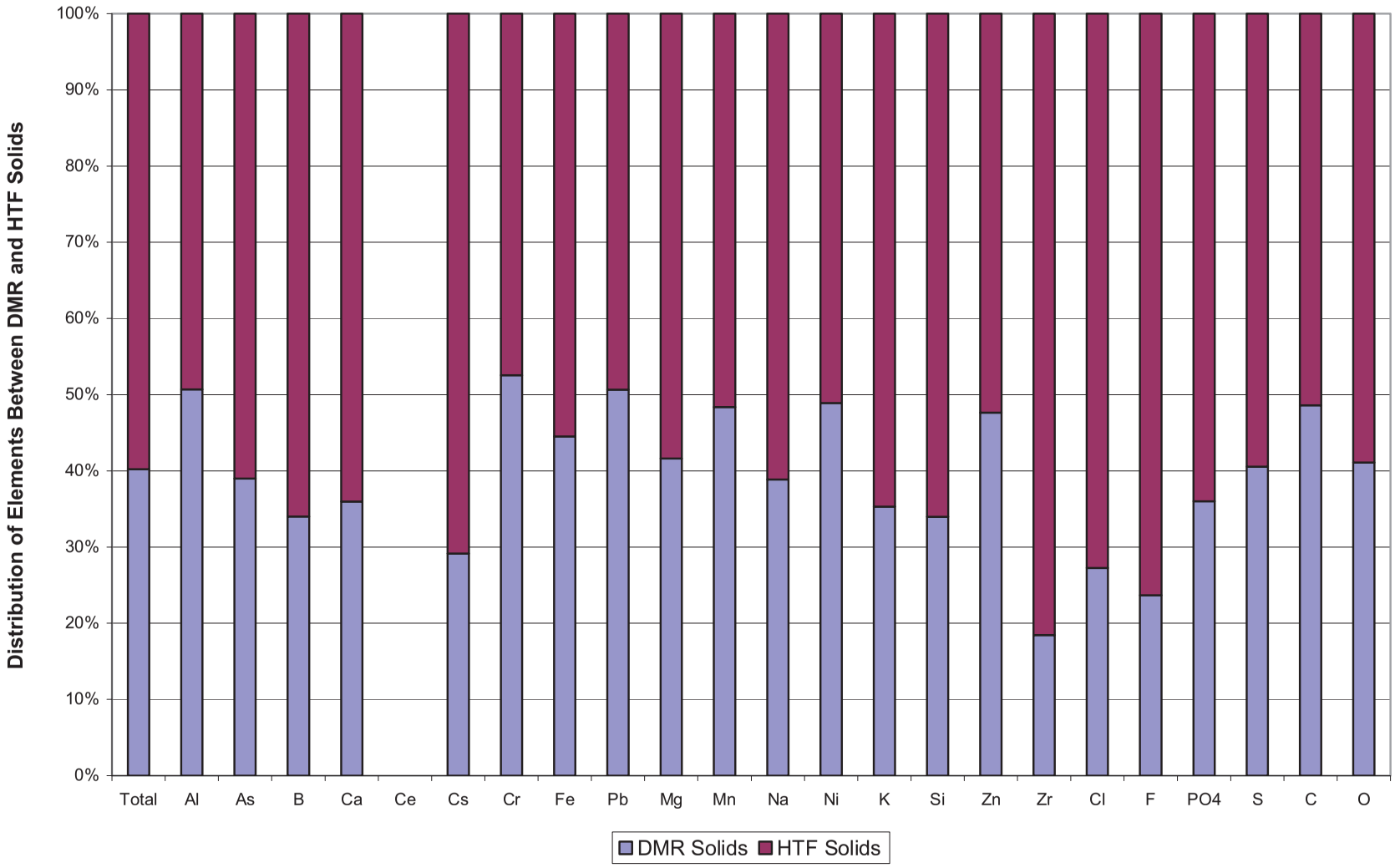

Note - Ce not included due to discrepencies in the analytical results for PR, DMR, and HTF solids

Figure 7-74. Elemental distribution of solids discharges from DMR and HTF for CP1.

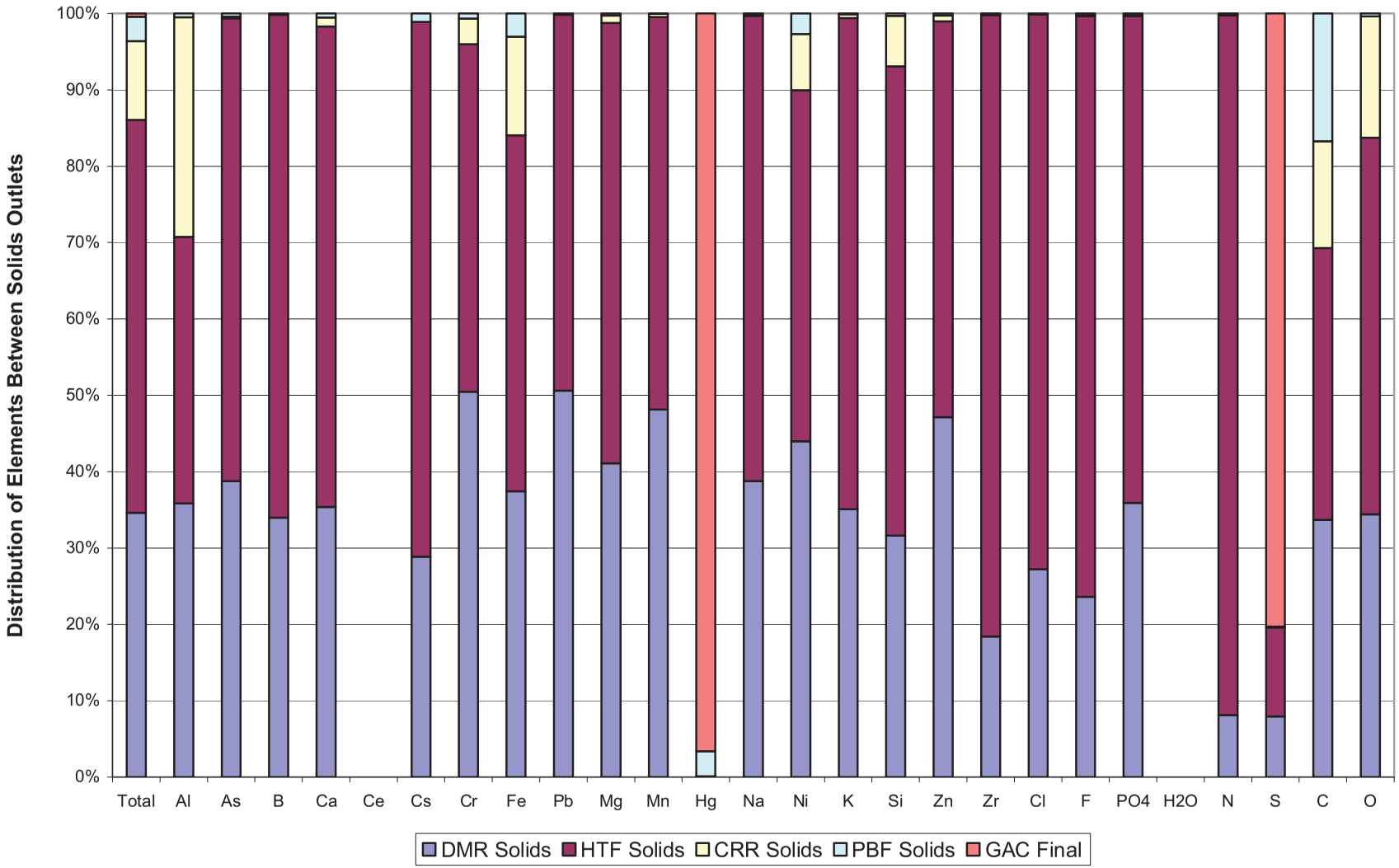

Note - Ce not included due to discrepencies in the analytical results for PR, DMR, and HTF solids

Figure 7-75. Elemental distribution of all solids discharges for CP1.

A small amount of sodium (0.3% of feed, about 4 pounds) is found in the CRR/OGC/PBF (Figure 7-75). There was only 0.5 pounds of sodium in the bed feeds to the CRR (starting bed, coke, and clay); therefore, most of the sodium found downstream of the HTF represents feed carry-over through the HTF. The partitioning of Na between the HTF fines (840 lb) and downstream of the HTF less the input Na in the CRR (3.7 lb) indicates an HTF filter efficiency of 99.7%.

Similar levels of other metals fed only to the DMR are found in the CRR/OGC/PBF, with levels ranging up to 1%. However, as the other components are minor constituents in the DMR feed, the sodium level of 0.3% is felt to be the most reliable representation of DMR feed carried to the CRR system. Combined with the indication of little difference in overall solids split in the DMR/HTF system, it is concluded that 0.3% of the feed solids carried through the HTF to the CRR. The Al, Ca, Fe Mg, and C in and downstream of the CRR primarily reflect the addition of these elements directly to the CRR. The Cr and Ni in and downstream of the CRR are primarily contaminants from the materials of construction of the CRR system.

7.8.2.2 CP-2 Mass Balance. The elemental distribution and mass balance for the CP2 test is shown in Table 7-63 and Table 7-64. The total mass balance closure is excellent with a difference of just 2.4% between feeds and discharges. The major gaseous components, including water, oxygen, nitrogen and carbon dioxide, account for 95% of the total mass. All the gaseous components show excellent mass balance closure with the greatest difference being just 2.3%. The solid components are judged based on the test objective of less than 10% closure for major components (Al, Na, and C) and 30% for minor components. Mass balance closure was achieved for all elements. As stated above for CP1, the overall excellence of the mass balance indicates that the measured masses of the product elements are reliable and that conclusions drawn on the fate of elements, based on these measurements, are valid.

Figure 7-76 shows the elemental distribution for all component discharges, including gases. The gases, at 96% of discharges, tend to dominate the figure which is why only the solids are shown in Figure 7-77 and Figure 7-78.

The non-volatile components including heavy metals and radionuclide surrogates in the SBW simulant are incorporated into the solid product and are either transferred out the bottom of the DMR to the PRR as product or elutriated by the fluidizing gas as fines which are then filtered out in the HTF. A small portion of the fines pass through the HTF and into the CRR. These fines either build-up in the CRR or elutriate out to be collected in the OGC and PBF. During the CP2 test, 7.6% of the solid product was elutriated to the HTF with the remaining 92.4% being transferred to the PRR as solid product (Figure 7-77). The majority of non-volatile components of the simulant feed tended to split with approximately 2%-10% percent being elutriated to the HTF and 90%–98% remaining in the DMR product. Only chlorine and fluorine split with a higher fraction being elutriated to the HTF (11% and 13%, respectively). There is little difference between the overall solids split and the individual elemental splits. Cerium splits in a similar fashion to other elements and it is expected that cerium in CP1 behaved similarly.

A small amount of sodium (0.1% of feed, about 1.2 pounds) is found in the CRR/OGC/PBF (Figure 7-78). There was only 0.2 pounds of sodium in the bed feeds to the CRR (starting bed, coke, carbo-ceramic, and clay); therefore, most of the sodium found downstream of the HTF represents feed carry-over through the HTF. The amount of Na captured in the HTF fines (82 lb) compared to the amount of Na in product streams downstream of the HTF, less the input Na in the CRR feeds (1.0 lb) indicates an HTF removal efficiency of 98.8%. The CP2 HTF removal efficiency is lower than the CP1 HTF removal efficiency (which was calculated using Na partitioning) because of the smaller amount of total CP2 HTF fines (356 lb) compared to CP1 HTF fines (4,614 lb). The CP2 HTF fines were less, in part because of the shorter feed duration, but more significantly because of the higher product to fines ratio during CP2.

Table 7-63. Elemental distribution and mass balance closure for CP2.

CP2 Tests		Total (lb)	Al (lb)	B (lb)	Ca (lb)	Ce (lb)	Cs (lb)	Cr (lb)	Fe (lb)	Pb (lb)	Mg (lb)	Mn (lb)	Hg (lb)	Na (lb)	Ni (lb)	K (lb)
5/30/06 14:57 to 6/8/06 13:25																
Feeds	DMR Bed	400	211	0.0858				0.112		0.0482						
	CRR Bed	874	460	0.187				0.245		0.105						
	Simulant Feed	28577	396	4.53	62.5	6.81	5.53	3.29	27.0	3.39	14.2	21.6	20.1	1031	1.93	179
	DMR Coal	6393	30.6	52.8				23.5		5.24			2.59		4.01	
	DMR Clay	47.0	24.8	0.0101				0.0131		0.00567						
	CRR Coke	4995										0.000225				
	CRR Carbo Ceramic	15.0	4.05					0.105								
	CRR Aluminum Hydroxide	101	37.2	0.00636									0.20			
	DMR Gas	19798														
	CRR Gas	24636														
	OGC Cooling Adds	48720														
	Purge N_2	33017														
	Unmonitored N_2 estimate	2970														
	Fan Air Leak Estimate	11616														
	Mercury Adsorber Adds	1742														
	Total	183902	1163	4.53	116	6.81	5.5	3.29	51.0	3.39	19.6	21.6	20.1	1034	1.93	183

Table 7-63. (continued).

CP2 Tests		Total (lb)	Al (lb)	B (lb)	Ca (lb)	Ce (lb)	Cs (lb)	Cr (lb)	Fe (lb)	Pb (lb)	Mg (lb)	Mn (lb)	Hg (lb)	Na (lb)	Ni (lb)	K (lb)
Outlet	DMR Solids	4325	645	4.29	111	5.66	4.4	2.67	44.6	2.93	14.8	19.6	0.00497	935	1.88	166.9
	HTF Solids	356	48.2	0.415	9.72	0.324	0.2	0.228	3.52	0.324	1.20	1.83	0.000677	82.2	0.171	15.2
	CRR Solids	943	356	0.00	0.676	0.0000486	0.002837	0.00381	3.67	0.00	0.0923	0.0287	0.0002721	0.700	0.1416	0.118
	PBF Solids	588	39.0	0.018	1.03	0.0034	0.02	0.0212	1.38	0.00163	0.0733	0.0414	2.246	0.516	0.093	0.0983
	OGC Solids	70.0														
	Mercury Adsorber Final	517										16.80				
	Stack 172653											0.000				
	Total 179453		1089	4.72	123	5.98	4.69	2.92	53.1	3.25	16.2	21.5	19.05	1018	2.29	182
Produced																
Reacted																
Mass Balance		-4448	-74.5	0.189	7.32	-0.825	-0.834	-0.369	2.14	-0.139	-3.48	-0.0784	-1.01	-16.1	0.355	-1.13

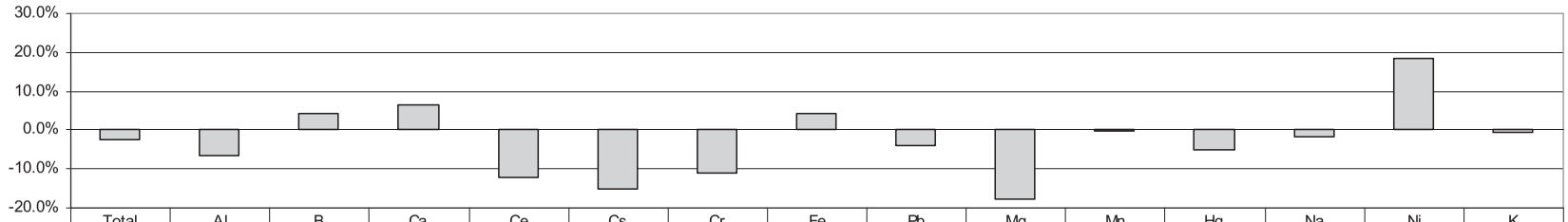

	Total	Al	B	Ca	Ce	Cs	Cr	Fe	Pb	Mg	Mn	Hg	Na	Ni	K
% Mass Imbalance	-2.4%	-6.4%	4.2%	6.3%	-12.1%	-15.1%	-11.2%	4.2%	-4.1%	-17.7%	-0.4%	-5.0%	-1.6%	18.4%	-0.6%

Table 7-64. Elemental Distribution and Mass Balance Closure for CP2.

CP2 Tests		Si (lb)	Zn (lb)	Cl (lb)	F (lb)	PO_4 (lb)	H+ (lb)	H_2O (lb)	Nitrogen Sulfur				Carbon			O_2 (lb)
									NO_3 (lb)	N_2 (lb)	SO_4 (lb)	SO_2 (lb)	Carbon (lb)	CO_3 (lb)	CO_2 (lb)	
5/30/06 14:57 to 6/8/06 13:25																
Feeds	DMR Bed	0.0935													187	
	CRR Bed	0.204													410	
	Simulant Feed	6.96		33.7	18.4	11.2	47.3	15566	9671	234						
	DMR Coal	81.3			2.07		77.6	393	192	99.7		4356			15.3	
	DMR Clay	0.0110													22.0	
	CRR Coke					14.5		1.50	7.74	3.74		4848			125	
	CRR Carbo Ceramic	3.16													7.27	
	CRR Aluminum Hydroxide	0.00142					33.6								31.0	
	DMR Gas						11539		5205						3054	
	CRR Gas								11169						13467	
	OGC Cooling Adds						34010		11283						3427	
	Purge N_2								33017							
	Unmonitored N_2 estimate								2970							
	Fan Air Leak Estimate								8910						2706	
	Mercury Adsorber Adds										1742					
	Total	84.8	6.96	33.7	18.4	13.2	139	61543	9870	72554	2080	0	9204	0.0	0	23452

Table 7-64. (continued).

CP2 Tests		Si (lb)	Zn (lb)	Cl (lb)	F (lb)	PO_4 (lb)	H+ (lb)	H_2O (lb)	Nitrogen Sulfur NO_3 (lb)	N_2 (lb)	SO_4 (lb)	SO_2 (lb)	Carbon Carbon (lb)	CO_3 (lb)	CO_2 (lb)	O_2 (lb)
5/30/06 14:57 to 6/8/06 13:25																
Outlet	DMR Solids	59.6	6.10	37.6	13.55	9.74		0.140		251		523		843	805	
	HTF Solids	5.85	0.58	4.65	2.30	0.92		0.235		23.4		29.7		72.3	63	
	CRR Solids	5.72	0.0356	0.00325	0.0166	0.107		0.0184		0.00556		244		0.699	325	
	PBF Solids	0.987	0.0125	0.0159	0.111	0.187		0.0277		1.32		505		0.900	36.4	
	OGC Solids															
	Mercury Adsorber Final									500						
	Stack		0.0					61592		74908		31.1			27653	8725
	Total	72.2	6.73	42.3	16.0	11.0	0.00	61591.86	0.421	74907.84	2324	31.1	1301	917	27653	9955
Produced							1246		2468		31.1		917		28287	8488
Reacted						139		9870		47.7			7903		22408	
Mass Balance		-12.6	-0.2294	8.64	-2.47	-2.30	0.00	-1197	-114		97.6		-173			423

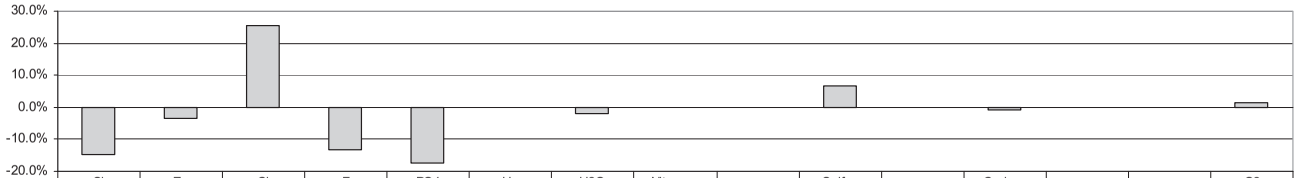

	Si	Zn	Cl	F	PO4	H+	H2O	Nitrogen		Sulfur		Carbon			O2
% Mass Imbalance	-14.8%	-3.3%	25.7%	-13.4%	-17.3%	0.0%	-1.9%	-0.1%		6.6%		-1.0%			1.3%

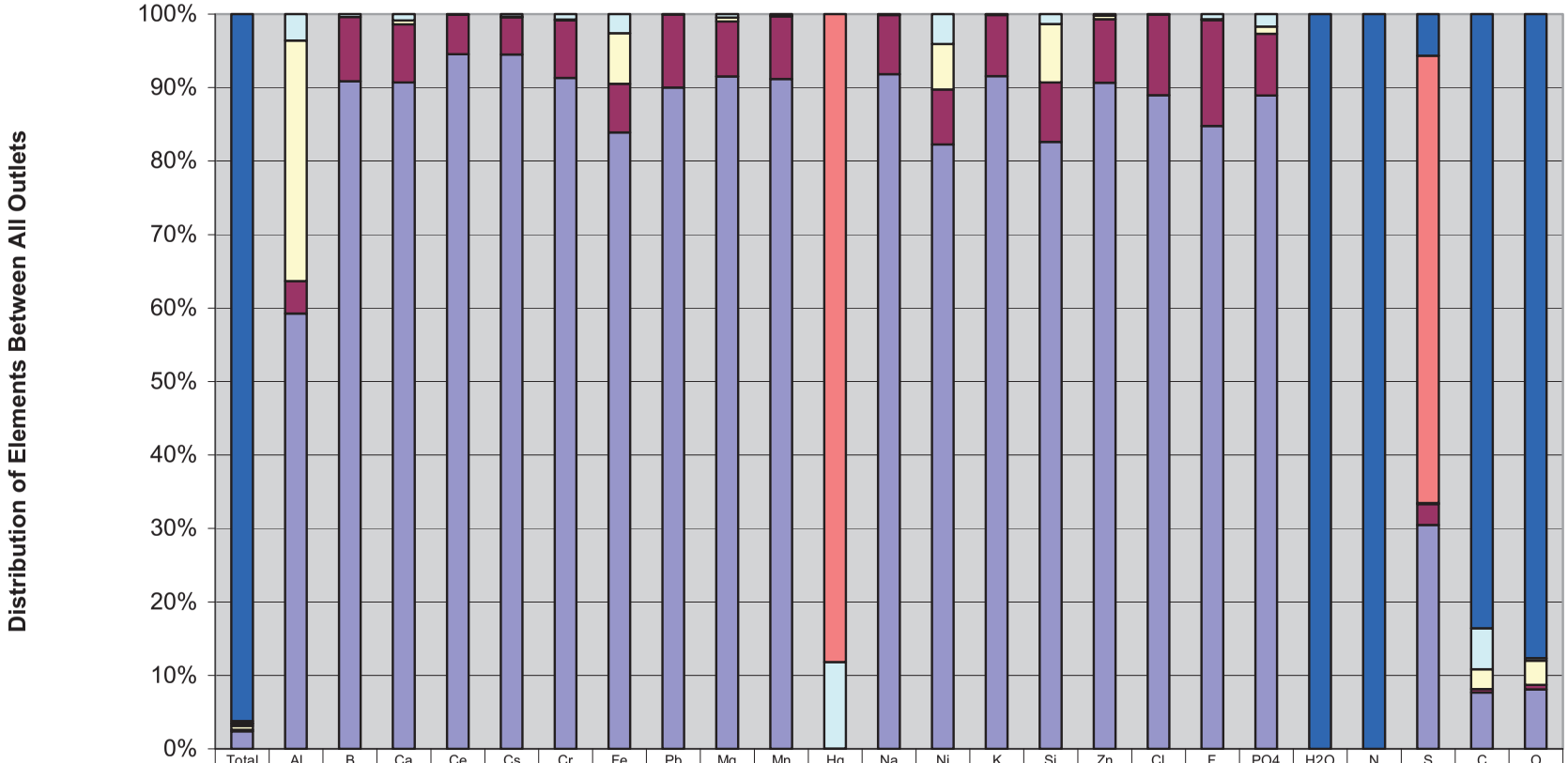

	Total	Al	B	Ca	Ce	Cs	Cr	Fe	Pb	Mg	Mn	Hg	Na	Ni	K	Si	Zn	Cl	F	PO4	H2O	N	S	C	O
Stack	96.2%	0.0%	0.0%	0.0%	0.0%	0.0%	0.0%	0.0%	0.0%	0.0%	0.0%	0.0%	0.0%	0.0%	0.0%	0.0%	0.0%	0.0%	0.0%	0.0%	100.0%	100.0%	2.0%	83.6%	87.6%
Mercury Adsorber Final	0.3%	0.0%	0.0%	0.0%	0.0%	0.0%	0.0%	0.0%	0.0%	0.0%	0.0%	88.2%	0.0%	0.0%	0.0%	0.0%	0.0%	0.0%	0.0%	0.0%	0.0%	0.0%	21.1%	0.0%	0.0%
OGC Solids	0.0%	0.0%	0.0%	0.0%	0.0%	0.0%	0.0%	0.0%	0.0%	0.0%	0.0%	0.0%	0.0%	0.0%	0.0%	0.0%	0.0%	0.0%	0.0%	0.0%	0.0%	0.0%	0.0%	0.0%	0.0%
PBF Solids	0.3%	3.6%	0.4%	0.8%	0.1%	0.4%	0.7%	2.6%	0.1%	0.5%	0.2%	11.8%	0.1%	4.1%	0.1%	1.4%	0.2%	0.0%	0.7%	1.7%	0.0%	0.0%	0.1%	5.6%	0.4%
CRR Solids	0.5%	32.7%	0.0%	0.6%	0.0%	0.1%	0.1%	6.9%	0.0%	0.6%	0.1%	0.0%	0.1%	6.2%	0.1%	7.9%	0.5%	0.0%	0.1%	1.0%	0.0%	0.0%	0.0%	2.7%	3.3%
HTF Solids	0.2%	4.4%	8.8%	7.9%	5.4%	5.1%	7.8%	6.6%	10.0%	7.5%	8.5%	0.0%	8.1%	7.5%	8.3%	8.1%	8.6%	11.0%	14.4%	8.4%	0.0%	0.0%	1.0%	0.5%	0.6%
DMR Solids	2.4%	59.3%	90.9%	90.7%	94.5%	94.5%	91.3%	83.9%	90.0%	91.5%	91.2%	0.0%	91.8%	82.2%	91.6%	82.6%	90.7%	89.0%	84.8%	88.9%	0.0%	0.0%	10.6%	7.7%	8.1%

Figure 7-76. Elemental distribution of all discharges for CP2.

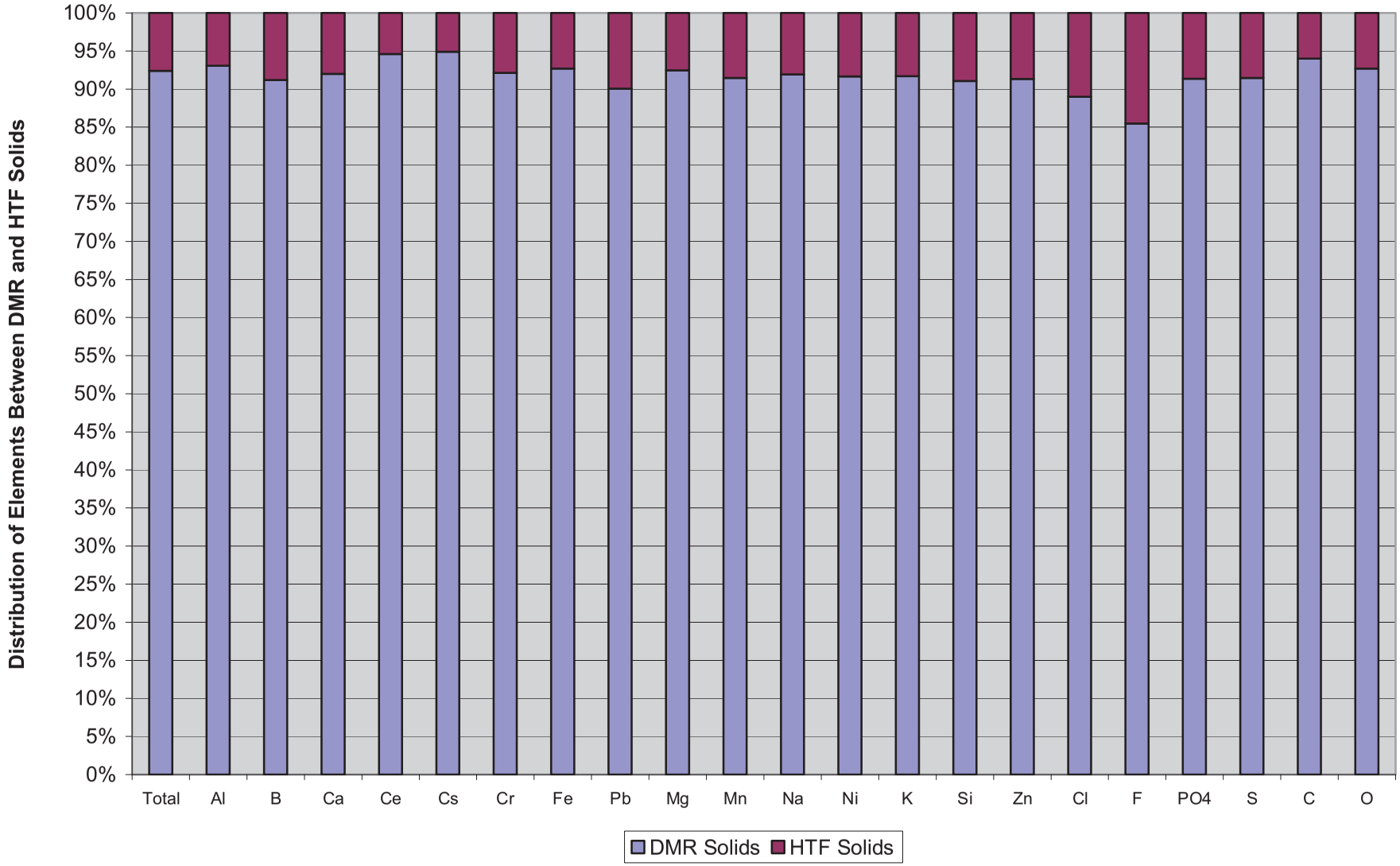

Figure 7-77. Elemental distribution of solids discharges from DMR and HTF for CP2.

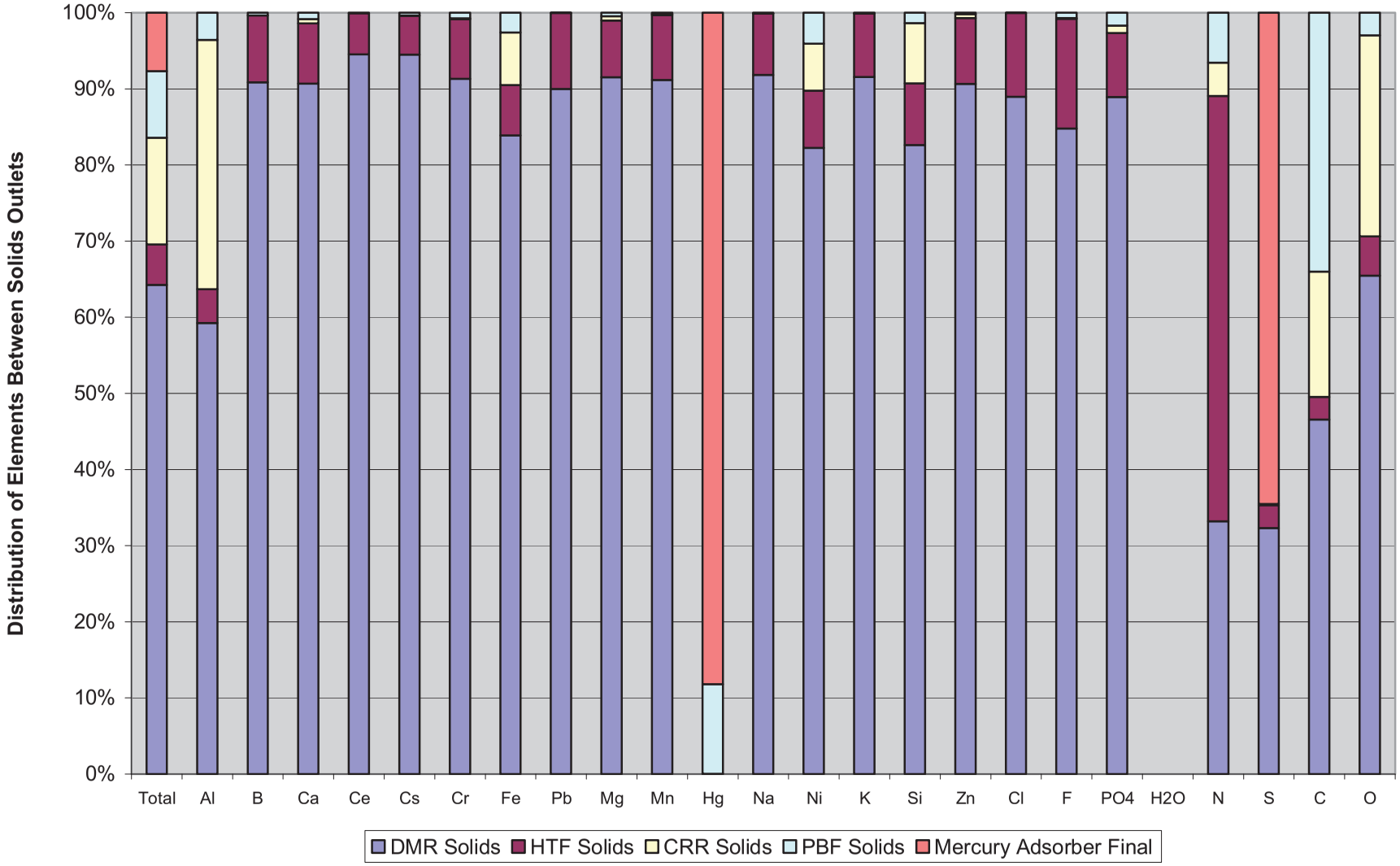

Figure 7-78. Elemental distribution of all solids discharges for CP2.

Similar levels of other metals fed only to the DMR are found in the CRR/OGC/PBF, with most levels less than 1%. However, as the other components are minor constituents in the DMR feed, the sodium level of 0.1% is felt to be the most reliable representation of DMR feed carried to the CRR system. Combined with the indication of little difference in overall solids split in the DMR/HTF system, it is concluded that 0.1% of the feed solids carried through the HTF to the CRR. The Al, Si, and C in and downstream of the CRR primarily reflect the addition of these elements directly to the CRR. The Fe, Cr, and Ni in and downstream of the CRR are primarily contaminants from the materials of construction of the CRR system.

CONTENTS

8. SOLID PRODUCT EVALUATION OF SUITABILITY FOR DISPOSAL 8-1

8.1 Primary Process Solids 8-1

8.1.1 Explosivity 8-1
8.1.2 Pyrophoricity 8-2
8.1.3 Ignitability 8-2
8.1.4 Reactivity 8-2
8.1.5 Detectable Liquids 8-4

9. METALLURGICAL ANALYSIS AND EVALUATION 9-1

10. COMPLETION OF TEST OBJECTIVES 10-1

11. CONCLUSIONS AND RECOMMENDATIONS 11-1

11.1 Lessons Learned 11-1

11.1.1 Integrated THOR® Process System 11-1
11.1.2 Waste Feed System 11-2
11.1.3 Denitration and Mineralization Reformer 11-4
11.1.4 High-Temperature Filter 11-9
11.1.5 Carbon Reduction Reformer 11-10
11.1.6 Off-Gas Cooler 11-12
11.1.7 Off-Gas System 11-13
11.1.8 Continuous Emissions Monitoring 11-15
11.1.9 Data Acquisition and Control System (DACS) 11-16

11.2 Conclusions 11-17

11.3 Recommended Path Forward 11-19

11.3.1 Testing Needs Prior To Integrated Process System Acceptance Test 11-19

12. REFERENCES 12-1

Appendix A—Summary of Data Validation Packages A-1

FIGURES

8-1. Effervescence of DMR Sample 1772 when mixed with water 8-3

TABLES

8-1. Summary of WIPP acceptability testing of SBW products 8-5

10-1. Testing program objectives, measurable parameters, and performance summary 10-2

8. SOLID PRODUCT EVALUATION OF SUITABILITY FOR DISPOSAL

8.1 Primary Process Solids

As discussed in Section 3.5, solid samples from the Hazen tests were collected and analyzed to determine their potential acceptability for disposal at WIPP. The analyses were performed to determine the presence or absence of certain characteristics that would preclude WIPP disposal of IWTU product material. These characteristics included explosivity, pyrophoricity, ignitability, reactivity, and detectable liquids. Although there is no intention of sending the material from the Hazen tests to WIPP, analyses of this material will provide information that will contribute to the Acceptable Knowledge/Process Knowledge for the IWTU waste products that must be qualified for disposal at WIPP.

Samples were collected from the DMR, PR, HTF, and PBF as the primary sources of product material from the SBW treatment process. Chilworth Laboratories in Plainsboro, New Jersey, was selected as the laboratory to conduct the required analyses. Chilworth is an ISO/IEC 17025 accredited laboratory with experience in the analysis of energetic materials. They were approved by the THOR® Treatment Technologies, LLC (TTT) Quality Assurance Manager to conduct these analyses.

Twenty-one product samples were obtained from CP1 Tests 4A-1 through 4A-6, which were the tests most representative of the intended operating conditions for the full-scale IWTU process. The liquid feed for these six tests included the supernatant solution, heavy metals, UDS, and POHC. Samples from the six tests were collected periodically, packaged, labeled, documented with Chain of Custody forms, and sent to Chilworth for analysis.

8.1.1 Explosivity

According to 49 CFR 173.57 [R38], a material is considered explosive if it fails any of four different tests: the Drop Weight Impact Sensitivity Test (Test Method 3(a)(i)), the Friction Sensitivity Test (Test Method 3(b)(iii)), the Thermal Sensitivity Test (Test Method 3(c)), and the Small-Scale Burning Test (Test Method 3(d)(i)). These test methods are described in Section 13 of "UN Recommendations on the Transport of Dangerous Goods, Manual of Tests and Criteria," Fourth Revised Edition, 2004 [R39].

The Drop Weight Impact Sensitivity Test required the use of a Bureau of Explosives impact machine, which caused a 3.63 kg weight to free fall 10 cm onto a 10 mg sample of the material to be tested. Any observation of smoke, flame, or audible report was an indication of shock sensitivity. The test was repeated ten times with ten different samples. A positive result (smoke, flame, or audible report) in at least 5 of the 10 trials would indicate that the material is too dangerous to transport. None of the 21 samples tested were positive for explosivity from the Drop Weight Impact Sensitivity Test.

The Friction Sensitivity Test required the use of a pendulum friction test apparatus. The test was run on twenty-five 20-mg samples. Evidence of explosion was determined if a flash, burn, or audible report was observed. The sample must have shown a negative result on all twenty-five trails for the material to be considered safe for transport. All 25 trials for all 21 samples were negative for friction sensitivity.

The thermal stability test required the use of an explosion-proof oven. A 50-g sample of the material was placed in the oven and heated to 75°C for a period of 48 hours. If there were no explosion or ignition and no evidence of thermal instability, e.g., flame or fuming, then no further testing was required. If there were evidence of thermal instability, then the instrumented test was conducted. If explosion, ignition, or self-heating greater than 3˜C were obser ved during the instrumented test, then the material

was considered too thermally unstable to transport. All 21 samples were shown to be resistant to ignition when exposed to an elevated temperature of 75°C.

The small-scale burning test determined the response of the sample to fire. The test was performed twice with a 10-g sample and twice with a 100-g sample. The test was considered positive if any indication of explosion occurred. Mere combustion of the sample did not constitute a positive result. All 21 samples did not explode or detonate when exposed to fire and were, therefore, negative.

8.1.2 Pyrophoricity

Solid samples were tested for potential pyrophoricity using EPA SW-846 Method 1050, "Test Methods to Determine Substances Likely to Spontaneously Combust" [R40]. Only Test Method A was conducted. A 1–2 g sample of the material was poured from a height of 1 meter onto a non combustible surface. If smoke, flame, incandescence, or other evidence of combustion were observed while the material was being poured or within five minutes of settling on the non combustible surface, then the material was classified as having pyrophoric properties. The test was repeated five times with five different samples or until a positive result was obtained. All 21 samples were negative for pyrophoricity.

8.1.3 Ignitability

Once it was determined that a given solid sample did not exhibit the characteristics of either explosivity or pyrophoricity, the ignitability of the material was determined. An ignitability test and, if necessary, a burning rate test, was accomplished using EPA SW-846 Method 1030, "Ignitability of Solids." [R40] A preliminary screening test was performed to determine if each sample was at all ignitable within the two minute test period and, if so, whether combustion propagated to the 200 mm mark on the test apparatus. All solid product samples were considered as non-metallic in nature. If the waste propagated burning of 200 mm or more of the test strip within two minutes, then the sample was evaluated by the burning rate test. If the burning rate test determined that flame propagated at a rate of 2.2 mm/sec or greater through the test sample, then the material was considered to test positive for ignitability. None of the 21 samples demonstrated a burning rate of greater than 2.2 mm/sec and were, therefore, determined to be negative for ignitability.

8.1.4 Reactivity

The determination of the characteristic of reactivity was qualitative rather than quantitative, as there is no current EPA method to establish reactivity. Certain aspects of reactivity were determined through the tests described above for explosivity, pyrophoricity, and ignitability. A material is considered reactive if: (1) it is normally unstable and readily undergoes violent change without detonating; (2) it reacts violently with water; (3) it forms potentially explosive mixtures with water; (4) when mixed with water, it generates toxic gases, vapors or fumes in a quantity sufficient to present a danger to human health or the environment; (5) it is a cyanide or sulfide bearing waste that, when exposed to pH conditions between 2 and 12.5 can generate toxic gases, vapors, or fumes in a quantity sufficient to present a danger to human health or the environment; (6) it is capable of detonation or explosive reaction if it is subjected to a strong initiating source or if heated under confinement; (7) it is readily capable of detonation or explosive decomposition or reaction at standard temperature and pressure; and (8) it is a forbidden, Class A, or Class B explosive as defined in 49 CFR 173. While it was not expected that the solid products generated from the SBW tests would exhibit any of the characteristics of reactivity other than those determined by the explosivity or pyrophoricity tests, qualitative tests were run to establish the presence or absence of the water-reactivity characteristics described in Items 2, 3, 4, and 5, above.

A series of simple screening tests was run to determine if the product materials were water reactive. First, a sample of the material (nominally 5 g) was added to water (50 ml) and stirred. The presence or absence of any violent reaction (including explosion, detonation, smoke, flame, or incandescence) was observed and recorded. Since the samples from the SBW tests contained significant quantities of water soluble salts, simple dissolution that was observed was not considered a violent reaction for purposes of this test. If effervescence (bubbling) was observed, then the screening test was repeated on a scale sufficient to obtain a sample of the generated gas in order to perform a quantitative analysis for hydrogen cyanide and hydrogen sulfide. None of the 21 samples exhibited any of the violent reactions associated with WIPP-prohibited water reactivity. Eight of the samples (two from the DMR and six from the PR) exhibited a slight amount of effervescence when mixed with water (Figure 8-1). This result was not unexpected due to the presence of carbonate and/or bicarbonate salts in the SBW product.

Figure 8-1. Effervescence of DMR Sample 1772 when mixed with water.

In order to establish the presence or absence of toxic gases in concentrations dangerous to human health and the environment (reactivity definitions 4 and 5), SW 846 7.3 analyses were performed on all 21 samples. In this analysis, an aliquot of the sample is acidified to pH2 in a closed system. The gas generated (if any) is swept into a scrubber where it is quantitatively trapped. The scrubber solution is then analyzed for cyanide via Method 9014 and for sulfide via Method 9034. None of the 21 samples tested positive for hydrogen sulfide. Four of the 21 samples exhibited detectable quantities of hydrogen cyanide in concentrations ranging from 0.6 to 2.4 mg/kg of sample. The other 17 samples had undetectable quantities of cyanide. In order for a material to be positive for water reactivity according to

definitions 4 and 5 from above, the cyanide concentration would have to be greater than 250 mg/kg. Due to the undetectable quantities of sulfide and the undetectable to trace quantities of cyanide found in the samples, the materials tested were determined to be negative for water reactivity.

8.1.5 Detectable Liquids

The current version of the WIPP waste acceptance criteria (WAC) requires that all waste materials sent to WIPP contain "no detectable liquids" [R12]. The pilot plant solid product materials removed from the process did not contain any free liquids, as they were generated at temperatures of 640°C or greater and were inspected and packaged as soon as they had cooled. The only way the product solids could contain free liquids is if they were extremely hygroscopic and were to pick up enough atmospheric moisture to actually exhibit free water. Since the SBW products contain anhydrous salts, it was fully expected that they would exhibit some degree of hygroscopic behavior and slowly gain weight up to a point when exposed to the atmosphere. If the weight gain proceeded without resulting in the appearance of water, then the material would not exhibit detectable liquids.

A small sample of the material (nominally 5 g) was placed in a vessel such as a watch glass or a weighing boat that allowed maximum exposure to air. The sample remained exposed to humid ambient air for a period of two months. None of the samples absorbed atmospheric moisture to the extent that they self-dissolved or exhibited detectable liquids. The presence or absence of detectable liquids and the tendency to generate them was also determined gravimetrically. A sample of the material was weighed on a regular basis until any weight gain due to hygroscopicity (or reaction with other atmospheric gases such as oxygen or carbon dioxide) ceased. The range of weight gains for samples from the various sources were as follows:

- HTF (6 samples) 5.2–7.0 wt%
- PR (5 samples) 3.2–4.6 wt%
- PBF (8 samples) -0.6 –0.6 wt%
- DMR (2 samples) 3.8–4.4 wt%.

Two of the PBF samples showed a slight weight loss (possibly due to experimental error), but none of the 21 samples were found to have detectable liquids.

A summary of the results of the WIPP acceptability testing performed on the 21 SBW product samples is shown in Table 8-1.

Table 8-1. Summary of WIPP acceptability testing of SBW products.

THOR Sample #	Sample Source	Chilworth Sample #	Explosivity Reactivity				Pyrophoricity	Ignitability				Detectable Liquids	
			Impact	Friction	Heat	Flame			Water Reaction	Sulfide (mg/kg)	Cyanide (mg/kg)	Presence of Detectable Liquids or Self-Dissolution	Wt. Gain (%)
1612 HTF		5763A	Neg.	Neg.	Neg.	Neg.	Neg.	Neg.	Neg.	U[2]	U[3] Neg.		6.0
1613 PBF		5763B	Neg.	Neg.	Neg.	Neg.	Neg.	Neg.	Neg.	U[2]	U[3] Neg.		0.0
1614 DMR		5763C	Neg.	Neg.	Neg.	Neg.	Neg.	Neg.	Effer.[1]	U[2]	U[3] Neg.		4.4
1634 PR		5763D	Neg.	Neg.	Neg.	Neg.	Neg.	Neg.	Effer.[1]	U[2]	U[3] Neg.		4.4
1639 PR		5763E	Neg.	Neg.	Neg.	Neg.	Neg.	Neg.	Effer.[1]	U[2] 0.6		Neg.	4.6
1640 HTF		5763F	Neg.	Neg.	Neg.	Neg.	Neg.	Neg.	Neg.	U[2]	U[3] Neg.		6.4
1641 PBF		5763G	Neg.	Neg.	Neg.	Neg.	Neg.	Neg.	Neg.	U[2]	U[3] Neg.		0.0
1666 HTF		5763I	Neg.	Neg.	Neg.	Neg.	Neg.	Neg.	Neg.	U[2] 1.5		Neg.	7.0
1667 PBF		5763J	Neg.	Neg.	Neg.	Neg.	Neg.	Neg.	Neg.	U[2]	U[3] Neg.		0.6
1668 PR		5763H	Neg.	Neg.	Neg.	Neg.	Neg.	Neg.	Effer.[1]	U[2]	U[3] Neg.		3.4
1710 PBF		5763K	Neg.	Neg.	Neg.	Neg.	Neg.	Neg.	Neg.	U[2]	U[3] Neg.		-0.6
1711 PR		5763L	Neg.	Neg.	Neg.	Neg.	Neg.	Neg.	Effer.[1]	U[2]	U[3] Neg.		3.2
1712 HTF		5763M	Neg.	Neg.	Neg.	Neg.	Neg.	Neg.	Neg.	U[2]	U[3] Neg.		6.8
1713 HTF		5763N	Neg.	Neg.	Neg.	Neg.	Neg.	Neg.	Neg.	U[2] 0.94		Neg.	5.6
1772 DMR		5763P	Neg.	Neg.	Neg.	Neg.	Neg.	Neg.	Effer.[1]	U[2]	U[3] Neg.		3.8
1774 PBF		5763O	Neg.	Neg.	Neg.	Neg.	Neg.	Neg.	Neg.	U[2]	U[3] Neg.		0.4
1821 PBF		5763Q	Neg.	Neg.	Neg.	Neg.	Neg.	Neg.	Neg.	U[2] 2.4		Neg.	0.2
1822 HTF		5763R	Neg.	Neg.	Neg.	Neg.	Neg.	Neg.	Neg.	U[2]	U[3] Neg.		5.2
1827 PR		5763S	Neg.	Neg.	Neg.	Neg.	Neg.	Neg.	Effer.[1]	U[2]	U[3] Neg.		4.2
1884 PBF		5763V	Neg.	Neg.	Neg.	Neg.	Neg.	Neg.	Effer.[1]	U[2]	U[3] Neg.		-0.2
1885 PBF		5763W	Neg.	Neg.	Neg.	Neg.	Neg.	Neg.	Neg.	U[2]	U[3] Neg.		0.4

Notes:

1. Effervescence (bubbling) observed on mixing with distilled water (pH 7).
2. Undetectable quantity when mixed with sulfuric acid (pH 2). Detection level is 10 mg/kg.
3. Undetectable quantity when mixed with sulfuric acid (pH 2). Detection level is 0.5 mg/kg

9. METALLURGICAL ANALYSIS AND EVALUATION

Corrosion coupons were installed during the CP1 and CP2 as discussed in detail in Section 3.6. Upon completion of the test program, selected coupons were removed from the process equipment and shipped to a qualified metallurgical lab at the Savannah River National Laboratory (SRNL) for analysis. Each coupon was measured and visually inspected by the laboratory. One of the coupons of each material in selected process locations was destructively examined to identify the corrosion mechanism and extent of corrosion. An estimate of the extent of corrosion and corrosion rate were made for each coupon examined. A second metallurgical professional independently examined the results of the analyses and evaluations.

The analyses have been completed and the results are provided in detail in the following two SRNL documents:

1. "Analyses of Hazen Corrosion Coupons (U), Rev. 1," WSRC-TR-2006-00142, Rev. 1, Karthik Subramanian, April 2006.

2. "Analyses of THOR Treatment Technologies CP2 Corrosion Coupons (U)," WSRC-TR-2006-00268, Karthik Subramanian, July 2006.

Metallurgical experts at the SRNL performed destructive analyses, inspections, and evaluation of the corrosion mechanisms, extent of corrosion, and have determined a corrosion rate for the coupons installed during CP1. Confirmatory analyses and evaluations were made on the CP2 corrosion coupons. See above referenced reports for details.

The results of the metallurgical evaluations performed by SRNL on the second set of corrosion coupons exposed during CP2 confirmed the selection of preferred alloys following CP1. Selection of the actual alloys for use in construction of the IWTU process systems and determination of the corrosion allowance for the IWTU systems are not part of the scope of the demonstration programs and are reported in separate IWTU project documentation.

10. COMPLETION OF TEST OBJECTIVES

The principal, overall objectives of the SBW testing program were to:

- Establish target steady-state system operating conditions
- Demonstrate integrated operation of the entire SBW treatment process, including serial operation of the DMR and CRR
- Demonstrate/confirm long-term system operability with respect to process chemistry, material flows, MEB, equipment durability, and particle size control
- Establish key operating parameters for the full-scale IWTU process
- Obtain operational data to confirm IWTU design parameters
- Gather off-gas emissions data for purposes of environmental permitting
- Confirm solid product data for requesting WIPP transportation and disposal.

The test conditions as specified in the pilot plant test plan were completed. Details concerning the overall objectives, along with quantifiable criteria where appropriate and an evaluation summary of the success in meeting the criteria are summarized in Table 10-1.

Table 10-1. Testing program objectives, measurable parameters, and performance summary.

Quantifiable Objective Target or Criteria	Measurable Parameters and Test Methods	Performance Achieved Against Objectives
Establish target steady-state system operating conditions		
1. Verify initial charcoal/carbon selections for DMR and CRR (steady autothermal process operation is maintained).	• Monitoring of charcoal/carbon types and addition rates. • CPMS gas monitoring at high-temperature filter outlet. • CEMS monitoring at stack.	**Objective was achieved** Steady autothermal operation of the DMR and CRR was demonstrated with GC-CRB and DeSulco products respectively. The CPMS and the CEMS provided gas composition results for the process gas and the stack gas. (Ref: Sections 7.4 & 7.5)
2. Verify adequacy of DMR startup bed media (bed does not agglomerate and sustainable DMR operation is maintained).	• Monitoring of thermocouples in DMR and CRR. • Monitoring of DMR bed particle appearance and size distribution.	**Objective was achieved** Scoping and initial production tests resulted in the selection of a starting bed with a 50% – 50% mixture of two different sizes of alumina particles, AGSCO 46 and AGSCO 80. The AGSCO alumina mixture provides a satisfactory startup bed for the DMR. (Ref: Sections 7.4 & 7.5)
3. Verify adequacy of CRR bed media (bed does not agglomerate and sustainable CRR operation is observed).	• Monitoring of thermocouples in CRR. • Monitoring of CRR bed particle appearance and size distribution.	**Objective was achieved** Both the Carbo Ceramics and AGSCO alumina starting bed materials performed well with minimal carryover and no significant agglomerations. (Ref: Section 7.4 & 7.5)
4. Optimize charcoal addition rate to DMR (maintain autothermal process operation while maintaining a NO_X concentration <500 ppm at the exhaust stack and <5 wt % C in solid product).	• Monitoring of charcoal/carbon types and addition rates. • CPMS gas monitoring at high-temperature filter outlet. • Monitoring of waste simulant feed rate. • Oxygen sensor at CRR gas outlet. • CEMS monitoring at stack.	**Objective was partially achieved** Sustained steady autothermal operations indicate that NO_X levels out of stack can be maintained at <500 ppm total NO_X. Average off-gas NO_X levels less <1000 ppm can be easily sustained with more moderate carbon and hydrogen levels in the DMR. ~10 wt% carbon in the product can be achieved with carbon separation from the PR product. <5% wt% carbon in the solid product could not be achieved. However, process performance is not affected. Waste canister count could increase by 10–20% because of increased carbon content. (Ref: Sections 7.6 & 7.7)

Table 10-1. (continued).

Quantifiable Objective Target or Criteria	Measurable Parameters and Test Methods	Performance Achieved Against Objectives
5. Optimize O_2 addition rate to DMR and carbon/O_2 addition rate to the CRR to maintain full autothermal operation while maintaining a feed rate of 0.25 ± 0.15 gpm, a DMR bed temperature of 640 ± 20°C, and CRR bed temperature of 1000 ± 20°C.	• Monitoring of thermocouples in DMR and CRR. • Monitoring of charcoal/carbon types and addition rates. • CPMS gas monitoring at high-temperature filter outlet. • Monitoring of DMR and CRR bed particle appearance and size distribution. • Monitoring of waste simulant feed rate. • Oxygen sensor at CRR gas outlet. • CEMS monitoring at stack. • Flow controllers for gas, oxygen, and water injection.	**Objective was achieved** Demonstrated consistent, reliable autothermal temperature control in the DMR and CRR by automatic control of the oxygen input to each reformer. DMR coal and CRR coke addition rates were manually adjusted to provide desired inventories. DMR and CRR bed temperatures were stable within operating guidelines over a range of waste feed rates including 0.25 to 0.35 gpm. CRR target temperature was changed to 950°C and the unit operated well at this temperature. (Ref: Section 7.5)
6. Achieve CO, H_2, and unburned hydrocarbon goals (see below) in gas downstream of CRR by optimizing air/oxygen injection rate to CRR.	• Monitoring of waste simulant feed rate. • Oxygen sensor at CRR gas outlet. • CEMS monitoring at stack. • Flow controllers for gas, oxygen, and water injection.	**Objective was achieved** Demonstrated consistent control of total hydrocarbon (THC) and CO emissions during production tests. THC levels averaged less than 0.4 ppm (dry, corrected to 7% O_2) and CO levels were readily controlled within regulatory limits by adjusting oxygen input to the CRR. (Ref: Section 7.7)
7. Establish water flow-rate to off-gas cooler necessary to achieve an off-gas temperature of 140-160°C downstream of the cooler.	• Monitoring of thermocouples in DMR and CRR. • Monitoring of waste simulant feed rate. • Flow controllers for gas, oxygen, and water injection.	**Objective was achieved** Demonstrated consistent, reliable control of off-gas temperature using the water spray quencher. Temperature control was within 5°C of set point. This set point was established at 170-180°C for optimal off-gas system operation. (Ref: Sections 7.4 & 7.7)

Table 10-1. (continued).

Quantifiable Objective Target or Criteria	Measurable Parameters and Test Methods	Performance Achieved Against Objectives
Demonstrate integrated operation of the entire SBW treatment system, including serial operation of the DMR and CRR		
8. Demonstrate that the operation of the DMR and CRR can be safely and consistently coordinated, while the DMR, CRR, and off-gas systems continue to perform their intended process functions at all test conditions shown in Tables 8 and 10 (in the test plan).	• Monitoring of all process instrument indications for the DMR, CRR, and off-gas systems to achieve and sustain steady process operations. • Monitoring of process parameters to confirm intended process operation, especially oxidation of hydrogen, carbon monoxide, and organics and reduction of nitrates to nitrogen gas.	**Objective was achieved** Demonstrated safe and reliable integrated operation of the DMR, CRR, filters, and off-gas system components. The GAC bed experienced a high temperature excursion during start-up of CP2 testing. This event is still under investigation, but the causes were conditions that occurred during start-up, not normal test conditions and not under conditions that would exist in the full-scale plant. Successful corrective action was taken in that the startup sequence was modified to isolate the GAC bed during start-up. Start-up and operation with the GAC bed within controlled temperature limits was demonstrated during CP1 and CP2. (Ref: Section 7.7)
9. Achieve a CRR bed attrition rate of less than 5% per day while maintaining CO, H_2, and unburned hydrocarbon concentrations at acceptable levels.	• Monitoring of all process instrument indications for the DMR, CRR and off-gas systems to achieve and sustain steady process operations. • Monitoring of CRR product and carryover to confirm attrition rate is acceptable. • Monitoring of process parameters to confirm intended process operation, especially oxidation of hydrogen, carbon monoxide, and organics and reduction of nitrates to nitrogen gas.	**Objective was achieved** Demonstrated low attrition and carryover of CRR bed (<1%/day), while maintaining CO and THC at acceptable levels. Testing shows that the carryover from the CRR is mainly carbon fines, not bed media. (Ref: Sections 7.4 & 7.6)

Table 10-1. (continued).

Quantifiable Objective Target or Criteria	Measurable Parameters and Test Methods	Performance Achieved Against Objectives
10. Demonstrate that the entire pilot plant can be operated as an integrated process without process trends or events that would lead to shutdown (e.g., no bed defluidizations or temperature excursions; no irrecoverable process line blockages).	• Monitoring of all process instrument indications for the DMR, CRR, and off-gas systems to achieve and sustain steady process operations. • Analysis of DMR product to confirm gradual replacement of the start-up bed with product bed, while monitoring all process operating parameters to confirm intended process operation. • Monitoring of CRR product and carryover to confirm attrition rate is acceptable. • Monitoring of process parameters to confirm intended process operation, especially oxidation of hydrogen, carbon monoxide, and organics and reduction of nitrates to nitrogen gas.	**Objective was achieved** With the implementation of corrective actions in response to operating issues, long-term integrated operation of the DMR, CRR, filters, and off-gas system components was demonstrated during the production runs, without process shutdown events, irrecoverable process line blockages, bed defluidizations, and temperature excursions. There were no irrecoverable process blockages or bed defluidizations during the production runs. There were several minor temperature variations during the production runs due to oxygen control input variations that resulted from DACS tuning iterations and inaccurate manual control inputs. There was also one loss of fluidizing steam due to shutdown of the steam boiler. Variation of CRR FG flows and bed media adjustments served to break up the two limited agglomerates in the CRR so no irrecoverable process shutdowns resulted. (Ref: Sections 7.4 & 7.5)
Demonstrate/confirm long-term system operability with respect to process chemistry, material flows, material and energy balance, equipment durability, and particle size control.		
11. Achieve >100 hrs continuous operation at an average waste simulant feed rate of 0.25 gpm, after complete turnover of DMR starting bed.	• System flow meters, temperature indicators and pressure transducers.	**Objective was achieved** This was achieved during CP1. DMR bed turnover was completed prior to start of the 100 hrs of continuous operation. (Ref: Section 7.4)
12. Confirm basic process chemistry and material flows as established in previous bench-scale tests.	• System flow meters, temperature indicators and pressure transducers. • Sampling and analysis of process solids and gaseous product streams. • Gravimetric measurement of 8-hr bed samples and fines samples. • Analysis of bed and fines samples for particle size distribution, bulk density, agglomeration, etc. • Solids material balances.	**Objective was achieved** Demonstrated process chemistry and materials flows that were consistent with previous bench-scale tests. New data provided by the tests on the formation of wall scale in the DMR are being evaluated. It was been determined that the wall scale does not form when GC-CRB is used in the DMR and UDS are in the stimulant feed. It has also been determined that the scale can be dissolved with hot water and dilute nitric acid. Findings of the additional evaluations will be presented in separate documents. (Ref: Sections 7.4, 7.5, 7.6, 7.7, & 7.8)

Table 10-1. (continued).

Quantifiable Objective Target or Criteria	Measurable Parameters and Test Methods	Performance Achieved Against Objectives
13. Achieve uniform temperature distribution in DMR and CRR beds with no greater than ±15°C axial temperature variation in either bed.	• System flow meters, temperature indicators and pressure transducers.	**Objective was achieved** Temperature profiles within the DMR and CRR beds during operation were well within the ±15°C axial temperature. (Ref: Sections 7.4 & 7.5)
14. Achieve DMR distributor pressure drop of <30 inches water column, and bed pressure drop of <60 inches water column.	• System flow meters, temperature indicators and pressure transducers.	**Objective was achieved** DMR FG distributor pressure drop ranged from ~5 up to 25 inch W.C. depending upon the FG flow. Bed pressure drop was a function of bed level, product density, and coal inventory. DMR bed pressure drop was maintained <60 inch W.C. (Ref: Section 7.5)
15. Achieve steady-state bed particle size distributions for the DMR and CRR (<5% bed agglomeration with <5% of particles greater than 1500 microns in diameter.	• System flow meters, temperature indicators and pressure transducers. • Sampling and analysis of process solids and gaseous product streams. • Gravimetric measurement of 8-hr bed samples and fines samples. • Analysis of bed and fines samples for particle size distribution, bulk density, agglomeration, etc. • Solids material balances.	**Objective was achieved** Particle size distribution data confirms that bed particle sizes in the DMR were stable and controllable within acceptable particle size ranges. CRR bed particles did not grow, remaining within the desired size range over the operating period. Three small agglomerates occurred during the CP1 production runs, which did not prevent continued operations, all associated with periods of infrequent high oxygen input to the DMR (1 agglomerate) and reduced fluidization for the CRR (2 agglomerates). Bed particle size data indicates that the larger particles in the DMR and CRR were substantially less than the 5% objective. (Ref: Section 7.5)
Establish key operating parameters for the full-scale IWTU process		
16. Determine optimum charcoal/carbon feed rates to DMR and CRR as a function of liquid feed rate to achieve required NO_X destruction and process heat generation. Determine maximum sustainable liquid feed rate as a function of DMR cross-sectional area (DMR operating temperature and required NO_X destruction is maintained).	• Charcoal/carbon feed rates to DMR and CRR, off-gas NO_X content, and DMR and CRR temperatures. • Liquid feed rate measurements, DMR bed temperatures, off-gas NO_X measurements, bed differential temperatures. • DMR and CRR particle size distributions, bed temperature spreads, and bed product general appearance as a function of fluidizing velocities.	**Objective was achieved** Demonstrated coal/coke addition rates to DMR and CRR respectively with waste feed rates between 0.25 and 0.35 gpm to provide desired NO_X destruction. Demonstrated that NO_X destruction is mainly a function of coal/coke inventory in the DMR, as indicated by the level of H_2 in the DMR process gas. Higher coal inventory in DMR can result in increased carryover of product fines to HTF for any given waste feed throughput. (Ref: Sections 7.4, 7.5, & 7.8)

Table 10-1. (continued).

Quantifiable Objective Target or Criteria	Measurable Parameters and Test Methods	Performance Achieved Against Objectives
17. Determine acceptable range of fluidizing velocities for DMR and CRR.	• Liquid feed rate measurements, DMR bed temperatures, off-gas NO_X measurements, bed differential temperatures. • DMR and CRR particle size distributions, bed temperature spreads, and bed product general appearance as a function of fluidizing velocities.	**Objective was achieved** Determined acceptable range of fluidizing velocities for the DMR (1.0-2.5 fps) and CRR (2 to 8 fps). DMR fluidizing velocities were minimized to reduce particle fines carryover to HTF and were a function of particle size and density in the DMR bed. Implemented improved fluidized range for CRR by using wider size range of alumina media than originally specified. (Ref: Section 7.5)
Obtain operational data to confirm IWTU design parameters		
18. Determine the better of two feed nozzle designs and establish optimal nozzle atomizing ratio (nozzle accretions <5% of bed product mass and particle size growth is stabilized).	• Monitoring of general process operation parameters and establish presence or absence of nozzle accretions by product examination. • DMR and CRR process parameters and general bed product appearance, post-test examination of distributors for plugging and erosion, and visual examination of residual bed solids. • Particle size distribution analysis of DMR bed material and Product Receiver output.	**Objective was achieved** Demonstrated progressively better nozzle designs as the testing proceeded. Demonstrated features that decreased nozzles tip plugging and methods to clear restrictions in the nozzle, waste feed system, transfer tubing, and pumps. Varied nozzle atomizing ratio (NAR) and determined that high NAR gas flows were not required to control particle size in DMR bed. Nozzle accretions were much less than 5% of bed product mass. (Ref: Sections 7.4 & 7.5)
19. Verify fluidizing gas distributor designs and configurations (agglomerates <5% of bed product mass, and erosion/corrosion rates support one year of IWTU operation).	• DMR and CRR process parameters and general bed product appearance, post-test examination of distributors for plugging and erosion, and visual examination of residual bed solids.	**Objective was achieved** Determined that DMR and CRR FG distributors performed within design basis operating parameters and did not appear to contribute to formation of agglomerates. The erosion resistance of planned IWTU DMR Haynes alloy FG distributors is well proven by the extended service of almost identical FG distributors at the Studsvik Processing facility, where the Haynes alloy FG distributors regularly achieve >2 year life. The small agglomerates that formed in the DMR were much less than 5% of the bed mass and the combined weight of the small agglomerates from the CRR were much less than 5% of the CRR bed mass. (Ref: Sections 7.4 & 7.5)

Table 10-1. (continued).

Quantifiable Objective Target or Criteria	Measurable Parameters and Test Methods	Performance Achieved Against Objectives
20. Determine if an off-gas scrubber system is required to meet acid gas emission standards shown below.	• Monitor HCl, Cl_2, and SO_2 stack emissions with scrubber system both on-line and off-line.	**Objective was achieved** Off-gas analyses indicate that no wet scrubber system is required for process off-gas to be MACT compliant or to meet anticipated IWTU off-gas emission permit limits. (Ref: Sections 7.4 & 7.7)
21. Determine capability of mercury removal GAC adsorber to meet emission standard shown below.	• Measurements of Hg concentration across GAC adsorber sections and analysis of Hg content of spent GAC beds at end of program.	**Objective was achieved** The Hg removal performance of the GAC bed met the objective criteria. (Ref: Section 7.7)
22. Determine if external classifier is needed to maintain DMR bed particle size control.	• DMR and CRR process parameters and general bed product appearance, post-test examination of distributors for plugging and erosion, and visual examination of residual bed solids. • Particle size distribution analysis of DMR bed material and Product Receiver output.	**Objective was achieved** Test results have shown that no external particle size classifier is required in order to achieve DMR particle size control. Three particle size control methods have been demonstrated for the DMR: use of a smaller alumina startup bed media, separation of the smaller fraction of product particles from the DMR bed solids drains and recycling the smaller fraction back to the DMR to serve as seed particles, and introduction of inert seed particles directly into the DMR bed during operation. (Ref: Sections 7.4 & 7.5)

Table 10-1. (continued).

Quantifiable Objective Target or Criteria	Measurable Parameters and Test Methods	Performance Achieved Against Objectives
Gather off-gas emissions data for purposes of environmental permitting		
23. $HCl + Cl_2$: <21 ppm (by volume, HCl equivalents, dry basis, corrected to 7% O_2).	• Measurement of emissions in stack gas via EPA designated methods using both CEMS and manual sample trains.	**Objective was achieved** Test results for stack emissions for all constituents using EPA designated methods met the applicable objectives. (Ref: Section 7.7)
24. Particulate matter: <3.4 mg/dscm, corrected to 7% O_2.		
25. Hg: <8.1 micrograms/dscm, corrected to 7% O_2.		
26. Pb: <10 micrograms/dscm, corrected to 7% O_2.		
27. Cr: <23 micrograms/dscm, corrected to 7% O_2.		
28. NO_X: <500 ppm (by volume, dry basis, corrected to 7% O_2).		
29. SO_2: <100 ppm (by volume, dry basis, corrected to 7% O_2).		
30. CO: <100 ppm over an hour rolling average (by volume, dry basis, corrected to 7% O_2.)		
31. Total Hydrocarbons (THC): <10 ppm (by volume, dry basis, corrected to 7% O_2).		
32. Organic Destruction Removal Efficiency (DRE): >99.99% for monochlorobenzene.		
33. Dioxins/furans: <0.11 nanograms TEQ/dscm, corrected to 7% O_2, where "TEQ" is the toxicity equivalent quotient that relates the total toxicity of all the dioxin/furan constituents to that for 2,3,7,8-TCDD.		

Table 10-1. (continued).

Quantifiable Objective Target or Criteria	Measurable Parameters and Test Methods	Performance Achieved Against Objectives
Confirm solid product data for requesting WIPP transportation and disposal.		
34. Solid products meet chemical composition requirements for shipment to and disposal at WIPP.	• Analysis of solid products for explosivity, pyrophoricity, ignitability, reactivity, and detectable liquids.	**Objective was achieved** Analytical tests on solid product samples from the DMR, HTF, and PBF were completed. Based on analytical results and process knowledge, the products do not exhibit any of the chemical characteristics prohibited by WIPP. (Ref: Section 8.0)
Minimize solid product carbon content and fines generation		
35. Carbon content of solid products remains below 5wt%.	• Carbon analysis of DMR and CRR products.	**Objective was not achieved** The carbon content in the DMR product generally exceeded the objective criteria. This is due to the presence of large-sized coal granules that were removed with the bed product when the bed solids were drained from the DMR. When the PR product was screened to less than 12-mesh to remove the larger carbon granules, the average carbon content of the PR product was ~10%. See item 4 in this table for more discussion. (Ref: Section 7.6)
Confirm high retention of inorganic feed constituents in bed product and removal of nitrates, nitrites, water, and organics in the solid products; generate acceptable bulk and true density data		
36. Chloride, sulfate, and non-volatile heavy metals in off-gas meet above emissions goals.	• Chemical analysis of product solids and off-gas stream.	**Objective was achieved** As indicated above, stack samples indicate that chloride, sulfate, and heavy metals emissions were within acceptable ranges. (Ref: Section 7.7)
37. <3 wt% nitrate in DMR product and fines.	• Chemical analysis of product solid. • SEM/EDX analysis of solids.	**Objective achieved** There were essentially no nitrates in the solids, with the nitrate content of the solids averaging less than 0.02% over the entire test. (Ref: Section 7.8)
38. <1 wt% organics in DMR product.	• Chemical analysis of product solids. • SEM/EDX analysis of solids.	**Objective was achieved** The mass balance indicates the total injected organic did not exceed 1 wt% in the DMR product. (Ref: Section 7.8)

Table 10-1. (continued).

Quantifiable Objective Target or Criteria	Measurable Parameters and Test Methods	Performance Achieved Against Objectives
39. Product bulk density 1.0–1.6 g/cm^3.	• Bed and fines density measurements.	**Objective was achieved** Solids sample analyses indicate that product bulk densities were within the objective range and varied from 1.029–1.560 g/cm^3. Results from solids sample analyses indicated that ~75% of the product particle densities are within the objective range of 1.8–2.8 g/cm^3. The remainder of the particle densities varied to a high of ~3.8 g/cm^3 (due to the presence of start-up bed material), which is completely acceptable. (Ref: Section 7.5)
40. Product particle density 1.8–2.8 g/cm^3.		
Demonstrate acceptable material balance closure for major and minor constituents		
41. Material balance closure of ± 10% for major constituents (Al, Na, NO_3^-, etc.).	• Analysis of bed samples, feed samples, fines samples, and scrubber solutions per sample collection log sheet. • Off-gas measurements and analysis.	**Objective was achieved** Material balance calculations were closed within the objective criteria for all major constituents. (Ref: Section 7.8)
42. Material balance closure of ±30% for minor constituents (K, Ca, P, Cl, F etc.).	• Analysis of bed samples, feed samples, fines samples, and scrubber solutions per sample collection log sheet. • Off-gas measurements and analysis.	**Objective was achieved with two exceptions** Material balance calculations were closed within the objective criteria with the exception of calcium and cerium for CP1. The calcium mass imbalance of 30.5% was likely due to high variability of the ash composition of the DMR coal. The cerium mass imbalance indeterminate was due to high scatter in the product analytical data. Material balance calculations were closed within the objective criteria for all minor constituents for CP2. (Ref: Section 7.8).
Demonstrate ability to process surrogates with varying concentrations of constituent chemicals and UDS		
43. Process operation continues without plugging or process upset at varying UDS concentrations (no process upsets due to atomizer plugging at maximum UDS concentration).	• Monitor feed system pressure measurements and feed flow rates. • Monitor product particle size distribution.	**Objective was achieved** Demonstrated reliable waste feed injector and overall process operation with UDS concentrations from 0-120 grams per liter. (Ref: Sections 7.4 & 7.5)

Table 10-1. (continued).

Quantifiable Objective Target or Criteria	Measurable Parameters and Test Methods	Performance Achieved Against Objectives
44. Process operations continue without process upset and in compliance with above emissions limits for surrogate feeds representative of tank farm flush solutions.	• Monitor feed system pressure measurements and feed flow rates. • Monitor product particle size distribution. • Monitor off-gas CEMS and grab sample results. • Monitor general process operation, including process temperatures and differential pressures.	**Objective was achieved** Demonstrated reliable process operations without process upset while feeding SBW surrogate without UDS and with high UDS concentrations, with the standard SBW simulant and with the simulant diluted 10x, but with high UDS, to simulate tank farm flush solutions. Particle size control was readily achieved when processing SBW with UDS. Off-gas emissions were well within target values and within the range of process operations while processing SBW with and without UDS. (Ref. Sections 7.4 & 7.5)

11. CONCLUSIONS AND RECOMMENDATIONS

11.1 Lessons Learned

The THOR® fluidized bed steam reforming (FBSR) process system installed and operated at Hazen Research, Inc. comprised each of the unit operations in the same process sequence that will be utilized at the IWTU for processing SBW. The thermal treatment process equipment sizing for the Hazen ESTD system was based on a 1:10 scale factor compared with the full-scale IWTU system. The scale basis was the DMR throughput, which is a proportional function of the cross-sectional area of the DMR vessel. The Hazen DMR was a 15-in. inside diameter fluidized bed that had 1/10th the area and hence 1/10th the SBW throughput capacity of the full-scale 48 in. inside diameter DMR planned for the IWTU processing facility. Other process equipment used during the Hazen ESTD program were also scaled to match the flow and thermal characteristics and functional requirements of the IWTU so that the system and component performance and operating characteristics were similar, comparable, and scalable between the ESTD and the IWTU. The successful extension of the ESTD test program and lessons learned to the full-scale IWTU facility seems probable because of the previous successful scale-up from the same Hazen test hardware to the commercially successful Studsvik Processing Facility located in Erwin, TN. The demonstrated scale-up from the Hazen 15-in. inside diameter DMR FBSR system to the Studsvik Processing facility main reformer (inside diameter of 45 in.) was a factor of 1:9, so the IWTU scale-up of 1:10 is a logical extension of previous successful work.

The purpose of the Lessons Learned section is to evaluate technical and performance successes and issues encountered during the pilot plant scoping and production tests. Issue resolutions are discussed. Each major process unit operation, mechanical equipment component, and the DACS are evaluated, and discussion is provided as to what worked well, what needs improvement, what improvements have already been made, what were the results of the modified system or component, and what additional testing is required prior to site acceptance testing (SAT) of the IWTU process. Design and performance impacts and modifications to the IWTU systems and components are discussed.

11.1.1 Integrated THOR® Process System

The integrated Hazen pilot plant process system demonstrated integrated operation of all process unit operations and major components that will be utilized at the IWTU, with the exception of the post-processing material handling and packaging equipment and the process HEPA filter.

Accomplishments of the pilot plant testing include the following:

- Demonstrated safe, reliable, predictable series operation of the DMR, CRR, and downstream off-gas system.
- Demonstrated that process gas from the DMR fully fluidized the CRR media at operating temperatures.
- Demonstrated that the DMR and CRR can be reliably operated with automatic temperature control, while maintaining the bed levels and system pressures within desired operating ranges.
- Demonstrated particle size control in the DMR when processing SBW simulant with and without UDS.

- Demonstrated that off-gas emissions of all potential pollutants are well below the MACT emission limit standards and anticipated IWTU air permit limits.

- Demonstrated that pressure drops across the process unit operations are within the design basis.

- Demonstrated that material flows, pressures, and temperatures from the DMR through the process system matched the MEB used to design both the ESTD and the IWTU.

11.1.1.1 Recommendations for Additional Testing. The integrated ESTD system performed as required during the CP1 test program. However, it was recommended that a Phase 2 carbonate test program be performed to provide additional confirmatory data. CP2 was successfully completed in June 2006. Based on the successful completion of CP1 and CP2, no additional integrated, full-system ESTD tests are required to complete the detailed design of the IWTU. Some individual subsystem and component tests are required. The performance of these subsystem and component tests is covered by a separate test program. See Section 11.3 for a summary of this follow-on testing.

11.1.1.2 Impact on IWTU. The integrated ESTD system performed as required, confirming the SBW thermal treatment process flowsheet for the IWTU. There are no changes that need to be made to the overall IWTU process flowsheet as a result of system and component performance and analytical data collected during the Hazen test programs. Any detailed changes to the overall process mass and energy balance resulting from the ESTD will be incorporated into the IWTU mass and energy balance, as appropriate. Modifications to individual pieces of equipment, as noted in the following sections, will need to be incorporated into the final IWTU design.

11.1.2 Waste Feed System

The waste feed system for the ESTD system included a series of mix tanks, pumps, transfer piping and tubing, flow controls, and two installed DMR waste feed atomizing injectors. One waste feed injector was on-line during waste feed operations and the other was off-line with nitrogen purge on to maintain flow paths clear. The majority of operational difficulties during the scoping and production tests, e.g., plugged lines, loss of waste feed, etc., occurred in the waste feed system.

A total of four waste feed injector designs were utilized during the performance of the Hazen scoping and production tests. The initial three waste feed injector designs were based on the successful injector designs used during previous STAR Center test programs. The first three waste feed injectors utilized a small bore waste feed tube internal to the injector with a reduced inside diameter tip that accelerates the waste feed solution as it enters the DMR bed. Considerable difficulty was encountered using these reduced tip size injectors during the scoping tests. The main problem was plugging of the small-bore tip with solids during waste feed operations. The reduced tip size injectors failed to adequately pass the SBW solution when the UDS was added to the surrogate. The system was then shutdown and a fourth waste feed injector design was fabricated. The fourth set of waste feed injectors utilized a multiple tube in tube axial assembly that also provided an insulated and water-cooled jacket near the tip of the injector. The central waste feed tube inside the injector was a straight tube with no flow restrictions. This set of injectors was used for most of CP1 and all of CP2. It appeared that this straight tube assembly solved the injector tip plugging problem, although occasional remotely initiated water flushing of the waste feed injection tubing and injector was required. However, other waste feed transfer system components and small bore transfer tubing did experience repetitive plugging during several production runs, due to the presence of the UDS in the feed, especially during feed tank and pump swap evolutions.

During CP1, one of the waste feed injectors had excessive erosion at the tip where the atomizing gas discharges. Examination of the erosion pattern at this location indicated that the secondary gas purge

(annulus between second and third co-axial tubes) caused bed solids to impact the part of the waste feed injector that extended past the gas purge tip. To minimize this erosion source, the gas purge flow was eliminated from the improved 4th generation waste feed injectors used during CP2. This erosion pattern was also seen on one earlier version waste feed nozzles where the nozzle extended too far beyond the atomizing gas discharge location. Inspection of the waste feed (WF) injector following CP2 operations indicated the presence of minor erosion at the atomizing gas tube discharge location. The elimination of the second gas flow has helped to minimize erosion at the atomizing gas tube tip.

The majority of the waste feed plugging problems occurred in the small bore (1/4 in.) tubing that supplied SBW surrogate from the T-101A and T-101B mix tanks to the DMR waste feed injectors. Frequent plugging of the tubing and peristaltic tubing pumps occurred during the initial operations when feeding SBW with UDS during CP1. Evaluation of the plugging problem determined that one of the UDS constituents was supplied with a small percentage of large oversize particles that would settle out and/or bridge in the small tubing and plug the lines. A strainer was installed between the two mix tanks and the tubing and waste feed pump to remove the largest fraction of the oversize materials. Subsequent batches of UDS surrogate were prepared using pre-screened materials, which greatly reduced line plugging.

11.1.2.1 Recommendations for Additional Testing. No additional testing is required for the WF injectors or other feed system components for the carbonate flowsheet using the pilot plant system. An improved WF injector design is recommended for use in the IWTU that will include improved materials with higher erosion resistance in the NAR gas tube tip and the elimination of water cooling. The IWTU mock-up test program will test and evaluate alternative erosion resistant nozzle tip materials such as ceramics and Haynes Alloy 25 that have been used successfully on the NWCF WF injectors to extend service life by more than a year.

It is also recommended that the full-scale IWTU WF injectors be independently evaluated and tested prior to use in the IWTU, including the following tests:

- Perform thermal analysis and actual hot furnace testing of heat transfer characteristics to determine the most efficient methods to keep the tips cool without the use of water cooling

- Test nozzles off-line to determine atomization patterns, pressure drops, and select atomization rates and flows as a function of WF injection rates

11.1.2.2 Impact on IWTU. The feed system utilized for the ESTD is not typical of the IWTU waste feed system due to the proportionately smaller tubing used for the ESTD compared with the 1/2 in. piping that will be used at the IWTU. The lessons learned from the ESTD test program that have been incorporated in the IWTU design include:

- Install a strainer in the waste transfer system to prevent oversized particles from entering the IWTU waste feed system.

- Install a high pressure nitrogen purge and a hot water and acid flush capability on both the feed atomizing gas and waste feed injector flow paths.

- Specify piping to minimize all line size changes, welds, etc., in the waste feed transfer lines that could serve as bridge initiators.

- Specify flow velocities in lines to prevent fine solids from dropping out and settling in lower flow velocity areas, and provide thorough flush capability. The feed lines in the IWTU are expected to be 1/2-in. schedule 80 pipes. The feed lines in the NWCF were 1/2-in. Schedule 80 pipe and did not experience feed line plugging, even though the calciner used a low-pressure gravity feed system and had solids loading equal to or greater than what the IWTU will experience when processing SBW.

- Install improved waste feed injectors that provide a single atomizing gas flow annulus, flush extension of the atomizing gas and waste feed tube tips to minimize erosion of tips, straight tube on waste feed bore to prevent solids bridging in tip, and active cooling and insulation on the end of the injector to prevent thermal related caking at the nozzle tip.

- Install automatic waste feed line nitrogen purge to keep bed solids out of the waste feed injector tips during periods when waste feed flow stops or fluctuates.

- Install waste feed flowmeters in vertical flow-up position to enhance air bubble release.

- Incorporate NWCF lessons learned on waste feed injector to provide improvements identified during the test program:

  - Waste feed injectors will be designed for remote replacement.

  - Successful methods used to maintain and unplug the NWCF calciner nozzles will be incorporated in the IWTU waste feed injectors. The NWCF calciner nozzle handled solids loading equal to or greater than will occur in the IWTU SBW processing. Calciner nozzle unplugging methods include automatic water purges and the ability to use high-pressure water and/or acid when needed to clear out nozzles.

11.1.3 Denitration and Mineralization Reformer

The DMR performed well within desired operating parameters during the ESTD test program, as expected. Production tests demonstrated that DMR operations are safe, reliable, and easily controlled. Accomplishments include:

- FG nozzle and waste feed injector nozzle placement (elevations) were acceptable.

- Bed levels were controlled by periodic removal of product solids out bottom of vessel.

- Bed temperatures were reliably controlled in automatic mode by controlling oxygen input to the FG.

- Hydrogen concentrations were controlled by adjusting coal input rate and inventory in the DMR bed.

- Demonstrated correlation of NO_X destruction to hydrogen levels in the DMR.

- Demonstrated safe correlation between hydrogen and oxygen in DMR at process temperatures from start-up conditions of 400°C up to normal maximum operating conditions of 670°C.

- The preferred range for DMR hydrogen is 0.5% to 1.5% on a wet basis at 640°C. Lower hydrogen levels do not support adequate NO_X destruction and carbonate product formation. Higher hydrogen levels result in little additional NO_X destruction and can only be achieved by maintaining an excessive coal inventory in the DMR.

- Coal reductant provided good NO_X reduction and needed energy in the bed, with low carbon fines carryover.

- Start-up alumina worked well with minimal carryover and no agglomerations. Preferred media is alumina with a particle size of 100 to 250 microns.

- Cyclone downcomer blockage prevented and cleared by use of three pulse jets.

- Cyclone achieved high efficiency removal of small particles, thereby limiting carryover of fines to downstream filter.

During the scoping tests when wood-based charcoal was used as the reductant and energy source in the DMR, two light bulk agglomerations (sandcastle-like) occurred in the DMR. Following a shutdown of the process, the sandcastle-like agglomerations were easily removed by light mechanical action. Analytical tests on the bed product indicated the presence of undesirable levels of Na-K-Ca eutectics on the surface of the product particles. The main source of calcium in the DMR was from the residues from the wood-based charcoal that was being used as the reductant. Accordingly, the wood-based charcoal was replaced by a coal reductant that had minimal calcium content. After changing to coal reductant in the DMR, no additional bulk agglomerations occurred in the DMR.

The coal worked very well as the reductant and energy source. The coal also was more dense and harder, so the carbon fines content of the product carryover to the HTF appeared to have been reduced. Due to the higher density of the coal, the coal inventory in the DMR bed was proportionately higher at the bottom of the fluidized section of the DMR bed; therefore, when bed product solids were removed from the bottom of the DMR, a larger than desired fraction of the coal was also removed with the carbonate product solids. In order to maintain the carbon fraction in the solid carbonate product as low as possible, it is recommended that a coal separation device be provided on the bottom solids outlet of the DMR to remove the large sized coal pieces and return them to the DMR for reuse.

Inspections of the DMR vessel following both CP1 and CP2 operations revealed a thin scale deposit on the internal walls and hardware of the DMR vessel. See Section 7.6 for a detailed treatment of the wall scale phenomenon and all appropriate references. A summary of this treatment follows.

The scale from the CP1 test was generally 1–6 mm thick. Scanning electron microscope (SEM) analyses indicated scale removed from the cyclone downcomer was made up mainly of sodium, potassium, calcium, aluminum, and sulfur, with minor amounts of silicon, potassium, and iron. X-ray diffraction (XRD) also revealed the presence of sodium aluminate. Further XRD analysis showed that this sample contained $Na2Mg(CO_3)_2$ (Eitelite), $Na_2(CO_3)\bullet H_2O$ (thermonatrite), $K_3Na(SO_4)_2$ (aphthitalite), $Al(OH)_3$ (bayerite), $NaAlSiO_4$ (nepheline), and Al_2SiO_5 (kyanite).

Another scale sample taken later during CP1 showed relatively high levels of alkalis and sulfates. The presence of increased levels of sulfate was likely due to the use of the GC-CRB coal as the reductant in the DMR, which has a higher sulfur content than the wood-based carbon used previously. A low-melting ternary eutectic mixture (Na_2CO_3-K_2CO_3-Na_2SO_4) was identified as the probable source of the "glue" in this wall scale material. The use of calcined mullite clay as a DMR bed additive seemed to exacerbate the formation of this scale by reacting in the bed to form Al_2SiO_5 (kyanite). Increasing the

reducing conditions in the DMR (higher H_2 concentrations), stopping of the use of the clay, and the addition of UDS in the DMR feed all seemed to contribute to cessation of wall scale formation in the DMR for the rest of the CP1 test.

After CP2 was concluded, a thin (1–6 mm) wall scale deposit was observed on the internal metal and refractory surfaces of the DMR. The CP2 wall scale was similar in appearance to the CP1 scale. The CP2 test did not use bed additives in the DMR and did not have UDS in the SBW feed. Microprobe and XRD analysis showed that the CP2 wall scale was comprised mainly of the bed solids sodium aluminate and sodium carbonate, and a Ca-Mg-Si mineral similar to merwinite, with an amorphous low-melting point eutectic binder of high sulfate. This analysis also indicated that the wall scale likely formed from residual ash constituents of the GC-CRB coal; in particular, the sulfate, calcium, and silicate in the coal ash. The sulfate in the SBW and most of the sulfate released into the DMR from the coal ash appears to readily combine with the SBW alkali metals to form higher melting sulfates in the majority of the product. However, a small amount of the sulfate from the coal ash apparently combines with other coal ash constituents, calcium and silicates to form low melting eutectics that tend to slowly accumulate and stick to the internal surfaces of the DMR. The presence of the small quantity of sticky sulfates and calcium silicates on the wall surfaces apparently attracts other fine solids in the bed to form a layered matrix of carbonates, aluminates, and calcium silicates that produces a gradual build up of the wall scale over time.

The scale was readily dissolved in hot water and in dilute nitric acid in 20 minutes. A simple wash of water and then dilute nitric acid was used to remove the scale from the inside surfaces of the DMR.

The mechanism of the CP2 DMR wall scale formation is being evaluated and analytical testing is still being performed. A separate detailed report will be prepared and issued that will address the composition and mechanism for development of the wall scale in the DMR.

To prevent or mitigate the formation of the scale, it is recommended that the coal for the IWTU be washed to remove the small amounts of sulfate, calcium, and silicates in the coal ash. This would prevent introduction of non-associated sulfate, calcium and silicates into the DMR and minimize potential wall scale formation. No additional ESTD or mockup testing is recommended, as the coal washing is expected to largely eliminate the potential for the sulfate, calcium, and silicate based wall scale formation in the DMR. In order to ensure that the coal is properly washed and subsequently dried prior to usage at the IWTU, it is recommended that a coal specification be prepared that will define what treatment methods can be used, what residual ash composition is allowed, and what quality control methods will be implemented for the DMR coal.. It may be necessary to perform lab-scale testing on coal washing and rinsing methods to identify the wash and rinse solution specifications and quality control standards that will be applied to coal procurement and receipt activities.

Towards the end of CP1, elevated temperatures were noted in the defluidized solids in the solids removal area above the auger at the bottom of the DMR bed. Apparently oxygen in the fluidizing steam entered the defluidized region and produced elevated temperatures in the product and coal solids that are present above the solids removal auger. The temperature excursion may have formed an agglomerate that prevented draining solids from the bottom of the DMR in the later part of CP1. An evaluation of this temperature excursion indicated that this type of temperature variation could be prevented by introducing a portion of the fluidizing steam in the bottom-most section of the fluidized region of the ESTD DMR and introducing the balance of the steam together with the autothermal oxygen just above the steam-only region for the ESTD DMR. The IWTU DMR FG distributors introduce only very low levels of oxygen in the bottom of the bed, as almost all oxygen is provided by the feed nozzle atomizing airflow. This type of temperature variation is, therefore, only a problem where the proportionately high heat losses from the ESTD refractory lined DMR must be balanced by proportionately higher inputs of oxygen with the

fluidizing steam in the bottom of the ESTD DMR. In addition, the IWTU DMR auger will have a much larger capacity and will be able to handle even large agglomerates if they form below the FG distributors.

11.1.3.1 Recommendations for Additional Testing. The ESTD auger/grinder assembly experienced occasional build-up of solids due to condensation of moisture in the cool exterior part of the auger and solids transport eductor. It is recommended that the lessons learned be incorporated into the design of the full-scale auger/grinder assembly that will then be fabricated and tested in an independent off-line mock up test. The full-scale, off-line tested grinder assembly would then be placed into the IWTU DMR.

Upon completion of CP1, it was recommended that the CP2 test program be performed to provide additional data on the carbonate product mass and density when processing SBW without UDS. In addition, the CP2 test program would quantify the amount of seed particles required to maintain the particle size in the DMR bed when processing SBW without UDS. The CP2 demonstration program was completed in June 2006 and the carbonate product mass and density data is presented in this report. In addition, the CP2 test program demonstrated that DMR carbonate particle size could be controlled without the addition of seed particles, but that seed particles could be added to the DMR if required.

No additional testing of the DMR in the ESTD is recommended or required in order to complete the IWTU detailed design. Testing of individual DMR components is recommended as discussed in Section 11.3.

11.1.3.2 Impact on IWTU. The lessons learned from the ESTD test program that have been incorporated in the IWTU DMR design include:

- Coal reductant, rather than a wood-based carbon, will be used in the DMR to prevent calcium-rich wall scale and bulk sandcastle agglomerate formation. The coal should be washed to remove sulfate, calcium, and silicate ash constituents prior to being used in the IWTU to minimize potential formation of wall scale.

- The PT ports on the DMR experienced partial blockage and flow restriction during early CP1 operations that affected the accuracy of PT instruments during portions of the CP1 production test program when high silicate wall scale formation was occurring. No PT port plugging was observed during the CP2 demonstration. The IWTU will provide high pressure nitrogen, water, and acid flush capability on DMR PT ports to clear potential plugs.

- The quantity of coal granules in the DMR bed solid product that was removed by the DMR grinder was above desired levels. In the IWTU, this would impact the final SBW waste volume and result in an increase in the final waste form canister count (estimated to increase canister count by 10% to 20%). Therefore, a coal separator will be installed external to the DMR to separate the larger coal from the smaller carbonate bed product solids removed from the DMR. Removed coal granules will be pneumatically returned to the DMR for reuse.

- When processing SBW without UDS during CP1, the product particles increased in size such that it was necessary to provide an external source of seed particles in the DMR bed. During CP2 operations, particle size was readily controlled in the DMR when processing SBW without UDS and without particle size addition. However, in the event that seed particles are required in the DMR to control bed particle size, the IWTU additive system will have the capability to introduce a metered input of inert seed particles into the DMR. CP2 demonstrated that seed particles can be added without problem to the DMR during operation and with minimal carryover of seed particles to the HTF/PGF. The IWTU additive system should include installation of a feeder and hopper on

the DMR solids addition airlock. The quantity of seed particle that could be required will vary, but could range up to 10% of the total bed product mass (up to ~25 lb/hr). Due to the small impact the occasional use of the inert seed particle addition will have on the final waste mass and volume, the process will utilize inert seed particle addition in lieu of separation and recycle of smaller bed product, which would significantly increase system complexity, cost, and maintenance.

- Occasionally the solids addition airlock valves that fed coal to the DMR would not actuate when the DACS signaled the valves to close. The specification of the IWTU solids shot-pot valves, therefore, has been upgraded to provide more powerful actuators, nitrogen purge to agitate non-flowing solids in valve bodies to clear valve disk closure path, and higher pressure air to actuators (Hazen used only 80 psig air). The valve type may be changed to a rotating disk instead of linear disk to provide improved solids closing capability.

- Temperatures in the DMR bed infrequently experienced some temperature non uniformity during off-normal operations. The introduction of higher FG flows near the internal wall of the DMR vessel appeared to improve in-bed mixing and reduce thermal gradients during these occurrences. The IWTU DMR should be modified to provide an auxiliary FG input through a ring sparge header located around the lower internal walls of the DMR to provide a means to better fluidize the wall-affected regions. Experience in the NWCF indicated that such a ring header could help stabilize in-bed temperatures during off-normal periods.

- During certain rapid off-normal shutdowns, it was possible for the DMR to have a higher pressure than the FG header. In unusual cases, this pressure reversal could result in bed solids being drawn into the FG distributor, which could impact distributor pressure drop and uniformity of FG distribution. Therefore check valves will be provided to minimize reverse flow potential into the IWTU FG header. The installation of a check valve in the Erwin facility has eliminated solids in the FG distributors.

- The DMR will be provided with the ability to remotely wash down the internal surfaces by means of hot water and/or dilute nitric acid. The DMR is provided with a drain to the cell sump so that wash down solutions can be pumped to NWCF tanks or the IWTU Waste Feed Tank for recycling of wash down solutions. By this means, any agglomeration or wall scale can be remotely removed by dissolution and the resultant liquid stored for recycle to the DMR.

- The IWTU superheater provides heat-up capability for start-up of the entire process system. The IWTU superheater specification has been increased in both capacity and upper temperature capability to reduce heat-up times to <30 hours.

- Cyclone downcomer plugging occurred during the scoping tests due to the small size and cohesive nature of the cyclone solids. Therefore, the ESTD and IWTU DMR cyclone design was modified to provide downcomer purge/pulse jet injectors on each cyclone for the IWTU DMR. Each downcomer purge jet line is provided with a continuous nitrogen purge and a timed nitrogen pulse to maintain solids movement in the downcomer. A high pressure nitrogen pulse system is provided with the capability to also perform off-line water and acid flush of pulse lines. Early operations of the DMR cyclone with the downcomer jet purges resulted in plugging of the jet purge lines. To prevent downcomer jet purge line plugging, the purge rates and pulse jet cycle frequency were increased to improve effectiveness.

11.1.4 High-Temperature Filter

The HTF performed well within desired operating parameters. The production tests demonstrated that HTF operations are reliable and easily controlled. Two types of sintered metal filters—sintered fiber and sintered powder—and one type of sintered silicon carbide filters elements were installed in the HTF during the tests.

Accomplishments include:

- Solids were effectively removed from the process gas stream by the sintered powder metal filter elements.
- Tubesheet seals (ceramic fiber rings) performed well with no apparent solids bypass around seals.
- Filter blowbacks were effective in removing product cake on external filter surfaces. No solids bridging was noted between adjacent filter elements when the filter vessel was opened for inspection.
- Filter blowbacks can be effectively automated by setting the start of pulse signal at 5 to 10 in. WC above the average filter differential pressure. Using this type of automatic filter back pulse initiation resulted in fewer blowback cycles, increased filtration efficiency, and lower nitrogen usage.
- Solids were collected in the bottom cone and were effectively removed without need for mechanical or pneumatic assistance.
- Sintered metal fiber filters are not suitable for use in the HTF. Upon completion of CP1, the sintered metal fiber filter elements were removed and inspected. It was found that the metal fibers had deteriorated to the point that continued use was impossible due to breaches in the filter media.
- Sintered powder metal and sintered silicon carbide filters are suitable for use in the HTF. These filter media were used exclusively during CP2 and performed well, experiencing negligible corrosion. The filter media found acceptable for use at the IWTU are sintered powder metal constructed of Inconel 600, Inconel 625, or Hastelloy X or sintered silicon carbide media.

11.1.4.1 Recommendations for Additional Testing. No additional testing of the HTF or filter element media is required using the ESTD.

11.1.4.2 Impact on IWTU. There is no impact on IWTU design. The IWTU design baseline for the PGF includes all major features of the HTF and will use standard dimensional filter media elements, 2.38 in. outside diameter and 59 in. long that are made of several different materials. The selected filter media elements will be incorporated into standardized filter tubesheet bundles that will all have the same dimensions and will utilize interchangeable tubesheet bundle assemblies that will not impact the design or construction of the PGF.

11.1.5 Carbon Reduction Reformer

The CRR performed well within desired operating parameters during CP1 and CP2. CRR operations were safe, reliable, and easily controlled. Accomplishments include:

- Demonstrated reliable, simple series operation of the DMR and CRR reformers. The CRR bed was well fluidized during operations by using process gases from the DMR.

- CRR alumina media had minimal attrition (<1% per day) and carryover of media to the off gas system was minimal. The CRR bed level changed little over time, as the alumina served as a semipermanent bed. The size of the alumina media was modified during the tests to provide a wider range of particle sizes. A minimum particle size of ~450 microns was determined to minimize elutriation of media. Maximum alumina size was set at 800 microns to improve ease of fluidization.

- CRR off-gas emissions were well within required MACT standards and anticipated regulatory limits.

  - Demonstrated that THC levels at the stack were near non-detection levels using the CEMS, well below MACT standard limit of 10 ppm.

  - Demonstrated that CO levels out of the CRR can be effectively controlled by controlling the oxygen concentration in the CRR process outlet gas. Increasing excess oxygen out of the CRR reduces CO levels. CO can be positively controlled, regardless of DMR operations, at levels below the MACT standard limit of 100 ppm.

  - Demonstrated that NO_X levels from the CRR can be controlled by adjusting coke inventory in the CRR bed and by controlling the coal/hydrogen levels in the DMR.

  - Demonstrated that emissions were effectively controlled at both higher and lower CRR bed depths.

- Demonstrated that automated in-bed oxygen input effectively controlled CRR bed temperature and excess free oxygen out of the CRR and, hence, CO levels at the stack. Middle and upper bed oxygen control were preferred and lower bed oxygen input was unnecessary.

- Petroleum coke worked well to provide the required energy in the CRR bed. The coke also provided the reducing conditions low in the bed to improve overall process NO_X destruction.

- Demonstrated effective heat-up of the CRR once the bed was >400°C by adding DMR carbon/coal and then at >700°C, the coke was used.

Two operational issues were noted and corrections incorporated during operation of the CRR: (1) coke versus oxygen control of CRR bed temperature and (2) small agglomerate formation caused by clay in the bed.

Initial CP1 CRR bed temperature control was performed by injecting a constant feed rate of oxygen into the bed and controlling the temperature by adjusting the coke feed rate and inventory in the bed. This method of temperature control was partially successful when the coke addition rate was manually controlled. During CP2 good operation was achieved by maintaining a higher bed level (>30 in.) and controlling the coke inventory in the bed. The CRR was successfully operated by manually maintaining

the bed level by adjusting the coke addition rate, automatically controlling the bed temperature via the in-bed oxygen injection rate, and automatically adjusting the over-bed oxygen (in CP1) or the upper-bed oxygen (in CP2) to maintain the desired levels of excess oxygen in the CRR outlet. Both modes of operation produced low CO emissions and steady CRR bed temperatures.

The DACS automated control functions did not adequately control coke addition due to the extended reaction times of coke in the bed. Accordingly, the CRR temperature control method was modified as described above. Automated oxygen control accurately controlled CRR bed temperature within a narrow band.

The bed level of the CRR was operated from a low of ~26 inches to a high of ~50 inches with reliable automated bed temperature control and with desired low CO emissions at all operating bed levels. The CRR operated with less frequent and reduced temperature and CO variations when the CRR was operated above the 30 inches bed level and with a low coke inventory.

There were several temperature excursions in the CRR bed that were the result of oxygen control input variations, which resulted from DACS control parameter tuning and iterative non-automated operational methods used during early operations. During two periods when the CRR FG flow was reduced, during process start-up and shutdown, localized CRR bed temperature excursions occurred due to continued oxygen input into the partially fluidized bed. Localized areas in the bed adjacent to the oxygen injector experienced elevated temperatures that caused clay in the CRR bed to fuse and form several small egg-sized to almond-sized agglomerates. Granular clay was the initial additive to the CRR bed to serve as a carbonate adsorbent to minimize agglomeration potential from fine carbonate particles that might pass through the HTF and enter the CRR bed. The clay agglomerates were broken up and removed without a need to shutdown the process. To prevent a recurrence, the clay additive was replaced with an aluminum hydroxide additive that has been used successfully to prevent carbonate and salt eutectic agglomerations in the Studsvik Processing Facility. In addition, the oxygen input injectors were relocated to provide improved mixing of the oxygen in the CRR bed and the oxygen/nitrogen input ratio was reduced to a maximum 50/50 mix ratio to prevent formation of localized hot spots. Additionally, the IWTU DACS will provide automated isolation of CRR oxygen input when CRR bed fluidization is below ~1.5 fps to further prevent hot spots.

The pilot plant CRR was not provided with an auger/grinder assembly that could size reduce and remove any accumulated agglomerates. Such an assembly proved unnecessary for the pilot plant, but the IWTU CRR will have an auger/grinder assembly that is identical to the DMR solids removal system that will be able to size reduce and remove agglomerates, if needed.

11.1.5.1 Recommendations for Additional Testing. With regard to the CRR, CP2 was conducted to incorporate lessons learned from CP1and improve operations. The following configuration changes were made:

- Lowered the elevation of the upper CRR oxygen injectors to reduce above-bed oxidation
- Modified the oxygen injection system to minimize the input of concentrated oxygen by limiting the oxygen/nitrogen mix ratio to 50/50.
- Added a third oxygen injection header to further distribute oxygen more uniformly in the lower bed area.

The CP2 operations demonstrated that the above listed modifications were successful in eliminating potential hot spots, providing more consistent bed temperature control, reducing above-bed oxidation, and achieving continued low CO emissions.

No additional ESTD testing of the CRR is recommended or required.

11.1.5.2 Impact on IWTU. The lessons learned from the ESTD test program that have been incorporated into the IWTU CRR design include:

- Incorporate automated oxygen input distributors in the middle and upper CRR bed regions to reduce oxygen input concentrations by spreading oxygen input over a larger, well fluidized bed volume. Modify the oxygen supply system to limit oxygen input to a maximum of 50/50 mixture with nitrogen. Provide nitrogen purge capability to purge oxygen headers during periods when oxygen flow is isolated.

- Provide, via the IWTU DCS, two coordinated oxygen controls. First, the upper oxygen distributor shall be controlled to provide the required level of excess free oxygen in the CRR outlet. Second, the middle and lower oxygen distributors shall be controlled to maintain the required bed temperature in the IWTU CRR.

- Utilize radially oriented ceramic or alloy oxygen injectors to provide high-temperature resistance and improved distributor life.

- Specify alumina bed media for CRR that has 450 to 800-micron particle size range.

- Utilize aluminum hydroxide as the carbonate mineralizing additive.

11.1.6 Off-Gas Cooler

The OGC performed well within desired operating parameters during the test program, as expected. CP1 and CP2 operations demonstrated that OGC operations were safe, reliable, and easily controlled. Accomplishments include:

- Off-gas cooler continuously quenched CRR outlet gases and maintained set point within 5°C.

- Auxiliary/standby water input effectively controlled off-gas temperature when the main water supply failed.

One operational issue was consistently present during the OGC operations—water collected in the bottom of the OGC. Water accumulation in the bottom of the OGC can occur as a result of the spray nozzle not completely atomizing the cooling water or the OGC not being of sufficient size such that some water droplets contact the wall and collect in the bottom cone of the OGC, and/or the bottom of the OGC is cool and moisture condenses in the bottom. The presence of water on the OGC internal surfaces tended to collect solids carryover from the CRR, and together with the water, formed a sludge that had to be periodically removed from the bottom of the OGC.

11.1.6.1 Recommendations for Additional Testing. No additional ESTD testing of the OGC is required or recommended.

11.1.6.2 Impact on IWTU. The IWTU design baseline for the OGC already incorporates features to prevent water collection in the OGC by implementing the following features:

- Improved spray nozzle that produces very fine water droplets that are completely evaporated before mist droplets can contact vessel wall and/or carryover to downstream off gas filter.
- The IWTU OGC vessel is substantially larger in diameter and height, such that water droplets are completely evaporated before the fine water mist can contact the vessel wall.
- The OGC is well insulated to prevent cool areas where moisture could condense.
- The IWTU OGC vendor will perform a full-scale hot functional test to demonstrate that the OGC will not experience undesirable water accumulation.

11.1.7 Off-Gas System

The off-gas system included two wet scrubbers, electrical reheater, off gas baghouse filter, blowers, ductwork, mercury adsorber, and the stack. The off-gas system blowers and temperature control performed well within desired operating parameters during the test program. The wet scrubber system was not used, as it was determined that the HCl and Cl_2 levels were very low and within the required emission limits without the use of the system. The reheater was provided to reheat the off-gas to prevent moisture condensation in the baghouse filter. The reheater and wet scrubber system operations are not discussed in this report, as they will not be part of the IWTU. With the exception of a hot spot in the GAC mercury adsorber during the initial heat-up for CP2, the off-gas and mercury adsorber operations were safe, reliable, and easily controlled. Accomplishments include:

- Demonstrated that wet scrubber system was not required to achieve emission limits that were MACT compliant.
- Demonstrated that the entire off-gas system can be maintained above 120°C to prevent moisture condensation.
- Demonstrated that the mercury adsorber effectively removed mercury from the off-gas such that mercury emissions were within MACT standard limits.
- The mercury adsorber (GAC) operated with a low pressure drop and consistent temperature control throughout the bed, with one exception as described below.
- Demonstrated that the GAC can be effectively pre-heated using off-gas flow through the cold bed. During such heat-up operations, steam FG to the DMR was switched to nitrogen to minimize moisture in the off-gas.

The mercury adsorber used sulfur-impregnated GAC media to adsorb gaseous mercury from the off-gas stream. Upon completion of CP1, it was found that the GAC bed bypass valve had not completely closed during CP1 operations due to a misaligned actuator. The partially opened valve allowed ~ 10% of the off-gas flow to bypass the mercury adsorber. This invalidated the use of the stack Hg measurement to determine the GAC bed Hg removal performance. The inter-bed Hg measurements, however, did indicate the expected GAC bed performance during CP1.

The GAC bypass valve actuator was repaired prior to CP2. Operation of the mercury adsorber during CP2 provided data that confirmed the incomplete results of CP1 and showed that the GAC bed provided the desired mercury removal efficiency.

During the initial heat-up for CP2, the GAC bed was valved on-line during the start-up period. During the heat-up of the CRR, a hot spot occurred in the top of the third bed. The GAC bed was isolated and a nitrogen purge introduced. The start-up was terminated and the GAC temperature event was investigated and evaluated prior to restart of CP2. See Section 7.7 for a detailed discussion of the GAC bed hot spot, including actions taken to prevent a recurrence, on going evaluations, and detailed references.

The GAC bed was heated-up several times and operated over extended periods with good temperature control during CP1 and during CP2 after the hot spot. Investigations have focused on differences between the successful GAC bed start-ups and the initial CP2 start-up that experienced the hot spot. The principal difference is that during the successful heat-ups the GAC bed had been off-line and was only valved on-line after the process system had been completely heated to normal operating conditions. In contrast, the GAC was on-line at the start of the initial CP2 heat-up and throughout the period of heat-up operation that resulted in the hot spot.

The events that lead up to the hot spot have been identified and appear to be related to conditions that occurred during the CRR heat-up. The test data, and supporting data from Nucon International, the GAC vendor, suggest that the GAC bed media was initially heated through exothermic sorption of water and possibly organic species from the CRR startup natural gas-fired burner. When localized hot spots were heated enough from heat of sorption of gas species, exothermic reactions between sorbed hydrocarbons and oxygen in the gas stream further heated those hot spots, eventually to a temperature high enough that some of the carbon in the heated area began to oxidize.

This hypothesis, which is supported by data and activated carbon industry experience, is being evaluated in detail, with additional sample analysis, by TTT and Nucon International. Evaluations shortly after the event lead to this hypothesis and identified corrective actions that were implemented for the successful restart and completion of the CP2 test. The GAC hot spot condition is covered in a separate report, which will be updated when analysis of the event is complete (See Section 7.7). Several lessons were learned from the GAC hot spot, which are discussed below.

11.1.7.1 Recommendations for Additional Testing. No additional testing of the ESTD mercury adsorber or off-gas system are required or recommended.

The causal factors related to the GAC temperature event continue to be evaluated. Analytical tests of the GAC media from the initial CP2 GAC bed during the hot spot and comparative analytical tests of the GAC media from the successful CP2 operations are in progress. The purpose of the continued investigation is to further develop the causal factors and to determine operating bounds for the IWTU GAC. Investigation of the causal factors is best accomplished by the use of lab-scale test equipment that has the accuracy to determine compositional analysis of adsorbed species and heats of adsorption of potential gases on the GAC media. Testing at the media vendor and at other laboratories is underway.

No additional testing of the ESTD GAC mercury adsorber is recommended as the ESTD has demonstrated reliable, safe operating methods for the GAC bed that will prevent potential risk of reoccurrence in the IWTU GAC bed. Several lessons learned have been incorporated into the IWTU GAC bed design to minimize the potential for a temperature excursion and to mitigate the impact of any potential event, as discussed below.

11.1.7.2 Impact on IWTU. The ESTD GAC bed was designed to use the same sulfur impregnated activated carbon media as will be used for the IWTU GAC bed. Specific design criteria that provided high mercury removal efficiency for the ESTD unit have been utilized for the IWTU baseline GAC bed design, including gas residence times and velocities through the bed. Lessons learned from normal ESTD GAC operation that are incorporated into the IWTU include the following:

- Provide redundant CO monitors on the inlet and outlet of the GAC to monitor for carbon oxidation that is not readily detected by in-bed and out-of-bed thermocouples.
- Utilize valves that have high sealing efficiency to prevent bypass around the GAC bed when in service and to provide positive isolation of the GAC bed when bypassed.
- Perform CFD analysis of the flow distribution media grid in the bottom media support in each of the GAC vessels. Verify that the gas flow distribution through the GAC beds is uniform across the width and length of the bed.
- Provide temperature sensors at the GAC bed inlet and outlet and at selected bed locations for enhanced temperature monitoring.
- Provide sequenced corrective actions in the event that outlet CO levels or bed temperatures rise above predetermined levels.

With the implementation of the above lessons learned for the IWTU GAC bed, it is very unlikely that there will be a temperature event, and in the unlikely case a higher than desired temperature or CO level occurs, the systems will be in place to safely reduce the in-bed temperatures, isolate the GAC, and prevent an excessive temperature event from occurring.

11.1.8 Continuous Emissions Monitoring

The ESTD system included two sets of gas monitoring analyzers: (1) The CPMS that monitors the process outlet gases downstream of the HTF as well as the off-gas oxygen content downstream of the CRR, and (2) The CEMS that monitors off-gas emissions at the process stack. The CEMS and CPMS systems performed well within desired operating parameters during the test program. Production tests demonstrated that CEMS and CPMS analyzer system operations were safe and generally reliable. Accomplishments include:

- CEMS and CPMS provided near-continuous indication of monitored gases that can be used reliably to monitor and/or control process parameters.
- Demonstrated that an SO_2 monitor is not required on process off-gas, as SO_2 levels are expected to be well below the significance level.
- Demonstrated that NO_X and CO monitors are likely not required on DMR process outlet gas, as the oxygen and combination hydrogen/CO_2 analyzers provide all required process control data needed to adjust coal inventory in the DMR.

Throughout all operations, the CPMS and CEMS required tuning, calibration checking, and sample conditioning system cleaning. Analyzer tuning and calibration checking were routine tasks that were performed during all system operations. However, sample conditioning system cleaning was problematic, particularly until modifications were made to facilitate removal of deposits from the sample conditioning system. In particular, operation of the CPMS was problematic and required frequent system cleaning to

remove ammonium carbonate particulates that formed in the conditioning system from the small amount of ammonia and abundant carbon dioxide in the DMR process gas. Additional in-line filters were added that helped reduce manual cleaning requirements.

11.1.8.1 Recommendations for Additional Testing. No additional ESTD testing needs to be performed, as the CPMS and CEMS system operated as required and design data was obtained that will provide input to the design, specification, and operation of the IWTU CPMS and CEMS.

11.1.8.2 Impact on IWTU. The IWTU design baseline for the CPMS and CEMS incorporates similar analyzers and sample conditioning systems as used for the ESTD. The following features should be incorporated into the IWTU CPMS and CEMS:

- Provide means to recycle the condensate from the CPMS and CEMS conditioning systems to the process to prevent the need for disposal of secondary waste streams.
- Ensure adequate primary and backup particulate filtration. Evaluate the potential use of NH_3 filtration to remove a precursor of solid ammonium species.
- Provide a minimum of three hydrogen detectors and two oxygen detectors on the DMR outlet process gas so one monitor can be calibrated or undergoing maintenance while the required number of monitors remain in service.
- Provide a minimum of three oxygen analyzers on the CRR off-gas for automated oxygen control in the CRR.
- Provide a minimum of two oxygen and two NO_X analyzers on the process off-gas so that one monitor of each type can be calibrated or undergoing maintenance while the other remains in service.
- Provide either two carbon monoxide analyzers or two THC analyzers and two NO_X monitors on the stack for confirmation of air permit limits for CO or THC.
- Provide nitrogen dilution on the CPMS conditioning system to reduce build-up of particulates in the conditioning system and if an ammonia scrubber is determined appropriate for this application, install and test the ammonia removal system during the SAT.

11.1.9 Data Acquisition and Control System (DACS)

The DACS performed within desired operating parameters during the test program following extensive debugging and tuning operations that impacted the efficiency of initial scoping tests. Through the upgrading of memory modules, reprogramming some control loops and interlocks, and significant tuning efforts during the scoping tests, the DACS performed well throughout the production tests with the exception of a few infrequent variations from stable operating conditions. Production tests demonstrated that the process systems can be safely and reliably controlled with a reliable control system. Accomplishments include:

- Uniform automatic temperature control of the DMR and CRR beds was achieved. The DACS automatically controlled oxygen input to the DMR and CRR to control temperatures.
- System pressures were maintained at desired levels by remotely adjusting blower speed (non automated input) from HMI.

- DMR fluidizing gases were maintained within desired flow ranges by controlling input of FG (automated steam and oxygen) to DMR.

- Uniform automatic temperature control was achieved by the OGC, off-gas reheater, and DMR FG superheaters.

- Carbon addition to the DMR and coke addition to the CRR were manually controlled remotely from the HMI.

The DACS was based upon LabView software that is designed to provide efficient, low cost control of smaller process systems. Significant effort was required to program and debug the DACS logic and control loops during initial scoping tests. LabView controller modules required memory upgrades and reprogramming of some control loops and logic to simplify the routines so the controllers performed more efficiently.

The DACS was a limited capacity system that was used to provide cost and schedule efficiencies compared with the fully hardened, industrial ABB Distributed Control System (DCS) that will be provided for the IWTU. Due to cost and schedule needs, the ESTD DACS utilized a limited level of interlocks, minimal automated shutdowns, and only one automatic waste feed cutoff; whereas, the IWTU DCS will have complete interlocks, fully automated control features, extensive safety shutdowns, alarm matrices with graded actions, and an automatic history system with redundant backup.

11.1.9.1 Recommendations for Additional Testing. No additional ESTD testing needs to be performed as the DACS performed as required, and the ESTD DACS limited interlock and rapid shutdown system programming is not representative of the extensive IWTU DCS programming.

11.1.9.2 Impact on IWTU. The IWTU design baseline for the DCS incorporates significant improvements in capabilities and redundancy, etc., compared with the ESTD DACS. The IWTU DCS will benefit from the ESTD DACS experience in the following areas:

- A program logic document has been prepared of the ESTD DACS programming, interlocks, control loop tuning parameters, etc., to serve as a starting point for programming of the IWTU DCS.

- It is recommended that the IWTU DCS be programmed well before the performance of the Site Acceptance Test (SAT), with off-line testing of the DCS software and hardware components prior to start of the SAT.

- Evaluate data archiving for IWTU operations so data retrieval and archiving is performed automatically with redundant databases.

11.2 Conclusions

The IWTU SBW carbonate testing program was performed at the Hazen Research facility in Golden, Colorado, during the period November 2005 through June 2006. The ESTD was a one tenth scale process, based on SBW throughput, of the planned IWTU facility for treating actual SBW for ultimate disposal at WIPP. The THOR® dual fluidized bed steam reforming technology employed in the ESTD was successful in generating data that supports full-scale process system design, permitting, and operation. The ESTD was functionally tested with regard to components and systems. Scoping tests were performed to determine appropriate process additives and operating parameters. Two production tests, CP1 and CP2, were performed at a variety of process conditions (e.g., reformer temperatures and liquid

simulant feed rates), during which numerous process gas, off-gas, and product solids samples were obtained to confirm compliance with MACT and other emissions regulations and general suitability of the product materials for disposal at WIPP. Process samples also supported mass balance determination and closure.

The operational data were collated, evaluated, and integrated with the analytical data. The documented performance and analytical data verifies that the testing activities were successful and no additional integrated ESTD testing is recommended to complete the IWTU final design and prepare the operating procedures, permits, and other project documentation. Although additional testing activities using the integrated ESTD process system is not necessary, a separate follow-on test program for individual full-scale IWTU components and subsystems is underway and is summarized in Section 11.3.

Specific achievements of the SBW ESTD demonstration program include:

- Approximately 500 hours of ESTD operation with simulant feed were logged, processing ~7,900 gallons (~89,000 pounds) of liquid SBW simulant into ~16,200 pounds of solid product.
- An overall input/output material balance closure of about 98% was achieved, with detailed material balances for individual elements being completed with excellent closure.
- It was determined that delivery of a constant/consistent simulant feed to the DMR is a key to stable operation. Four waste feed injection nozzle designs were evaluated and nozzle performance was substantially improved during the course of operations. Knowledge gained will be valuable when scaling up to the IWTU waste feed injectors.
- Process additives in the form of carbon and fluidized bed stabilizers were evaluated. Carbon types and bed media materials were selected for the DMR and CRR. Some additives were shown to be more desirable than others with regard to stabilizing the fluidized beds and enhancing process performance.
- The off-gas system, including the mercury adsorber GAC bed, operated well over the course of the test program. Off-gas emissions were demonstrated to be within MACT or other expected permit levels for the IWTU.
- The product solids generated were demonstrated to be chemically and physically compatible with WIPP disposal.
- Corrosion coupons were placed in strategic locations throughout the process system. These coupons were removed and selected coupons submitted to SRNL for metallurgical analysis. The metallurgical analyses are completed and have provided required data to select IWTU process system materials of construction and corrosion rates.
- Numerous challenges were met with regard to process equipment, chemistry, and operating parameters. A great deal has been learned about the process and how best to operate it.
- The entire suite of test objectives, as discussed in Section 10, was achieved.
- Lessons learned have been recorded, as described in Section 11.1. The incorporation of the ESTD lessons learned will provide confidence that the IWTU final design will proceed without open concerns and that the IWTU will operate in a safe and reliable manner.

In general, it has been shown that the integrated ESTD process system can provide safe, reliable, and predictable operation for the processing of SBW simulant over a wide range of waste feed variation and within a set of well defined and robust operating parameters.

11.3 Recommended Path Forward

A significant amount of performance and analytical data have been generated and evaluated during the course of the SBW carbonate scoping and production runs. The discussion in this section is based upon the final analytical results, operating data, and lessons learned during course of the testing program.

11.3.1 Testing Needs Prior To Integrated Process System Acceptance Test

The ESTD carbonate test program has provided the technical data, operating parameter guidelines, principal product characteristics, product masses and volumes, gaseous emissions data, and data on component and integrated system performance needed to complete the IWTU process system and component designs. However, there are several specific full-scale IWTU components and subsystem designs that would benefit from additional individual testing. This additional testing will be performed prior to the IWTU SAT. For the components and systems designated to be tested during the SAT program, no additional discussion is provided in this report.

The following list of testing recommendations is a summary of the recommendations for additional testing of individual full-scale IWTU components and subsystems during the Mockup Test Program (See detailed discussions in Section 11.1 and below):

- Integrated Process System
  - No additional integrated process system testing is recommended or required prior to the IWTU SAT. The THOR® SBW carbonate flowsheet and integrated FBSR process have been well demonstrated. Lessons learned will be incorporated into IWTU components and systems and the integrated IWTU process will be tested during the SAT.
- Denitration and Mineralization Reformer
  - Grinder and coal granule separation: Perform off-line full-scale grinder and coal granule separator test using prototype of full-scale grinder and coal separator with solids at temperature. Test to be performed using a mockup of the bottom of the DMR with heaters to provide hot solids to grinder and coal separator. Work to be included in the Mock-Up Test Program.
  - Waste feed injectors: Perform thermal performance test on full-scale waste feed injectors using heated oven and test apparatus. Perform ambient temperature atomization tests to define range of atomizing gas and waste feed flows that provide desired level of atomization.
  - Additive solids addition airlocks: Incorporate lessons learned into IWTU solids additive airlock and provide seed particle addition feeder to airlock. Test full-scale additive feeders and airlock at vendor's facility.
- High-temperature Filter
  - No additional ESTD testing is required.

- Carbon Reduction Reformer
  - No additional ESTD testing is required.
- Off-gas Cooler
  - Incorporate lessons learned into IWTU OGC and perform computational fluid dynamics modeling of IWTU OGC to ensure that water droplets are fully evaporated in the OGC. Perform full-scale test of OGC performance at vendor's facility.
- Off-gas System
  - No additional ESTD testing is required.
  - Perform necessary lab-scale evaluations of adsorption in GAC bed media and causal factors of the temperature excursion. Perform computational fluid dynamics modeling of IWTU GAC to verify uniform gas flow distribution. Incorporate lessons learned into IWTU GAC design and operational methods.
- CEMS and CPMS
  - No additional ESTD testing is required.
- Data Acquisition and Control System
  - No additional ESTD testing required. Perform logic check and implement simulator to verify programming and logic of full-scale ABB DCS for the IWTU.
- Product Solids Handling and Packaging Subsystem
  - Not part of ESTD objectives; no ESTD testing is required.

12. REFERENCES

1. C. M. Jantzen, "Engineering Study of the Hanford Low Activity Waste (LAW) Steam Reforming Process (U)," WSRC, TR, 2002, 00317, Rev. 0, Savannah River Technology Center, July 12, 2002.

2. D. W. Marshall, N. R. Soelberg, K. M. Shaber, "THOR® Bench, Scale Steam Reforming Demonstration," INEEL/EXT-03-00437, Idaho National Engineering and Environmental Laboratory, May 2003. (Phase 1 Report)

3. C. M. Jantzen, "Disposition of Tank 48-H Organics by Fluidized Bed Steam Reforming (FBSR) (U)," WSRC, TR, 2003, 00352, Rev. 0, Savannah River Technology Center, September 18, 2003.

4. B. P. McGrail, et al., "Initial Suitability Evaluation of Steam Reformed, Low Activity Waste for Direct Land Disposal," PNWD, 3288, WTP, RPT, 097, Rev. 0, Battelle, Pacific Northwest Division, January 2003.

5. B. P. McGrail, "Laboratory Testing of Bulk Vitrified and Steam, Reformed Low, Activity Forms to Support a Preliminary Assessment for an Integrated Disposal Facility," PNNL, 14414, Pacific Northwest National Laboratory, September 2003.

6. F. M. Mann, "Risk Assessment Supporting the Decision on the Initial Selection of Supplemental ILAW Technologies," RPP, 17675, Rev. 0, CH2M-HILL Hanford Group, Inc., September 29, 2003.

7. C. M. Jantzen, "Characterization and Performance of Fluidized Bed Steam Reforming (FBSR) Product as a Final Waste Form (U)," WSRC, MS, 2003, 00595, Revision 0, Savannah River National Laboratory.

8. N. R. Soelberg, D. W. Marshall, S. O. Bates, D. D. Taylor, "Phase 2 THOR® Steam Reforming Tests for Sodium, Bearing Waste Treatment," INEEL/EXT-04-01493, Idaho National Engineering and Environmental Laboratory, January 30, 2004.

9. B. P. McGrail, D. H. Bacon, R. J. Serne, K. M. Krupka, R. J. Puigh, R. Khaleel, and S. Finfrock, "Risk Assessment Supporting the Decision on the Initial Selection of Supplemental ILAW Technologies," F. M. Mann, CH2M Hill Hanford Group, Inc., Pacific Northwest National Laboratory and Fluor Federal Services, Inc., RPP, 17675, Rev. 0, September 2003.

10. "Pilot Plant Testing Plan for Treating Sodium-Bearing Waste Surrogates Using the THOR® Steam Reforming Process," TP 1.1, Revision 3, February 14, 2006.

11. D. Kunii and O. Levenspiel, Fluidization Engineering, 2nd Ed., Butterworth-Heinemann, Boston, 1991, p 70.

12. Remote-Handled Transuranic Waste Acceptance Criteria for the Waste Isolation Pilot Plant, DOE/WIPP-Draft-23-3123, Rev. 0 Draft 23, U.S. Department of Energy, Carlsbad Field Office.

13. "Feed Composition for the Sodium-Bearing Waste Treatment Process," INEEL/EXT 2000-01378, Revision 4, June 2004.

14. OI 1.3, "Sodium Bearing Waste Pilot Plant Normal Operations," Revision 3, February 9, 2006.

15. OI 1.5, "Sodium-Bearing Waste Pilot Plant Solids and Liquid Sampling," Revision 2, December 14, 2005.

16. 40 CFR 264.342, "Principal Organic Hazardous Constituents (POHCs)," Code of Federal Regulations, Office of the Federal Register, July 14, 2006.

17. "Hazardous Waste Incineration Measurement Guidance Manual," Volume III of the Hazardous Waste Incineration Guidance Series, EPA/625/6-89/021, June 1989.

18. "Demonstration Testing for Mixed Waste Thermal Treatment Technologies," National Technical Workgroup on Mixed Waste Thermal Treatment, sponsored through an Interagency Agreement between the EPA and DOE, May, 27, 1997.

19. "Guidance on Setting Permit Conditions and Reporting Trial Burn Results," EPA 625/6 89/019, January 1989.

20. "Pre-Start and Checkout of Pilot Plant Equipment," GWI 1.3, Revision 0, November 2, 2005.

21. "Calibration and Control of In-Process Instrumentation," GWI 1.2, Revision 0, November 11, 2005.

22. "Pilot Plant Testing Sequence for Sodium-Bearing Waste Surrogates Using the THOR® Steam Reforming Process," TSD 1.1, Revision 3, February 17, 2006.

23. "Quality Assurance Project Plan for Treating Sodium Bearing Waste Using the THOR® Steam Reforming Process," QAPP 1.1, Revision 0, November 11, 2005.

24. "LabView Developer Suite Software Qualification Plan," GWI 1.6, Revision 0, December 5, 2005.

25. EDF-6923, 2006, "Hydrogen Generation and Fate for the Sodium-Bearing Waste Integrated Waste Treatment Unit," Revision 0, Idaho Cleanup Project, April 25, 2006.

26. Hazen CP2 Granular Activated Carbon (GAC) Bed Over-temperature Condition Joint Test Group Action Form No. 7, Washington Group International, May 17, 2006.

27. C. M. Jantzen letter report to B. Mason, SRNL-PSE-2006-00044, Rev. 1, "Characterization of Hazen Pilot Scale Demonstration Waste Form Products, Agglomerates, and Scale," March 20, 2006.

28. C. M. Jantzen, J. C. Marra, J. M. Pareizs, "Analysis of Raw Materials for Fluidized Bed Steam Reforming (FBSR)," SRNL-ITB-2004-0004, June 30, 2004.

29. Superior Graphite, Desulco 9005 Product Certification, August 10, 2005.

30. "Design Basis Document for Engineering Scale Test Demonstration at Hazen Research for Treating Sodium-Bearing and Drummed Waste Surrogates," DB-21-001, Revision 03, December 14, 2005.

31. "Outokumpu HSC Chemistry® for Windows," Chemical reaction and equilibrium software with extensive thermochemical database, Version 5.11, copyright ˜ 1974—2002 by Outokumpa Research Oy, 2002,

32. Hazen Memo from Bob Johnson to Harry Mudget, "Microprobe and XRD analysis of Sample No. 2334-PR, Hazen Project No. 10386-05, "dated August 11, 2006.

33. Hazen Memo from Bob Johnson to Larry May, "Summary of Samples Analyzed from Pilot Plant Operations," dated May 5, 2006.

34. Hazen Memo from Bob Johnson to Harry Mudget, "Sample 2376 Bark, Hazen Project 1-386-05," dated July 21, 2006.

35. "Design of the ESTD Mercury Adsorption Activated Carbon Bed Vessel," DB 21 002-00, Washington Group, November 2005.

36. Boardman, R.D., L. J. Young, N. R. Soelberg, M. L. Abbott, and D.V. Croson, "Summary of NWCF Calciner Emissions Inventory Data," INEEL/EXT-99-1190, November 1999.

37. Young, L. J., N. R. Soelberg, B. H. O'Brien, R. D. Boardman, L. A. Matejka, M. L. Abbott, and G. R. Hassel, "NWCF Calciner Emissions Inventory – Final Report for Test Series 1, 2, and 3," INEEL/EXT-2000-00114, January 2000.

38. 49 CFR 173.57, 2006, "Acceptance Criteria for New Explosives," Code of Federal Regulations, Office of the Federal Register, June 12, 2006.

39. "UN Recommendations on the Transport of Dangerous Goods, Manual of Tests and Criteria," Section 13, Fourth Edition, 2004.

40. Test Methods for Evaluating Solid Waste, Physical/Chemical Methods, SW-846, 3rd Edition, Revised, U.S. Environmental Protection Agency, Washington, DC, November 1986. (Available with updates at: http://www.epa.gov/epaoswer/hazwaste/test/under.htm.)

Appendix A

Summary of Data Validation Packages

Appendix A

Summary of Data Validation Packages

A level "A" validation, as defined by Sample and Analysis Management (SAM) guide document (GDE)-7003,[1] was performed on off-gas sample analysis data generated by Severn Trent Laboratories, Inc. SAM implements the applicable criteria mandated by the U.S. Environmental Protection Agency's Contract Laboratory Program at INL. The data were validated in accordance with the applicable procedures instituted by SAM for performing analytical method data validation as outlined in the following guides (GDEs): GDE-201, "Inorganic Analyses Data Validation for Sample and Analysis Management,"[2] for data packages pertaining to inorganic analyses; GDE-239, "Validation of Volatile Organic Compounds Data Analyzed Using Gas Chromatography/Mass Spectrometry,"[3] GDE-240, "Validation of Gas and Liquid Chromatographic Organic Data,"[4] and GDE-241, "Validation of Semivolatile Organic Compounds Data Analyzed Using Gas Chromatography/Mass Spectrometry,"[5] for organic data packages and GDE-205, "Radioanalytical Data Validation,"[6] for radiological data packages, the SBW Test Plan (Document No. 28276-21-0015-01), and Quality Assurance Project Plan 1.1 (QAPP). This section provides a summary of the Limitations and Validation reports for these data. The complete set of data validation reports is available in CWI project files.

A total of fifteen (15) samples for hydrochloric acid and fifteen (15) samples for chlorine were analyzed using laboratory Standard Operating Procedures (SOPs) equivalent to specified test methods, i.e., SW-846 Method 9057. The validation results were reported in files *idvsbwoffgasdnt06147.pdf*, *idvsbwoffgasdnt06148.pdf*, and *idvsbwoffgasdnt06149.pdf*. All initial calibration verification (ICV) standards and continuing calibration verification (CCV) standards percent recoveries were within the control limits of 90–110%. All initial calibration blanks (ICBs) and continuing calibration blanks (CCBs) were non-detects. All reported sample results for hydrochloric acid and chlorine were verified and confirmed from the raw data. The relative percent differences were all within the 20% control limit. All sample results were assessed and remain unqualified.

Twelve (12) fiIter/XAD/solvent/H20 samples were collected and analyzed for Semivolatile Organic Compounds by SW-846 8270C/EPA 0010. The validation results were reported in files *TS0019_G6A250261.pdf*, *TS0020_G6B070348.pdf*, *TS0027_G6B100336.pdf*, and *TS0021_G6B170239.pdf*. The target compound analyses of these samples showed compliance with the quality control (QC) requirements of SW- 846 Method 8270C, and all data are valid and acceptable, with the following exceptions:

- According to the laboratory, all matrices (filter, methanol/$MeC1_2$, acetone/$MeC1_2$, XAD) were extracted separately, combined, and then analyzed as a single sample.

- The initial and continuing calibrations were below the 0.05 relative response factor (RRF) quality control criterion for 1,3,5-trinitrobenzene and pentachloronitrobenzene. Non detected results for these compounds were rejected, "R," in all samples.

- Di-n-butylphthalate was detected in the method blank. The positive result for di n butylphthalate below the action level was qualified as non-detected, "U," in sample 1. The field blanks were not qualified for method blank contamination. Positive results for di n butylphthalate were qualified as estimated, "J," in samples TB1 and TB2.

- The percent recovery of hexachlorocyclopentadiene exceeded the quality control standards in the blank spike. Non-detected results for hexachlorocyclopentadiene were rejected, "R," or qualified "UJ" in all samples.

- The percent recovery of phenol was below the quality control criterion in the blank spike and blank spike duplicate. Non-detected results for phenol were qualified as estimated, "UJ," in all samples. The qualified data have been reported for completeness and would not have affected the validity of the sample results.

- Several tentatively identified compounds (TICs) were detected in the method blank at various retention times. TICs with similar retention times were lined out of the samples. TICs identified with a CAS number were qualified as presumptively present "NJ." The amounts of all TICs were near or below detection limits. The appearance of a few TICs, and the occurrence of a few low surrogate recoveries, are common.

Ten (10) samples were collected and analyzed for Polychlorinated Dibenzodioxins (PCDD) and Polychlorinated Dibenzofurans (PCDF) by SW-846 Method 8290 and eleven (11) samples for Dioxin-like Polychlorinated Biphenyl (PCB) congeners using EPA Method 1668 were collected and analyzed. The validation results were reported in file *TS0032_G6B100306rev1.pdf*. The target compound analyses of the samples showed compliance with the QC requirements of SW 846 Method 8290 and EPA Method 1668. No qualification of the data was necessary.

Twenty six (26) samples were collected and analyzed for antimony (Sb), arsenic (As), barium (Ba), beryllium (Be), cadmium (Cd), cerium (Ce), cesium (Cs), chromium (Cr), cobalt (Co), copper (Cu), lead (Pb), manganese (Mn), mercury (Hg), nickel (Ni), phosphorus (P), selenium (Se), silver (Ag), thallium (Ti), and zinc (Zn) using SOPs equivalent to specified test methods, i.e., SW-846 Method 7470A for mercury and Method 6020 for the remaining metals. Results of the validation effort were reported in file *idvsbwoffgasdnt06157.pdf* and shown in Table A-1.

Table A-1. Sample data results that received validation qualifying flags.

Analy te	Blank Contamination	Quality Control
As	U	
Ce		UJ
Cu		J
Hg		J
P		J
Se		J
Ag	U	
Zn	U	

U = The material was analyzed for and was detected at or above the applicable detection limit. However, the associated value was less then 5 times the highest positive amount in any laboratory blank.
UJ = The material was analyzed for, but was not detected. The associated value is an estimate and may be inaccurate or imprecise. A "UJ" validation flag is not differentiated from the combined action of both a "U" and "J" validation flag.
J = The material was analyzed for and was detected at or above the applicable detection limit. The associated value is an estimate and may be inaccurate or imprecise.

The results for the remaining constituents were considered valid and acceptable. Those constituents which received qualifiers were detected at or near the range of detectability and would therefore not have significantly affected the results. The results have been included in the report for completeness of the dataset.

Validation files *idvsbwoffgasdnt06150.pdf* and *idvsbwoffgasdnt06151.pdf* report the results of forty (40) and forty-three (43) samples, respectively, that were collected and analyzed for mercury by using laboratory Standard Operating Procedures (SOPs) equivalent to specified test methods, i.e., SW-846 Method 7470A. All ICV and CCV percent recoveries were within the control limits of 90-110%. All ICB and CCB results were non-detects. All reported sample results for mercury were verified and confirmed from the raw data. All samples were analyzed for mercury after the 28-day holding time had expired. Therefore, all mercury results that were reported as non-detects ("ND" on the report forms) were assigned a "UJ" validation flag and all mercury results that were reported as positive detections were assigned a "J" validation flag. It is recognized that the hold time was exceeded: however, the data are reported for completeness. Subsequent results obtained in the CP2 test are valid and are also presented.

Eleven (11) samples were collected and analyzed for total chromatographable organics (TCOs) and total gravimetric organics (TGOs) by EPA Method 018. The validation results were reported in file *TS0028_H6A250122.pdf*, *TS0030H6A300137.pdf*, *TS0024_H6B080113rev1.pdf*, *TS0025_H6B080115.pdf*, and *TS0026_H6B170307.pdf.* The target compound analyses of the samples showed compliance with the QC requirements of EPA Method 018 and all data are valid and acceptable with the following exceptions:

- Surrogate recoveries were validated using the surrogate recoveries reported on the Form Is.
- The laboratory combined the filter, XAD, solvent, and condensate media together in one extract, which was then analyzed.
- The method blanks associated with QC batches contained TCO at a concentration of ~1.0 mg. The laboratory blanks corrected the positive results.
- The method blanks associated with QC batches contained TCO at a concentration of ~0.028 mg.
- According to the laboratory, samples 4A-1, 4A-2, 4A-3, 4A-3B, 4A-4, 4A-5, and 4A-6 required a dilution ranging from 5X to 40X because of the sample matrix. The surrogate n heptadecane for all samples was diluted out due to the sample dilution. No action was taken on this basis. The result calculation for TCO in all samples was checked and verified. No action was taken on this basis. The data are considered valid as the sample results were corrected using the blank values.

Six (6) Tenax® tube, six (6) Anasorb® tube, and one (1) condensate samples were collected and analyzed for Volatile Organic Compounds by EPA 0031/SW-846 8260B. The validation results were reported in file *TS0029_H6A250128rev1.pdf*. Twenty-seven (27) additional Tenax® tube, twenty-seven (27) Anasorb® tube, six (6) condensate, and two (2) solvent (reagent blank) samples were collected and analyzed by the same method. The validation results were reported in file *TS0031_H6B070219rev1.pdf*. The target compound analyses of the samples showed compliance with the QC requirements of EPA 0031/SW-846 8260B, and all data are valid and acceptable, with the following exceptions:

- The initial calibration performed on November 28, 2005, was below the 0.05 relative response factor (RRF) quality control criterion for 2-butanone. Non-detected results for 2 butanone were rejected, "R," in all samples.

- The initial calibration performed on November 28, 2005, exceeded the 15% relative standard deviation (RSD) quality control criterion for 1,2 dibromo 3 chloropropane and naphthalene. The positive result for naphthalene in sample 1A Tenax was qualified as estimated, "J." Non-detected results for 1,2 dibromo 3 chloropropane and naphthalene were qualified as estimated, "UJ" in all samples except the Anasorb portion of IA, 1B, and 1C because the results were rejected for surrogate recovery non-compliance.

- The continuing calibration performed on January 27, 2006, exceeded the 20% difference quality control criterion for dichlorodifluoromethane. No action was taken for non-detected results on this basis. Positive results for dichlorodifluoromethane were qualified as estimated "J."

- All surrogates were outside the quality control criteria in the Anasorb portion of samples IA, IB, and 1C. In addition, the surrogate 1,2-dichloroethane-d4 was not recovered. Non-detected results were rejected, "R," and positive results were qualified as estimated, "J," in the aforementioned samples.

- The surrogates dibromofluoromethane and 1,2 dichloroethane-d4 exceeded the quality control criteria in the Tenax portion samples 1 FB and A-5296. No action was taken on this basis because all results were non-detected in the aforementioned samples.

- The surrogate 1,2-dichloroethane-d4 exceeded the quality control criterion in the Anasorb portion of sample 1 FB. No action was taken on this basis because all results were non detected in the aforementioned sample.

- All internal standards were below the quality control criterion in the Anasorb portion of samples IA, IB, and 1C. In addition, the internal standards fluorobenzene and chlorobenznene-d5 were ~25% recovered. Non-detected results for all compounds except 1,2,3-trichloropropane, 1,3,5-trimethylbenzene, 1,3 dichlorobenzene, 1,4-dichlorobenzene, 1,2-dichlorobenzene, 1,2-dibromo-3-chloropropane, 1,2,4-trichlorobenzene, hexachlorobutadiene, naphthalene, and 1,2,3-trichlorobenzene were rejected, "R, in the aforementioned Anasorb samples. Positive results were qualified as estimated, "J," in the Anasorb samples IA, 1 B, and 1 C. No action was taken for nondetected results of 1,2,3 trichloropropane, 1,3,5-trimethylbenzene, 1,3-dichlorobenzene, 1,4 dichlorobenzene, 1,2-dichlorobenzene, 1,2-dibromo-3-chloropropane, 1,2,4 trichlorobenzene, hexachlorobutadiene, naphthalene, and 1,2,3-trichlorobenzene because they were rejected for surrogate recovery non-compliance.

- The off-gas sample Anasorb tube analyses generally had low recoveries of sampling surrogates and internal standards, causing all of the reported values to be flagged as estimated or rejected. This has been noted in other test programs and may be due to NO_X levels in the off-gas that were high enough to interfere with the analysis of those surrogates. Since the Anasorb tube is a backup for the Tenax tubes, and the Tenax tube and condensate analyses generally had good surrogate and internal standard recoveries, the flags on the Anasorb tube results have not been propagated to the test total values that include the Anasorb, Tenax, and condensate analyses.

TICs were detected in the method blanks at various retention times. TICs with similar retention times were lined out of the samples. TICs identified with a CAS number were qualified as presumptively present "NJ." The result calculation for dichlorodifluoromethane in sample 1A was checked and verified. The amounts of all TICs were near or below detection limits. The appearance of a few TICs, and the occurrence of a few low surrogate recoveries are common using this method.

Seven (7) condensate samples were collected and analyzed for Unspeciated Volatile Organic Compounds by EPA 0040/SW-846 5030B/8015B. The validation results were reported in files *TS0022_H6A250131pdf*, and *TS0023_H6B070208.pdf*. The target compound analyses of the aqueous samples showed compliance with the QC requirements of EPA 0040 / SW-846 5030B/8015B, and all data are valid and acceptable, with the following exceptions:

- C6 was detected in the field blank. The positive result for C_6 below the action level was qualified as non-detected, "U," in Sample 1. The result calculation for C_6 in Sample 1 field blank was checked and verified.

- According to the chain of custody, the samples arrived without custody seals. No action was taken on this basis.

- The continuing calibration performed on February 9 at 0918 exceeded the 10% difference quality control criterion for C_4. Non-detected results for C_4 were qualified as estimated, "UJ," in all samples. These data are reported for comparison and completeness, as the results are generally consistent with the results of the other test conditions. The C_4 compound results for the condensate are flagged as UJ, because the continuing calibration exceeded the 10% difference QC criterion, however, these non-detects do not significantly contribute to the total C_4 results so the flag does not propagate to the total C_4 values.

Table A-2 provides a listing of the data validation files with corresponding sample data package information.

Table A-2. Data packages.

Data Validation File	STL Project Code (Sample Delivery Group)	Production Condition	Method Description	Date Sampled
idvsbwoffgasdnt06147.pdf G	6A210169	1	M 26A	1/18/2006
TS0019_G6A250261.pdf	G6A250261	1	M 0010 - Spec. VOCs	1/19/2006
	G6A250261	1	M 0010 - Train Blanks	1/26/2006
	G6A260335	1	M 29	1/19/2006
TS0020_G6B070348.pdf	G6B070348	4A-1 through 4A-3	M 0010 - Spec. VOCs	1/29-30 & 2/1/2006
idvsbwoffgasdnt06148.pdf	G6B100258	2A, 3B, 4A-1 through 4A-6	M 26A	1/27-30 & 2/1-4/2006
TS0032_G6B100306rev1.pdf	G6B100306	4A-1 through 4A-6	M 0023A	1/29-30 & 2/1, 2, 4, 8, 16/2006
TS0027_G6B100336.pdf	G6B100336	4A-4 through 4A-6	M 0010 - Spec. VOCs	2/2, 4, 8/2006
idvsbwoffgasdnt06157.pdf	G6B100373	2A, 3B, 4A-1 through 4A-6, 5, 6	M 29	1/27-30 & 2/1-4/2006
idvsbwoffgasdnt06150.pdf	G6B130215	3B, 4A-1 through 4A-6, 5, 6	OHM - 2nd Stage GAC	1/28-30 & 2/1-5, 9, 10/2006
idvsbwoffgasdnt06151.pdf	G6B130217	3B, 4A-1 through 4A-6, 5, 6	OHM - 1st Stage GAC	1/28-30 & 2/1-5, 9, 10/2006
TS0021_G6B170239.pdf	G6B170239	Reagent Blanks	M 0010 - Spec. VOCs and TCO-Grav.	2/16/2006
idvsbwoffgasdnt06149.pdf	G6C010220	5 and 6	M 26A	2/9-10/2006
	H6A250122	1	M 0010 - TCO-Grav.	1/19/2006
TS0028_H6A250122.pdf H	6A250122	1	Media Checks	1/20/2006
TS0029_H6A250128rev1.pdf H	6A250128	1	M 0031	1/19/2006
	H6A250128	1	Train Blanks, Media Checks	1/19/2006
TS0022_H6A250131.pdf	H6A250131	1	M 0040 Condensate	1/19/2006
TS0030_H6A300137.pdf	H6A300137	1	M 0010 - TCO-Grav.	1/26/2006
	H6A300137	1	Train Blanks	1/26/2006
TS0023_H6B070208.pdf	H6B070208	4A-1 through 4A-4	M 0040 Condensate	1/29 through 2/2/2006

Table A-2. (continued).

Data Validation File	STL Project Code (Sample Delivery Group)	Production Condition	Method Description	Date Sampled
TS0031_H6B070219rev1.pdf, TS0031_H6B070219PARTB.pdf TS0031_H6B070219PARTC.pdf	H6B070219	4A-1 through 4A-4	M 0031	1/29 through 2/2/2006
TS0024_H6B080113rev1.pdf	H6B080113	4A-1, 4A-2, 4A-3 (Day 2)	M 0010 - TCO-Grav.	1/29-30 & 2/1/2006
TS0025_H6B080115.pdf	H6B080115	4A-3 (Day 1)	M 0010 - TCO-Grav.	1/30/2006
TS0026_H6B170307.pdf	H6B170307	4A-4 through 4A-6	M 0010 - TCO-Grav.	2/2, 4, 8/2006
	H6C300257	4A5 and 4A6	M 0031 (Condensates Only) and M 0040	2/4/2006
	H6D070261	4A5 and 4A6	M 0031 (Tubes Only), Media Checks	2/4, 5, 7, 8/2006

REFERENCES

1. GDE-7003, Bechtel BWXT Idaho, LLC (BBWI) Environmental Operations Division Sample, Management Office, "Levels of Analytical Method Data Validation," Rev. 3, March 2005.

2. GDE-201, "Inorganic Analyses Data Validation for INEEL Sample and Analysis Management," Sample and Analysis Management, current revision.

3. GDE-239, "Validation of Volatile Organic Compounds Data Analyzed Using Gas, Chromatography/Mass Spectrometry," Sample and Analysis Management, current revision.

4. GDE-240, "Validation of Gas and Liquid Chromatographic Organic Data," Sample and Analysis Management, current revision.

5. GDE-241, "Validation of Semivolatile Organic Compounds Data Analyzed Using Gas Chromatography/Mass Spectrometry," Sample and Analysis Management, current revision.

6. GDE-205, "Radioanalytical Data Validation," Sample and Analysis Management, current revision.